Compartment Fire Toxicity: Measurements and Aspects of Modelling

Abdulaziz Abdulrahman S Alarifi

Submitted in accordance with the requirements for the degree of Doctor of Philosophy

The University of Leeds

Energy Research Institute
School of Chemical and Process Engineering

February 2016

The candidate confirms that the work submitted is his/her own, except where work which has formed part of jointly-authored publications has been included. The contribution of the candidate and the other authors to this work has been explicitly indicated below. The candidate confirms that appropriate credit has been given within the thesis where reference has been made to the work of others.

I. A. Alarifi, H. N. Phylaktou and G. E. Andrews (2015) **What Kills People in a Fire? Heat or Smoke?**, Proceedings of the 9th Saudi Students Conference, 13-14 February, 2016. University of Birmingham, Birmingham, UK. (submitted)

(Included in Chapter 1)

The candidate led the writing up of the publication. Dr Phylaktou and Prof Andrews supervised the research work and proof-read the publication.

II. A. Alarifi, H. N. Phylaktou and G. E. Andrews (2015) **Toxic Gas Analysis from Compartment Fires using Heated Raw Gas Sampling with Heated FTIR 50 Species Gas Analysis**, Proceedings of the *International Fire Safety Symposium*, 20-22 April, 2015. University of Coimbra, Coimbra, Portugal.

(Included in Chapter 3)

The candidate led the experimental procedures, development of techniques and writing up of the publication. Dr Phylaktou and Prof Andrews supervised the research work, participated in the analysis of results and proof-read the publication.

III. A. Alarifi, H. N. Phylaktou and G. E. Andrews *[Poster]* (2015) **Heated Raw Gas Sampling with Heated FTIR Analysis of Toxic Effluents from Small and Large Scale Fire Tests**, presented at the 10th Asia-Oceania Symposium on Fire Science and Technology, 5-7 October, 2015. Tsukuba, Japan.

(Included in Chapter 3)

The candidate led the experimental procedures, development of techniques and writing up of the publication. Dr Phylaktou and Prof Andrews supervised the research work, participated in the analysis of results and proof-read the publication.

IV. A. Alarifi, J. Dave, H. N. Phylaktou, O. A. Aljumaiah and G. E. Andrews (2014) **Effects of fire-fighting on a fully developed compartment fire: temperatures & emissions**, Fire Safety Journal (2014;68: 71-80), http://dx.doi.org/10.1016/j.firesaf.2014.05.014

(Included in Chapter 5)

The candidate participated in carrying out the experimental procedures, development of techniques and setup and led the writing up of the publication. J. Dave contributed greatly in securing the experiments site, the experimental setup and procedure. D. O. Aljumaiah participated in carrying out the experimental procedures. Dr Phylaktou and Prof Andrews supervised the research work, participated in the analysis of results and proof-read the publication.

V. A. Alarifi, H. N. Phylaktou, G. E. Andrews, J. Dave and O. A. Aljumaiah (2015) **Developing and post-flashover fires in a full scale room. Thermal environment, toxic emissions and effects of fire-fighting tactics**, Proceedings of the 2nd European Symposium in Fire Safety Science, 16-18 June, 2015. European University of Cyprus, Nicosia, Cyprus.

(Included in Chapter 5)

The candidate participated in carrying out the experimental procedures, development of techniques and setup and led the writing up of the publication. Dr Phylaktou and Prof Andrews supervised the research work, participated in the analysis of results and proof-read the publication. J. Dave contributed greatly in securing the experiments site, the experimental setup and procedure. Dr O. Aljumaiah participated in carrying out the experimental procedures.

VI. A. Alarifi, H. N. Phylaktou, G. E. Andrews, J. Dave and O. A. Aljumaiah (2015) **Toxic Gas Emissions from a Timber-Pallet-Stack Fire in a Full Scale Compartment**, Proceedings of the 10th Asia-Oceania Symposium on Fire Science and Technology, 5-7 October, 2015. Tsukuba, Japan.

(Included in Chapter 8)

The candidate participated in carrying out the experimental procedures, development of techniques and setup and led the writing up of the publication. Dr Phylaktou and Prof Andrews supervised the research work, participated in the analysis of results and proof-read the publication. J. Dave contributed greatly in securing the experiments site, the experimental setup and procedure. Dr O. Aljumaiah participated in carrying out the experimental procedures.

Acknowledgements

Special appreciation goes to my supervisors, Dr Roth Phylaktou and Prof Gordon Andrews, for their supervision and constant support. Their invaluable help of constructive comments and suggestions throughout the experimental and thesis works have contributed to the success of this research. I also thank SCAPE labs staff, especially Robert Boreham and Edmund Woodhouse.

Sincere thanks to all my friends and colleagues especially Omar, Jim, Hamid, Clara, Abdul, Bala, Ali, Mike and many others for their kindness and moral support during my study. Thanks for the friendship and memories.

Last but not least, my deepest gratitude goes to my beloved parents; Mr. Abdulrahman S. Alarifi and Mrs. Nawal A. Alarifi and also to my siblings; Areej, Sager, Saad and Abdulilah for their endless love, prayers and encouragement.

To those who indirectly contributed in this research, your kindness means a lot to me. Thank you very much.

Abstract

Fire statistics from the UK and the USA attribute 60% to 70% of fire fatalities in dwellings to the inhalation of fire toxic smoke. The objective of this project was to provide more toxic yield data from typical compartment fires and in the process develop a methodology for faster generation of such data on bench scale apparatus.

The models for overall toxicity assessment (for irritants and asphyxiants) were reviewed and the reported threshold limits for typical smoke toxicants, were collected, categorised and compared for increasing levels of harm. An extensive database was created of yields of toxic species from different materials and under different fire conditions. This highlighted the need for more yield data for under-ventilated fires in compartments.

Eight full scale tests were carried out in a room enclosure with ventilation through a corridor to a front access door. Fire loads were wood pallets, cotton linen and towels, typical living room furniture and diesel. The fires were allowed to become fully developed before extinguishment by the local FRS team. Toxic concentrations were monitored in the hot layer and the corridor (through a heated sampling line) using a heated FTIR analyser, calibrated for 65 species. An emissions based model, developed as part of this work, was used to quantify the equivalence ratio and also the toxic species yields, even for the cases where the fuel mass loss rate was unknown. An important finding was the overwhelming contribution of Acrolein and Formaldehyde in most tests, in exceeding the impairment of escape threshold.

The modified controlled atmosphere cone calorimeter showed comparable results to the full scale tests for lean burning combustion however it proved difficult at this stage to produce combustion in the rich burning regime and further development of the methodology is needed.

Table of Contents

List of Tables

List of Figures

Chapter 1
Introduction

Fire is one of the first discoveries of humanity, and arguably the most important one. The known hazards of fire for the early generations of humanity were limited to thermal hazards only. With the advancement in civilization and the increase of population, the way people live their lives has changed, including the structure of their homes i.e. space, ceiling heights, insulation, and ventilation. With the modern way of living accidental fires are more probable to occur and potentially can be more hazardous in compartments rather than in open outdoor areas. The production of toxic smoke in fires has (in the last few decades) been recognised as a major threat to people during accidental fires.

The need for effective assessment, measurement and quantification of the toxic hazards to which humans can be exposed during a fire event has become an integral and necessary requirement for the development of safe building designs and fire safety strategies

Fire toxicity is part of the developing wider fire science field which is an interdisciplinary subject with contributions from a range of different fields including physiology, human psychology, combustion science, fluid dynamics, thermodynamics and optics, computing, statistics, material science, ecology, toxicology, and most forms of engineering and forensic science.

The understanding being developed from the application of the topics on fire contributes to and influences the design of buildings and the development of materials and/or systems for preventing, detecting and mitigating fire hazards. Fire science can be crucially important in management areas such as risk analysis and designing safe evacuation plans for challenging building designs and is also important for fire-fighting operations. Fire science can contribute even after the fire incident where understanding the causes, development and impact of the fire are required.

The main objective of fire science is to provide a safer environment and reduce losses by utilising scientific evidence to produce practical solutions. Fire toxicity research has a significant role in achieving this objective.

1.1 Fundamentals of fires in enclosures

One of the major challenges of studying fires is their randomness. Studies of combustion and combustion fundamentals provide an important understanding of the actual physics and scientific fundamentals that are applicable to fires. However, combustion studies are mainly targeted to systems that seek the improvement of combustion efficiency and reduction of environmental emissions, and as such do not produce data that are relevant real fires. With

fires there are no designed systems to be perfected but a large degree of randomness as to the physical boundaries and environmental conditions in which fires occur.

Therefore one main task is to understand fire development and evaluate the hazards generated under different conditions that are representative of the a wide range of practical circumstances. This should result in the formulation of practical solutions that can manage these hazards to acceptable levels.

The combustion fundamentals should not be ignored as they are the driving principles but rather we should be aware that for correct application to fires we most likely need to produce more relevant combustion data and knowledge.

1.1.1 Idealised fire growth stages in an enclosure

The majority of fire fatalities (more than 75%) occur in buildings [1, 2]. Enclosure fires begin typically by ignition and a small fire [3-5], which then start growing by producing more heat and smoke (illustrated in Figure 1-1). In this early stage, the fire would not be affected by the enclosure element in the process, as it is fuel-controlled. Then, the fire grows at a slow or fast rate, depending on the fuel type and/or the ventilation conditions. A smouldering fire may have a very long growth period, and may extinguish itself without reaching the subsequent stages (shown in Figure 1-1). On the other extreme a flaming fire could progress to a fully developed fire after experiencing flashover.

Flashover is the transition between the growth period and the fully developed fire stage which is defined in the literature in many ways. Once a fire reaches a certain size it becomes affected by the enclosure and especially the ventilation. If the ventilation is restricted the fire becomes ventilation controlled at a small size but if the ventilation is sufficient the fire may progress to flashover at the transition from fuel-controlled to ventilation-controlled. A formal definition given by the International Standards Organisation, British Standards Institute and European Committee for Standardization [6] is the “transition to a state of total surface involvement in a fire of combustible materials within an enclosure.” Flashover characteristics are temperature of the upper layer is 500 – 600 ˚C, radiation at the ground level of the compartment reaches 15 – 20 $kW \cdot m^{-2}$, or flames appearing from the compartment vents.

Fully developed fire stage (post-flashover) is the phase when the heat release rate in an enclosure fire peaks and often the fire size inside the compartment would be restricted by the availability of the oxygen. This is a ventilation-controlled fire. Unburnt pyrolysis gases are mixed with the combustion products and are hot (700-1200 ˚C) and as they leave through the openings they mix with the external air and burn creating flames outside the enclosure openings. Most of the fire load in the compartment is consumed during fully developed fire stage.

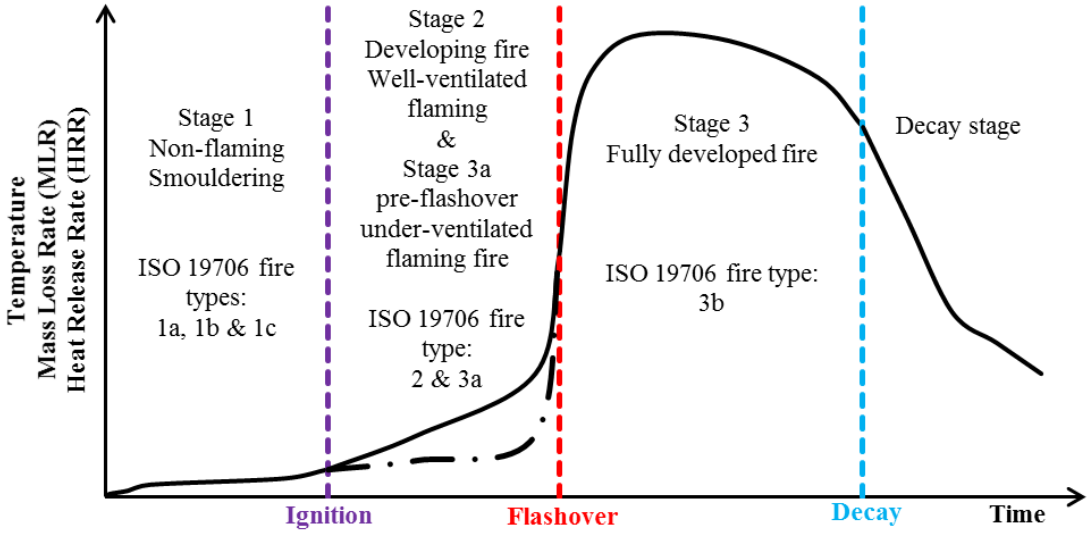

Figure 1-1: Different phases in the development of a compartment fire.

In both the growth period and in particular the fully developed stage the combustion is incomplete resulting in yields of toxic products that are much larger during the fully developed stage than at the growth stage of the fire.

Subsequently the heat release rate diminishes as the fuel is consumed, cooling down the temperature of the upper layer entering the decay stage of the fire. Typically at this phase the fire turns from a ventilation-controlled fire to a fuel-controlled fire.

The toxic gases produced by the fire will initially affect any people inside the fire compartment but as the fire grows if the smoke spills out in corridors and other parts of the building it can affect people in these areas. Even if the smoke spills, say through a window into the atmosphere for large fires the toxic content of the plume may have an effect on the surrounding population or in high rise building it may be entrained into that building at higher levels and affect the people there.

1.2 Brief case studies of fires that contributed to highlighting the significance of fire smoke toxicity.

Toxic products from fires started to be recognized as a major threat to fire victims in the 1970s and 1980s, calling for the attention of the scientific community to study and analyse this hazard [7]. The driving forces behind this recognition were fire disasters where the majority of victims died as a result toxic smoke inhalation. Also statistical reviews of fire casualties highlighted (at the time) the increased risk of smoke on fires victims [8]. This section will show-case some of these major incidents with the outcomes of the main investigation reports. This will be followed by a review of relevant fire statistics..

1.2.1 Beverly Hills Supper Club, Kentucky, USA (1977)

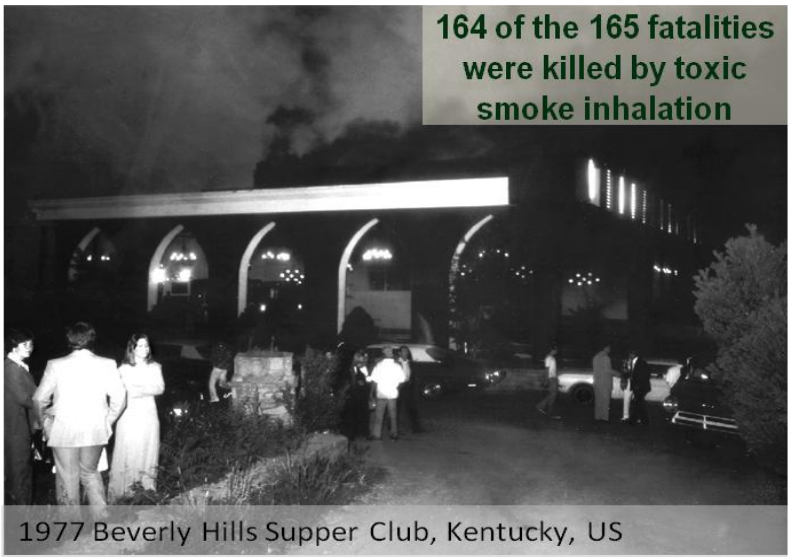

Figure 1-2 Survivors outside the Beverly Hills Supper Club [9].

This was one of the early incidents that raised alarms about the importance of understanding fire toxicity and its impact. The Beverly Hills Supper Club had number of annexes and expansions to the main building, which created a complex layout and challenging means of escape in general. The fire started around 8:40 pm on the evening of May 28, 1977. The origin of the fire was the zebra room (marked in Figure 1-3) which is a small L-shaped room. On the same night the facility was hosting a very popular act in the showroom known as the Cabaret room where the majority of the victims were located (134 bodies recovered from that room). A follow up study focusing on the long-term effects of the smoke inhaled by the survivors was conducted in the 1980s [10].

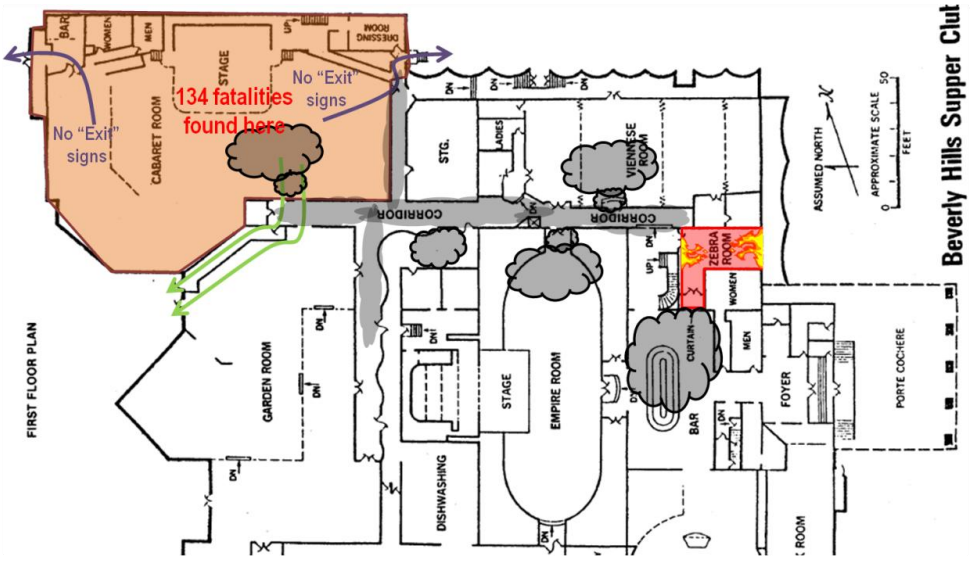

Figure 1-3: Fire scenario marked on the plans of the building, original building plans taken from [9].

The main conclusions of the investigations highlighted the following factors as main contributors to the loss of lives; delayed detection of the fire, no evacuation training given to staff, overcrowding (the legal capacity of the cabaret room was about 550 but it is believed that between 900 – 1,300 people were in the showroom that night) and safe exits and means of escape were not adequate. The total amount of compensation paid to the victims and their families was $50 million (equivalent to about $200 million of today's money) [11].

1.2.2 Cinema Statuto Fire, Turin, Italy (1983)

Figure 1-4: One of the first pictures from inside the cinema during rescue [12].

The largest disaster since the second world war (until now) hit Turin on the evening of February 13, 1983, when a fire broke out during the screening of "La chèvre" (Knock on Wood) at Cinema Statuto. In total 64 people died, the main cause of death for all the victims found in the gallery was toxic gas inhalation. Luckily the venue wasn't packed that day as it can accommodate for up to a thousand spectators. Press reports [12, 13] suggest that only a hundred were attending the showing of the French comedy film. The fire started by a spark from a short circuit which caught the curtains on the ground floor spreading the fire to the seats, which resulted in the production of toxic emissions (namely Hydrogen Cyanide) killing most of the people in the upper gallery. All the five fire exits were locked, the only way out was the main entrance. The owner of the picture house was held responsible and sentenced eight years (reduced to two years) and ordered to compensate victims and their families with 3 billion Italian Lire (equivalent to £3.2M of today's GBP). Many of the Italian health and safety laws related to public places were changed subsequently in response to this fire.

1.2.3 Saudi Airline Flight SV163, Riyadh, Saudi Arabia (1980)

Figure 1-5: Debris of Saudi Airline SV163 airplane [14].

The 1980 Saudi Arabian Airline flight 163 [15], pictured in Figure 1-5, is an example of the large number of deaths that can occur from toxic gases in aircraft passenger compartment fires. The fire broke through from a cargo hold into the main cabin through the cabin floor. The pilot managed to land the aircraft but no one managed to open the airplane door to escape, as everybody was incapacitated by toxic emissions. The doors remained closed until they were opened by the rescue services from outside.

1.2.4 British Airtours Flight 28M, Manchester, England (1985)

Figure 1-6: Aftermath of British Airtours flight 28M accident [16].

On August 22nd, 1985, Boeing 737-236 was set to fly from Manchester to Corfu (Greece) and during the take off, the left engine caught fire forcing the pilot to abort the take off and stop the aircraft to undertake the evacuation plan. According to the official investigations, it is believed that after a minute from stopping the aircraft the fire penetrated the passengers' cabin sidewalls in the area between seats 17A to 19A as shown in Figure 2-15. Then, the

fire started burning the interior furniture of the cabin producing highly toxic emissions. This incident claimed the lives 55 people toxic gas inhalation was the cause of death for 48 of them while 15 other person suffered severe injuries.

This incident had a significant impact on the air safety as the investigation report concluded that stricter limitations on the toxic gases emissions from the aircrafts' interior cabin materials should be applied [17].

1.2.5 MGM Grand Hotel, Las Vegas, NV (1980)

Figure 1-7: Picture of the MGM hotel during the fire showing the smoke dispersing from various areas in the building [18].

The fire broke out in the Casino at the ground level of the MGM Grand Hotel in the morning of November 21st, 1980, the Casino was closed at that time which resulted in the late discovery of the fire. Of the 85 people killed and more than 600 injured (including 318 were admitted to hospital) most were in the top high-rise tower floors who suffered from smoke inhalation. Even though the development of the fire was limited by the horizontal expansion, that did not prevent the toxic smoke emissions from travelling vertically through the elevators' shafts, (designed to be smokeproof) stairwells, and the air conditioning system (Figure 1-8).

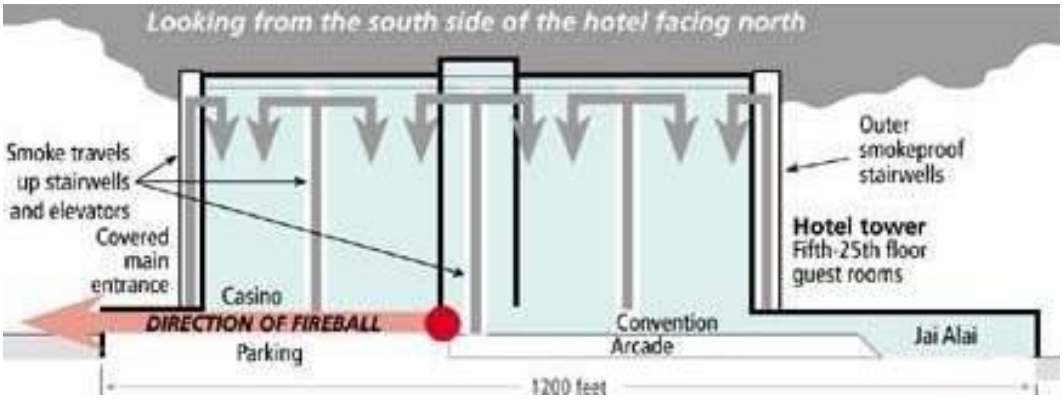

Figure 1-8: Fire and smoke spread in MGM Grand Hotel fire **[18]**.

Toxic smoke inhalation was the cause of death for 79 of the people killed that day, 3 killed because of burns and smoke inhalation, while different causes of death for each of the left three fatalities; burns, skull fracture and myocarditis. As part of the official investigation a full toxicological blood tests have been under taken for victims [19, 20]. The owners of the hotel paid $140 milion ($337 million of today's money) in compensations for the victims and their families [21].

1.2.6 Rosepark care home, Uddingston, Scotland (2004)

On the morning of January 21, 2004, a fire broke out at Rosepark care home claiming the lives of 14 residents. According to the official investigation report by Brian Lockhart [22] which includes experimental research conducted by BRE, the origin of the fire was found to be an electric fault in the back the cupboard shown in Figure 1-4. The cupboard contents were reported by Strathclyde Police to be flammable materials in the form of aerosols and a fair amount of combustible material such as, books cardboard game boxes, disposable aprons, and body care products which produced a sustainable flaming fire. The reported main cause of death for all the fatalities was toxic smoke inhalation.

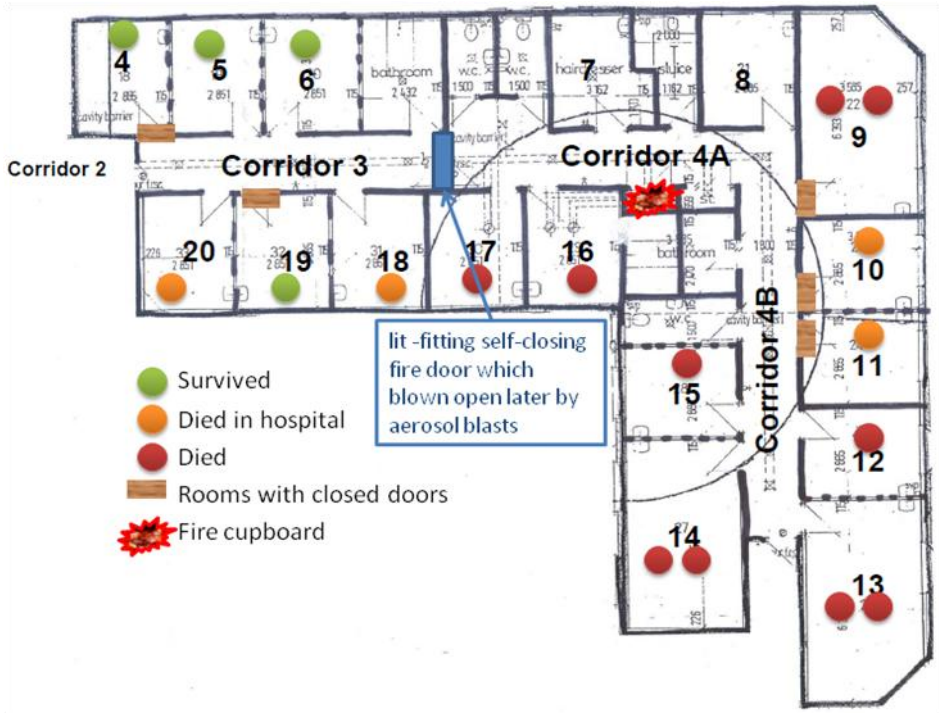

Figure 1-9: Schematic of the upper floor part involved in Rosepark care home fire. original plans taken from **[23]**.

The report addressed the electrical installation hazards and recommended proper safety measures to be maintained. Also the provision of self-closing fire doors with smoke seals for all the bedrooms was recommended as most of victims who died in the premises had their doors wedged open or ajar as shown in Figure 1-4. Subdividing of corridor 4 was also strongly recommended as it can be seen the effect of even the poorly fitted fire door between corridor 3 and corridor 4 where four of corridor 3 residents survived and the other

two died in the hospital, while all corridor 4 residents were killed in the incident (except for two with room doors closed, who were rescued alive but died in hospital). The report also raised the concerns of the management level as the incident was reported to the fire service after ten minutes of the first fire alarm activation at 4:28 am which believed that some victims have died by that time the fire brigade arrived as a clock in room 12 found burnt and stopped at 4:40 [23].

1.2.7 New York Telephone Exchange Fire, New York, USA (1975)

Figure 1-10: Pictures of the fire-fighting efforts on the scene of New York telephone exchange fire.

While no fire-fighters were killed at the fire that took place on February 27th, 1975, many suffered long-term health effects from their exposure to the smoke that was generated from the compartment fire involving electric cables (around 100 tonnes of PVC cables) as the main fire load, was monitored and recorded by experts in occupational health [10, 24]. It is believed that fire-fighters who were involved in fighting this fire have developed various cancer related diseases and about 40 of these fire-fighters died from cancer related diseases. According to the New York Daily News [25], a telephone fire veteran's leukaemia was linked to the combustion products from the telephone exchange fire by Professor Stephen Levin of occupational medicine at Mount Sinai School of Medicine.

1.3 Review of fire statistics: Causes of fatalities and injuries in domestic fires

Recent official statistics of cause of deaths for fire fatalities released by the UK and USA authorities [1, 2] show that toxic smoke inhalation was partially or wholly the leading contributor to fire fatalities. When looking into the cause of death in fire fatalities a "Smoke/Burns" category represents victims with blood samples showing incapacitating levels of toxic species and not fatal threshold levels and evidence of burnt parts of the body is present. For such category, it is important to highlight that toxic smoke products are the main cause of incapacitation and impairment of movement, which consequently results in the fatal thermal damage to the fire victim. Therefore, it is reasonable when looking into the

impact of fire toxicity on fire victims to include victims under both categories; Smoke inhalation and Smoke/Burns. By reviewing most recently published official fire statistics in the United Kingdom and United states of America for fire fatalities shown in Figure 1-11, toxic products released from fires were responsible for 61% of the total fire fatalities (322) in the UK from April 2013 to March 2014 (41% Smoke and 20% Smoke/Burns) [1]. While in the USA, toxic products released from fires were responsible for 85% of the total fire fatalities (2,530 per annum) from 2011 to 2013 (39% Smoke and 46% Smoke/Burns) [2].

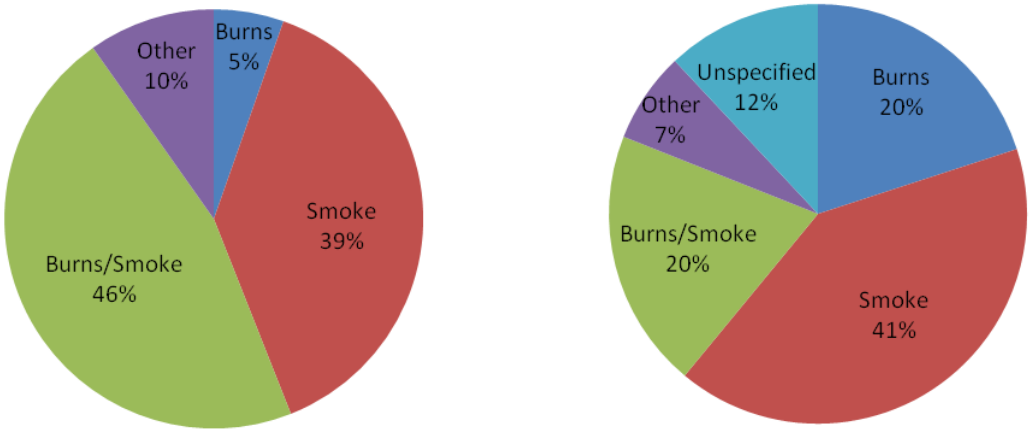

Figure 1-11: Cause of death for fire Fatalities from; Left: USA between 2011 and 2013 [2]. Right: UK 2013/14 [1].

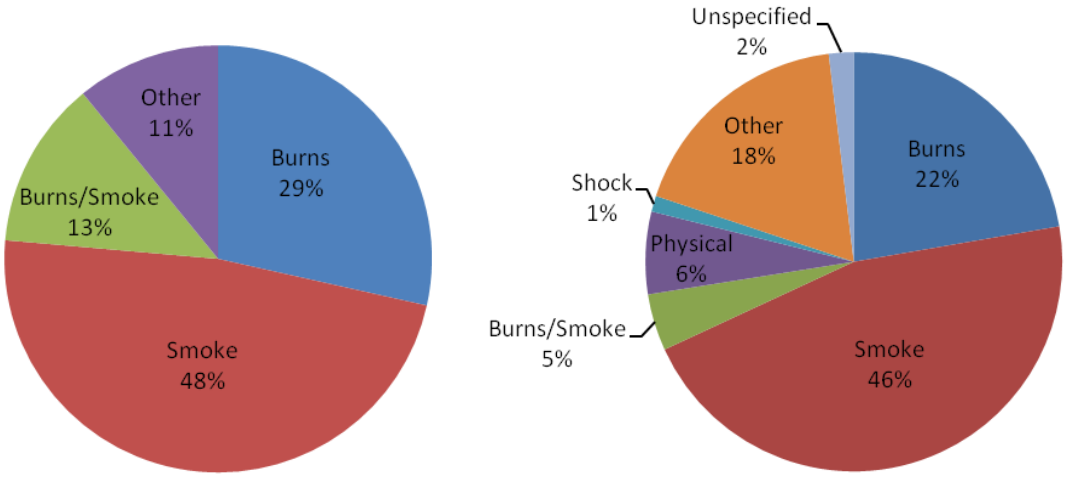

Figure 1-12: Cause of injury for non-fatal fire casualties from; Left: USA between 2011 and 2013 [26]. Right: UK 2013/2014 (excluding first aid and precautionary checkups) [1].

By Looking at the collected statistics for non-fatal casualties (excluding any first aid and precautionary checkups) for the same period, presented in Figure 1-12. Inhaling smoke products in fires caused 51% of the total fire injuries (5,401) in the UK between April 2013 and March 2014 (46% Smoke and 5% Smoke/Burns) [1]. While in the USA, toxic products released from fires were responsible for 61% of the total fire fatalities (13,125 per annum) from 2011 to 2013 (48% Smoke and 13% Smoke/Burns) [26].

Figure 1-11 and Figure 1-12 clearly demonstrate that a fire victim, at the present time, is more likely to die or get seriously injured from inhaling toxic emissions released in fires rather than any other factor.

A historical statistical review of cause of death for UK fire fatalities between 1955 and 2007 was conducted by Purser [27], which was used in addition to other recent official fire statistics reports [1, 28-32] to produce Figure 1-13. The percentile distribution by cause of death for fire victims is shown in Figure 1-14. Two main observations are important to highlight; firstly the gradual reduction of the overall fire fatalities combined with stable share of fire victims dying every year because of smoke inhalation in the period between 1980s and nowadays. Secondly, the sudden increase of smoke inhalation contribution as a cause of death to the overall fire fatalities combined with an overall increase in the total fire victims between 1950s and early 1970s.

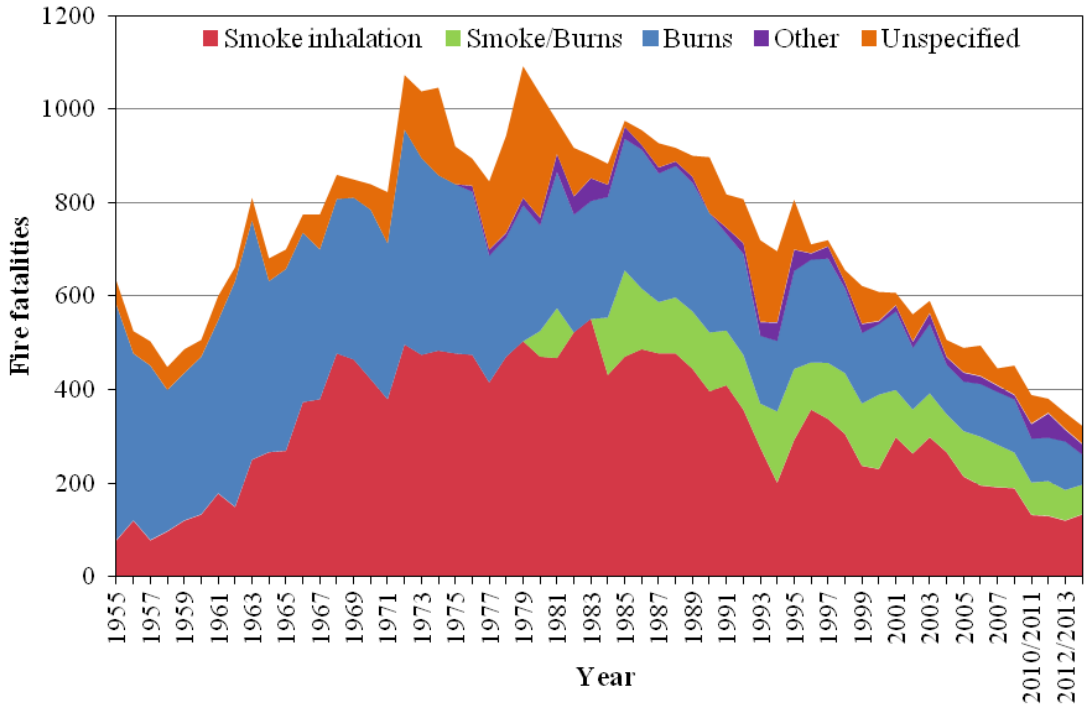

Figure 1-13: UK fire fatalities between 1955 - 2014, collected from [1, 27-32]

Similar review was conducted by Hall [33] based on the USA death certificates database issued cause of death for fire victims in the period from 1979 until 2007, summarised in Figure 1-15 and Figure 1-16 in comparable format to the previous figures from the UK. The patterns of both data are the same, even though Hall's review was limited to year 1979, the same gradual reduction of overall fire victims is observed with smoke inhalation causing death to more victims than any other factor. The gradual drop observed in fire fatalities between 1980s and present time can be attributed to the regulations that were introduced in 1988 for the UK [34] outlawing renting furnished property containing non-fire retardants

furniture, as well as banning the sale of such furniture. In the USA, similar regulations were introduced in 1953 initially targeting manufacturing of flammable clothing and amended in 1967 to include all furnishing materials [35]. Also, the introduction of low-cost smoke alarms to the market in the 1980s played a significant role in reducing the overall total of fire fatalities.

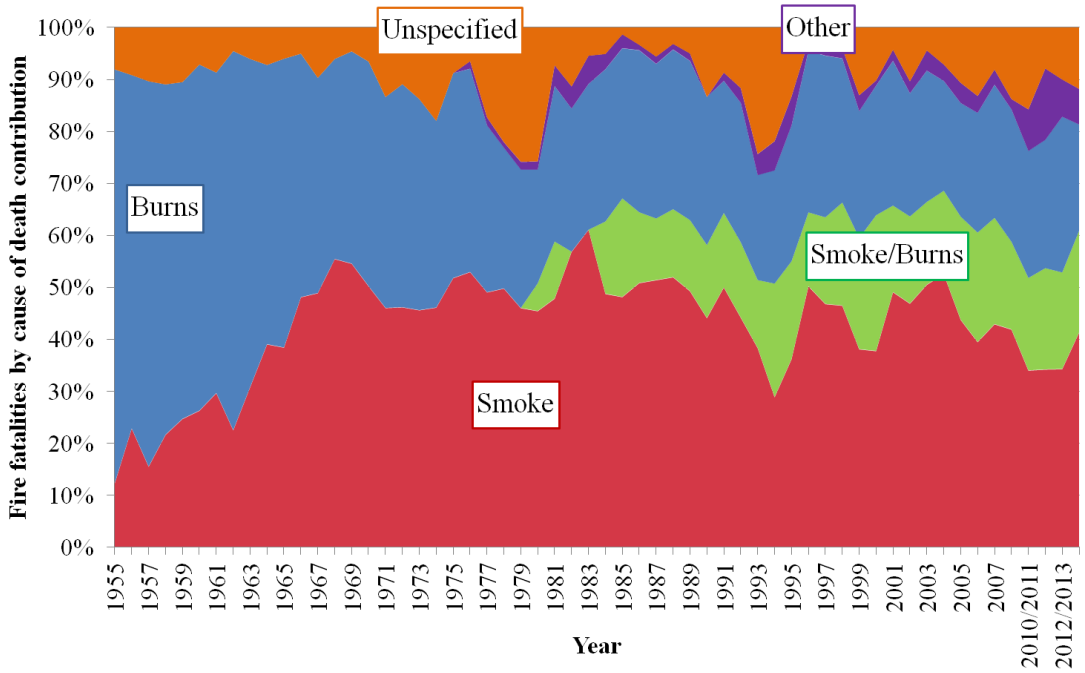

Figure 1-14: UK fire fatalities by cause of death contribution between 1955 - 2014 based on Figure 1-13.

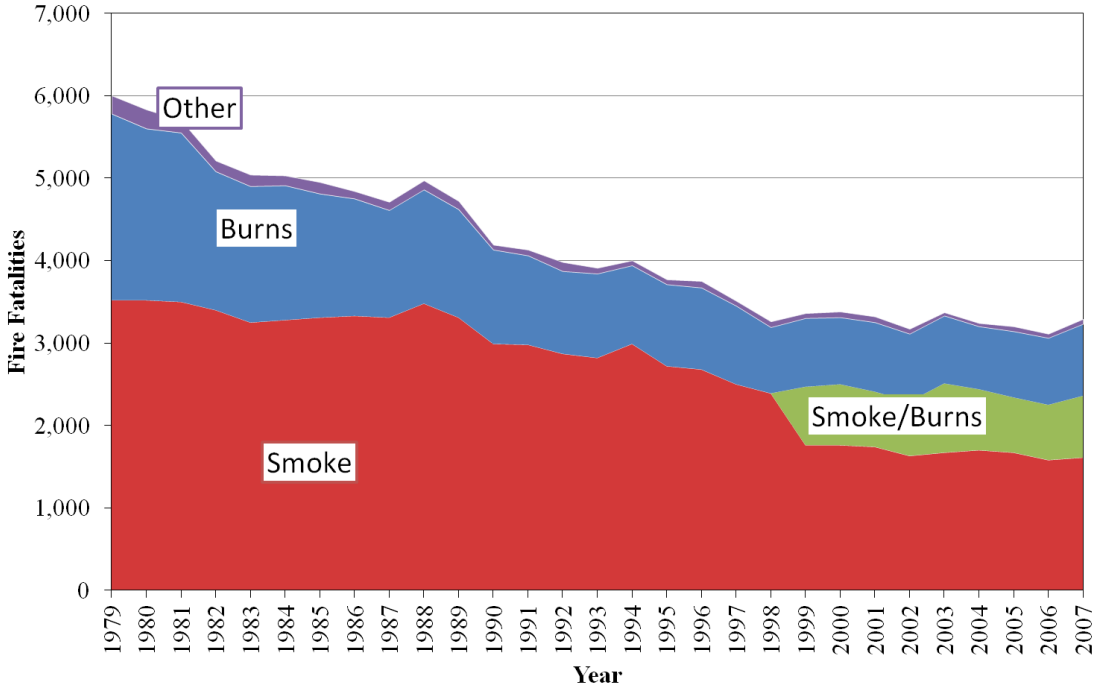

Figure 1-15: US fire fatalities between 1979 and 2007, data collected via [33] from The US National Center for Health Statistics (NCHS) death certificate database

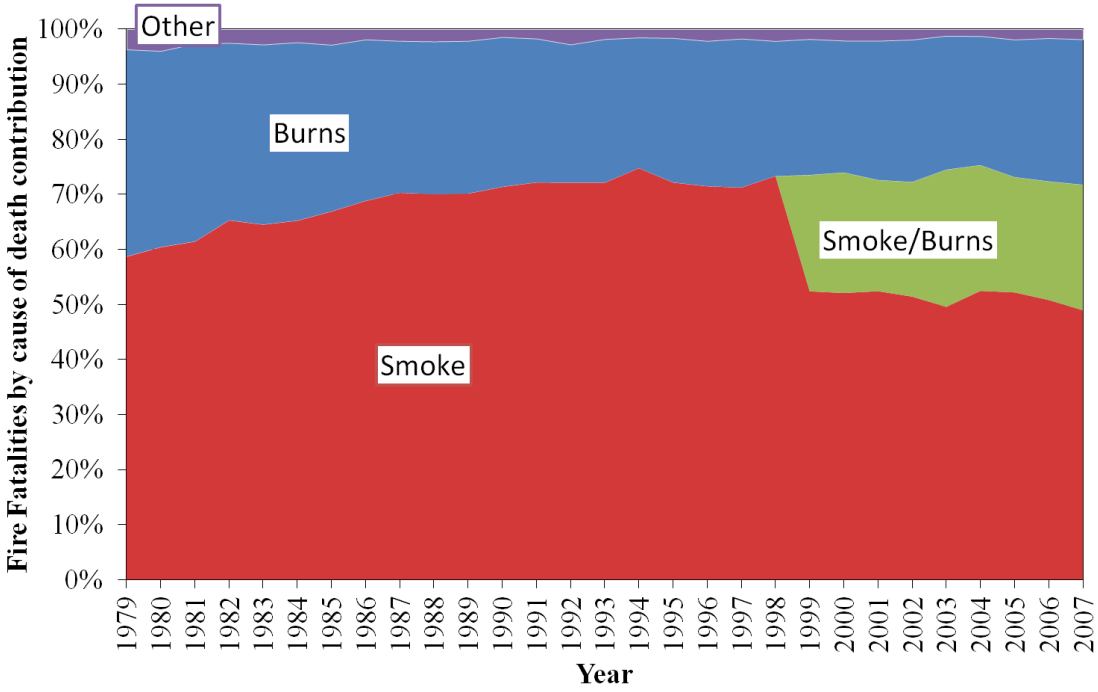

Figure 1-16: US fire fatalities by cause of death contribution between 1979 - 2007 based on Figure 1-15.

There are a few explanations for the statistical increase between 1950s and 1970s, one of the explanations was that this rise is a result of increasing the awareness of the fire department of the toxic smoke effect on victims, implying that this rise is not real and can be considered "statistical anomaly". Purser [36] dismissed this reasoning attributing the increase to three major factors that contributed to the rise of fire toxicity victims. Firstly, the increased use of complex materials e.g. polymers that burn inefficiently and produce incomplete complex combustion emissions. Secondly, the influence of modern energy efficient building construction, smaller rooms and lower ceiling heights for conserving energy that would increase the temperature of burning creating a faster fire growth. Finally, ventilation restrictions of modern day designs can aid in slowing down the fire spread, by not having enough oxygen, however this also complicates the combustion process and enhances the production of incomplete combustion products. These factors aided with the change in the lifestyle, such as the increase in the amount of furniture (fire loads), its layout and material composition are the main reasons for the increase of fire causalties from toxic smoke inhalation.

Based on these factors the fire toxicity research agenda should follow certain directions. Firstly, we need to understand and quantify the toxicity potential of the different materials that we use in our buildings and develop suitable models that allow the toxic exposure levels to be quantified within the fire compartment but also within the rest of the building and ultimately beyond the building geometry to the outside environment. This will allow the evaluation and implementation of suitable protection strategies such smoke control measures that reduce the exposure of people to levels that are not harmful. Secondly,

research should be directed towards developing materials and products that are inherently safer by having a slower burning rate and low toxic species yields.

1.4 The importance of fire toxicity in assessing fire hazards

One of the most common approaches to assess the fire hazards on survivability of occupants is quantifying the Available Safe Egress Time (ASET) and the Required Safe Egress Time (RSET) [36-47]. In the designing stage ASET must be longer than RSET with a margin of safety.

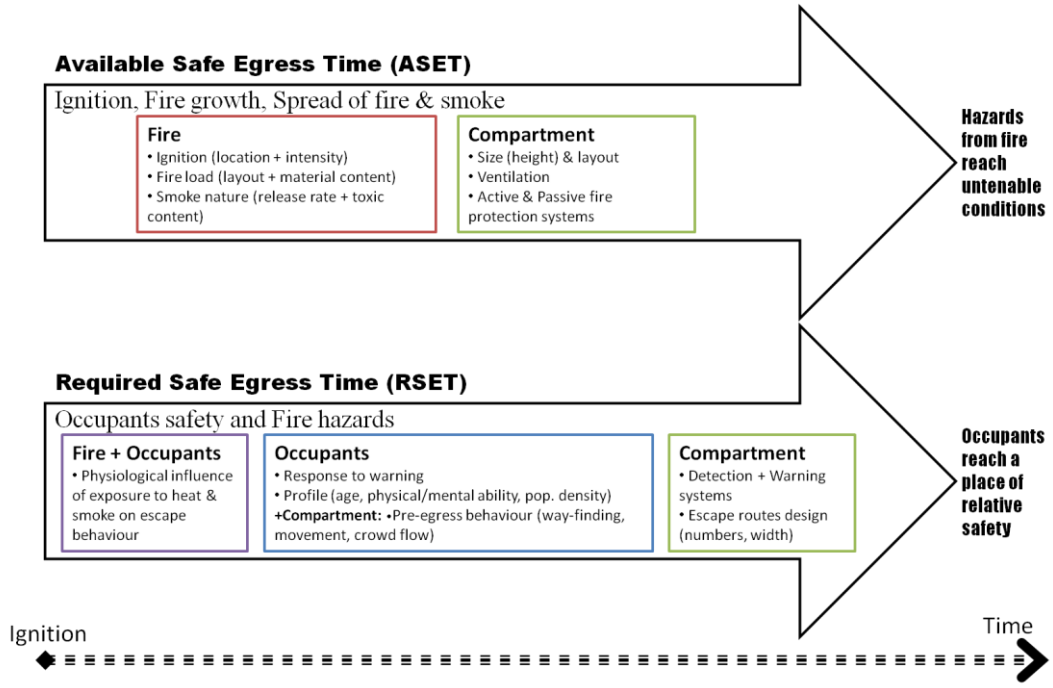

Figure 1-17: ASET and RSET (processes, factors, and results).

ASET depends on the development of fire hazards involving fire characteristics and compartment effects. The significance of the fire characteristics on the development of fire hazards can be summarised in three main areas;

Firstly, ignition source (in terms of location and intensity).

Secondly, fire load involved (in terms of layout and material content that influence the spread of the fire, heat released and burning behaviour).

Finally, nature of smoke produced (in terms of release rate and toxic species that control the overall toxicity level of emissions produced).

The impact of the compartment orientation on the development of fire hazards can be summarised into three factors;

Firstly size and layout (in terms of height, shape and location of openings that also influence the spread of fire hazards).

Secondly, ventilation (in terms of rate and locations of feed and exhaust points that influence the spread of the fire, nature of smoke produced, spread of smoke within other parts of the building).

Finally, the provision and activation of active and passive fire protection systems e.g. suppression systems (including fire-fighting) and structural fire protection, these systems can have great influence on the containing the fire with its hazards or possibly extinguishing the fire. ASET's end point is defined by reaching untenable conditions within a specified space.

RSET is more complicated as it depends on many variables that are not easily quantified, these variables can be summarised in three main categories; firstly, the development of fire hazards and their interaction with occupants that potentially affect the evacuation efficiency. Secondly, the human factor, in terms of the profile of the occupants, their response to warning, pre-egress behaviour which depends on the compartment in terms of way-finding task and crowd flow. Finally, the compartment design can influence the effectiveness of the evacuation process based on the provision of detection and warning systems and the design of the escape routes. RSET's end point is defined by occupants reaching a place of relative safety.

Figure 1-17 illustrates the main factors that influence the time for fire hazards to reach ASET & RSET analysis also used in performance based design which is widely accepted in the statutory documents especially for buildings not covered by the prescriptive standards. However ASET and RSET concept has been scrutinised by researchers [48-50] on the basis of interpretation and applicability, highlighting the lack of quantified available data. This work aims to aid in providing accurate yield data to be easily implemented in such analysis in order to deliver safer designs.

1.5 Simulating fire toxicity in virtual environment (CFD)

Fire models are used for the purpose of establishing and assessing the potential fire hazards in buildings but such models, for example FDS [51], are not capable of predicting,from first principles, the incomplete combustion products relevant to fire smoke hazard in terms of acute lethal toxicity and/or severe irritation. Such data are typically entered by the user as fixed yields usually based on published data from well ventilated bench scale tests. The area of fire toxicity modelling is in its infancy, and model developers are restricted by the lack of information on toxic products in general and in particular for under-ventilated compartment fires.

The lack of information on fire smoke toxic species, not only affects the fire modelling development, but also affects the fire safety engineering practice in a wider sense. For example, the British Standards Institution [40], in its latest guidance on initiating a fire

within the enclosure of origin for fire safety engineering analysis, recommends the use of 0.13 g/g as the generic CO production yield from the design fire. It also reports a range of CO yields for different fuels ranging from 0.004 to 0.063 g/g based on Tewarson's [52] data for well ventilated fires with samples usually taken from heavily diluted flows. The provided figures are not representative of the toxicity problem in present-day ventilation controlled fires.

More experienced engineers, who use CFD techniques, adopt what might be considered a better industry practice, which starts with specifying a fixed fire heat release rate fire, typically ranging from 1-5 MW, depending on the building occupancy, and assume a fixed production yield of carbon monoxide appropriate to fully developed compartment fires typically at yields of 0.2 g/g [53]. Based on this, engineers, more often than not, restrict smoke hazard analysis to visibility and carbon monoxide levels (this is an under-estimate of the smoke hazard which is frequently reported by surviving fire victims as irritant and impairing escape). They use the output information for establishing the effectiveness of smoke ventilation systems proposed to provide clear and safe means of escape and/or validate the building compartmentation. This is an under-estimate of the smoke hazard which is frequently reported by surviving fire victims as irritant and impairing escape.

Progress in fire toxicity modelling, is impaired by the limited available information on fire smoke gases produced by the combustion of different materials and under different conditions, including ventilation restricted fires. There is an urgent need for precise experimental quantification of toxic yields, especially irritant species under variable conditions an there is shortage of labs producing such measurements. Many fire laboratories do however have cone calorimeters which could be adjusted to make meaningful toxicity measurements routinely, particularly if combined with an FTIR spectrometer.

1.6 Aim of the project

The main aim of the project is to identify and measure toxic yields in full scale under-ventilated fires and develop and to develop and validate a suitable bench-scale test setup (based on the popular apparatus Cone Calorimeter) as a method for evaluating toxicity of materials in enclosed air starved compartment fires.

Such setup would enable the fast production of detailed toxicity data in relevant and varied fire scenarios.

Chapter 2
Literature review

2.1 Ventilation, Equivalence Ratio and Toxic Yields

Fires occurring in enclosed compartments have unique characteristics in comparison to those occur in the open. These differences have significant impact on production of toxic emissions in fires. Factors that govern the production of the toxic emissions can be limited to three main factors; material content, equivalence ratio and temperature. Interestingly these factors are related to the traditional fire triangle main elements; fuel, oxygen and heat. These three factors shown in Figure 2-1 influence other important fire characteristics such as the continuity of the combustion chain reaction and deciding whether the fire is a flaming or non-flaming one. In this section these factors are reviewed in the context of compartment fires, in order to draw the full picture of combustion conditions in compartment fires.

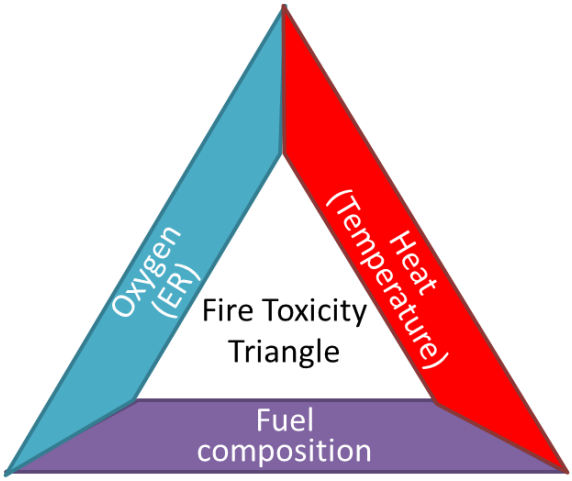

Figure 2-1: Fire toxicity triangle showing the main general factors that influence toxic emissions in fires.

2.1.1 Typical ventilation rates and fire loads in compartment fires

Figure 2-2 was constructed using engineering recommendations for ventilation rates for buildings and rooms [54-56] . It is clear that most of **residential** building spaces (which is where the majority of fire fatalities occur, as discussed earlier in Chapter 1) are associated with highly restricted ventilation conditions, typically less than 4 Air Changes an Hour (ACH) apart from kitchens which are in the 15-20 ACH category. It is very important when simulating compartment fires in an experimental or virtual environment to apply appropriate ventilation conditions rather than default to well-ventilated conditions. Although fire damage may result in additional ventilation being provided to the fire this usually occurs at a later stages of the fire. In the early stages of the fire (which are critical for life safety) ventilation to the space is likely to very limited. Hence, toxic emissions data produced in

well-ventilated conditions are not appropriate to be used in predicting toxic hazards from fire effluents for compartment fires. Further discussion on the influence of ventilation and equivalence ratio on the production of asphyxiant and irritant fire emissions is presented later in this chapter.

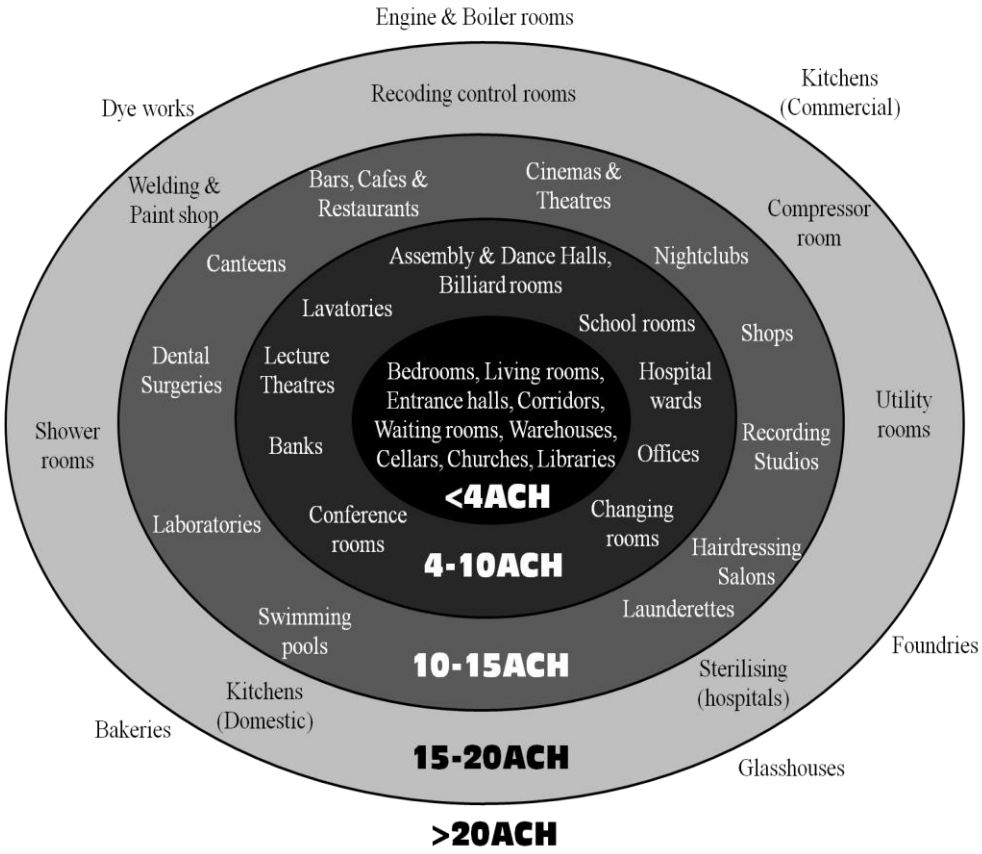

Figure 2-2: Typical ventilation rates for buildings and rooms. Data collected from engineering standards recommendations [54-56]

Fire load content contribute significantly on the severity of hazards generated from compartment hazards. A survey has been done in Sweden on buildings combustible contents. The results of a Swedish survey [57] on the combustible contents of buildings are summarised in Table 2-1 where wood is shown to be the major fire load in residential buildings by 40 times the nearest other fuel type (polyurethane PUR). Figure 2-3 shows that in schools, where PVC has significant presence with 20%. Where cellulosic materials in the form of wood and paper are forming 70% of the combustible content within schools. These surveys support the direction of focusing fire toxicity research on these materials in addition to monitoring new materials, introduced by manufacturers, which may contain super toxicants that could contribute significantly to the overall toxicity.

Table 2-1: Relative distribution of combustible materials for dwellings [57]

Material type	Material distribution (furniture + TV + flooring) [%mass]
Wood materials	79.2
Cotton	3.1
Polyurethane (PUR)	5.2
ABS – plastic	0.08
Polypropylene	0.97
Polyethylene	0.009
Nylon	0.13
Polyester	0.85
Melamine	1.1
Polystyrene	0.62
Acrylic	0.008
Wool	0.23
PVC (flooring)	4.3
Linoleum (flooring)	4.3

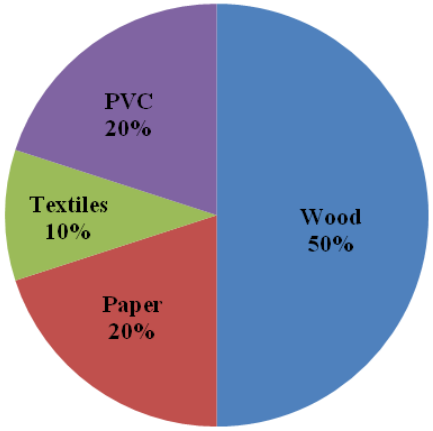

Figure 2-3: Relative distribution of combustible materials for schools [57]

2.1.2 ISO classification of combustion conditions in compartment fires

Combustion conditions in compartment fires have a major influence on the toxic emissions produced by the fires. These conditions can be characterised by a number of parameters including; temperature, heat flux, oxygen concentration, CO_2:CO and the equivalence ratio. In the course of the development of the fire, these characteristics can significantly. For the purpose of relating the bench-scale to the large-scale toxicity test methods the International Standards Organisation classified each stage and identified the associated conditions as shown in Table 2-2 [45, 58-60]. Purser et.al explained each classification thoroughly in [61].

Table 2-2: ISO 19706 classification of fires [58]

	Fire type	Heat flux to fuel surface [kW/m^2]	Max. temperature [°C]		Oxygen [%vol.]		ER ϕ	$\frac{[CO]}{[CO_2]}$ [v/v]	$\frac{[CO_2]}{([CO_2]+[CO])} \times 100$ [% Combustion efficiency]
			Fuel surface	Upper layer (smoke)	Entrained (in)	Exhausted (out)			
1. Non-flaming	1a. Self-sustained smouldering	N/A	450-800	25-85	20	0-20	–	0.1-1	50 – 90
	1b. Oxidative, external radiation	–	300-600	–	20	20	–	–	–
	1c. Anaerobic external radiation	–	100-500	–	0	0	–	–	–
2. Well-ventilated flaming		0-60	350-650	50-500	≈20	0-20	<1	<0.05	>95
3. Under-ventilated flaming	3a. Low-ventilation room fire	0-30	300-600	50-500	15-20	5-10	>1	0.2-0.4	70-80
	3b. Post-flashover	50-150	350-650	>600	<15	<5	>1	0.1-0.4	70-90

2.1.3 Equivalence ratio (ϕ or ER)

The equivalence ratio ER is a critical factor in the combustion process and consequently the production of toxic gases. It is defined as:

$$\phi = \frac{\text{actual fuel to air ratio}}{\text{stoichiometric fuel to air ratio}} = \frac{\text{stoichiometric air to fuel ratio}}{\text{actual air to fuel ratio}}$$

$$\text{When; } \begin{cases} \phi < 1 \text{ fuel} - \text{lean fire} \\ \phi = 1 \text{ stoichiometric fire} \\ \phi > 1 \text{ fuel} - \text{rich fire} \end{cases}$$

The stoichiometric air to fuel ratio on mass basis is the mass of air needed for to completely oxidise a unit mass of fuel. The actual air to fuel ratio is the ratio of the masses of air and fuel actually involved in the reaction.

Forell in his PhD thesis titled "A methodology to assess species yields of compartment fire by means of an extended global equivalence ratio concept" [62] discussed the different methods available for measuring or estimating ER in fire enclosures. Forell presented the phi meter (discussed in more detail in section 2.4.7) which measures ER based on burning the gas sample with induced oxygen in catalytic combustor. He also presented four other methods to estimate the flow in and out of the compartment utilising different techniques consisting of thermocouple trees at different locations within the compartment and at the openings with and without bi-directional pressure probes along the openings. Alternatively, having metered forced supply of air to the compartment would provide a control and a measure of $\boldsymbol{\phi}$.

However, there is significant confusion in definition of equivalence ratios reported in published experiments. It is important for users of the data to know exactly what the reported values represent.

The global equivalence ratio concept and its influence on carbon monoxide was defined and reviewed by Pitts in [63]. He stated that "For hood experiments it is possible to define several different phi, herein we will consider two". These were Plume Equivalence Ratio (PER) and Global equivalence ratio (GER). PER was defined as "the fuel mass-flow rate divided by the air mass-entrainment rate into the plume below the layer, normalized by the stoichiometric ratio for the fuel".

Some researchers defined the upper layer equivalence ratio ULER as follows, "GER refer[s] to the ratio of the mass of gas in the upper layer derived from the fuel divided by that introduced from air normalized by the stoichiometric ratio" [63].

Gottuk and Lattimer [64] suggested that if "one uses the term GER it must be associated with a defined control of volume". Then they defined PER, in the context of the hood experiments [65, 66], as "the ratio of the mass of fuel burning to the mass of oxygen entrained into the fire plume (below the upper layer) normalized by the stoichiometric fuel-to-oxygen ratio". They also gave a definition for the ULER as "the ratio of the mass of the

upper layer that originates from fuel sources, to the mass of the upper layer that originates from any source of air into the upper layer, divided by the stoichiometric fuel-to-air ratio" [64]. Then as an example of using the upper layer equivalence ratio in compartment fires, compartment equivalence ratio (CER) was introduced where the control volume is the whole compartment and CER was defined as "the ratio of the mass of any fuel entering or burning in the compartment to the mass of air entering the compartment normalized by the stoichiometric fuel-to-air ratio".

Pitts [63] noted that the two equivalence ratios PER and GER/ULER are identical in some cases specifically when combustion is in a steady state (referring to zonal modelling), Gottuk and Lattimer explained the relationship between PER and ULER further [64]. The main difference between the plume and upper layer equivalence ratios is that PER is the undiluted ER of the fire, while the ULER is the ER including any dilution if present.

Wang et al. [67] presented definitions of PER and ULER similar to Pitt's definitions, but they also added a definition of the Local Equivalence Ratio (LER) over a small volume and defined it as "the ratio of the mass in this volume that originates from fuel sources to the mass in the same volume that originates from the natural air stream divided by the stoichiometric fuel-to-air ratio". They went on to suggest that GER for the ISO 9705 room tests by Fardell et.al [68] should be referred to as LER because the reported equivalence ratio was based on a gas sample at a local position within the compartment. The reason why Wang and his colleagues suggested that the reported ER should be called local rather than global is that as a modeller global means a single value for the whole compartment, while local means a defined volume within the compartment and can be represented as contours of different values to represent the dilution effect on ER.

In this work three Equivalence ratios will be defined and used where applicable;

Firstly, the Reaction Equivalence Ratio (RER), this represents the actual reaction equivalence ratio and can be defined as the ratio between mass of fuel that was lost/burnt during the fire to the oxygen consumed in the reaction normalized by the stoichiometric fuel-to-oxygen ratio. This can be quantified experimentally as follows, the mass of fuel consumed in the reaction can be measured from a load cell monitoring the mass loss rate (MLR). The mass of oxygen consumed in the fire can be quantified in exactly the same way that oxygen consumption principle for heat release rate HRR is used, by utilizing the duct flow rate and oxygen concentration measured to quantify the mass of oxygen consumption. Hietaniemi et al. [69] have identified this RER term as the "local" equivalence ratio because it "reflects the local fuel and oxidizer balance in a restricted volume enclosing the flames", this has been avoided herein, because of the mix-up between equivalence ratio terms as discussed earlier. This RER is equivalent to the normalised oxygen depletion measurements inverted. Normalised oxygen depletion is defined as the mass of the

actual oxygen consumed divided by the mass of actual fuel consumed in the fire normalised to the maximum theoretical oxygen consumption in mass per unit mass of fuel consumption. The following equation is presented to demonstrate that relationship

$$RER = \frac{\dot{m}_f/\dot{m}_{O2}}{(m_f/m_{O2})_{Stoich.}} = \left(Y_{O2,norm.}\right)^{-1}$$

$$Y_{O2,norm.} = \frac{\dot{m}_{O2}/\dot{m}_f}{(m_{O2}/m_f)_{Stoich.}}$$

Where;

RER is the reaction equivalence ratio, $_{Stoich.}$ refers to stoichiometric ratio, m_{O2} is the mass of oxygen consumed, m_f is the mass of fuel consumed, $Y_{O2,norm.}$ is the normalised yield of oxygen depletion.

Secondly, the Metered Equivalence Ratio (MER), this is the most commonly used method for compartment fires where MER can be quantified by controlling/measuring the supply of fuel and air to the fire compartment. And can be defined exactly as Gottuk and Lattimer's definition of CER, "the ratio of the mass of any fuel entering or burning in the compartment to the mass of air entering the compartment normalized by the stoichiometric fuel-to-air ratio" [64]. The difference between the RER and MER is important to be highlighted, RER is only quantifying ER for the actual reaction or reactions (post-oxidation is counted for here), and even if there is excess oxygen supplied to the combustion zone but not used it would not be quantified in the RER. Hence RER values, theoretically, are 1 or above but not below 1 because any excess oxygen cannot be consumed by the combustion reaction. On the other MER is taking into account all air supplied to the whole compartment, even if it was not near the combustion zone and only acting as dilutor. Both terms are useful, however it is important to highlight that RER is too specific to the actual reaction (or chain of reactions), while MER is too general can be effected by the geometry of the test compartment more than the actual reaction and production of species.

$$MER = \frac{\dot{m}_f/\dot{m}_{air}}{(m_f/m_{air})_{Stoich.}}$$

Where;

MER is the metered equivalence ratio, $_{Stoich.}$ refers to stoichiometric ratio, $\dot{m}_{air}$ is the rate mass of air supplied, $\dot{m}_f$ is the rate mass of fuel consumed.

Thirdly, the newly proposed concept in this work (see Chapter 4), the Emission-Based Equivalence Ratio (EBER), this is a complicated method to back calculate the equivalence ratio based on the products sampled. Emission based equivalence ratio is defined as the ratio of the mass of fuel involved in the reaction that produced the

sampled mixture to the mass of air involved in producing the sampled mixture normalised by the stoichiometric fuel-to-air ratio. This is introduced herein for the purpose of being utilized in the fire research, with the capability of handling complex fuels and not only hydrocarbons. The advantage of this equivalence ratio model, is utilizing this EBER in producing yield data (g/g) from concentration measurements of gases, see further discussion in chapter 4.

2.1.4 Influence of equivalence ratio on toxic yields

Equivalence ratio variations undoubtedly have a major impact on the toxic species produced in fires, some researchers introduced models for predicting species yields based on equivalence ratio, fuel type and temperature.

Gottuk & Lattimar [64] have presented two versions of carbon monoxide yield models for compartment fires based on the compartment equivalence ratio (CER) if there was no external flames and , the choice between the two version depends on the upper layer temperature (one for below 800 K and the other for above 900 K). In the following models the fuel composition influence was deemed insignificant on CO yields, although that was contradicted by Tewarson's FPA data [70]. Gottuk & Lattimer's equations are as follows;

$Y_{CO} = (0.19/180)\ \tan^{-1}(10(\boldsymbol{\phi} - 0.8)) + 0.095$ when $T_{ul} < 800K$

$Y_{CO} = (0.22/180)\ \tan^{-1}(10(\boldsymbol{\phi} - 1.25)) + 0.110$ when $T_{ul} > 900K$

Where; Y_{CO} is carbon monoxide yield, $\tan^{-1}$ is in degrees, $\boldsymbol{\phi}$ is the equivalence ratio, and T_{ul} is the upper layer temperature.

Tewarson produced empirical correlations for predicting yields (carbon dioxide, carbon monoxide, total hydrocarbons and soot) as a function of equivalence ratios for halogenated and non-halogenated polymers [70]. Tewarson's empirical correlations were based on experimental values obtained using ASTM E2058 fire propagation apparatus [71]. These correlations are presented as following;

$$Y_{CO2} = Y_{CO2,wv}\left(1 - \frac{1}{\exp\left(\phi/2.15\right)^{-1.2}}\right)$$

Where; Y_{CO2} is the predicted carbon dioxide yield on mass bases grams of CO_2 per grams of fuel, $Y_{CO2,wv}$ is the carbon dioxide yield measured in well ventilated FPA tests (data presented in Table 2-3) in [g/g], and ϕ is the equivalence ratio.

$$Y_{CO} = Y_{CO,wv}\left(1 + \frac{\alpha}{\exp\left(2.5\phi^{-\zeta}\right)}\right)$$

Where; Y_{CO} is the predicted carbon monoxide yield on mass bases grams of CO per grams of fuel, $Y_{CO,wv}$ is the carbon monoxide yield measured in well ventilated FPA tests in [g/g], α and ζ are correlation coefficients (data presented in Table 2-3), and ϕ is the equivalence ratio.

$$Y_{THC} = Y_{THC,wv}\left(1 + \frac{\alpha}{\exp\left(5.0\phi^{-\zeta}\right)}\right)$$

Where; Y_{THC} is the predicted total hydrocarbon yield on mass bases grams of THC per grams of fuel, $Y_{THC,wv}$ is the total hydrocarbon yield measured in well ventilated FPA tests in [g/g], α and ζ are correlation coefficients (data presented in Table 2-3), and ϕ is the equivalence ratio.

$$Y_S = Y_{S,wv}\left(1 + \frac{\alpha}{\exp\left(2.5\phi^{-\zeta}\right)}\right)$$

Where; Y_S is the predicted soot yield on mass bases grams of soot per grams of fuel, $Y_{S,wv}$ is the soot yield measured in well ventilated FPA tests in [g/g], α and ζ are correlation coefficients (data presented in Table 2-3), and ϕ is the equivalence ratio.

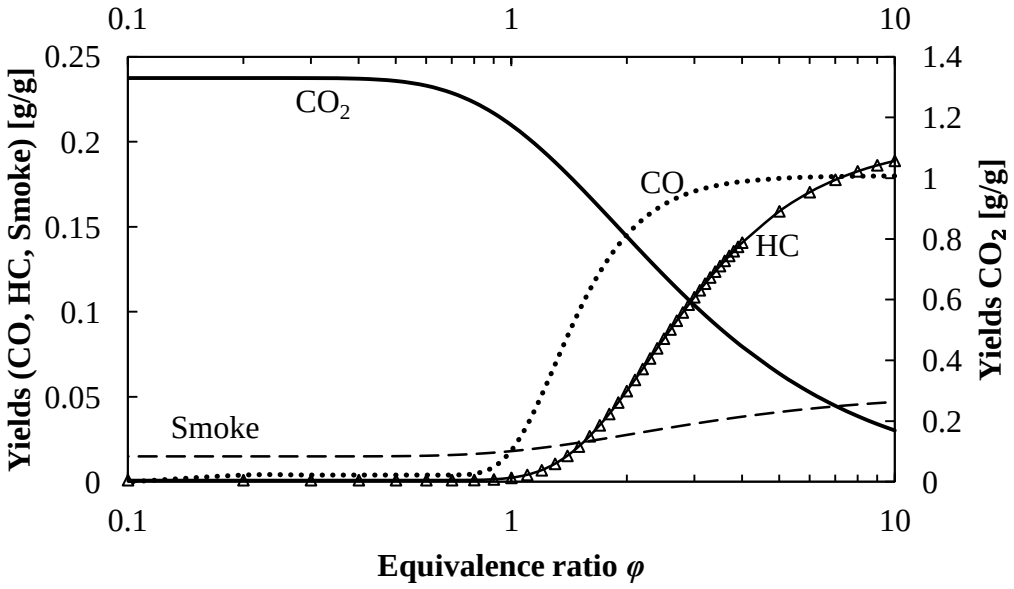

Figure 2-4: Tewarson's empirical correlations for (CO, CO_2, total hydrocarbons and soot) yields as a function of equivalence ratio for pine wood.

Table 2-3: Input values for Tewarson's yields empirical correlations [70].

Fuel	CO_2	CO			THC			Soot		
	$Y_{CO2,wv}$	$Y_{CO,wv}$	α	ζ	$Y_{THC,wv}$	α	ζ	$Y_{S,wv}$	α	ζ
PS	2.33	0.060	2	2.5	0.014	25	1.8	0.164	2.8	1.3
PP	2.79	0.024	10	2.8	0.006	220	2.5	0.059	2.2	1.0
PE	2.76	0.024	10	2.8	0.007	220	2.5	0.060	2.2	1.0
Nylon	2.06	0.038	36	3.0	0.016	1200	3.2	0.075	1.7	0.8
PMMA	2.12	0.010	43	3.2	0.001	1800	3.5	0.022	1.6	0.6
Wood	1.27 - 1.33	0.004 - 0.005	44	3.5	0.001	200	1.9	0.015	2.5	1.2
PVC	0.46	0.063	7	8.0	0.023	25	1.8	0.172	0.38	8.0

PS: Polystyrene, PP: Polypropylene, PE: Polyethylene, PMMA: Polymethylmethacrylate, PVC: Polyvinylchloride.

Tewarson's correlations for yields emitted from burning pine wood with varied equivalence ratios are presented in Figure 2-4 to showcase the use of the correlations. Karlsson and Quintiere [4] have produced Figure 2-5 for Tewarson's correlations for different materials as normalised yields to the well ventilated yield values. Tewarson's findings highlight the general trend of evolved fire effluent from most combustible materials that with higher equivalence ratios carbon monoxide and soot yields increase while carbon dioxide yields and oxygen consumption decrease.

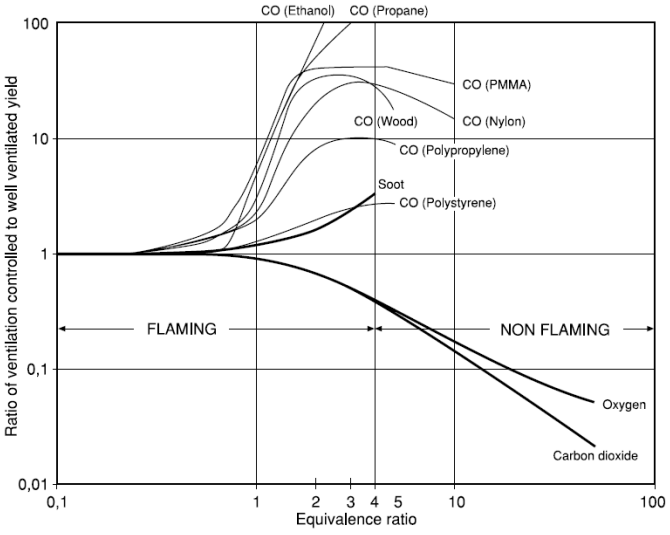

Figure 2-5: Tewarson's yields correlations for different materials as presented by Karlsson and Quintiere [4].

2.1.5 Yields vs. Concentrations

In fire toxicity field, gas yields, also known as emission factors or indices in environmental pollution literature, are the ratios between mass discharge rate of the specific gas from the combustion reaction and the mass burning rate of the fuel expressed in [$g_{species}/g_{fuel}$]. Toxic gas concentrations are known to be the volumetric ratio of the gas in the sampled air, and usually expressed in [ppm or %].

The hazardous effects of the toxic products on people depends on the amount of gases (concentration) inhaled. Exposure threshold values for toxic gases are defined in terms of concentration and dose (concentration × time) measurements and used in the FED hazard assessment calculation methods. It is crucial to understand that the concentrations measured in full scale experiments are only relevant to the sampling location used. As concentrations measured depend on the fire development and the geometry of the building that the generated smoke would travel through, taking into account any additional dilution to the smoke, before the point of exposure/sampling.

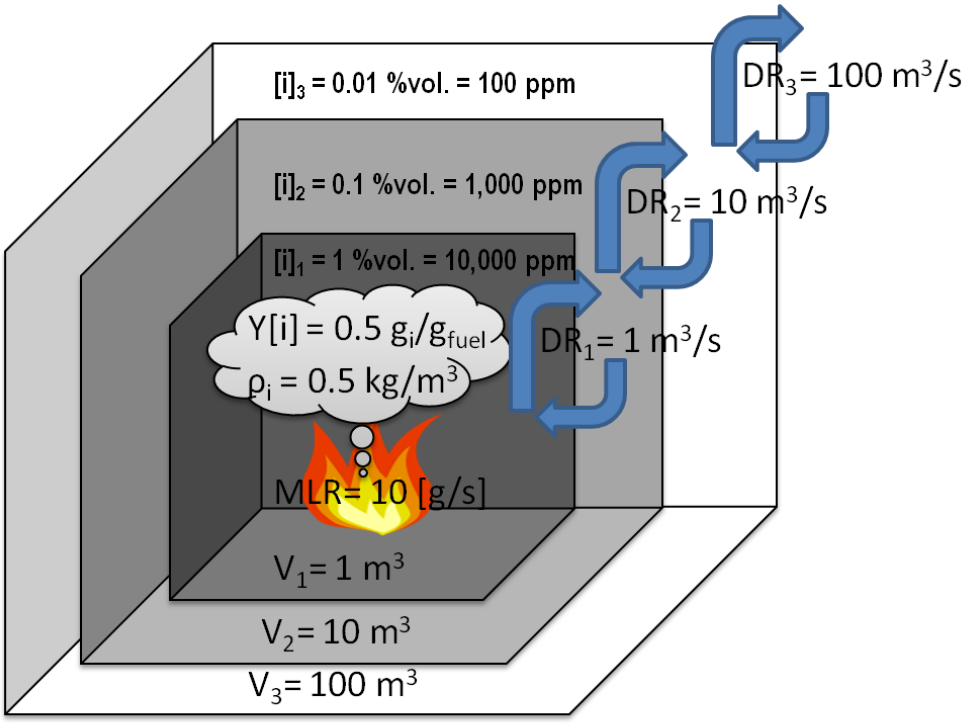

Where;
MLR is mass loss rate, ρ_i is the density of gas i
Y[i] is the mass yield of gas i in g/g
V_n is the volume of the zone n
$[i]_n$ is the volumetric concentration of gas i in zone n
DR_n is the dilution air supply rate for smoke in zone n

Figure 2-6: Scenario demonstrating the difference between yield data and concentration data.

The production of the toxic emissions from a fire can be quantified by yields values, this term is only dependent on the fire development and can be considered as a fire characteristic that develops as the fire grows and changes collectively with other fire characteristics. Yield data do not change by changing the sampling point location unless a post-oxidation reaction occurs. This important quality is required for reporting data from experimental tests at different scales.

The emission rate (yields of the gas × mass burning rate) and the dilution rate as the smoke moves away from the source will determine the exposure concentration at different locations within the building and beyond. It is important to highlight that yields discussed above are the mass loss yields, however some data may be reported as "mass charge yields" referring to the available specimen mass in the test regardless of how much has decomposed during the test.

A hypothetical example presented in Figure 2-6, shows that at certain moment the mass burning rate (MLR) was 10 g/s and yield of gas i was 0.5 g/g that had a density of 0.5 kg/m^3 (assuming constituent density for the purpose of the exercise). Then by having three different zones with variation in size and ventilation rate (assumed to be only a dilution rate and not interfering with the oxidation process), this showed that differences in concentration/exposure could occur for the same fire if they were sampled/inhaled at different locations, with the assumption that no post-oxidation occurred.

Concentrations are measured normally as volumetric ratio in % or ppm that are usually measured by chemical analysis (discussed later in section 2.4) which represent the volume of the measured gas as a ratio to total volume of the sample (gas cell size). However, sometimes concentrations are expressed in mg/m^3 that can be converted to volumetric ratio in ppm using the following relationship:

$$[ppm] = \frac{[mg/m^3] \times 24.45[m^3/kmol]}{M_W[kg/kmol]}$$

Yields are usually determined on the basis of the concentration measurements and then translated to mass based ratio e.g. grams of gas emitted per gram of fuel burnt.

Practical guidance for calculating yields is given in the literature, two main approaches are the most common. Firstly, the following method presented in ISO 19700 [72] and BS 7990 [73] to be used specifically for the tube furnace test however only minor modifications are needed for it to be used in other dynamic small-scale tests with fixed flow rates. Secondly, the approach used by Gottuk and Lattimer [64], Tewarson [74] and others [62, 75] the depends on air to fuel ratio rather than fixed flow rate of exhaust. For the first method, two options for yields are given; mass charge yield and mass loss yield; the former is most useful for ranking and comparing materials as it would take into account the reactivity of the specimen in the tested fire conditions. While the latter is most useful for actual

representation of the combustion and more relevant to fire toxicity scaling and modelling studies. The following steps are followed to calculate both yields in the Purser furnace [72] [73];

1) Calculate the mass charge concentration;

$$C_{m.charge} = \frac{\dot{m}_{charge}}{A}$$

Where; $C_{m.charge}$ is the mass-charge concentration in grams of the test specimen charged into the furnace per cubic meter of dispersed volume, $\dot{m}_{charge}$ is the rate of introduced specimen mass into the furnace in milligrams of the test specimen charged into the furnace per minute, A is the total air flow rate through the mixing and measurement chamber in litres per minute i.e. 50 L/min for the tube furnace.

Then, mass charge yield can be calculated as follows;

$$Y_i(t) = \left(\frac{g_i(t)}{C_{m.charge}(t)}\right) \times \frac{M_{W,i}}{V_{ideal\ gas}} \times 10$$

Where; Y_i gas yield in ($g_i \cdot g_{fuel}^{-1}$) at the time *t*, g_i Gas *i* concentration at time *t* in %(l_i/l_{air}), $C_{m,charge}$ is the mass charge concentration in grams of fuel per cubic meter of dispersed space [$g_{fuel} \cdot m^{-3}_{air}$], $Mw_i/V_{ideal\ gas}$ is in ($g_i \cdot l_i^{-1}$), 10= 1000[$l_{air}^{1} \cdot m^{-3}_{air}$]/100[%].

2a) Calculate the mass loss per unit length;

$$m_{loss} = m_{load} - m_{res}$$

Where; m_{loss} is the mass loss per unit length in milligrams of specimen burnt per millimetre of boat advancement, m_{load} is the specimen mass loading per unit length in milligrams of the specimen introduced per millimetre of boat advancement, m_{res} is the specimen mass residue (at the end of the test) per unit length in milligrams of the specimen left unburnt per millimetre of boat advancement.

2b) Calculate the mass loss rate;

$$\dot{m}_{loss} = m_{loss} \times \dot{b}$$

Where; $\dot{m}_{loss}$ is the rate of specimen mass loss in milligrams of specimen burnt per minute, $\dot{b}$ is the boat advancement rate in millimetres per minute.

2c) Calculate the mass loss concentration;

$$C_{m.loss} = \frac{\dot{m}_{loss}}{A}$$

Where; $C_{m.loss}$ is the mass-loss concentration in grams of the test specimen burnt per cubic meter of dispersed volume.

Finally, mass loss yield of each gas measured is calculated as follows;

$$Y_i(t) = \left(\frac{g_i(t)}{C_{m.loss}(t)}\right) \times \frac{M_{W,i}}{V_{ideal\ gas}} \times 10$$

The main limitation of this formula is that it requires constant flow rate of effluents e.g. for ISO 19700 tube furnace test 50 L/min [72] and for ISO 5660 cone calorimeter 24 L/sec [76]. Consequently, there is limited application of this equation in situations where constant flow rate of effluents is not achievable, for instance, in full scale experiments without hoods.

An alternative method presented by Gottuk and Lattimer [64], Tewarson [74] and others [62, 75].

$$Y_i(t) = [g_i(t)] \times \frac{Mw_i}{Mw_{mix}} \times \{1 + AFR(t)\} \quad g/g$$

Where;

$Y_i(t)$ gas yield in (g_i/g_{fuel}) at the time *t*, Mw_{mix} is the molecular weight of the mixture assumed to be that of air = 28.96 [g/mol], Mw_i molecular weight of the gas in [g_i/mol_i], [$g_i(t)$] Gas *i* concentration at time *t* in (ppm vol.)×10^{-6} or in (%vol.)×10^{-2}, AFR(t) mass-based actual air to fuel ratio g_{air}/g_{fuel}.

This method can be used without the need for a defined flow rate of effluents, however it requires actual air to fuel mass ratio. The author is presenting as part of this work a model in Chapter 4 for an emission-based actual air to fuel ratio on mass basis for different fuels. Following this procedure provides wider applicability for analysing fire emissions without the need for additional dilution that can potentially cause post-oxidation especially for under-ventilated fire emissions. Further details about dilution in small-scale tests are presented in Chapter 3 and Chapter 6.

Yields are sometimes presented as "normalised" yields or as a ratio to their corresponding well ventilated yields as shown in Figure 2-5 that was adapted from [4]. Normalising the yields means that the measured yields are divided by the maximum theoretical (notional) yield calculated from the fuel composition. Usually researchers use normalised yields to compare yields of specific species from different fuels.

2.1.6 Temperature influence on fire effluent

Temperature may influence the production of toxic fire effluents in a number of ways [64]. For example, in the actual combustion zone, depending on the temperature, the combustion conditions can change (e.g. flaming and non-flaming combustion) influencing the combustion efficiency and reaction rate characteristics (e.g. MLR). Additionally, temperature may influence toxic fire effluents beyond the combustion zone (i.e. smoke transport). At high temperatures the reactivity of incomplete combustion products increases. This encourages incomplete combustion toxic products (e.g. CO) to be converted to

complete combustion, less-toxic products (e.g. CO_2) where the chemical kinetics characteristics are influenced greatly by temperature of the surrounding environment.

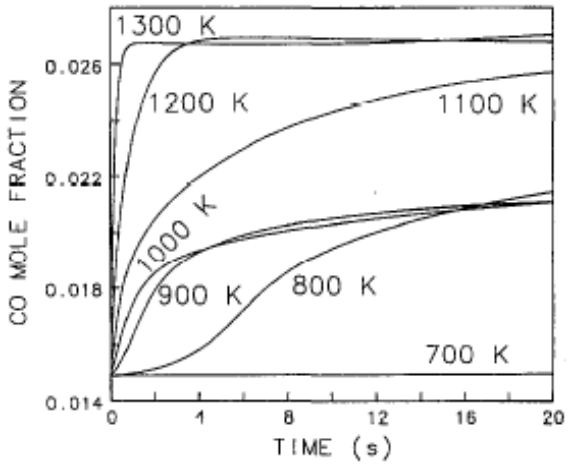

Figure 2-7: Pitt's comparison of calculated CO concentrations at different temperatures. GER = 2.17. from [77].

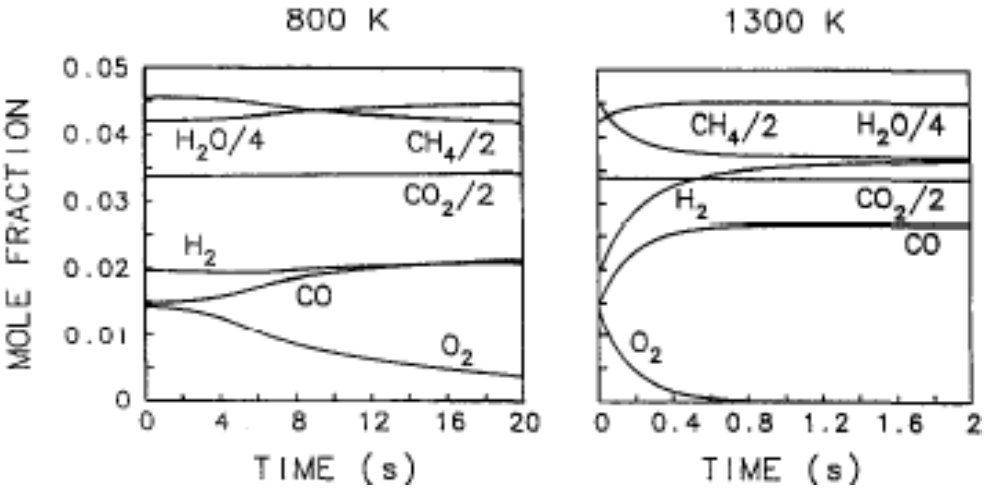

Figure 2-8: Pitt's comparison of calculated time behaviour of major gas species. GER = 2.17. Left: low temperature (800 K), Right: high temperature (1300 K), from [77].

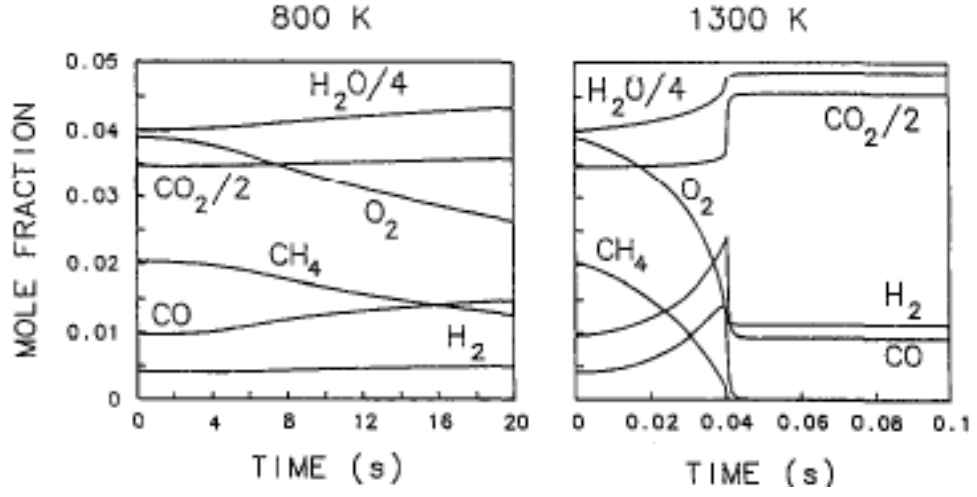

Figure 2-9: Pitt's comparison of calculated time behaviour of major gas species. GER = 1.09. Left: low temperature (800 K), Right: high temperature (1300 K), from [77].

Pitts investigated the chemical kinetics influence on fire effluents [63, 77, 78], main findings of his study can be summarised as follows; firstly, fire effluents are frozen (unreactive) when the temperature of the gas is below 700 K (426.85 C), these effluents start to be reactive in temperatures above 800 K (526.85 C), see Figure 2-7. Secondly, the reaction rates or conversion rates of the combustion products increase as temperature increases beyond the reactive temperature (i.e. 800 K), see Figure 2-8 (note the residence time scale on the x-axis). Pitts noticed the influence of the equivalence ratio on the reaction rate, it was shown that a dramatic change occur with rich mixtures, see Figure 2-9. Pitts findings were highlighted experimentally by Zukoski et al. [66] using hood experiments as shown in Figure 2-10.

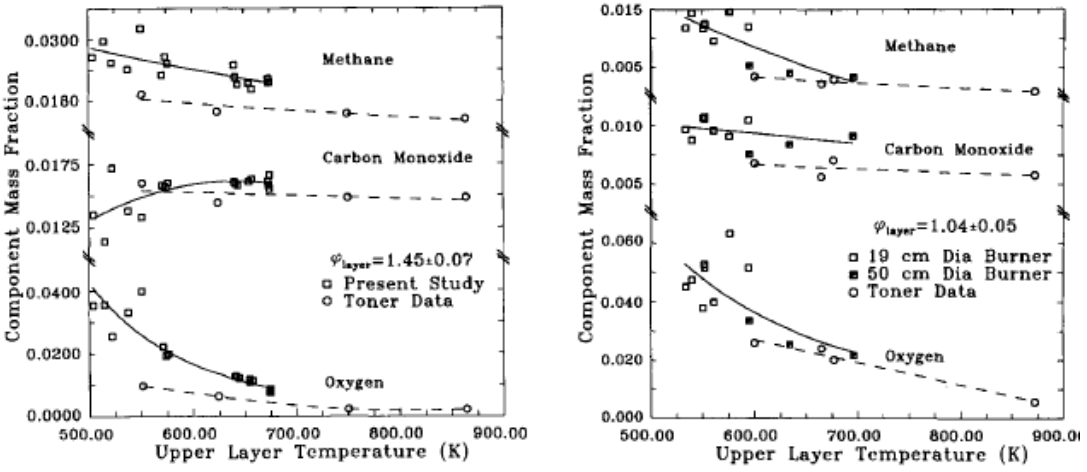

Figure 2-10: Experimental temperature dependence of product species measurements; Left: $\boldsymbol{\phi}$ = 1.45, Right: $\boldsymbol{\phi}$ = 1.04, from [66].

It is clear that by increasing the temperature of the atmosphere where the fire products are released into, the reactivity of these products increases causing quicker oxidation of the fire effluents. In other words if the fire effluents are pyrolysed in a higher temperature atmosphere, as opposed to a lower temperature atmosphere, more unoxidised products will be oxidised in less time, assuming that pyrolysis rate, effluent composition and oxygen availability are all the same. With richer mixtures the reactivity increases. These observations are very relevant to compartment fires, where the smoke products are released into other parts of the building or to the outer atmosphere. Gottuk and Lattimer [64] experimentally measured Carbon monoxide yield inside the compartment and downstream the hood (after dilution). The results, presented in Figure 2-11, show that post-oxidation outside the compartment zone happens with rich mixtures (compartment ER above 1.6) in Gottuk's setup for hexane compartment fire.

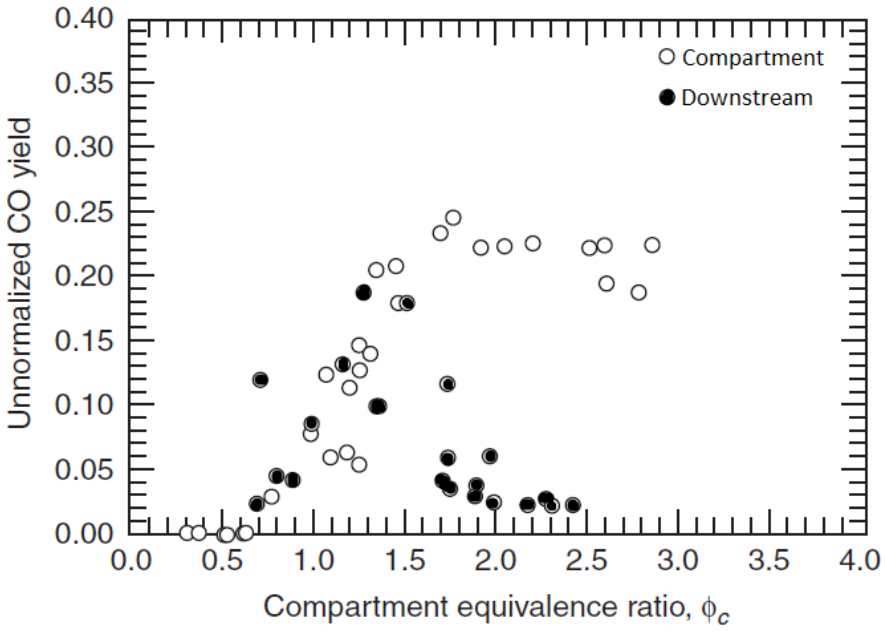

Figure 2-11: CO yields as measured inside the compartment (raw) and downstream (diluted) as a function of compartment ER burning hexane. External flames were visible above $\boldsymbol{\phi}$ =1.6. Adapted from [64].

2.2 Fire emissions that are harmful to people

This section details the health challenges that fire effluents can cause to people who are exposed to them. There are two main classifications for these effects, as outlined in Figure 2-12.

- Firstly, acute effects that affect the majority of immediate fire victims as discussed earlier in 1.3, from impairment of escape to eventually death.
- Secondly, long-term effects which are relevant to occupational health of those exposed to fires regularly i.e. fire fighters and also for the health concerns from reduction of air quality as a result of large fires that sustain themselves for lengthy periods [79, 80]. For example; Kuwait oil fires [81], Buncefield fire [82, 83], and wildfires [84, 85].

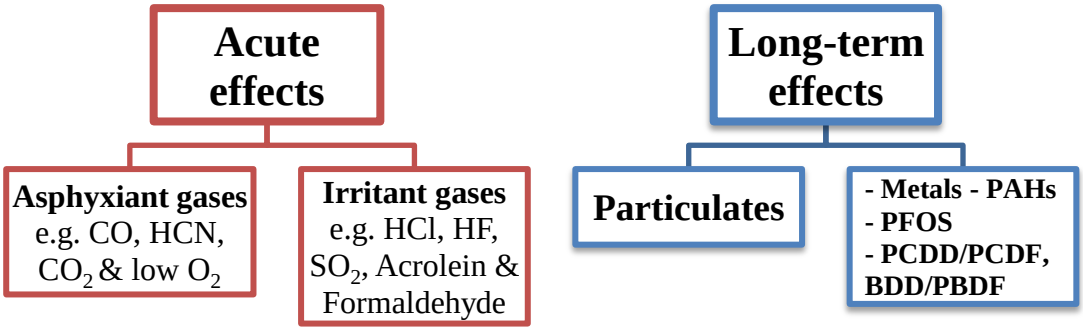

Figure 2-12: Classification of fire effluents based on their effects on people.

2.2.1 Asphyxiants

Asphyxiation is the condition where severe deficiency of oxygen supply to the body tissues and organs [45, 86-90]. For fire victims asphyxiation is the main cause of death as a result of smoke inhalation. Technically, inhaling toxic smoke replaces oxygen in the blood causing reduction to the amount of oxygen supplied to vital body organs. Initially, asphyxia causes body parts to start shutting down causing unconsciousness. Then, different degrees of damage to body-parts occur. These damages might be fatal depending on the time of rescue. Main gases produced in fires that cause asphyxiation are carbon monoxide (CO) and hydrogen cyanide (HCN). While carbon dioxide (CO_2) and reduction in oxygen (O_2) are major contributing factors - they are not as significant as CO and HCN and are difficult to trace in post-mortem analysis for fire victims [7, 91]. Specific details of the mechanism that these gases affect human body at different levels of exposure is given in this section.

2.2.1.1 Carbon monoxide

Carbon monoxide is a primary product from any incomplete combustion of most common fuels. It is produced in significant quantities in every rich (under ventilated) fire. Inhaling carbon monoxide can form carboxyhaemoglobin (COHb) in the red blood cells, which reduces oxygen uptake and hence delivery of oxygen to body organs. Ultimately, if sufficient amount of COHb is formed, a lethal effect can be caused. However depending on the exposure dose, different levels of effects can be experienced [92, 93]. Purser [7, 94] reviewed the relationship between concentration and exposure dose (concentration multiplied by the exposure time) that causes loss of consciousness. He showed that the CO exposure dose for losing consciousness is almost independent of the concentration applied. Purser reported exposure values between 26,000 and 28,000 ppm.min. For concentrations from 1,000 to 8,000 ppm the reported time for loss of conscious from 26.6 min for the lowest concentration to 3.24 min for the highest. With higher concentrations loss of conscious can occur after 2 or 3 breaths, a scenario that could occur when opening the door of a smoke-filled room [7, 94]. It is important to highlight that these effects depend on many factors such as body weight, age and breathing rate that depends on the level of activity of the subject at the time of exposure.

Table 2-4: Effects of carbon monoxide inhalation on susceptible subpopulations as reported in [95]

Blood %COHb saturation	**Symptoms experienced by susceptible subpopulations**
2	During physical exertion reduced time to onset of angina and electrocardiogram signs of myocardial ischemia in subjects with coronary artery disease.
5-6	Increase in cardiac arrhythmias in subjects with coronary artery disease
7	Headache, nausea in children
13	Cognitive development deficits in children
15	Myocardial infarction in subjects with coronary artery disease
25	Syncope in children
25	Stillbirths

Blood carboxyhaemoglobin saturation is the main measure of the body absorption of carbon monoxide gas, and consequently it is more accurate in assessing the effects of the human body from exposure to such a toxic gas. Purser [86] reviewed these effects, where 30% COHb was considered the threshold for the risk of collapsing and 50%COHb was the threshold for coma and irreversible damage to body organs. These figures are in agreement with published data of 260 carbon monoxide poisoning cases by Pach et.al [96] and reproduced in [86]. It was highlighted that the proportion of survivors starts dropping after 30%COHb, reaching only 15% survivors of cases with carboxyhaemoglobin up to 55%COHb. It is important to highlight that most of the previous data are for healthy adults and is not representative of the most vulnerable population. The US Environmental Protection Agency in their report of the AEGLs for carbon monoxide [95], presented the effects/symptoms that different levels of carboxyhaemoglobin would cause for healthy adults (which are in agreement with other sources presented earlier) in addition to the symptoms for susceptible subpopulations. The effects on vulnerable people can start from 7%COHB for children to start feeling headache and nausea. Higher levels i.e. 25%COHb may cause stillbirths. Full symptoms for susceptible groups are presented in the Table 2-4.

2.2.1.2 Hydrogen cyanide

HCN is considered approximately 35 times more lethally dangerous than carbon monoxide (based on LC50 values - defined later in section 2.3) [97]. Cyanide ion formed in the blood is the key factor of its effect. When HCN is inhaled, its toxic effect is applied in two main mechanisms; when first inhaled a rapid increase in respiration is observed (for up to 5 minutes), followed by a sharp depression of the respiratory system [98]. The other mechanism is diminishing the use of oxygen at the effected tissues and organs causing asphyxiation. Purser reviewed the relationship between concentration and exposure dose that cause loss of conscious. He showed that, unlike CO, HCN's exposure dose for losing conscious depends significantly on the HCN concentration applied. Purser [94] reported high exposure values (i.e. 2,610 ppm.min) for low HCN concentrations (i.e. 87 ppm) that can cause loss of consciousness when applied for a lengthy time (i.e. 30 minutes). However, as the concentration level increases the exposure dose required to cause loss of conscious decreases e.g. 200 ppm concentration can cause loss of conscious within 1.9 minutes giving an exposure dose of 380 ppm.min. Higher concentrations are reported to cause loss of conscious in less than a minute of exposure and fatal consequences may follow rapidly. These findings support the earlier explanation of HCN exposure mechanism in the respiratory system, the initial hyperventilation means that higher HCN levels will be inhaled in the lungs in the initial period of exposure. Symptoms/effects of different levels of HCN were reviewed in details by Purser and others in the literature [86, 94, 99-101].

2.2.1.3 Carbon dioxide

The major effects of carbon dioxide exposure are hyperventilation for the victim and subsequent increased uptake rate of other toxic gases [36, 87-90]. Exposure to CO_2 concentration level of 3% can double the rate of breathing. Levels up to 5% CO_2, can cause headache, dizziness, increase in blood pressure and pulse rate. Exposure to levels between 5 and 10% CO_2 causes extreme laboured breathing, visual impairment, ringing in the ears, impaired judgement followed by loss of consciousness and stopping of respiration. Exposure to levels beyond 10% CO_2 can have fatal consequences, however in reasonable fire environments fatal outcomes are produced mainly by other fire products before CO_2 become fatally toxic on its own. CO_2 main threat in fire environment is the hyperventilation effect that can increase uptake of the other toxic fire effluents.

2.2.1.4 Oxygen depletion – Hypoxia

Oxygen depletion can effect victims in a similar way as the CO_2 in the sense that it is very difficult to be a major cause of death for smoke inhalation victims in fires. But the main concern is to be acting as additive to the other toxic gases in the fire environment. Reduction in oxygen levels causes hyperventilation that would become more rapid as the oxygen percentage decreases. Below 12 $\%O_2$ when serious symptoms start appearing such as tiredness, dizziness and unconsciousness, oxygen levels below 6 % are lethal [86].

2.2.2 Irritant gases

In fires, irritant gases are generally not fatal but incapacitating and impairing the escape effort, leading to death by other toxic gases. Irritant gases are difficult to trace in a victim's body in post-mortem analysis [7, 45, 91, 102-104].

It is very important to assess the hazard posed by irritant gases in fires, because they can impair escape by their effects on the eyes and respiratory system [105]. The two major effects of irritant gases on human body are painful sensory irritation, occurring on initial exposure and lung inflammation, occurring after a longer exposure. A good example to understand this irritants effect is when smoke produced from barbeque or cigarettes and how eyes and nose start feel the pain almost immediately. A study presented by purser [106] highlighted the effects of irritant gases on walking speed and presented two empirical equations to resemble the walking speed in humans when irritant and non-irritant smoke is experienced;

Walking speed non-irritant [m/s] = $1.36 - 1.9 \times \text{smoke}_{\text{optical density}}$ [OD/m]

Walking speed irritant [m/s] = $2.27 - 9 \times \text{smoke}_{\text{optical density}}$ [OD/m]

The above experimental equations illustrate the effect of these irritants on reducing walking speed, however they are considered very generic and not representative of different levels of irritancy. So Purser [45] introduced another equation to predict walking speed based on the

level of irritancy of the gases, that can be determined using FIC (Fractional Irritation Concentration) model and can be applied for compounds of different irritants. The model is;

$$W_{irr} = e^{-(1000FIC/160)^2} + (-0.2FIC + 0.2)$$

$$\text{Overall walking speed} = 1.2 - (1.2 - W_s) - (1.2 - W_{irr})$$

Where; W_{irr} is walking speed adjusted for irritant compounds effects.

W_s is walking speed adjusted for smoke obscuration effects.

There are other health effects that are posed by irritants gases such as, upper respiratory tract and pulmonary irritations and in serious situations oedema may develop in the lungs [107]. These symptoms occur depending on the exposure level (concentration and time).

Irritant gases that can be produced in fires are classified in two types; inorganic or organic irritants. Inorganic irritants that include hydrogen halides (e.g. HCl, HB and HF), Nitrogen oxides and sulphur dioxide. While most significant organic irritants are acrolein and formaldehyde [7]. It is very important to highlight that the existence of most inorganic irritant gases depends mainly on the material composition e.g. HCl is produced only when chloride forms part of the fuel e.g. PVC [108]. While organic irritants (partially oxidised organic species) e.g. unsaturated aldehydes of isocyanate-derived compounds are the main source of irritancy of mixed fire effluents.

An environment rich in partially oxidized organic species is highly irritant while an environment with low organic content or lacking of partially oxidized organic species is relatively non-irritant. Polypropylene with the chemical formula $(C_3H_6)_n$ is a good example for that conclusion [7], when polypropylene was decomposed under inert atmosphere (nitrogen) it produced an environment rich in organic compounds without any oxidised organic species, this was non-irritant.

Under non-flaming oxidative decomposition conditions (with air as surrounding atmosphere), the environment produced is highly irritant. With flaming conditions (at higher temperature), 'cleaner' emissions are produced with lower irritancy but asphyxiant.

High yields of irritant emissions produced when wood and flexible polyurethane foam are decomposed even in an inert environment, due to the existence of oxygen as part of these materials' composition. Therefore, the existence of irritants is inevitable, their rate of production depends on amount of oxygen involved in the reaction (i.e. the fire).

The most significant species based on exposure limits (IC_{50} values [109]) are sulphur dioxide (inorganic) and acrolein (organic) as their incapacitation threshold are very low; IC_{50} for SO_2 is 120 ppm (7 times more impairing than HCl) and 30 ppm for acrolein (33 times more impairing than HCl). Exposure limits (lethality and impairment) have many variations depending on; the original data (bioassay) used, the extrapolation factors and the

definition of the threshold level. These factors will be discussed in detail later in this chapter.

2.2.3 Smoke particulates

Smoke particulates are the airborn solid and liquid particles produced by the fire and are responsible for obscuring vision for victims resulting in reduction of their evacuation speed and ultimately forcing them to turn back and look for an alternative route to a place of relative safety. Obscuration has been the main hazard of emphasis of particulate matter in fire studies. The health hazards posed by particulates have not been prioritised in the research and limited investigations have been conducted on quantifying the characteristics smoke particulates (size, distribution and composition) that can have damaging health effects on the exposed population.

Figure 2-13 shows the influence of the particle size on the location of deposition in the respiratory system. Particles with size less than 0.5 μm are able to penetrate into the lung interstitium, causing interstitial and luminal oedema. Additionally particulates can play a significant part in transporting poisonous molecules (by adsorption) to different parts of the body (most significantly the respiratory system) causing toxicological effects. However, limited quantitative information is available about these hazards in fire environments.

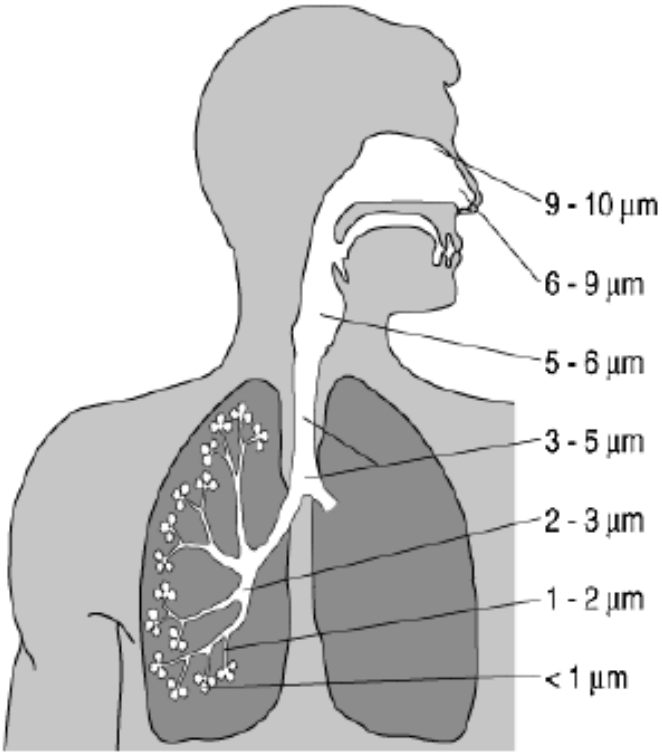

Figure 2-13: Particles deposition in respiratory system [110].

The Swedish National Testing and Research Institute (SP) conducted a research project [110] investigating the generation of particulates alongside isocyanates from burning 24 different building materials using multi scale testing, mainly small scale tests (cone

calorimeter ISO 5660 [76]) but larger experiments were used as well (intermediate-scale; SBI method EN 13823 [111], and full-scale; room-corner ISO 9705 [112]) and it was found that materials that do not burn well (fire retarded materials) produce more particles than materials that do burn well (combustibles), see results in Figure 2-14. Blomqivst et al. [113] tested Polyurethane and FR polyethylene cable insulation materials in in the Purser furnace (ISO 19706 tube furnace [58]) at different fire conditions. They concluded that in well ventilated conditions particulate size is smaller than vitiated fires.

The above measurements of particulates in fires report the total particulates which are effectively PM_{10}. The most harmful $PM_{2.5}$ is supported by the available measurements in EMEP/EEA document 5.C.2 [114]. Kang et al. also measured a $PM_{2.5}/PM_{10}$ ratio of the order 0.91 downwind of forest fires in Quebec in 2002 and 2010 [115].

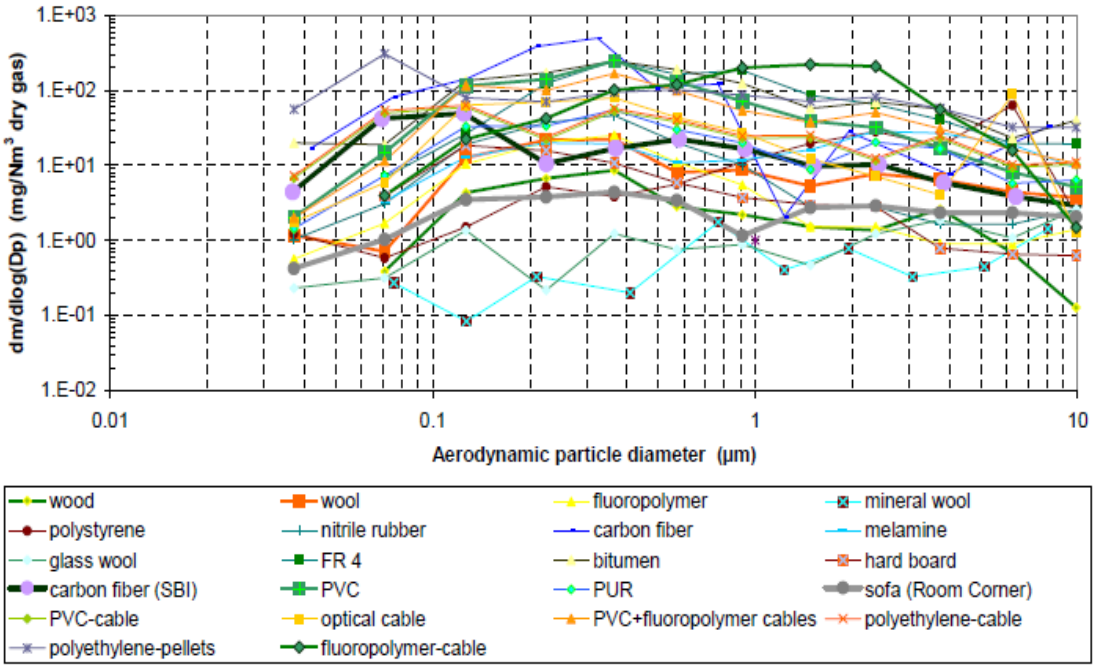

Figure 2-14: Mass size distribution of particles produced in SP testing program [110].

2.2.4 Determination of death cause as toxic smoke inhalation through forensic analysis

When CO is inhaled it substitutes oxygen and form carboxyhaemoglobin reducing the amount of oxygen delivered to tissues and organs. Carbon monoxide has been considered as the main cause of death in fires since COHb is very stable in victims' blood. Alarie [87] reviewed post-mortem blood analysis of fire victims from four major fire incidents and other collective databases of fire victims from different incidents. Alarie concluded that the levels of COHb in fire victims have decreased over the years while the levels of cyanide in blood have increased. He also highlighted that the sensitivity of young adults to carbon monoxide was quite narrow. Purser and McAllister [116] reviewed other databases of fire fatalities in buildings and post-crash vehicle fires. Lundquist et al. [117] presented blood

cyanide and carboxyhemoglobin data for 18 buildings fire fatalities. Figure 2-16 shows the post-mortem analysis of blood samples from 54 (including a single inconclusive sample with no data) victims of British airtours fire in Manchester airport 1985 (discussed earlier in Chapter 1) that measured the levels of COHb, CN, toluene, and benzene in the blood of the victims [17].

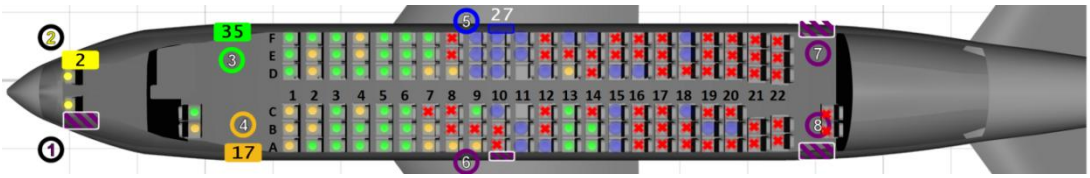

Figure 2-15: Passengers seating plan by exit used – red crosses represent fatalities **[118]**. Other colours and annotations as per original reference.

The reported levels were referenced to the seat locations of the victims as booked in their tickets (see Figure 2-15 and Figure 2-16). Since the flight was fully booked, it is reasonable to assume that the victims stayed in those seats at least until the start of evacuation process. It can be noticed that the samples from victims who were sat in the back of the airplane (near the left engine that caught fire) had lower toxic content than those further away from the burning engine. Probably because those at the back died rapidly, partly from heat while those at the front had longer to inhaled the gases.

In the official investigation, incapacitation threshold used was 30%COHb and CN 0.135 mg/100ml while lethal threshold used was 50%COHb and CN 0.270 mg/100ml. Table 2-5 shows the breakdown of the data based on these two thresholds showing that definitely 25 samples exceeded the lethal threshold of carboxyhaemoglobin or cyanide while 48 samples exceeded at least one of the incapacitation thresholds. Cyanide levels were above threshold levels in more samples than COHb, indicating that cyanide was a significant contributor to incapacitation, thereby preventing escape and leading to the death of these victims. Figure 2-17 shows the distributions of COHb levels in the blood samples of the victims.

Table 2-5: Summary of post-mortem toxicological analysis of British Airtours flight 28M (Manchester, 1985) victims

	Incapacitation; COHb 30%, CN 0.135 mg/100ml	**Fatal; COHb 50%, CN 0.270 mg/100ml**
# of samples with COHb above threshold	40	13
# of samples with CN above threshold	43	21
# of samples with COHb and CN combined above threshold	35	9
# of samples with either COHb or CN above threshold	48	25

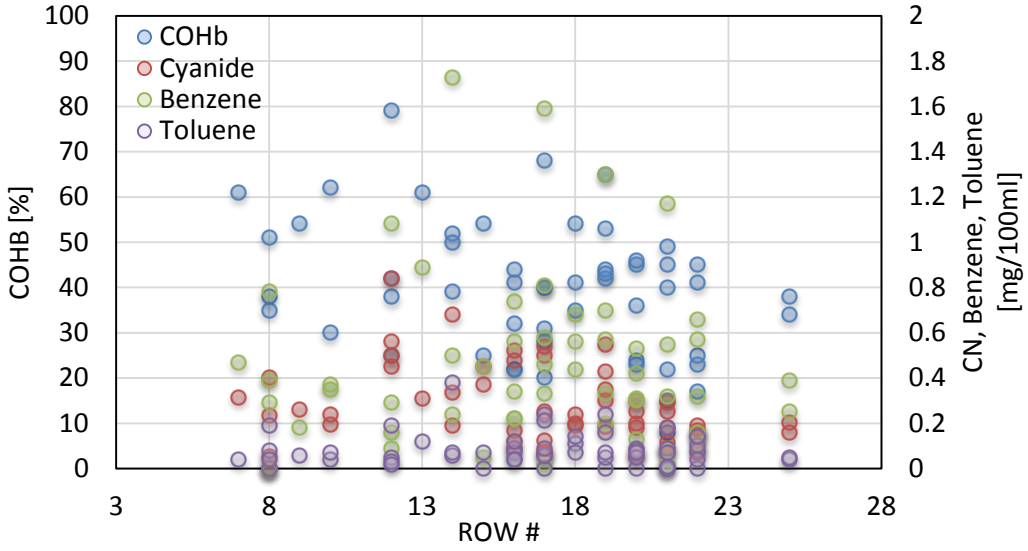

Figure 2-16: Pathological analysis of 53 blood samples from the victims of the British Airtours Flight 28M fire in Manchester in 1985. Row # refers to the row number of the seat allocated to the victim (see Figure 2-15).

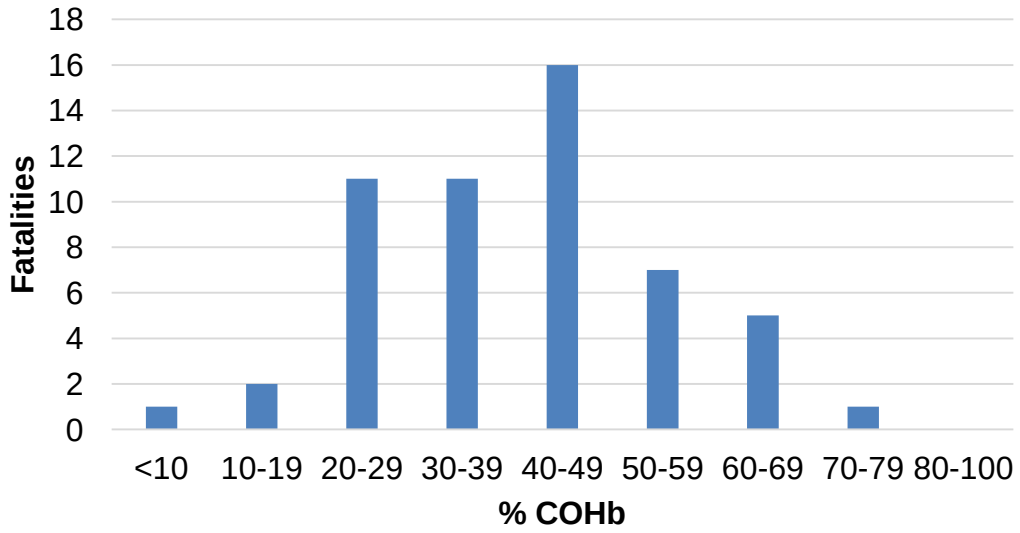

Figure 2-17: Distributions of %COHb in 53 blood samples from British Airtours flight 28M fire fatalities. original data were published in the official investigation report [17].

Experimental human exposure studies were used to extrapolate a prediction of carboxyhaemoglobin formed based on carbon monoxide exposure, the linear uptake Stewart model [86] takes into account the variation of breathing rate in addition to the exposure dose as follows;

$$COHb = 3.317 \times 10^{-5} [CO\ ppm]^{1.036} \times VE \times t$$

Where; VE in volume of air inhaled [Litres of Air breathed/min], t is exposure time [minutes]

Realistic values of VE can be obtained from [119]. Purser [116] suggested the use of three VE benchmarks (based on values obtained from [119]) for 70Kg human representing three levels of activities; 8.5 L/min for rest sitting, 25 L/min for light work (e.g. walking), and 50 L/min for heavy work (e.g. slow running).

2.2.5 List of emissions of interest for fire toxicity hazards assessment

It is crucially important for fire toxicity assessment to identify the main emissions produced in fires and their effects on people. The species listed below were compiled based on two main rationales; the possibility of their existence within products released from fires (any fire). Secondly, the existence of their acute effects on humans. If both these aspects are available for any species then it is included in the list below. Other fire products that are important to quantify for assessing long term effects are not included in this list, such as soot, and metals. The species listed below in Table 2-6 have been grouped in three classifications based on their nature and effects on humans; asphyxiants, inorganic irritants, and organic irritants.

Table 2-6: List of emissions of interest for fire toxicity hazards assessment

Asphyxiants	Inorganic irritants	Organic irritants
Carbon monoxide	Hydrogen chloride	Acrolein
Hydrogen cyanide	Hydrogen bromide	Formaldehyde
Carbon dioxide	Hydrogen fluoride	Benzene
Oxygen	Nitrogen dioxide	Acetaldehyde
	Nitric oxide	Acetic acid
	Sulphur dioxide	Styrene
	Ammonia	Phenol
	Carbon disulphide	Toluene
	Chlorine	Formic Acid
	Phosgene	Acrylonitrile
	Hydrogen sulphide	

2.3 Quantification of toxic hazards from fires effluents

Quantifying toxic hazards from fire effluents has been the subject of research interest since the 1960's utilizing bioassay experiments that often involve animals and rarely humans. This research was pioneered by Alaire [120-122], Tsuchiya [123, 124], Purser [99, 104, 125-128], Levin [129-131], Hartzell [132-134] and others [135, 136] that focussed on developing experimental methodologies to establish effective doses of fire products. These resulted in additive models for assessing toxic effluent from fires on humans [46, 127, 130, 136]. The work of these researchers and other experimentalists [137-142] resulted in establishing toxic exposure threshold limits that were compiled by different bodies such as HSE (COSHH) [143], OSHA (PEL) [144], ACGIH (TLV) [145], NIOSH (IDLH) [146], AEGL [147], ISO (IC50 [109] and LC50 [97]), and SFPE (impairment of escape, incapacitation, and lethality) [7, 116]. These limits are discussed below and their use in the additive models for assessing toxic effluent from fires for the purpose of fire safety engineering calculations is described.

2.3.1 Toxic threshold levels of exposure to fire effluents

Based on the definitions of toxic threshold levels of the available 13 datasets that are included in this review, four threshold levels are proposed, each to be for the purpose of the different levels of fire toxicity hazard assessment as summarised in Figure 2-18 with more detailed explanations following below;

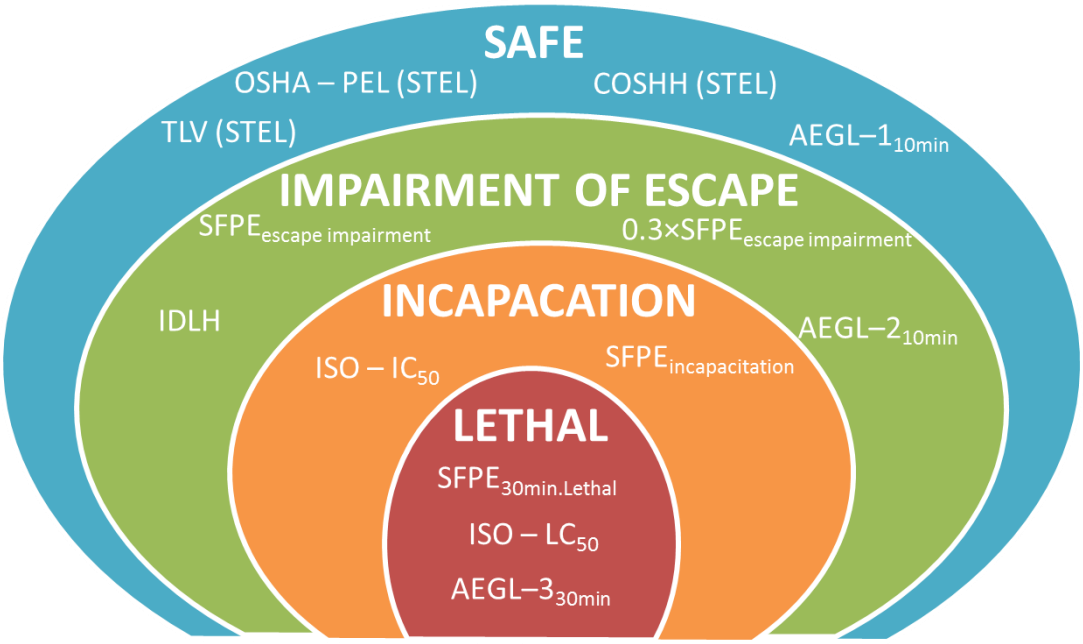

Figure 2-18: Toxic exposure threshold classification for fire toxic hazards assessment and associated datasets.

2.3.1.1 Safe Exposure levels

Safe level of exposure that any fire safety design should achieve for protected areas. Values for emissions of interest for fire toxicity hazards assessment from the relevant datasets are compiled in Table 2-7. The following toxic threshold exposure levels were deemed most appropriate to represent Safe level of exposure based on their definitions;

a) COSHH (STEL); is the legal limit in the UK for short term exposures (15 minutes) of an employee to a chemical substance. Published by the UK Health and Safety Executive (HSE) for the purpose of regulating the Control of Substances Hazardous to Health (COSHH) to ensure occupational health. The extensive database for COSHH values is published by the UK HSE [143], and is regularly reviewed. The classification of Short Term (15 minutes) Exposure Limit (STEL) is the most relevant here for the safe exposure because they "are set to help prevent effects such as eye irritation" [143]. COSHH (STEL) values for emissions of interest for fire toxicity hazards assessment are presented in Table 2-7.

b) OSHA – PEL (STEL); US equivalent of COSHH limits, as it is the US legally approved limit for safe exposure to toxic gases. Established by the Occupational Safety and Health Administration (OSHA) that provides an extensive database of Permissible Exposure Limits (PELs) for different chemical substances [144]. The STEL classification (15 minutes) is the most relevant here to the safe exposure of fire effluents. OSHA – PEL (STEL) values for emissions of interest for fire toxicity hazards assessment are presented in Table 2-7.

c) TLV (STEL); published by the American Conference of Governmental Industrial Hygienists (ACGIH), a non-governmental entity. Threshold Limit Value (TLV) is defined as the recommended level that a worker can be exposed to (for defined time limits) without adverse health effects [145]. The classification of the 15 minute STEL is the most relevant here for the safe exposure to fire effluents. TLV (STEL) values for emissions of interest for fire toxicity hazards assessment are presented in Table 2-7.

d) AEGL–1_{10min}; part of the Acute Exposures Guidelines (AEGLs) published by US Environmental Protection Agency [95, 101, 147-151]. Defined as "is the airborne concentration of a substance above which it is predicted that the general population, including susceptible individuals, could experience notable **discomfort**, **irritation**, or certain **asymptomatic non-sensory** effects. However, the effects are not disabling and are transient and reversible upon cessation of exposure". Purser [7] recommended the use of these exposure limits because they are based on a detailed review of the toxicity data from both human and animal studies with carefully justified opinion on extrapolation of data and application to the choice of guideline ceiling levels. The 10 minutes exposure limit for level 1 is considered most appropriate to be in the safe classification for fire effluents exposure (see Figure 2-18). AEGL–1_{10min} values for emissions of interest for fire toxicity hazards assessment are presented in Table 2-7.

2.3.1.2 Impairment of escape threshold exposure levels

Impairment of escape level, implying that reaching these exposure levels would start causing impairment of escape for exposed subjects. Values for emissions of interest for fire toxicity hazards assessment from the relevant databases are compiled in Table 2-8.

a) AEGL–2_{10min}; [147]. Defined as "is the airborne concentration of a substance above which it is predicted that the general population, including susceptible individuals, could experience **irreversible** or other serious, **long-lasting** adverse health effects or an **impaired ability to escape**". Purser [7] recommended the use of AEGL-2 exposure limits for impairment of escape. The 10 min. exposure limit for level 2 is considered most appropriate to be in the impairment of escape classification for fire effluents exposure (see Figure 2-18). AEGL–2_{10min} values for emissions of interest for fire toxicity hazards assessment are presented in Table 2-8.

b) SFPE $_{escape\ impairment}$; these values are presented by Purser [7] showing the predicted concentrations that can cause impairment of escape to half the exposed population, for that reason it is considered the most appropriate to be in the impairment of escape classification for fire effluents exposure (see Figure 2-18). SFPE $_{escape\ impairment}$ values for emissions of interest for fire toxicity hazards assessment are presented in Table 2-8.

c) 0.3 x SFPE $_{escape\ impairment}$; a factor of 0.3 is recommended by Purser [7] to be applied on the presented impairment of escape SFPE threshold limits to allow "for safe escape of nearly all exposed individuals". This level is considered most appropriate to be in the impairment of escape classification for fire effluents exposure (see Figure 2-18). SFPE $_{escape\ impairment}$ values multiplied by a factor of 0.3 for emissions of interest for fire toxicity hazards assessment are presented in Table 2-7.

c) IDLH; Immediately Dangerous for Life or Health (IDLH) values are published by the US National Institute for Occupational Safety and Health (NIOSH) [146]. IDLH values represent the level that poses "a threat of exposure to airborne contaminants when that exposure is likely to cause death or immediate or delayed permanent adverse health effects or prevent escape from such an environment". The definition of IDLH data set is ambiguous in clarifying the effect of the reported data, making it difficult to classify it within a distinguished threshold level in the purposed scheme. Therefore even though it was placed in the impairment of escape (see Figure 2-18), its data are not necessarily represent that level of threat and should be used with caution. Compared to the other data on the same Table the threshold values for asphyxiants based on the IDLH are too high and this may not be a suitable choice for asphyxiant threshold values for escape impairment. IDLH values for emissions of interest for fire toxicity hazards assessment are presented in Table 2-8.

Table 2-7: Concentrations reported by the available databases for the Safe level of exposure from fire effluents

	Species	SAFE [ppm]			
		COSHH (STEL)	OSHA PEL (STEL)	TLV (STEL)	AEGL-1_{10min}
asphyxiants	Carbon monoxide	200	200	NR	NR
	Hydrogen Cyanide	10	4.7	4.7	2.5
	Carbon dioxide	15k	30k	30k	NA
	Oxygen	NA	NA	NA	NA
inorganic irritants	Hydrogen chloride	5	5	5	1.8
	Hydrogen bromide	3	3	3	1
	Hydrogen fluoride	3	1	3	1
	Nitrogen dioxide	NA	1	5	0.5
	Nitric oxide	NA	NR	NR	NR
	Sulphur dioxide	NA	5	5	0.2
	Ammonia	35	35	35	30
	Carbon disulphide	NR	12	NR	17
	Chlorine	0.5	1	1	0.5
	Phosgene	0.06	NR	NR	NR
	Hydrogen sulphide	10	15	15	0.75
organic irritants	Acrolein	0.3	0.1	0.3	0.03
	Formaldehyde	2	2	0.3	0.9
	Benzene	NR	5	2.5	130
	Acetaldehyde	50	25	25	45
	Acetic Acid	NA	15	15	NA
	Styrene	250	100	40	20
	Phenol	4	NR	NR	19
	Toluene	100	150	0.02	67
	Formic Acid	NR	10	10	NA
	Acrylonitrile	NR	60	NR	1.5

NR: Not recorded, meaning that the species are available but the measurement for the needed classification is not recorded.

NA: Not available, meaning that the species needed is not available in that database.

Table 2-8: Concentrations reported by the available databases for the Impairment of escape level of exposure from fire effluents

	Species	Empirical formula	Impairment of escape [ppm]			
			AEGL-2_{10min}	SFPE $_{escape\ impairment}$ *	0.3×SFPE $_{escape\ impairment}$ †	IDLH
asphyxiants	Carbon monoxide	CO	420	NA	NA	1,200
	Hydrogen Cyanide	HCN	17	NA	NA	50
	Carbon dioxide	CO_2	NA	NA	NA	40k
	Oxygen	O_2	NA	NA	NA	NA
inorganic irritant	Hydrogen chloride	HCl	100	200	60	50
	Hydrogen bromide	HBr	250	200	60	30
	Hydrogen fluoride	HF	95	200	60	30
	Nitrogen dioxide	NO_2	20	70	21	20
	Nitric oxide	NO	NR	NA	NA	100
	Sulphur dioxide	SO_2	0.75	24	7.2	100
	Ammonia	NH_3	220	NA	NA	300
	Carbon disulphide	CS_2	200	NA	NA	500
	Chlorine	Cl_2	2.8	NA	NA	10
	Phosgene	$COCl_2$	0.6	NA	NA	2
	Hydrogen sulphide	H_2S	41	NA	NA	100
organic irritants	Acrolein	C_3H_4O	0.44	4	1.2	2
	Formaldehyde	CH_2O	14	6	1.8	20
	Benzene	C_6H_6	2000	NA	NA	500
	Acetaldehyde	C_2H_4O	340	NA	NA	2000
	Acetic Acid	$C_2H_4O_2$	NA	NA	NA	NA
	Styrene	C_8H_8	230	NA	NA	700
	Phenol	C_6H_6O	29	NA	NA	250
	Toluene	C_7H_8	1400	NA	NA	500
	Formic Acid	CH_2O_2	NA	NA	NA	30
	Acrylonitrile	C_3H_3N	8.6	NA	NA	85

NR: Not recorded, meaning that the species are available but the measurement for the needed classification is not recorded.

NA: Not available, meaning that the species needed is not available in that database.

*: SFPE $_{escape\ impairment}$ is for escape impairment of average subjects (50% of the population).

†: 0.3×SFPE $_{escape\ impairment}$ is for escape impairment of population including sensitive individuals.

Table 2-9: Concentrations reported by the available databases for the Incapacitation level of exposure from fire effluents

	Species	CAS number	Empirical formula	Incapacitation [ppm]	
				SFPE $_{incapacitation}$ *	ISO - IC_{50}
asphyxiants	Carbon monoxide	630-08-0	CO	3400	NA
	Hydrogen Cyanide	74-90-8	HCN	130	NA
	Carbon dioxide	124-38-9	CO_2	7.5%	NA
	Oxygen	7782-44-7	O_2	(21-10.2)	NA
inorganic irritant	Hydrogen chloride	7647-01-0	HCl	900	1000
	Hydrogen bromide	10035-10-6	HBr	900	1000
	Hydrogen fluoride	7664-39-3	HF	900	500
	Nitrogen dioxide	10102-44-0	NO_2	350	250
	Nitric oxide	10102-43-9	NO	1000	NA
	Sulphur dioxide	7446-09-5	SO_2	120	150
	Ammonia	7664-41-7	NH_3	NA	NA
	Carbon disulphide	75-15-0	CS_2	NA	NA
	Chlorine	7782-50-5	Cl_2	NA	NA
	Phosgene	75-44-5	$COCl_2$	NA	NA
	Hydrogen sulphide	7783-06-4	H_2S	NA	NA
organic irritants	Acrolein	107-02-8	C_3H_4O	20	30
	Formaldehyde	50-00-0	CH_2O	30	250
	Benzene	71-43-2	C_6H_6	NA	NA
	Acetaldehyde	75-07-0	C_2H_4O	NA	NA
	Acetic Acid	64-19-7	$C_2H_4O_2$	NA	NA
	Styrene	100-42-5	C_8H_8	NA	NA
	Phenol	108-95-2	C_6H_6O	NA	NA
	Toluene	108-88-3	C_7H_8	NA	NA
	Formic Acid	64-18-6	CH_2O_2	NA	NA
	Acrylonitrile	107-13-1	C_3H_3N	NA	NA

NR: Not recorded, meaning that the species are available but the measurement for the needed classification is not recorded.

NA: Not available, meaning that the species needed is not available in that database.

*: SFPE $_{incapacitation}$ is for incapacitation of average subjects (50% of the population).

Table 2-10: Concentrations reported by the available databases for the Lethal level of exposure from fire effluents

	Species	CAS number	Empirical formula	Lethal [ppm]		
				AEGL-3_{30min}	SFPE $_{30min.lethal}$	ISO-LC_{50}
asphyxiants	Carbon monoxide	630-08-0	CO	600	5705	5700
	Hydrogen Cyanide	74-90-8	HCN	21	165	165
	Carbon dioxide	124-38-9	CO_2	NA	NA	NA
	Oxygen	7782-44-7	O_2	NA	(21-5.4)	(21-5.4)
inorganic irritant	Hydrogen chloride	7647-01-0	HCl	210	3800	3800
	Hydrogen bromide	10035-10-6	HBr	250	3800	3800
	Hydrogen fluoride	7664-39-3	HF	62	2900-3000	2900
	Nitrogen dioxide	10102-44-0	NO_2	25	63-170	170
	Nitric oxide	10102-43-9	NO	NR	1000	NA
	Sulphur dioxide	7446-09-5	SO_2	30	400-1400	1400
	Ammonia	7664-41-7	NH_3	1600	NA	NA
	Carbon disulphide	75-15-0	CS_2	600	NA	NA
	Chlorine	7782-50-5	Cl_2	28	NA	NA
	Phosgene	75-44-5	$COCl_2$	1.5	NA	NA
	Hydrogen sulphide	7783-06-4	H_2S	59	NA	NA
organic irritants	Acrolein	107-02-8	C_3H_4O	2.5	150	150
	Formaldehyde	50-00-0	CH_2O	70	750	750
	Benzene	71-43-2	C_6H_6	5600	NA	NA
	Acetaldehyde	75-07-0	C_2H_4O	1100	NA	NA
	Acetic Acid	64-19-7	$C_2H_4O_2$	NA	NA	NA
	Styrene	100-42-5	C_8H_8	1900	NA	NA
	Phenol	108-95-2	C_6H_6O	NR	NA	NA
	Toluene	108-88-3	C_7H_8	5200	NA	NA
	Formic Acid	64-18-6	CH_2O_2	NA	NA	NA
	Acrylonitrile	107-13-1	C_3H_3N	50	NA	NA

NR: Not recorded, meaning that the species are available but the measurement for the needed classification is not recorded.

NA: Not available, meaning that the species needed is not available in that database.

2.3.1.3 Incapacitation threshold exposure levels

Incapacitation level, implying that exposure would cause incapacitation to subjects. Unless the affected subjects are rescued by others they may continue to breathe in the toxic emissions leading to death eventually by either smoke inhalation or burns. Values for emissions of interest for fire toxicity hazards assessment from the relevant databases are compiled in Table 2-9.

a) ISO – IC_{50}; introduced the International Standards Organisation (ISO) in the published standard 13571 [109]. IC_{50} is defined as "the concentration that is expected to seriously compromise occupants' ability to take effective action to accomplish escape". Hence, it has been included in the incapacitation classification for fire effluents exposure (see Figure 2-18). ISO – IC_{50} values for emissions of interest for fire toxicity hazards assessment are presented in Table 2-9.

b) SFPE $_{incapacitation}$; these values were presented by Purser in [7] showing the predicted concentrations that can cause incapacitation to **half** the exposed population. Hence, it is considered the most appropriate to be in the incapacitation classification for fire effluents exposure (see Figure 2-18). SFPE $_{incapacitation}$ values for emissions of interest for fire toxicity hazards assessment are presented in Table 2-9.

2.3.1.4 Lethality threshold exposure levels

A lethal level implies that being exposed to this level would most likely result in death. This level is most useful to post-incident investigations that focus on understanding the circumstances and conditions suffered by victims before their death. Values for emissions of interest for fire toxicity hazards assessment from the relevant databases are compiled in Table 2-10.

a) SFPE $_{30min.Lethal}$; these values were presented by Purser in [7] showing the concentrations that cause death to **half** the population. SFPE $_{30min.Lethal}$ values for emissions of interest for fire toxicity hazards assessment are presented in Table 2-10.

b) ISO – LC_{50}; introduced by the International Standards Organisation (ISO) in the published standard 13344 [97]. Defined as the concentration of an individual toxic gas or fire effluent, statistically calculated from concentration-response data, responsible for the death of **50%** of a population of a given species (mostly rodents) within 30 minutes exposure and 14 days post-exposure. ISO – LC_{50} values for emissions of interest for fire toxicity hazards assessment are presented in Table 2-10.

c) AEGL–3_{30min}; Defined as "the airborne concentration of a substance above which it is predicted that the general population, including **susceptible individuals**, could experience life-threatening health effects or death". Purser [7] recommended the use the use of AEGL–3 for the periods 10 and 30 minutes for lethal fire hazards assessment. The 30 minute

exposure limit for level 3 is considered most appropriate threshold to be part of the lethal classification for fire effluents exposure threshold (see Figure 2-18). AEGL–3_{10min} values for emissions of interest for fire toxicity hazards assessment are presented in Table 2-10.

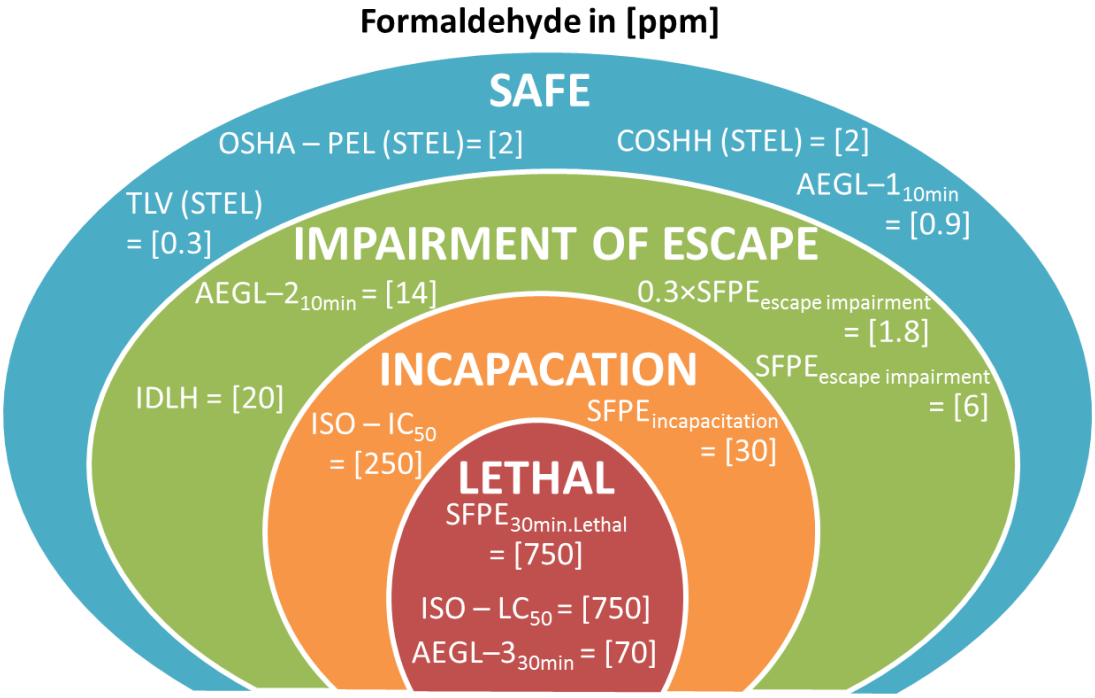

Figure 2-19: Toxic exposure thresholds of formaldehyde for fire toxic hazards assessment.

In order to showcase and compare the reported values from the reviewed databases, using the fire toxicity hazards classification presented in Figure 2-18, Figure 2-19 is produced for formaldehyde (organic irritant). It can be seen that the safe level for formaldehyde exposure ranges from 0.3 to 2 ppm with 3 important sources agreeing on a value of around 2 ppm. However as the severity of the effect increases it is clear that the recommended threshold values become sparser and significant differences between the relevant values from the various databases.

It is not the intention in this section to distil down to specific recommendations for each level of effect but rather to collate and present the relevant values from the different data bases so it becomes easier for relevant parties (designers, regulators, investigators,) to make judgements and assessments with clear collective overview of the pertinent data.

It is worth highlighting that Level 1 (Safe) in Figure 2-18, is an appropriate target for fire safety design using the instantaneous fire effluents toxic hazards assessment models (i.e. Fractional Effective Concentration). The other levels 2, 3, and 4 are important in post-incident investigations using the instantaneous FEC models for the impairment of escape and incapacitation, levels 2 and 3 respectively. For determination of the combined lethality hazard, cumulative fire effluents toxic hazards assessment models (i.e. Fractional Effective Dose) are used. These assessment approaches are discussed in the following section.

2.3.2 Additive models for the assessment of toxic effects from fire effluents

Methods for assessing the toxic hazards generated by fires are called the “additive” models. Most models are similar and based on two main concepts;

- Firstly, there is a limited number of gases (key toxic gases) that are responsible for the overall lethal toxicity.
- Secondly, the interaction between these “key toxic gases” is mainly additive with possible synergic effects from CO2.

A number of researchers [97, 109, 116, 127, 129, 134, 136, 152] have examined the interaction between different types of fire effluents in terms of the overall toxicity and concluded that the additive models are the most accurate tool in predicting the overall toxicity for fire effluents mixtures. However, it was acknowledged by the creators of these models that the predicted overall toxicity is always less than the actual overall toxicity because of other toxic species are usually present that are not considered “key toxic species”. Also in some circumstances there may be species in the effluent whose toxicity effects are unknown.

The applications and differences between the instantaneous fractional effective concentration model and the cumulative fractional effective dose models are important to be clarified. The instantaneous Fractional Effective Concentration (FEC) model is appropriate to be used for assessing the instantaneous toxicity effects, making it the suitable tool for determining the level of hazards posed by toxic exposure of fire effluents (safe, impairing of escape and incapacitation). The Fractional Effective Concentration value is very useful for the fire safety engineering calculations of the required ventilation rate to dilute the toxic emissions below threshold concentrations, in order to keep protected areas in the safe level.

While the cumulative Fractional Effective Dose (i.e. concentration in ppm multiplied by time of exposure in minutes) model is suitable for assessing the cumulative effect from being exposed to toxic atmospheres generated by fires (lethality) where breathing rates can be applied to predict the inhaled dose. The Fractional Effective Dose (FED) [36, 47, 97, 116, 130, 136] which is the usual parameter for quantifying the hazard magnitude is defined as the ratio of the exposure dose (integrated over time) to the exposure dose necessary to produce incapacitation. To deal with the mixture of threats presented by the fire products the FED from each threat/hazard needs be evaluated then all the FEDs need to be appropriately combined on the basis of the physiological effects on humans and a combined FED determined. This would represent a combined effective dose in terms of heat (radiation, convection and possibly conduction), visibility (related to particulate yields), the effective dose from asphyxiants (e.g. CO, HCN, CO_2 low O_2), and the effective dose from irritants (hydrogen fluoride, hydrogen chloride, hydrogen bromide, nitrogen oxides, phosphoric acid, sulphur dioxide, acrolein, formaldehyde, etc.). There is greater confidence when dealing

with the thermal or visibility effects of fires rather than the toxicity aspects mainly because of the lack of data and understanding of the interactions. In particular there very are few measurements of irritant gases.

In the following section two most commonly used tools in the fire toxicity assessment as FED models are discussed (Purser's rat LC50 model and Levin's N-gas model both are recommended by the ISO 13344 [97]).

2.3.2.1 Purser's LC50 model

Purser's model is different from Levin's model in a number of ways; firstly, CO_2 is dealt with mathematically as a multiplicative factor of the uptake of all toxic gases and as additive factor of enhancing the metabolic acidosis. Secondly, low oxygen hypoxia is also an additive factor independent of CO_2 hyperventilation synergic factor. Thirdly, the correction of NOx gases protective effect from HCN toxic effect. Finally, taking into account the toxic effects of all possible irritants (organic and inorganic).

Purser's FED model for lethality in its most recent form [127] is presented as follows;

$$L_{FED} = \left(\frac{[CO]}{LC_{50,CO}} + \frac{[CN] - [NO_x]}{LC_{50,HCN}} + \sum_{i=1}^{n} \frac{[I_A]_i}{LC_{50,I_{Ai}}} + \sum_{i=1}^{n} \frac{[I_O]_i}{LC_{50,I_{Oi}}} \right) \times VCO_2 + A + \frac{1}{H}$$

[CN]=[HCN]+[R-C≡N] in ppm,

[NOx]= [NO] + [NO_2] in ppm,

VCO_2=1+(exp(0.14×[CO_2]) -1)/2,

A=[CO_2]×0.05,

H = exp(8.13 – 0.54 x [21 – [O_2]), H term included only if [O_2] is less than 12%, then otherwise the term is omitted.

[CN] is concentration of cyanide, [NO_x] is the sum of [NO] and [NO_2],

[I_A] is irritant acid gas i.e. (HCl, HBr, HF, SO_2) in ppm,

[I_O] is irritant organic gas i.e. (Acrolein & Formaldehyde) in ppm,

VCO_2 is multiplication factor for hyperventilation caused by CO_2,

A is an acidosis factor.

Values as recommended in [127] for LC50 to be used in the above Purser's FED model for lethality are;

$LC_{50,CO}$ = 5,705 ppm

$LC_{50,HCN}$ = 165 ppm

$LC_{50,HCl}$ = 3,800 ppm [inorganic irritant]

$LC_{50,HF}$ = 2,900 ppm [inorganic irritant]

$LC_{50,HBr}$ = 3,000 ppm [inorganic irritant]

$LC_{50,SO2}$ = 400 ppm [inorganic irritant]

$LC_{50,NO2}$ = 170 ppm [inorganic irritant]

2.3.2.2 Levin's N-Gas model

Levin's N-Gas model is different from Purser's model in few features; firstly, CO_2 influence on toxicity is dealt with as an exclusive enhancement of CO toxicity only. Secondly, the way it deals with NO_2 influence on the overall toxicity. Thirdly, the mathematical term for low oxygen hypoxia effect on the overall toxicity. Finally, it is restricted to only 7 "key toxic gases".

Levin's N-Gas model for lethality in its most recent form as reported in [131] and [127] is presented as follows;

$$N-Gas = \frac{m[CO]}{[CO_2]-b} + \frac{21-[O_2]}{21-LC_{50,O_2}} + \left(\frac{[HCN]}{LC_{50,HCN}} \times \frac{0.4 \times [NO_2]}{LC_{50,NO_2}}\right) + \frac{0.4 \times [NO_2]}{LC_{50,NO_2}} + \frac{[HCl]}{LC_{50,HCl}} + \frac{[HBr]}{LC_{50,HBr}}$$

Values as recommended in [127] for LC50 to be used in the above Levin's N-Gas model for lethality are;

If $[CO_2] \leq 5\%$, then m = -18 and b = 122,000

If $[CO_2] > 5\%$, then m = 23 and b = -38,600

$LC_{50,O2}$ = 5.4% (21 -5.4 = 15.6% depletion)

$LC_{50,HCN}$ = 150 ppm

$LC_{50,HCl}$ = 3,700 ppm

$LC_{50,HBr}$ = 3,000 ppm

$LC_{50,NO2}$ = 200 ppm

2.3.2.3 Applications of the additive models in the assessment toxic hazards of fire effluents

Based on the above discussion, Purser's model is chosen because of its inclusivity of all possible toxic effects and its wider applicability on different types of fires as validated in [127]. Based on the 4 levels of toxicity threshold for assessment of toxic hazards of fire

effluents (Safe, Impairment of escape, Incapacitation, and Lethality), the following additive models are suggested to be applied for their appropriate levels as detailed next;

Level 1 instantaneous **Safe** fractional exposure concentration model (FEC_{safe}) is applied as follows;

$$FEC_{Safe} = \left(\frac{[CO]}{TLC_{Safe,CO}} + \frac{[CN] - [NO_x]}{TLC_{Safe,HCN}} + \sum_{i=1}^{n} \frac{[I_A]_i}{TLC_{Safe,I_{Ai}}} + \sum_{i=1}^{n} \frac{[I_O]_i}{TLC_{Safe,I_{Oi}}} \right)$$

Where;

[CO] is the CO concentration in ppm,

[CN] is the cyanide concentration =[HCN]+[R-C≡N], in ppm,

[NOx] is the sum of NO and NO_2 concentrations in ppm,

$[I_A]$ is the concentration of irritant acid gas i.e. (HCl, HBr, HF, SO_2, etc.) in ppm (see Table 2-6),

$[I_O]$ is the concentration of irritant organic gas i.e. (Acrolein, Formaldehyde, etc.) in ppm (see Table 2-6),

TLC_{safe} is the threshold limit concentration for safe exposure, it is recommended to use the most available conservative value from Table 2-7 for each considered species.

Level 2 instantaneous **Escape Impairment** fractional exposure concentration model (FEC_{EI}) is applied as following:

$$FEC_{EI} = \left(\frac{[CO]}{TLC_{EI,CO}} + \frac{[CN] - [NO_x]}{TLC_{EI,HCN}} + \sum_{i=1}^{n} \frac{[I_A]_i}{TLC_{EI,I_{Ai}}} + \sum_{i=1}^{n} \frac{[I_O]_i}{TLC_{EI,I_{Oi}}} \right)$$

Where;

Same as above apart from, TLC_{EI} is the threshold limit concentration for exposure causing impairment of escape, it is recommended to use the most available conservative value from Table 2-8 for each considered species.

Level 3 instantaneous **Incapacitation** fractional exposure concentration model (FEC_I) is applied as following:

$$FEC_I = \left(\frac{[CO]}{TLC_{I,CO}} + \frac{[CN] - [NO_x]}{TLC_{I,HCN}} + \sum_{i=1}^{n} \frac{[I_A]_i}{TLC_{I,I_{Ai}}} + \sum_{i=1}^{n} \frac{[I_O]_i}{TLC_{I,I_{Oi}}} \right)$$

Where;

Same as above apart from, TLC_I is the threshold limit concentration for exposure causing incapacitation, it is recommended to use the most available conservative value from Table 2-9 for each considered species.

Level 4 cumulative **Lethal** fractional exposure dose model (FED_{Lethal}) is applied as following:

$$FED_{Lethal} = \left(\frac{[CO]_d}{TLD_{L,CO}} + \frac{[CN]_d - [NO_x]_d}{TLD_{L,HCN}} + \sum_{i=1}^{n} \frac{[I_A]_{i,d}}{TLD_{L,I_{Ai}}} + \sum_{i=1}^{n} \frac{[I_O]_{i,d}}{TLD_{L,I_{Oi}}} \right) \times VCO_2 \times VE + A + \frac{1}{H}$$

Where;

$[CO]_d$ is the CO dose in ppm.min,

$[CN]_d$ is the cyanide dose =$[HCN]_d$+$[R\text{-}C{\equiv}N]_d$, in ppm.min,

$[NOx]_d$ is the sum of NO and NO_2 doses in ppm.min,

$[I_A]$ is the dose of irritant acid gas i.e. (HCl, HBr, HF, SO_2, etc.) in ppm.min (see Table 2-6),

$[I_O]$ is the dose of irritant organic gas i.e. (Acrolein, Formaldehyde, etc.) in ppm.min (see Table 2-6),

TLD_{Lethal} is the threshold limit dose for lethal exposure, it is recommended to use the most available conservative value multiplied by the time of exposure in minutes (30 minutes for the values from Table 2-10) for each considered species.

VCO_2 is the multiplication factor for hyperventilation caused by CO_2 =1+(exp(0.14×$[CO_2]$) - 1)/2, $[CO_2]$ concentration in %,

A is the acidosis factor = $[CO_2]$×0.05,

H = exp(8.13 – 0.54 x [21 – $[O_2]$]), H term to be included only if $[O_2]$ is less than 12%, otherwise the term is omitted.

VE is the breathing rate in L/min, realistic values of VE can be obtained from [119]. Purser [116] suggested the use of three VE benchmarks (based on values obtained from [119]) for 70Kg human representing three levels of activities; 8.5 L/min for rest sitting, 25 L/min for light work (e.g. walking), and 50 L/min for heavy work (e.g. slow running).

2.4 Review of chemical analytical methods for measuring fire effluents

For the purpose of reviewing the chemical analysis commonly used in the literature for quantifying fire effluents, it is important to review the different sampling methods of the fire effluents and understand their influence on the results presented. That will eventually aid in evaluating the available options for designing the sampling and analysis systems in fire models at different scales.

Sampling methods can be classified into two major methods continuous online sampling and batch sampling which has two types, depending on sampling time interval, instantaneous/grab batch sampling and average/integrated batch sampling.

Continuous online sampling is the ideal method for rapidly changing environment e.g. Fires. It has the advantage of enabling the production of a representative concentration profile during different phases of the fire test. Typically used for most non-dispersive infrared (NDIR) analysis, where a consistent flow of the sample is fed to the analyser for instant measurements.

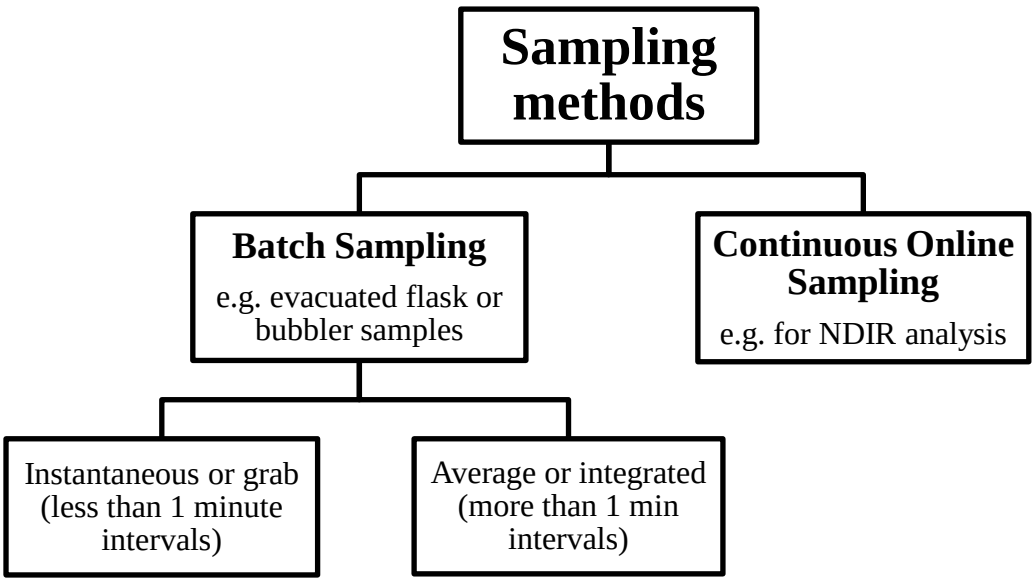

Figure 2-20: Fire effluents sampling methods.

Each sampling method is suitable for specific analysis methods, however it is very important to highlight that understanding the capabilities and limitations of these sampling and analysis methods is crucial to evaluate the accuracy of the results obtained. In the following section most commonly used chemical analysis methods in the fire research fields are discussed in terms of principle of operation and their capabilities.

2.4.1 Non-Dispersive Infra-Red (NDIR)

Non-dispersive infrared gas analysis is based on the optical dispersion of the light through the gas sample. This technique is widely used in different fields (e.g. continuous emission

monitoring and combustion research) and is recommended for fire effluents analysis by the international standards organization [153, 154]. Each species has its own finger print when light is applied on them. And this finger print can be recorded by the absorbance of light at specific wavelength ranges, and depending on the intensity of the absorbance the magnitude of the concentration is determined. NDIR usually have a limited number of species to be analysed and depending on the targeted species its wavelength will be the focus of the light absorbance measurement and eventually a volumetric concentration measurement can be achieved. For example to measure CO_2, the targeted wavelength normally is 4260 nm (equivalent to 2347 cm^{-1}). According to the ISO 19701 [153] NDIR is recommended to be used for CO and CO_2, however there are some NDIR manufacturers that produce NDIR analysers that could measure also NO, SO_2, and CH_4. The main source of limitation is the interference between the gases. Others requirements to be considered such as, minimum flow rate required, temperature, pressure, dust-free sample, dry sample, and other conditions. However, each design of manufactured NDIRs deal with these limitations with their unique solutions, which gives different accuracy levels [155-158]. The main advantages of NDIR is that it can provide a continuous measurement of the gas sampled online, minimal servicing and consumable requirements, and the fact that it is legally approved equipment in different countries for compliance with emissions control requirements [159, 160].

2.4.2 Paramagnetic

Paramagnetic oxygen analyser main components are: magnetic field, diamagnetic substance (nitrogen), turning dumbbell (with two glass spheres filled with the diamagnetic substance and a mirror fix in the middle of the rod), light source and light receiver (photocell).

The pair of magnets creates a magnetic field across the gas cell where the sample is introduced. When there is no oxygen in the gas cell the dumbbell is static as the diamagnetic substance (nitrogen) inside the spherical glass on both ends of the dumbbell will be held in the middle by the magnetic field, where the photo cell can detect that based on the reflected light on the mirror. As soon as oxygen is introduced it will start create a layer between the diamagnetic spherical glass and the magnetic field oxygen is paramagnetic and depending on the quantity of oxygen the dumbbell turning torque will vary, the photo cell can monitor and measure the oxygen concentration based reflected light on the rotating mirror [154, 161, 162].

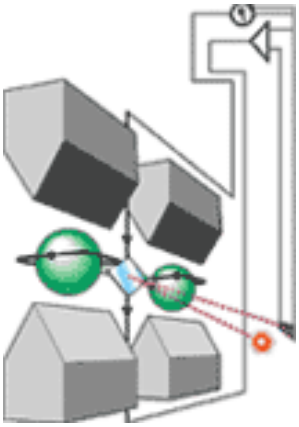

Figure 2-21: Schematic diagram of the paramagnetic oxygen analysis concept from [163].

2.4.3 FTIR

FTIR has been used in fire research for 15 years and was extensively investigated in the European SAFIR project, as summarised by Mikkola [164] and Hakkarainen et al. [165]. In SAFIR project, the sample line and filter were hot >150 ^{o}C, but the pump was downstream of the FTIR which is not recommended due to problems of sample cell pressure control [166]. A PTFE sample tube was used inside the heated sample line, as in the present work. However, the detector was not liquid nitrogen cooled and the minimum detection limit was about 10 times that in the present work. This work showed that by using quantitative target factor analysis (QTFA) there was no need for external calibration of the instrument in use. Once the instrument was calibrated this was fixed and only zero gas was required on a daily basis. This is the principle on which the Gasmet FTIR, made in Finland, operates and was a direct outcome of the SAFIR project which was led by researchers in Finland. FTIR for fire toxicity research was verified and validated by a number of research projects [167, 168], and in this work further validations using certified bottles and a comparison with measurements of other analysers were conducted and presented in 3.1.3. An international standard for the usage of FTIR to assess fire effluents was first published in 2006 [169] and updated in 2015 [170].

In 2005, Andrews et al. [171] in Leeds used the Temet Gasmet CR-2000 FTIR analyser to present under-ventilated fire toxic gas results for organic irritants such as acrolein and formaldehyde for different fuels. All toxic gases that occur in fires can be analysed simultaneously, also the instrument can be used to measure the total unburnt hydrocarbons by summation of the individual hydrocarbons. The main advantage of the heated FTIR is that it can measure high temperature raw sample gases [171]. The high sample temperatures (180 ^{o}C) keep all the toxic gases of interest in the gas phase and also enable all unburnt hydrocarbons to be measured so that the fire compartment combustion efficiency can be correctly determined. Another important advantage is that FTIR can quantify concentrations of a wide range of toxic gases with a very high accuracy using the same heated sample and as a function of time. The present FTIR can be operated with full spectral scans at 10Hz and

spectral averages every 1 or 2s can be used. However, fire transients do not occur on this time scale and time averaging every 5s or 50 scans gives good resolution of the toxic gases. In the experimental section, it is shown how to take the advantage of the high temperature analysis to achieve accurate measurements of raw fire toxic gases, in order to minimise potential post oxidation of the gases as air dilutes the products of the fire is avoided.

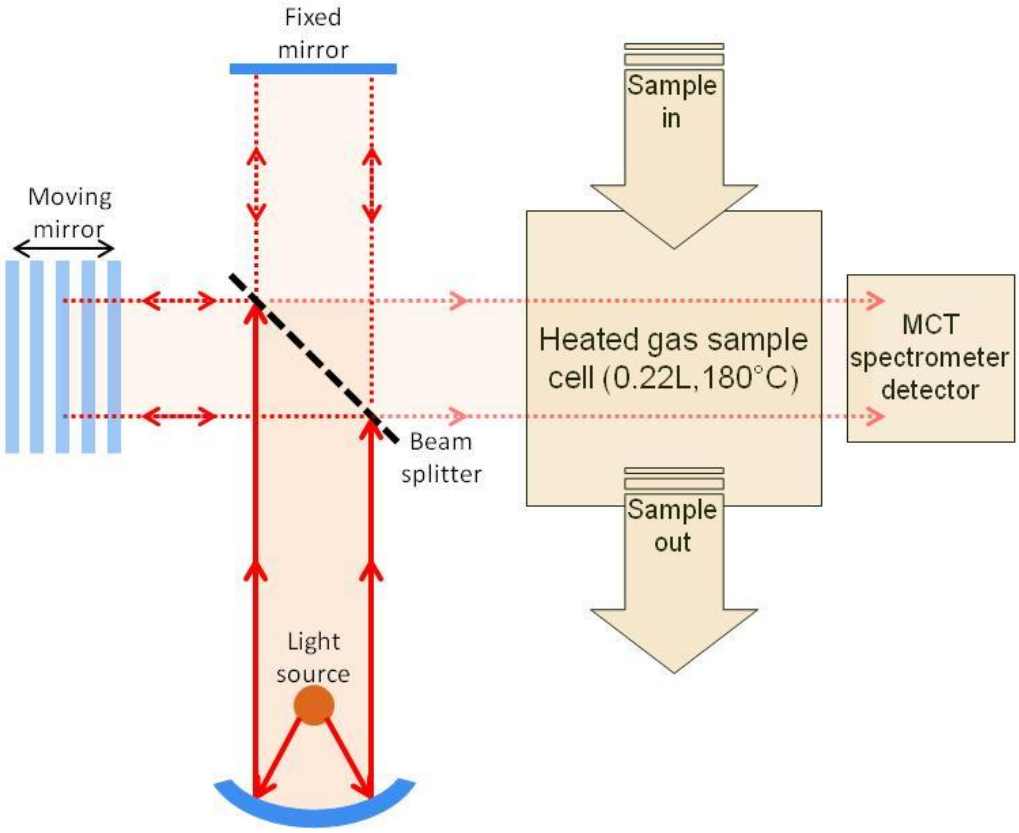

Figure 2-22: FTIR working principle.

Fourier transform infrared (FTIR) is an infrared spectroscopy technique for chemical analysis compounds. The technique is based on two basic principles; firstly, molecular vibrations take place in the infrared region, secondly, each compound has a characteristic absorption frequency and the intensity of absorption is correlated to the concentration of that compound. Most targeted gases have their peak vibrations in the wavelength range from 2.5 – 16 μm equivalent to the wave number range 4000 – 625 cm^{-1}.

The Gasmet FTIR CR-2000 (used in this work) consists of two main parts (illustrated in Figure 2-22). Firstly, the heated detection cell (up to 180 ^{o}C), which has a multi-pass fixed 2 m path length and a sample cell volume of 0.22 litres. In the detection cell all three parts (sample cell body and 2 mirrors) have a special rhodium coating and gold layers to achieve high corrosion resistance. Secondly, the liquid nitrogen cooled MCT (mercury-cadmium telluride) spectrometer detector enables the resolution of 8 or 4 cm^{-1}, with a minimum scan frequency of 10 Hz and covers wave number range from 600 to 4200 cm^{-1}. The motion of the moving mirror creates the optical path difference required to generate wavelength range.

2.4.4 Colourimetry

The colourimetry technique depends on the formed colour and its intensity of the trapped gas sample in solution after applying the specific reagents for species monitored. The intensity of the colour formed can be evaluated visually by comparison to standard coloured glass benchmarks, in its simplest form using human eye. Or with more sophisticated technique by using a photoelectric cell including a filter photometer or a spectrophotometer, this version of the technique called a photoelectric colorimeter. Colourimetry technique deals with a solution sample, meaning that averaged batched samples are required from the fire effluents produced by the fire test. This is a major disadvantage specifically for fire research where the environment and smoke production rates are rapidly changing. However, the ISO 19701 standard [153] recommends the use of this methodology for wide range of fire effluents; HCN, ammonia, acrolein, formaldehyde, total aldehydes, and phosphates. This method is rightly recommended by ISO 27368 [172] for post-mortem analysis of fire victims' blood samples for the cyanide content.

2.4.5 Chromatography

Chromatography generally refers to the separation process of the sample with the objective of quantifying targeted components that are present in the sample. The separation process occur in the especially designed column where the sample is carried by the mobile phase (this is the carrier gas in the gas chromatography and eluent in the liquid chromatography) over the stationary phase which acts as a trap for the targeted components. The choice of the materials used to act a mobile phase and stationary phase vary depending on the application and the targeted components. Then different types of detection techniques can be used to quantify the separated components [154]. The ISO 19701 [153] recommended the use of three types of chromatography for certain fire effluents, these recommendations are detailed next.

2.4.5.1 High Performance Ion Chromatography (HPIC)

HPIC is a liquid chromatography that requires the sample to be in a solution form. HPIC's mobile phase is an ionic solution while its stationary phase is an ion-exchange resin located in the column. It is recommended, by ISO 19701 [153], for measuring wide range of species; HCN, HCl, HBr, HF, NO_2, SO_2, H_2S, NH_3, phosphates, and formic acid. Setup, capabilities, and limitations differ depending on the targeted component. Detailed guidance is provided by the ISO 19701 [153]. However, the main disadvantage is that the analysed sample is a time-integrated solution sample, which is not appropriate for a rapidly changing environment that fire tests create.

2.4.5.2 High Performance Liquid Chromatography (HPLC)

HPLC is also a liquid chromatography that also uses a time-integrated solution sample. HPLC's setup can have the mobile phase as non-polar and the stationary phase as polar or vice versa. ISO 19701 recommends the use of HPLC to measure acrolein, formaldehyde, acetaldehyde, phenol, benzene, toluene, styrene, and formic acid. HPLC's setup, capabilities, and limitations also differ depending on the targeted component. Detailed guidance is provided by the ISO 19701 [153].

2.4.5.3 Gas Chromatography

Gas chromatography (GC) can be packed (short with ID 2-5 mm) column or capillary (longer with ID < 1 mm) column. The type of carrier gas (mobile phase) and column built material (stationary phase) are decided based on the targeted species and detection requirements. Gas chromatography coupled with mass spectrometry detector (GC-MS) is one of the most prominent analysis methods in the combustion science, ISO 19701 [153] recommends it for measuring acrolein, acetaldehyde, carbon disulphide, phenol, benzene, toluene, styrene, and acrylonitrile. However the same disadvantage of other chromatography techniques is present with GC that it is the limited applicability for continuous measurements, and lengthy time-integrated batches are used.

2.4.6 Flame Ionization Detector (FID)

The flame ionization detector (FID) is one of the most popular analysers to measure the concentrations of total unburnt hydrocarbon (THC). By burning a heated sample of the fire effluents in a hydrogen flame which yields ionised products that correlated to the concentrations of these hydrocarbons and measured the two electrodes in the detector. THC concentration measurements normally are presented as CH_4 equivalent.

2.4.7 Phi-meter

The phi meter instrument was developed by Babrauskas et al. [173] with the objective of providing "a simple, fuel-independent" approach to measure equivalence ratio as an alternative to metered control of air and fuel supply of the combustion. However, Babrauskas and his colleagues acknowledged the limitations of the phi meter approach to hydrocarbon fuels (containing only C, H, and O). Later, Lonnermark et al. [174] used the approach with other materials containing other elements (such as; nitrogen, sulphur, and chlorine) and stated that after "some investigations" [175] there was "no proof of influence by these elements" on phi measurements.

The approach, shown in Figure 2-23, uses unfiltered heated full gas sample (minimum of 100C to avoid condensation) fed into a catalytic combustor. This has shown to be problematic in practical applications as the soot caused clogging in sample probe [62]. Then oxygen is induced in the combustor producing "ideally" a complete combustion with the

simple products consisting only H_2O, CO_2 and excess O_2. Then H_2O and CO_2 are removed, and the left oxygen concentration is measured using a paramagnetic oxygen analyser.

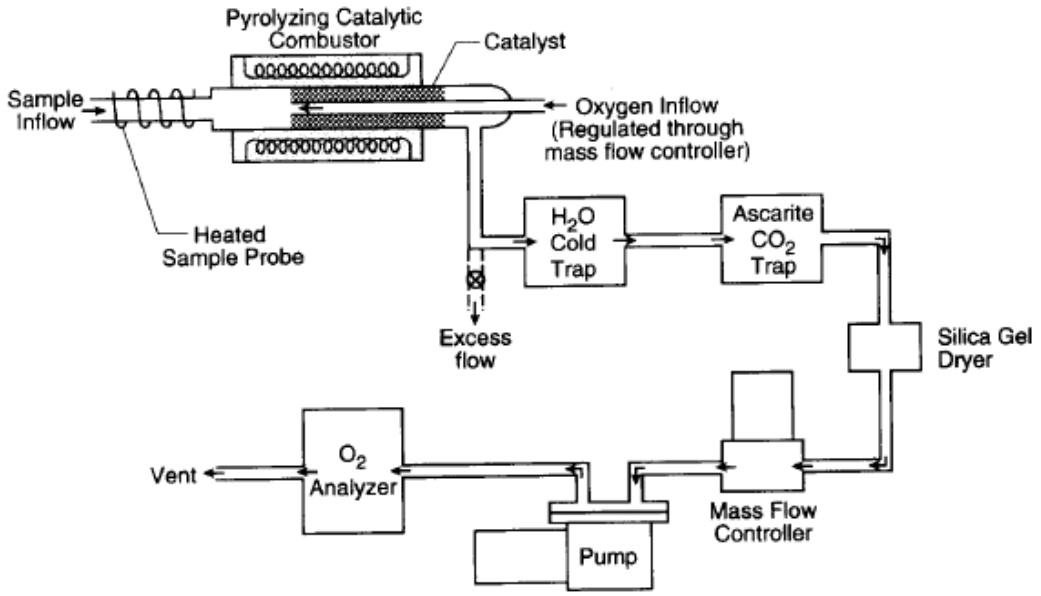

Figure 2-23: Schematic of Phi meter reproduced from [173].

By utilising reference oxygen measurements and online measurements of oxygen concentration, local equivalence ratio measurement is achieved using the following equation:

$$\phi_L = \frac{X_{O2}^{l} - X_{O2}}{X_{O2}^{a} \cdot (1 - X_{O2})}$$

X_{O2}^{a} is oxygen volumetric concentration in ambient air.

X_{O2}^{l} oxygen volumetric concentration from ambient air with induced oxygen.

X_{O2} oxygen volumetric concentration from burnt gas sample with induced oxygen.

2.4.8 Ion-Selective Electrodes (ISE)

ISE technique requires a solution sample for its analysis, meaning that averaged batched samples are required from the fire effluents produced in by the test. This is a major disadvantage specifically for fire research where the environment and smoke production rates are rapidly changing. However, the ISO 19701 standard [153] recommends the use of this methodology for wide range of fire effluents; HCl, HBr and HF.

These were the main techniques recommended by the ISO 19701 [153] and ISO 19702 [170] for gases of interest produced in fires. In the experimental part of this work FTIR, NDIR, Paramagnetic analysis were used for analysing fire effluents produced in those tests, as detailed in chapter 3.

2.5 Review of experimental methods used for quantifying fire toxic hazards

Fires are random phenomena, and experimental methods used in the literature to resemble them are as random as the phenomena. This randomness may have been the caused by the fact that fire science is the interdisciplinary field that it is, resulting in having different (sometimes conflicting) objectives and approaches to quantify fire hazards. Other geopolitical/commercial reasons may have also played a role in the adoption/promotion of specific test methods over others. However, it is very important to highlight that many concepts in fire toxicity were established from different test methods and setups. And the variety of available test methods data can be the source of creative thinking that is able to overcome the challenges that face fire toxicity research. Number of reviews on the available fire toxicity testing from different scales are available in the literature [7, 59, 176-178].

Fire toxicity test methods can be classified to static and dynamic physical models. The smoke produced from static fire physical model accumulates in a smoke chamber without exhaust, where bioassay or chemical analysis is used. Sampling methods (see Figure 2-20) used are normally batch sampling for static models, and data collected are average of the whole experiment results. While dynamic fire physical model would mean that the smoke produced is dynamically flowing through the sampling system enabling online sampling and measurements of the fire effluents as they are produced. The main advantage of using dynamic approach is the capability of incorporating concurrent fire characteristics changes with smoke production changes in the physical fire test model.

In this review the most common fire experiments that had fire toxicity as a major objective will be highlighted. Starting with bench/small scale experiments and intermediate scale testing to real/full scale experiments that provided useful fire toxicity data. In terms of the data a specific focus will be on toxic emission mass yields data for the reasons discussed in the previous sections. Finally a survey of the available of mass yield data is presented to help identifying the available data in the literature from different scale tests. Such data should be used with care, and going back to the original source referenced is strongly encouraged, in order for the user to stay away from assumptions (as discussed earlier certain terms were used in the literature to describe completely different characteristics).

2.5.1 Bench scale apparatus

In this review the focus will be on describing the design of the fire model for the bench-scale fire toxicity tests that provided toxicity yield data or used to obtain lethality data and their potential modifications to resemble ISO 19706 [58] classification of fires conditions presented in Table 2-2. The role of these bench-scale toxicity testing has been identified by Purser [7] to be serving at least one of the following four objectives;

1. Development of FED expressions:

That includes determining threshold values for incapacitation and lethality for individual gases generated in fires by exposing bioassay subjects and understanding the influence of the interaction between those gases on the overall toxicity. The findings of these tests allowed for the development of the additive models for toxic effects assessment of fire effluents presented earlier in section 2.3.2 and applied in accordance with ISO 13571 [109].

2. Determination of the simplified mass loss FED for application in fire safety engineering calculations:

These are the tests where FED of specified material is expressed in their mass loss rate per volume of dispersion. This method has limited application in real scale fires as stated by Babrauskas [179] few years after he presented the methodology [180, 181]. Also, the procedure to be followed for producing such data is described by the ISO 13344 [97].

3. Generation of yield data for toxic gases produced in fires:

This is the main objective of this work to establish yield data that are valid for implementing in modelling full-scale fires. In order to reach this objective it is important to identify the combustion conditions relevant to the intended fire to be modelled. The modelled fires with the relevant yield data then can produce suitable prediction of concentration-time curves at the required location of monitoring. This type of approach is becoming the main focus of many multi-scale testing which was able to explain many aspects of the relationship between combustion conditions and the production of toxic species in fires. Hence, the crucial importance of defining the combustion conditions in details for any reported toxic yields i.e. flaming/non-flaming, temperature/heat flux, equivalence ratio, fuel composition, and sampling and analysis methods.

4. Product specification (e.g. producing a toxicity index);

This approach utilizes number of small-scale toxicity tests to produce toxicity data. These toxicity data are then input in a toxicity index calculation method that influences the choice of products in specific applications. This approach is common in the transport industry [182, 183]. However, it has limited applicability in the general fire safety engineering calculations due to the fact that its combustion scenarios are not well defined that makes it difficult to decide the relevancy to real compartment fires [7].

2.5.1.1 NBS cup furnace test

The NBS cup furnace test shown in Figure 2-24, was first used by Levin et al. [129] for bioassay tests that yielded LC50 data [152] for the N-gas model [131] presented in ISO 13344 [97], discussed earlier in section 2.3.2.2.

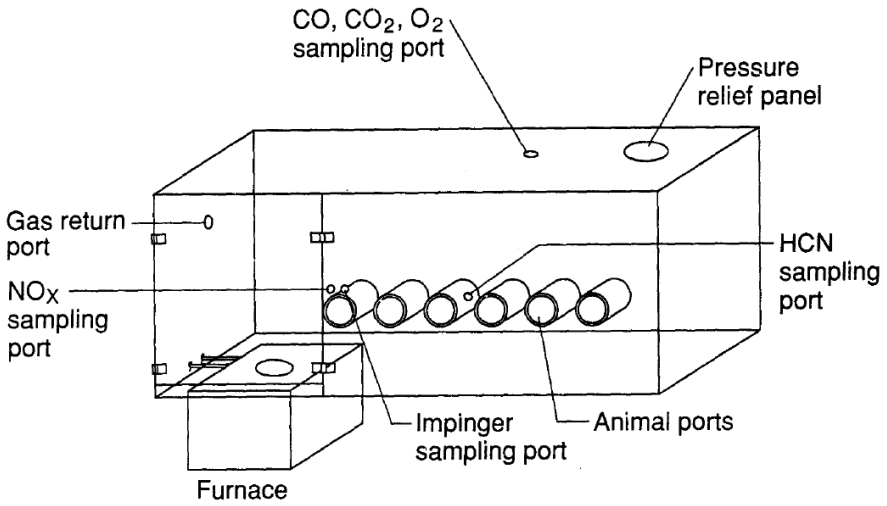

Figure 2-24: NBS cup furnace test method reproduced from [184].

The test method comprises a crucible furnace where the sample (around 10 g) burnt/decomposes depending on of two setups of furnace temperature; non-flaming (ISO 19706 class 1b and 1c (by replacing air with nitrogen)) and flaming (ISO 19706 class 2 or 3a) based on the auto-ignition temperature of the subjected materials. Non-flaming setup the temperature would be set at 25C less than the auto-ignition temperature, while for flaming setup the temperature would be set at 25C more than the auto-ignition temperature. The produced smoke would accumulate in the 200 L exposure chamber where the animals would be exposed to the produced fire effluents for 30 minutes and observed for 14 days post-exposure. Continuous chemical analysis of different toxic gases may be used to monitor the chamber atmosphere as can be seen in Figure 2-24. This equipment was used as the main toxicity assessment test for NBS (NIST now) in the 1980s [129, 185, 186] however its evolvement resulted in the introduction of the SwRI/NIST radiant test (NFPA 269 [187]/ ASTM E1678 [188]) in the 1990s [184, 189].

2.5.1.2 NIST radiant test (ASTM E1678 – NFPA 269)

This test shown in Figure 2-25 is a current standard test method endorsed by the American Society for Testing and Materials (ASTM E 1678 [188]) and the National Fire Protection Association (NFPA 269 [187]). It is a developed version of the NBS cup furnace discussed earlier. The main difference between the two is the thermal decomposition arrangement.

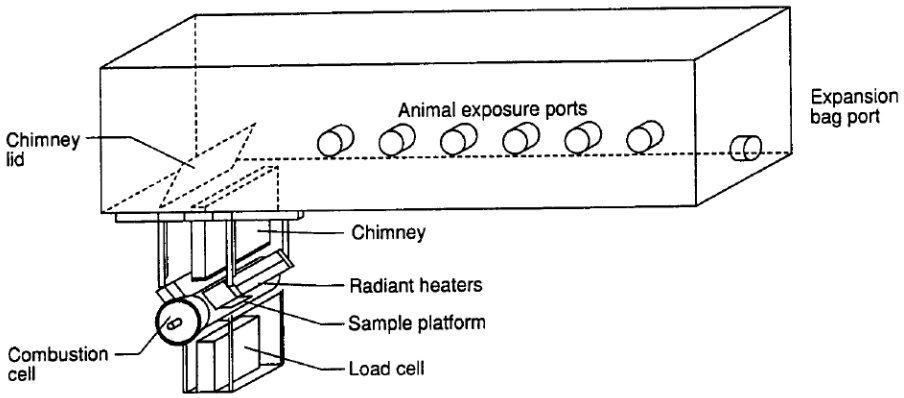

Figure 2-25: NIST test method reproduced from [136].

In this test, two radiant elements are used to heat the sample (76 x 127 mm and maximum 50 mm depth). The sample is mounted on a load cell that monitors the mass loss while 50 kW/m^2 heat flux is applied on the sample for 15 minutes then switched off for another 15 minutes. The evolved products enter the same static 200 L smoke camber as in the cup furnace discussed earlier where similar toxicity analysis is conducted. The ASTM E1678 test has been used (mainly by NIST) to generate toxicity potency (LC50, IC50) and yield data [136, 184, 190].

2.5.1.3 NBS smoke density chamber (ISO 5659-2 – ASTM E662)

The NBS smoke density chamber, shown in Figure 2-26, is a very widely used test apparatus, with the main purpose of measuring the specific smoke density, was developed by the US National Bureau of Standards (NBS) now known as the National Institute of Standards and Technology (NIST) [191]. The apparatus has two versions for the fire model; vertical and horizontal sample orientations (see Figure 2-27) both are adopted by many different standardising bodies for different purposes. For example; the vertical setup is adopted for aircraft materials by BS EN 2824 [192], BS EN 2825 [193], BS EN 2826 [194], Airbus ADB3, and Boeing BSS 7239, and for general building materials by BS 6401 [195], and ASTM E 662 [196]. While the horizontal setup is adopted for plastics by BS EN ISO 5659-2 [197], for railway products by BS EN 45545-2 [183] and for marine industry products by IMO MSC 41 (64) [198].

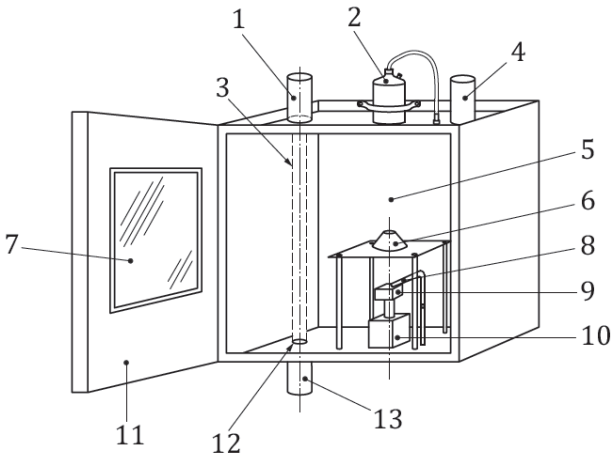

Figure 2-26: Schematic for the NBS smoke density chamber test as presented in ISO 5659-2 [197].

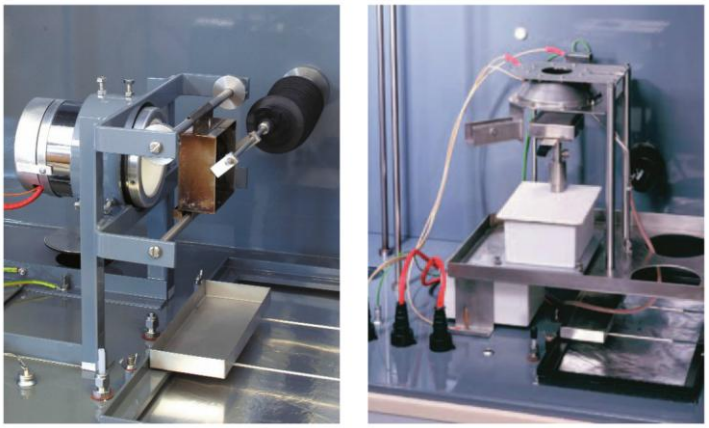

Figure 2-27: Pictures of the vertical orientation (left) and horizontal orientation (right) for the NBS smoke density chamber as presented by [199].

The NBS smoke density chamber is a static fire model where the smoke produced accumulates in 0.51 m^3 chamber until the end of the test. The specimen size is 76 x 76 mm^2 with a maximum thickness of 25mm. The vertical orientation applies radiated heat flux of 25 kW/m^2 on the sample, while the horizontal orientation applies heat flux of 50 kW/m^2. Some test protocols (listed above) require flames to be applied on the bottom edge of the sample, while others use pilot flame or none relaying on self-igniting the specimen from the radiated heat. Different smoke and toxicity analyses are required (depending on the standard chosen) ranging from ion chromatography, ion specific electrodes, and optical measurement system to FTIR analyser. The main concern with this apparatus is its static nature meaning that availability of air in the chamber changes during the test creating more than one ISO 19706 fire class ranging from 1b (for non-flaming) to 2, 3a and 3b (for flaming specimens) or only 1c (by replacing air with nitrogen). While the smoke from these different burning behaviours is accumulating in the smoke chamber making it difficult to determine the yields of smoke produced in relation to the mass loss behaviour. In addition of other concerns regarding stratification of the fire effluent creating a non-mixed representative smoke sample.

2.5.1.4 University of Pittsburgh (UPITT) test (ASTM E981)

UPITT test [200] is a dynamic test where the sample (around 5 g) is mounted on a load cell inside a furnace with 11L/min air supply as can be seen in Figure 2-28. Then the smoke produced is diluted with further 9 L/min dry air before entering the smoke chamber where animals are exposed to the fire effluents, also gas samples are collected there for chemical analysis. This test method was pioneered by Alarie to establish LC50 and RD50 data [122, 137]. It has been adopted by the New York State regulations for building materials and ASTM E981 [ref]. The furnace heat the sample using constant heating rate 20C/min of the sample thermal decomposition is monitored making it difficult to relate it to the ISO 19706 classes, theoretically it can go through stages 1b, 1c (by replacing air with nitrogen), 2 and 3a however it is impossible to differentiate between the stage in this setup.

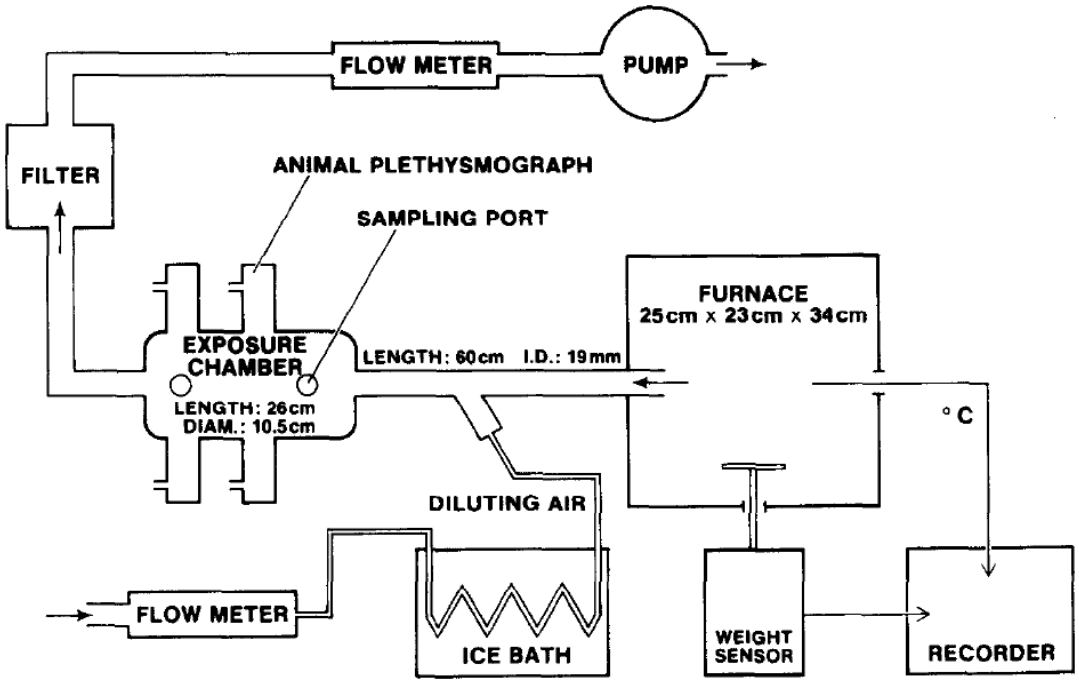

Figure 2-28: Schematic for the UPITT test method as presented in [200].

2.5.1.5 Steady state tube furnace (Purser's furnace) test method (BS 7990)

The tube furnace method is dynamic test that is widely used in fire toxicity research, it has a long history of being used in the obtaining toxicity exposure data (LC50 and IC50) [128]. Its origins go back to the DIN 53436 moving furnace (with stationary tube) test method [201]. Another static version of the test method (NFX 70-100) is adopted by the European railway standard BS EN 45545 [183]. Purser's furnace is adopted as a recognised test method for determining toxic product yields of fire effluents by the British Standard Institution as a current standard BS 7990 [73]. Other international standardization organisations used to recommend the method as a fire toxicity test [72, 202], however both standards from IEC and ISO are withdrawn now. Purser's furnace underwent regress validation and verification processes which yielded many data published in the literature. Stec PhD thesis titled "Fire Toxicity and its Measurement" focused on utilising purser's furnace coupled with FTIR analyser to investigate the yields of toxic emissions from testing different materials [203].

The steady-state tube furnace test method (shown in Figure 2-29) requires a strip specimen or pieces are spread in a silica boat over a length of 800 mm with a loading density of at least 25 mg/mm and fed into a tube furnace at a rate of 1 g/min with adjustable primary flowing air depending on the intended ISO fire stage chosen to be replicated, as detailed in Table 2-11. Secondary air is introduced in a mixing chamber to give a total gas flow of 50 L/min for analysis [73]. The furnace adjustable temperature and air flow makes it applicable to meet ISO fire stages 1b, 1c (by replacing air with nitrogen), 2, 3a and 3b. It is crucially important to satisfy the ISO fire stage, desired to simulate, conditions in terms of; steady flaming or non-flaming and equivalence ratio.

Table 2-11: Purser's furnace combustion conditions as recommended by ISO 19700:2007 [72].

ISO 19706 class	Test conditions			
	Mass loading [mg/mm]	Temperature of the furnace [C]	Primary air supply rate [L/min]	Secondary (dilution) air supply rate [L/min]
1b	25	≤ 350 (non-flaming)	2	48
2	25 – 50	≥ 650 (flaming)	10 – 15	35 – 40
3a	25	≥ 650 (flaming)	2.15 – 3.75	46.25 – 47.85
3b	25	825	2.15 – 3.75	46.25 – 47.85

The tube furnace method has been used by many researchers to determine toxic yield data, creating a very useful database of toxic emission [59, 113, 203-205]. It is important to highlight at this point, that some of these yield data were reported as mass charge yield data while others as mass loss yield data, so careful consideration to the definition of the data supplied is very advisable before to ensure that the data is fit for the application intended.

There are few concerns regarding the smoke produced and measured using Purser's furnace; firstly, the temperature at the end of quartz tube before the dilution chamber is too low, as detailed in [206], potentially causing condensation and loss of products this should be above 200 C (see section 3.1.1.2). Secondly, Mass loss rate (MLR) cannot be measured instantaneously, and mass charge rate is used from the feeding rate. In order to consider the unpyrolysed char residue for the yield (g/g) measurements, average MLR is used [73], which is acceptable if the steady state phase is achieved abruptly but in the tube furnace the steady state phase is much shorter than the total test time starting from feeding the sample into the furnace till the end of the test. Thirdly, the specimen is too small; the low production of fire effluents in the test restricts the sampling process to be only diluted. Also, low flow rate of primary air feed may potentially result on secondary air supplied to the dilution chamber to be drawn into the quartz tube.

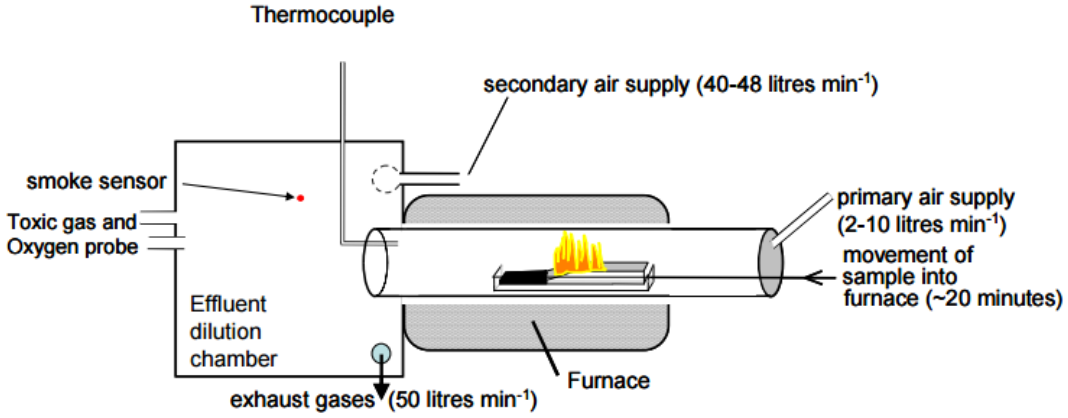

Figure 2-29: Steady state tube (Purser) furnace [207].

2.5.1.6 Fire propagation apparatus (ISO 12136 – ASTM E2058)

Fire Propagation Apparatus (FPA) [208] shown in Figure 2-30, was developed by FM global in the 1980s, it is recognised test method for heat release rate measurements and limited CO and CO_2 estimations by international standardisation organisations as BS ISO 12136 [209] and ASTM E2058 [208]. It consists of a 172 mm diameter vertical silica tube containing the sample holder. Four sample orientations are suggested by the ASTM E 2058; Horizontal Square specimen (100 x 100 mm^2 and maximum 25 mm thickness), Horizontal circle (for liquids), vertical specimen, and vertical cable specimen. The sample is mounted on the load cell, while the four IR heaters apply radiated heat flux up to 65 kW/m^2 from outside the quartz tube. The length of the vertical tube (65 cm) is to eliminate any interference by any post-oxidations from entrained air. Tewarson [70] used FPA to produce his fire toxicity yields database for many common fuels, which was in a well-ventilated conditions. Also he presented correlations for predicting toxic yields for richer fires (reviewed earlier in section 2.1.4). the apparatus is not the most popular in the literature for generating toxicity yield data, not many data from outside FM global are available beyond Tewarson's SFPE data [210, 211].

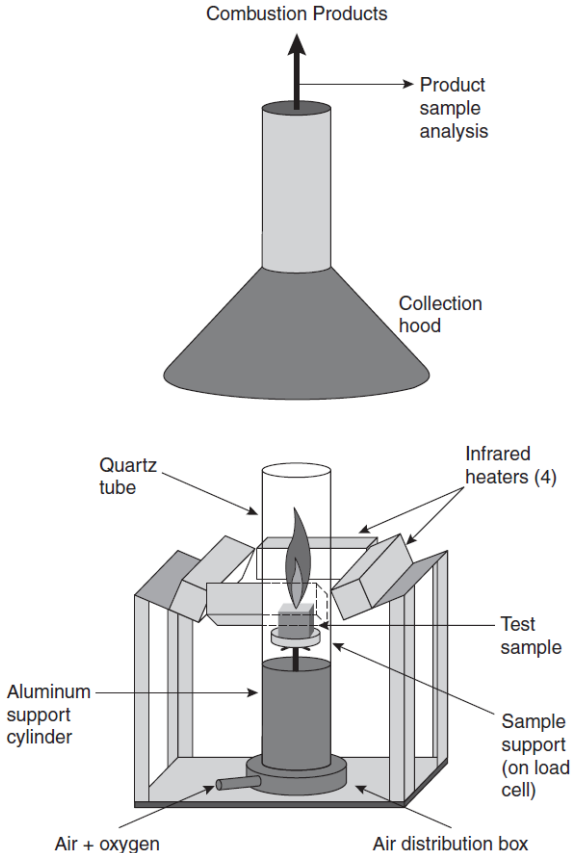

Figure 2-30: Fire Propagation Apparatus as presented in [70]

2.5.1.7 Cone Calorimeter (ISO 5660 – ASTM E1354)

The standard setup of the cone calorimeter test method according to BS ISO 5660 [76] and ASTM E1354 [212] would test samples with a 100 mm by 100 mm and a depth from 5 to 50 mm mounted on a load cell measuring the loss of weight as it burns during the test. The Leeds cone calorimeter is the standardised version, purchased from FTT (Fire Testing Technology Ltd.) [213]. An electric conical heater (capable of producing heat flux from 0 to 100 kW/m^2 on the surface of the sample) with 80 mm diameter for the top opening and 177 mm for the bottom one with 65 mm depth for the conical heater. The sample is mounted 25 mm below the conical heater, this distance is vital for ensuring that the designated heat flux is applied to the sample surface uniformly. Piloted spark ignition or auto self-ignition may be used. The smoke released by the sample travels through the conical heater and then mixed with diluting fresh air. All the smoke is collected by the metal hood aided by the fan motor pulling the smoke through the exhaust duct with the standard flow of 24 L/s measured and recorded during the test. The cone calorimeter is one of the most popular apparatus in the fire research and industry yielding around 400 paper a year (on ScienceDirect.com).

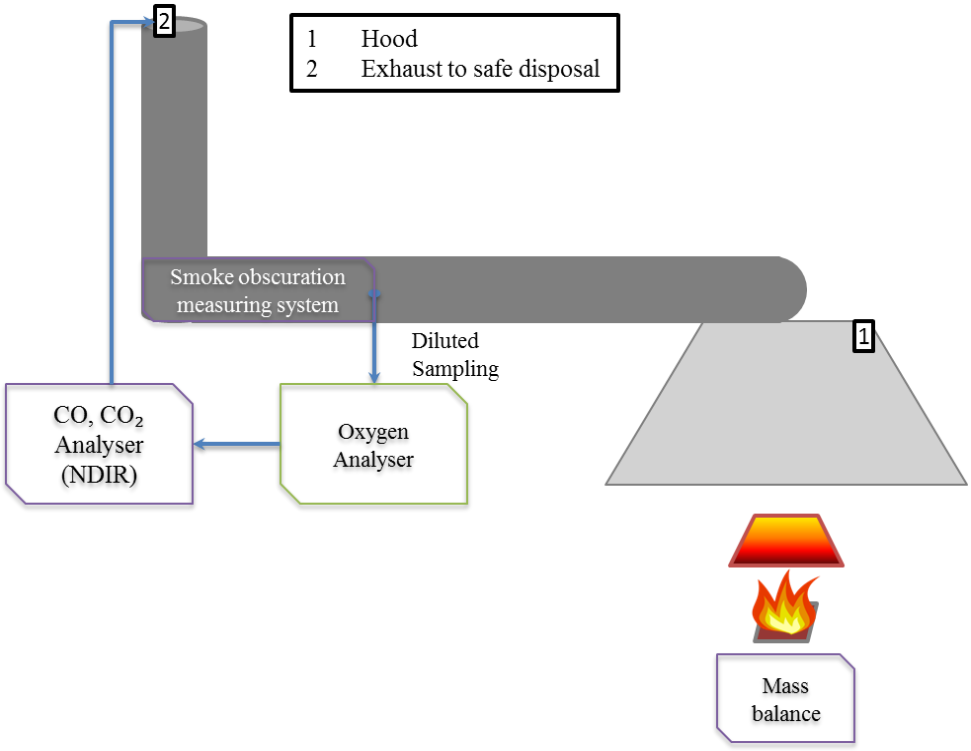

Figure 2-31: Main parts of the ISO 5660 cone calorimeter equipment.

2.5.1.8 Controlled Atmosphere Cone Calorimeter (CACC)

The Controlled Atmosphere Cone Calorimeter standardised setup is not defined yet. There are efforts to establish an ISO standard for using CACC for toxicity measurements, final version is yet to be produced. The main modification is to introduce an enclosure around the combustion zone to enable control of the surrounding atmosphere as can be seen in Figure 2-32. Some setups used by researchers to establish toxic yields are shown in Figure 2-33 [214-218]. The clear benefit of using CACC instead of the standard cone calorimeter is the ability to control the combustion conditions in accordance with ISO 19706 classifications.

Challenges related to quantification of equivalence ratios have been observed in the literature [69], which can be rooted to the reliance on metered ER rather than reaction ER and emission based ER discussed earlier in section 2.1.3. The major concern regarding toxicity measurement in this setup is the massive dilution occurring outside the burning chamber before the diluted sampling point, this issue can be resolved by introducing raw sampling, further details is discussed in 3.1.1. Other concern is the influence of using inert atmosphere on the HHR measurements via oxygen consumption principle as the reference oxygen should not use standard 20.95%vol. of oxygen in air, further discussion and details of solutions to the issue are presented by Werrel [219]. Mass yield data of toxic emissions have been produced in the literature [207, 220-225]. The popularity of the original standard apparatus can be a motivator to mass production of useful toxic yield measurements, once a robust measurement method is established.

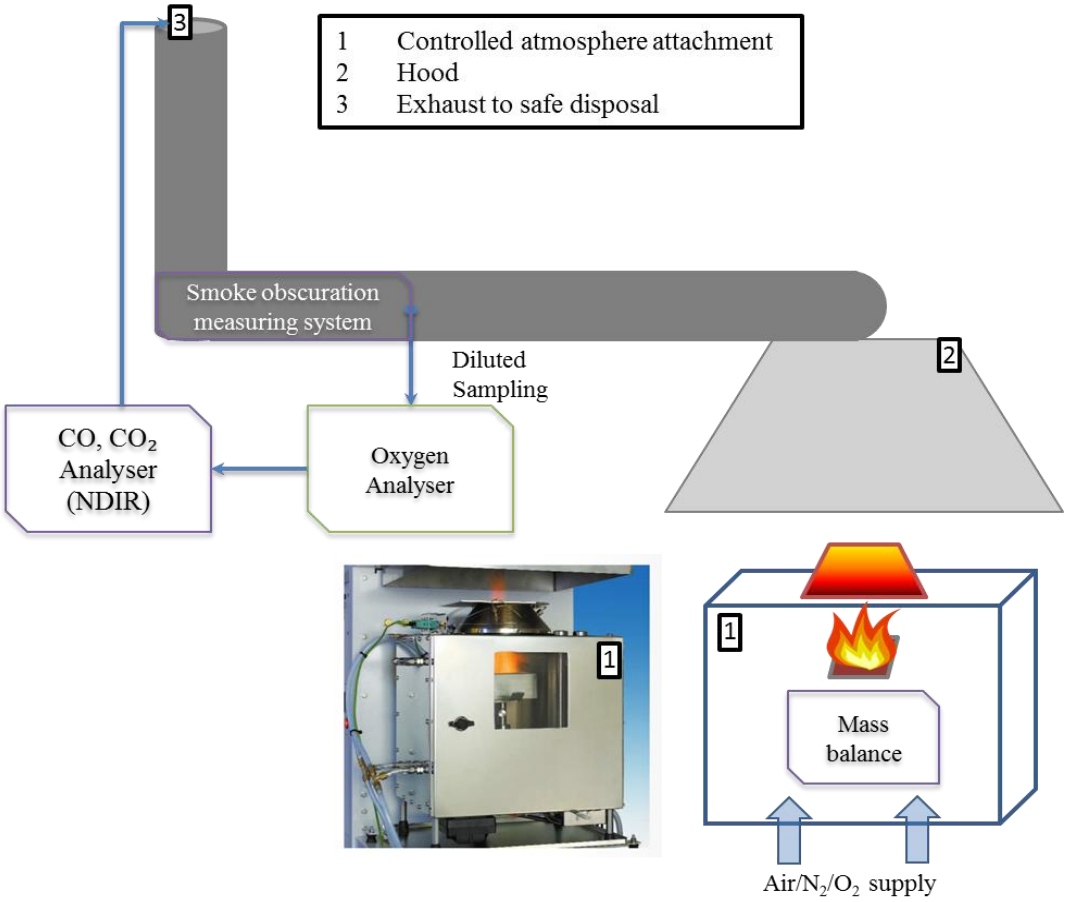

Figure 2-32: The controlled atmosphere enclosure attached to the cone calorimeter. Picture taken from [226].

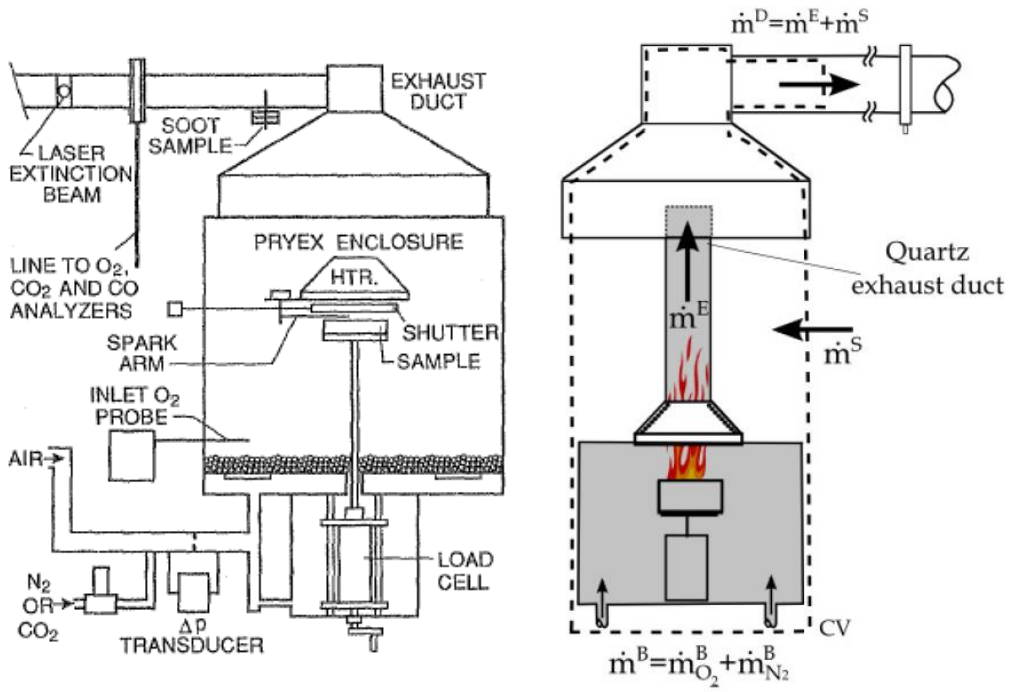

Figure 2-33: Schematic of controlled atmosphere cone calorimeter used in the literature by Mulholland et al. [215] (left) and Marquis et al. (right) [216].

2.5.2 Intermediate-scale experiments

In this section the experimental setup for what is considered intermediate-scale experiments that were used for toxicity measurements are explored. Generally, intermediate-scale fire experiment is a term used to describe what is larger than bench/small scale fire tests but not large enough to resemble a full scale compartment fire test. The main advantage of using intermediate-scale experiments is that the sample size is more representative to real fire scenarios (than small-scale tests) combined with the ability to isolate test conditions from other factors, to some extent, which enables analysis of factors influencing toxicity characteristics.

2.5.2.1 Single burning item test (SBI) – (BS EN 13823)

The single burning item (SBI) is European standard test method (BS EN 13823 [111]) for testing most building products except flooring materials. SBI main objective is to examine the behaviour of building materials when exposed to heat produced from a single burning item (simulated by a 31 kW propane burner). The total test duration is 25 minutes where the subjected sample is mounted in a corner orientation in the same configuration as in end use application, the sandbox propane burner is positioned at the bottom of that corner. The specimen used of 1.5 m height and maximum thickness of 200 mm. Combustion products are collected in the hood above the sample with pre-set flow rate of 60 L/s. SBI addresses the toxicity hazard in the form of smoke production rate, measured by optical measurement system installed in the exhaust hood (see Figure 2-34). Oxygen, CO and CO_2 analysers sampling from the exhaust hood are used for heat release calculations.

The ISO 19706 fire stage resembled by the standard SBI test is 2 for flaming well ventilated conditions. SBI was utilised in a multi-scale investigation by the Swedish SP of particles and isocyanates generated from fires [110].

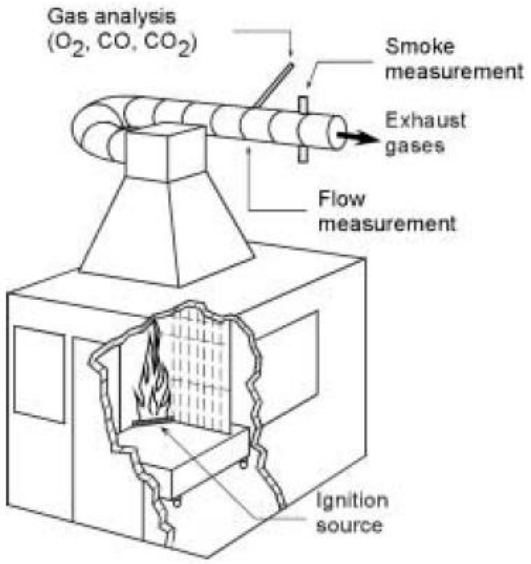

Figure 2-34: Single burning item EN 13283 test method from [227].

2.5.2.2 Furniture calorimeter test

Developed by the US NBS (NIST now) as method for measuring heat release rate by furniture items and their contribution to the overall fire size [228]. The targeted item is positioned on the top of the load platform (2.64 by 1.73 m). The ignition source is not defined but a 50 kW burner is suggested to be applied for 200 seconds, then the smoke is collected in the hood of at least the same size as the load platform with recommended flow rate of 1.7 m^3/s. Gas analyses and soot sampling ports are measured in the exhaust duct. It has been used as part of a multi-scale fire toxicity investigation where three materials were tested (Douglas fir, rigid polyurethane foam, and PVC) conducted by Babrauskas et al. [184]. In terms of ISO 19706 stages it represent a well ventilated flaming fire stage 2, however it has been observed that depending on the material smouldering stage can initially be dominant, and (sometimes) followed by a transaction to a flaming fire occur [229].

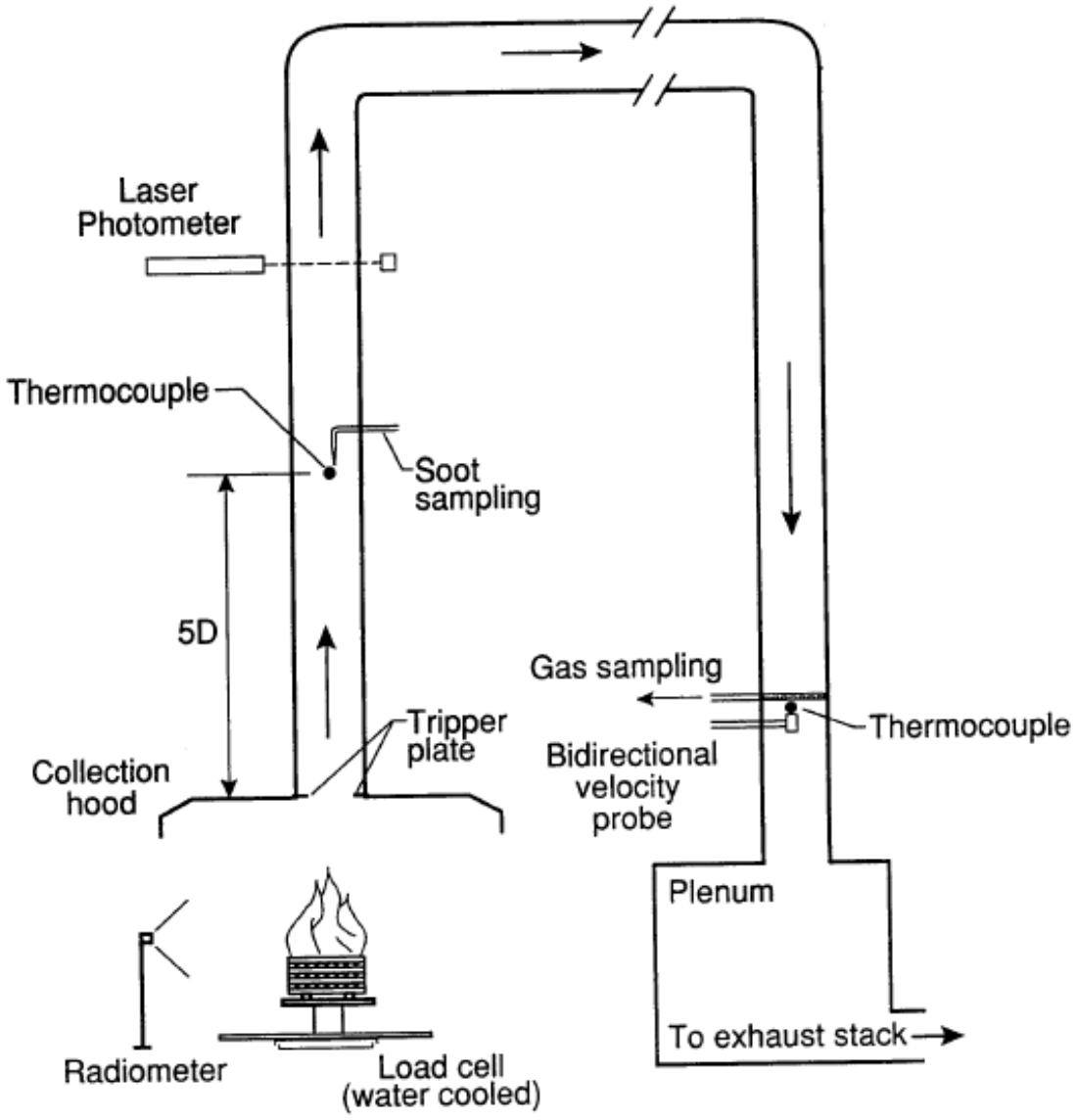

Figure 2-35: Furniture calorimeter test used in [184].

2.5.2.3 Hood tests

Hood experiments conducted in Harvard university by Beyler [65, 230] and California institute of technology by group of researchers led by Zukoski [66, 231-234]. These experiments shared the objective of understanding the influence of the reduced oxygen diffusion flame on the combustion products. These studies focused on measuring yields of incomplete combustion as a function of equivalence ratio. This kind of experiments has the advantage of creating a steady flow situation creating two distinct layers, which was very important for zonal modelling investigations. Pitts [63, 77] reviewed these studies and developed the global equivalence ratio concept in relation to enclosure fires, discussed earlier in section 2.1.3.

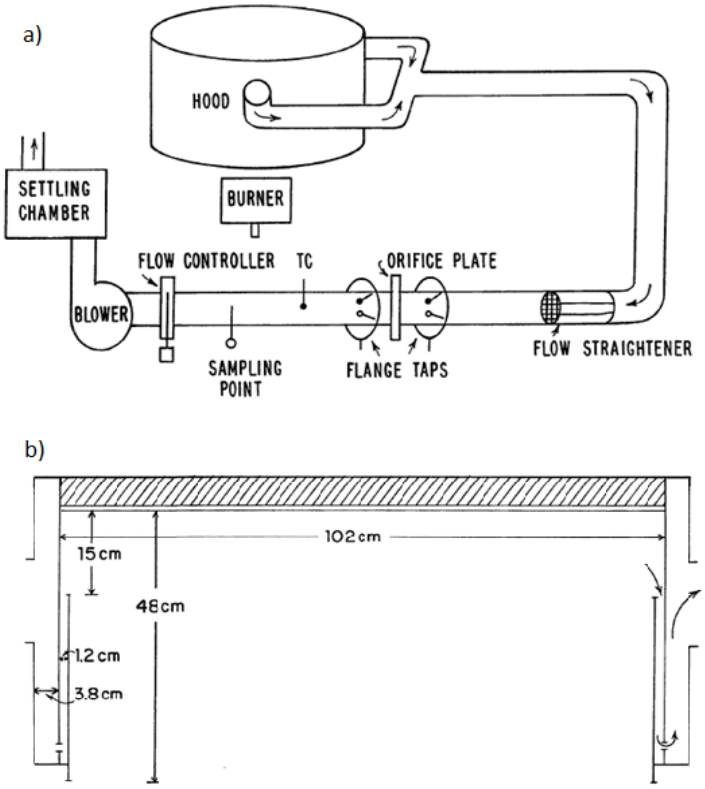

Figure 2-36: Schematic of Beyler's hood apparatus reproduced from [65].

Beyler's hood [65, 230] was cylindrical with 1 m diameter and height of 0.5 m where the smoke from the upper layer is collected on the sideways as shown in Figure 2-36b. The sampling system is shown in Figure 2-36a does not involve any further dilution. Beyler's hood was used to burn different hydrocarbon fuels both gaseous such as (propane, propene) and liquid such as (hexanes, toluene, methanol, ethanol, isopropanol, acetone) using gas burners and shallow 22 cm diameter pool fed from the centre [65], as well as burning ponderosa pine as a solid wood fuel [235]. Other hoods were used in the literature had slightly different setup for example; the researchers from California Tech. used 1.2 m^3 hood for their early work on steady flows, then they had to expand it to 2.2 m^3 to accommodate for studies related to the unsteady flows [233].

2.5.2.4 Reduced-Scale Enclosure (RSE) tests

Reduced-scale enclosures have been used for generating toxicity measurements in many projects in the past few decades. This section shows some examples of the work that have been done using such configuration. Fuels studied ranged from liquid hydrocarbons burnt as pool fires to solid materials. There is no clear rationale behind choosing the size of the reduced scale compartment, most commonly 2/5 ratio is used for scaling fire experiments from the ISO room with 3.6 x 2.4 m^2 to 1.44 x 0.96 m^2 for the RSE [236, 237]. Different configurations were utilised for supplying air and collecting and measuring gas samples ranging from raw heated sampling systems to diluted hood sampling systems.

2.5.2.4.1 Leeds' 1.6 m^3 RSE

Leeds' 1.6 m^3 reduced scale enclosure, shown in Figure 2-37, has been used for over 15 years for studying the influence of ventilation restriction on the fire, primarily focusing on gas analysis [171, 238-245].

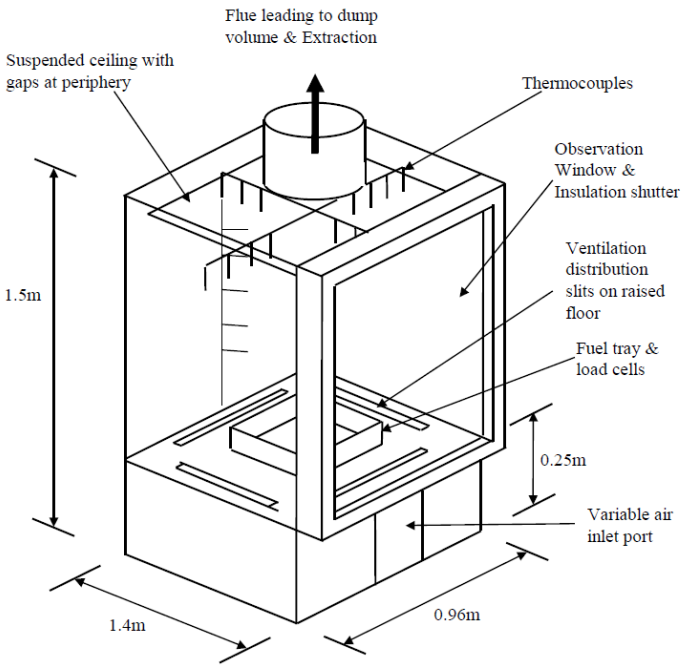

Figure 2-37: Leeds' 1.6 m^3 RSE from [243].

The used enclosure is actually has the potential to be expanded to a larger compartment with triple the width, which is the current direction in Leeds, with the objective of evaluating the smoke layer development. The 5 cm suspended ceiling gives the fire effluents the opportunity to mix well before being sampled by the x-ring sample probe, without any additional dilution. The materials burnt in this apparatus in Leeds ranged from hydrocarbon pool fires of kerosene, toluene, heptane and diesel to solid fuels of wood, polyethylene, cotton textiles, acrylic curtains including a mix of aircraft interior materials [171, 238-245]. The load platform gives continuous measurements of the mass loss rate, the controlled air supply system enables different ISO 19706 stages to be created.

2.5.2.4.2 Gottuk's 2.2 m^3 compartment fire tests

Gottuk used a 2.2 m^3 compartment, shown in Figure 2-38, for his experimental work in his PhD titled "Generation of Carbon Monoxide in Compartment Fires" [235].

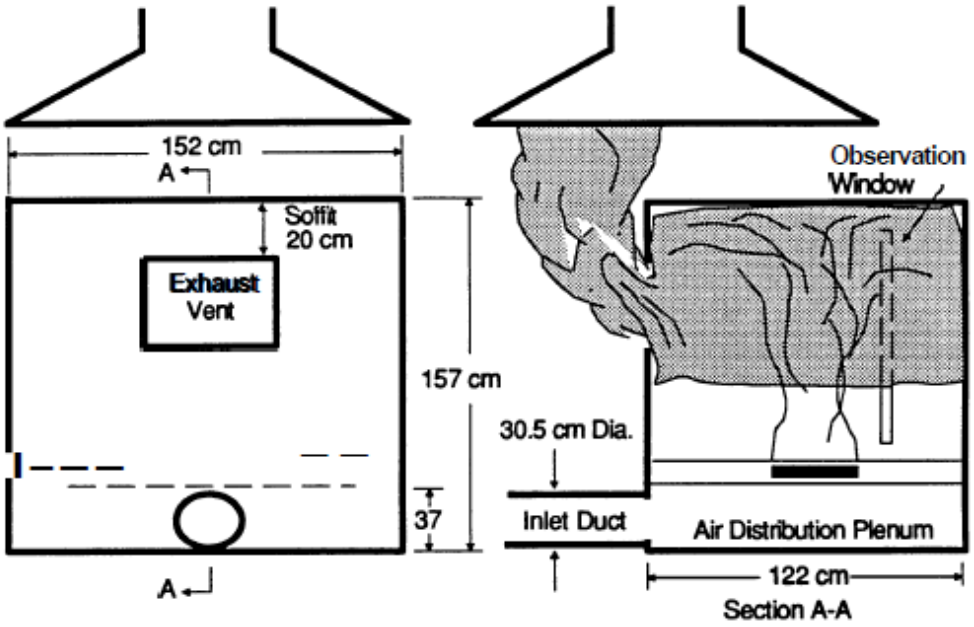

Figure 2-38: Schematic of the Gottuk's reduced scale enclosure (RSE) from [235].

In that project variety of fuels in solid and liquid forms was used, namely hexane, PMMA, spruce wood, and flexible polyurethane foam. Two sampling points were used in these tests; raw and diluted sampling points. The former located 13 cm into the compartment from the exhaust vent, while the latter is located downstream after the hood where also optical measurement system is installed. The sampling lines from both points were unheated and meet at sample selection valve which is connected to the gas analysers. Heated sampling lines from the sampling points to the FID analyser were used only for hexane tests. Gottuk's work yielded a model for predicting carbon monoxide yields based on equivalence ratio and temperature of the upper layer [64, 246], discussed earlier in section 2.1.4.

2.5.2.4.3 Lattimar's RSE with connected hallway

Lattimar's PhD thesis [247] titled "The Transport of High Concentrations of Carbon Monoxide to Locations Remote from the Burning Compartment" followed up on Gottuk's research by using the same compartment with the introduction of a hallway (see Figure 2-39) between the exhaust vent and the hood collecting the smoke emissions to study the toxic emissions transportation from the fire compartment [248].

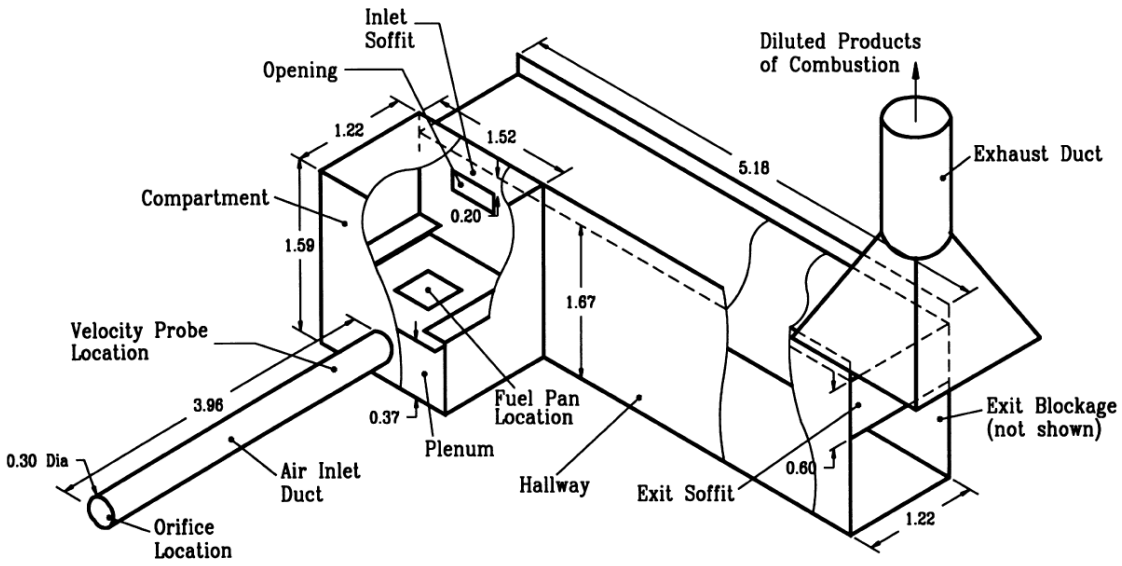

Figure 2-39: Lattimer's RSE with connected hallway setup as presented in his thesis [247].

Fuels used in this study were; hexane, polyurethane foam, and Douglas fir plywood. Sampling systems used two sampling points; downstream diluted sampling point similar to Gottuk's while the other sampling point was from the hallway using an automated sampling cart. In terms of gas analysis heated lines with heated filters were used for FID analysis, while dry gas samples were used for NDIR (CO, CO_2) and paramagnetic O_2 analysers. Yields data were presented as function of global equivalence ratios for different opening configurations. In that study it was claimed that CO yields measured in certain locations within the upper layer of the hallway are greater than CO yields inside the compartment by up to 23%, suggesting that unburnt hydrocarbons produced are more reactive to be converted to CO using the additional oxygen entrained in the hallway before CO is converted to CO_2.

2.5.2.4.4 NIST's 2007 1.4 m^3 Reduced-Scale Enclosure tests

NIST performed a series of tests on a 1.4 m^3 compartment shown in Figure 2-40 [237, 249]. The main objective of these tests was to guide the development and validation of CFD field models namely NIST's Fire Dynamics Simulator (FDS) [250, 251]. These tests were following on from the 1994 NIST's tests conducted using the same compartment to burn natural gas at different heat release rates (HRR) ranging from 7 to 650 kW [236]. While in this test series more fuels were tested including natural gas, such as; heptane, ethanol, polystyrene, methanol, and toluene. Gas measurements of CO, CO_2, O_2, and unburned hydrocarbons were measured from samples at two location inside the compartment as indicated in Figure 2-40. Mass yield measurements as a function of mixture fraction were reported from both sampling points.

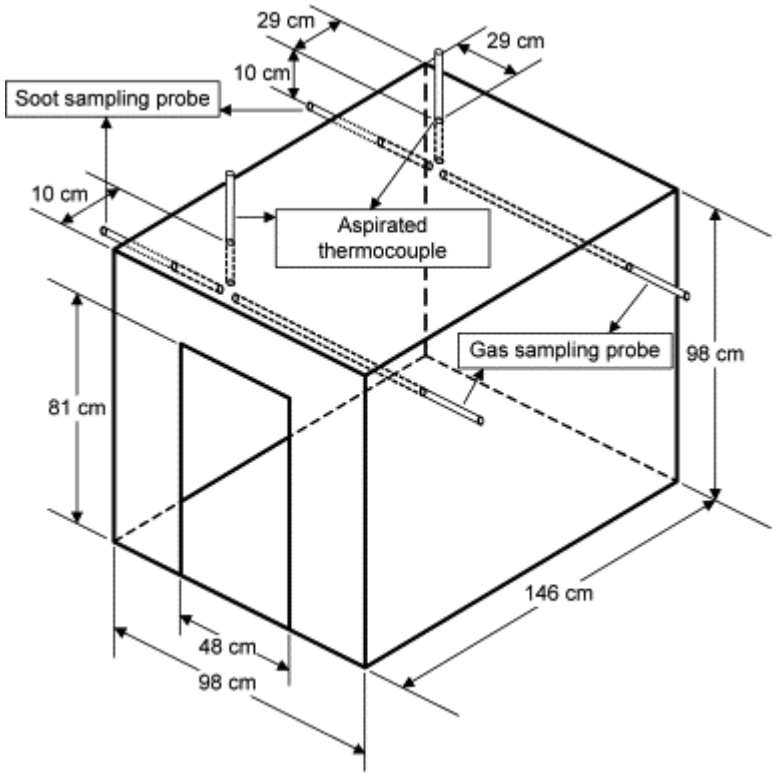

Figure 2-40: schematic of NIST 2007 [237] RSE test facility with sampling probes locations reproduced from [249].

2.5.3 Full scale experiments

Full scale experiments is the ultimate simulation of real compartment fire scenarios. Full scale experiments can be in real (disused) building or in specifically built tests compartments. The toxicity data collected from such experiments are rare and extremely valuable. Other full scale experiments were used for the purpose of other fire studies, as well as fire-fighting training, that can be wasted opportunities for fire toxicity measurements to be produced. It is important that whenever possible to present a useful quantification of mass yield of toxic emissions in compartment fire tests with a clear definition of the fuel involved, ventilation conditions, the geometry of the compartment and specific identification of the sampling location. Incorporating these data with other thermal measurements can present a beneficial full scale fire experiment to fire toxicity research and other areas of fire science.

The major challenge in conducting such experiments is the repeatability due to the limited possibility of repeating tests with exactly the same conditions. Generally, by the end of an intense flashover test, it is difficult to use the same compartment again. So a new one needs to be built or the equipment need to be dismantled and reinstalled in a new location. The costs of conducting such full scale tests are very expensive, it may include the need for hiring professional fire-fighting team on standby during the tests in order to satisfy safety precautions.

This section will review the efforts for producing toxicity data from full scale compartment fire experiments including the standardised ISO 9705 full scale room test.

2.5.3.1 ISO Room 9705

The standard ISO room fire 9705 [112] is defined for surface products to evaluate their contribution to the fire growth within the compartment by utilising floor heat flux measurements, fire size using the overall HRR measurements, toxic emission by gas analysis measurements, and the reduction of visibility by the optical density measurements. The test room dimensions are 3.6 x 2.4 m^2 with a height of 2.4 m with a single opening of 0.8 x 2 m^2, as shown in Figure 2-41. The standard ignition method is applying 100 kW for the first ten minutes and then increased to 300 kW for another ten minutes using a burner. The test is stopped as soon flashover occur (according to the standard this occur when HRR reaches 1 MW). The exhaust hood collects the fire effluents where all gas analyses occur. Several projects used the ISO 9705 setup for their full scale testing with various deficiencies from the actual standard testing different materials, and different sampling points.

SP testing program TOXFIRE in 1996 [174, 175, 252-255] used the ISO 9705 and a larger compartment (8.9 x 6 m^2 and 4.8 m high) setup shown in Figure 2-42 for investigating fires in chemical warehouses. The materials tested were polypropene, nylon 66, tetramethylthiuram monosulphide (TMTM), 4-chloro-3-nitrobenzoic acid (CNBA), and

chlorobenzene. Sampling gases was taken from two locations; at the compartment opening and at the exhaust duct using FTIR, FID, phi-meter, and NDIR analysers to quantify equivalence ratio, soot, NOx, CO, CO_2, O_2, and THC. Mass yield data v equivalence ratio were reported, also other thermal characteristics such as HRR and temperature inside the compartment [256]. Data from these tests have been used in comparisons with other bench-scale yield measurements from purser furnace [203, 204].

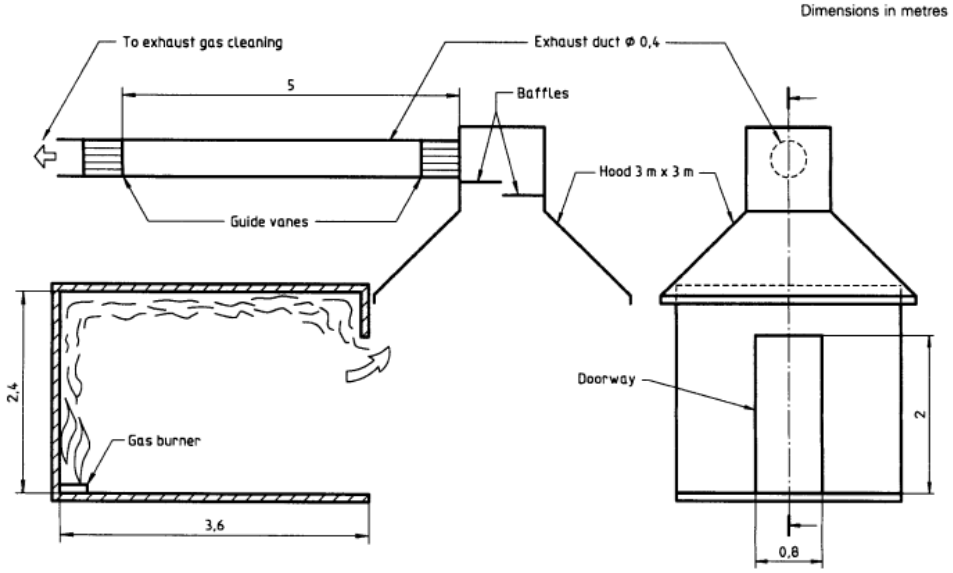

Figure 2-41: Schematic of the ISO 9705 room fire test, reproduced from [112].

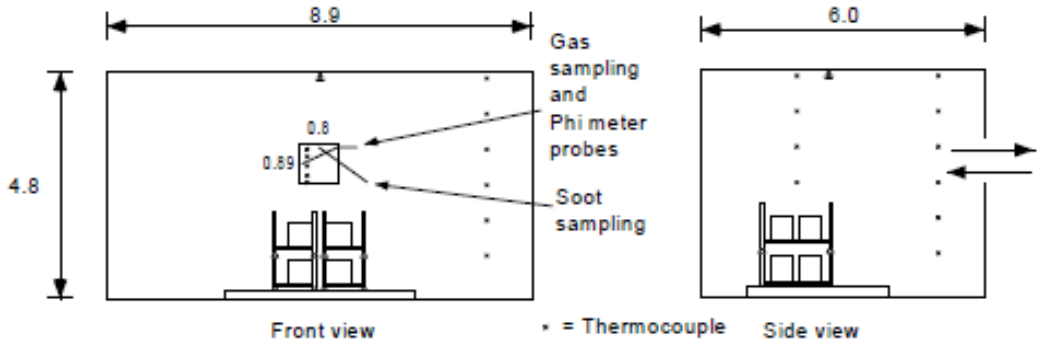

Figure 2-42: The storage (larger scale) TOXFIRE test compartment from [253].

NIST testing program in 2008 [257], Lock et al. used the ISO 9705 with heated gas sampling probes inside the compartment to burn natural gas, heptane, nylon, polypropylene, propanol, polystyrene, toluene, and polyurethane foam. This work is continuing the work on scaling by Bundy et al. [237] in the RSE for the purpose of generating data for validating FDS models, as discussed in 2.5.2.4.4.

NIST multi scale testing program in 1991 [184] used the ISO 9705 room to investigate the role of bench scale testing in predicting fire toxicity. In that study, three materials were tested; Douglas fir (wood), rigid polyurethane foam, and PVC sheets. Five different tests were used in that study; NBS cup furnace test (see section 2.5.1.1), SwRI/NIST radiant test

(see section 2.5.1.2), Cone Calorimeter (see section 2.5.1.7), Furniture calorimeter (see section 2.5.2.2), and ISO 9705 room connected with a 4.6 m corridor before the sampling room (see Figure 2-43). In all these tests (except cone and furniture calorimeters), animal toxic analyses were conducted to determine LC50 measurements along chemical analyses. Useful gas concentration measurements were reported at the different scales for CO, CO_2, O_2, HCN, HCl, and NOx and their corresponding mass yield measurements. Other fire characteristics were reported as well such as HRR curves, HRR and duration of steady state [184].

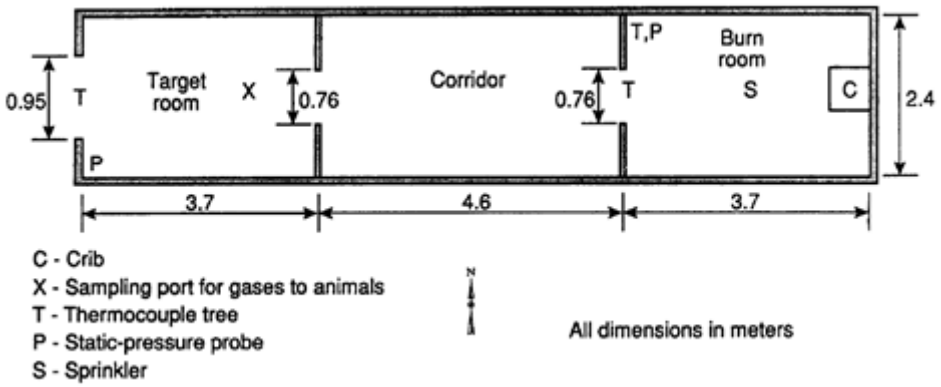

Figure 2-43: NIST 1991 full-scale testing facility from [184].

NIST testing program in 2003 [53], titled "the international study of sub-lethal effects of fire smoke on survivability and health (SEFS)" utilised full scale testing for the determination of the sub-lethal levels for fire products from burning sofas, bookcases, and PVC cables. The compartment used was similar setup to the NIST 1991 testing facility however the corridor, this time is much longer (9.75 m). With an exhaust vent just outside the fire compartment doorway that could be opened for HRR measurement through the hood. Four sampling points were used at different locations as can be seen in Figure 2-44. The results were recently used by Marsh et al. [258] in a multi-scale comparison project, investigating mass yield data produced from; the SwRI/NIST radiant furnace [190], the controlled atmosphere cone calorimeter (CACC) [223], and purser furnace [205].

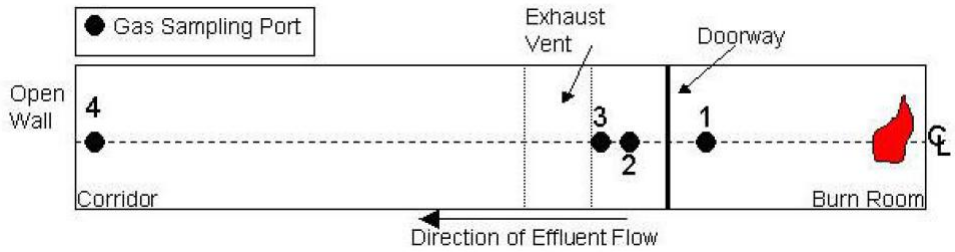

Figure 2-44: NIST 2003 full-scale testing facility, Burn room is of the ISO 9705 size while the attached corridor is 9.7m length. Adapted from [53].

2.6 Literature survey of experimental emissions yields

In this part a selected published toxic yields from burning wood are used to highlight the current available published data from different fire test scales. A larger list is presented in Appendix A, it is important to highlight that this not a complete list of all toxic yields from burning any material that have ever been published in the literature, but best efforts were made to compile a useful list from relevant sources. It is acknowledged that such a full database should be available to researchers and more importantly to modellers of fire safety engineering solutions to be used in their calculations and designs. It is even more important to highlight that such database should provide clear "best practice" guidelines that spell out how to use such a database, as the risk of misusing and bias in picking the "useful" data is greatly acknowledged in many relevant situations.

Yields presented herein are mass yields as reported in the referenced published papers if more than a single value is reported then the endpoints of the range are reported. ISO 19706 classifications (ISO stage column) were judged by the author based on the information available. The most relevant information from the published references were summarized in the comments sections, the reader is encouraged to read the full published paper referenced to form a better understanding of the conditions for the experiments, including measurement methods, specimen specifications, and calculations used to present the data.

The abbreviations used in the equipment column in the tables below are explained as follows;

- CC: Cone calorimeter (ISO 5660)
- CACC: Controlled-atmosphere cone calorimeter
- FPA: Fire propagation apparatus – ASTM E2058
- SSTF: Steady state tube furnace (Purser furnace) – ISO TS 19700
- NIST: NIST radiant test – ASTM E1678/NFPA 269
- RSE: Reduced scale enclosure
- 9705: ISO 9705 room fire test
- FC: Furniture calorimeter
- FS: Full scale
- NBS-CF: NBS cup furnace

The abbreviations used in the equipment column in the tables below are explained as follows;

- DF: Douglas fir
- MDF: Medium density fibreboard
- PB: Particleboard
- ACH: Air changes per hour
- L/min: Unit for quantifying the air supply rate
- kW/m^2: Unit for quantifying the applied heat flux

Table 2-12: Carbon monoxide mass yields for burning wood in different scales and conditions as published in the literature.

Equip.	Y_{CO} [g/g]	ISO stage	Comments	Ref.
CC	0.13	1b	Pine, 15kW/m^2, non-flaming	[259]
CC	0.017- 0.023	1b	Douglas fir, 15kW/m^2, non-flaming	[259]
CC	0.071- 0.092	2	Ponderosa Pine, 35kW/m^2, flaming	[259]
CC	0.087- 0.093	2	Douglas fir, 35kW/m^2, flaming	[259]
CC	0.003- 0.005	2	DF, 35, 50, 75kW/m^2, flaming	[184]
CC	0.05	2	Plywood, 35kW/m^2, flaming	[110]
CACC	0.004 - 0.09	3b	PB, 50kW/m^2, vitiated (10,15, 17, 18, 19, 21%O_2), 150 L/min	[222]
CACC	0.005 - 0.16	3b	PB, 50kW/m2, under-ventilated (10, 20, 30, 50, 110, 130, 150, 170 L/min)	[222]
FPA	0.005	2	Pine, well ventilated	[70]
FPA	0.004	2	Red oak, well ventilated	[70]
FPA	0.004	2	Douglas fir, well ventilated	[70]
SSTF	0.005 - 0.01	2	Pine wood	[113]
SSTF	0.1 - 0.14	3b	Pine wood	[113]
SSTF	0.002 - 0.23	2 - 3b	MDF	[204]
NIST	0.03 - 0.04	2	Douglas fir,	[184]
NBS-CF	0.2	ND	Douglas fir, flaming	[184]
RSE 1.6m^3	0.002- 0.262	2 - 3b	Pine, 11, 21, 37 ACH, flaming	[242]
RSE 1.6m^3	0.02 - 0.123	1a	Pine, 5 ACH, non-flaming	[242]
RSE 2.2m^3	0.008- 0.165	2 - 3b	Spruce wood	[235]
FC	0.012- 0.013	2	Douglas fir	[184]
Hood	0.004- 0.143	2 - 3b	Ponderosa Pine	[65]
9705	0.007 - 0.23	2 - 3b	MDF	[204]
FS	0.04 - 0.27	2 - 3b	41 m^3	[260]
FS	0.072 - 0.12	2 - 3b	Douglas fir	[184]

Table 2-13: Hydrogen cyanide mass yields for burning wood in different scales and conditions as published in the literature.

Equip.	Y_{HCN} [g/g]	ISO stage	Comments	Ref.
9705	0.001 - 0.005	2 - 3b	MDF	[204]
SSTF	0.00003 - 0.008	2 - 3b	MDF	[204]

Table 2-14: Acrolein mass yields for burning wood in different scales and conditions as published in the literature.

Equip.	$Y_{Acrolein}$ [g/g]	ISO stage	Comments	Ref.
RSE 1.6m^3	0.001- 0.008	2 - 3b	Pine, 11, 21, 37 ACH, flaming	[242]
RSE 1.6m^3	0.001- 0.002	1a	Pine, 5 ACH, non-flaming	[242]
FS	0.001- 0.006	2 - 3b	41 m^3	[260]

Table 2-15: Formaldehyde mass yields for burning wood in different scales and conditions as published in the literature

Equip.	$Y_{Formaldehyde}$ [g/g]	ISO stage	Comments	Ref.
RSE 1.6m^3	0.001- 0.006	2 - 3b	Pine, 11, 21, 37 ACH, flaming	[242]
RSE 1.6m^3	0.001- 0.014	1a	Pine, 5 ACH, non-flaming	[242]
FS	0.002- 0.013	2 - 3b	41 m^3	[260]

Table 2-16: Total unburnt hydrocarbon mass yields for burning wood in different scales and conditions as published in the literature

Equip.	Y_{THC} [g/g]	ISO stage	Comments	Ref.
FPA	0.005	2	Pine, well ventilated	[70]
FPA	0.004	2	Red oak, well ventilated	[70]
FPA	0.004	2	Douglas fir, well ventilated	[70]
SSTF	0.01 - 0.11	2 - 3b	MDF	[204]
RSE 1.6m^3	0.001- 0.08	2 - 3b	Pine, 11, 21, 37 ACH, flaming	[242]
RSE 1.6m^3	0.004- 0.048	1a	Pine, 5 ACH, non-flaming	[242]
FS	0.001- 0.052	2 - 3b	41 m^3	[260]

Table 2-17: Particulate mass yields for burning wood in different scales and conditions as published in the literature

Equip.	Y_S [g/g]	ISO stage	Comments	Ref.
FPA	0.015	2	Red oak, well ventilated	[70]
FPA	0.015	2	Hemlock, well ventilated	[70]
CC	0.0024	2	Plywood, 35kW/m^2, flaming	[110]
SSTF	0.002 - 0.02	2 - 3b	MDF	[204]
9705	0.01 - 0.04	2 - 3b	MDF	[204]

2.7 Aims and objectives

From the discussion throughout this chapter the following aims and objectives were identified for this work:

1. FTIR is a powerful tool for determining concentrations of species, that's why it should be used after validation and verification in this project,
2. CACC is a prominent apparatus for a small-scale toxicity yields measurements, however, it has some problematic issues with the diluted sampling, solutions to these problems are investigated and clear guide is provided. Including, the development of a full mass balance equivalence ratio model based on emissions measurements.
3. Establishing a scientific method for measuring the produced toxicity yields tested in the Controlled-Atmosphere Cone Calorimeter is part of reaching this goal.
4. Full scale fire experiments are the ultimate simulations of a real fire, and such experiments are very important in providing toxic yield data for comparison with small scale tests.

Chapter 3
Experimental Methodologies

This chapter focus is on the experimental methodologies used by the author in conducting experiments and analysis presented in this work. Since gas analysis have a significant role in achieving the objectives of this project, it will be discussed and detailed thoroughly first. Starting with detailing the specifications of the sampling systems used and explaining the rationale behind choosing those systems. Then techniques used to analyse smoke emissions from fires in this work will be discussed in terms of working principle, analysis methods, validations of measurements, advantages and limitations in comparison to other alternative techniques. One of the unique aspects of this work is taking the advantage of the state of the art Fourier transform infrared (FTIR) gas analysis technique to measure smoke emissions from different scales of fire testing. In all the tests presented in this work, the more common (in fire research) non-dispersive gas analysis technique that was also used to verify FTIR measurements for CO and CO_2. The paramagnetic analysis technique for measuring oxygen was the only method used to quantify oxygen levels in the samples analysed. Then, details of the experimental setup tests presented in this work are specified for both, full scale tests and bench scale tests. Finally, analytical testing (proximate and ultimate analysis) for determining the fuel characters are discussed and examples of typical calculations methods are presented.

3.1 Gas analysis

The need for raw fire product gas analysis for true toxic gas measurements in the room of origin in the fire is explained. All current methods of fire toxic gas analysis involve some dilution of the fire products prior to analysis and this is likely to promote oxidation of the toxics and re-equilibration of CO. The hot gas handling requirements for raw fire product gas analysis are outlined. Heated Fourier Transform Infrared (FTIR) analysers are available capable of analysing raw hot samples gases, these were developed for automotive direct exhaust gas analysis but are shown to be ideally suited to fire toxicity analysis in raw fire gases.

3.1.1 Raw sampling and the dilution effect on effluents of under-ventilated fires

3.1.1.1 Toxic Gases in Compartment Fires with Restricted Ventilation

All current methods of assessing the quantities of toxic gases from compartment fires use some form of fire product dilution with air and do not measure the actual concentration in compartment fires or in smaller scale toxic gas fire simulation equipment. The classic

technique is fire calorimetry where small or full scale specimens are burnt in an open air configuration under a hood that collects all the combustion products with additional air entrained into the hood. The total mass flow of the mixed air and fire gases is measured and the oxygen concentration in the mixed gases is determined. This enables the mass of oxygen consumed in the fire to be determined and from this the fire HRR can be calculated. This is known as the oxygen consumption calorimetry approach to the measurement of the HRR from burning materials. One of the advantages of these techniques is that they measure the maximum heat release rate, in a freely ventilated fire. A modified version of the techniques is used in compartment fires where the fire products leaving a compartment through a door or window are collected in a large hood which has entrained dilution air as well as the fire products. However, the technique in this case does not determine the HRR in the compartment fire but determines the sum of the HRR in the compartment and in the external fire. The analysis of the raw gas sample from inside a compartment fire enables the HRR in the compartment to be determined by oxygen consumption and often this is much lower than the total heat released.

If the aim of the test is to determine the maximum HRR of materials or whole pieces of furniture, then the standard Cone Calorimeter test under free ventilation conditions is a good method. However, it is not a suitable method for fire toxicity studies that are relevant to restricted ventilation compartment fires i.e. the type of fires in which casualties from inhaling toxic gases occurs. The reason is that in ventilation controlled compartment fires there is either insufficient air or insufficient temperature to burn the entire fire load to completion in the original compartment. This leads to inefficient combustion and the partial burning or inefficiency in burning of the fire load results in the formation of the toxic products that cause harm in a fire.

Aljumaiah et al. [242] showed for pine crib compartment fires with restricted ventilation that all the fires were fuel rich with very high levels of CO and hydrocarbons, HC. The energy content of these gave combustion efficiencies between 45% and 90% at the peak HRR, or 55% and 10% of the total HRR occurred outside the compartment as the discharge gases mixed with additional air. The combustion efficiency deteriorated as the ventilation increased as the burning rate increased faster than the air supply. These fires had peak global equivalence ratios, Ø, of 2 - 3.5, with richer mixture for higher ventilation. Among the products of inefficient wood combustion in addition to high levels of CO, that can cause death in fires, were significant yields of acrolein, formaldehyde, benzene and acetic acid, which are irritant gases that impair escape from fire. Outside the compartment, as occurs in real fires once a window breaks, combustion was completed with the external entrained air. Similar work by Aljumaiah et al. [241] was undertaken in the same fire compartment for hanging acrylic curtains and at 11 and 21 ACH the combustion efficiency at the peak HRR was 85% and in addition to CO, acrolein and formaldehyde there was a high yield of HCN

from the acrylic organic nitrogen content of the curtains. Again in these air starved fires the peak Ø was 2 – 2.5. The final toxic gases after the fire products burn in the external air has very little relationship with the toxic products inside the compartment or the toxic products that leak around the door into corridors and then disperse into other rooms causing fatalities there. Any measurements of toxic gases in fires should account for the impact of compartment fire ventilation on the toxic gas yield. Most laboratory measurements of toxic gases do not simulate real fires and all dilute the products of the fire prior to analysis and thus allow post fire oxidation. Standard tests with dilution of the fire product gases are summarised in Table 3-1.

The standard cone calorimeter test is a freely ventilated fire test; the air supply indicated in Table 3-1 is based on the flow of the products through the conical heater. Introducing "raw" (pre-dilution) sampling points to these tests for heated gas analysis is appropriate and achievable.

It should be noted that for the Cone Calorimeter as well as the other apparatuses in Table 3-1 the air supply to the fire zone is actually in excess of that entrained and participating in the actual combustion of the pyrolysed fuel. In fact the combustion products are effectively already diluted by approximately a factor of 40 to 50 by the time of exit at the top of the cone heater. So by the time the combustion gases reach the normal sampling point the overall dilution factor is of the order of 300 to 400.

Table 3-1: Standard sampling point locations and dilution ratios for fire toxicity bench-scale tests.

Test	Standard sampling point location	Air supply to the fire zone	Total flow rate at sampling point	Dilution ratio
Purser furnace **ISO 19700** [72]	Effluent dilution chamber	2 – 10 [L/min]	50 [L/min]	25-5
Cone Calorimeter **ISO 5660** [261]	Exhaust duct	3 [L/s]*	24 [L/s]	8
Fire propagation apparatus (FPA) **ASTM E2058** [71]	Exhaust duct	3.3 [L/s]	150 [L/s]	45

* Based on experimental measurements by the author shown in Chapter 6.

The Controlled Atmosphere Cone Calorimeter (CACC) is not included in Table 3-1 since there is no agreed standard method yet. The dilution ratio in CACC is based on the air supply flow rate to the enclosure around the fire sample and the total flow rate by the exhaust fan. CACC has been used with various supply rates creating vitiated (reduced oxygen levels) and ventilation restricted conditions and total flow rates at the exhaust duct has been reduced [216, 222]. Raw sampling coupled with heated FTIR analysis has been used for fire toxicity assessment in CACC apparatus in previous work by the author and others [171, 224, 262].

Tewarson [263] was the first to show on a laboratory scale that the local Ø of the fire influenced the fire toxic gas yield. Tewarson [263] used the Fire Propagation Apparatus, FPA, [71] where a fire sample on a load cell is placed in a vertical quartz tube with an external conical heater and metered airflow up the quartz tube. Alarifi et al. [224] have shown that the cone calorimeter can be modified to be similar to the FPA by using the controlled atmosphere version of the cone calorimeter. This places an airtight box around the cone fire specimen with a controlled air flow. A short chimney was fitted to the exit from the cone heater, which enabled a raw gas sample to be obtained and transmitted for gas analysis via a heated sampling system. Andrews et al. [225] have used the same system to investigate the toxic gas emissions from acrylic blanket fires. These modifications to the cone calorimeter enable it to meet ISO 19706 fire stages 3a & 3b [58] for under ventilated flaming tests.

For large scale compartment fires Bundy et al. [237] have developed raw gas analysis techniques for sampling from the internal compartment ceiling gases as well as the standard calorimetry method of sampling the diluted gases. For the diluted gases they used 93 ^{o}C heated teflon sampling lines to a water condenser and then Nafion tube drier to remove the water vapour and this was followed by dry gas analysis. This technique was used to avoid the sample losses that occur if the more conventional condensation of water in the sample is used, by cooling the sample to 2 ^{o}C in an ice bath. Unfortunately this type of water condenser also removes all toxic gases that dissolve in water, which are shown in Table 3-2. For the raw ceiling gas analysis in the work of Bundy et al. [237] the sample condenser was removed and the gases were kept at 60 ^{o}C in an oven and all the water was removed using a membrane drier, this avoided the sample coming into contact with liquid water and hence kept the toxic gases in the sample. However, there was no heated FTIR to measure the toxic gases but there was a total hydrocarbon flame ionisation detector, FID, operated without sample heating. All the gases were still analysed on a dry gas basis, but without the loss of gases by solution in water. The weakness of this method is that in many fires, particularly the pool fires that Bundy et al. [237] investigated, there would be hydrocarbon condensation in the sample lines and filters at 60^{o}C. To avoid this all sample lines, filters and pumps should be heated to 180 – 190^{o}C, as has been done for many years for this type of measurement in automotive exhaust gas analysis.

By surveying the aqueous solubility of common fire products in gas phase and their boiling points [264-267], Table 3-2 was created. Solubility were calssified using the common US-Pharmacopeia solubility definition, as described in the highly cited paper by Stegemann et.al [268]. Table 3-2 illustrates the signifcance of using heated sampling and analysis systems to avoid any sample loss with possible condensation of water.

Table 3-2: The problem of sample losses in unheated raw gas sampling and analysis systems collected from [264-267], solubility classified using USP definitions [268].

Species	Boiling Point	Solubility in Water
Carbon monoxide	-191 °C	Practically insoluble
Carbon dioxide	-79 °C	Slightly soluble
Nitrogen monoxide (Nitric oxide)	-152 °C	Practically insoluble
Oxygen	-183 °C	Practically insoluble
Methane	-161 °C	Practically insoluble
Ethane	-88 °C	Practically insoluble
Propane	-42 °C	Practically insoluble
Benzaldehyde	178 °C	Slightly soluble
Benzene	80 °C	Slightly soluble
Toluene (Methylbenzene)	111 °C	Very slightly soluble
Sulfur dioxide	-10 °C	Soluble
Acrylonitrile	77 °C	Soluble
Propionaldehyde	48 °C	Very soluble
Ammonia	-33 °C	Very soluble
Acrolein (2-propenal)	53 °C	Very soluble
Hydrogen bromide	-67 °C	Very soluble
Hydrogen chloride	-85 °C	Freely soluble
Hydrogen cyanide	26 °C	Miscible
Hydrogen fluoride	20 °C	Miscible
Nitrogen dioxide	21 °C	Hydrolysis
Formaldehyde (Methanal)	-19 °C	Miscible
Acetaldehyde (Ethanal)	20 °C	Miscible
Formic acid	101°C	Miscible
Acetic acid	118 °C	Miscible

3.1.1.2 The Problem of Water Vapour in Fire Product Gases

There are two ways of dealing with water vapour in the sample gases from fires that do not simultaneously lose unburnt high MW hydrocarbon. Firstly, heated raw gas sampling systems, could be used and secondly gas dilution can be used. With gas dilution the concentration of the water vapour is reduced and this reduces the dewpoint of the gas mixture, such that water does not condense as it is cooled by dilution as illustrated in Figure 3-1. Both methods have been used in automotive emissions measurement, but for passenger cars only the dilution method is recognised for legislative purposes. The heated exhaust sample line has to be used for large offroad and marine engines as the dilution systems would be too large. The reason for this approach is that the automotive emissions legislation involves testing vehicles over a highly transient load cycle and it is considered that gas sample systems could not follow these transients adequately. For fire applications there are no equivalent fast transients and so no reason to use a dilution method to overcome the water vapour problems in raw gas analysis.

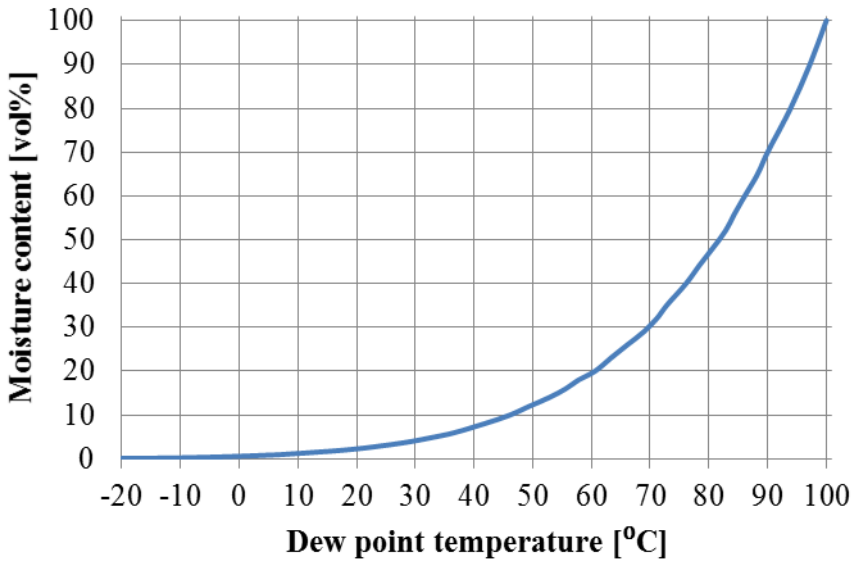

Figure 3-1: Moisture content as a function dew point temperature [269].

A further problem with the dilution method is that dilution obviously reduces the concentration of the gases to be measured in proportion to the dilution factor. This is a further reason for not using dilution, as some toxic gases such acrolein are toxic at very low concentrations. For example the SFPE impairment of escape limit for acrolein is 4ppm [36] and for the COSHH 15 min. exposure limit it is 0.3ppm. The lower limit of measurement in the present FTIR is about 0.3 - 2ppm, depending on the gas, and in raw gases from fires acrolein is present well above these impairment of escape limits and can be reliably determined, but they would be very difficult to determine after dilution.

3.1.1.3 Raw gas sampling

To avoid sample losses of the toxic gases in Table 3-2 using raw gas sampling, heated sample systems are required and these have rarely been used in fire toxic gas research. The sample collected should give an accurate representation of the fire toxic gases, without the sampling system altering their concentration through condensation, solution in water or absorption on surfaces or particulates. There is a further problem with fire gas analysis and that is the non-uniformity of the fire. Normally a mean gas sample that is representative of the fire ceiling gases is used as multipoint sampling is too expensive.

The use of multi-hole gas sample probes to obtain a mean ceiling layer gas sample is the best approach [237, 260]. In large room fires a single gas sample tube is placed across the width of the ceiling with 10 or more equi-spaced holes along the length of the tube [237, 260]. It would be better if there were several of these tubes along the length of the chamber so that a better mean ceiling layer gas sample was achieved, but this procedure has not been used to the authors knowledge. In the compartment fires of Aljumaiah et al. [241, 242] the mean ceiling gas samples was achieved by the ceiling gases flowing across the ceiling, then turned through 180^{o} to flow along the back side of the ceiling to an exit through a 140mm chimney with a water cooled 'X' configuration gas sample probe with 40 gas sample holes on centres of equal area. This was considered sufficiently mixed to give a mean ceiling layer sample. In fire testing with dilution of the fire products it is usually assumed that the dilution process and the distance from the fire discharge to the gas sample point is sufficient for the gases to be mixed, although definitive proof of this has not been demonstrated in the fire literature.

Assuming that a well-mixed ceiling layer gas sample has been achieved, the task is now to transfer this to analytical equipment without changing the composition. For fire ceiling temperatures above 200 ^{o}C this normally involves cooling the sample, as most heated gas sample lines will melt above this temperature. The cooling can be achieved using water cooling, but this can lead to overcooling and so steam cooling at the desired sample temperature of 180 ^{o}C – 190 ^{o}C if no high boiling point hydrocarbon losses are to occur and this method is used in gas turbine combustor test rig emissions monitoring. This is far too complex and expensive for fire toxic gas analysis. Instead an uncooled sample probe is used in the fire compartment and outside the compartment wall there is a length of uncooled stainless steel pipe that loses heat by convection to ambient air. The length of this (typically of the order of 0.5m) is empirically adjusted to achieve a measured temperature of 190 ^{o}C into the sample probe.

The aim of the gas transfer system is to keep the sample at close to 180 ^{o}C all the way to the hydrocarbon analyser (heated FTIR or heated flame ionisation detector, FID). The determination of the fire combustion efficiency in the compartment depends on the hydrocarbon analysis being made without losses. For air starved fires the hydrocarbon

contribution to the combustion inefficiency is significant [241, 242]. A further problem with raw gas analysis is that the gas sample is transferred by a pump to the gas analysis equipment and this pump is always upstream of the gas analysis equipment [166]. Also no gas analysis equipment can cope with soot or other particles in the sample line and so there must be a fine filter in the sample line. To avoid any losses due to condensation in the pump and filter, these must be in an oven at 180^{o}C. The simplest way to achieve this is to place the heated pump and filter in an oven close to the fire gas sample point and also to mount the heated hydrocarbon analyser immediately downstream of the heated pump and filter. This requires two short heated lines to achieve, one from the mean gas sample probe to the pump unit and one from the pump unit to the hydrocarbon analyser. After this point the sample does not need to be at 180^{o}C. This is the procedure used in automotive engine test cell gas analysis. However, it is impractical for large scale compartment fires, due to the risk of damage to the equipment by fire radiation. Thus in fire research with raw hot gas sampling it is usual to use at least a 5m heated sample line between the test compartment and the analytical instruments, as used by Aljumaiah et al. [241, 242] for a 1.6 m^3 experimental compartment fire and by Alarifi et al. [224] and Andrews et al. [225] for raw gas sampling from the cone calorimeter with a ventilation controlled enclosure around the test specimen. For full scale room fire raw gas analysis Alarifi et al. [260] used a 25m long heated sample line. It is important in all uses of heated sample lines that the junctions at the end of the line to the heated filter units and the analytical equipment are insulated to avoid cold spots in the gas sample transfer lines.

After the heated pump and filter unit there is a further heated sample line that transfers the hot sample to the heated hydrocarbon analyser (FTIR or FID). Normally the heated sample would be split inside the heated pump and one line would go to the heated FID (or FTIR) and the other to a heated chemiluminescence NOx analyser. The NOx analyser is not normally used in fire research, but is useful as NOx is generated by the peak flame temperature in a fire and so NOx emissions give useful information on fire dynamics [270]. Also NO_2 is one of the toxic gases in fires and this can be determined by chemiluminescence analysers. A further sample line usually goes from the heated pump and filter unit to a condenser or membrane water removal device. The subsequent low temperature dry sample is then analysed by NDIR for CO and CO_2. If a heated FTIR was used, this would not be necessary as these are measured hot and wet by the FTIR. However, the one gas that currently has to be measured with water removed is oxygen, as a paramagnetic analyser is usually used. For hot analysis a heated zirconia electrochemical cell could be used, but to the authors knowledge no one in fire research is using this at present, but it would be a good method for raw oxygen analysis. The problem is that the removal of water from the hot sample increases the concentration of oxygen and the oxygen measured dry has to be converted to a wet oxygen concentration if oxygen mass

consumption HRR calculations are to be carried out on the raw samples. None of this is necessary if the sample is diluted as the mixture is cooled to room temperature by dilution.

This type of raw gas oxygen consumption analysis is required if the proportion of the total HRR inside a compartment is required to be measured [241, 242]. The total heat release is after secondary heat release in the compartment discharge gases as they mix with external air and this is the procedure used in fire calorimetry. Although it is possible to calculate the production of water in a fire if the global equivalence ratio is known together with the fuel composition, as in the work of Chan [271], this is more difficult for fire fuels such as wood, where the wood has significant water content. It is considered the best way to correct a dry measured oxygen to a wet basis in fire is to use a heated FTIR and measure the water vapour, which the heated FTIR does routinely. However, direct raw gas hot oxygen measurement is preferable.

Andrews et al. [171] were one the first groups to demonstrate the use of raw fire gas analysis using full heated gas sample system, as used in the automotive industry, in fire toxicity research. This was for diesel pool fires in a 1.6 m^3 compartment. Recent developments in the automotive area for on board exhaust emissions measurement (PEMS) has led to the development of heated wet gas analysis for CO, CO_2, oxygen and as well as hot chemiluminescence analysis for NOx. These are ideally suited to fire investigation for HRR inside compartments [241, 242] but they only measure one toxic gas, CO. Where a wider range of toxic gases is required heated FTIR analysers are ideally suited to raw gas analysis from fires, as demonstrated by the Andrews et al. [171] using the Temet Gasmet CR-2000 heated FTIR analyser. Other heated FTIRs are available, such as the Horiba MEXA-6000FT, which has pre-calibration of the toxic gases.

Heated FTIR gas analysis combined with heated gas sampling systems is able to provide reliable raw gas measurements of fire toxic species. The introduction of a raw (pre-dilution) sampling point to fire toxicity tests for heated gas analysis enables the toxic conditions in the room of origin to be determined and not the post dilution oxidation of these conditions as in most current fire toxicity research. A significant problem is obtaining a mean ceiling gas composition and two techniques for this were shown to be viable. Raw gas oxygen analysis is a further problem if this is done using a dry sample using a paramagnetic analyser, as the water content has to be corrected for water loss which is difficult to calculate. Raw gas analysis using heated zirconia electrochemical probes is recommended. To obtain the HRR inside a compartment by oxygen consumption calorimetry raw oxygen analysis on a wet basis is required together with either the measured fire sample mass loss or the compartment air mass flow rate. However, both measurements are recommended as this enables the fire equivalence ratio to be determined, which is difficult to do by carbon balance for fuels that may have mixed composition and with significant water content (e.g. wood).

3.1.2 Sampling systems

This work used online (continuous) sampling method for spectrometric analysis. This method is considered more appropriate for sampling products from a rapidly changing phenomenon such as fire in comparison to other batch sampling methods (i.e. sampling using solution or solid absorbers and sampling using gas bags) which are considered to be collecting integrated or average samples [153] that can be useful for monitoring other phenomena such as monitoring industrial emissions for environmental purposes.

Generally, sampling systems include the following parts: Probe, Sampling line, pump, filters and sample treatments (drying agents and cold traps). This section will identify the specifications of the sampling system parts that were used in this work. Set up arrangements (location, length, etc...) of the sampling system for each experiment will be identified later within this chapter.

3.1.2.1 Sample probe

Sampling probes used in the experimental work of this thesis were:

a) Sampling from the real scale experiments: two stainless steel tubes (with an outer diameter of 8mm and inner diameter of 6mm) were used, each had ten 2mm holes for collecting samples however the spacing between the holes was different. One had 33 cm spacing length (ideal for sampling from the centre of the room), while the other had 8cm spacing length (ideal for sampling from door opening or the corridor).

b) Sampling from the bench scale experiments (standard cone calorimeter tests, and modified controlled atmosphere cone calorimeter CACC): two sampling points were used; raw and diluted sampling points (discussed in 3.1.1). The diluted sampling point is the standard sampling probe of the cone calorimeter apparatus. Located at the end of the exhaust duct, a ring sampler with 12 holes facing downstream, minimizing the chances of blockage by soot particles. Secondly, the introduced raw sample point which is a 5mm inner diameter stainless steel probe with an open end, sampling from the added chimney (see Section 3.3.3) on the top of the conical heater.

3.1.2.2 Sampling lines

Sampling lines used in this work are made of PTFE (Polytetrafluoroethylene) with an outer diameter of 6 mm and an inner diameter of 4.5 mm. When used as heated sampling lines it was aimed to be heated to 180 ^{o}C during tests. PTFE sampling lines are capable of handling temperatures up to 200 ^{o}C.

PTFE tubes are non-reactive material especially with acid gases, PTFE sampling tubes are considered suitable especially for minimizing acid gases losses due to condensation and reactivity. However, it was suggested [153] that HCl and HBr losses are imminent particularly due to adsorption onto soot particles and gas sampling lines, therefore it is recommended for sampling lines to be shorten as much as possible to reduce the chances of these loses. Also it is important to highlight that these recommendations are directed at unheated sampling systems. Using heated sampling systems would reduce adsorption in the sampling systems.

3.1.2.3 Sampling pump

Pumps used as part of the sampling system have to supply a consistent volume of the gas sample to gas analysers. In this work the two main types of pumps were used; heated and unheated pumps depending on the sampling system. Details of each pump used in the experimental work of this thesis would be specified later in this chapter in 3.2.3.3.

The location of the pump is very important; having the pump located upstream from the analyser can eliminate the chances of creating a pressure drop in the analyser's gas cell, which consequently can severely affect the accuracy of the gas analysis [166]. For all the experimental work in this thesis, the pump has always been located before gas analysers. And when needed a heated pump is used to supply a heated gas sample to the gas analyser with the same temperature of the heated sampling system.

3.1.2.4 Soot filters and sample treatments

Gas analysers require the gas sample to be soot-free in order to eliminate the chances of soot deposition inside the gas cell which can have a severe impact on the optical measurements of gas concentrations. Therefore, soot filters are essential for all sampling systems, heated soot filters can be used for heated sampling lines.

For gas analysers with ambient temperature gas cells (unheated gas cells) additional sample treatments to ensure that the gas sample is dry (water free) are required. Condensing the water contained in the gas sample can be achieved by passing the gas sample through two main gas treatments; cold traps and desiccants. Cold trap is an area of the sampling system where the gas sample would pass by very low temperature atmosphere forcing any condensation to occur. This can be achieved by using a refrigeration unit set temperature below 4 ^{o}C or by using an ice bath where the moisture can condense. Desiccants or drying agents are used as well to remove moisture from the gas sample, Silica gel is very common desiccant due to its porosity and efficiency in capturing moisture.

Paramagnetic oxygen analysers normally use soda lime to remove CO_2 however there are evidence that soda lime also removes NO_2, both gases can interfere with oxygen measurements [161, 272-274].

3.1.3 Fourier transform infrared (FTIR) gas analysis technique

FTIR has been used in fire research for 15 years and was extensively investigated in the European SAFIR project, as summarised by Mikkola [164] and Hakkarainen et al. [165]. In this work (SAFIR project) the sample line and filter were hot >150 ^{o}C, but the pump was downstream of the FTIR which is not recommended due to problems of sample cell pressure control. A PTFE sample tube was used inside the heated sample line, as in the present work. However, the detector was not liquid nitrogen cooled and the minimum detection limit was about 10 times that in the present work. This work showed that by using quantitative target factor analysis (QTFA) there was no need for external calibration of the instrument in use. Once the instrument was calibrated this was fixed and only zero gas was required on a daily basis. This is the principle on which the Gasmet FTIR, made in Finland, operates and was a direct outcome of the SAFIR project which was led by researchers in Finland. FTIR for fire toxicity research was verified and validated by a number of research projects [167, 168], Also an international standard for the usage of FTIR to assess fire effluents was published in 2006 [169].

In 2005 Andrews et al. [171] were the one of early groups to publish fire toxic gas results using the pre-calibrated Temet Gasmet CR-2000 analyser. All toxic gases that occur in fires can be analysed simultaneously, also the instrument can be used to measure the total unburnt hydrocarbons by summation of the individual hydrocarbons. The Temet Gasmet CR-2000 has liquid nitrogen cooling of the detector, which gives 0.3 – 2 ppm minimum detection limits, depending on the gas. The main advantage of the heated FTIR is that it can measure high temperature raw sample gases [171]. The high sample temperatures (180 ^{0}C) keep all the toxic gases of interest in the gas phase and also enable all unburnt hydrocarbons to be measured so that the fire compartment combustion efficiency can be correctly determined. Another important advantage is that FTIR can quantify concentrations of a wide range of toxic gases with a very high accuracy using the same heated sample and as a function of time. The present FTIR can be operated with full spectral scans at 10Hz and spectral averages every 1 or 2s can be used. However, fire transients do not occur on this time scale and time averaging every 5s or 50 scans gives good resolution of the toxic gases.

As with any newly introduced technique, the main limitation of the application of the FTIR is that it is not the most common gas analysis technique. Also the ability of modern FTIR analysers to be calibrated once, normally at the manufacturers, and to not need recalibration has been difficult for researchers in fire toxicity to accept [169, 171, 241, 242]. It is shown how to take the advantage of the high temperature analysis to achieve accurate measurements of raw fire toxic gases, so that post oxidation of the gases as air dilutes the products of the fire is avoided.

3.1.3.1 Principles of FTIR measurements

Fourier transform infrared (FTIR) is an infrared spectroscopy technique for chemical analysis compounds. The technique is based on two basic principles; firstly, molecular vibrations take place in the infrared region, secondly, each compound has a characteristic absorption frequency and the intensity of absorption is correlated to the concentration of that compound. Most targeted gases have their peak vibrations in the wavelength range from 2.5 – 16 μm equivalent to the wave number range 4000 – 625 cm^{-1}.

The Gasmet FTIR CR-2000 consists of two main parts (illustrated in Figure 2-22). Firstly, the heated detection cell (up to 180 ^{o}C), which has a multi-pass fixed 2 m path length and a sample cell volume of 0.22 litres. In the detection cell all three parts (sample cell body and 2 mirrors) have a special rhodium coating and gold layers to achieve high corrosion resistance. Secondly, the liquid nitrogen cooled MCT (mercury-cadmium telluride) spectrometer detector enables the resolution of 8 or 4 cm^{-1}, with a minimum scan frequency of 10 Hz and covers wave number range from 600 to 4200 cm^{-1}. The motion of the moving mirror creates the optical path difference required to generate wavelength range.

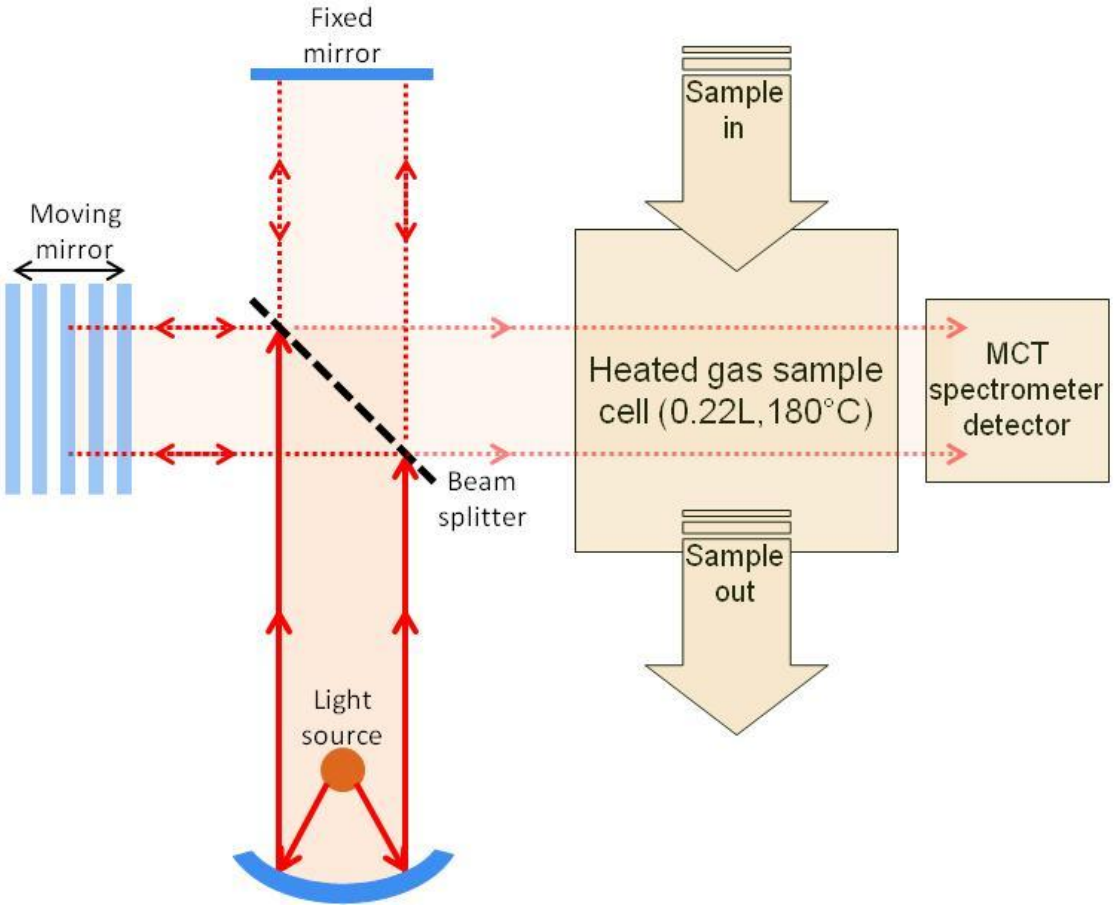

Figure 3-2: FTIR working principle.

The Gasmet portable 180 ^{o}C heated system enables sampling undiluted hot wet gases. PTFE heated lines connected to the FTIR gas cell through heated pump and heated cylindrical filter. A heated pump located before the gas cell has the advantage of preventing pressure drop at the gas cell [168]. The detection chamber of the FTIR is also heated at 180^{o}C so that all gases are analysed and calibrated in the presence of water vapour.

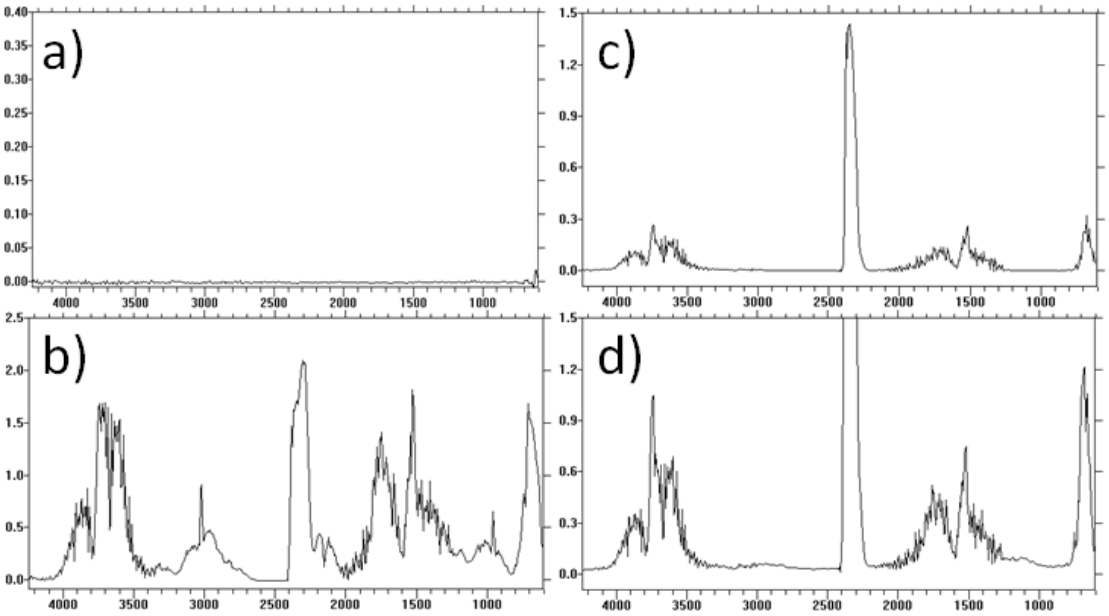

Figure 3-3: FTIR spectrums collected; a) while zeroed by flushing the nitrogen gas. b) From a full scale fire test 3. c & d) From cone calorimeter tests using raw and diluted sampling points**.**

Figure 3-3a shows a typical FTIR spectrum resolution for zero nitrogen. Figure 3-3b shows a full scale compartment fire test [260] with multi-hole fire compartment ceiling gas sample probe. All the peaks in this spectrum have to be in the instruments calibration for the quantitative analysis to be valid. It is not sufficient to calibrate for the species of interest, all the significant species in the spectrum have to be calibrated for. Figure 3-3c shows a diluted gas sample spectrum from a cone calorimeter pine wood fire tests. Figure 3-3d shows the spectra for the raw gases from a pine wood fire taken from a chimney mounted on the cone discharge. The similarity in the raw and diluted spectra can be seen, but the raw spectra have higher concentrations and better resolution of the spectra.

3.1.3.2 FTIR measurements validation

The Gasmet FTIR used in the present work has also been used by Andrews, for exhaust emissions measurement in on-road vehicles and there was an extensive calibration exercise undertaken for this application [275, 276]. This included comparison over a legislated transient test for vehicle emissions on a legislated test facility. This demonstrated good agreement with the legislated measurement techniques for CO, CO_2 and NOx. The Gasmet FTIR had reference gases calibrated by the manufacturer for 63 different gases. Also the annual maintenance and water calibration is carried out by the manufacturer. The FTIR was validated again for this work using different methods. Firstly, certified bottles of mixed gases (e.g. 16.23% CO_2, 1063ppm Hexane and the rest Nitrogen) were used. Figure 3-4 shows a demonstration of the accuracy of the FTIR calibration when compared with certified gas bottle concentrations. There was no need for daily calibrations of the FTIR as there is of more conventional gas analysis instruments. Secondly, during fire tests an NDIR was connected to the outlet of the FTIR. The outlet gas sample was dried using an ice bath and drying agent before it enters the NDIR to be analysed for CO and CO_2. Figure 3-5 shows very good agreement between the two independent gas analysers for CO under fire conditions in laboratory test (cone calorimeter) and full scale test (Jersey test 8) see Figure 3-6. It can be seen in both examples that FTIR is more sensitive to sudden changes in concentrations, this can be attributed to the low flow required for the NDIR (eighth FTIR's minimum flow required). Meaning that it would take longer for the gas cell to be filled with gas sampled which can influence measurements from rapidly changing environment generated in a fire compartment. However these differences between FTIR and NDIR are only observed when there is an abrupt change in gases production occur (ignition or flashover).

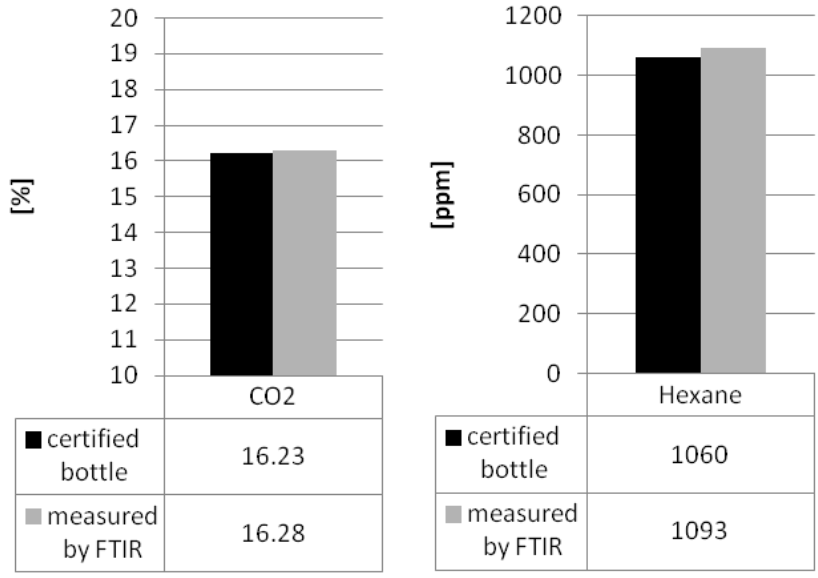

Figure 3-4: Certified mixture bottle validation results.

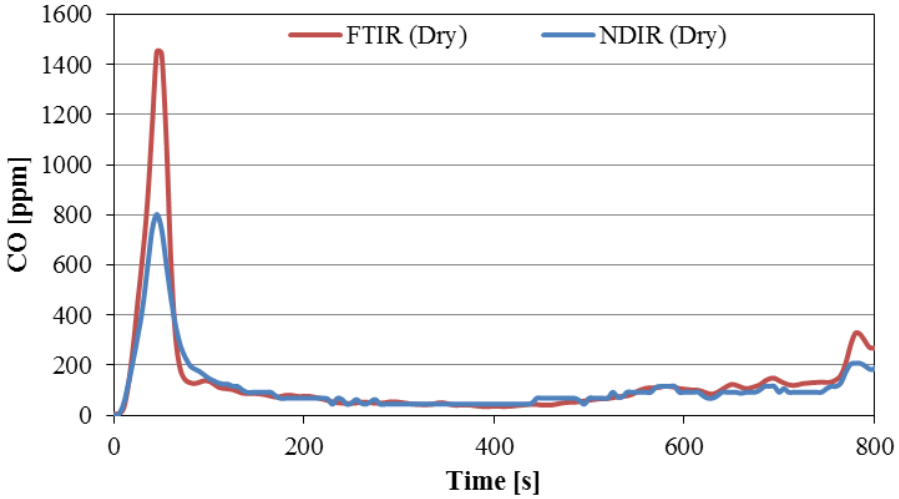

Figure 3-5: Carbon monoxide measurements (FTIR & NDIR) from cone calorimeter test.

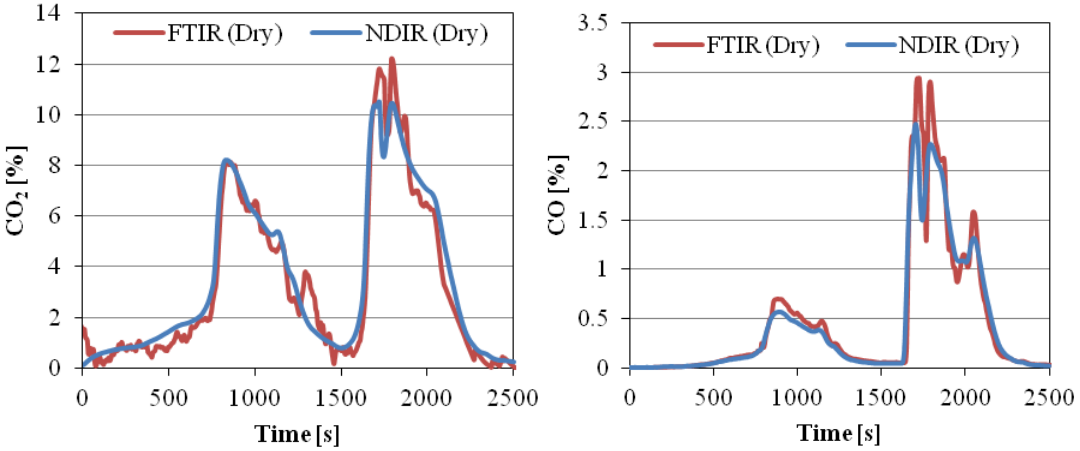

Figure 3-6: FTIR & NDIR measurements for fire emissions sampled from full scale test; Left: Carbon dioxide. Right: Carbon monoxide.

3.1.3.3 Analysing FTIR spectra

The recorded FTIR sample spectra were analysed (qualitatively and quantitatively) using Calcmet software [277]. Calcmet was developed by Gasmet the manufacturer of the CR 2000 FTIR gas analyser and uses modified Classical Least Square (CLS) algorithm. Calcmet can analyse the sample for more than 50 components. However, it is not recommended to analyse more than 50 components at one time for the best accuracy of analysis. Calcmet provides many useful features, such as simultaneous analysis, identification of gas components using a library search routine and ensuring quality of analysis by monitoring residual absorbance. The maximum acceptable value for overall residual is 0.2, when it is exceeded the spectrum is reanalysed with less interfering species to improve the quality of the readings by reducing the residual value, if that cannot be achieved then the analysis are ruled out as inconclusive and discarded [277].

Table 3-3: Concentration Ranges and Number of Data Points for FTIR Calibration Curves.

Gas name	formula	No of calibration points	Calibration range [ppm]
Carbon dioxide	CO_2	10	3% – 30.1%
Carbon monoxide	CO	26	20 – 9,960
Nitrogen monoxide	NO	36	20 – 10,032
Nitrogen dioxide	NO_2	9	20 – 4,885
Sulfur dioxide	SO_2	12	20 – 1,000
Hydrogen chloride	HCl	7	20 – 489
Hydrogen Fluoride	HF	4	33.9 – 100
Hydrogen Bromide	HBr	6	20 – 592
Formaldehyde	CH_2O	5	39.8 – 218.8
Hydrogen cyanide	HCN	6	20 – 500
Acrolein	C_3H_4O	5	50 – 500
Hexane	C_6H_{14}	3	50 – 500
Water	H_2O	22	0.1% – 40%
Nitrous oxides	N_2O	20	20 – 5,000
Ammonia	NH_3	12	20 - 1000
Methane	CH_4	21	20 – 5,000
Ethane	C_2H_6	9	20 – 1,000
Propane	C_3H_8	13	20 – 2,000
Ethylene	C_2H_4	13	20 – 2,000
Benzen	C_6H_6	5	50 – 500
Formic acid	CH_2O_2	5	50 – 500
Acetic acid	$C_2H_4O_2$	5	50 – 500
Acetylene	C_2H_2	8	20 – 1,000
Acrylonitrile	C_3H_3N	2	50 – 200

The Gasmet FTIR used in the present work had the calibration points and ranges of main components frequently used in fire research FTIR gas analysis is shown in Table 3-3. The Gasmet CR2000 FTIR used in the present work was calibrated for 64 gases at variable concentrations totalling 411 calibration curves available to be used for qualitative or quantitative analysis.

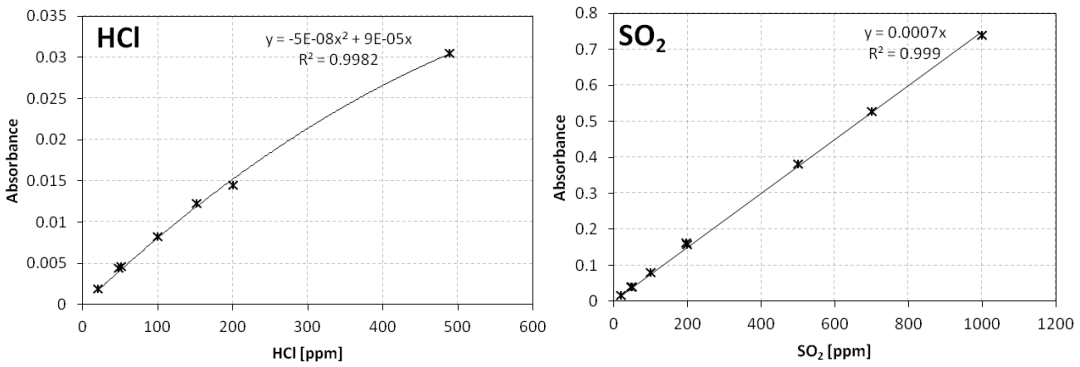

Figure 3-7: **Left:** HCl non-linear calibration (20 – 500 ppm). **Right:** SO_2 linear calibration (20 – 1000 ppm).

Examples of these calibration spectra are shown in Figure 3-8. A typical calibration of one of the compounds in Figure 3-8 is that for HCl which is shown in Figure 3-7 and is a slightly non-linear calibration. A linear calibration for SO_2 is shown in Figure 3-7. All the calibrations in the instruments have a best fit equation which is used to extrapolate the calibration beyond the specific gases used. The instrument indicates when this has been done and the accuracy of this has been tested using a Dekati 10/1 diluter to show that extrapolation by a factor of 10 above the maximum concentration range has an error of <10% and the instrument was therefore used beyond its calibration range where necessary in some fires [278].

Understanding the interference between different gas spectrums is very crucial for the analysis process of the captured spectrums. Figure 3-9 is created based on the active regions for each of the 64 gases that can be observed from reference spectrums shown in Figure 3-8.

Figure 3-10 illustrates the identification of SO_2 in the raw toxic gases for an aircraft fabric seat cover in the cone calorimeter test with controlled air supply [244]. An example of the SO_2 yields as a function of time is shown in Figure 3-11.

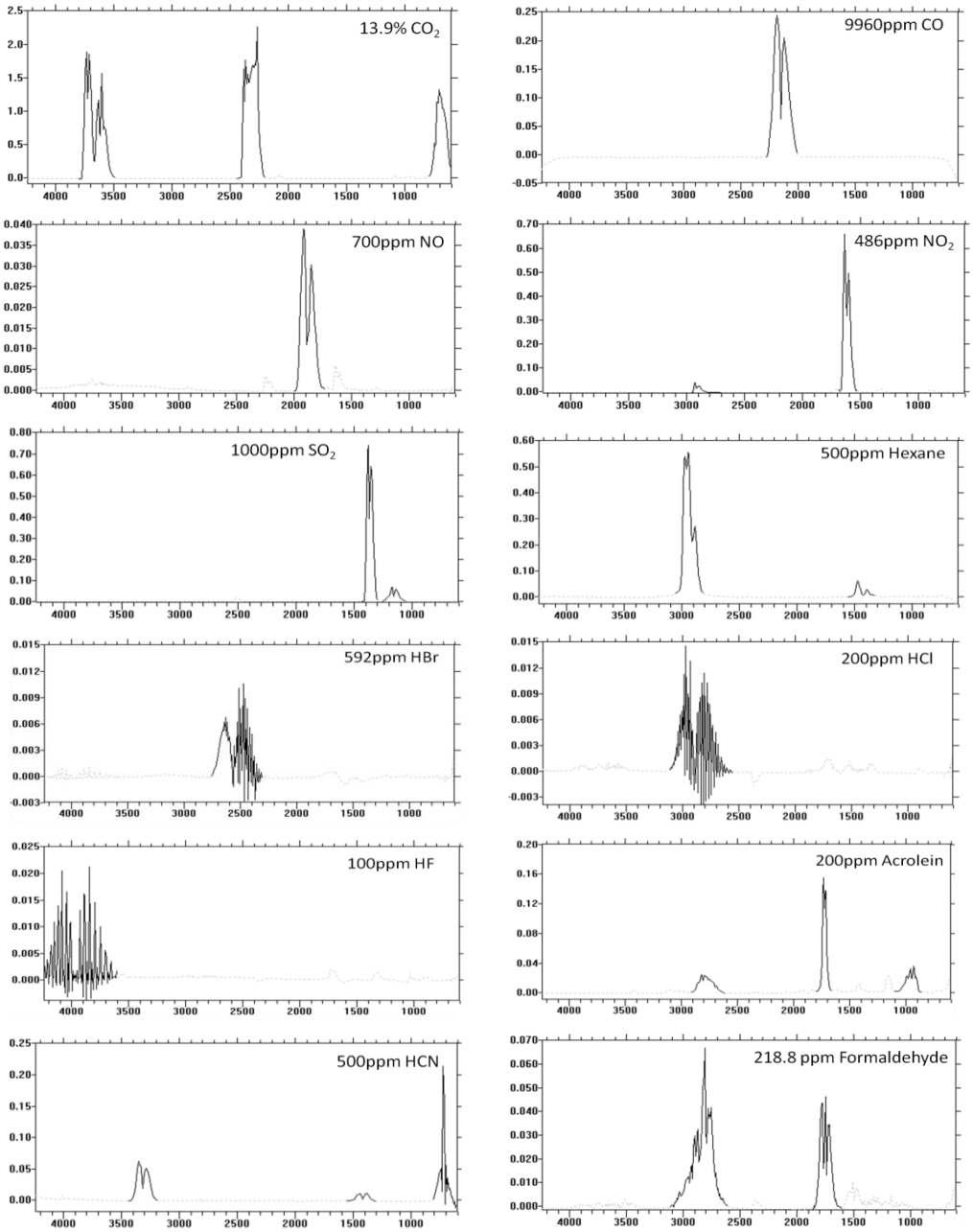

Figure 3-8: Examples of calibration curves used for FTIR analysis.

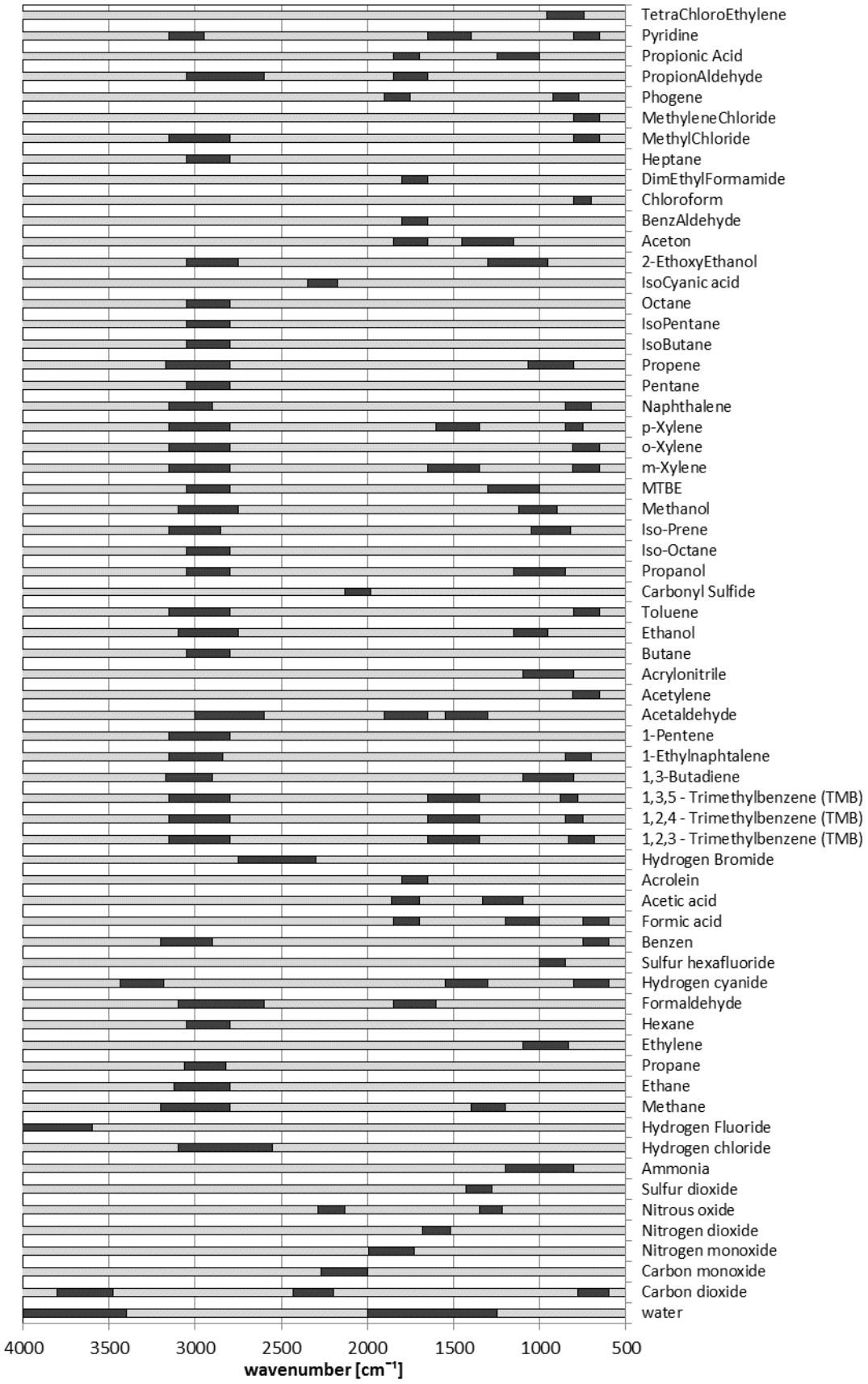

Figure 3-9: Spectral absorption regions for each gas component

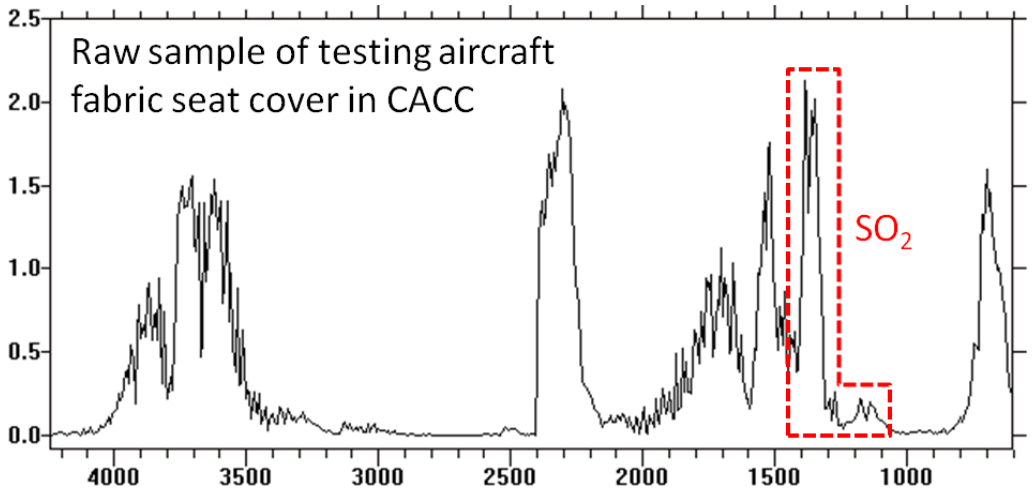

Figure 3-10: Absorption spectra for a raw CACC hot gas sample analysed by the FTIR showing the SO_2 absorption peak used for SO_2 quantification [224].

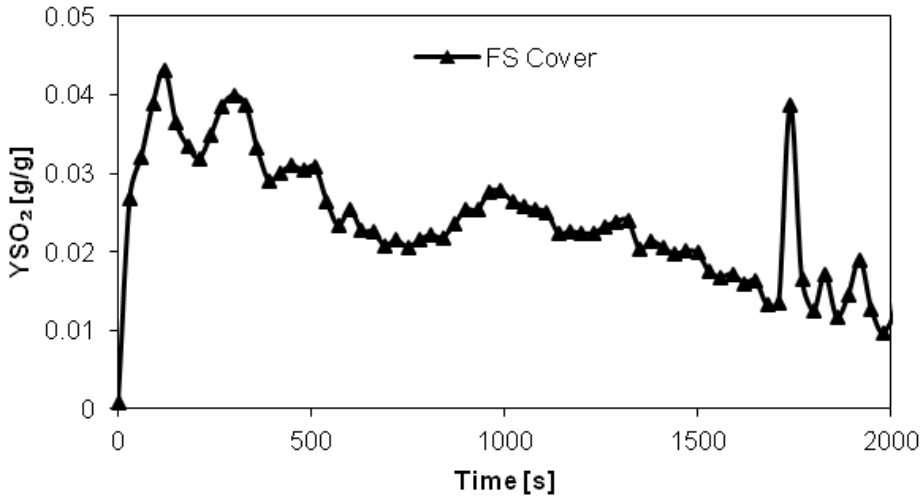

Figure 3-11: The SO_2 yield as a function of time for an aircraft fabric seat cover [224].

This Gasmet FTIR when adequately calibrated and used with appropriate hot sample gas transfer equipment, it form a valuable instrument in fire toxicity research. FTIR of this type with similar software is a powerful tool for fire toxicity research. This equipment has been utilised in Leeds for researching fire toxicity in large scale room compartment wood fires [260, 279, 280], pine wood crib fires [171, 242], pool fires [171, 244, 270] cotton towel fires [240], acrylic curtain fires [241] and aircraft passenger car material fire [224, 225, 281]. These publications show the versatility of this instrument for practical fire toxicity research.

3.1.4 Other gas analysis techniques used in this work

3.1.4.1 Non-dispersive infrared (NDIR) gas analysis technique

Non-dispersive infrared gas analysis is based on the optical dispersion of the light through the gas sample. This technique is widely used in different fields (e.g. continuous emission monitoring and combustion research) and is recommended for fire effluents analysis by the international standards organization [153, 154]. As mentioned earlier in the FTIR section, each species has its own finger print when light is applied on them. And this finger print can be recorded by the absorbance of light at specific wavelength ranges (each species has its own range as shown earlier in Figure 3-9). NDIR usually have a limited number of species to be analysed and depending on the targeted species its wavelength will be the focus of the light absorbance measurement and eventually a volumetric concentration measurement can be achieved. For example to measure CO_2, the targeted wavelength normally is 4260 nm (equivalent to 2347 cm^{-1}).

In this work, a Hartmann & Braun URAS-10E analyser was used in most tests for both full-scale and bench-scale tests. This analyser can measure CO at different ranges (0-1000ppm and 0-5%) and CO_2 at 0-20%. URAS-10E can handle sample temperature between -25 and +65 C as long as it is a dry sample with a dew point of 5 degrees below ambient temperature, in order to avoid condensation. The analyser operational flow rate range is between 20 to 60 L/hr equivalent to 0.33 and 1 L/min. It has a zero drift up to ± 1% of span per week and non-linearity of less than or equal to ± 2% of span [282].

3.1.4.2 Paramagnetic oxygen analysis

Paramagnetic oxygen analyser main components are: magnetic field, diamagnetic substance (nitrogen), turning dumbbell (with two glass spheres filled with the diamagnetic substance and a mirror fix in the middle of the rod), light source and light receiver (photocell).

The pair of magnets creates a magnetic field across the gas cell where the sample is introduced. When there is no oxygen in the gas cell the dumbbell is static as the diamagnetic substance (nitrogen) inside the spherical glass on both ends of the dumbbell will be held in the middle by the magnetic field, where the photo cell can detect that based on the reflected light on the mirror. As soon as oxygen is introduced it will start create a layer between the diamagnetic spherical glass and the magnetic field oxygen is paramagnetic and depending on the quantity of oxygen the dumbbell turning torque will vary, the photo cell can monitor and measure the oxygen concentration based reflected light on the rotating mirror [154, 161, 162].

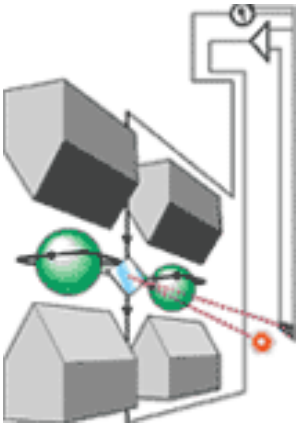

Figure 3-12: Schematic diagram of the paramagnetic oxygen analysis concept from [163].

The Paramagnetic Spectrometer instrument used was a Series 1400 made by SERVOMEX [274]. It reads oxygen levels for a range of 0 to 100%. The oxygen concentration was presented as a percentage with a resolution of 0.01 percent. The measurements from these detectors were taken from a dry analysis so they will need to be converted to wet analysis if they are to be used for comparison.

3.2 Full scale experiments (Jersey tests)

Eight full scale experiments were conducted for the purpose of comparing measurements to reduced scale lab experiments, from the literature as well as from experiments conducted by the author. This section will detail the experimental setup used for conducting the full scale tests. These tests were carried out in abandoned bungalow in St. Helier, Jersey, about to be demolished. The results of these tests are presented primarily in Chapter 5 and are referred to elsewhere within the thesis as the "full scale experiments" or "Jersey tests". The building details will be presented in terms of layout, size and materials. Then the experimental plan and setup of the equipment will be detailed.

Figure 3-13: View of School road bungalows starting from #68 (used for Test 8) on the right then #67 (used as a control room for test 8) and sequence continues till #58 on the far left.

3.2.1 The buildings

The tests were carried out in abandoned bungalows about to be demolished. The bungalows were constructed in the 1960's and were of traditional build, 100 mm brick wall outside and 100 mm concrete block work inside with 50 mm cavity between the two layers. The bungalow consisted of a 1.1 m wide hallway connecting the main entrance (sole source of air) to the bungalow with the burn room door (0.8 m width by 2 m height), sealed kitchen and bathroom on either sides of the corridor. The ceilings in the burn room (living room) were double lined with 12.5 mm plaster board. The back wall to the living room was also double lined. This effectively gave the room one hour fire protection and also ensured that any air for the fire was only coming from the hallway. The burn room was 17.4 m^2 in floor area (4.2 m width x 4.15 m depth) and 2.35 m in height. The burn room within the bungalow layout is shown in Figure 3-14.

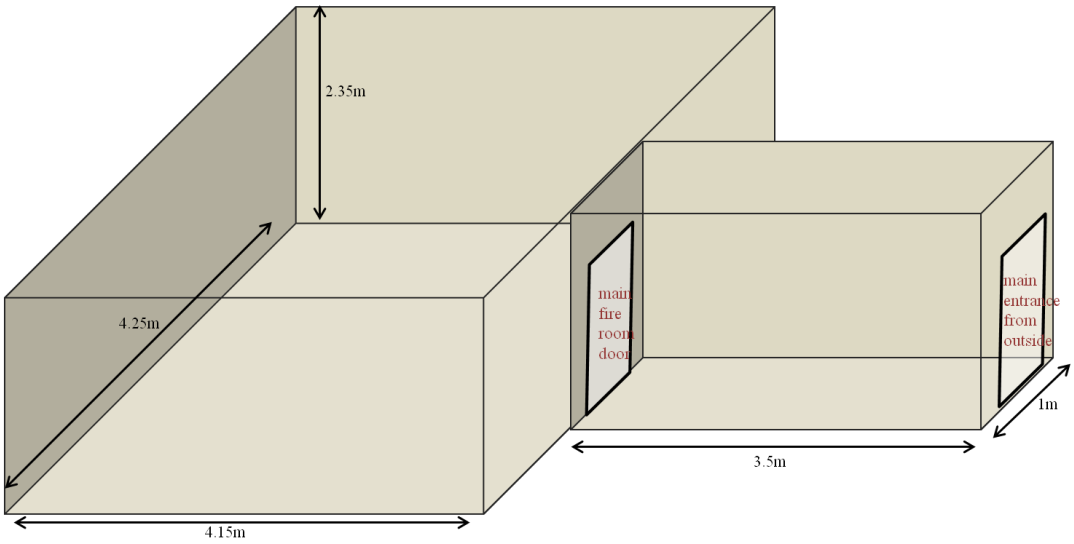

Figure 3-14: geometry and dimensions of the full scale experiments.

3.2.2 Design of experiments

While designing Jersey tests, the main aim was to produce toxicity measurements of real scenarios of compartment fires, comparable to bench scale fire tests and useful for modelling purposes. So the concept followed in designing these tests focused in single item fuels, making it possible to produce a comparable bench-scale fire tests. However mixture of typical fire loads with different compositions was also included in the test plan in order to study similarities and differences of compartment fires and their overall toxic products. The main disadvantage of testing mixed items with diverse compositions is that during the spread of the fire different items would burn and produce cumulative mixed emissions, making it difficult to separate and trace the emissions released back to their origin fuel. This disadvantage means that results from tests with such mixed fuel load are not the most practical way to determine key toxic emissions characteristics for specific materials such as yields, however these results can add to the literature data in terms of concentrations emissions yielded during realistic mixture of fuels compartment fires. Table 3-4 details the test plan that was conducted, showing the fuel load type and the specific bungalow used for each test. Details of each fuel and layout of the fire load will be detailed later in this chapter. Thermal and emissions' products monitoring equipment setup for each bungalow will be detailed later in this chapter.

Table 3-4: Full-scale (Jersey) tests list.

Test #	Date	Fuel	Ventilation	Bungalow #
1 1a / 1b	2nd July 2011	Cotton towels	Door closed / Door open	64
2 2a / 2b	3rd July 2011	Settee	Door closed / Door open	64
3 3a / 3b	4th July 2011	Wooden pallets stack	Door closed / Door open	64
4 4a / 4b	6th July 2011	Cotton towels	Door closed / Door open	66
5	6th July 2011	Wooden pallets stack	Door open	66
6	7th July 2011	Pool fire	¼ Door open	66
7	7th July 2011	Pool fire	½ Door open	66
8 8a / 8b	8th July 2011	Full living-room furniture	Door closed / Door open	68

3.2.3 Instrumentation

Instrumenting the full scale fire tests is crucial element in providing the targeted results for these tests. This section details equipment configurations and their accuracies that were used in monitoring the compartment fire characteristics and its emissions. Starting with detailing the configuration of the weighting platform used that was an important element in determining the heat release rates of compartment fires through mass loss rates measured. Then details of thermocouples used and the influence of compartment fires on their readings are explained. After that the configuration of the gas sampling system used to collect and convey smoke sample to gas analysers is detailed. Finally details of the equipment used for visual imagery for the tests are given.

3.2.3.1 Mass balance

Fire load is mounted on an insulated weighting platform supported on four load cells, in order to monitor the burning rate of the fire load. The load cells were used with the single item tests (all tests except test 8). Four 80 kg, NovaTech, F256 DFSOKN compression load cells were used at the 4 corners of the fire platform, which was a steel frame covered with two layers of plaster board on which the fire load was placed. Up to 320 kg of fuel could be supported and the mass loss monitored to a combined output resolution of 10g and maximum non linearity error at around 40 g. The load cells were protected by a thick high temperature resistance Morgan ceramic fibre ‘super-wool’ blanket. As a safety precaution a thermocouple was positioned underneath the platform to monitor insulation efficiency and temperature around the load cells, all four load cells survived the extreme fire conditions.

3.2.3.2 Thermocouples

Temperatures within the fire compartment were monitored using type K mineral insulated exposed junction, 1.5mm bead, 613 stainless steel sheathed thermocouples. The thermocouple temperature readings are used to represent the surrounding gas temperature when in fact they are the temperatures of the metal thermocouple junctions themselves which are different to the actual gas temperatures. The main heat transfer mechanisms are convective heat exchange between the gas and the thermocouple bead, and radiative heat exchange between the bead and the surrounding environment (which is usually taken to be the enclosure walls). In the hot gas layer the thermocouple tends to lose heat by radiation while it gains heat by radiation in the cold layer. Accurate evaluation of the errors requires full knowledge of local convective heat transfer coefficients, temperatures of the bead and of the surrounding surfaces and gases, their respective emissivities (as well as the temperature dependence of these emissivities). Evaluation of such errors is therefore not a routine task.

Based on the work of Blevins [283] and Pitts et. al [284] it is possible to get an approximation of the error for the range of conditions in the present tests. For upper layer temperatures of 900-1000K, lower layer temperatures of 500-600K and wall temperatures assumed below 600K, the absolute error at upper layer measurement was 10-15% and of the order of 5% at the lower layer but increases significantly if the walls are taken to be at higher temperatures. However, the assumption of a clear gas volume (non-participating media) on which Blevins [283] and Pitts et. al [284] used is not really valid in typical compartment fires as the flame and smoke would have a high soot content and thus would be involved in radiation exchange with the thermocouples.

In more realistic full scale sooty (polyurethane and furniture) fires Luo [285] showed that the reading from a bare thermocouple could be more than 100 K higher than the gas temperature obtained from the suction pyrometer during the flaming fire stage and more than 200 K higher during the flashover stage. For a clean burning propane burner flame at steady-state the radiation error was negligible in the hot upper level near the ceiling. However, the thermocouple significantly overestimated the gas temperature by more than 80 K in the cool lower level near the floor because of the radiation effects.

The 26 thermocouples used were divided into; central vertical tree (9 Thermocouples), sidewall vertical tree (8 Thermocouples), a ceiling array on a diagonal axis (5 Thermocouples) and three other ceiling thermocouples; inside the room before the door, in the corridor close to the door and closer to the exit door in the corridor. In addition to a thermocouple positioned underneath the weighting platform to ensure a safe environment of operation for the load cells. Thermocouples were positioned as identical as possible for all bungalows however that slight differences were imminent that will discussed thoroughly for each bungalow later in Section 3.2.4.

3.2.3.3 Gas analysis

Heated sampling system was used for transferring emissions to gas analysers. Compiling two sampling probes, 26 m heated sampling lines, two way switching valve and two heated pumps with heated filters in addition to condensing sample treatments before any unheated gas analysis (NDIR and paramagnetic analysers). Gas sample collected were analysed using a combination of heated (FTIR) and unheated (NDIR and Paramagnetic) gas analysers. Figure 3-15 below shows the layout of the gas analysis system in relation to gas sampling probes inside the test compartment. The default setting of the two way switch valve was the central sampling probe of the room and the result presented in the results section are for the raw sample collected by the central probe unless mentioned otherwise. The second sampling probe was positioned above the door for the first four tests (Bungalow #64). For the following tests (Bungalows #66 and #68) the second sampling probe was positioned in the corridor as clearly described in the following Section 3.2.4. Detailed technical discussion of each element of the gas analysis used is covered thoroughly earlier in Section 3.1.

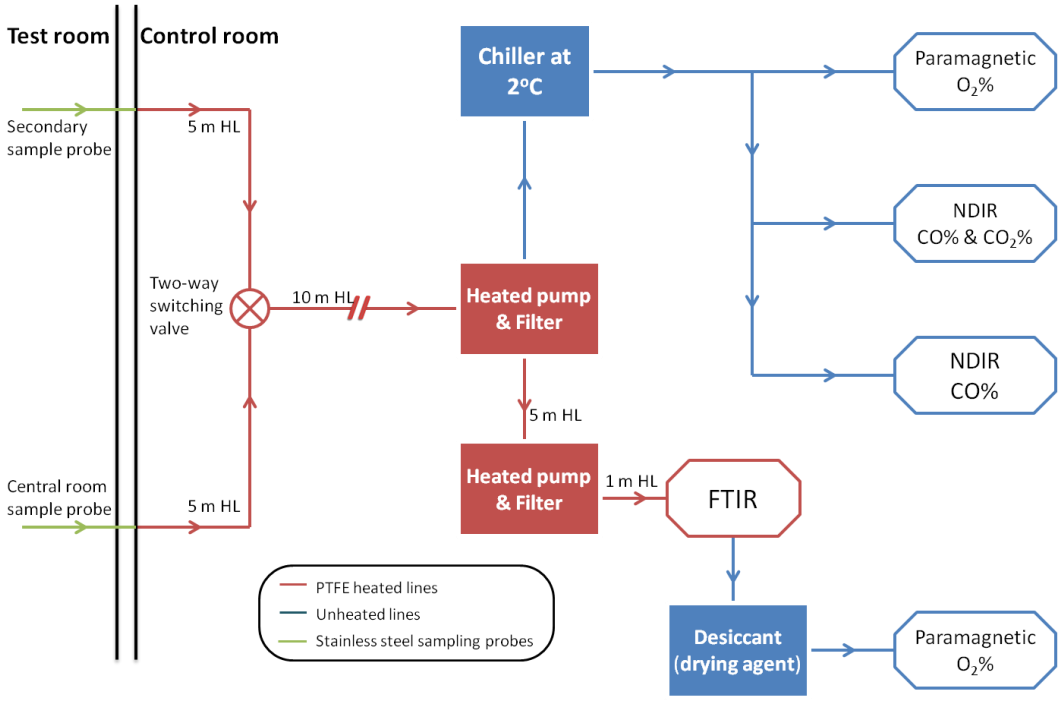

Figure 3-15: **Gas analysis system configuration used in Jersey tests.**

3.2.3.4 Visual monitoring

Visual phenomena are monitored using video recording equipment in addition to still pictures giving an insight to specific compartment fire characteristics such as smoke layer height. These equipment were used generally from the outside of the bungalow looking into the burn room through the main corridor. However, in the first test a video camera was fixed on the helmet of a fire-fighter which gave a good insight into the fire-fighting activities however the stand used could not stand the heat and melted during that test. So the decision was made to protect the equipment by not repeating that trial in the following tests. These images will be presented in the results and discussion section where they fit. Also LED lights were used to aid determining the smoke layer depth when photographs were taken during tests from outside the bungalow, they were positioned at predetermined heights on the opposite wall from the corridor. Details of the LED heights will be given for the relevant imagery when they are presented in the results and discussion section. It is important to mention that these lights are not heat resistant and in most cases they melt down by the end of each test. Examples of these LED lights setup are shown in Figure 3-16.

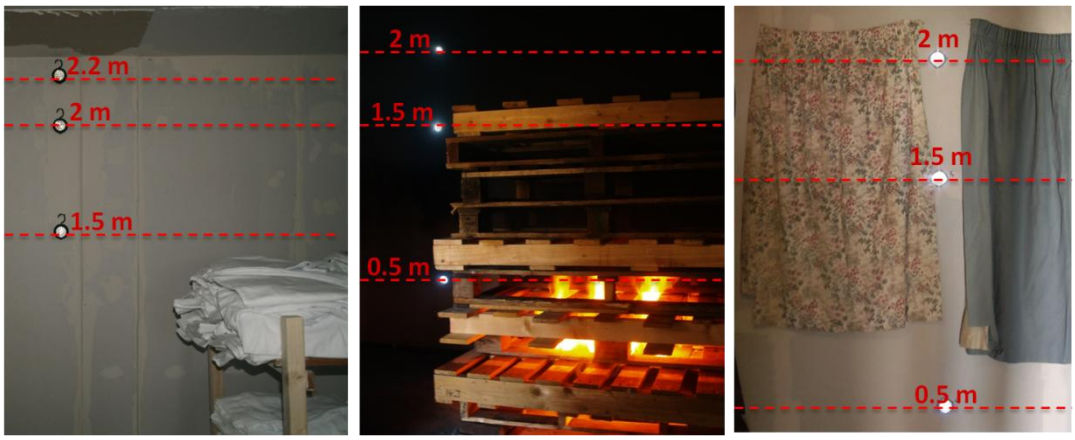

Figure 3-16: LED lights setup for Left: test 1, Middle: test 5 and Right: test 4.

3.2.4 Equipment setup

This part will detail the positioning of the measurements probes within the compartment. Each bungalow of the three bungalows had slightly different setups, this section will detail the setup for each bungalow. The same thermocouple vertical trees configuration used for all the bungalows so the heights of each thermocouple within those trees are detailed in Table 3-5. the positioning of the sidewall tree has changed only at Bungalow #68 (used for Test 8) due to the existence of an electric fireplace on the middle of the sidewall full details of the positioning of both thermocouples tree at each bungalow are discussed below.

Table 3-5: Heights of thermocouples used for vertical thermocouples trees inside the burn room used in all bungalows.

Thermocouples height (central) [m]	**Thermocouples height (sidewall) [m]**
2.31	2.08
2.07	1.83
1.82	1.59
1.58	1.11
1.33	0.86
1.09	0.62
0.84	0.38
0.60	0.13
0.36	

Ceiling thermocouple tips were 155 mm below the ceiling. For ceiling thermocouples fitted inside the burn room were positioned in a diagonal configuration, the positioning of these thermocouples was the same for Bungalows #64 and #66 and for Bungalow #68 the diagonal configuration was turned 90 degrees making the reference wall is the right sidewall instead of the left sidewall in Table 3-6.

Table 3-6: Position of ceiling thermocouples inside the burn room. The reference sidewall for Bungalows #64 and #66 was the northern (left) sidewall while for Bungalows #68 the southern (right) side wall was used as reference for measurements.

Thermocouple name	**From sidewall [m]**	**From back wall [m]**
A1	3.33	0.89
A2	2.69	1.55
A3	1.64	2.71
A4	1.04	3.13
A5	0.34	3.65
Door room	2.26	3.73

3.2.4.1 Bungalow #64 (used for tests 1, 2 and 3)

Schematic diagram shown as Figure 3-17 showing the approximate positioning of monitoring instruments inside the burn compartment. For Bungalow #64 weighing platform was positioned near the right far corner. Ceiling thermocouples positioned in the middle of the corridor 0.7 m and 2.1 m away from the burn room door as shown in Figure 3-18. Central sampling probe was positioned above the sidewall thermocouple tree and hanging 90 mm below ceiling. Secondary sampling probe was fixed to the wall above the door, spacing between the probe and the wall was 20 mm while positioned 200 mm below the ceiling.

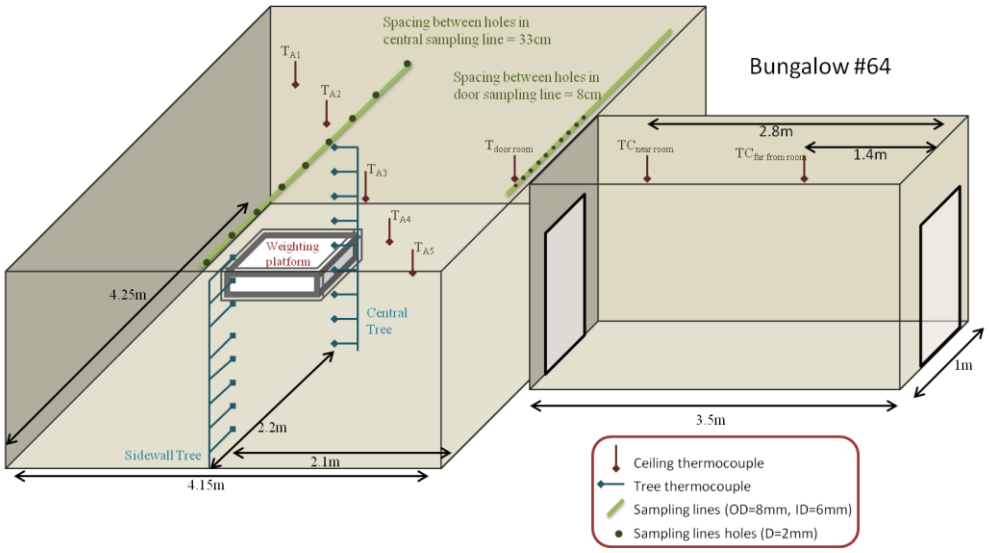

Figure 3-17: Instrumentation of Bungalow #64 (used for tests 1, 2 and 3).

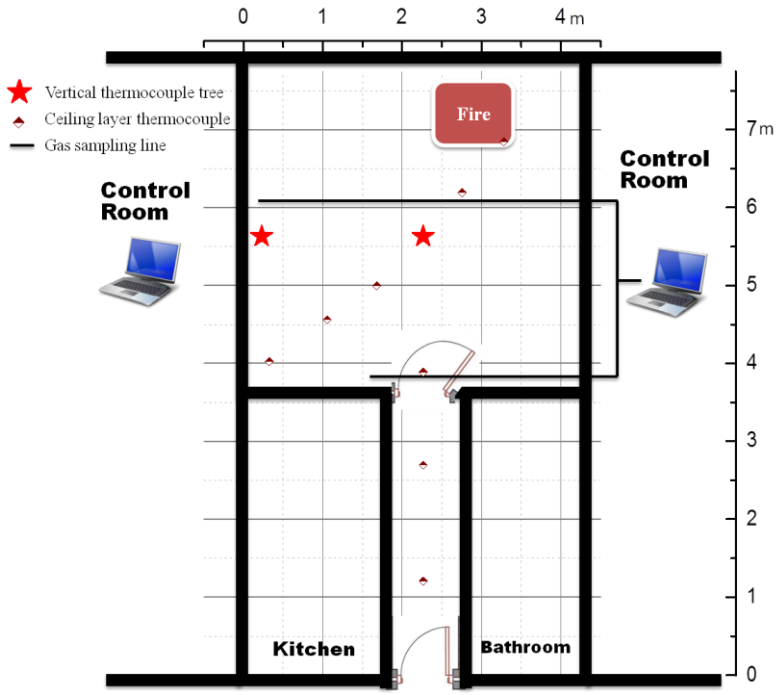

Figure 3-18: A 2-D plan view of instrumentation in Bungalow #64 (used for tests 1, 2 and 3) demonstrating locations of probes.

3.2.4.2 Bungalow #66 (used for Tests 4, 5, 6 and 7)

The approximate positioning of monitoring instruments inside the burn compartment For Bungalow #66 was almost the same as Bungalow #64. However slight changes were made, weighing platform position was changed to be near the left near corner for the purpose of measuring pyrolysis rates for the unignited pile of timber pallet in test 5 (repeat of test 3). Ceiling thermocouples were positioned exactly the same as Bungalow #64 as shown in Figure 3-19. Central sampling probe also had the same arrangement . However secondary sampling probe was moved to be outside the burn room in the corridor 0.8 m away from the burn room door hanging 90 mm below the ceiling, in order to position the secondary sampling probe at a location that can collect the fire emissions leaving the burn room. During test 4 the cupboard door next to the fire load was involved in the fire, the influence of that involvement on the measurements is assessed in the results section. After test 4 the damaged door was removed and the opening was sealed using fire resisted plasterboard for the following tests. During test 7 the ceiling collapsed over the weighting platform and the test was abandoned at that stage.

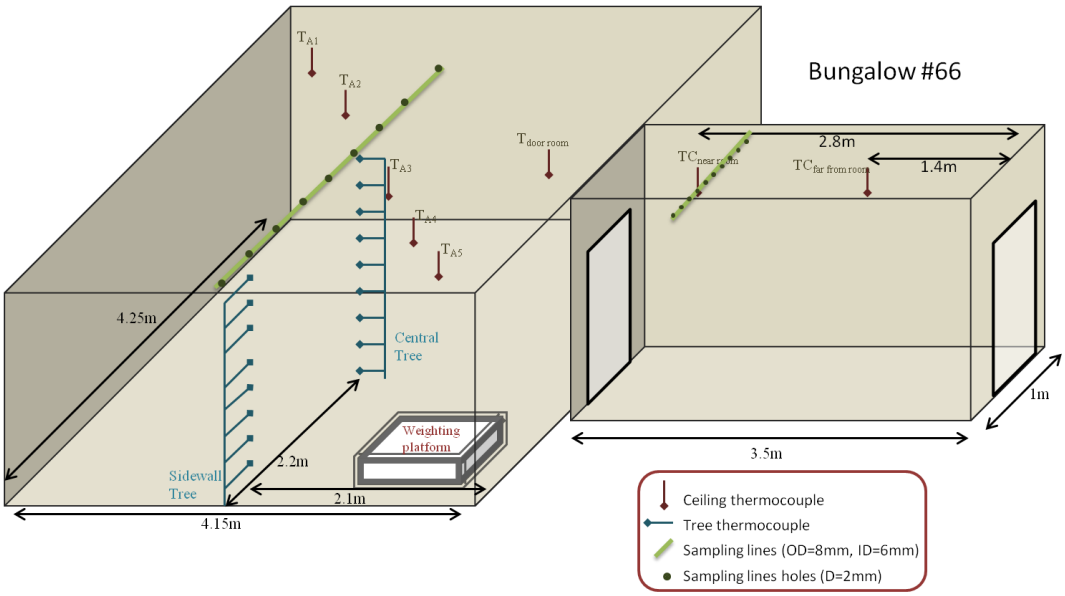

Figure 3-19: Instrumentation of Bungalow #66 (used for tests 4, 5, 6 and 7).

3.2.4.3 Bungalow #68 (used for Test 8)

Bungalow #68 was used for the living room furniture test (test 8) where mixed items at different configurations were placed inside the burn room, more details on the fire load are discussed in Section 3.2.5. As the fire load for this test was much larger than previous experiments it was decided that weighting platform would not be used for test 8. Same vertical thermocouple trees were used heights are shown in Table 3-5, however the position of sidewall tree has been moved to be 0.8 m from the start of the wall) due to an electric fireplace that was fixed on the middle of the sidewall. Ceiling thermocouples inside the room were arranged in the same diagonal configuration (in terms of dimensions, see Table 3-6) however 90^{o} tilted so it will be from the far-left corner to the near-right corner instead of far-right corner to near-left corner used in Bungalows #64 and #66, as demonstrated in Figure 3-20. Same configuration as Bungalow #66 was used to setup emissions sampling probes with the central probe in the middle of the room and the secondary probe in the corridor.

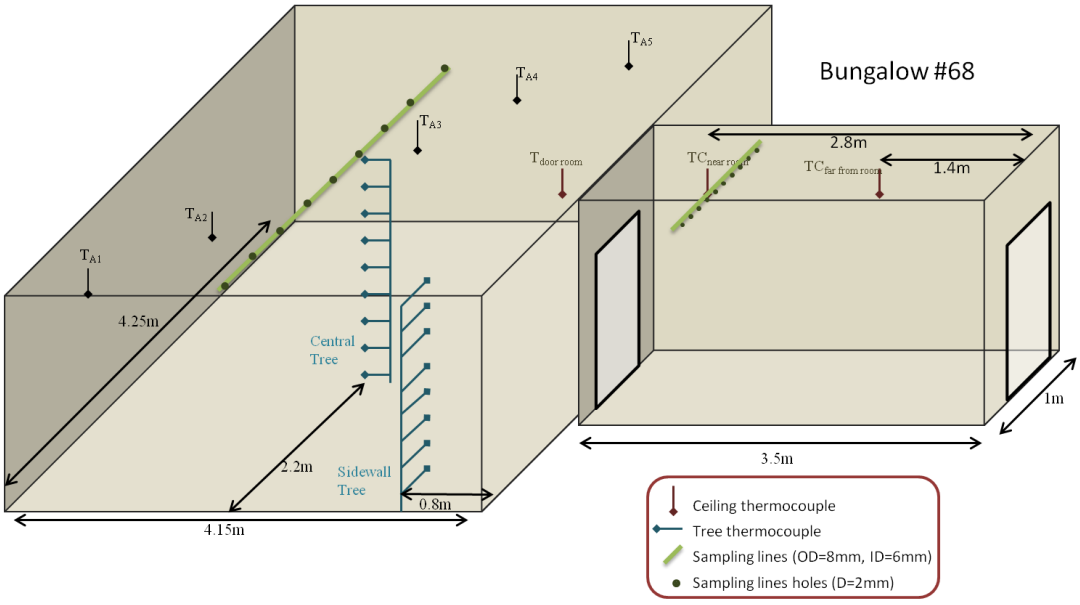

Figure 3-20: Instrumentation of Bungalow #68 (used for test 8).

3.2.5 Fire loads

This part provides details of fire loads used for each test (combination and composition) and their orientation within the burn room.

3.2.5.1 Test 1 (Cotton linings and towels)

The test was intended to be a simulation of a smouldering fire of linen, as a common scenario (fire load) for storage rooms in hospitals, care homes, and hotels. The full setup of the test is illustrated in Figure 3-21 showing the location of the fire load within the burn room. Two-shelf wooden structure was used to mount the fire load on a similar orientation to a storage room as shown in Figure 3-22. Ultimately the wooden structure was involved in the fire especially in the later stages when ventilation become unrestricted when the door was open. The top two sections of the door were glazed which enabled capturing photos even when the door is closed.

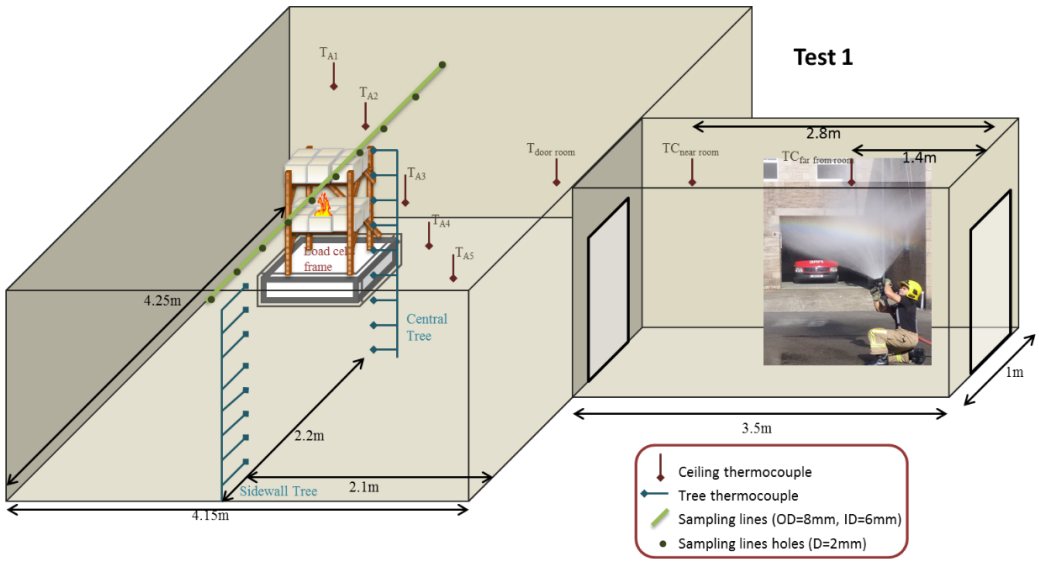

Figure 3-21: Test 1 full setup showing fire load, instrumentation and fire-fighting entrance.

Figure 3-22: Photographic image shows the orientation of the fire load (used in Test 1) on the top of the weighting platform.

During this test a leak was discovered in the gas sample system particularly at the first heated filter, it was fixed by the 25th minute from initiating data logging for the test. This means that the smoke analysis results for the first phase of the test would not cover the initial propagating phase of test 1A (with the door closed). However the smoke analysis of the later stage test 1B (after opening the door) would not be affected by this leak. A combustion based ultimate analysis test was conducted on sample from Test 1 fire load, showing that the bed sheet has mass based composition of 47.09% of carbon, 5.26% of hydrogen and 47.65% oxygen. While the wooden structure showed a mass based composition of 44.86% of carbon, 5.45% of hydrogen and 49.69% oxygen.

Table 3-7: Details of the fire load orientation within the two-shelf wooden structure for test 1.

Position		Fuel type	Weight [kg]
		Wooden shelf support	17.2
Bottom shelf	Centre - front	White cotton towels	1.7
	RH&LH Sides - front	2 piles of white cotton towels (with blue strips)	3.6
	RH&LH Sides - back	2 piles of bedcovers	8.0
Top shelf	LH Side – Front & back	2 piles of bottom sheets	17.5
	RH side – Front & back	2 piles of top sheets	14.3
	Centre – Front & back	2 piles of pillow cases	6.3
		Total weight	**68.6**

3.2.5.2 Test 2 (Settee)

The test was intended to be a simulation of a single item from living rooms furniture which was a three-person-settee shown in Figure 3-25. The settee used for this test was complying with furniture regulations and was fully fire retarded. The total weight of the settee was 52.59 kg including 19.13 kg of the removable cushions. Flashover targets, consisting of crumpled A4 printing papers (shown in Figure 3-24), were located on the floor underneath the lowest thermocouple of the sidewall vertical tree. The ignition of these targets was taken as the onset of flashover (a criterion similar to [286-288]). The ignition of these targets was clearly recorded by an abrupt rise in the output of the lowest thermocouple on the tree.

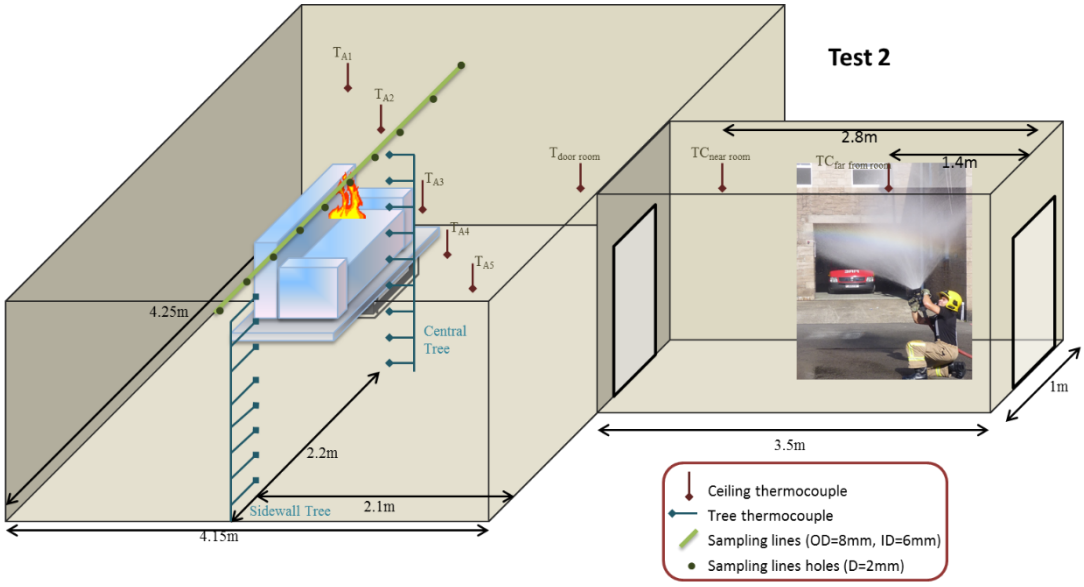

Figure 3-23: Test 2 full setup showing fire load, instrumentation and fire-fighting entrance.

Figure 3-24: Flashover target located at the bottom of the sidewall thermocouple tree.

Figure 3-25: Photographic image shows the orientation of the fire load for test 2 on the top of the weighting platform.

Table 3-8: Details of the fire load composition for test 2.

Fuel		Weight [kg]	Mass ratio	C [g/g%]	H [g/g%]	N [g/g%]	O [g/g%]
Removable cushions 19.13 kg	cushions foam (85%)	16.26	0.33	60.37	4.18	0.13	35.32
	Fabric (15%)	2.87	0.06	39.96	5.65	2.18	52.22
Settee body 33.46 kg	wooden frame (60%)	20.08	0.41	49.17	6.30	0	44.53
	settee foam (20%)	6.69	0.14	52.65	6.93	15.41	25.01
	Fabric (10%)	3.35	0.07	39.96	5.65	2.18	52.22
	metal springs (10%)	3.35	N/A	N/A	N/A	N/A	N/A
Total combustible materials		***49.24***	1	***52.18***	***5.60***	***2.41***	***39.81***

The settee consisted of a wooden frame, metal springs, and foam covering the arm with two layers of fabric covering the main body of the settee. It is assumed that the wooden frame counts for 60% of the total weight of the settee without the cushions, the metal springs count for 10%, the foam for 20% and the two-layer fabric for 10%. Samples of the cushions outer cover, top foam and bottom foam were cut out for ultimate analysis. The settee had a wooden frame which could not be weighed without its attached covering. The arms of the settee had foam attached which. Samples of the base settee or the wood frame were not taken. The combustion based ultimate analysis conducted on the samples collected from the fire load before the test, shows that the average mass based composition for outer and inner cover fabrics was 39.96% of carbon, 5.65% of hydrogen, 2.18% nitrogen and 52.22% oxygen. Two samples of foam were taken, one from the removable cushions showing a mass based composition of 60.37% of carbon, 4.18% of hydrogen, 0.13% nitrogen and

35.32% oxygen, while foam collected from the actual body of the settee showed a mass based composition of 52.65% of carbon, 6.93% of hydrogen, 15.41% nitrogen and 25.01% oxygen. Assuming that the wooden frame was made of pine wood the mass based composition of pine wood is 47.38% of carbon, 6.36% of hydrogen and 46.25% oxygen. A mass relative composition average of the whole settee found to be 52.18% of carbon, 5.60% of hydrogen, 2.41% nitrogen and 39.81% oxygen, giving an estimated air to fuel stoichiometric ratio of 6.13 g/g, as detailed in Table 3-8.

3.2.5.3 Test 3 (Wooden pallets)

The test was intended to be a simulation of a smouldering fire of two stacks of wooden pallets, as a common fire load (more than 80% of furniture is made of wood [57]) for residential buildings with door closed after igniting the stack on the load cell. Two stacks of wooden pallets were used one to be ignited while the other stack was positioned on the opposite corner. First stack had 8 pallets (with a total mass of 143 kg) and was mounted on the load cell (to enable measurements of mass loss rate from the original fire). While the second stack had 9 pallets (with a total mass of 144 kg) both stacks had total height of 1.29 m from the floor level. The sidewall vertical thermocouple tree was 20 cm away from the second pile enabling picking any flaming combustion spreading to the second stack of wooden pallets (which was not the case for this test). Figure 3-26 illustrates the fire load distribution within the compartment. Flashover targets similar to the ones used in test 2 and shown in Figure 3-24 were used in this test, however thermocouples did not show a clear indication of the targets being ignited during the test, this was caused by the falling wall papers from the wall that shielded the flashover targets from any radiation emitted by the fire or the hot smoke layer. As a result, flashover targets were to be displaced to be at the bottom of the central thermocouple tree instead of the sidewall tree for all the following tests (4, 5, 6, 7 and 8). Figure 3-28 is a post-test photograph showing the wall papers shielding the flashover targets from the hot layer radiation.

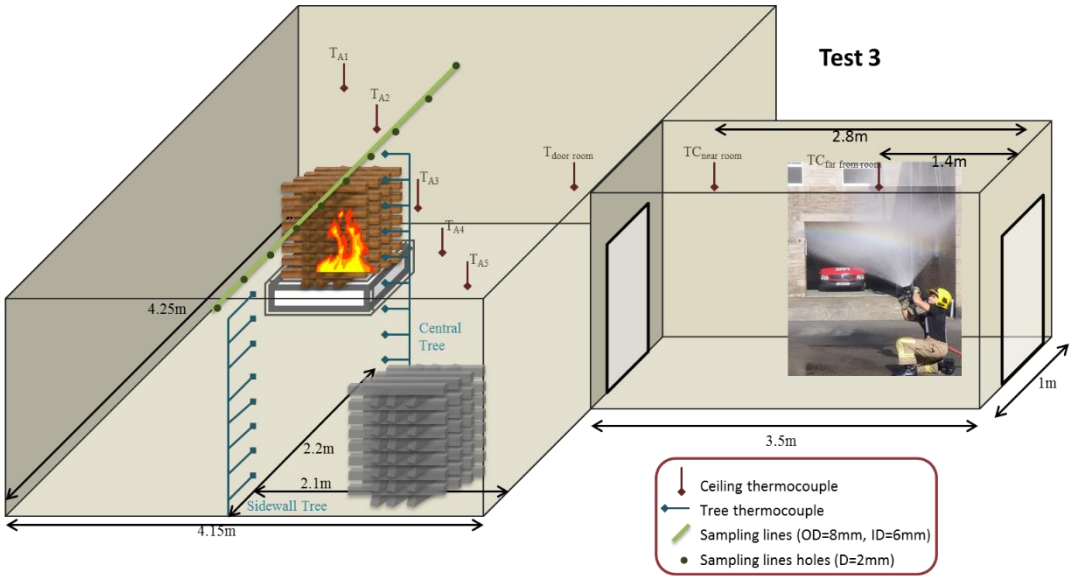

Figure 3-26: Test 3 full setup showing fire load, instrumentation and fire-fighting entrance.

Figure 3-27: Photographic image shows the orientation of the fire load for test 3 on the top of the weighting platform and away on the opposite corner.

Figure 3-28: Post-test photograph of the flashover targets showing the wall papers covering the targets

The combustion based ultimate analysis conducted on samples collected from the fire load before the test showing an average mass based composition for wooden pallets as 45.2% of carbon, 5.58% of hydrogen and 49.22% oxygen, giving the formula of $CH_{1.54}O_{0.82}$ and from this the stoichiometric A/F by mass was determined as 5.0.The net calorific value (CV) of the material was 15.4 MJ/kg, based theoretical oxygen consumption requirements [15].

3.2.5.4 Test 4 (Cotton linings and towels)

The test was intended to be a repeat of Test 1 with some variations such as the location of the fire would be on the opposite corner and of the far wall four curtains (total mass of 3.2 kg) were hanged as an extra fire load. Curtains were used in this test to demonstrate fire spread in compartment fires. The location of the curtains (on the opposite wall) can be clearly viewed (photographed) from the outside when they catch fire. The top two sections of the door were glazed which enabled capturing photos even when the door is closed.

Figure 3-29: Photographic image shows the orientation of the fire load for test 4 on the top of the weighting platform and curtains hanging on the opposite wall.

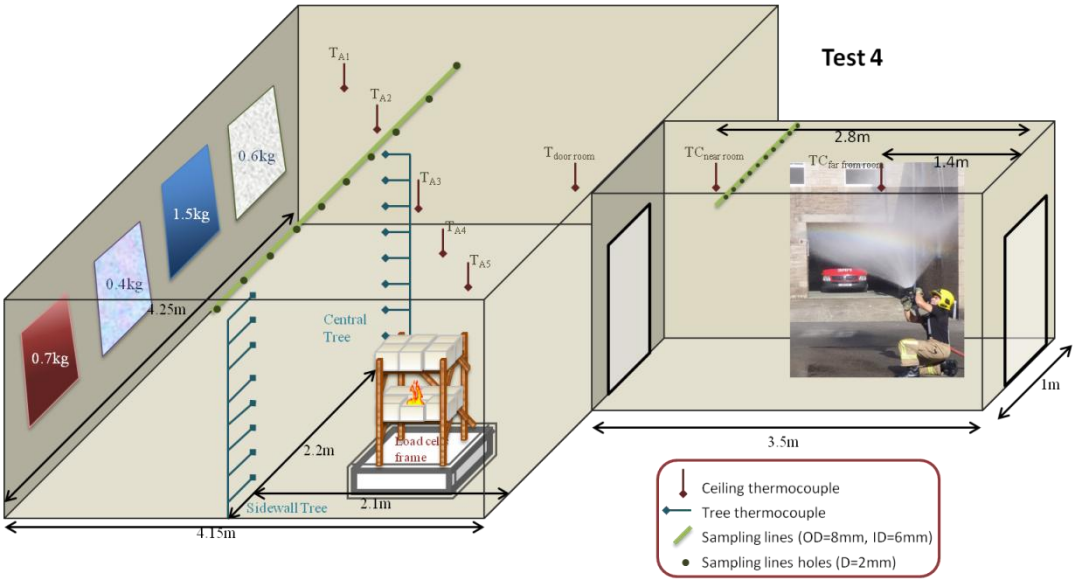

Figure 3-30: Test 4 full setup showing fire load, instrumentation and fire-fighting entrance.

Table 3-9: Details of the fire load orientation within the two-shelf wooden structure for test 4.

Position	Fuel type	Weight [kg]

		Wooden shelf support	15.5
Bottom shelf	Centre - front	White cotton towels	1.4
	RH&LH Sides - front	2 piles of white cotton towels (with blue strips)	3.7
	RH&LH Sides - back	2 piles of bedcovers	6.2
Top shelf	LH Side – Front & back	2 piles of bottom sheets	15.3
	RH side – Front & back	2 piles of top sheets	14.8
	Centre – Front & back	2 piles of pillow cases	5.8
		Total weight	**62.7**

3.2.5.5 Test 5 (Wooden pallets)

The test was intended to be a repeat of Test 3 while the weight balance will be monitoring the un-ignited stack. The test didn't consist of a smouldering (closed door) phase, and the door was kept open after igniting the stack on the far corner. The data logger responsible for recording the smoke analysis measurements from the paramagnetic oxygen and NDIR analysers (all gas analysis apart from FTIR) has malfunctioned for this test and data were lost, however some of the oxygen measurements were noted down with an approximation of the time (by the minute). Consequently this test measurements presented in the results section 5.1 will be consisting of the thermocouple, mass balance, and FTIR data. Fire-fighters were instructed not to put any water on the un-ignited stack if no visible flame can be seen (which was the case here), to enable post-test weight measurement of the pallets and understanding of the pyrolysis phenomenon.

Figure 3-31: Photographic image shows the orientation of the fire load for test 5 on the top of the weighting platform and away on the opposite corner.

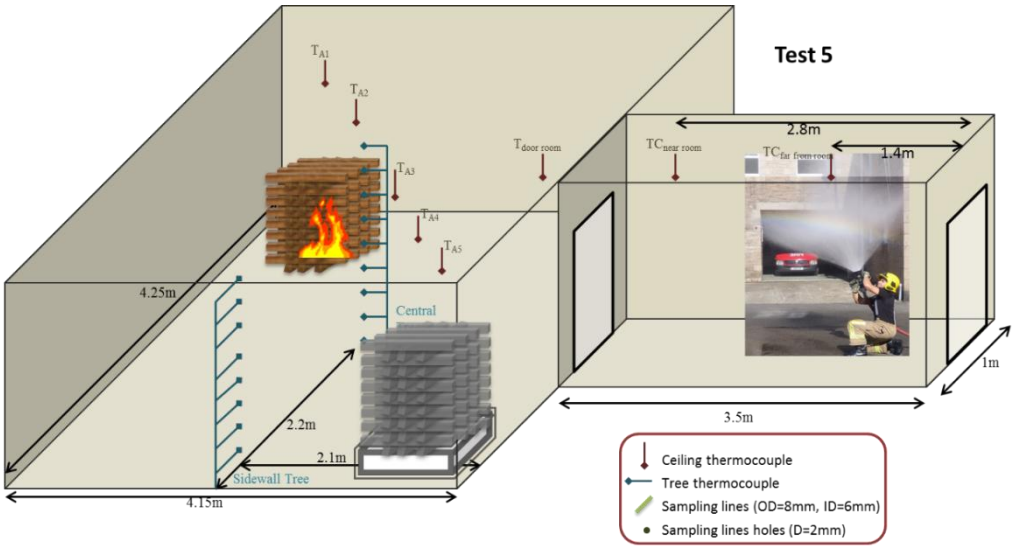

Figure 3-32: Test 5 full setup showing fire load, instrumentation and fire-fighting entrance.

3.2.5.6 Test 6 (Diesel pool)

The test simulates an oil spillage fire in a compartment for industrial application. A tray with the dimensions 1.2 x 1.2 m^2. It was mounted on the top of the weighting platform in the near corner to the door. The ventilation for the compartment was restricted to smaller than quarter of the door as shown in Figure 3-34 (total area of ventilation was (0.28 x 0.82 = 0.23 m^2). The ventilation was expected to keep the HRR to a maximum value of 340 kW based on the fire dynamics calculations explained in [289]. No fire-fighting activity was required as the test was planned for the diesel to burn out by the end of the test, however fire-fighting teams were on standby.

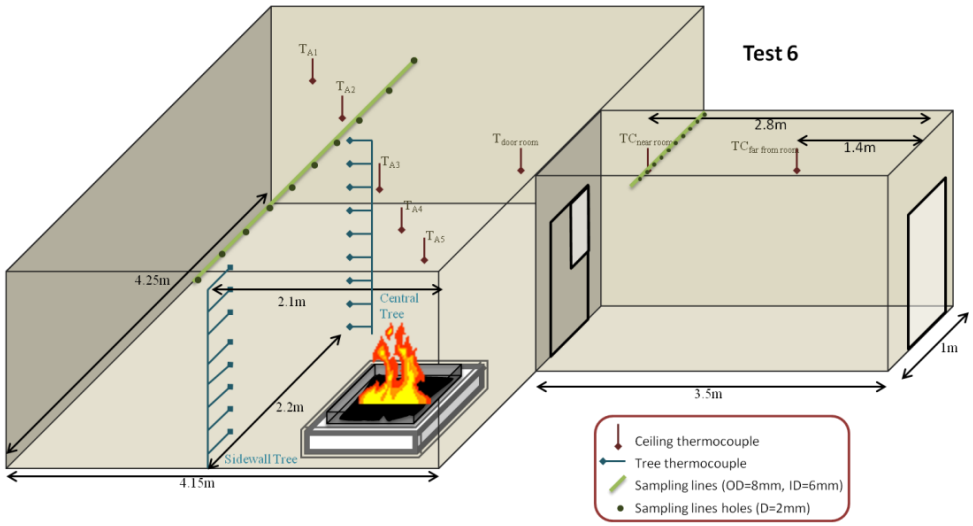

Figure 3-33: Test 6 full setup showing fire load, instrumentation and ventilation openings.

The tray had 3 supporter beams (to prevent the tray from bending) in the middle of the tray dividing the tray into 4 sections. Also four bricks were put on each corner of the tray to prevent bending as well. Total weight of diesel burnt was 8.5 kg. An additional thermocouple was added to measure the temperature of the diesel pool, the thermocouple was fixed to its position by one of the bricks . Also it was bent away from the metal base to ensure that the thermocouple measurement is for the fluid temperature not the metal tray temperature, a photographic image was taken of that setup and shown in Figure 3-35.

Figure 3-34: Photographic images showing the quarter of the door opening (on the left-hand side) and the diesel tray is shown on the top of the weighting platform for test 6.

Figure 3-35: Photographic image of the pool thermocouple (no diesel is poured yet) for test 6 and 7.

3.2.5.7 Test 7 (Diesel pool)

Using the same compartment and tray as test 6 this test was conducted however the amount of diesel was doubled to be 16.2 kg and the ventilation opening was doubled by extending the opening to double the height for the total area of opening to be 0.28 x 1.64 = 0.46 m^2. During the test due to the excessive heat of the previous tests the fire managed to penetrate the plasterboard ceiling above the weighting platform which eventually collapsed on the tray and weighting platform, at this stage the test was suspended (this was about 20 minutes into the test) and fire-fighters had to extinguish the pool fire using foam. The control room had to be evacuated due to the risk of the fire spreading through the roof space.

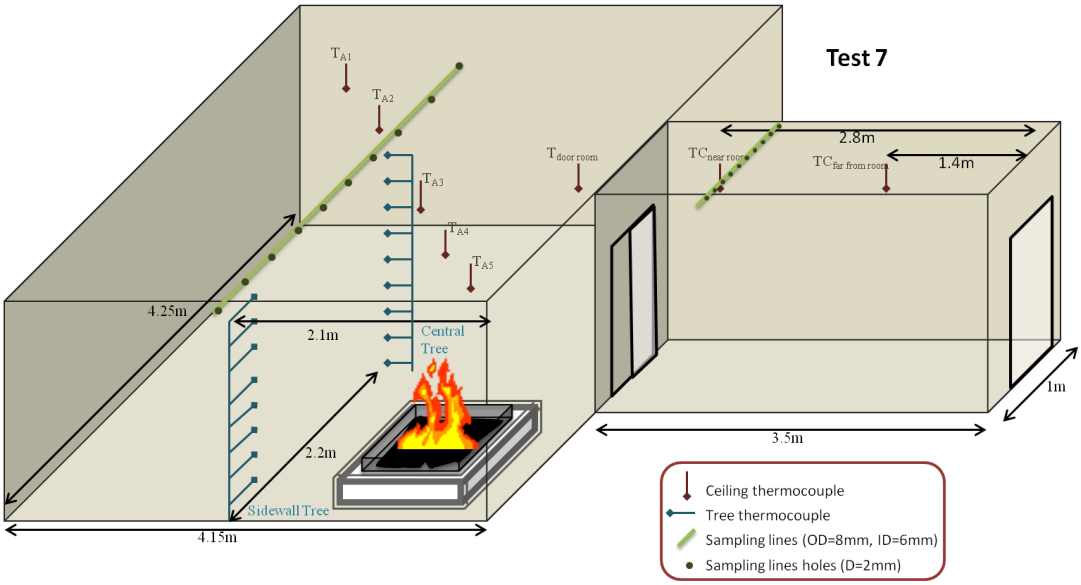

Figure 3-36: Test 7 full setup showing fire load, instrumentation and ventilation openings.

3.2.5.8 Test 8 (Living room furniture)

The test was designed to simulate a home living-room fire and measure the effectiveness of fire-fighting tactics on a fully developed post-flashover fire, in terms of temperature and toxic emissions within the compartment. The effect of almost complete air restriction was also simulated at the start of the test before allowing the fire to develop. The fuel load was typical living-room furniture. Table 3-10 shows the list of the individual fuel items and their corresponding mass. The total weight was 255.25 kg which was equivalent to 14.6 kg/m^2. If 20 MJ/kg is taken as an average heat of combustion this gives 293 MJ/m^2. Figure 3-38 shows the pictures of the arrangement of the furniture showing that there was no space for any additional furniture. However the European code (BS EN 1991-1-2 [290]) recommends using 780 MJ/m^2 as fire load average for dwellings (excluding any construction elements, linings and finishing) and suggesting 948 MJ/m^2 for 80% fractile. This is more conservative than published figures in PD 7974 -1 [39] which suggests 870 MJ/m^2 for 80% fractile, but agrees with the 780 MJ/m^2 as average fire load density for dwelling. Based on this test, it is clear that these values are very difficult to achieve especially with the contemporary minimalistic trend in furnishing houses and offices. In terms of the composition of this test fire load, cellulosic materials (mainly wood) were dominant, then plastics from the TV & PC equipment, in addition to some minor synthetic fabrics from curtains and seat covers and polyurethane foam from cushions. A recently published report by the Swedish SP [57] suggests that wood is accountable for approximately 80% of combustible interior furniture of dwellings.

Table 3-10: Itemized list of fuel load detailing weight for test 8.

Item (composition)	**Weight [kg]**
Dining table and coffee table (wood)	27.85
4 chairs (wood, PU cushions, fabric cover)	26.10
White sideboard (wood)	33.20
3-seater + 1 single seat sofas (wood frame, metal springs, PU cushions, fabric cover)	66.00
Bookshelf, 2 baskets and a chair (bamboo wood)	13.05
Wooden folding chair	3.80
Magazines (paper)	9.85
Curtains (synthetic fabrics)	5.90
TV & computer equipment (plastic, metals)	41.90
Plastic flower tubs (plastic)	1.20
Carpet (synthetic fabrics)	26.40(est.)

Total = 255.25 kg ~ 293 MJ/m^2

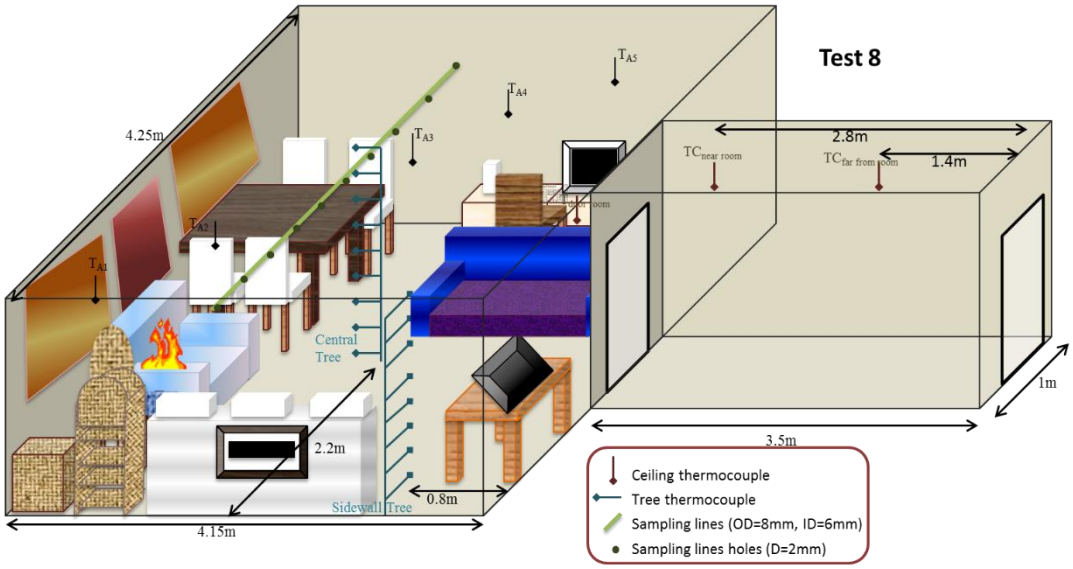

Figure 3-37: Test 8 full setup showing fire load, instrumentation and fire-fighting entrance.

Figure 3-38: Photographic image of the contents of the burn room for test 8.

3.3 Bench scale experiments (cone calorimeter)

The cone calorimeter is used to develop a method to generate practical toxic emission yields at bench-scale lab equipment. This section details the technical details of the standard cone calorimeter design and its implications on emissions measurements. Then the modifications implemented in order to improve these measurements on the standard test method and the modified controlled atmosphere cone calorimeter (CACC) would be detailed.

The cone calorimeter was developed with the purpose of determining heat release rate (HRR) of small samples of materials, other characteristics can also be measured using the apparatus such as effective heat of combustion, mass loss rate, ignitability and smoke generation for small samples of materials used in furniture and building materials [291]. According to Babrauskas [292], the major developer of the apparatus, the design of the conical heater was an improved version of the ISO 5657 (BS 476-13). Other empirical measurements were also been thoroughly collected in the literature using the cone calorimeter such as the critical heat flux which indicates minimum external radiant flux required to produce pilot ignition. The oxygen consumption principle for solid fuels introduced by Huggett in 1980 [293] is applied in the cone to estimate a time dependent HRR - therefore an O_2 analyser is an integral part of the equipment. It is very important to highlight here that the main purpose of creating the cone calorimeter, in the developing stage of the original standard method, was to enable measurement of the maximum HRR. Excessive dilution (pre-sampling) ensures that maximum possible heat released from the sample is measured. However, that standard setup not necessarily would provide a realistic approach in evaluating the potential harmful emissions from burning the sample. Since excessive dilution would encourage complex incomplete combustion products to further react producing simple (less toxic) complete combustion products (i.e. CO_2 and H_2O).

The cone calorimeter test was firstly adopted by the American Society for Testing and Materials in 1986 [212] and then was standardized by the International Organization for Standardization in 1990 as ISO 5660 [294]. The cone calorimeter has been the subject of many standards such as CAN/ULC S135, ASTM E1474, ASTM E1740, ASTM E1995, ASTM E20102, ASTM E2536, ASTM F1550 and ASTM D6113. However, apart from its use to measure soot yields through laser obscuration measurements and the optional CO and CO_2 analyser, the cone calorimeter standard test is not recognised as an official method for evaluating harmful emission yields for materials.

Previous studies used the cone calorimeter to quantify CO and CO_2 yields for different fire loads. Babrauskas et al. in [184] compared CO, CO_2, HCN and HCl yields among other fire variables for three materials Douglas fir, rigid polyurethane and PVC tested in the cone calorimeter at three different heat fluxes (35, 50 and 75kW/m^2) with multi scale standard fire tests. Another study [295] conducted in NIST (NBS at the time) compared the fire

hazards of fire retarded against non-fire retarded materials using the cone calorimeter among other equipment. Reporting toxic yields of toxic species (CO, CO_2, HCN, HBr and HCl) for different household furniture products e.g. TV cabinet, chair, cable and others.

Numbers of issues were identified in regards to toxic gas measurements using the cone calorimeter apparatus:

1. The standard equipment set-up represents a freely ventilated fire which is very important to achieve the peak heat release rate, as by supplying excessive air the combustion would be leaner consuming more oxygen. Hence data collected from such test cannot represent the influence of confinement and limited supply of air. In terms of evaluating the potential production of toxic emission this setup would underestimate these emissions, as excess air supply leads to efficient combustion with ideal products of CO_2 and water. Alternative setups have been introduced previously where the air supply can be restricted however none of these setups has been standardised yet apart from the IEC BS EN 60695 (focusing on electro-technical products) .
2. Even in the standard set-up with open ventilation around the burning specimen the distance between the combustion and the sampling point results in significant dilution of the fire gases and resulting in gas concentrations in many cases are too low to measure with the analysis equipment, as reported in [296]. It should be noted that the dilution and cooling of the combustion products is intentional as this brings the sample temperature down and also reduces the dew point of the water vapour and enables the sample to be transported to the analysers without the water vapours condensing which would also result in many of the toxic gases - such as HCl, HCN, Aldehydes, benzene and SO_2 - to dissolve in water. To avoid this is a fully heated system including the measuring cell needs to be heated and that is normally the arrangement used with the FTIR analyser, discussed thoroughly in Section 3.1.
3. Diluting the smoke too early while its temperature is still high, can induce oxidation of the toxic gases leaving the conical heater, as the fire emissions at these temperatures would be highly reactive. Thereby altering the actual emissions produced from the sample in the burning zone by the time it reaches the standard sampling point of the cone calorimeter apparatus. This was noted by Kallonen [296] as mentioned earlier, and by a number of other workers [165, 218, 222, 297], when working with the controlled atmosphere cone calorimeter (CACC). In an attempt to reduce the oxidation and burning of gaseous fuels produced by thermal degradation of the solid material tested, outside the test chamber (when meeting fresh air) an exhaust chimney was attached to the conical heater to enable dilution-free reduction of temperature for the smoke emitted from the burning sample which would reduce the reactivity of these emissions when excess air is introduced.

Another important argument is that using diluted sampling resembles the travelling smoke inhaled by victims in rooms away from the origin of the fire, this is a board assumption that only be applicable at specific conditions that the apparatus was not designed to resemble. The dilution in the cone calorimeter and other toxicity tests were introduced to the smoke products for technical purposes; either for reducing oxygen measurements errors or for convenience with handling the hot gas sample. Simulating the real case scenario should be a case by case exercise, data of emission yields at the origin room (outside the combustion zone) should be used and based on the ventilation conditions within the case scenario. In the current situation of bench-scale data being reported for a certain dilution levels (that might not be applicable for all scenarios), fire engineers performing the fire risk assessment for a certain scenario would feed these data into a CFD package as the fire origin emission yields and based on the geometry of the scenario and ventilation conditions the computer program would calculate the levels of emissions at the user specified locations based on the actual dilution factors of the actual design. With the previous exercise it is evident that dilution has been overestimated resulting in an overall lenient approach in evaluating the toxicity emission risk. Another important aspect of implementing data from standard diluted samples is that in real case scenario, the smoke temperature would be lowered gradually as the smoke travels in the hot layer which is normally would have a limited amount of oxygen. Meaning that post-oxidation outside the combustion zone is limited, and possibly be experienced only by the first wave of smoke if it occurs, which is a very minimal if taken into the context of a full fire scenario.

3.3.1 cone calorimeter (CC) setup – BS ISO 5660

The standard setup of the cone calorimeter test method according to BS ISO 5660:2015 [63] would test samples with a 100 mm by 100 mm and a depth from 5 to 50 mm mounted on a load cell measuring the loss of weight as it burns during the test. The Leeds cone calorimeter is the standardised version, purchased from FTT (Fire Testing Technology Ltd.) [213]. An electric conical heater (capable of producing heat flux from 0 to 100 kW/m^2 on the surface of the sample) with 80 mm diameter for the top opening and 177 mm for the bottom one with 65 mm depth for the conical heater. The sample is mounted 25 mm below the conical heater, this distance is vital for ensuring that the designated heat flux is applied to the sample surface uniformly. The standard method would require a piloted ignition via an electric spark which is mounted on the top of the sample (13 mm gap) positioned centrally. the smoke released by the sample travels through the conical heater and would be mixed with more fresh air after exiting the cone all the smoke then is collected by the metal hood aided by the fan motor pulling the smoke through the exhaust duct in flow recommended by the standard to be 24 l/s which is measured by the thermocouple and pressure ports fitted across the orifice plate at the exhaust stack (see Figure 3-39). A sampling ring is positioned further down the exhaust duct by 685 mm where 12 holes facing

downstream collect a representative homogeneous smoke sample which then goes through soot filters and sample treatments to remove water (cold trap and drying agent) before it reaches gas analysers. A laser system is applied on the smoke, just after the ring sampler, monitoring the obscuration and smoke production. An optional sampling port is available at the bottom of the exhaust duct midway between the fan and the hood, which can be used to collect soot for gravimetric analysis. Figure 3-39 is produced by the manufacturer FTT. showing the main components of the standard cone calorimeter.

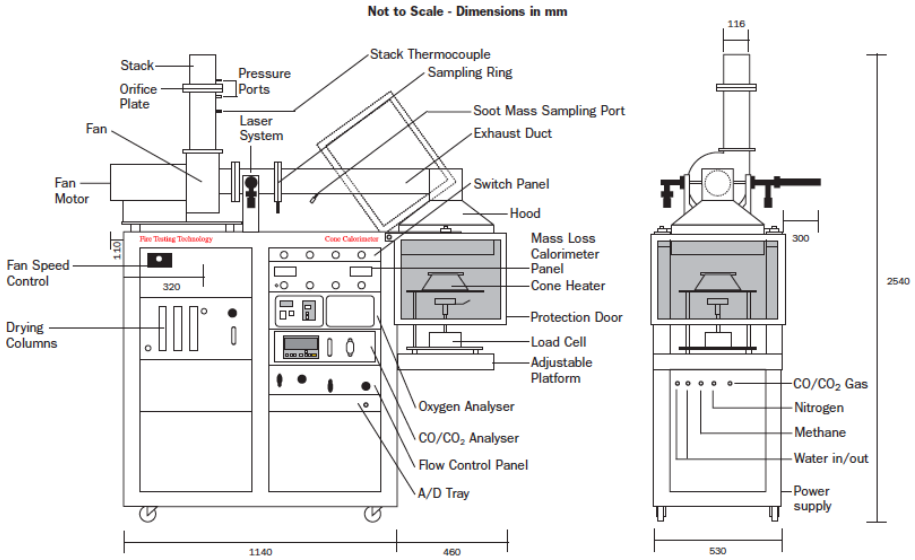

Figure 3-39: Schematic of a standard FTT cone calorimeter [213].

3.3.2 Controlled atmosphere cone calorimeter (CACC) setup

The various modifications has been introduced to the cone calorimeter in order to create a reduced oxygen environment for testing materials as discussed in the literature review section 2.5.1.8. In this work the modification used is a manufacturer supplied enclosure with the conical heater fitted to the top side. ISO 19706 classified fires into six types, detailed in earlier in the literature review section 2.1.2, these are classifications of combustion conditions. The standard ISO 5660 cone calorimeter setup is capable of creating combustion conditions that would satisfy classifications 1b (oxidative pyrolysis) and 2 (well ventilated flaming fires). Introducing the enclosure to the cone calorimeter to become CACC would make the apparatus capable of creating the combustion conditions for classifications 1c (anaerobic pyrolysis) and both 3a (low ventilated fires) and 3b (post-flashover fires). Utilizing the controlled atmosphere attachment would enable testing materials almost in every possible stage apart from stage 1a (self-sustained smouldering fires).

Controlled atmosphere cone calorimeter can control the atmosphere thorough the atmosphere supply port at the bottom of the enclosure in order to conduct under-ventilated tests (where reduced flow rate of fresh air supplied) or vitiated tests (where air supplied would have reduced percentage of oxygen). In this work CACC is used to test materials in under-ventilated environments.

3.3.3 Raw sampling point for the cone calorimeter

The importance of raw sampling and the advantages of collecting smoke sample as early as possible are discussed earlier in 3.1.1. the influence of diluting smoke generated in a rich environment such as those created in the controlled atmosphere cone calorimeter This section discusses the technical issues of introducing raw sampling point to the cone calorimeter. The solution is to mount the probe above the conical heater and before the secondary dilution by fresh air under the hood by introducing a chimney to the cone calorimeter as shown in Figure 3-40. Introducing the chimney or extended exhaust has been adopted by other researchers and standards [216, 298] for different purposes.

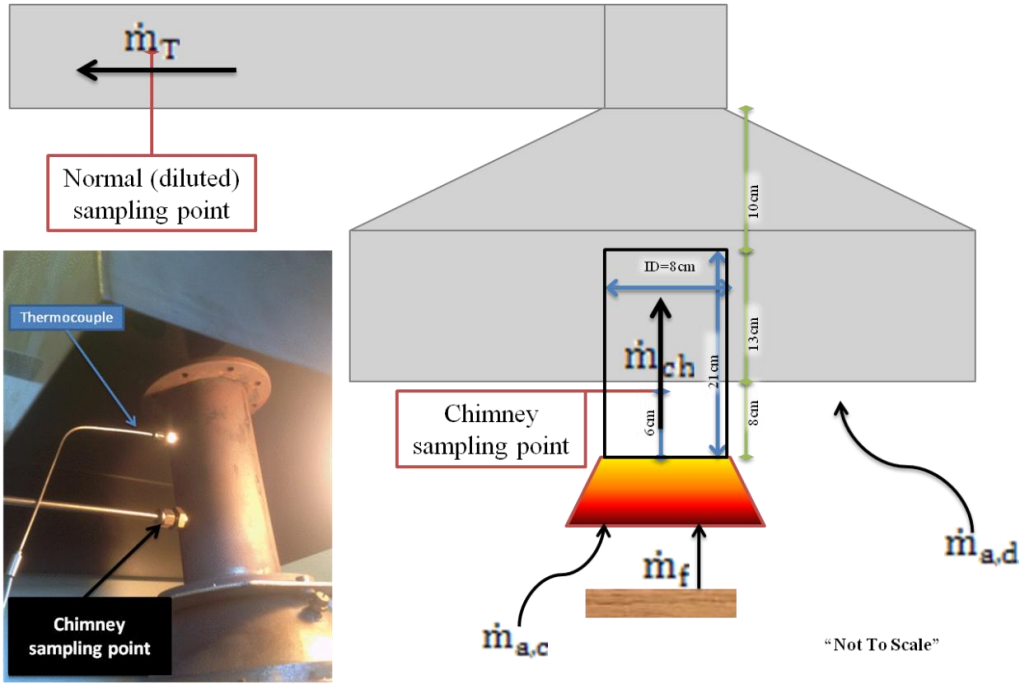

Figure 3-40: Schematic (and photographic) of the chimney extension added to the cone heater with indications and relative positioning of the sampling points and indications of the mass flows and dimensions.

As discussed earlier for raw gas analysis it is imperative that the gas sample line is fully heated, with heated filters and pumps. In this work the cone was connected to a heated TEMET GASMET CR2000-Series portable FTIR, sample cell volume 0.22 L, multi-pass fixed path length of 2 m. It had a separate heated sample line, as illustrated in Figure 3-41, filter and pump and the FTIR sample cell was also heated, all at 180 ºC, so that all analysis was on a hot wet basis with no acidic gas loss by condensation. In addition to the standard O_2 analyser sampling from the normal position, an additional Servomex paramagnetic oxygen analyser was used to take a continuous sample from the exhaust chimney to enable (in conjunction with the FTIR concentrations of other species) calculating the Equivalence Ratio (ER) based on the emission based model (developed specifically for fire research studies) that would detailed in the following Chapter 4.

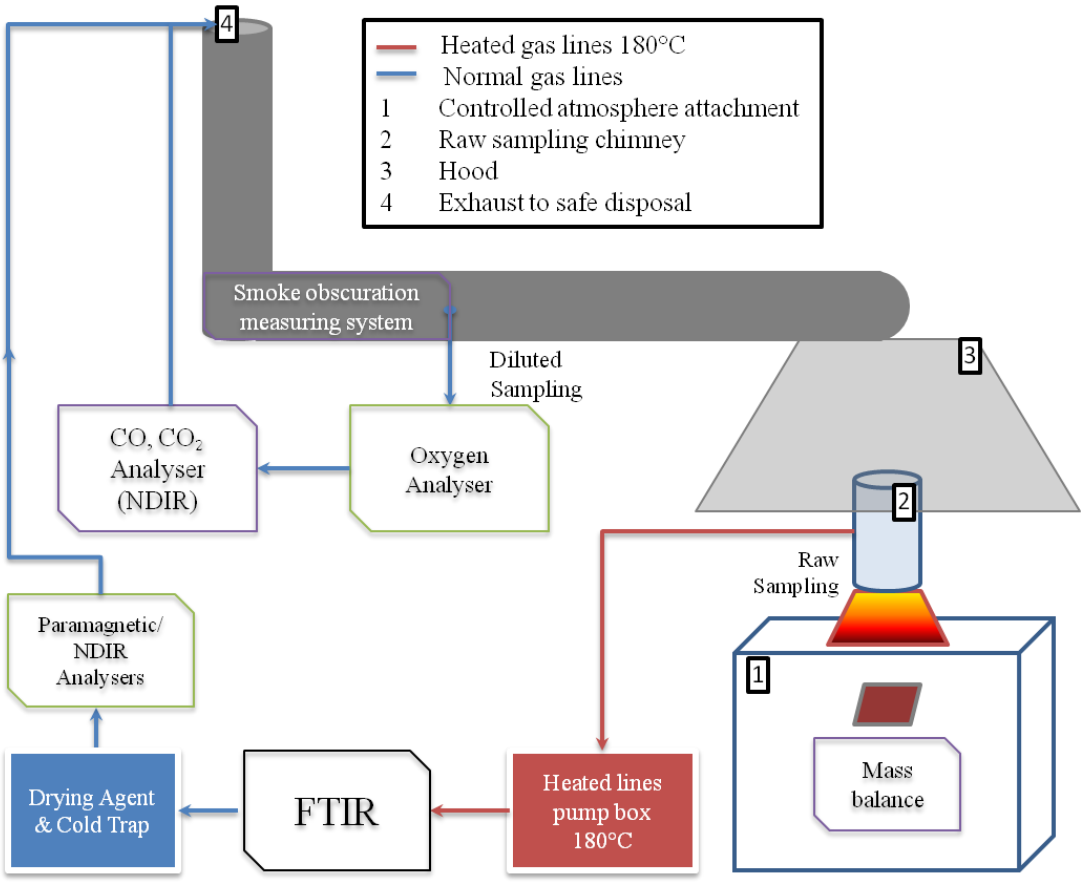

Figure 3-41: Gas sampling system used on the cone calorimeter

Series of tests were conducted to investigate the effect of introducing the raw sampling support in the form of a chimney as shown in Figure 3-40 is presented in the results Chapter 6. This chimney is made of stainless steel with an internal diameter of 8 cm and height of 21 cm. Two thermocouples have been added to detect any invisible combustion or exothermic reactions in the chimney or the hood space (see Figure 3-42). The first (chimney) thermocouple was added in the chimney at a fixed location 90 mm above the raw sampling point. The second (hood) thermocouple was added in the space above the centre of the chimney and has adjustable location in respect to the top of the chimney. The position of this thermocouple is critical, as it is important to measure the space when the exhaust flow interacts with air entrained in the hood as early as possible to eliminate the cooling effect from fresh air. Two thermocouples were fitted with the chimney, to monitor and record any changes in temperature (indication of flames) in the chimney, one is fixed at 15 cm above the conical heater and the second is flexible but in these tests it was positioned 4 cm above the chimney. It is possible to determine if the raw sample collected is from the combustion zone or outside the combustion, by monitoring temperatures in these two zones.

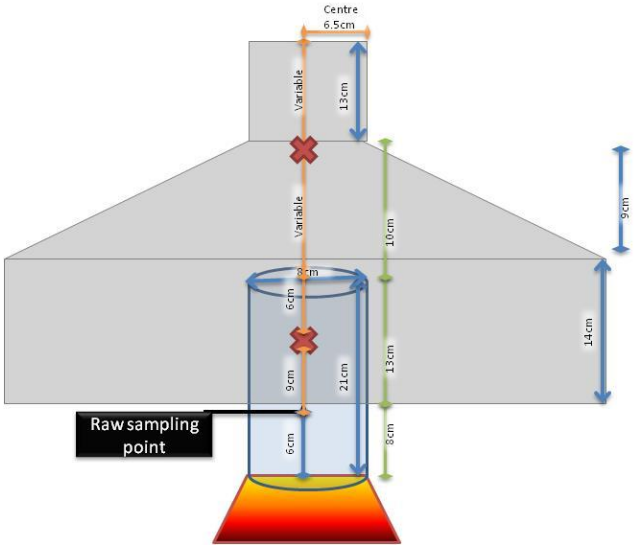

Figure 3-42: Schematic of the chimney extension mounted on the cone heater with relative positioning of thermocouples added.

3.4 Analytical laboratory tests

In this work analytical laboratory tests and techniques were used mainly to identify the characteristics of materials used as fuel in the experimental part. The techniques used in this work will be identified and explained in this section and examples of the output results of these techniques will be presented. In order to be able model the combustion reaction, quantifying the content of the reactants crucial activity to achieve that goal. In this work, ultimate analysis of targeted materials were conducted using organic (combustion based) elemental analysis in order to identify the content of the sample. ASTM standard D 5373 [299] details the test methods than can be followed to perform ultimate analysis, while ASTM standards D 3176 and D 3180 [300, 301] offer standard practices for conducting Ultimate analysis and presenting results. Advantages and limitations are discussed below as well as alternative tests. Additionally, proximate analysis were performed by well-known thermogravimetric analysis (TGA), it can provide measurements of materials' physical characteristics during degradation, where surrounding temperature and environment are controlled. ASTM standard D 7582 [302] details the test methods than can be followed, while ASTM standards D 3172, D 3173, D 3174, D 3175 and D 3176 [300, 303-306] offer standard practices for conducting proximate analysis and presenting final results. This section details the test methods for these techniques and show examples of the data output.

3.4.1 Proximate TGA analysis – Mettler Toledo TGA/DSC 1

Proximate analysis were conducted using Mettler Toledo TGA/DSC 1 [307]. The Thermogravimetric heating process used is detailed as follows; The sample is heated under inert atmosphere at a rate of 10 ^{o}C/min from room temperature to 105 ^{o}C temperature is held for 10 minutes to obtain the weight loss associated with moisture vaporisation. Then the temperature is raised at the rate of 20 ^{o}C/min to 700 ^{o}C (still under inert environment) to obtain the weight loss associated with volatiles discharge in this phase. Then air is introduced into the furnace to oxidise the carbon residue available in the sample in order to obtain the weight loss associated with fixed carbon in this phase. The remaining weight by the end of the test represents the ash content in the sample. The results offered by the instrument are on ***as-determined (ad)*** bases that can be converted to ***dry (d)*** or ***dry ash-free (daf)*** bases using the guideline suggested by the ASTM standard D 3180 [301].

3.4.2 Organic elemental analysis – Flash 2000 elemental analyser

The technique is designed for organic materials with assumption that all the sample is oxidised within the test period. This particular analyser, named Flash 2000 EA and manufactured by Thermo Scientific, is the single reactor CHNS analyser, that was made to measure the mass content of the sample for only these elements (carbon, hydrogen, nitrogen and sulphur) while oxygen is determined by subtraction based on the assumption that remaining mass is oxygen which is applicable for organic materials. Alternative methods

should be used for complex materials, such as Field Emission Gun Scanning Electron Microscopy (FEG-SEM) with Energy Dispersive X-ray Detection (EDX) analysis. The EDX analyser is able to detect all elements in the periodic table except H, He, Li, and Be (any element without electrons in the p shell i.e. elements with atomic number less than 5) [224, 308].

The Flash 2000 Elemental analyser requires the sample to be finely grinded in order to improve its reactivity ultimately reaching a complete combustion in the test chamber. The sample is dropped, encapsulated in an airtight tin, by the auto-sampler into the furnace through a quartz reactor where the sample would combust reaching 1800 ^{o}C, all in a rich pure oxygen environment inside the reactor. Then Helium is switched on to convey combustion products to the Chromatographic Column (CC). Nitrogen oxides are reduced to N_2. Then N_2, CO_2, H_2O & SO_2 are separated in the Chromatographic Column. Where the products would pass Thermal Conductivity Detector (TCD) to determine the content of carbon, hydrogen, nitrogen and sulphur [309] as illustrated in Figure 3-43. The results offered by the instrument are on ***as-determined (ad)*** bases that can be converted to ***dry (d)*** or ***dry ash-free (daf)*** bases using the guideline suggested by the ASTM standard D 3176 [300]. Oxygen is determined following the same ASTM standard D 3176 using the following equation:

$$O_{ad} = 100\% - A_{ad} - C_{ad} - H_{ad} - N_{ad} - S_{ad} \qquad [300]$$

Where; O is oxygen in [wt.%], A is ash as determined by proximate analysis in [wt.%], C is Carbon as determined by ultimate analysis in [wt.%], H is hydrogen as determined by ultimate analysis in [wt.%], N is nitrogen as determined by ultimate analysis in [wt.%] and S is sulphur as determined by ultimate analysis in [wt.%].

The material composition results are important for different exercises and application such as; determining the stoichiometric air to fuel (or fuel to air) ratio, and calculating the gross calorific value based on the material contents. Both applications will be exercised on the example illustrated below in section 3.4.1.1 for results from pine wood samples.

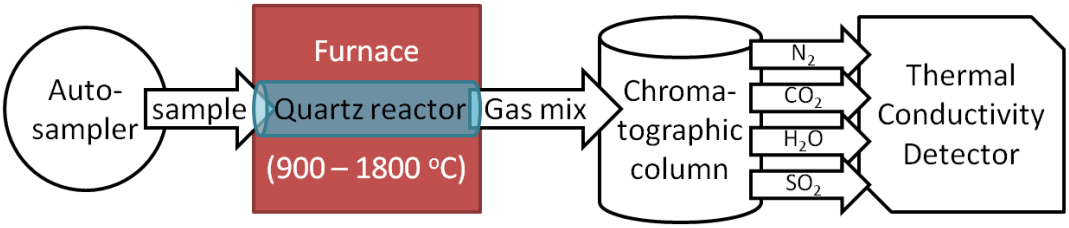

Figure 3-43: Organic elemental analysis (Combustion-based EA). Flowchart of Flash 2000 EA apparatus and its main parts illustrating the testing process.

3.4.3 Example of utilising proximate (TGA) and ultimate (elemental) analysis results – pine wood

This exercise shows real output from pine wood proximate and ultimate analysis as described above in Section 3.4.1 and 3.4.2 It is a standard protocol in Leeds analytical laboratory to always test two samples of each material, however as part of this research eight pine wood samples underwent the ultimate analysis, while three samples used to determine the proximate analysis.

Table 3-11: direct output of TGA and combustion based elemental analysis.

TGA				EA	
M_{ad} [wt.%]	VM_{ad} [wt.%]	FC_{ad} [wt.%]	A_{ad} [wt.%]	C_{ad} [wt.%]	H_{ad} [wt.%]
2.56	81.99	14.39	1.06	47.39	6.36

Where; M_{ad} is moisture as determined by TGA in [wt.%], VM_{ad} is volatile matters as determined by TGA in [wt.%], FC_{ad} is fixed carbon as determined by TGA in [wt.%], A_{ad} is ash as determined by TGA in [wt.%], C_{ad} is carbon as determined by EA in [wt.%] and H_{ad} is hydrogen as determined by EA in [wt.%].

standards published by ASTM D 3176 [300] and D 3180 [301] can be used for converting outputs from as-determined base to different bases. List of equations used to produce proximate and ultimate analysis in different bases in Table 2.2 are shown below;

$A_d=A_{ad} \times(100/(100-M_{ad}))$

$C_d=C_{ad} \times (100/(100-M_{ad}))$

$C_{daf}= C_{ad} \times (100/(100-M_{ad} - A_{ad}))$

$H_d=H_{ad} – 0.1119\ M_{ad} \times (100/(100-M_{ad}))$

$H_{daf}= H_d \times (100/(100 - A_d))$

$O_{ad} = 100\% – A_{ad} – C_{ad} – H_{ad} – N_{ad} – S_{ad}$ [300]

$O_d = 100\% – A_d – C_d – H_d – N_d – S_d$

$O_{daf} = 100\% – C_{daf} – H_{daf} – N_{daf} – S_{daf}$

Table 3-12: Proximate and ultimate analysis in different bases for pine wood.

Bases	M [wt.%]	A [wt.%]	C [wt.%]	H [wt.%]	O [wt.%]
ad	2.56	1.06	47.39	6.36	*45.19*
d	--	*1.09*	*48.62*	*6.23*	*44.06*
daf	--	--	*49.17*	*6.30*	*44.53*

Molar volume equivalent of each element for 100 grams of the sample on dry-ash free bases (daf) is calculated based on the molecular weight of each element. Giving 4.09 moles of carbon, 6.25 moles of hydrogen and 2.78 moles of oxygen. Then the molar ratios for all elements to a single carbon mole give the empirical formula for pine wood tested as $CH_{1.53}O_{0.68}$.

Then using the empirical formula stoichiometric air to fuel ratio can be determined through the following equation:

$C_\alpha H_\beta O_\gamma N_\delta + x\,(O_2 + 3.76\,N_2) \rightarrow \alpha\,CO_2 + (\beta/2)\,H_2O + (\delta/2 + 3.76x)\,N_2$

Where; $x = \alpha + \beta/4 - \gamma/2$

then stoichiometric air to fuel (AFR) ratio on mass bases can be calculated based on the following formula:

$$AFR_{Stoich.}\left[g_{air}/g_{fuel}\right] = \frac{x \cdot 4.77 \cdot 28.8}{12.011\alpha + 1.008\beta + 15.999\gamma + 14.007\delta}$$

Where;

4.77 is the molar ratio of oxygen in air and 28.8 is air molecular weight.

AFR stoichiometric = 5.86 [g_a/g_f]

Which can be converted to stoichiometric fuel to air (FAR) ratio by inversing AFR that gives $FAR_{stoich.}$= 0.171 grams of fuel for each single gram of air.

FAR stoichiometric = 0.171 [g_f/g_a]

Higher heating value (HHV) or gross calorific value (GCV) is an important fuel characteristic. The typical test method to quantify HHV is bomb calorimetry that relies on measurements of change in temperature of the 2 litres of water surrounding the pressurized vessel where a small sample (1-1.5g) of the material is ignited. However estimating such a value from the elemental composition is a useful practice [310]. Channiwala and Parikh [311], in their highly cited paper, reviewed more than 22 calculations from the literature then established a unified correlation for different fuels with average error of 1.45% and bias error of 0.00%. The unified correlations is shown below;

$$HHV\ [MJ/kg] = 0.3491\ C_d + 1.1783\ H_d + 1.005\ S_d - 0.1034\ O_d - 0.0151\ N_d - 0.0211\ A_d \quad [311]$$

Channiwala and Parikh [311] gave the following limitations to the equation:

0 wt.% ≤ C_d ≤ 92.25 wt.%, 0.43 wt.% ≤ H_d ≤ 25.15 wt.%, 0 wt.% ≤ S_d ≤ 94.08 wt.%, 0 wt.% ≤ O_d ≤ 50.00 wt.%, 0 wt.% ≤ N_d ≤ 5.60 wt.%, 0 wt.% ≤ A_d ≤ 71.4 wt.% and 4.745 MJ/kg ≤ HHV ≤ 55.345 MJ/kg.

Where; C_d is carbon in dry basis in [wt.%], H_d is hydrogen in dry basis in [wt.%], S_d is sulphur in dry basis in [wt.%], O_d is oxygen in dry basis in [wt.%], N_d is nitrogen in dry basis in [wt.%] and A_d is ash in dry basis in [wt.%].

HHV = 19.74 [MJ/kg]

Chapter 4
Emission-Based Equivalence Ratio (EBER) model for fire research

4.1 Introduction

Quantification of the combustion equivalence ratio is important in the determination and interpretation of toxic emissions in compartment fires. A comprehensive review of the various approaches on the evaluation of ER was given in Chapter 2. Most of these approaches are based on the evaluation of the supply rate of air to the fire (or the total mass of exhaust and dilution gases) and the mass loss rate of the fuel in the fire. These methods assume complete combustion, which rarely occurs in compartment fires. As an example, the oxygen consumption method in conjunction with an external collection hood, assumes that combustion is complete and that all oxygen consumed reacted within the compartment and this allows the determination of the HRR. This is not the case in ventilation controlled fires where a large proportion of the combustion may occur outside the compartment. There are have been modifications to improve the prediction of the HRR based on CO and CO_2 concentrations as well as O_2 [312].

The Emission-Based Equivalence Ratio (EBER) approach, presented here, is based on taking into account all the species concentrations that can be measured with modern techniques and knowledge of the fuel composition. It has the advantage that it determines the actual fuel to air ratio involved in producing the effluents at the point of measurement, which with suitable sampling distribution can be representative of the overall combustion reactions within the enclosure. This can then give important information about the conditions responsible for the toxicity of the fire products. Importantly it also enables the evaluation of toxic yields without the need for any data on mass burning rate or effluent mass flow rate.

4.2 The EBER model

This is a mass/species balance approach to quantify the equivalence ratio based on emission measurements and knowledge of the fuel composition. Emission based equivalence ratio is defined as the ratio of the mass of fuel involved in the reaction that produced the sampled mixture to the mass of air involved in producing the same sampled mixture normalised by the stoichiometric fuel-to-air ratio.

Emission-based equivalence ratio models are well established in the field of vehicle emissions research [313, 314] for HC and HCO fuels and used previously by the author for wood fires [260]. However, in compartment fires, involved fuels are more complex and the significant amount of water usually exists in wood and this needs to be taken into account as well as the presence of chlorine, organically bound nitrogen, sulphur and other elements in the fuel.

4.2.1 The reaction:

A fuel with an elemental composition potentially comprising of up to 17 elements is assumed to be oxidised in air to form up to 31 fully and partially oxidised products as shown below.

$$C_{x1}H_{x2}O_{x3}N_{x4}S_{x5}Cl_{x6}Br_{x7}F_{x8}Si_{x9}K_{x10}Ca_{x11}Mg_{x12}Na_{x13}P_{x14}Fe_{x15}Al_{x16}Ti_{x17} + A(O_2 + 3.7292N_2 + 0.0444Ar + 0.0019CO_2) + BH_2O \rightarrow n_1CO + n_2CO_2 + n_3H_2O + n_4O_2 + n_5HCN + n_6HCl + n_7HBr + n_8HF + n_9NO_2 + n_{10}NO + n_{11}C_3H_4O + n_{12}CH_2O + n_{13}C_2H_4O + n_{14}C_7H_6O + n_{15}C_3H_6O + n_{16}SO_2 + n_{17}NH_3 + n_{18}C_6H_6 + n_{19}C_7H_8 + n_{20}C_3H_3N + n_{21}CH_2O_2 + n_{22}N_2 + n_{23}N_2O + n_{24}H_2 + n_{25}C + n_{26}KCl + n_{27}K_2SO_4 + n_{28}Ar + n_{29}CH_4 + n_{30}C_2H_6 + n_{31}C_3H_8$$

Where; x_i is the molar ratio for element (i), n_i is the number of moles of product (i).

By assuming the following:

- The reaction formula above represents the overall combustion reaction. There are no other products of the combustion.

Composition of the fuel element is known i.e. x_1, x_2, …., x_{17} are known (for example from elemental of the sample)

- The molar fractions of all the products are known (e.g. from FTIR measurements) apart from H_2, N_2, Ar and KCl.

Then the next step is to identify elemental balance equations and relationships to be used on an overall balance approach to quantify the ratio of fuel to air involved in the combustion.

4.2.1.1 Elemental balance equations

Carbon balance:

$x_1+0.0019\ A= n_1+n_2+n_5+ (3*n_{11}) + n_{12} + (2*n_{13}) + (7*n_{14}) + (3*n_{15}) + (6*n_{18}) + (7*n_{19}) + (3*n_{20}) + n_{21} + n_{25}+ n_{29} + (2*n_{30}) + (3*n_{31})$

Hydrogen balance:

$2B + x_2 = (2*n_3) + n_5 + n_6 + n_7 + n_8 + (4*n_{11}) + (2*n_{12}) + (4*n_{13}) + (6*n_{14}) + (6*n_{15}) + (3*n_{17}) + (6*n_{18}) + (8*n_{19}) + (3*n_{20}) + (2*n_{21}) + (2*n_{24}) + (4*n_{29}) + (6*n_{30}) + (8*n_{31})$

Oxygen balance:

$x_3 + 2.0038A+B = n_1+(2*n_2) + n_3 + (2*n_4) + (2*n_9) + n_{10} + n_{11} + n_{12} + n_{13} + n_{14} + n_{15} + (2*n_{16}) + (2*n_{21}) + n_{23} + (4*n_{27})$

Converting the equation to molar fraction (concentrations):

y_i is the "wet" molar fraction (as measured concentration) of species (i), and since; n_i is the number of moles of species sampled and $\sum_{i=1}^{31} n_i$ is the total number of moles sampled.

The following conversion can be used to convert number of moles of species to molar fraction:

$$y_i = \frac{n_i}{\sum_{i=1}^{31} n_i}$$

Wet to dry conversion and vice versa

Heated sampling systems measurements usually measure on a wet basis, however measurements performed using dry basis instruments can be incorporated in the calculations by converting the dry measurements to wet measurements.

So: y_i^0 is defined as the "dry" molar fraction of species (i)

to convert from wet to dry, the following equation can be used:

$$y_i^0 = \frac{y_i}{1-y_3}$$

where; y_3 is water's molar fraction

to convert from dry to wet the following equation can be used:

$$y_i = y_i^0 \times (1 - y_3)$$ where; y_3 is water's molar fraction

Converting elements balance from atomic to molar fractions

Carbon molar balance:

$x_1+0.0019\ A=[\ y_1+y_2+y_5+\ (3*y_{11}) + y_{12} + (2*y_{13}) + (7*y_{14}) + (3*y_{15}) + (6*y_{18}) + (7*y_{19}) + (3*y_{20}) + y_{21} + y_{25}+ y_{29} + (2*y_{30}) + (3*y_{31})]*\sum_{i=1}^{31} n_i$

Hydrogen molar balance:

$2B + x_2 = [(2*y_3) + y_5 + y_6 + y_7 + y_8 + (4*y_{11}) + (2*y_{12}) + (4*y_{13}) + (6*y_{14}) + (6*y_{15}) + (3*y_{17}) + (6*y_{18}) + (8*y_{19}) + (3*y_{20}) + (2*y_{21}) + (2*y_{24}) + (4*y_{29}) + (6*y_{30}) + (8*y_{31})]* \sum_{i=1}^{31} n_i$

Oxygen molar balance:

$x_3 + 2.0038A+B = [\ y_1+(2*y_2) + y_3 + (2*y_4) + (2*y_9) + y_{10} + y_{11} + y_{12} + y_{13} + y_{14} + y_{15} + (2*y_{16}) + (2*y_{21}) + y_{23} + (4*y_{27})\ ] * \sum_{i=1}^{31} n_i$

4.2.1.2 Other equations & relationships

The above elemental balance equations are not sufficient to solve all the unknowns in the reaction formula. So humidity relationship with air can formulated using the vapour pressure Antoine equation [315], and the water-gas shift reaction equation [316] are used to solve the overall equation;

Equation for humidity B in air A

$$B = 4.7755 \frac{P_v}{P_a - P_v} A$$

where; P_a is the atmospheric pressure in [Pa] = 100000Pa, P_v is the partial pressure of water vapour in [Pa];

$$P_v = \phi P_g$$

Where; ϕ is the relative humidity in [%] (typically 60%), P_g is the saturated water vapour pressure at ambient temperature in [Pa].

Using Antoine's equation for calculating vapour pressure:

$$\log_{10} P_g = A - \frac{B}{C + T}$$

where; P_g is the water vapour pressure in [mmHg], T is atmospheric temperature in [^{o}C] (ambient = 20^{o}C), A, B and C are Antoine Constants for water, dependant on temperature as shown in the following table;

T_{min} [°C]	T_{max} [°C]	A	B	C
1	99	8.07131	1730.63	233.426
100	374	8.14019	1810.94	244.485

Taking into account the water-gas shift reaction:

$$CO_2 + H_2 \leftrightarrow CO + H_2O$$

having an equilibrium constant K:

$$K = \frac{n_1 n_3}{n_2 n_{24}} = \frac{y_1 y_3}{y_2 y_{24}}$$

where K is a function of the equilibrium temperature T_{eq} ,

K values of 3.5 and 3.8 obtained from the JANAF tables, are commonly used, corresponding to equilibrium temperatures at 1738K and 1814K. Generally the following equation can be used [317];

$$\ln K = 2.743 - \frac{1.761}{0.001T_{eq}} - \frac{1.611}{(0.001T_{eq})^2} + \frac{0.2803}{(0.001T_{eq})^3}$$

for $400K < T_{eq} < 3200K$

4.3 The solution:

The following equation represents the combustion reaction with components marked in red being unknowns.

$$C_{x1}H_{x2}O_{x3}N_{x4}S_{x5}Cl_{x6}Br_{x7}F_{x8}Si_{x9}K_{x10}Ca_{x11}Mg_{x12}Na_{x13}P_{x14}Fe_{x15}Al_{x16}Ti_{x17} + A(O_2 + 3.7292N_2 + 0.0444Ar + 0.0019CO_2) + BH_2O \rightarrow n_1CO + n_2CO_2 + n_3H_2O + n_4O_2 + n_5HCN + n_6HCl + n_7HBr + n_8HF + n_9NO_2 + n_{10}NO + n_{11}C_3H_4O + n_{12}CH_2O + n_{13}C_2H_4O + n_{14}C_7H_6O + n_{15}C_3H_6O + n_{16}SO_2 + n_{17}NH_3 + n_{18}C_6H_6 + n_{19}C_7H_8 + n_{20}C_3H_3N + n_{21}CH_2O_2 + n_{22}N_2 + n_{23}N_2O + n_{24}H_2 + n_{25}C + n_{26}KCl + n_{27}K_2SO_4 + n_{28}Ar + n_{29}CH_4 + n_{30}C_2H_6 + n_{31}C_3H_8$$

Unknowns:

- Major unknown is air coefficient (A) which relates to the number of moles of Air involved in the reaction
- Other unknowns that are needed to quantify A:
  - (B) humidity in air or moles number of water in air.
  - y_{24} (H_2) is the 'wet' hydrogen concentration
  - $\sum_{i=1}^{31} n_i$ total number of moles in the products.

Finally the linear equations to be used to solve unknowns;

1) Carbon balance

x_1+0.0019 A = [y_1[CO]+y_2[CO_2]+y_5[HCN]+ (3*y_{11}[C_3H_4O]) + y_{12}[CH_2O] + (2*y_{13}[C_2H_4O]) + (7*y_{14}[C_7H_6O]) + (3*y_{15}[C_3H_6O]) + (6*y_{18}[C_6H_6]) + (7*y_{19}[C_7H_8]) + (3*y_{20}[C_3H_3N]) + y_{21}[CH_2O_2] + y_{25}[Fixed C] + y_{29}[CH_4] + (2*y_{30}[C_2H_6]) + (3*y_{31}[C_3H_8])]* $\sum_{i=1}^{31} n_i$

2) Hydrogen balance

2B + x_2 = [(2*y_3[H_2O]) + y_5[HCN] + y_6 [HCl]+ y_7 [HBr]+ y_8 [HF]+ (4*y_{11}[C_3H_4O]) + (2*y_{12}[CH_2O]) + (4*y_{13}[C_2H_4O]) + (6*y_{14}[C_7H_6O]) + (6*y_{15}[C_3H_6O]) + (3*y_{17}[NH_3]) + (6*y_{18}[C_6H_6]) + (8*y_{19}[C_7H_8]) + (3*y_{20}[C_3H_3N]) + (2*y_{21}[CH_2O_2]) + (2*y_{24}[H_2]) + (4*y_{29}[CH_4]) + (6*y_{30}[C_2H_6]) + (8*y_{31}[C_3H_8])]* $\sum_{i=1}^{31} n_i$

3) Oxygen balance

x_3 + 2.0038A+B = [y_1[CO]+(2*y_2[CO_2]) + y_3[H_2O] + (2*y_4[O_2]) + (2*y_9[NO_2]) + y_{10}[NO] + y_{11} [C_3H_4O]+ y_{12}[CH_2O] + y_{13}[C_2H_4O] + y_{14} [C_7H_6O]+ y_{15}

$[C_3H_6O]+ (2*y_{16}[SO_2]) + (2*y_{21}[CH_2O_2]) + y_{23}[N_2O] + (4*y_{27}[K_2SO_4])] * \sum_{i=1}^{31} n_i$

4) Air humidity and air relationship

$$B = 4.7755 \frac{P_v}{P_a - P_v} A$$

5) water-gas shift equilibrium constant

$$K = \frac{n_1 n_3}{n_2 n_{24}} = \frac{y_1 y_3}{y_2 y_{24}}$$

By rearranging the five linear equations above the problem can be presented and solved in a matrix form;

	1st unknown	2nd unknown	3rd unknown	4th unknown	5th unknown	
C – balance	$\frac{x_1}{\sum_{i=1}^{31} n_i}$	$+\frac{0.0019\ A}{\sum_{i=1}^{31} n_i}$				= Eq1 = y_1[CO] + (2*y_{13}[C_2H_4O]) + (7*y_{19}[C_7H_8]) + (3* (2*y_{30}[C_2H_6]) + (3*
H – balance	$\frac{x_2}{\sum_{i=1}^{31} n_i}$		$+\frac{2B}{\sum_{i=1}^{31} n_i}$		- (2*y_{24}[H_2])	= Eq2 = (2*y_3[H (4*y_{11}[C_3H_4O]) + ((6*y_{15}[C_3H_6O]) + (3*y_{20}[C_3H_3N]) + (8*y_{31}[C_3H_8])
O – balance	$\frac{x_3}{\sum_{i=1}^{31} n_i}$	$+\frac{2.003\ A}{\sum_{i=1}^{31} n_i}$	$+\frac{B}{\sum_{i=1}^{31} n_i}$			= Eq3 = y_1[CO]+(y_{10}[NO] + y_{11} [C_3 [C_3H_6O]+ (2*y_{16}[SC
Humidity				B/A		$= 4.7755\frac{P_v}{P_a - P_v}$
Water-gas shift					y_{24}[H_2]	$= \frac{y_1[CO]y_3[H_2O]}{y_2[CO_2]\ K}$

$$\begin{bmatrix} x_1 & 0.0019 & 0 & 0 & 0 \\ x_2 & 0 & 2 & 0 & -2 \\ x_3 & 2.003 & 1 & 0 & 0 \\ 0 & 0 & 0 & 1 & 0 \\ 0 & 0 & 0 & 0 & 1 \end{bmatrix} \cdot \begin{bmatrix} \frac{1}{\sum_{i=1}^{31} n_i} \\ \frac{A}{\sum_{i=1}^{31} n_i} \\ \frac{B}{\sum_{i=1}^{31} n_i} \\ B/A \\ y24[H2] \end{bmatrix} = \begin{bmatrix} Eq1 \\ Eq2 \\ Eq3 \\ 4.7755 \frac{P_v}{P_a - P_v} \\ \frac{y_1[CO] y_3[H_2O]}{y_2[CO_2]\, K} \end{bmatrix}$$

Using matrix solver (Microsoft Excel used here) values of all unknowns are determined and most importantly A value, then the following steps are followed to determine the instantaneous EBER;

1. Determine fuel to air ratio:

$$FAR = \frac{F}{138.3237A}$$

Where; Fuel mass (F) $=12.011x_1 + 1.0079x_2 + 15.9994x_3 + 14.0067x_4 + 32.065x_5 + 51.9961x_6 + 79.904x_7 + 18.9984x_8 + 28.0855x_9 + 39.0983x_{10} + 40.078x_{11} + 24.305x_{12} + 22.9897x_{13} + 30.9738x_{14} + 55.845x_{15} + 26.9815x_{16} + 47.867x_{17}$

2. Normalise the actual fuel to air ratio by the stoichiometric air to fuel ratio:

$$EBER = \frac{FAR}{FAR_{Stoich}}$$

Assumptions and limitations

- Fuel involved in the reaction is based on the 17 elements included in the reaction formula.
- All products evolved are covered by the 31 species.
- The EBER model's accuracy depends crucially on the species concentration measurements (the square bracketed terms in the Equations above).

4.4 Validation

A Leeds University in house programme for the calculation of adiabatic flame temperature and thermodynamic equilibrium composition "FLAME" was used to produce equilibrium combustion products from the combustion of theoretical fuel having a typical elemental composition of wood, at variable combustion equivalence ratios.

The fuel composition used was C:47.39 wt.%, H: 6.08 wt.%, O: 42.91 wt.%, Moisture: 2.56 wt.%, Ash: 1.06 wt.%, and GCV: 18 MJ/kg. note that as determined moisture was compensated from as determined hydrogen and oxygen weight percentages (2.56% water = 0.285% hydrogen + 2.275% Oxygen). While the oxidant mixture as follows; O_2: 20.946 vol.%, N_2: 78.084 vol.%, Ar: 0.937 vol.%, and CO_2: 0.033 vol.%. For the species products the following list were used for this run; O_2,CO_2, CO, C, H_2, H_2O, N_2, NO, NO_2, N_2O, Ar, SO_2, SO, S, H_2S, HS, HCl, Cl_2, HF, F_2, CH_2O, CH_4, and NH_3. Standard atmospheric pressure and ambient temperature at 20oC was and pressure for the fuel and the oxidant. The only variable was equivalence ratio from ER 0.5 to 3.0.

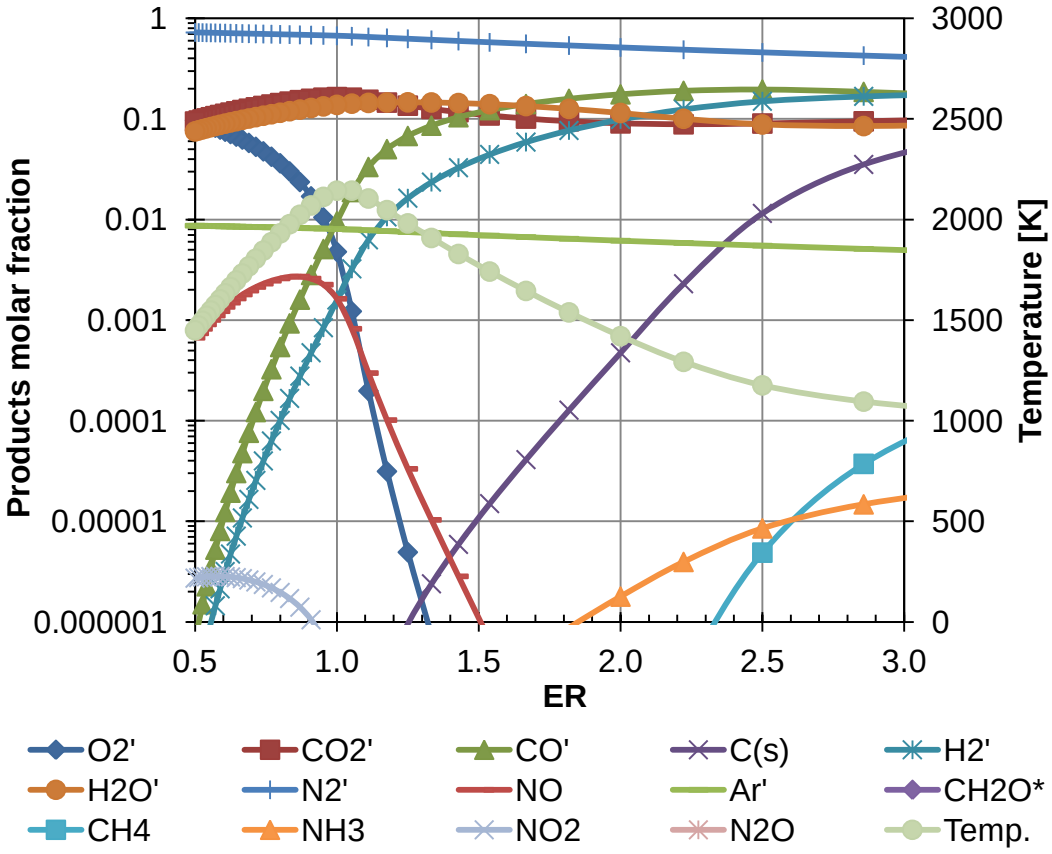

Figure 4-1: Results produced by FLAME for ER from 0.5 to 3.0; concentrations as molar fraction on a logarithmic scale (Left) and adiabatic temperature (Right).

The “FLAME” calculated equilibrium product concentrations are presented in Figure 4-1 as function of ER.

These theoretical product concentrations were then fed into the present EBER model and used a matrix solver to back calculate the ER and compare with corresponding input value into “FLAME”, as shown in Figure 4-2.

As a further comparison/validation Chan’s Air to fuel ratio model (used by the author and the Leeds group previously) was also used to compute the original equivalence ratio from the theoretical product data.

The results are showing that up to ER of 1.54 both models were able to back calculate the input ER with good accuracy. Beyond 1.54 both models started under predicting the input ER reaching 10% deviation at ER 2.0 input and higher deviations were reached with higher FLAME input ER. It should be noted that FLAME was created with the purpose of predicting equilibrium products, normally used for designing combustion systems with the objective of being near unity ER. Products from “very rich mixtures” such as soot are not “well defined” according to the manual. It is believed that where the deviations start is when the “not well defined” parts of the model start affecting the predicted emissions. Based on these findings, it is concluded that both (EBER and Chan’s AFR) models are valid for at least emissions with ER below 2.

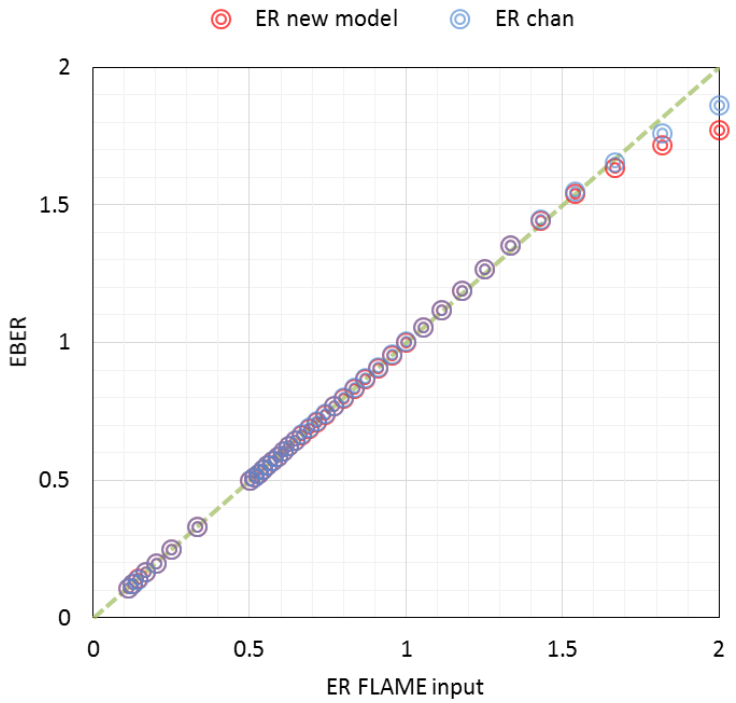

Figure 4-2: Results from the emission based equivalence ratio based on FLAME predicted equilibrium concentrations shown in Figure 4-1. ER FLAME input is the prescribed ER (independent) while EBER is the emission based calculations of ER (dependent). The green dotted line to highlight deviation from unity.

A further validation exercise was performed against experimental emission data measured at different gasoline engines [314, 316-320].

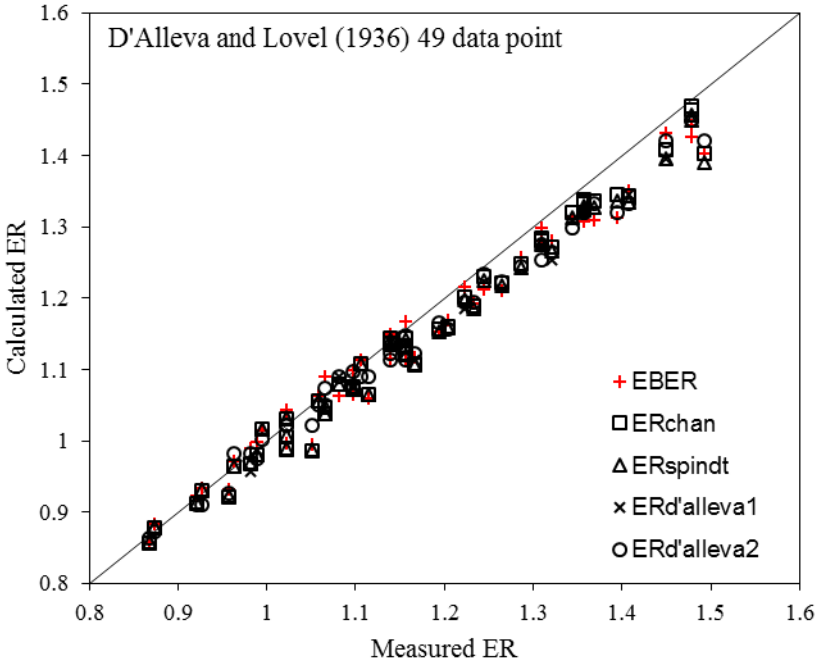

Figure 4-3: Comparison of emission-based equivalence ratio models for data (49 data point) from burning in engines from D'Alleva and Lovell [316].

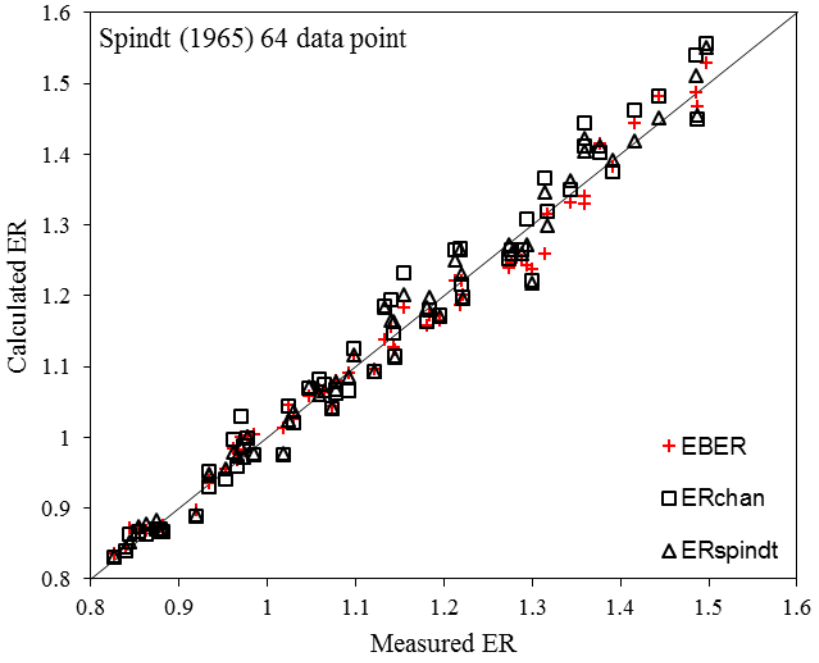

Figure 4-4: Comparison of emission-based equivalence ratio models for data (64 data point) from burning in engines published by Spindt [314].

4.5 Concluding comments.

As discussed in the literature review, EBER is unlike other ERs in that it quantifies the ratio of the mass of the fuel to the mass of air that were involved in producing the species concentrations in the sampled smoke..

By quantifying the mass based fuel to air ratio (or air to fuel ratio), toxic yields can be determined based on the volumetric concentrations measured as discussed earlier, without the need for constant flow to measure the total flow rate that is usually achieved by having collecting hood with a constant blowing fan.

Additionally, from the incomplete combustion species concentrations near the source of the fire, the combustion efficiency can also be calculated. The HRR inside the fire compartment can then be determined if the fuel mass loss rate and calorific value are known, corrected for the combustion efficiency. Hence the air consumed in the fire can also be determined from the EBER. This procedure enables full scale fire compartment tests in real buildings to be undertaken without the need for the conventional exhaust gas oxygen consumption calorimetry hood. Also it enables the total heat release to be split between internal compartment and external HRR if the exhaust calorimetry hood is used for the total HRR.

The procedure presented is also able to take into account more complex /realistic fuel compositions in fires and the determination of the fire A/F and equivalence ratio from heated gas sampling of the mixed ceiling layer fire product gases prior to external dilution.

The information produced using direct raw gas ceiling layer sampling in full and reduced scale compartment fires will be used to illustrate the application of the technique to the determination of internal fire compartment equivalence ratio prior to any external dilution of the fire product gases and this will allow the calculation of toxic yields from more reliable measurements of higher concentration values prior to dilution.

Chapter 5
Full scale experiments

This Chapter presents, analyses and discusses the results from the large scale experiments. The experimental setup and fuel characteristics for each experiment were presented in Chapter 3 in detail. Eight tests were conducted as part of this study (see Table 3-4.) and presented here sections based on the fuel type;

- Wooden pallets (tests 3 and 5)
- Cotton linen and towels (tests 1 and 4)
- Three seater sofa (test 2)
- Fully furnished living room (test 8)
- Diesel pools (tests 6 and 7)

The analyses focus on the toxic emission measurements that were taken from these tests. It utilises the EBER concept presented in Chapter 4 to establish mass yields of toxic emissions. The thermal environment conditions is presented with smoke layer height and temperature analyses. Additionally heat release rate values are estimated using mass burning rates and calorific value concept.

5.1 Wooden pallets I

Wood is the dominant fuel in residential buildings, almost 80% of homes' furniture is wood, see section 2.1.1. Therefore, it is important to understand the composition of combustion products produced by wood in different fire scenarios. Test 3 had two scenarios; firstly (T3a), a door closed scenario, where shortly after ignition the only door to the room was closed in order to restrict ventilation. Secondly (T3b), with the door fully open which was conducted here by the end of the first scenario.

The fire load was wood pallets which were stacked on top of one another (9 in total) with a total weight of 143 kg; each pallets dimensions were measured to be 1.22 m x 1.22 m x 0.140 m and located on the corner opposite the door see Figure 3-26. The stack was ignited using a small metal tray (200 mm square) with 400 ml of methanol to the centre of the fuel mass. Another wooden pallet stack (intended to be identical to the first one) with a total weight of 144 kg was positioned on the opposite corner, to assess the pyrolysis effect between the two stacks, this did not ignite in the fire. The British Standards guidance [19] suggests that the average fuel load in dwellings is 780 MJ/m^2, which for this compartment is 786 kg of wood, so that the fire is lightly loaded. The front door was the main ventilation path and it will be shown that the fire was ventilation controlled so that the relatively low fire loading was not a major factor in the fire development.

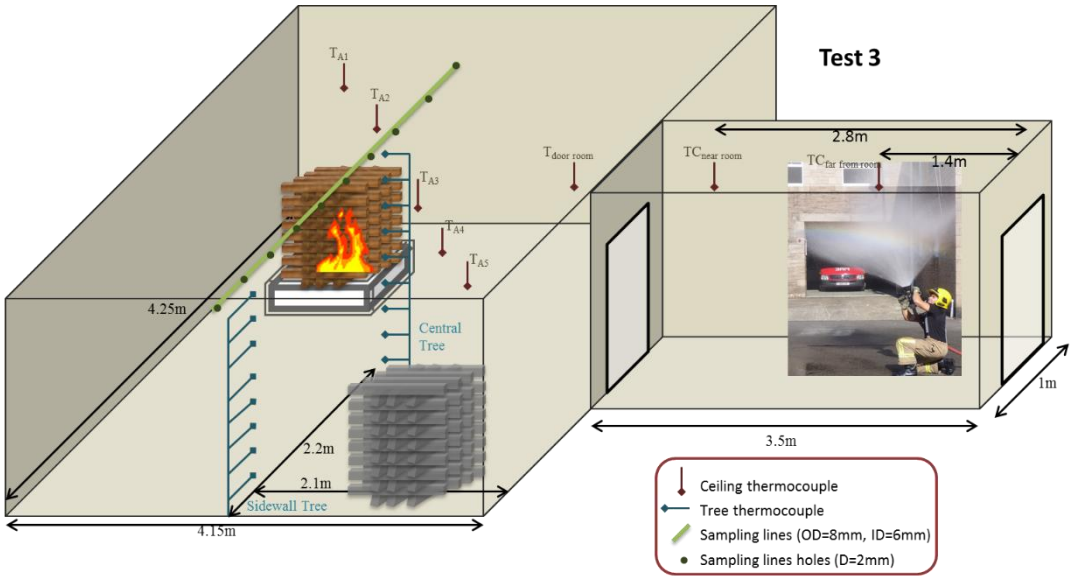

Figure 5-1: Test 3 full setup showing fire load, instrumentation and fire-fighting entrance.

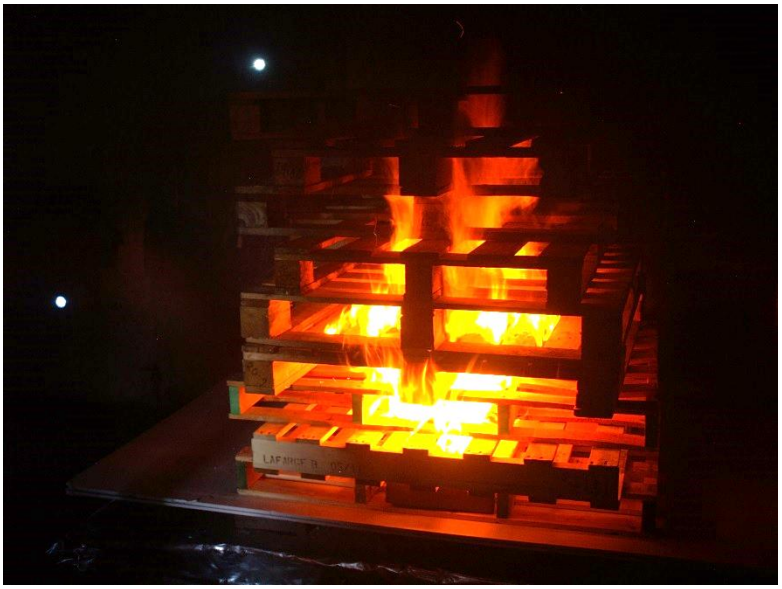

Figure 5-2: Picture of the fire in Test 3, 46 seconds after ignition.

The fire load was ignited 420 seconds (7min 45sec) from the start of logging. Pictures of the fire were taken before closing the door e.g. Figure 5-2.The door was shut 2 minutes later at the 590th second (9min 50sec). Then after temperatures dropped in the compartment to below 60 C the door was opened at 2060 seconds (34min 60sec) for T3b scenario to start. The fire was left for over twenty minute to give a chance for any smouldering fire to propagate after opening the door. At 3600th second (60min) the fire was reignited using 400 mL of meths poured into the metal tray, it propagated straight away reaching flashover conditions. Then fire-fighting activities started at 3920 seconds (65min 20sec). The time line of Test 3 is graphically demonstrated in Figure 5-3 and measurements of mass of the fire load throughout the test is shown in Figure 5-4.

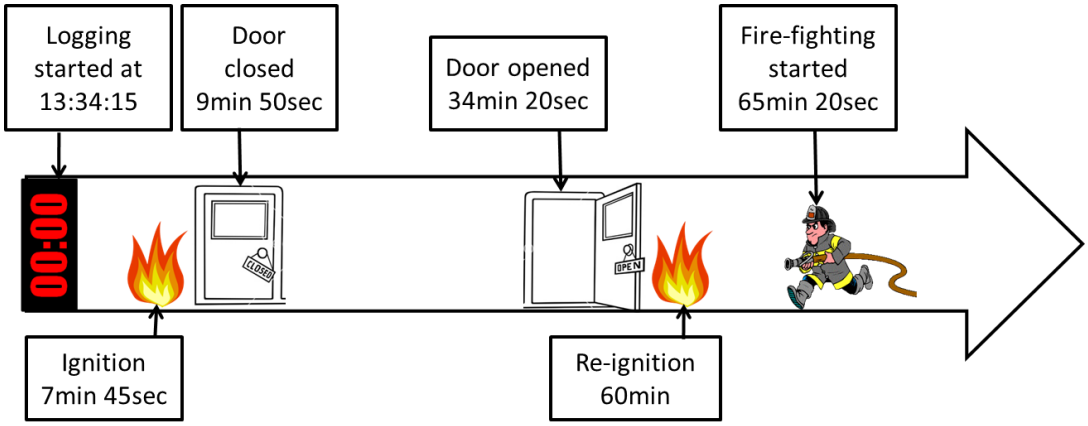

Figure 5-3: Timeline of the main events for Test 3.

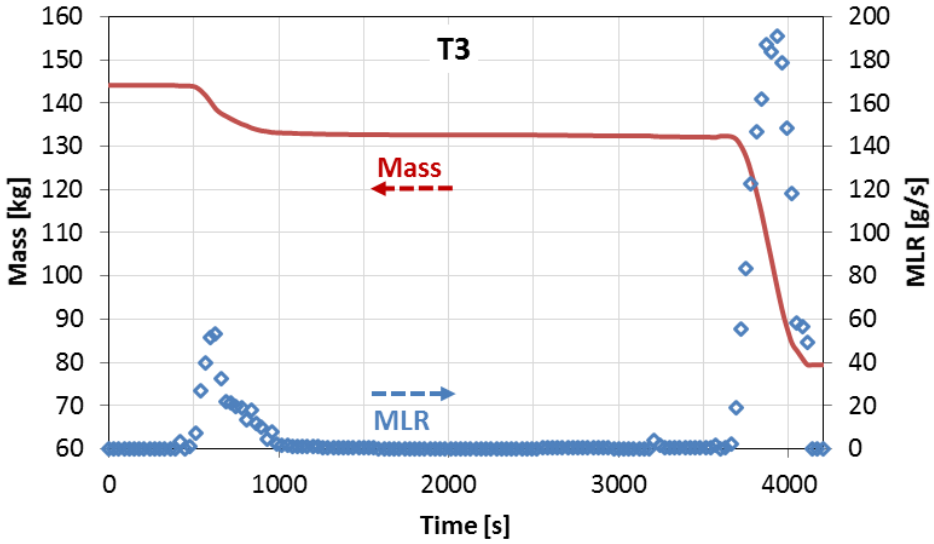

Figure 5-4: Total mass of the fire load (Red) and mass loss rate (Blue) for Test 3.

5.1.1 Results and analysis for the first part of Test 3 (T3a)

During this part of the test the fire started initially with a well ventilated flaming fire (ISO stage 2) until oxygen available was used (reaching peak temperatures and heat release rate). Deprived oxygen levels at this point were unable to sustain the fire at the same burning rate so it transformed to be under-ventilated pre-flashover flaming fire (ISO stage 3a). With more oxygen being used, oxygen reached the level to be unable to sustain a flaming fire to transform to a slower non-flaming smouldering fire (ISO stage 1a) until it was fully extinguished by the 1200th second. In the following sections thermal and toxic environment results and analysis for this phase (T3a) are discussed (from 0 seconds till 2060 seconds).

5.1.1.1 Mass loss and heat release rate (HRR) – Test 3a

Heat release rate can be quantified by the use of mass loss data and calorific values of the materials. And can be corrected for inefficiencies using the mass yields data of incomplete combustion products. A calorific value of 15.4 MJ/kg were used to produce Figure 5-5. The correction of the HRR data is based on inefficiency as derived from unburnt hydrocarbons

and carbon monoxide measurements as used by the author in [260]. Initially, the burning rate was propagating rapidly (due to the existence of the fire load and oxidizing agent). Then, the level of oxygen dropped (due to the lack of ventilation) and the fire slowed down. Till eventually it was unable to sustain any flaming fires, to transform to a smouldering fire with a very slow burning rate until ultimately it self-extinguished.

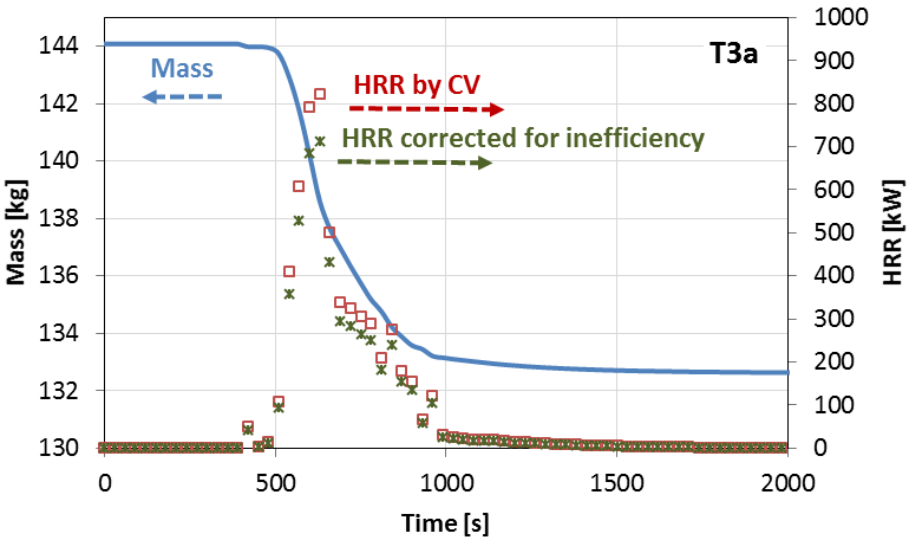

Figure 5-5: Mass change with time and associated HRR based on the mass loss rate for Test 3a. Also shown is an adjusted HRR, based on inefficiency of combustion as derived from the unburnt hydrocarbons and CO measurements.

5.1.1.2 Thermal environment – Test 3a

Temperature inside the room followed similar patterns to the HRR discussed above. Figure 5-6 shows temperature measured at the ceiling level, where temperatures at the highest point dropped lower than 100 C just after the 1200th second mark. Before opening the door to end phase a of Test 1, the vertical temperature gradient throughout the room showed very little variation (max. 25 C) at the 1800th second, as can be seen in Figure 5-7.

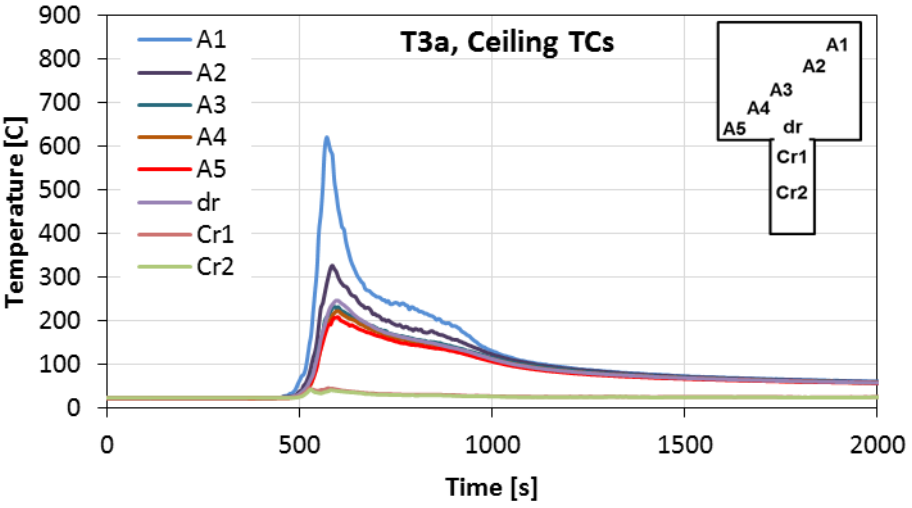

Figure 5-6: Ceiling layer temperature measurements at different positions inside the compartment and corridor during Test 3a.

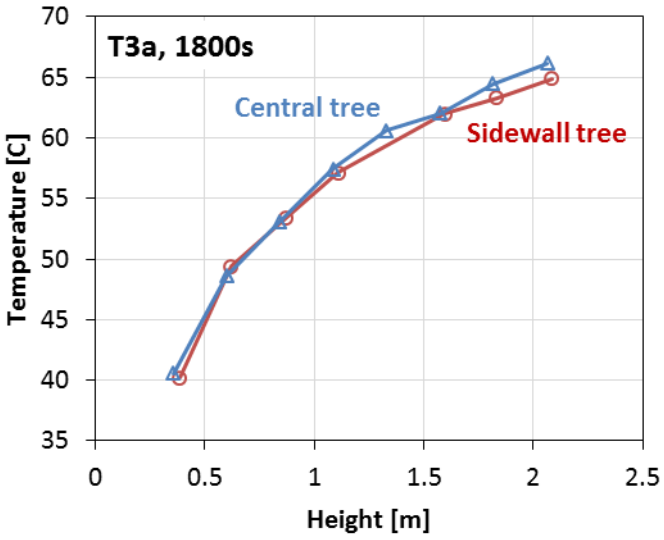

Figure 5-7: Vertical temperature variation at 1800th second from central and sidewall thermocouple trees.

5.1.1.3 Toxic environment – Test 3a

Gas analyses for products from the first part of the test (T3a), while the door was closed, cannot be treated as a dynamic process due to the lack of exhaust and fresh air supply, which is important for sustaining a flaming combustion. So the gas concentration measurements given by the instruments in that period were for a static situation of the fire where the smoke is accumulating in the room space. So for the purpose of establishing yield data, concentration measurements were taken at the point when the fire died down and before opening the door.

Table 5-1: Concentrations of major combustion emissions produced in Test 3a at the 1800th second, with their ratios to relevant toxic exposure thresholds. and average mass yield data for each species.

Species	Conc. [ppm]	R-Safe	R-Escape impairment	R-Lethal	R-LC50	Yield [g/g]
CO	19,381	97	46	32.3	3.4	0.0869
Acrolein	541	18,033	1,229	216	3.6	0.0049
Formaldehyde	560	1,867	93	8	0.75	0.0027
HCN	99	40	5.9	4.8	0.6	0.0004
THC	13,719					0.0352

At that point (1800th second), the deviation for the vertical temperature gradient was minimal between top and bottom thermocouples (less than 25 ^{0}C), hence it was assumed that the collected sample was representative of the whole 41 m^3 compartment. And by quantifying the total mass of fuel burnt during that period (11.43 kg), then mass yields of each toxic gas can be quantified, as presented in Table 5-1. The fractional effective concentration of the sampled gas in respect to the different levels of effects discussed earlier in section 2.3.2.3 were established the contribution of each species is demonstrated in Figure 5-8.

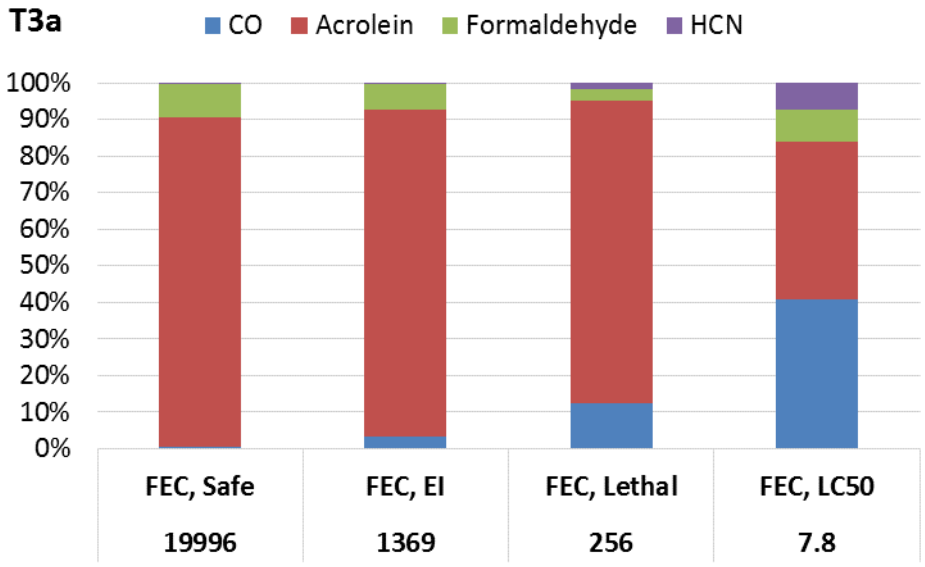

Figure 5-8: The main toxic products released in Test 3a in respect to their contribution to the overall Fractional Effective Concentration (FEC).

5.1.2 Results and analysis for the second part of Test 3 (T3b)

As discussed earlier Test 3b started by reigniting the stack while the door was open allowing unlimited supply of air to the fire. The fire propagated quickly reaching flashover, it was left to stabilise for 5 minutes before the start of the fire-fighting activities (3920th second on the global timeline). The following sections present the results for that part of the test (T3b) by discussing the thermal and toxic environment produced within the compartment and the influence of the fire-fighting activities.

5.1.2.1 Mass loss and heat release rate (HRR) – Test 3b

The mass of the pallet-stack as a function of time is shown in Figure 5-9, which also shows the onset of flashover and the start of fire-fighting activities. Approximately 50 kg of wood was consumed in the duration of Test 3b, 60% of which was lost before the start of the fire-fighting operations.

The elemental analysis of the wood gave the formula of $CH_{1.54}O_{0.82}$ in a dry ash free basis (daf) and from this the stoichiometric A/F by mass was determined as 5.0.The net calorific value (CV) of the material was 15.4 MJ/kg , based theoretical oxygen consumption requirements [15].

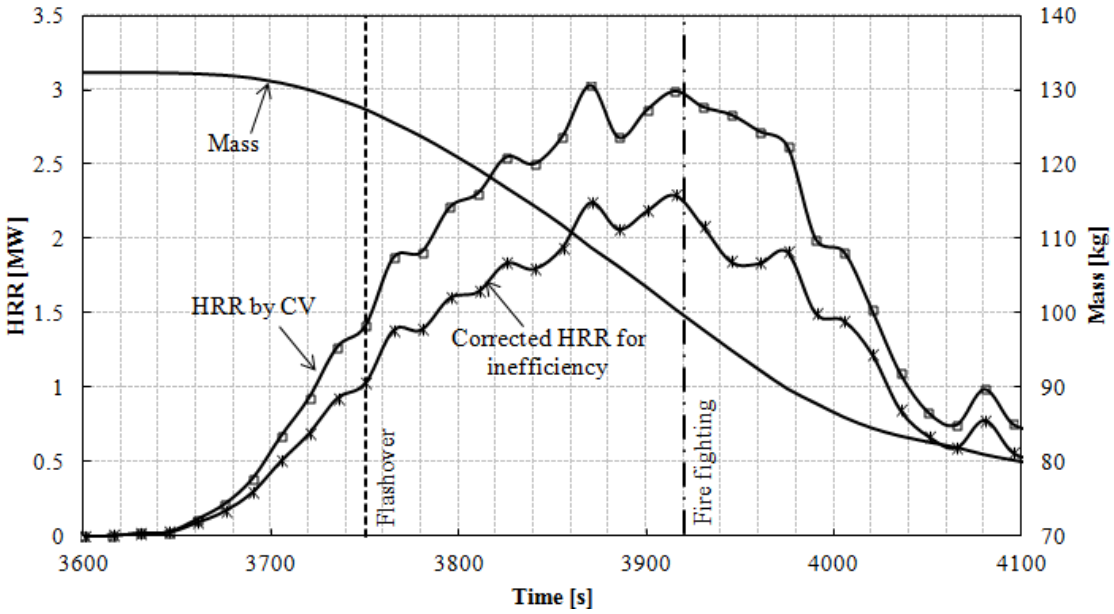

Figure 5-9: Mass change with time and associated HRR based on the mass loss rate. Also shown is an adjusted HRR, based on inefficiency of combustion as derived from the unburnt hydrocarbons and CO measurements.

The heat release rate (HRR) based on the mass loss rate and the Calorific Value (CV) of the wood is shown in Figure 5-9. This evaluation of the HRR effectively assumes complete combustion and release of all the available energy. Carbon monoxide, unburnt hydrocarbons (Total Hydrocarbons, THC) and soot are all evidence of incomplete combustion and therefore unreleased energy, which is quantified as the combustion inefficiency. Soot yields need to be >1% to be significant, but were not determined in the present work which based the combustion inefficiency on the CO and THC using procedures common in the automotive emissions area [75]. Aljumaiah et al. [242] showed that THC were particularly important in correctly evaluating the HRR in under-ventilated wood crib fires. The combustion efficiency deteriorated as the compartment ventilation increased and was as low as 50% for the highest ventilation rate (all fires were under-ventilated overall) [242]. The flame seen outside the compartment in real fires is the combustion of the unburnt CO, HC and hydrogen released in the rich burning fires, it is also the source of backdraft when air is admitted through opening a door to a fire burning with low combustion efficiency.

In the present full scale work only CO and THC yields, presented in Figure 5-19 were taken into account in correcting the HRR shown in Figure 5-9. The combustion inefficiency is shown in Figure 5-10 to grow relatively quickly to over 20% and to stabilize between 20 and 30% for the test duration. Figure 5-10 clearly demonstrates the large contribution of the THC to the combustion inefficiency.

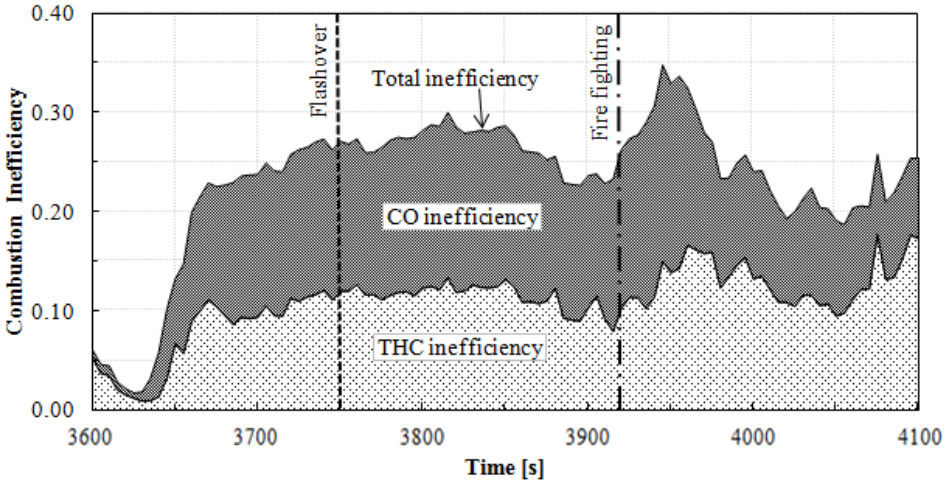

Figure 5-10: Total combustion inefficiency as a function of time with contributions from CO and THC.

These combustion inefficiencies are similar to those found by Aljumaiah et al. [242] for ventilation controlled pine wood crib fires. On the onset of the fire-fighting operations the combustion inefficiency was increased to a peak of 35% for a short period after the onset of fire-fighting, as the fire fighters blocked the entrainment of air into the fire from the air feed corridor. Once the fire fighters were out of the corridor and in the room this air blockage ceased and the combustion inefficiency fell back to near 20%.

The HRR corrected for the combustion inefficiency in Figure 5-9 reached 1 MW in about 140 seconds from ignition which, on the basis of a t^2 fire, would give a growth rate of about 0.05 kW/s^2. This is the fire growth rate of a "fast" fire and is similar to the measurement of Alpert & Ward [321] for stacks of wood pallets of different heights, burning in the open, see Figure 5-11. The corrected maximum HRR per unit area in the present tests was less than half the corresponding value for the open tests [321] demonstrating the effects of ventilation control and combustion inefficiency.

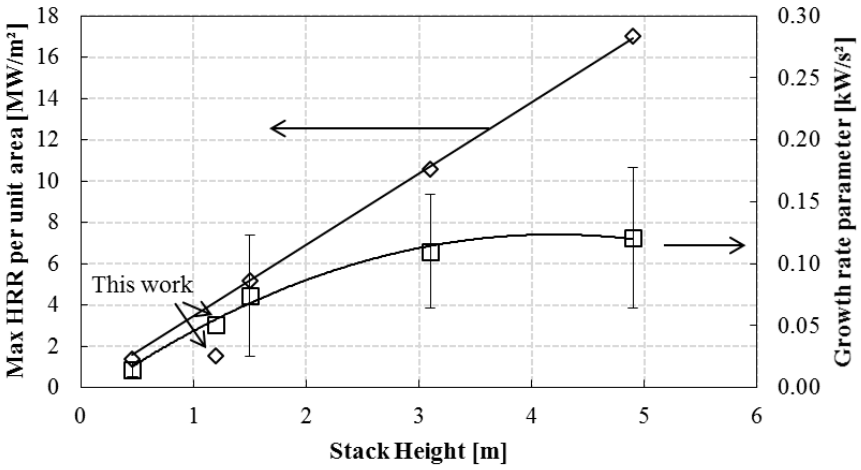

Figure 5-11: Maximum heat release rates per unit area and growth rate parameter from T3b compared with data for burning freely ventilated wood stacks with different heights reported by Alpert & Ward [321].

5.1.2.2 Thermal environment – Test 3b

Figure 5-12 shows the fire temperatures as a function of time, from the thermocouples at different heights on the sidewall tree. After 100 seconds from ignition, there was a rapid rise in temperature for all the thermocouples above 1.5 m, indicating the fast descent of the hot layer. Hot layer temperatures were fairly uniform with height from the start of the combustion with maximum temperatures between 650 and 730 °C after the onset of flashover. Figure 5-12 also shows that the lower level (below 1.2 m) temperatures were high at over 400 °C and these would have generated a hazardous convective heat environment for the fire-fighters – even if in the crouching position.

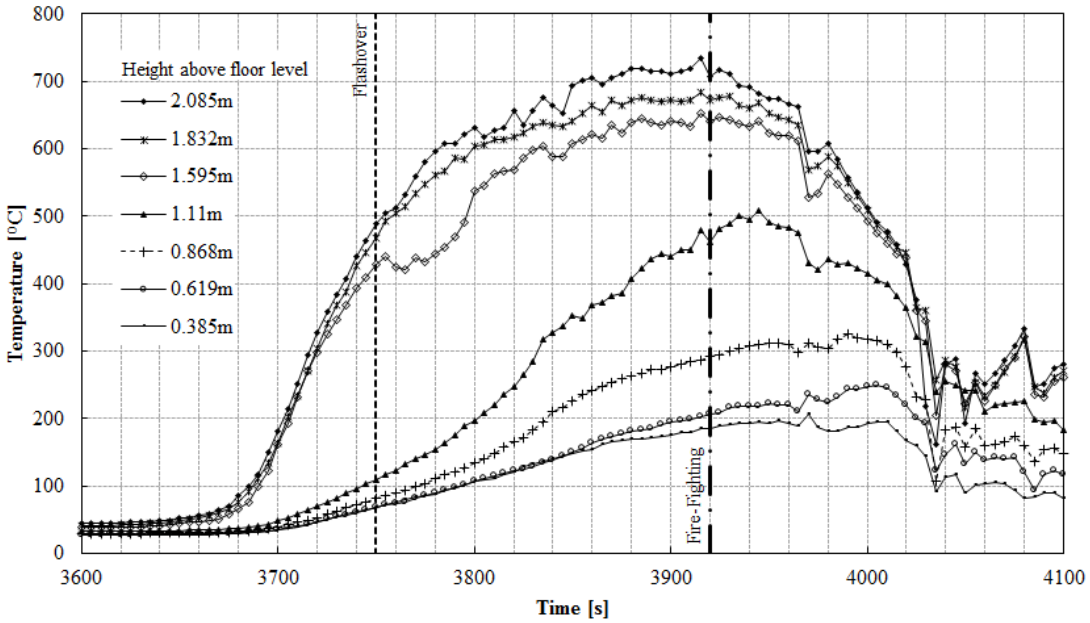

Figure 5-12: Temperatures at different heights from floor level in the fire room as measured by the vertical thermocouple tree on the sidewall of the compartment during test 3b.

The central vertical-thermocouple-tree recorded a similar range of temperatures from the bottom to the top of the compartment. However the temperature vertical gradients were more uniform for the central tree as shown in Figure 5-13. This was due to the position of this tree in the path of the main flows in and out of the compartment which resulted in more mixing of the layers.

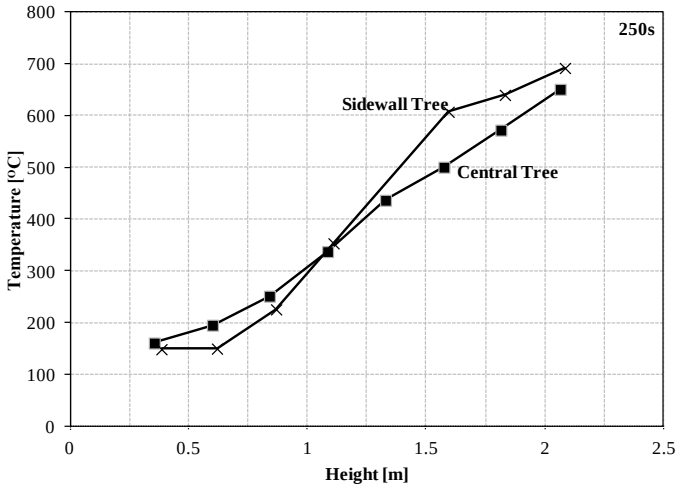

Figure 5-13: Vertical temperature variation at 3750th second (250s from ignition)

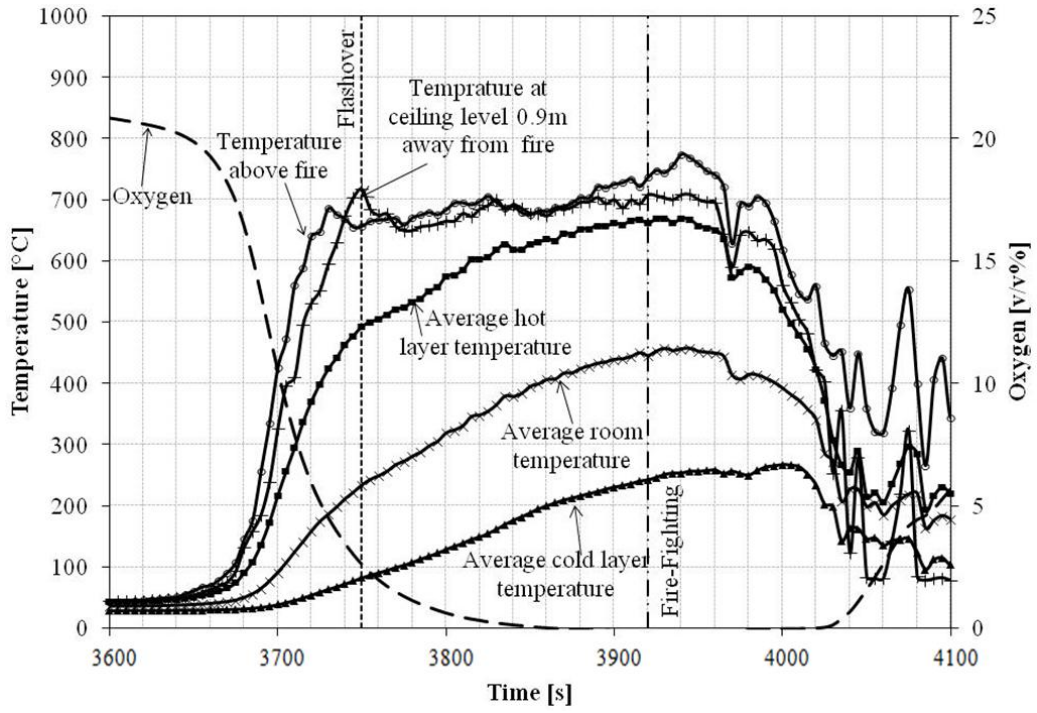

Figure 5-14: Temperatures and Oxygen levels, Top ceiling temperatures in the vicinity of the fire and average hot layer temperatures (top 3 thermocouples from each vertical tree plus thermocouples T1, T2, T3 at ceiling level), average cold layer temperature (bottom 3 thermocouples from each vertical tree), average room temperature (average of all thermocouples on the two vertical trees).

Figure 5-14 shows that the temperature of the ceiling thermocouple T1, nearest to the burning stack plume, reached a maximum of 780 ^{o}C. For most of the "steady" burning period this temperature was 680 to 730 °C, which is comparable to the top sidewall and central tree temperatures, similar range was produced in other full scale experimental fires [322]. This indicates a fairly uniform temperature across the room near the ceiling plane. In contrast, the temperature of the upper layer in the corridor (shown in Figure 5-15) was significantly lower than the room temperature, indicating a higher degree of mixing of the exiting hot gases with the incoming cold air.

5.1.2.3 Onset of Flashover

The most commonly accepted definition of flashover is “transition to a state of total surface involvement in a fire of combustible materials within an enclosure” [6]. In the present test this definition would have corresponded with the ignition of the second stack. There was no clear evidence of this happening, although there was charring at the top of the stack. The fire-fighters reported that there were no flames on top of the second stack when they entered the compartment. However, there was an overall reduction of the weight of the stack by 5.1 kg (3.68% of the overall stack weight) or in terms of the top pallet on its own, the mass loss was 1.45 kg or 12.4% of the original mass. Thus the top pallet average pyrolysis rate was 3.4 g/m^{2}s over the 300 s (from 3600 to 4000 seconds). This was sufficiently high to support ignition [323] under normal oxygen concentrations and therefore this would be evidence of sufficient heat to cause ignition of the second stack. The top of the stack was immersed in the hot layer which had low oxygen to support combustion. Delichatsios [323] showed that for non–flame–retarded plywood the critical mass flux for ignition (at high heat fluxes) was raised from about 3 to 7 g/m^{2}s as oxygen was reduced from 21 to 15%. Therefore at oxygen concentration levels below 15%, pyrolysis mass fluxes higher than 7 g/m^{2}s would be needed for ignition to occur.

Other phenomena associated with onset of flashover include

- Upper layer between 500 – 600 °C [4, 324] – in this test the average upper layer temperature reached 500 °C at around 155th second from ignition (3755th second on the global timeline)
- Heat flux of 20 kW/m² at floor level [3, 4] – this was not measured in the present tests (flashover targets were shielded by wall paper during this test as discussed and shown earlier in Figure 3-28). Calculation of the heat flux at floor level from the hot layer at 1.2 m above floor level (based on visual evidence) and at temperature of 500 °C and using view factors between finite parallel plates [325] and an emissivity of 0.8 gives a value of 13 kW/m^2 at floor level. This would appear lower than expected but it does not account for radiation from the fuel package and the flames through and above it, which can be shown to contribute an additional 4 to 10 kW/m^2 to floor targets depending on the distance from the flame – this part of the calculation was performed using view factors between perpendicular finite rectangles [325], to represent the vertical flame and a target on the floor, a flame temperature of 900 °C and a calculated flame emissivity of 0.5.

On this basis it was considered that the most likely timing of the onset of flashover and ventilation controlled burning occurred at 155th second from ignition (3755th second on the global timeline).

5.1.2.4 Fire-fighting and thermal environment

Fire-fighting was initiated when it was deemed that the fire had reached steady burning rate, which was at 3920th second as shown in Figure 5-15. The progress into the access corridor and the room, of a group of 3 fire-fighters (with one charged water line) was tracked from the video recordings and the length of hose fed into the enclosure and is shown in Figure 5-15 by the star symbols. The bar lines in Figure 5-15 are an indication of the spray pattern, timing and duration of water spray discharge by the advancing team. The short bars indicate a short water pulse towards the ceiling while the longer bars indicate longer pulses directed onto the fire seat.

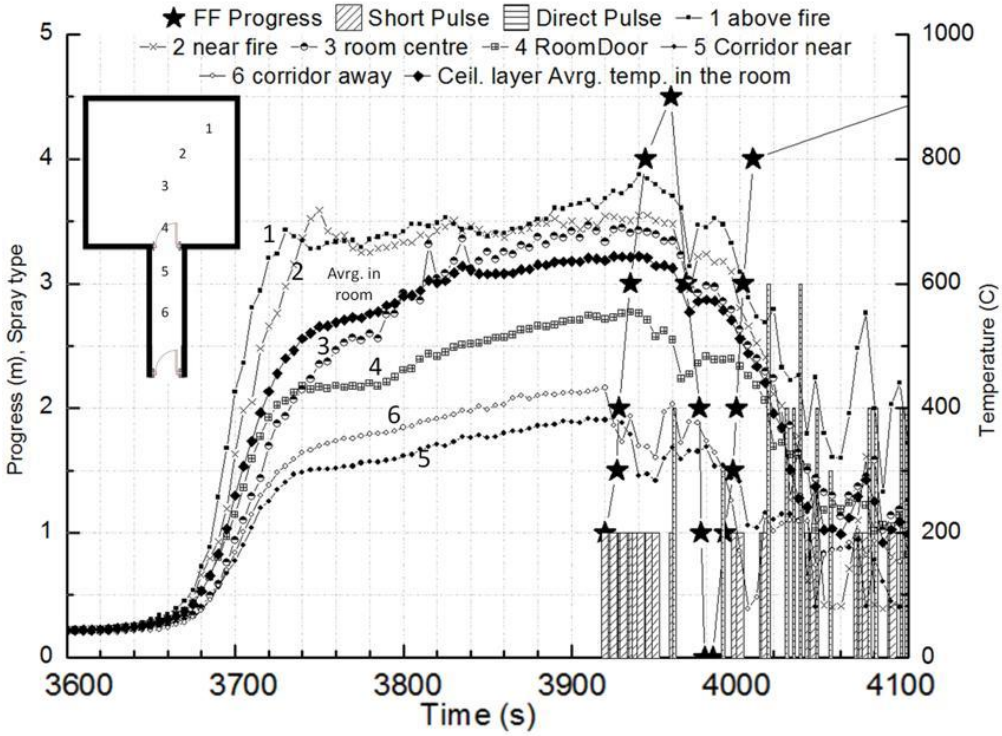

Figure 5-15: Ceiling temperature along the corridor and into the fire room.

On entering the corridor the fire-fighting team adopted the crouching or kneeling position, trying to keep below the outflowing smoke layer, whilst directing a series of short water pulses towards the corridor ceiling and then the compartment ceiling ahead of them. The spray had an immediate effect in reducing the smoke layer temperature as shown in Figure 5-15 from the temperatures in the ceiling layer. It can be seen that the water pulses were more effective in dropping the temperature in the corridor by about 100 degrees, but the temperature drop achieved by the spray in main fire compartment was much smaller.

On entering the fire compartment the fire fighters tried to manoeuvre and position themselves in the near right hand corner of the room close to the door. This would have allowed all three men to be inside the room during fire extinguishment. However, for the few seconds that it took the leader to adjust his position he stopped pulsing water and this, in combination with the prevailing conditions resulted in the team experiencing unbearable

heat levels and an immediate retreat was ordered, accompanied by a long water pulse directly to the seat of fire. From the fire room entry to room exit there was only a 20 s interval.

The team retreated all the way to the outside regrouped and re-entered the corridor immediately starting with a direct pulse towards the fire and then 3 short pulses as they positioned themselves in the entrance just inside the room. Figure 5-14 the average lower layer temperature of the gases surrounding the crouching fire-fighters was in the range of 242 to 267 °C. This is above the 235 °C limit and therefore in the critical range, as defined by DCLG [326] and shown in Figure 5-16.

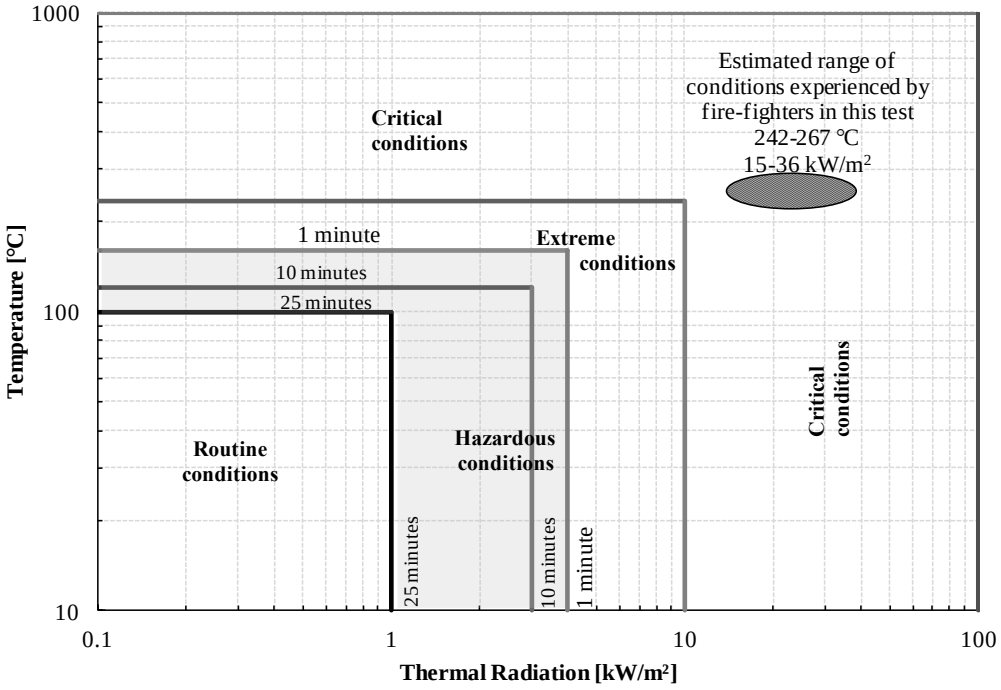

Figure 5-16: Fire-fighters exposure conditions in standard BA kit with proposed time limits [326]. Conditions estimated to be faced by fire-fighters in this test, are presented by the highlighted area.

To define the locus of the thermal conditions experienced we also needed to determine the likely heat flux at the fire-fighter level within the fire compartment, both from the hot layer and the flames, using view factors and flame and hot layer temperatures and emissivities. This resulted in estimates of heat fluxes ranging from 15 to 36 kW/m^2, for vertical and horizontal body parts at varying heights from the floor, as depicted in Figure 5-16. This heat flux is well above the 10 kW/m^2 limit delineating the extreme from the critical conditions [326].

In terms of the thermal dose received by the fire fighters it was estimated that during the first 15 seconds in the compartment they received 1800 TDUs which built up to around 2400 TDUs during the next 5 seconds of retreat time. This is marked on Figure 5-17. The calculation shows that they would have exceeded the threshold limit of damage to their

protective equipment (PPE) if they delayed their exit by 10 seconds more. This is congruent with the very fast build-up of physical discomfort that the fire-fighters reported on debrief. They also reported experiencing hot temperatures on their knees where their clothing was compressed against the skin. This again agrees with the high ambient temperatures measured at low level.

The very short time to unbearable conditions experienced by the team and the estimate of 30 s to PPE thermal damage levels, demonstrates and quantifies the very short time available for fully protected fire-fighters to move to a safer location in an escalating or fully developed fire.

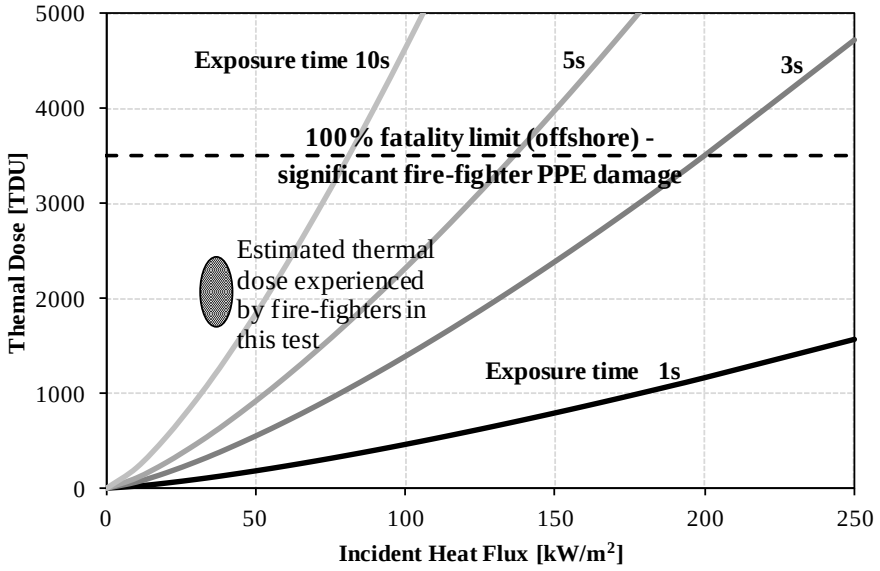

Figure 5-17: Thermal dose as a function of incident flux and exposure time, and in the shaded area the thermal dose estimated to have been experienced by the fire fighters in this test in their first attempt (15-20 s exposure).

5.1.2.5 Toxic environment – Test 3b

The combustion Equivalence Ratio (ER) was calculated as a function of time and is shown in Figure 5-18. The ER plot shows that the fire started burning rich after 50 seconds from ignition and reached a value of near 1.8 and steadied off at this value, indicating that the fire reached a ventilation controlled steady state earlier than our estimated timing for flashover. On entry of the fire-fighters in the corridor there was a further increase of ER due to the physical blockage to the incoming fresh air path by the bodies of the fire crew. The combustion became even richer at the initial application of water, this effect was due to the increase in the combustion inefficiency, as shown in Figure 5-10. After the second fire attack the ER dropped as the fire was brought under control.

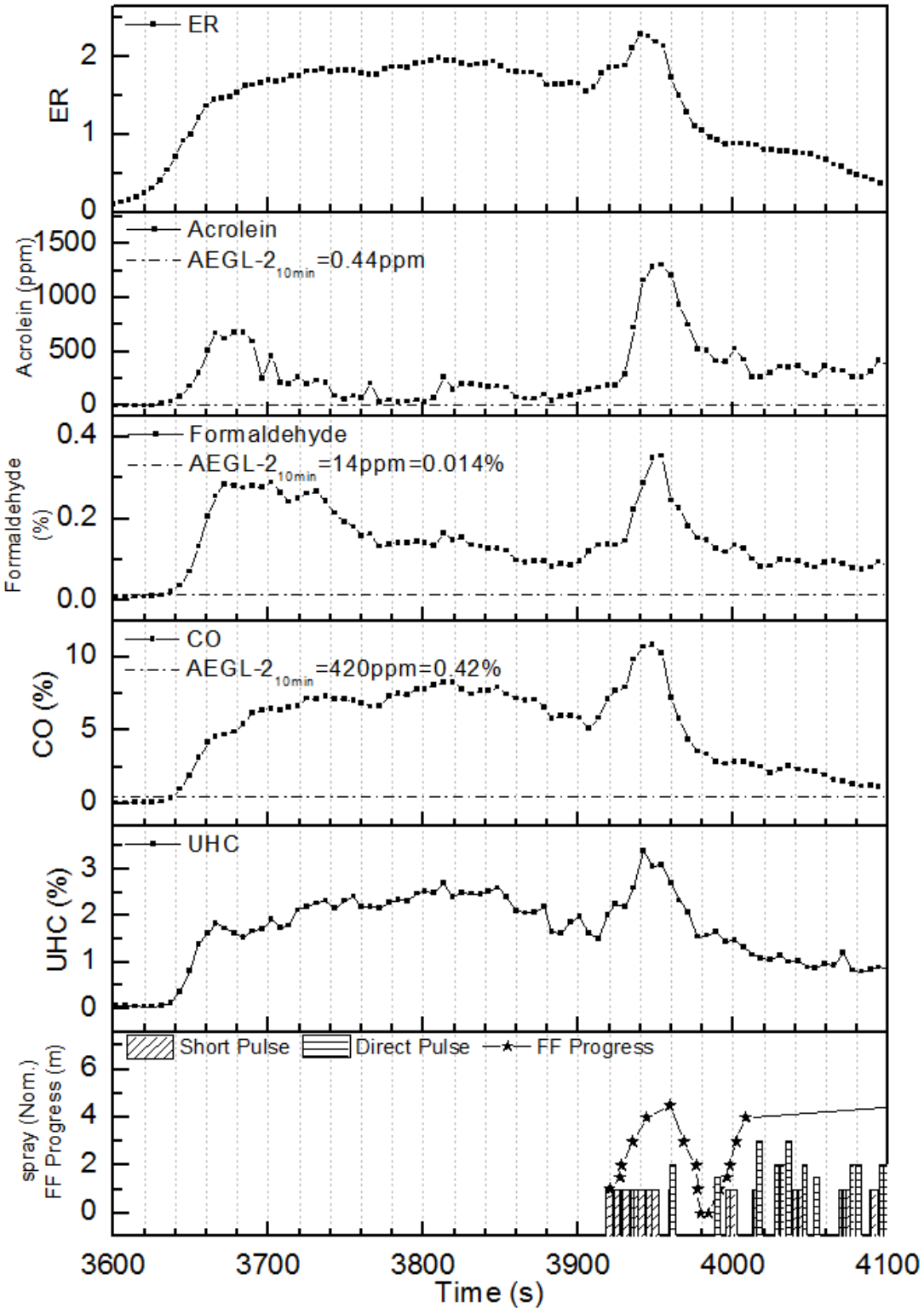

Figure 5-18: Combustion toxic products concentrations in volume basis [v/v] in line with equivalence ratio and fire-fighting activities.

Figure 5-18 also shows the variation of the concentrations of the main toxicants. Carbon monoxide and THC showed similar behaviour with a rapid increase after 40 seconds reaching steady high levels during the steady state period of the fire. Acrolein and formaldehyde showed a reduction of concentrations during the steady state phase. This

occurred at the same time as the oxygen was reduced to its minimum value and flashover occurred. Aldehydes form at low temperatures in the presence of hydrocarbons and oxygen. Comparison with the oxygen levels in Figure 5-14 aldehydes peaked at about 400 ^{o}C and 10% oxygen, at the start and end of the fire. It is the peak early in the fire which is of most concern as this occurs pre-flashover and would tend to impair escape from the fire.

The relative toxicity of each species is usually determined by the ratio to an appropriate standard concentration with known effects to humans [36]. There is considerable debate and development in this area [242]. For the purposes of this work the species concentrations were compared to the AEGL-2_{10min} values which are particularly relevant to impairment of escape in fires. "AEGL-2 is the airborne concentration of a substance above which the general population could experience an impaired ability to escape" [327]. This limit is marked on Figure 5-18 as a straight line and it is shown to have been exceeded for most of the duration of the fire.

In designing suitable ventilation systems computational fluid dynamics software (such as FDS) are usually used and an important input in these models are the species mass yields such as soot and CO. Most measurements of such yields have been performed under well ventilated conditions (such as the Cone Calorimeter) [328-331] and these are not suitable for compartments fires due to the effect of inadequate ventilation on these emissions. A number of researchers [240-242, 329, 332-337] have in recent years reported toxic species yields under variable ventilation conditions that show much higher yields than measured under free ventilation conditions.

The main toxic species yields in the present experiment are given in Figure 5-19. Tewarson [263] empirically (based on FPA tests) correlated the main species emissions to the equivalence ratio for different fuels. His predictions for CO and THC yields from wood combustion for the equivalence ratios in the present experiment, are also shown in Figure 5-19. The Tewarson THC predictions show remarkable agreement with the present measurements. The CO predicted yields however fall short (about half) of those measured, suggesting that a refinement to the model is needed.

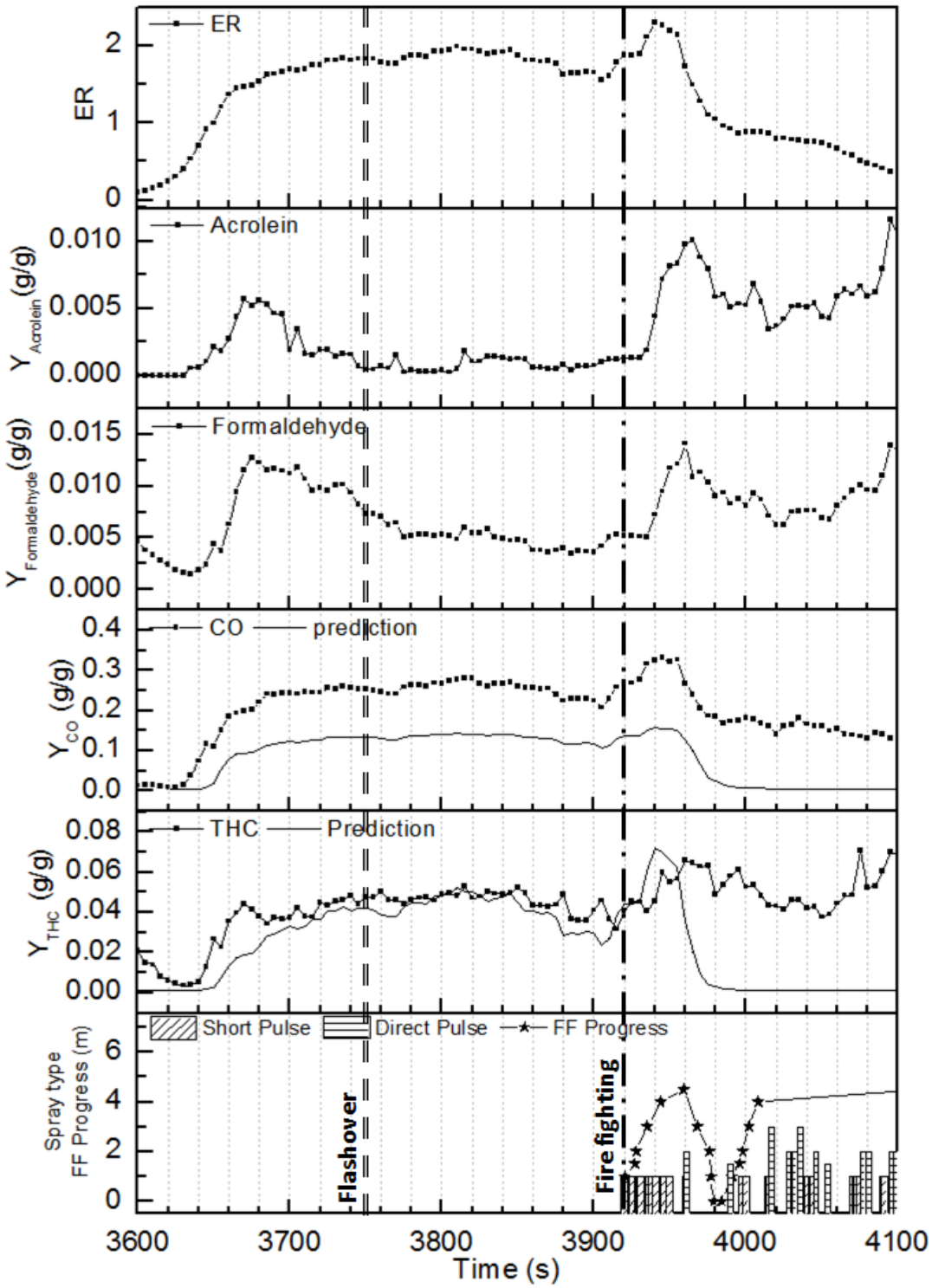

Figure 5-19: Combustion toxic products mass yields and Tewarson's yield prediction in line with equivalence ratio and fire-fighting activities.

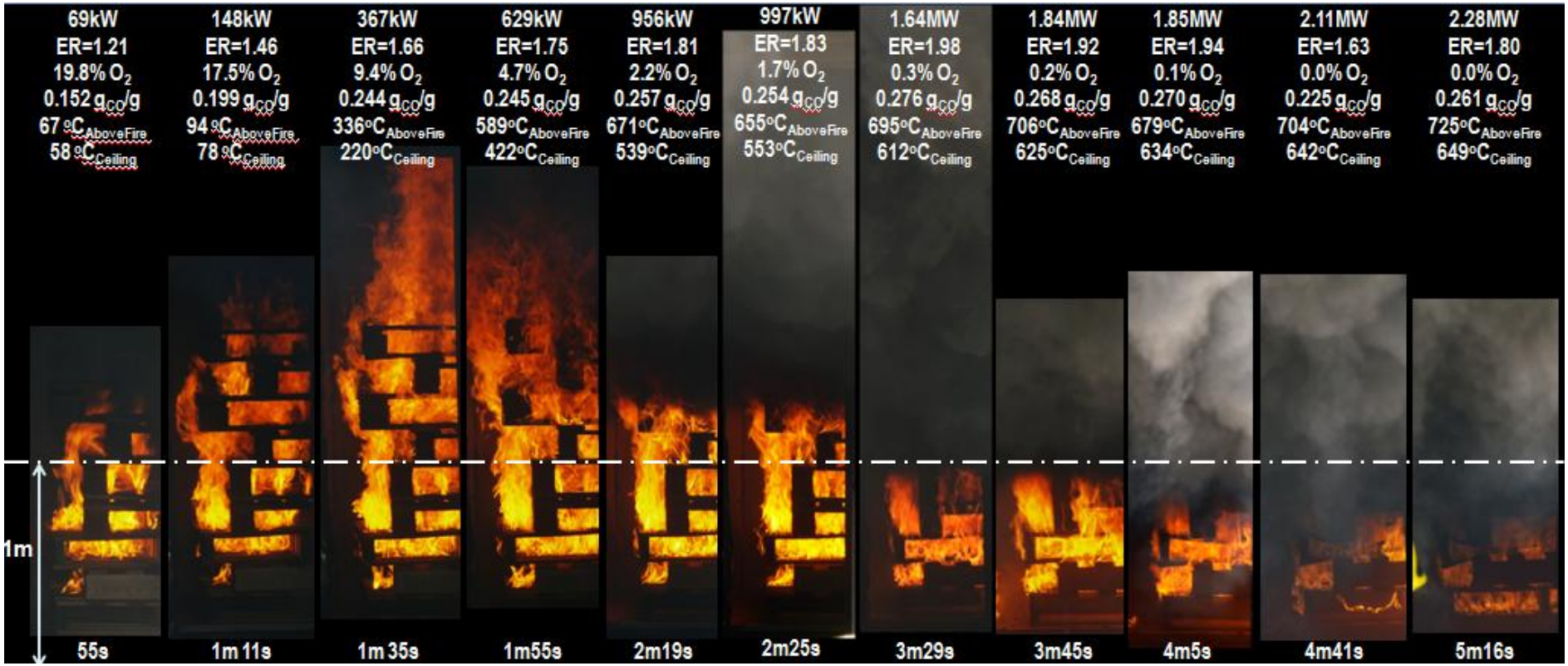

Figure 5-20: Summary of results corresponding to photographs taken through the corridor of the compartment fire development at progressive timings. Showing the related measurements of; HRR, Equivalence Ratio (ER), oxygen level, carbon monoxide yield, temperature above the fire, and ceiling temperature. Also a reference height 1 m from floor level is drawn in order to indicate the smoke layer height. Photographs times are shown at the bottom in reference to the ignition time.

Figure 5-21 presents FEC for safe level by the combustion products from Test 3b in the stacked graph (Figure 5-18). Figure 5-22 shows the composition of the contributing toxic emissions by percentage, where acrolein is dominating while formaldehyde is contributing third of the total influence of the smoke based on the safe exposure thresholds.

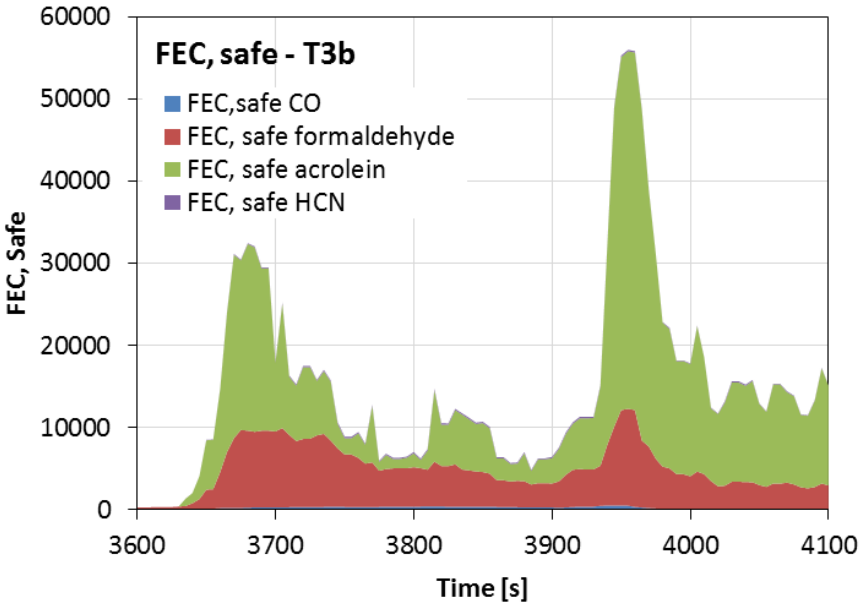

Figure 5-21: Instantaneous total fractional effective concentration (FEC) for safe level during Test 3b.

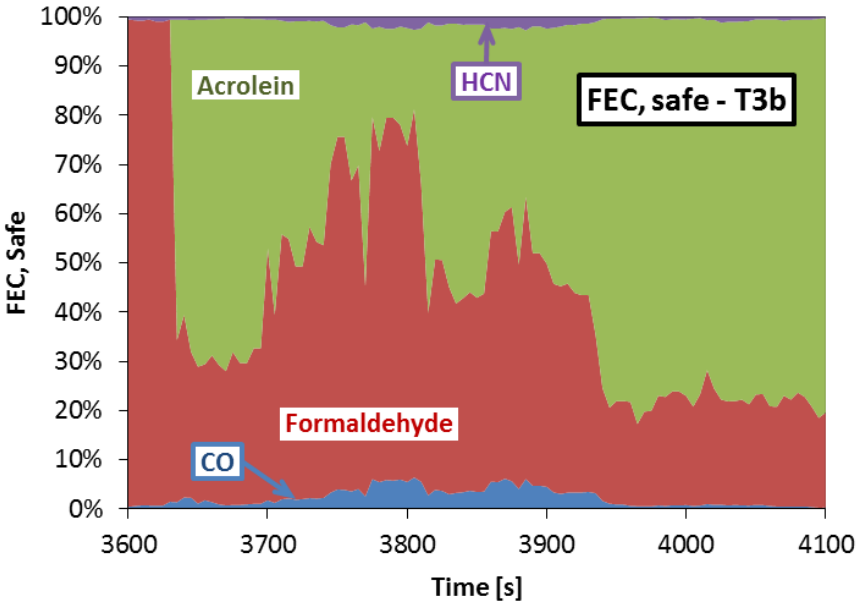

Figure 5-22: Major toxic emissions contribution by species to the fractional effective concentration for safe level in Test 3b.

Secondly, FEC for escape impairment (EI) that is important for post-accident investigations to understand the development of the evacuation plan and the point where victims were trapped. Figure 5-23 shows FEC for escape impairment from Test 3b in the stacked graph

(Figure 5-18).These ratios are effectively the dilution levels required for any ventilation system to bring the concentration of the individual species below the critical limit being considered. It can be seen that for CO this dilution level is of the order of 200 whilst for acrolein the dilution required is of the order of several hundred rising to about 3000 during fire-fighting operations. Figure 5-24 shows the composition of the contributing toxic emissions by percentage based on escape impairment exposure thresholds.

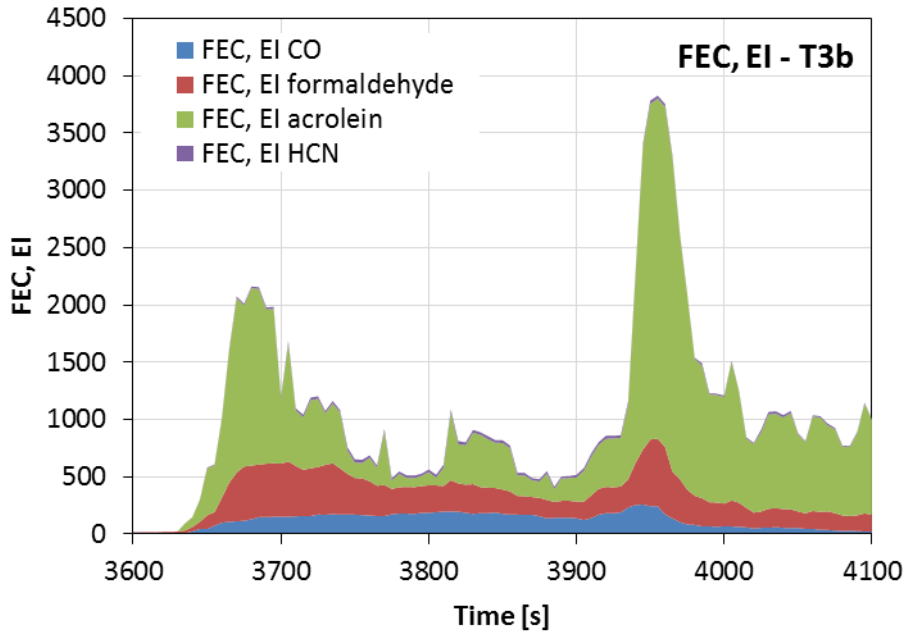

Figure 5-23: Instantaneous total fractional effective concentration (FEC) for escape impairment (EI) level during Test 3b.

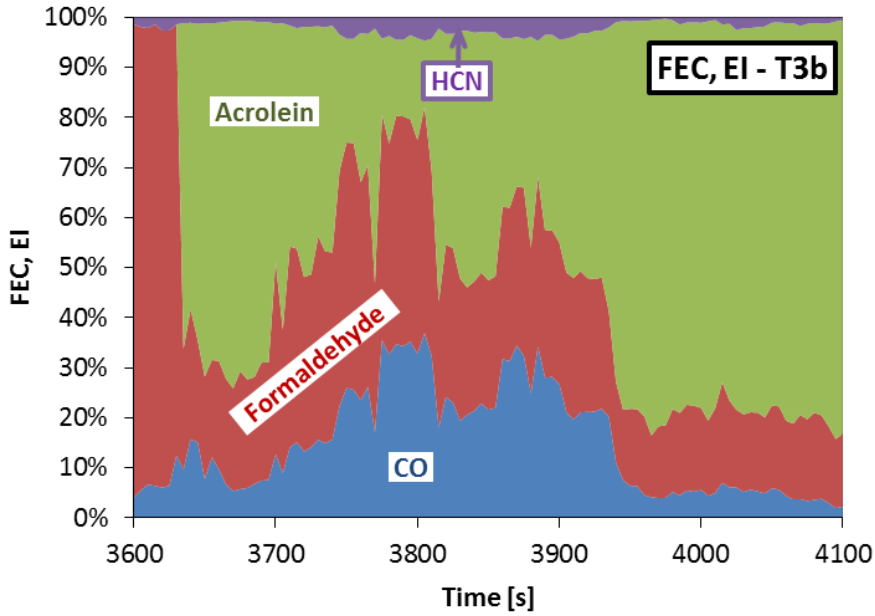

Figure 5-24: Major toxic emissions contribution by species to the fractional effective concentration for escape impairment (EI) level in Test 3b.

Thirdly, FEC for lethality that is useful for post-accident investigations. Figure 5-25 shows the instantaneous FEC for lethality from Test 1b in the stacked graph (Figure 5-18). The total value for lethal FEC stabilised at around 200 in the steady state phase and peaked reaching 750 during fire-fighting activities. Figure 5-26 shows the composition of the contributing toxic emissions by percentage based on lethal exposure thresholds.

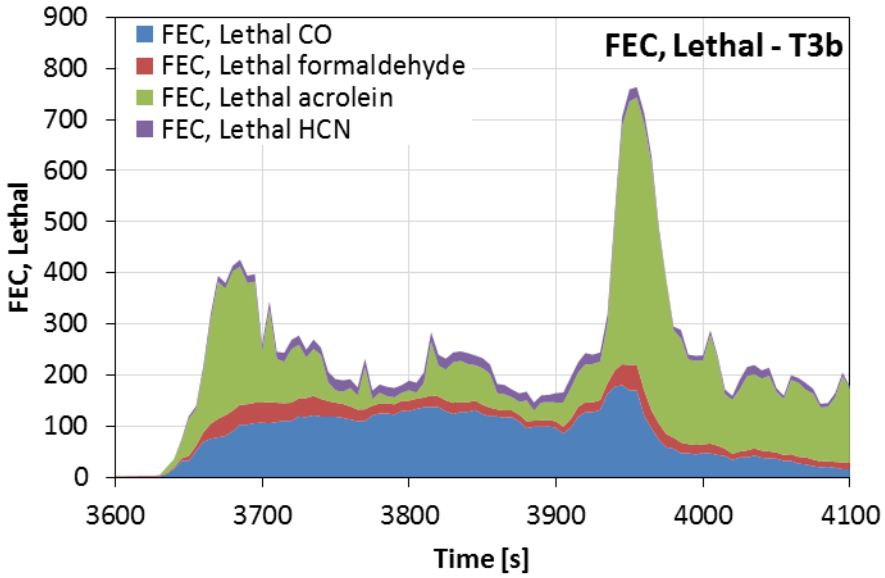

Figure 5-25: Instantaneous total fractional effective concentration (FEC) for lethal level during Test 3b.

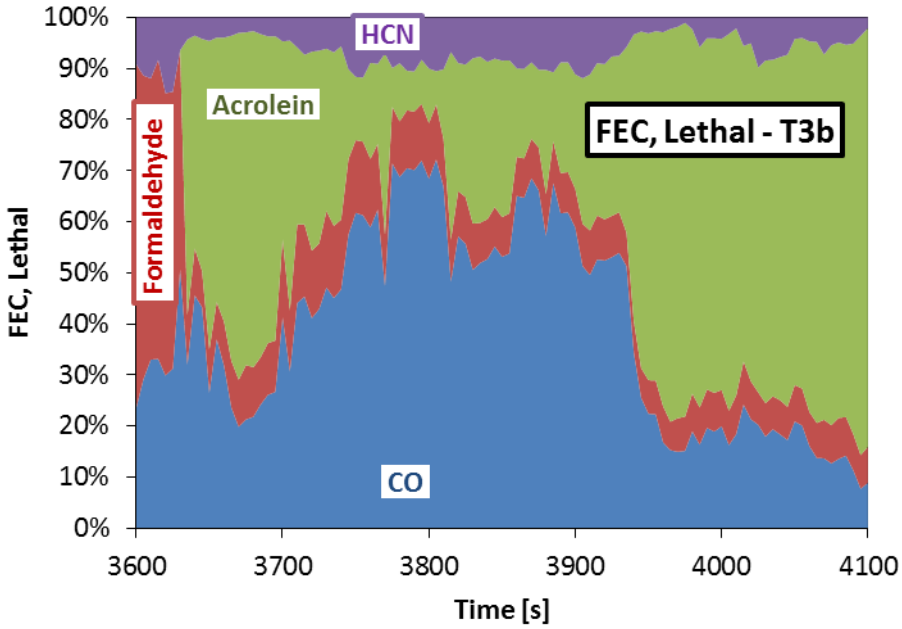

Figure 5-26: Major toxic emissions contribution by species to the fractional effective concentration for lethal level in Test 3b.

Finally, FEC for lethality based on the values purposed by ISO 13344 for LC50 the lethal concentration for half the population, as discussed earlier in section 2.3.2.3. Figure 5-27

shows the instantaneous FEC for lethality (based on LC50) from Test 1b in the stacked graph (Figure 5-18). The total value for lethal FEC stabilised to be less than 1 in the steady state phase (post 4500th second). Figure 5-28 shows the composition of the contributing toxic emissions by percentage based on lethal exposure thresholds of LC50. The comparison between FEC for lethality based on the most conservative threshold shown in Figure 5-25 and Figure 5-26 on one hand and FEC for lethality based on LC50 shown in Figure 5-27 and Figure 5-28 on the other, is important to demonstrate the difference between the two. As discussed earlier in section 2.3.2.3, the most conservative threshold database for lethality used was AEGL-3_{30min} is defined to be the minimum exposure to cause life-threatening health damage or death, while LC50 is defined to be the concentrations that cause death to half the population.

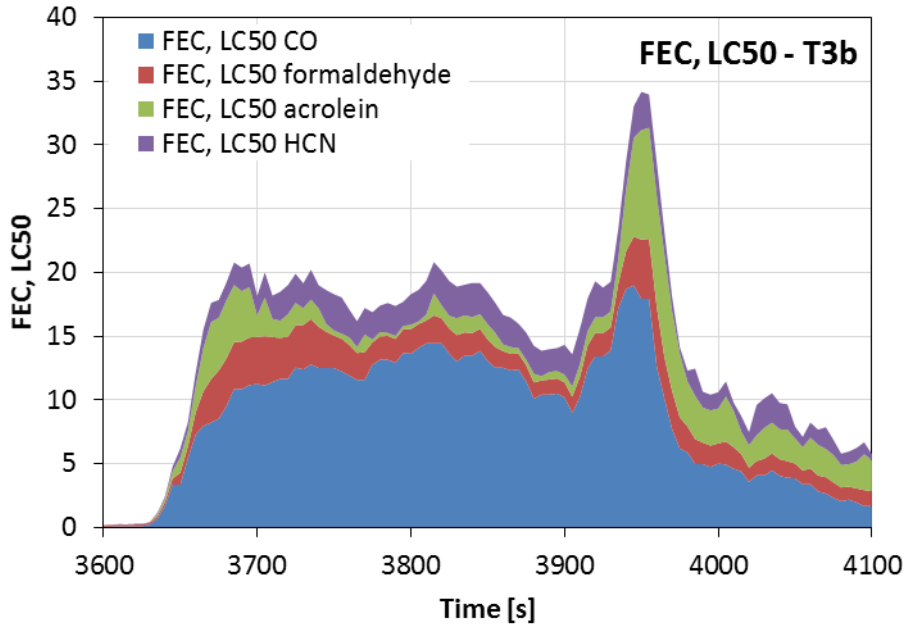

Figure 5-27: Instantaneous total fractional effective concentration (FEC) for lethal level (using LC50 values) during Test 3b.

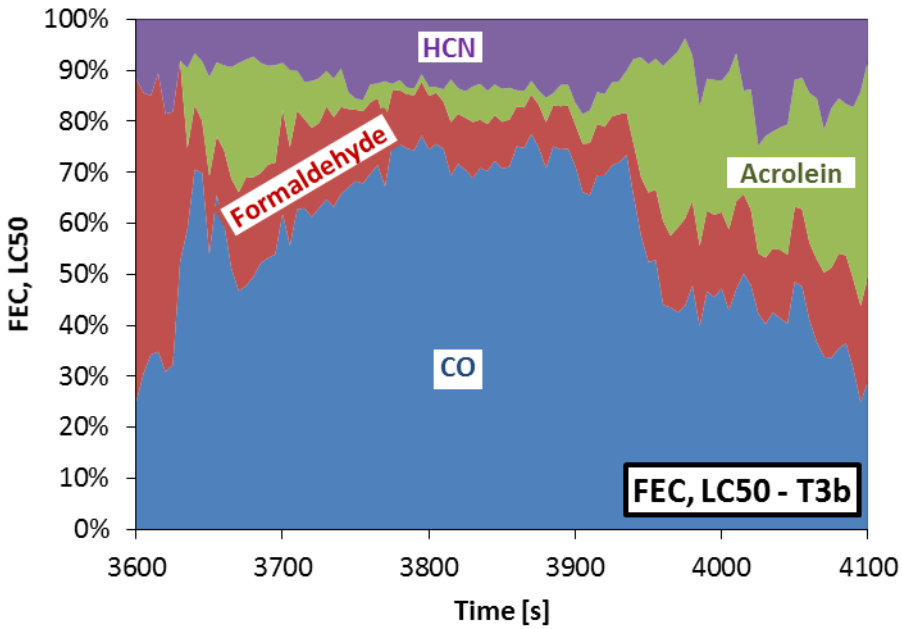

Figure 5-28: Major toxic emissions contribution by species to the fractional effective concentration for lethal level (using LC50 values) in Test 3b.

5.2 Wooden pallets II

The test was intended to be a repeat of Test 3 while the weight balance will be monitoring the un-ignited stack. The test didn't consist of a smouldering (closed door) phase, and the door was kept open after igniting the stack on the far corner. The data logger responsible for recording the smoke analysis measurements from the paramagnetic oxygen and NDIR analysers (all gas analysis apart from FTIR) has malfunctioned for this test and data were lost.

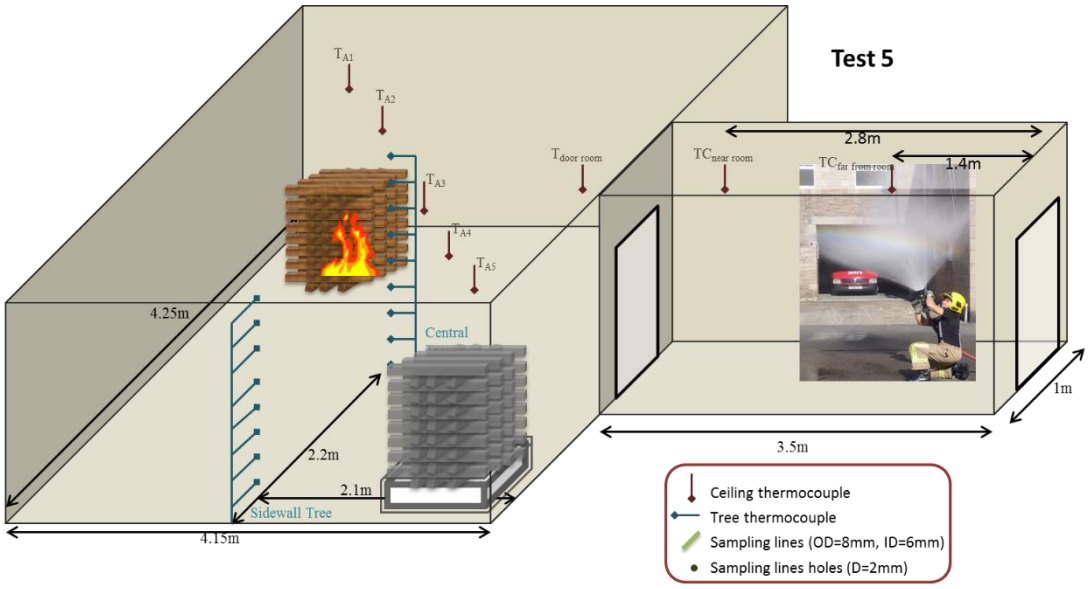

Figure 5-29: Test 5 full setup showing fire load, instrumentation and fire-fighting entrance.

Figure 5-30: Picture of the fire in Test 5, 88 seconds after ignition.

The fire load was ignited 90 seconds (1min 30sec) from the start of logging. Pictures of the fire were taken before closing the door e.g. Figure 5-30.The door was left open to propagate to reach post-flashover conditions for 6 minutes before fire-fighting activities started at the 440th second (7min 20sec). The time line of Test 5 is graphically demonstrated in Figure 5-31.

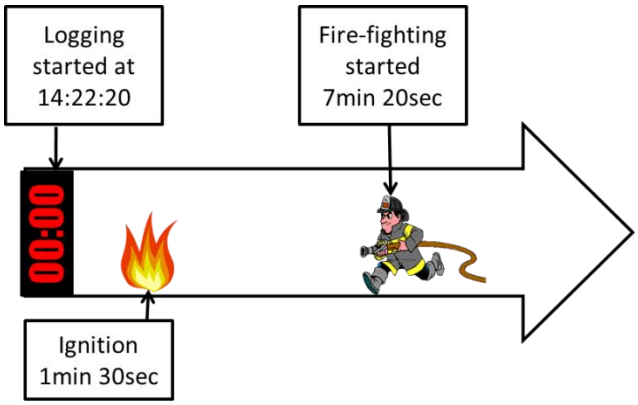

Figure 5-31: Timeline of the main events for Test 5.

5.2.1 Thermal environment – Test 5

Temperatures measured inside the room followed similar patterns to observed in Test 3b. However, thermocouples above the ignited stack (see Figure 5-32) showed measurements stabilising at 900 C during the post-flashover steady state phase (between the 260th – 440th second) this exceeds maximum temperatures measured in Test 3b for the same location and phase, where maximum temperature measured was 700 C.

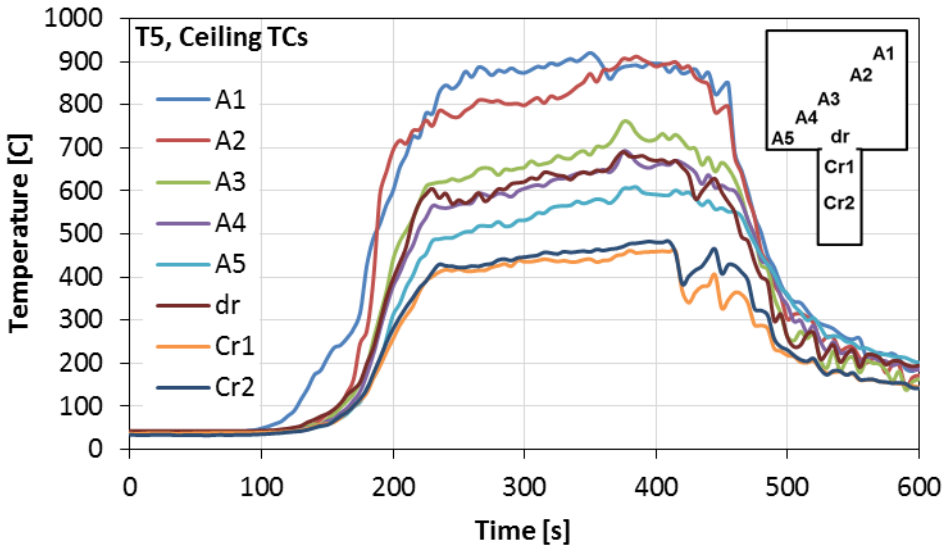

Figure 5-32: Ceiling layer temperature measurements at different positions inside the compartment and corridor during Test 5.

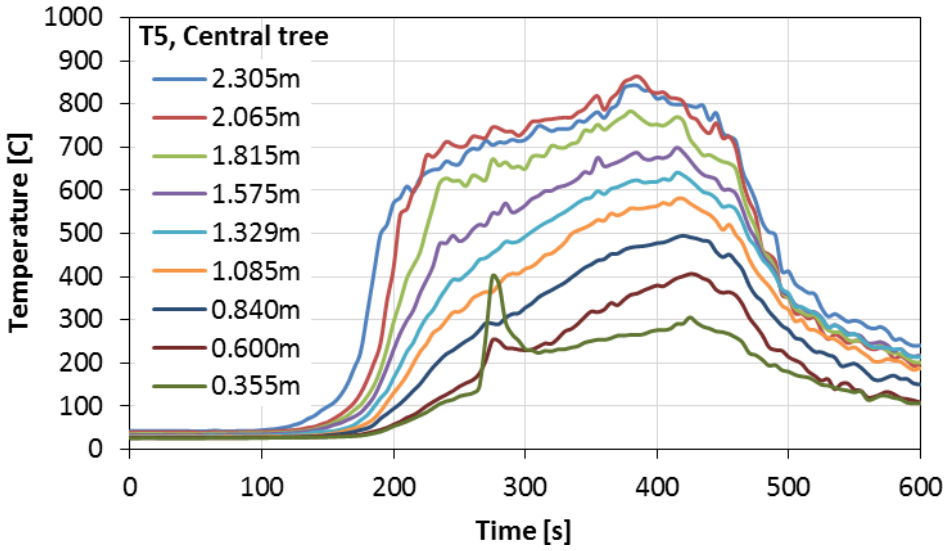

Figure 5-33: Temperatures at different heights from floor level in the fire room as measured by the central vertical thermocouple tree on during test 5. The lowest thermocouple was flashover indicator.

Figure 5-33 and Figure 5-34 show temperatures recorded by the central and sidewall thermocouple trees. Flashover targets, consisting of crumpled A4 printing papers, were located on the floor underneath the lowest thermocouple of the central vertical tree. These flashover indicators were ignited at the 265th second as demonstrated in Figure 5-33. The vertical temperature gradients can indicate the height of the smoke layer, therefore gradients at different times (before and after flashover) are presented in Figure 5-35 from both sidewall and central vertical trees. However the temperature vertical gradients were more uniform for the central tree as shown in Figure 5-35. This was due to the position of this tree in the path of the main flows in and out of the compartment which resulted in more mixing of the layers.

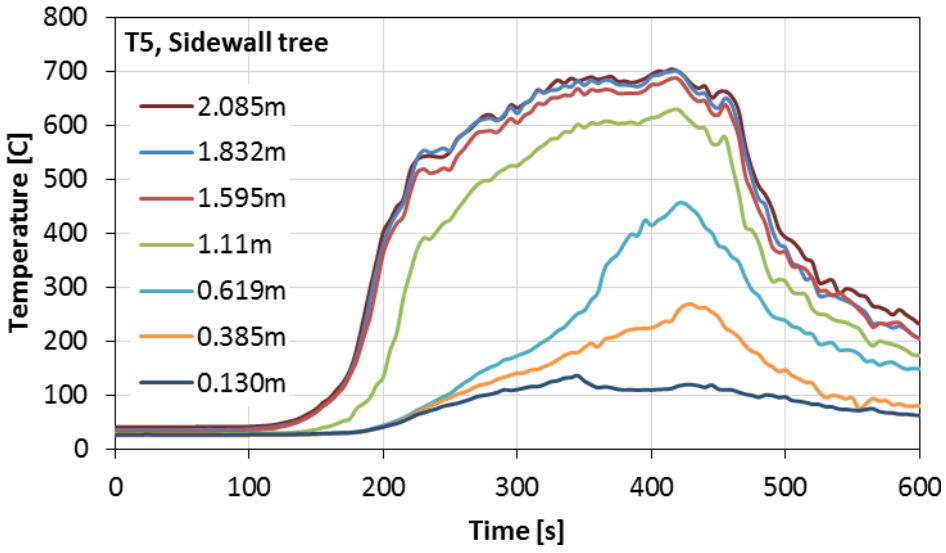

Figure 5-34: Temperatures at different heights from floor level in the fire room as measured by the vertical thermocouple tree on the sidewall of the compartment during test 5.

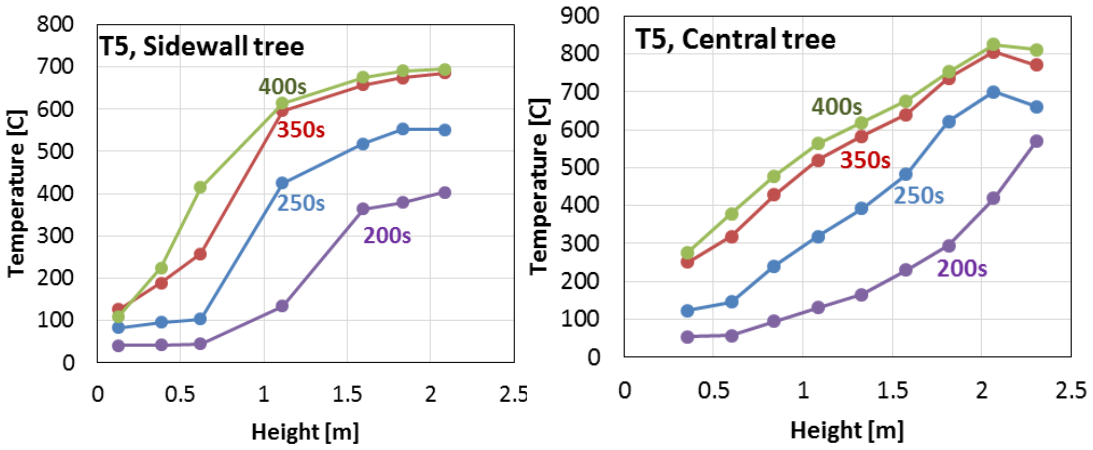

Figure 5-35: Vertical temperature variation by the sidewall (left) and central (right) thermocouple trees at different times during Test 5.

5.2.2 Toxic environment – Test 5

Losing the oxygen measurements data inside the compartment during Test 5, meant that it is impossible to establish emission-based equivalence ratio values for the combustion. Concentrations measurements from FTIR are presented in Figure 5-36, in general the patterns for concentrations observed were similar to those measured in Test 3b. Although, the magnitude of the concentrations measured were lower in Test 5 than those measured in Test 3b. Carbon monoxide and THC showed similar behaviour with a rapid increase after the 200th second reaching steady high levels during the steady state period of the fire. Acrolein and formaldehyde showed a reduction of concentrations during the steady state phase. This occurred at the same time as flashover occurred.

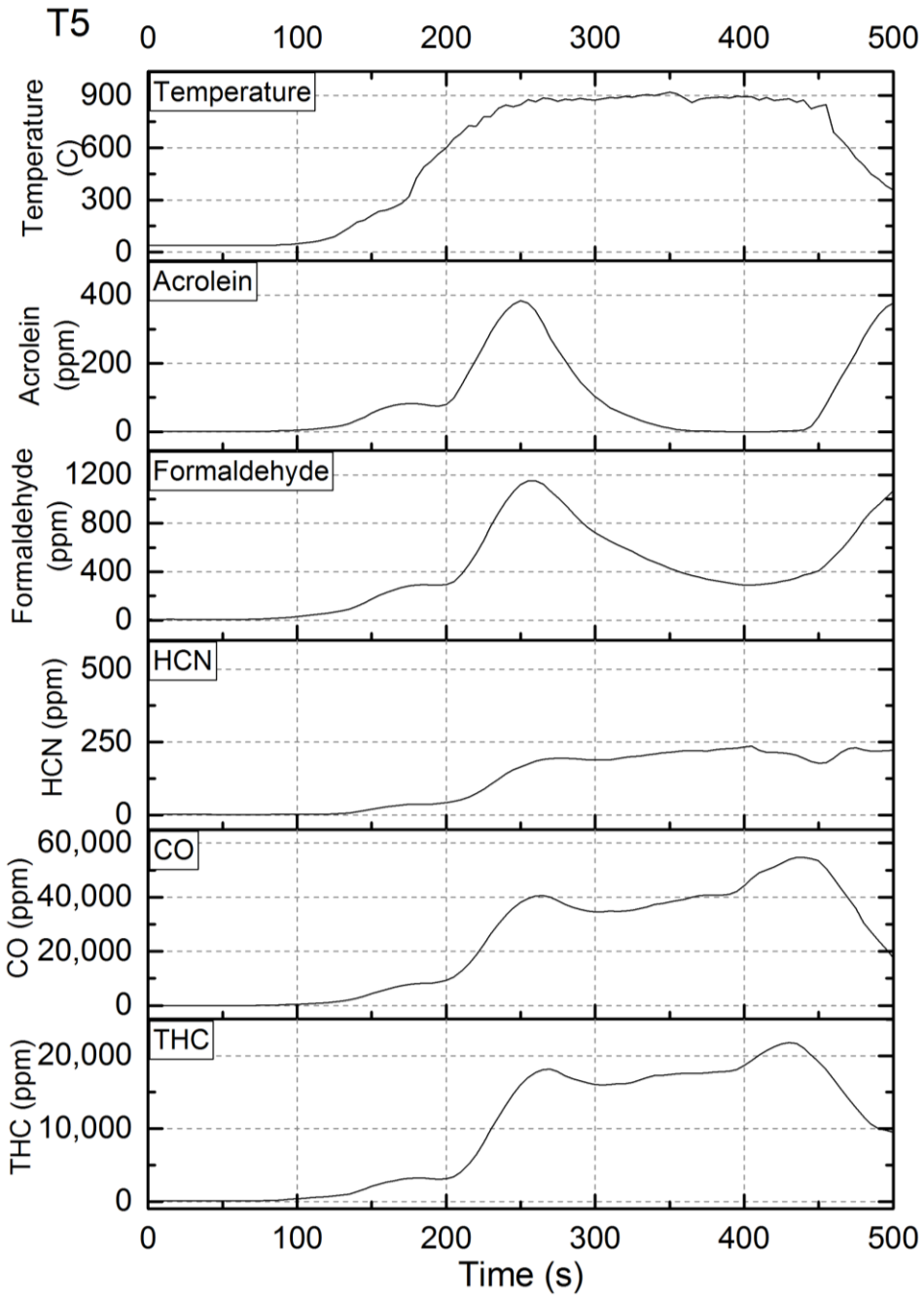

Figure 5-36: Combustion toxic products concentrations in volume basis in line with equivalence ratio and Oxygen concentration for Test 2b.

The instantaneous fractional effective concentration FEC for different levels were calculated in accordance with the guidelines presented earlier in section 2.3.2.3 to demonstrate the health effects of the smoke produced at the point of sampling. Firstly, FEC safe that is important for designing purposes to ensure a safe environment in protected structures such as corridors and staircases. Figure 5-37 presents FEC for safe level by the combustion products from Test 5 in the stacked graph (Figure 5-36). Figure 5-38 shows the composition of the contributing toxic emissions by percentage, where acrolein is dominating while formaldehyde is contributing about quarter at the peaks of the total influence the smoke based on the safe exposure thresholds.

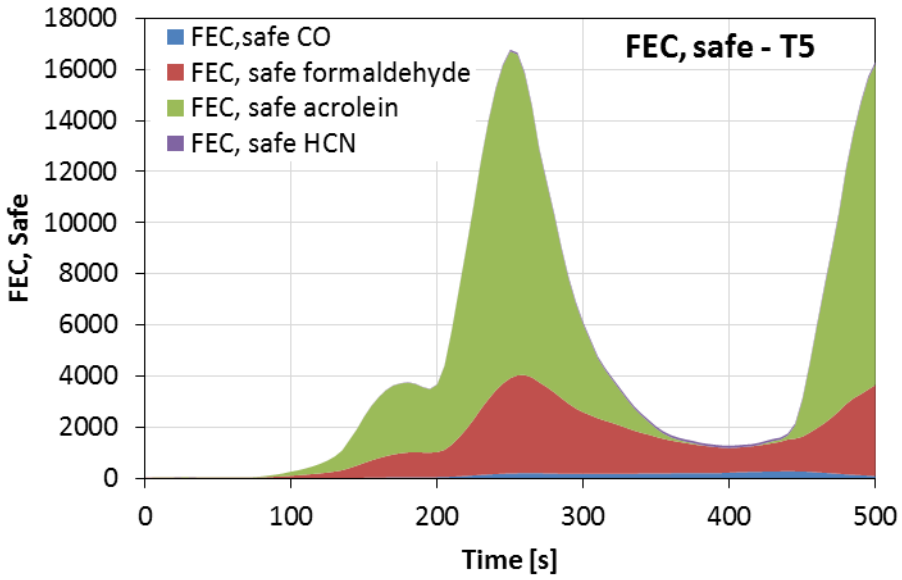

Figure 5-37: Instantaneous total fractional effective concentration (FEC) for safe level during Test 5.

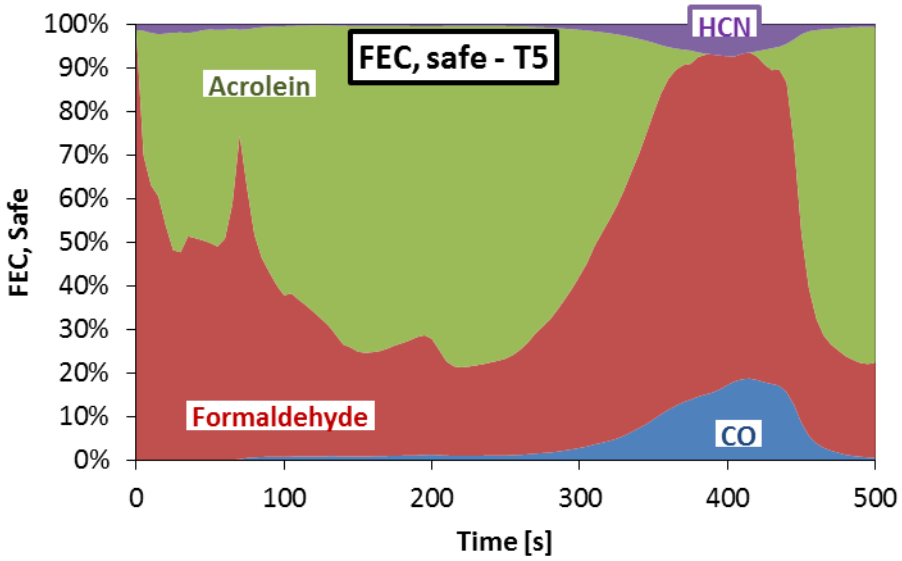

Figure 5-38: Major toxic emissions contribution by species to the fractional effective concentration for safe level in Test 5.

Secondly, FEC for escape impairment (EI) that is important for post-accident investigations to understand the development of the evacuation plan and the point where victims were trapped. Figure 5-39 shows FEC for escape impairment from Test 5 in the stacked graph (Figure 5-36). While Figure 5-40 shows the composition of the contributing toxic emissions by percentage based on escape impairment exposure thresholds.

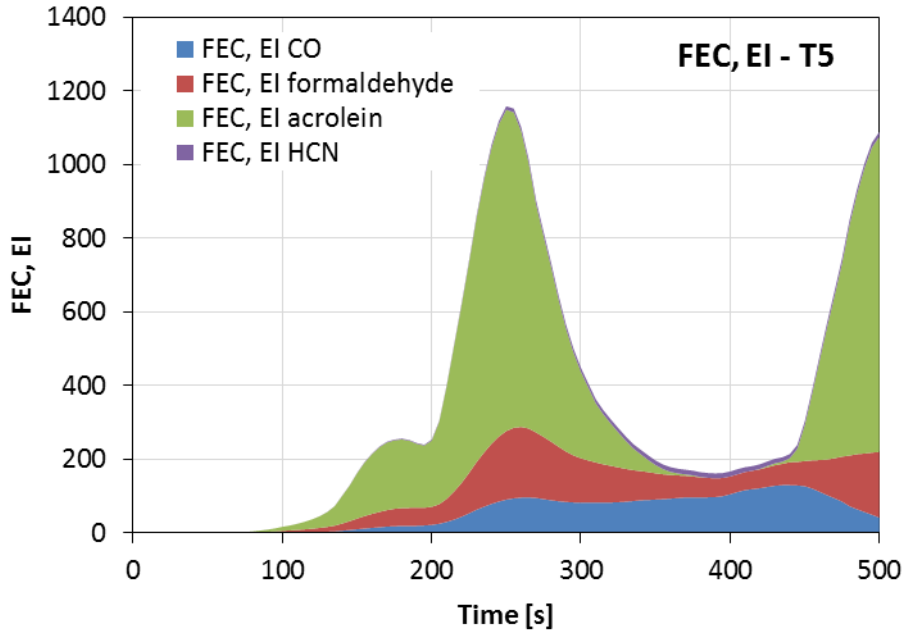

Figure 5-39: Instantaneous total fractional effective concentration (FEC) for escape impairment (EI) level during Test 5.

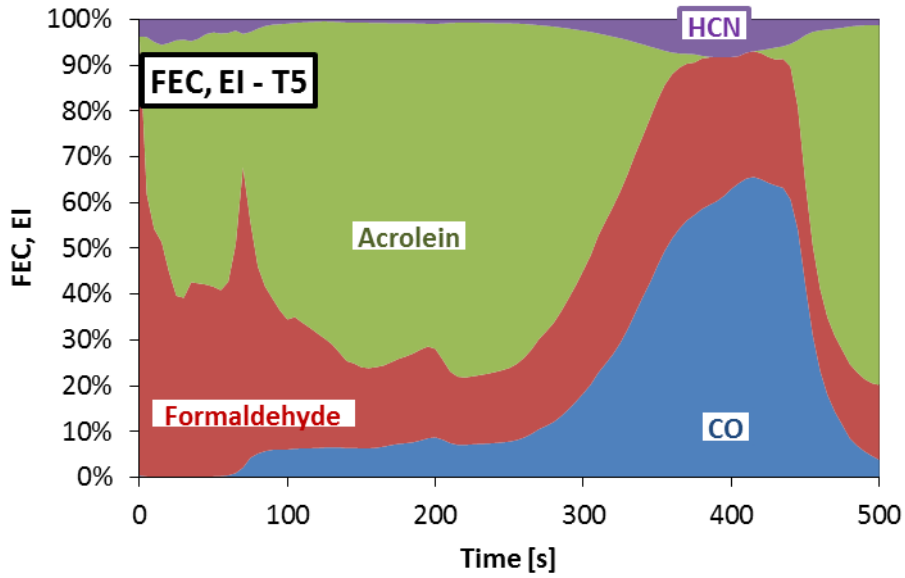

Figure 5-40: Major toxic emissions contribution by species to the fractional effective concentration for escape impairment (EI) level in Test 5.

Thirdly, FEC for lethality that is useful for post-accident investigations. Figure 5-41 shows the instantaneous FEC for lethality from Test 5 in the stacked graph (Figure 5-36). The total value for lethal FEC peaked initially at the flashover point to reach 240, then dropped to less than 100 during the steady state phase (post 300th second) until the fire-fighting intervention where it peaked again to reach about 200. Figure 5-42 shows the composition of the contributing toxic emissions by percentage based on lethal exposure thresholds discussed in section 2.3.2.3.

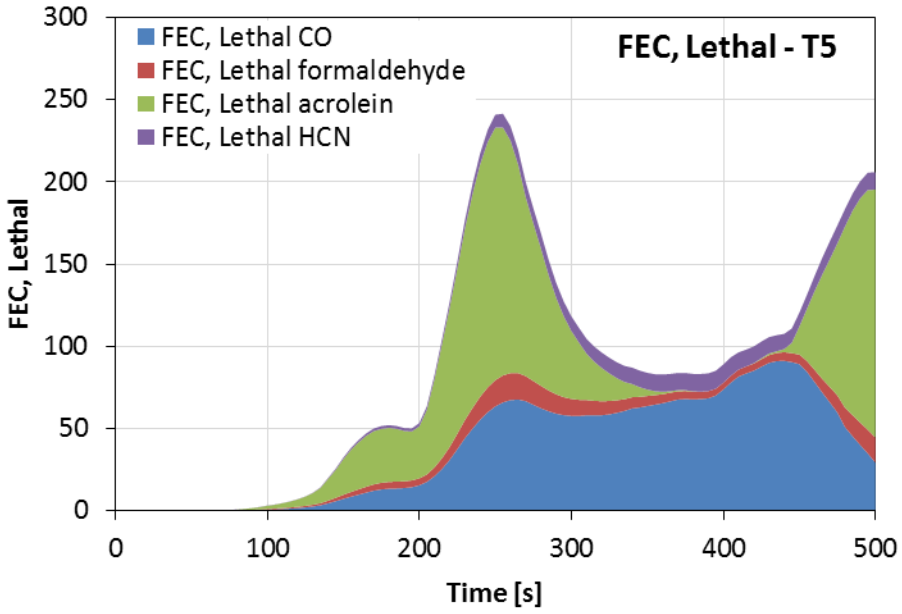

Figure 5-41: Instantaneous total fractional effective concentration (FEC) for lethal level during Test 5.

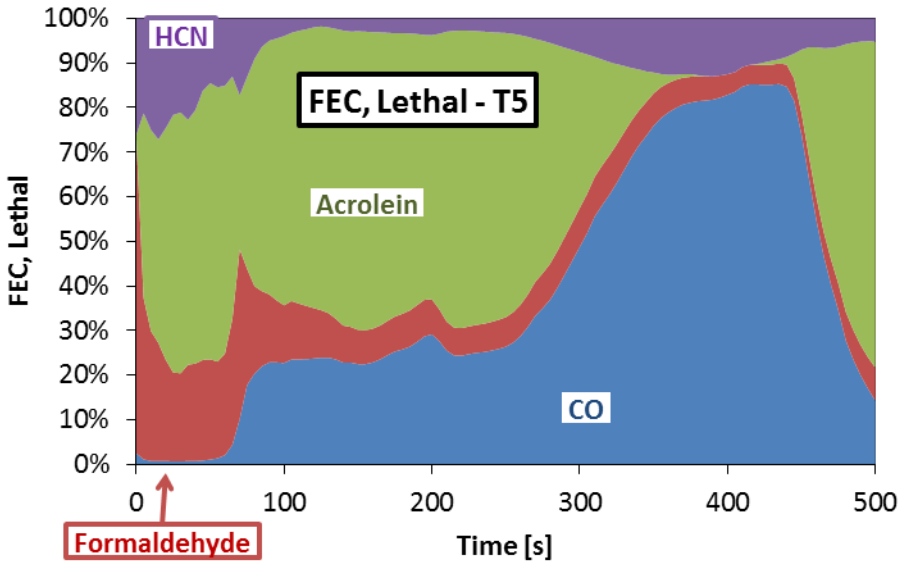

Figure 5-42: Major toxic emissions contribution by species to the fractional effective concentration for lethal level in Test 5.

Finally, FEC for lethality based on the values purposed by ISO 13344 for LC50 the lethal concentration for half the population, as discussed earlier in section 2.3.2.3. Figure 5-43 shows the instantaneous FEC for lethality (based on LC50) from Test 5 in the stacked graph (Figure 5-36). The total value for lethal FEC peaked initially at the flashover point to reach 12, then dropped to about 8 during the steady state phase (post 300th second) until the fire-fighting intervention where it peaked again to reach 11. Figure 5-44 shows the composition of the contributing toxic emissions by percentage based on lethal exposure thresholds of LC50. The comparison between FEC for lethality based on the most conservative threshold

shown in Figure 5-41 and Figure 5-42 on one hand and FEC for lethality based on LC50 shown in Figure 5-43 and Figure 5-44 on the other, is important to demonstrate the difference between the two. As discussed earlier in section 2.3.2.3, the most conservative threshold database for lethality used was AEGL-3_{30min} is defined to be the minimum exposure to cause life-threatening health damage or death, while LC50 is defined to be the concentrations that cause death to half the population.

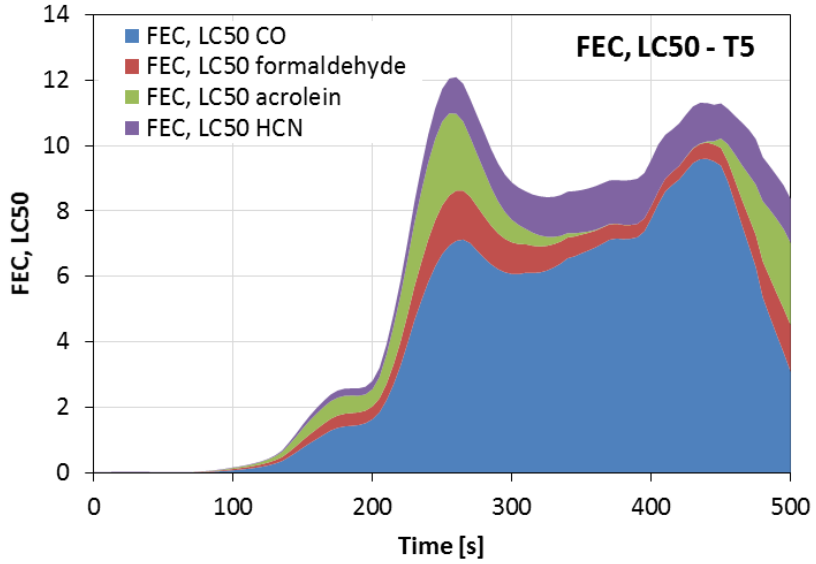

Figure 5-43: Instantaneous total fractional effective concentration (FEC) for lethal level (using LC50 values) during Test 5.

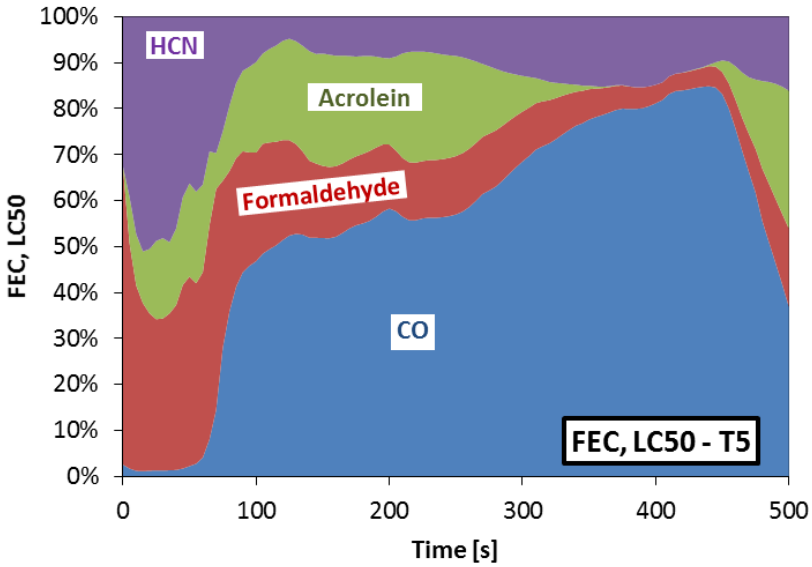

Figure 5-44: Major toxic emissions contribution by species to the fractional effective concentration for lethal level (using LC50 values) in Test 5.

5.3 Cotton linen and towels

The test was intended to be a simulation of a smouldering fire of linen, as a common scenario (fire load) for storage rooms in hospitals, care homes, and hotels. The test had two scenarios; firstly (T1a), a door closed scenario where shortly after ignition the only door to the room is closed in order to restrict ventilation. Secondly (T1b), with the door fully open which was conducted here by the end of the first scenario.

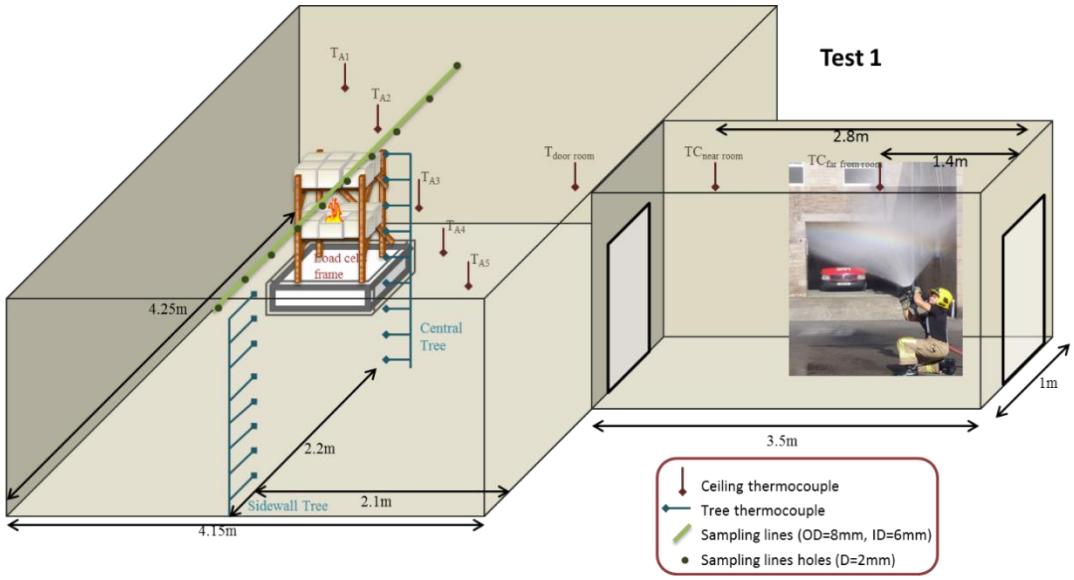

Figure 5-45: Test 1 full setup showing fire load, instrumentation and fire-fighting entrance.

Figure 5-46: Picture of the fire in Test 1, 220 seconds after ignition. The room door was closed and the pictures were taken from the corridor through the glazed window in the door.

The elemental analysis of the linen used showed the mass based composition to be 47.09% carbon, 5.26% hydrogen, and 47.86% oxygen. The room setup is shown in Figure 3-21, a full description of the room setup and fuel was discussed earlier (see section 3.2.5.1). The ignition source used was 250 ml of meths poured at the centre of the lower shelf, as can be seen in the picture shown in Figure 5-46.

The fire load was ignited 150 seconds (2min 30sec) from the start of logging. The door was shut 5 seconds later (2min 35sec). Pictures were taken from the corridor through the glazed section of the door e.g. Figure 5-46. A leakage was discovered in the sampling system and it was fixed around 1440 seconds (24min) from the start of the logging time. Therefore, no data for gas analysis is reported before this point. Then after temperatures dropped in the compartment to around 50C the door was opened at 3910 seconds (65min 10sec) for T1b scenario to start. Then the fire self-reignited within two minutes to propagate reaching flaming fully involved fire. Then fire-fighting activities started at 5150 seconds (85min 50sec). The time line of Test 1 is graphically demonstrated in Figure 5-47 and measurements of mass of the fire load throughout the test is shown in Figure 5-48.

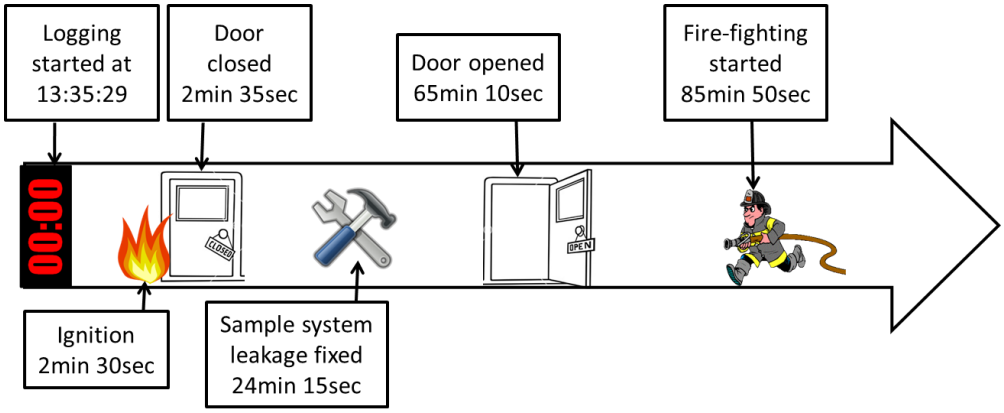

Figure 5-47: Timeline of the main events for Test 1.

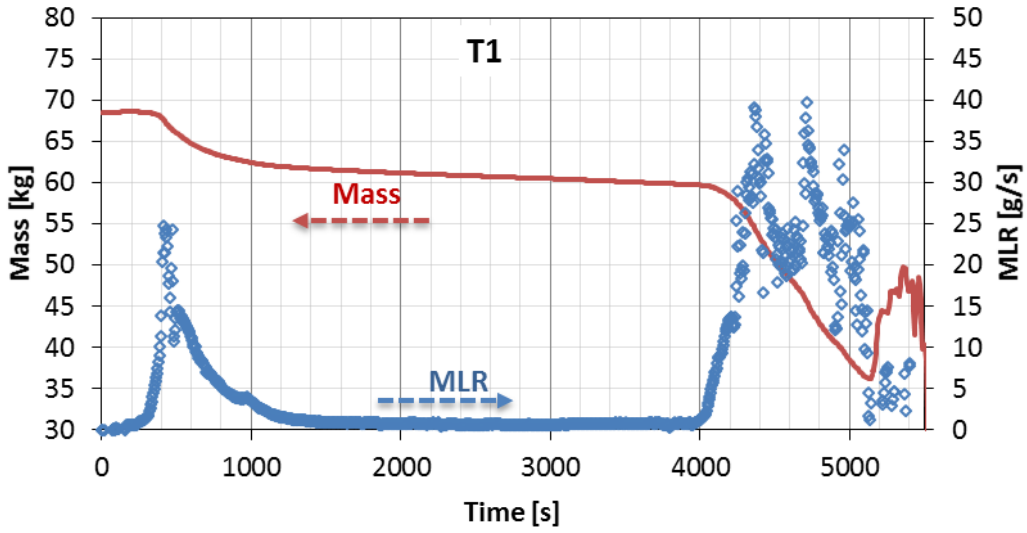

Figure 5-48: Total mass of the fire load (Red) and mass loss rate (Blue) for Test 1 from start till fire-fighting.

5.3.1 Results and analysis for the first part of Test 1 (T1a)

During this part of the test the fire started initially with a well ventilated flaming fire (ISO stage 2) until oxygen available was used (reaching peak temperatures and heat release rate). Deprived oxygen levels at this point were unable to sustain the fire at the same burning rate so it transformed to be under-ventilated pre-flashover flaming fire (ISO stage 3a). With more oxygen being used, oxygen reached the level to be unable to sustain a flaming fire to transform to a slower non-flaming smouldering fire (ISO stage 1a). In the following sections thermal and toxic environment results and analysis for this phase (T1a) are discussed (from 0 seconds till 3910 seconds).

5.3.1.1 Mass loss and heat release rate (HRR) – Test 1a

Heat release rate can be quantified by the use of mass loss data and calorific values of the materials. And can be corrected for inefficiencies using the mass yields data of incomplete combustion products. A calorific value of 18 MJ/kg were used for cotton to produce Figure 5-49. The correction of the HRR data is based on inefficiency as derived from unburnt hydrocarbons and carbon monoxide measurements as used by the author in [260]. Initially, the burning rate was propagating rapidly (due to the existence of the fire load and oxidizing agent). Then, the level of oxygen dropped (due to the lack of ventilation) and the fire slowed down. Till eventually it was unable to sustain any flaming fires, to transform to a smouldering fire with a very slow burning rate.

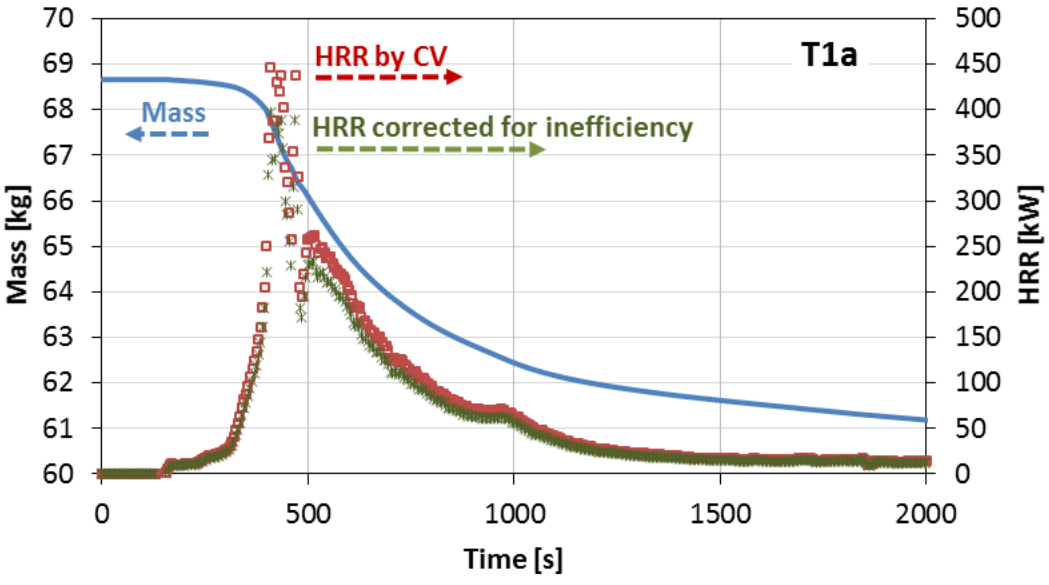

Figure 5-49: Mass change with time and associated HRR based on the mass loss rate for Test 1a. Also shown is an adjusted HRR, based on inefficiency of combustion as derived from the unburnt hydrocarbons and CO measurements.

5.3.1.2 Thermal environment – Test 1a

Temperature inside the room followed similar patterns to the HRR discussed above. Figure 5-50 shows temperature measured at the ceiling level, where temperatures at the highest point dropped lower than 100 C just after the 1000 seconds mark. Before opening the door to end the first part of Test 1, the vertical temperature gradient throughout the room showed very little variation (max. 25 C), demonstrated in Figure 5-51.

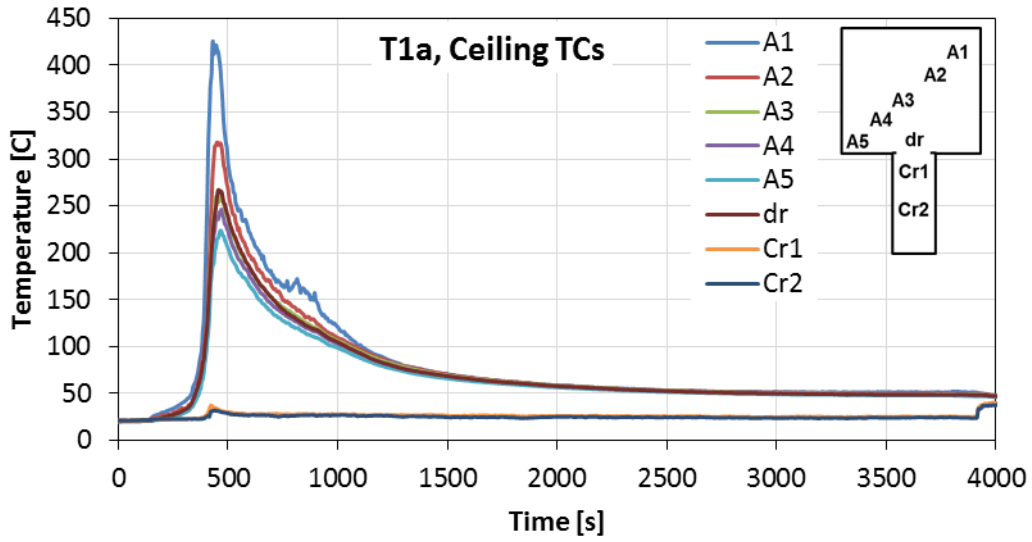

Figure 5-50: Ceiling layer temperature measurements at different positions inside the compartment and corridor during Test 1a.

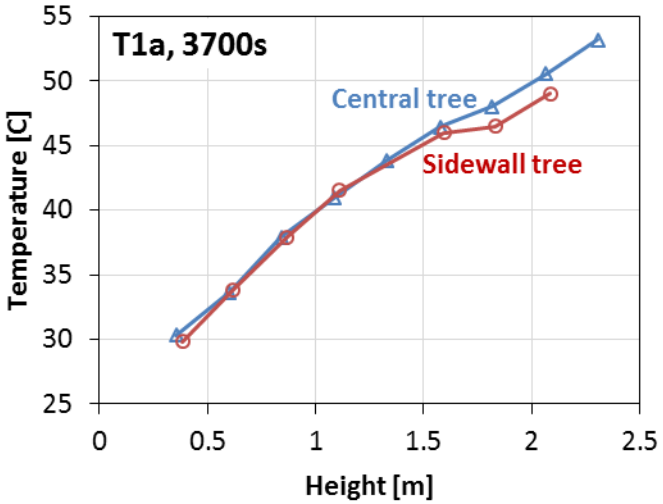

Figure 5-51: Vertical temperature variation at 3700s from central and sidewall thermocouple trees.

5.3.1.3 Toxic environment – Test 1a

Gas analyses for products from the first part of the test (T1a), while the door was closed, cannot be treated as a dynamic process due to the lack of exhaust and fresh air supply, which is important for sustaining a flaming combustion. So the gas concentration measurements given by the instruments in that period were for a static situation of the fire where the smoke is accumulating in the room space. So for the purpose of establishing yield data, concentration measurements were taken at the point when the fire died down and before opening the door.

Table 5-2: Concentrations of major combustion emissions produced in Test 1a at the 3700th second, with their ratios to relevant toxic exposure thresholds. and average mass yield data for each species.

Species	Conc. [ppm]	R-Safe	R-Escape impairment	R-Lethal	R-LC50	Yield [g/g]
CO	13,078	65.4	31.1	21.8	2.3	0.0787
Acrolein	509	16,960	1,156	204	3.4	0.0061
Formaldehyde	701	2,336	117	10	0.9	0.0045
THC	8,032					0.0277

At that point (3700 seconds), the deviation for the vertical temperature gradient was minimal between top and bottom thermocouples (less than 25 C), hence it was assumed that the collected sample was representative of the whole 41 m^3 compartment. And by quantifying the total mass of fuel burnt during that period (8.5 kg), then mass yields of each toxic gas can be quantified, as presented in Table 5-2. The fractional effective concentration of the sampled gas in respect to the different levels of effects discussed earlier in section 2.3 were established the contribution of each species is demonstrated in Figure 5-52.

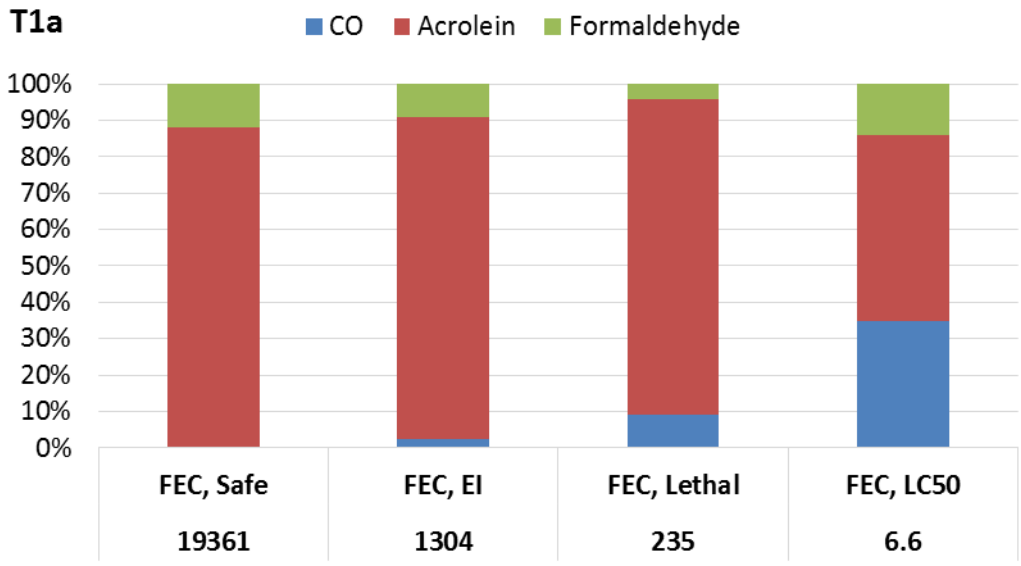

Figure 5-52: The main toxic products released in Test 1a in respect to their contribution to the overall Fractional Effective Concentration (FEC).

5.3.2 Results and analysis for the second part of Test 1 (T1b)

As discussed earlier Test 1b started by opening the door and allowing the supply of air to the smouldering fire. Because the fire load was cotton with such a high porosity, it sustained the smouldering fire for a lengthy period. When the door was opened and fresh air started reaching the combustion zone, the fire propagated rapidly to a well ventilated flaming fire. The fire was left to stabilise and reach its peak, however a flashover did not occur in this test, and fire-fighting activities started about 20 minutes from opening door (5150 seconds on the global timeline). The following sections present the results for that part of the test (T1b) by discussing the thermal and toxic environment produced within the compartment.

5.3.2.1 Mass loss and heat release rate (HRR) – Test 1b

Using the calorific value approach combined with the mass loss data, online heat release rate is established. Additionally, using the incomplete combustion products measurements carbon monoxide and total unburnt hydrocarbons. During Test 1b, about 22 kg of the fire load was consumed giving a peak corrected HRR of 700 kW, demonstrated in Figure 5-53. In terms of inefficiency, Figure 5-54 shows the combustion reached above 20% at the start of the test before the fire propagated to a well ventilated flaming fire, when inefficiency dropped to be below 5%.

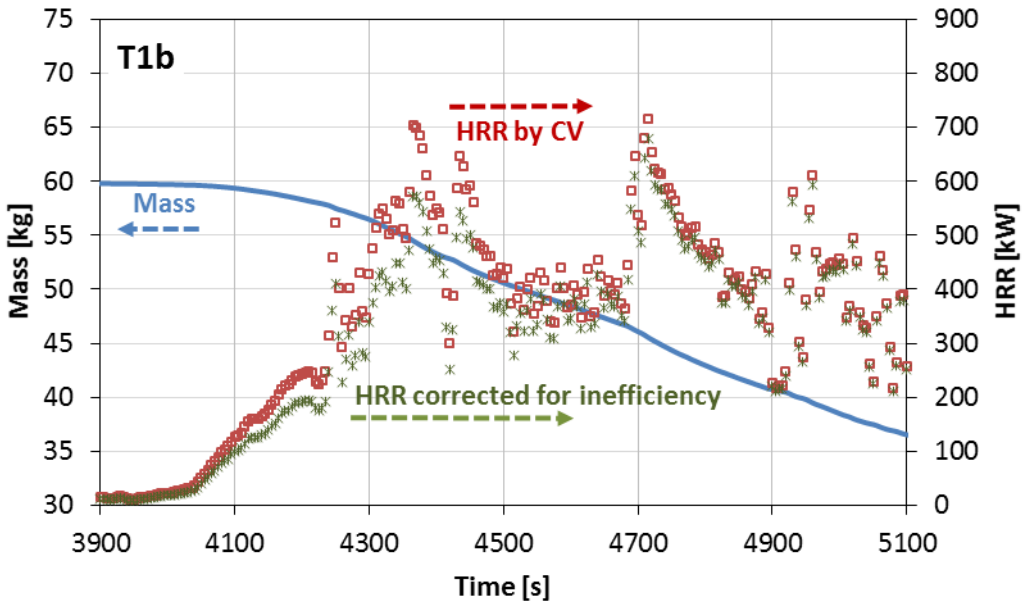

Figure 5-53: Mass change with time and associated HRR based on the mass loss rate for Test 1b. Also shown is an adjusted HRR, based on inefficiency of combustion as derived from the unburnt hydrocarbons and CO measurements.

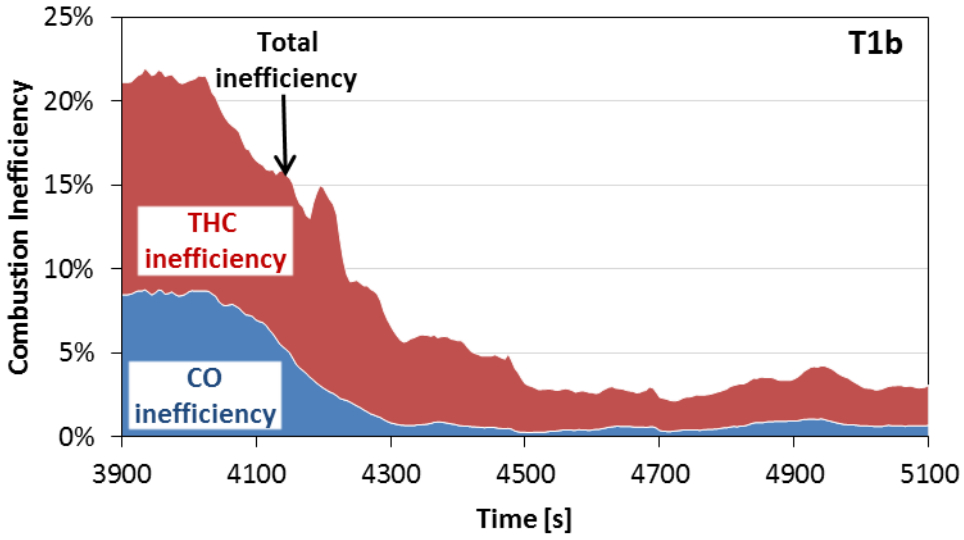

Figure 5-54: Total combustion inefficiency as a function of time with contributions from CO and THC for Test 1b.

5.3.2.2 Thermal environment – Test 1b

Temperatures inside the room followed a similar pattern as the HRR shown in Figure 5-53 where upper layer temperature peaked at 4350th second and started stabilising afterwards, as can be seen in Figure 5-55.

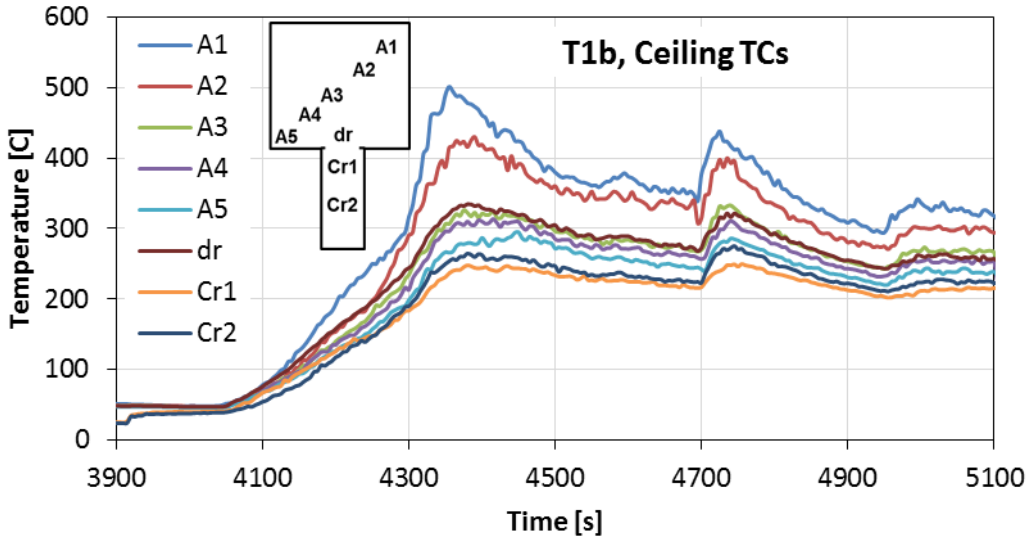

Figure 5-55: Temperature profile at ceiling level across the room and corridor for Test 1b.

The vertical gradient of the room temperature from both vertical trees can indicate the smoke layer height. However, the sidewall vertical temperature variations (see Figure 5-56) show clearer distinction between upper and lower layers than those observed by the central vertical tree due to the central location in the path of the flows in and out of the compartment through the corridor. The smoke layer started to descend from 1.6 m at the 4400th second to 1.1 m by the 4750th second. The smoke layer stayed at that level till fire-fighting started.

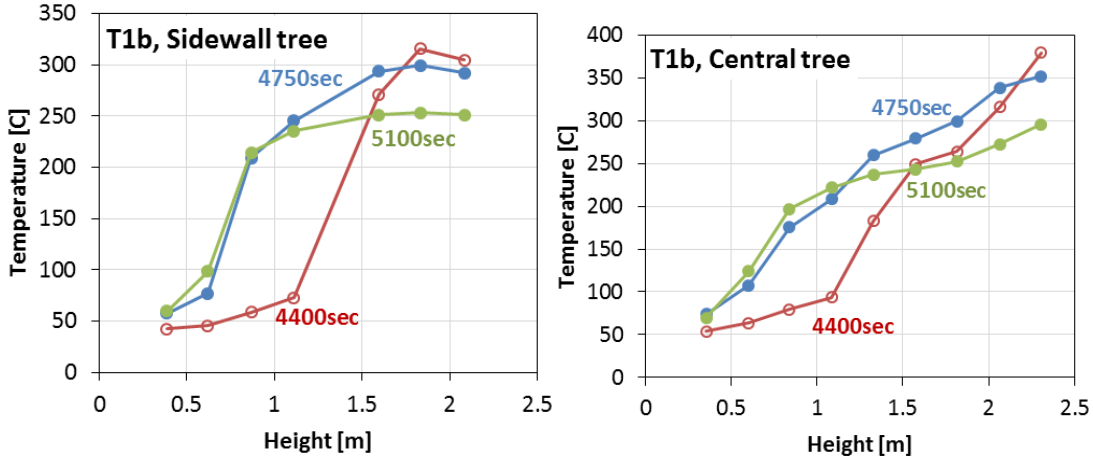

Figure 5-56: Vertical temperature variation at 4400th, 4750th, and 5100th seconds from the sidewall (left) and the central (right) tree for Test 1b.

5.3.2.3 Toxic environment – Test 1b

The combustion emission-based equivalence ratio (EBER) was calculated as a function of time and is presented at the top of Figure 5-57. The EBER shows that the fire was lean (less than 0.4) throughout Test 1b. Measurements of the concentrations of the combustion products are presented in Figure 5-57. The initial concentrations needed some time for the accumulated smoke from the first part of the test (T1a) to be vented out and replaced by fresh air and smoke produced from T1b fire, this took about three minutes.

In general the fire was fuel controlled, air supplied to the compartment was in excess creating a lean combustion as shown by the equivalence ratio values. Toxic oxygenated hydrocarbons (acrolein and formaldehyde) are formed in low temperatures, so couple of peaks are observed at the initial propagating stage (4100th – 4400th seconds), as can be seen in Figure 5-57 and Figure 5-58. Carbon monoxide and unburnt hydrocarbons production were very low due to the excess air supplied by opening the door, this was enough to ensure a lean combustion with minimal incomplete combustion production. Oxygen levels measured in the sampled smoke show that in the period between (3900th – 4100th seconds) oxygen levels inside the compartment were recovering due to the introduction of fresh air by opening the door at the 3910th second, then a drop of oxygen level was observed between (4250th – 4400th seconds) this is the same time when peak HRR and temperatures inside the compartment, shown in Figure 5-53 and Figure 5-55. After that a stable oxygen concentration was observed between 16 and 18%vol. the fire was left for about 20 minutes to develop to a larger fire before starting the fire-fighting activities to extinguish the fire however it reached a steady state fuel controlled fire situation. And it was proven that the fire load used was too small to produce enough HRR to achieve flashover conditions and ventilation controlled fire conditions.

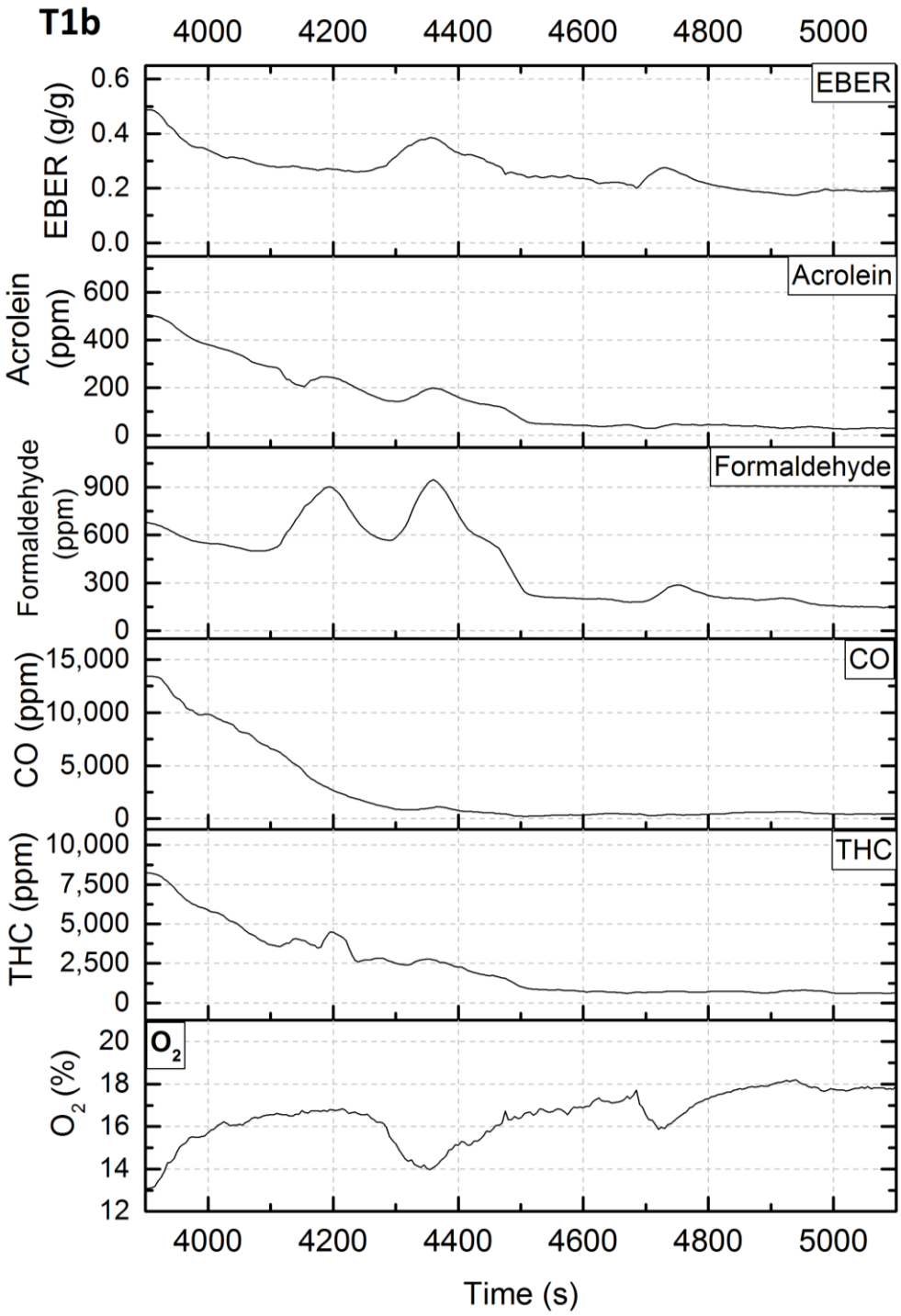

Figure 5-57: Combustion toxic products concentrations in volume basis in line with equivalence ratio and Oxygen concentration for Test 1b.

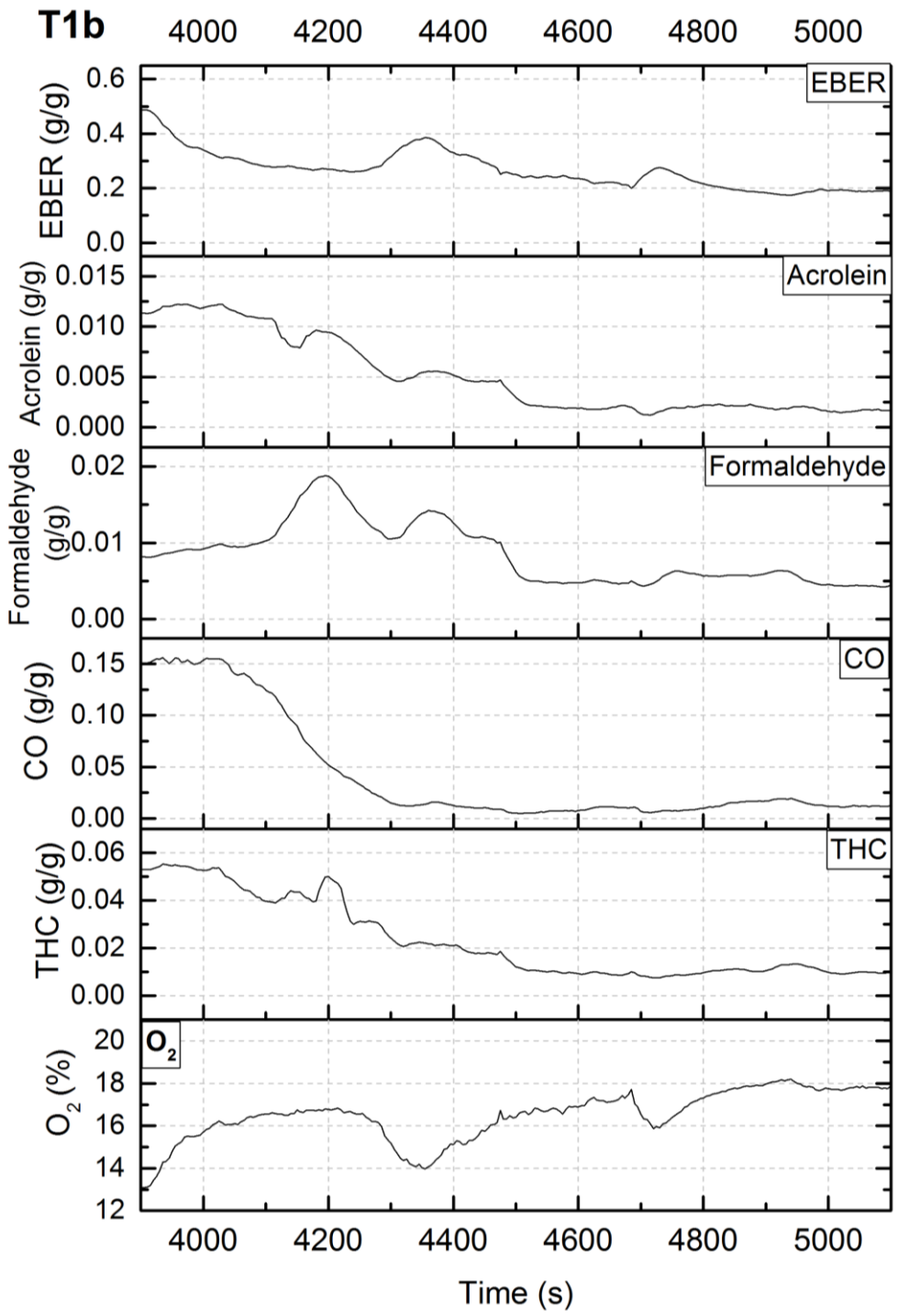

Figure 5-58: Combustion toxic products mass yields in line with equivalence ratio and Oxygen concentration for Test 1b.

The instantaneous fractional effective concentration FEC for different levels were calculated in accordance with the guidelines presented earlier in section 2.3 to demonstrate the health effects of the smoke produced at the point of sampling. Firstly, FEC safe that is important for designing purposes to ensure a safe environment in protected structures such as corridors and staircases. This value (total FEC safe) is the dilution factor required to achieve a safe environment as discussed earlier in section 2.3.

Figure 5-59 presents FEC for safe level by the combustion products from Test 1b in the stacked graph (Figure 5-57). As discussed earlier that the concentrations observed before 4300th seconds are partially from the accumulated smoke in the first part of the test T1a. However these values show the effect of inhaling the smoke after opening the door of a closed room that inhabits a smouldering fire, compared to a well ventilated fire. Figure 5-60 shows the composition of the contributing toxic emissions by percentage, where acrolein is dominating while formaldehyde is contributing third of the total influence of the smoke based on the safe exposure thresholds.

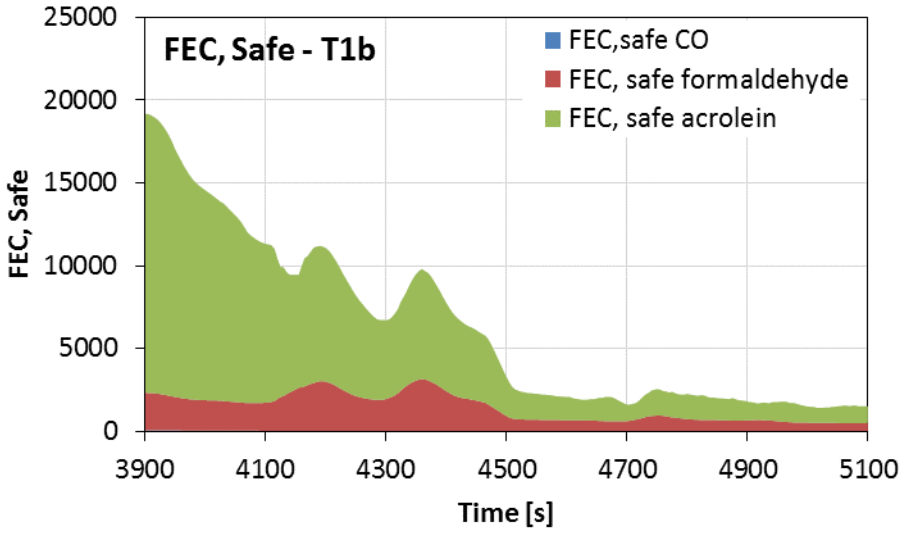

Figure 5-59: Instantaneous total fractional effective concentration (FEC) for safe level during Test 1b.

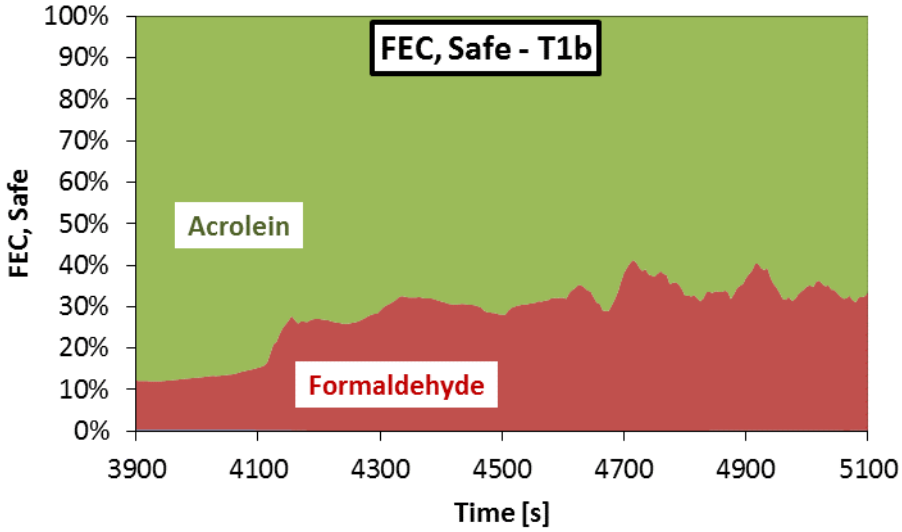

Figure 5-60: Major toxic emissions contribution by species to the fractional effective concentration for safe level in Test 1b.

Secondly, FEC for escape impairment (EI) that is important for post-accident investigations to understand the development of the evacuation plan and the point where victims were

trapped. Figure 5-61 shows FEC for escape impairment from Test 1b in the stacked graph (Figure 5-57). While Figure 5-62 shows the composition of the contributing toxic emissions by percentage based on escape impairment exposure thresholds.

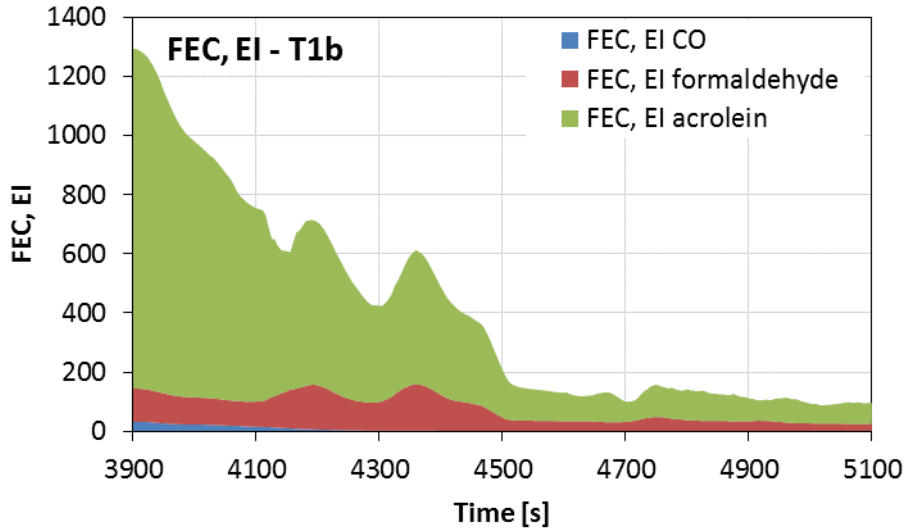

Figure 5-61: Instantaneous total fractional effective concentration (FEC) for escape impairment (EI) level during Test 1b.

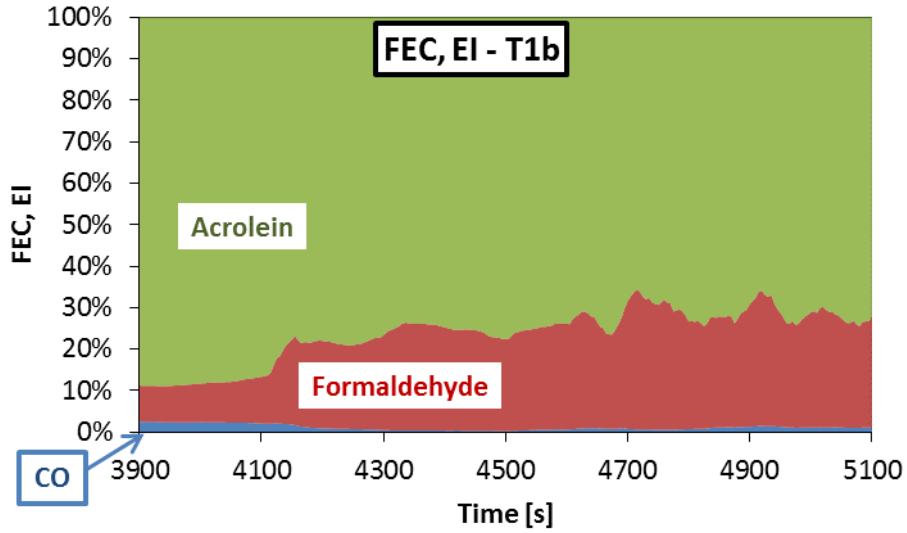

Figure 5-62: Major toxic emissions contribution by species to the fractional effective concentration for escape impairment (EI) level in Test 1b.

Thirdly, FEC for lethality that is useful for post-accident investigations. Figure 5-63 shows the instantaneous FEC for lethality from Test 1b in the stacked graph (Figure 5-57). The total value for lethal FEC stabilised at around 20 in the steady state phase (post 4500th second). Figure 5-64 shows the composition of the contributing toxic emissions by percentage based on lethal exposure thresholds discussed in section 2.3.

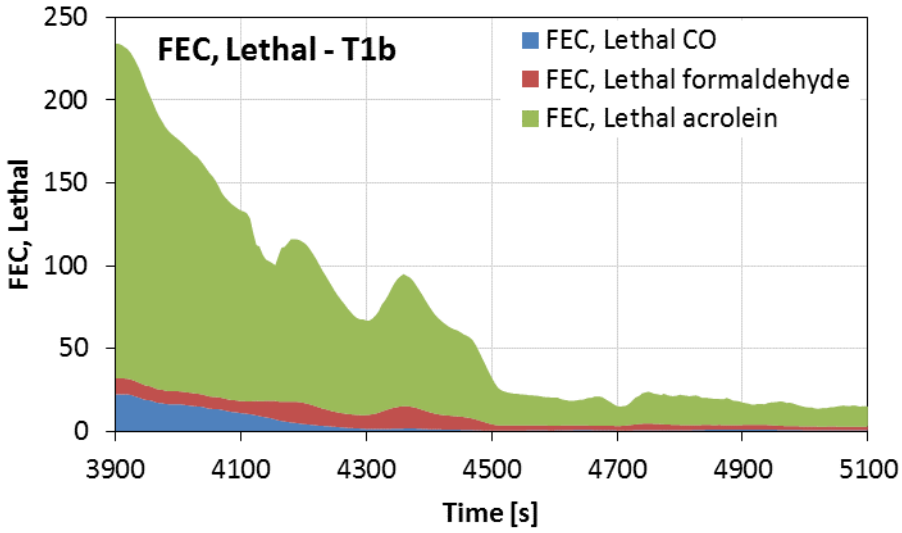

Figure 5-63: Instantaneous total fractional effective concentration (FEC) for lethal level during Test 1b.

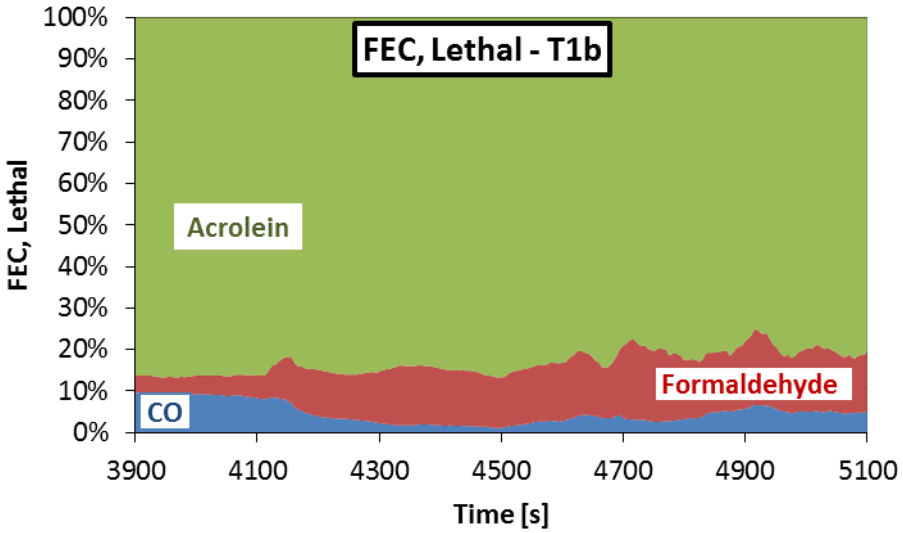

Figure 5-64: Major toxic emissions contribution by species to the fractional effective concentration for lethal level in Test 1b.

Finally, FEC for lethality based on the values purposed by ISO 13344 for LC50 the lethal concentration for half the population, as discussed earlier in section 2.3. Figure 5-65 shows the instantaneous FEC for lethality (based on LC50) from Test 1b in the stacked graph (Figure 5-57). The total value for lethal FEC stabilised to be less than 1 in the steady state phase (post 4500th second). Figure 5-66 shows the composition of the contributing toxic emissions by percentage based on lethal exposure thresholds of LC50. The comparison between FEC for lethality based on the most conservative threshold shown in Figure 5-63 and Figure 5-64on one hand and FEC for lethality based on LC50 shown in Figure 5-65 and Figure 5-66 on the other, is important to demonstrate the difference between the two. As discussed earlier in section 2.3, the most conservative threshold database for lethality used was AEGL-3_{30min} is defined to be the minimum exposure to cause life-threatening health

damage or death, while LC50 is defined to be the concentrations that cause death to half the population.

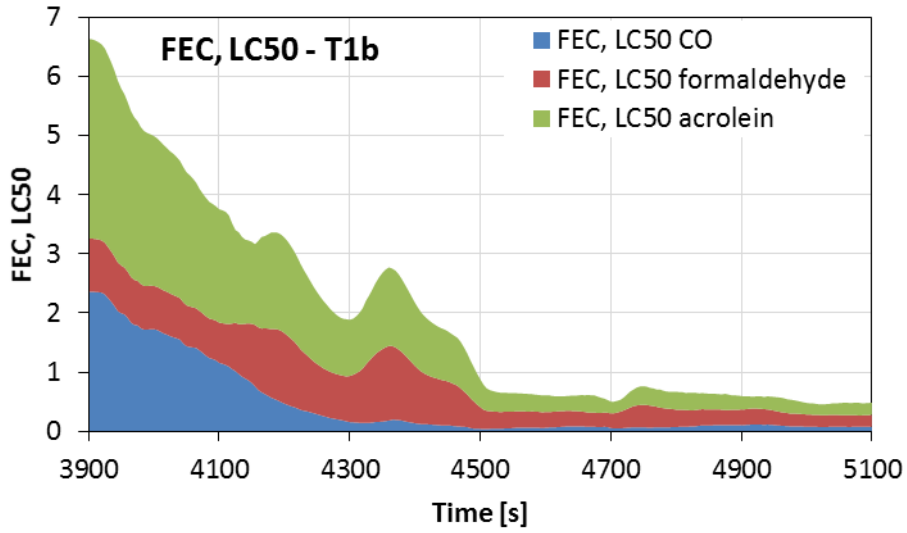

Figure 5-65: Instantaneous total fractional effective concentration (FEC) for lethal level (using LC50 values) during Test 1b.

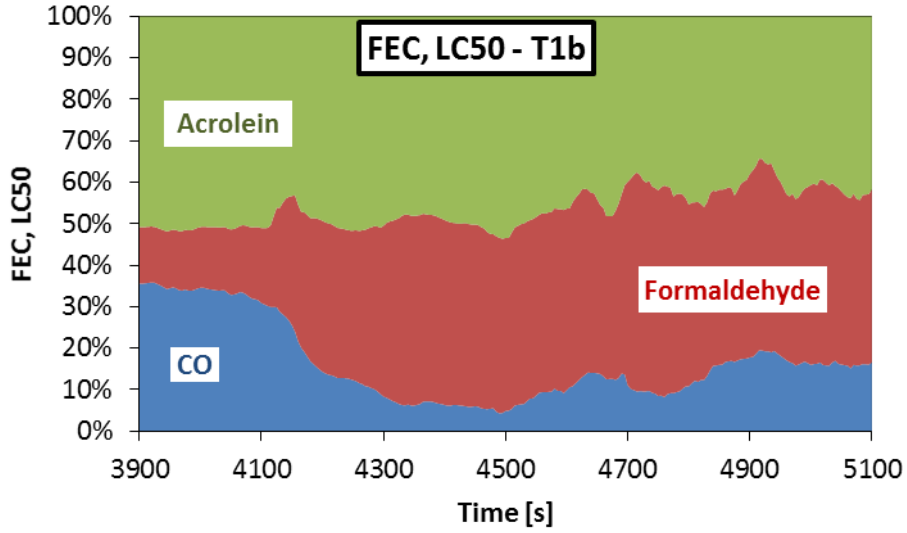

Figure 5-66: Major toxic emissions contribution by species to the fractional effective concentration for lethal level (using LC50 values) in Test 1b.

5.4 Cotton linen and towels II

The test was intended to be a semi-repeat of Test 1, however few changes were implemented in the setup of the test (shown in Figure 5-67); four curtains were hanged on the opposite wall to demonstrate the spread of fire to items away from the fire origin via the smoke hot layer. Additionally the location of the fire load was changed to be in the left hand side near corner from the corridor. Moreover the secondary sampling line locate in the corridor was used for few intervals to measure smoke products in corridor. However, other unplanned major changes occurred as well, namely; the spread of the fire to involve a door for an inside-wall storage space, located next to the fire load. This involvement meant more air was supplied, additionally the main door to the room was very leaky where considerable amounts of the smoke were measured in the corridor, while the door was closed. Other technical difficulties resulted in the loss of mass balance data. The results in this section are presented for test 4 with these changes taken into consideration.

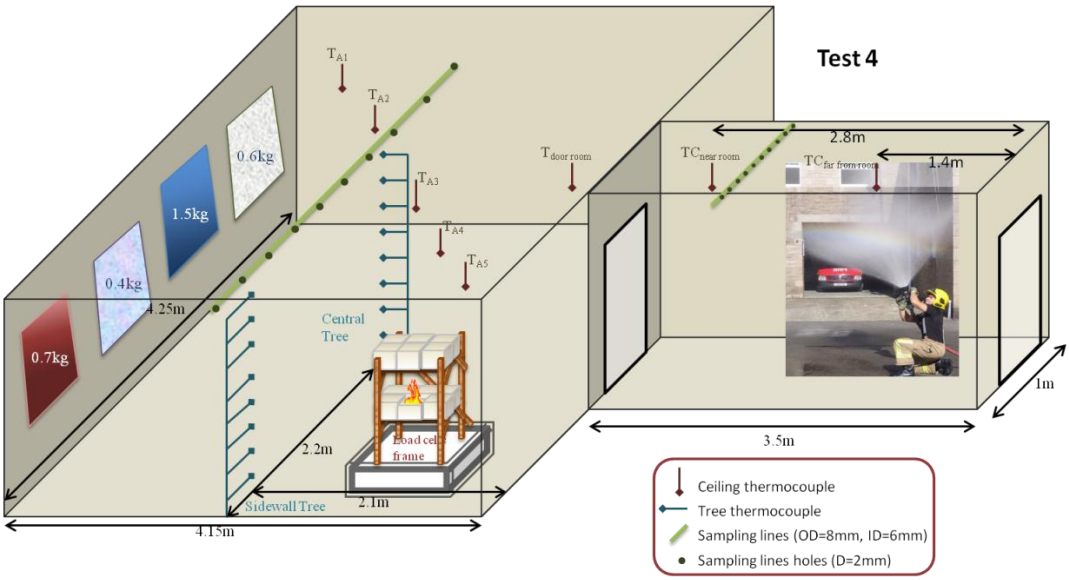

Figure 5-67: Test 4 full setup showing fire load, instrumentation and fire-fighting entrance.

The elemental analysis of the linen used showed the mass based composition to be 47.09% carbon, 5.26% hydrogen, and 47.86% oxygen. The room setup is shown in Figure 5-67, a full description of the room setup and fuel was discussed earlier (see section 3.2.5.4). The ignition source used was 250 ml of meths poured at the centre of the lower shelf. The fire load was ignited 140 seconds (2min 20sec) from the start of logging. The door was shut 273 seconds later (6min 53sec). Pictures were taken from the corridor through the glazed section of the door e.g. Figure 5-68. Then it was apparent that door for the storage space (located next to the fire load, in the left hand side of the picture presented as Figure 5-68) was involved in the fire after the 1500th second which developed to be another peak in the temperature profile inside the room.

Figure 5-68: Picture of the fire in Test 4, 291 seconds after ignition. The room door was closed and the pictures were taken from the corridor through the glazed window in the door.

The door was left closed till 2820th second (47min) when door was opened. Then the fire rapidly propagated within three minutes to spread reaching the curtains in the opposite corner and ignite them. Then fire-fighting activities started at the 3250th second (54min 10sec). By the end of the test it was concluded that no flashover occurred during the test, as the flashover targets were intact. The time line for Test 4 is graphically demonstrated in Figure 5-69. The influence of these developments, on the temperature at celling level, was recorded by the fitted thermocouples and demonstrated in Figure 5-70.

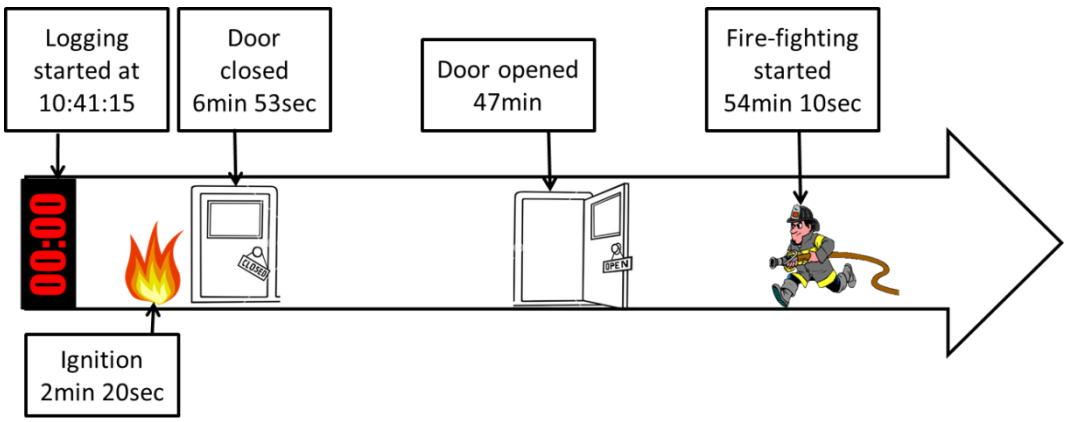

Figure 5-69: Timeline of the main events for Test 4.

Based on the developments of test 4, it can be split into three distinctive parts for the purpose of presenting results and analysis;

First, T4a (from 0 to 1500th second) – initial fire involving only the fire load on the mass balance while the door is closed,

Second, T4b (from 1500th to 2820th second) – during the spread of the fire to other items in the room while the door is closed until opening the door,

Third, T4c (from 2820th to 3250th seconds) – with compartment door fully open until fire-fighting activities started.

Mass measurements (if they were available) would have been very useful in establishing HRRs during the first part of the test T4a. But for the other parts of the test, this helpfulness is limited due to the spread of the fire to other items that their burning rates are not quantified by the mass balance.

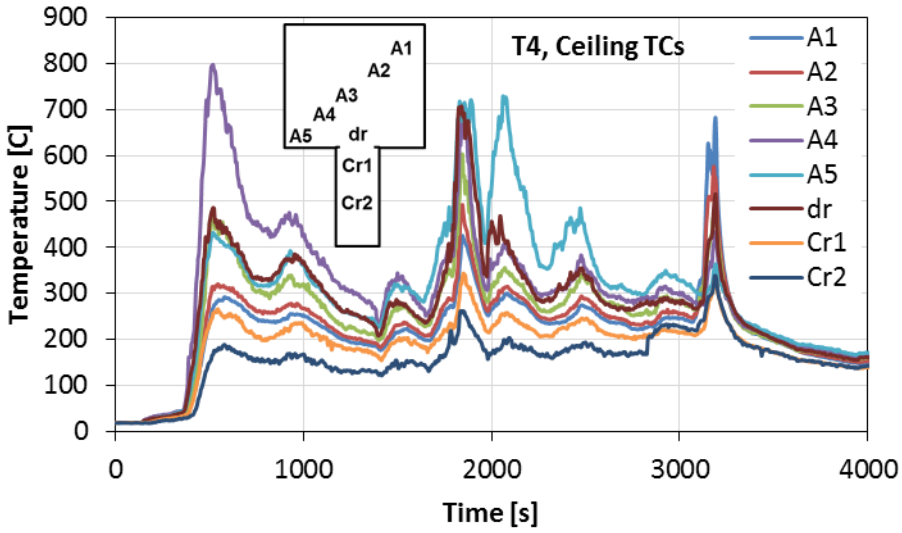

Figure 5-70: Ceiling layer temperature measurements at different positions inside the compartment and corridor during Test 4.

5.4.1 Results and analysis for the first part of Test 4 (T4a)

During the first part of test 4 the door was closed, but the restriction of air supply was not as in test 1. In test 4a the fire was involving only the main fire load (cotton towels and linen), the endpoint for this part of the test was the involvement of other items in the fire (specifically the storage door next to the fire load).

5.4.1.1 Thermal environment – Test 4a

During this part of the test the fire started initially with a well ventilated flaming fire (ISO stage 2) until oxygen available was used (reaching peak temperatures around at the 500th second). Up to this point, this is a very similar pattern to the initial stages observed in Test 1, however in this test after the 500th second peak point temperatures measured in the upper

layer started stabilising above 250 C unlike Test 1 where temperatures dropped straight away to below 100 C. Figure 5-71 shows temperature measurements at ceiling level, two interesting observations worth highlighting in this graph; firstly, the ceiling thermocouple (A4) peak at 800 C indicates that it was located exactly above the fuel. Secondly the temperature profile (Cr1) and (Cr2) located in the corridor behind a closed door, it is clear that the door was not stopping the hot smoke from traveling through the corridor to the outside. This is backed by the oxygen measurements inside the compartment which recovered rapidly after the initial ignition meaning that smoke was freely travelling outside the room and air was drawn in almost freely throughout Test 4.

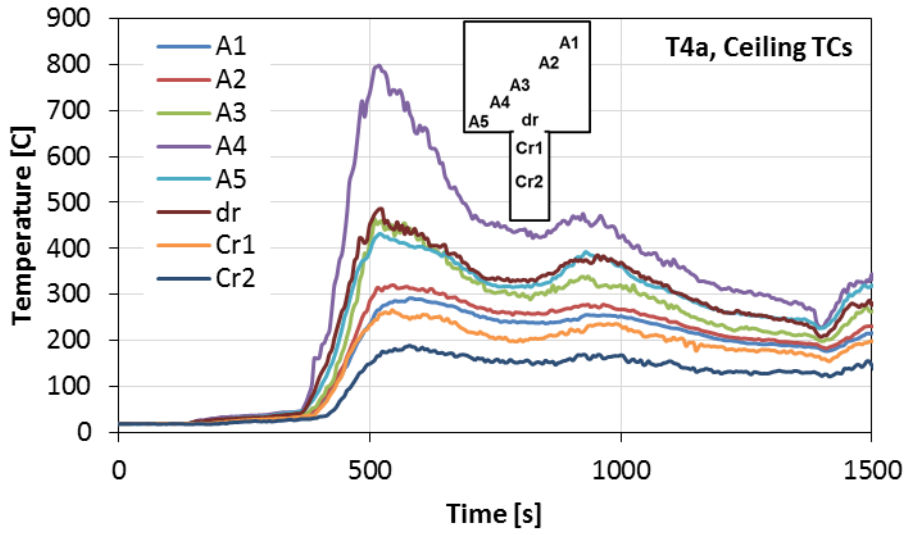

Figure 5-71: Ceiling layer temperature measurements at different positions inside the compartment and corridor during Test 4a.

5.4.1.2 Toxic environment – Test 4a

During Test 4 the gas sampling system was mainly set on the central sampling line inside the room and switched to sample from the corridor briefly once for 5 minutes during test 4a (between 750th – 1050th seconds). Measurements from the corridor were cropped out and treated as a single point measurement at the 1000th second. Table 5-3 presents the gas concentration measurements in the corridor and their corresponding yields based on the emission-based equivalence ratio (EBER) at the point of sampling that was 0.19. Ratios to the relevant exposure thresholds are presented. The composition of the overall fractional effective concentration (FEC) are presented in Figure 5-72: The main toxic products measured in the corridor during Test 4a at 1000th second in respect to their contribution to the overall Fractional Effective Concentration (FEC).. These data useful for studying situations of exposure away from the room of origin where the required dilution rate is indicated by the FEC values for different levels of exposure effects.

Table 5-3: Concentrations of major combustion emissions measured in the corridor during Test 4a at 1000th second, with their ratios to relevant toxic exposure thresholds and mass yield data for each species.

Species	Conc. [ppm]	R-Safe	R-Escape impairment	R-Lethal	R-LC50	Yield [g/g]
CO	729	3.6	1.7	1.2	0.13	0.0201
Acrolein	26	876	60	11	0.18	0.0014
Formaldehyde	34	115	5.7	0.5	0.05	0.0010
HCN	5	1.8	0.27	0.22	0.03	0.0001
THC	372					0.0059

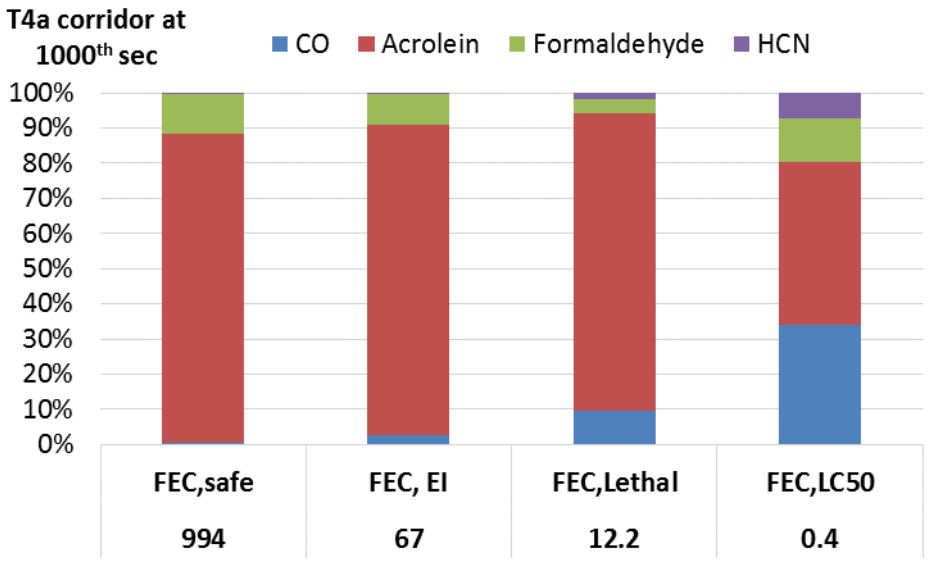

Figure 5-72: The main toxic products measured in the corridor during Test 4a at 1000th second in respect to their contribution to the overall Fractional Effective Concentration (FEC).

The measurements from inside the room were analysed separately, for the gap measurements (due to sampling from the corridor, not for the room) the data points were linked based on before and after switching in order to estimate these measurements. Due to the fact that the room was not completely confined from ventilation, the data were treated as a dynamic online gas measurements. The combustion emission-based equivalence ratio (EBER) was calculated as a function of time and is presented at the top of Figure 5-73. The EBER shows that the fire was lean throughout Test 4a with a 0.4 peak around the 500th second. Main toxic species measured at this stage (T4a) are presented as well in Figure 5-73. Oxygen levels dropped to 13% similar to Test 4a around the 500th second. Corresponding mass yields are presented in Figure 5-74.

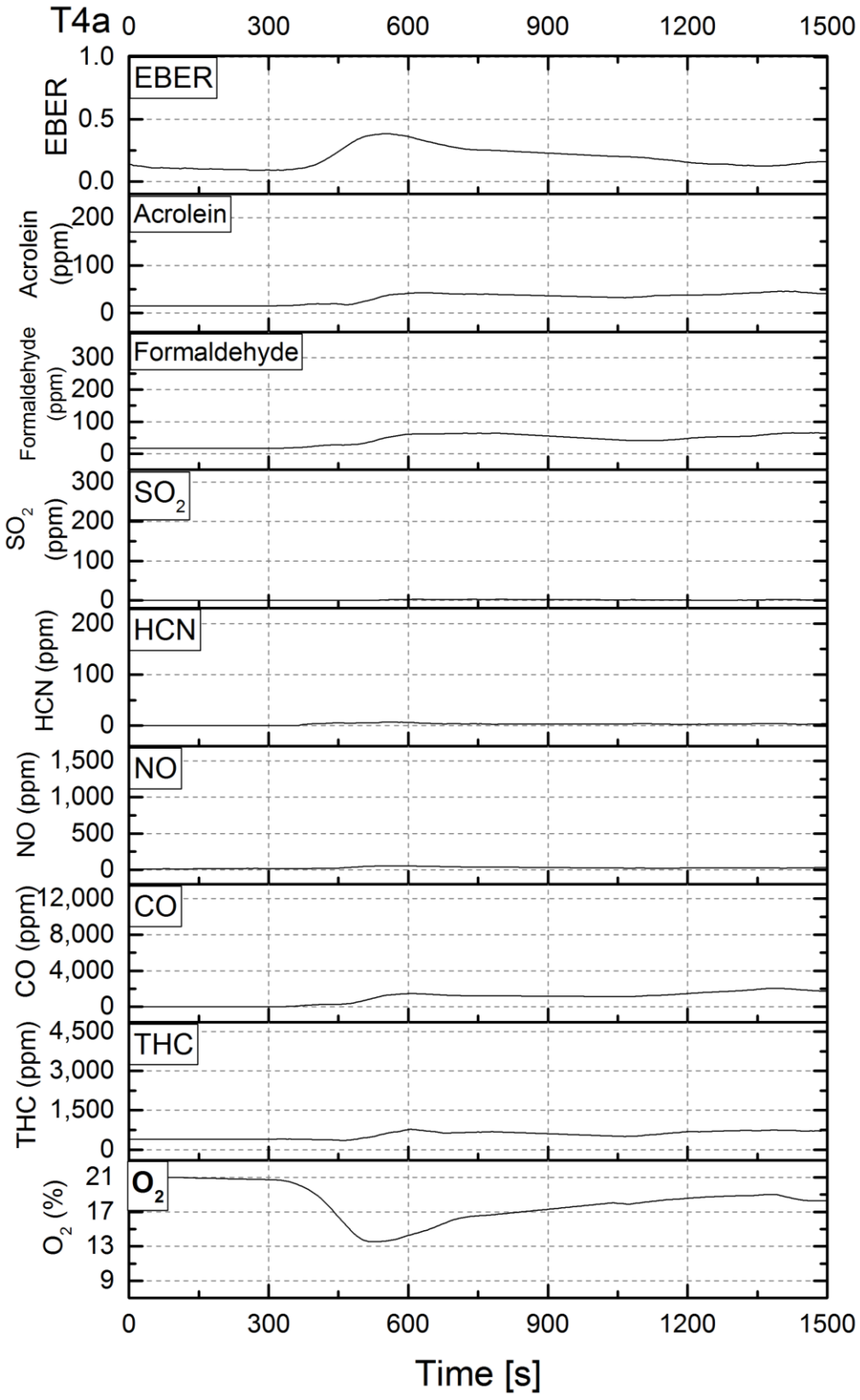

Figure 5-73: Combustion toxic products concentrations in volume basis in line with equivalence ratio and Oxygen concentration for Test 4a.

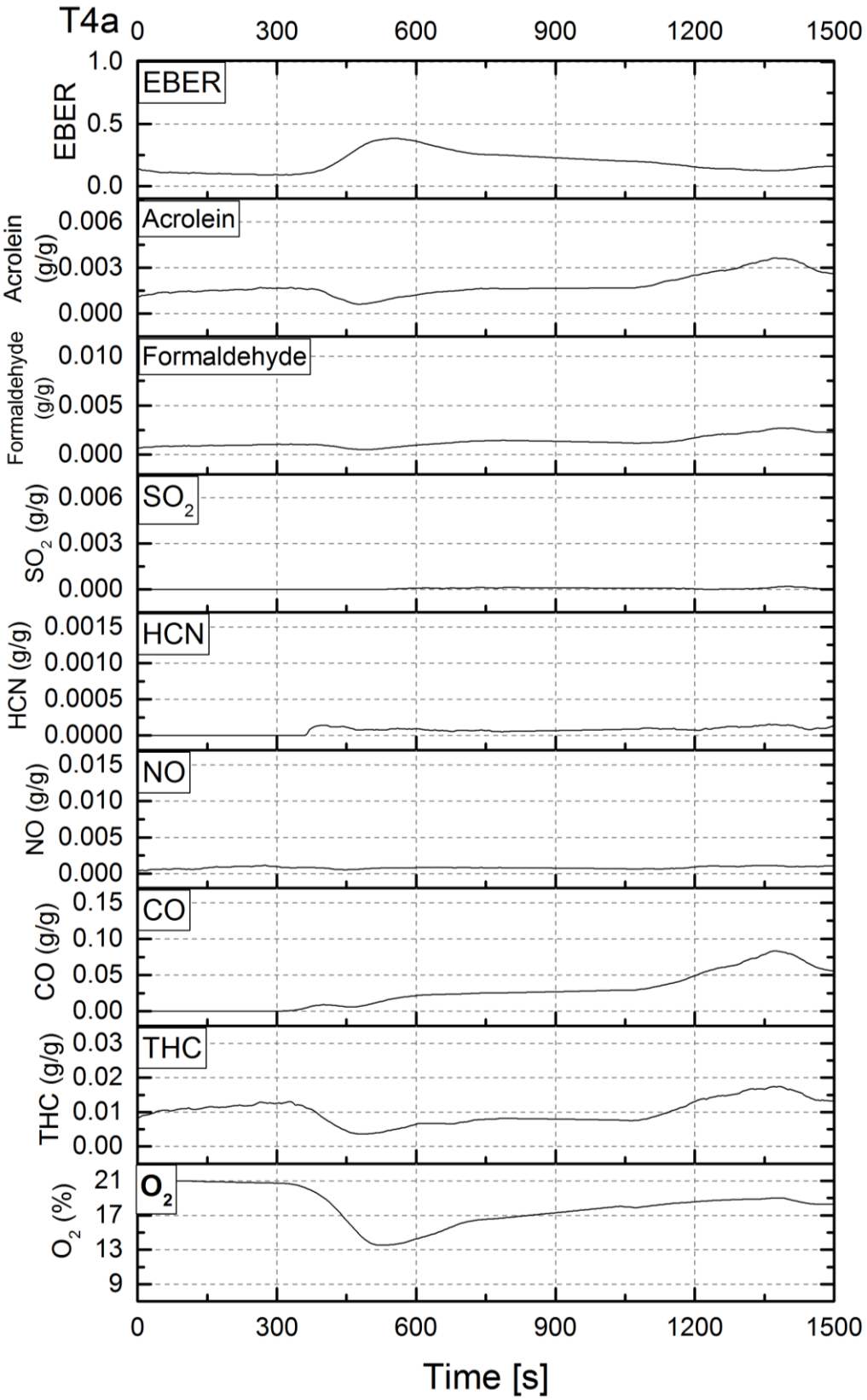

Figure 5-74: Combustion toxic products mass yields in line with equivalence ratio and Oxygen concentration for Test 4a.

The instantaneous fractional effective concentration FEC for different levels were calculated in accordance with the guidelines presented earlier in section 2.3 to demonstrate the health effects of the smoke produced at the point of sampling. Firstly, FEC safe that is important for designing purposes to ensure a safe environment in protected structures such as corridors and staircases. This value (total FEC safe) is the dilution factor required to achieve a safe environment as discussed earlier in section 2.3.

Figure 5-75 presents FEC for safe level by the combustion products concentrations from Test 4a in the stacked graph (Figure 5-73). Figure 5-76 shows the composition of the contributing toxic emissions by percentage, where acrolein is dominating while formaldehyde is contributing 10% to the total influence of the smoke based on the safe exposure thresholds.

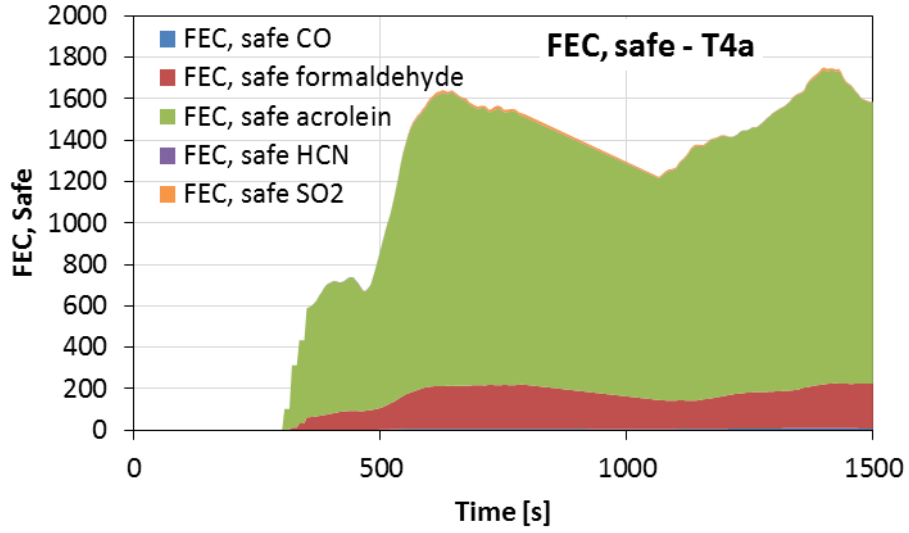

Figure 5-75: Instantaneous total fractional effective concentration (FEC) for safe level during Test 4a.

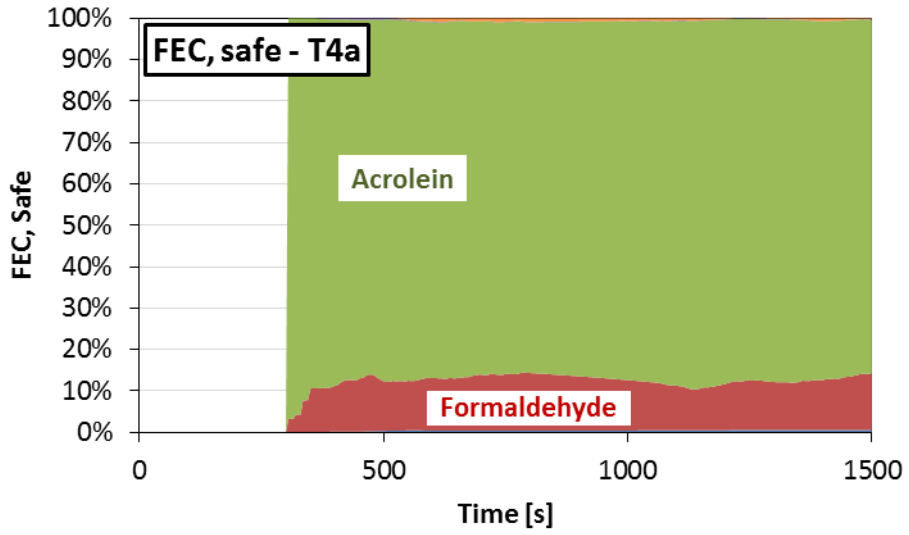

Figure 5-76: Major toxic emissions contribution by species to the fractional effective concentration for safe level in Test 4a.

Secondly, FEC for escape impairment (EI) that is important for post-accident investigations to understand the development of the evacuation plan and the point where victims were trapped. Figure 5-77 shows FEC for escape impairment from Test 4a in the stacked graph (Figure 5-73). While Figure 5-78 shows the composition of the contributing toxic emissions by percentage based on escape impairment exposure thresholds.

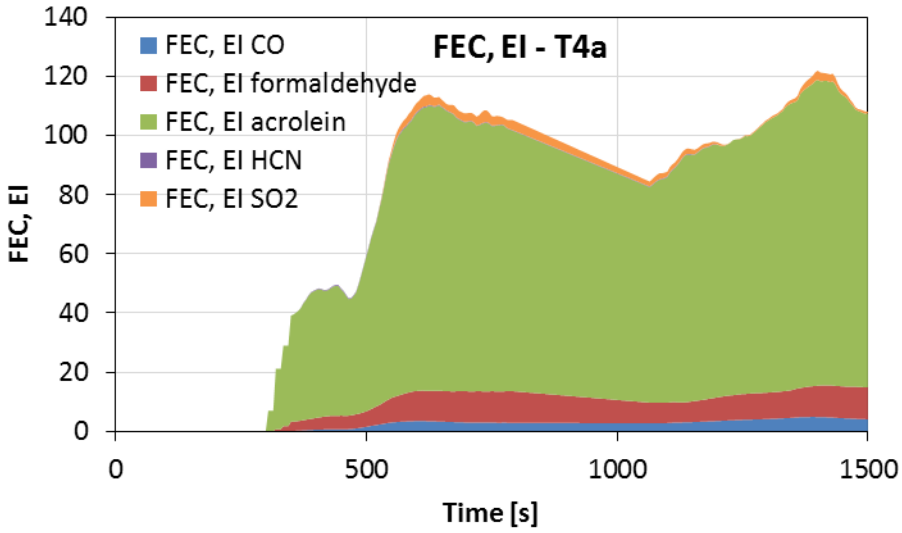

Figure 5-77: Instantaneous total fractional effective concentration (FEC) for escape impairment (EI) level during Test 4a.

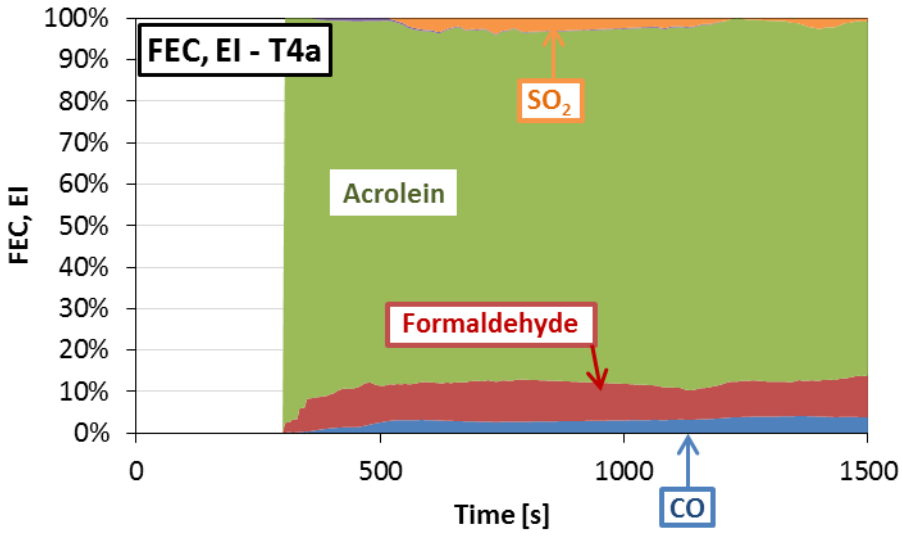

Figure 5-78: Major toxic emissions contribution by species to the fractional effective concentration for escape impairment (EI) level in Test 4a.

Thirdly, FEC for lethality that is useful for post-accident investigations. Figure 5-79 shows the instantaneous FEC for lethality from Test 4a in the stacked graph (Figure 5-73). The total value for lethal FEC reached 20. Figure 5-80 shows the composition of the contributing toxic emissions by percentage based on lethal exposure thresholds discussed in section 2.3.

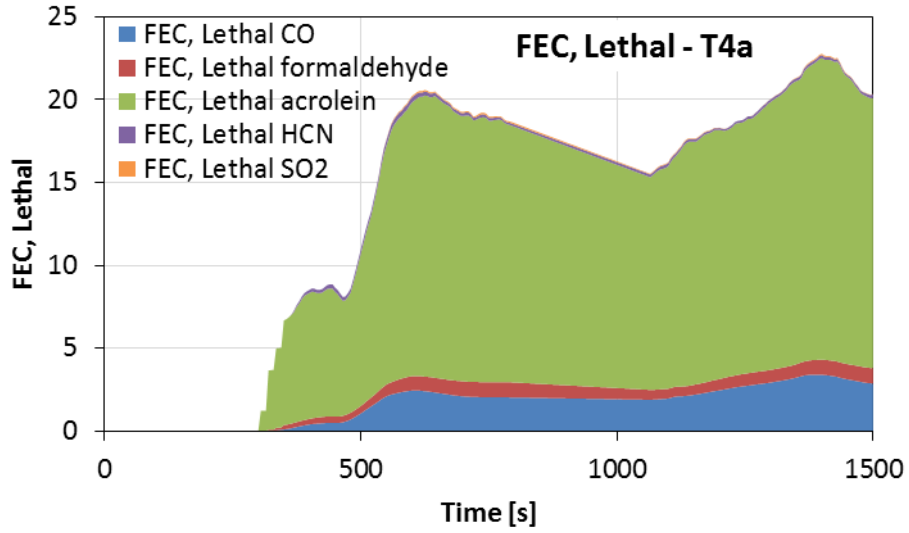

Figure 5-79: Instantaneous total fractional effective concentration (FEC) for lethal level during Test 4a.

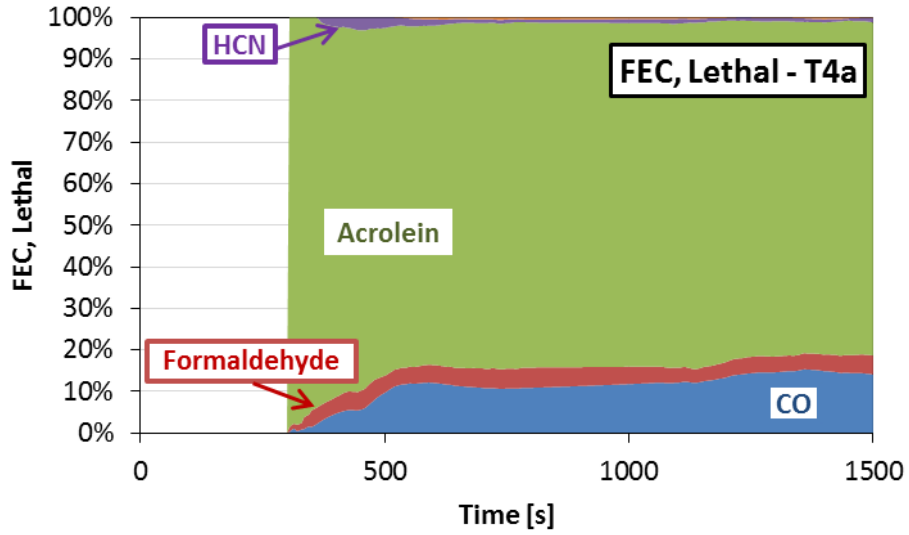

Figure 5-80: Major toxic emissions contribution by species to the fractional effective concentration for lethal level in Test 4a.

Finally, FEC for lethality based on the values purposed by ISO 13344 for LC50 the lethal concentration for half the population, as discussed earlier in section 2.3. Figure 5-81 shows the instantaneous FEC for lethality (based on LC50) from Test 4a in the stacked graph (Figure 5-73). The total value for lethal FEC reached 0.7. Figure 5-82 shows the composition of the contributing toxic emissions by percentage based on lethal exposure thresholds of LC50. The comparison between FEC for lethality based on the most conservative threshold shown in Figure 5-79 and Figure 5-80 on one hand and FEC for lethality based on LC50 shown in Figure 5-81 and Figure 5-82 on the other, is important to demonstrate the difference between the two. As discussed earlier in section 2.3, the most conservative threshold database for lethality used was AEGL-3_{30min} is defined to be the minimum exposure to cause life-threatening health damage or death, while LC50 is defined to be the concentrations that cause death to half the population.

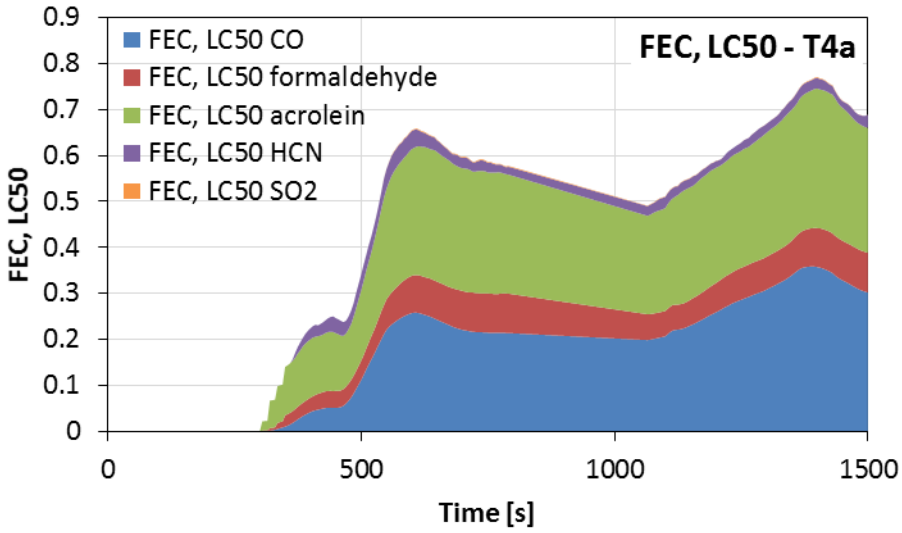

Figure 5-81: Instantaneous total fractional effective concentration (FEC) for lethal level (using LC50 values) during Test 4a.

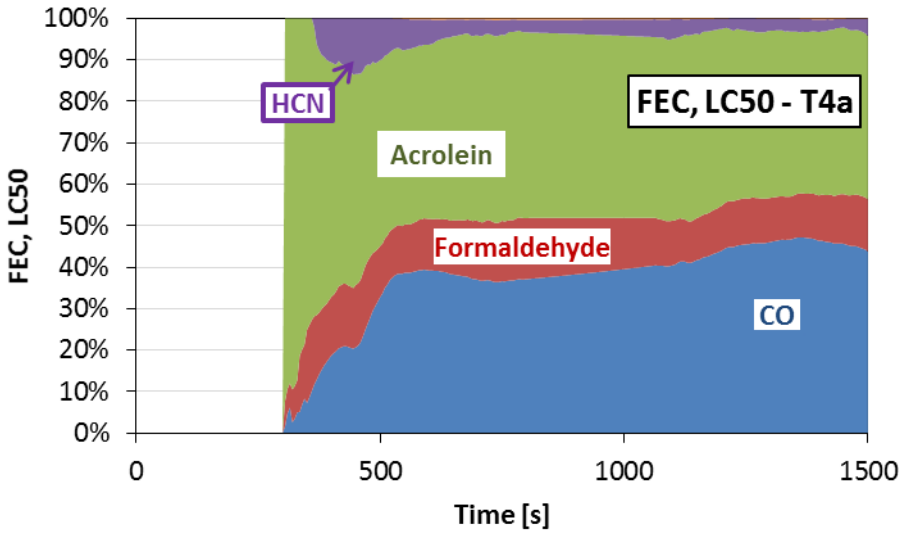

Figure 5-82: Major toxic emissions contribution by species to the fractional effective concentration for lethal level (using LC50 values) in Test 4a.

5.4.2 Results and analysis for the second part of Test 4 (T4b)

The second part of test 4 started by the involvement of the storage door next to the fire load. The end point of test 4b was opening the door at the 2820th second. By that time the temperatures inside the compartment stabilised below 300 C at the ceiling level.

5.4.2.1 Thermal environment – Test 4b

During this part of the test the fire started with a dying down pattern till the 1700th second when temperatures started to rise top peak at the 1850th second reaching 700 C at ceiling level as can be seen in Figure 5-83. A second peak occurred at the 2100th second observed significantly by thermocouple (A5), nearest to the storage door. Temperature profile in the corridor measured by (Cr1) and (Cr2) were following the same pattern inside the room with a lesser magnitude. By the end of this part of the test T4b, temperatures at the ceiling level were settling below 300 C. then, the door was opened for the third part of the test T4c to begin with the door open.

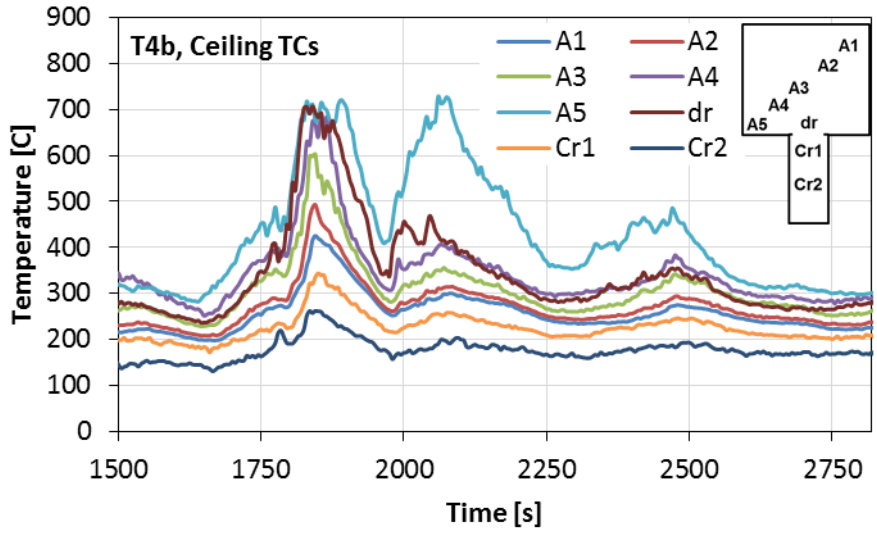

Figure 5-83: Ceiling layer temperature measurements at different positions inside the compartment and corridor during Test 4b.

5.4.2.2 Toxic environment – Test 4b

During Test 4 the gas sampling system was mainly set on the central sampling line inside the room and switched to sample from the corridor briefly twice during test 4b (1550th – 1800th seconds and 2350th – 2550th second). Measurements from the corridor were cropped out and treated as a single point measurements at the 1700th and 2400th second. Table 5-4 presents the gas concentration measurements in the corridor for the first single point measurement (1700th second) and their corresponding yields based on the emission-based equivalence ratio (EBER) at the point of sampling that was 0.14. Ratios to the relevant exposure thresholds are presented. The composition of the overall fractional effective concentration (FEC) are presented in Figure 5-84. These data are useful for studying situations of exposure away from the room of origin where the required dilution rate is indicated by the FEC values for different levels of exposure effects.

Table 5-4: Concentrations of major combustion emissions measured in the corridor during Test 4b at 1700th second, with their ratios to relevant toxic exposure thresholds and mass yield data for each species.

Species	Conc. [ppm]	R-Safe	R-Escape impairment	R-Lethal	R-LC50	Yield [g/g]
CO	1,624	8.1	3.9	2.7	0.28	0.0579
Acrolein	38	1,279	87	15.3	0.26	0.0027
Formaldehyde	36	120	6	0.5	0.05	0.0014
HCN	3	1.3	0.18	0.15	0.02	0.0001
THC	655					0.0134

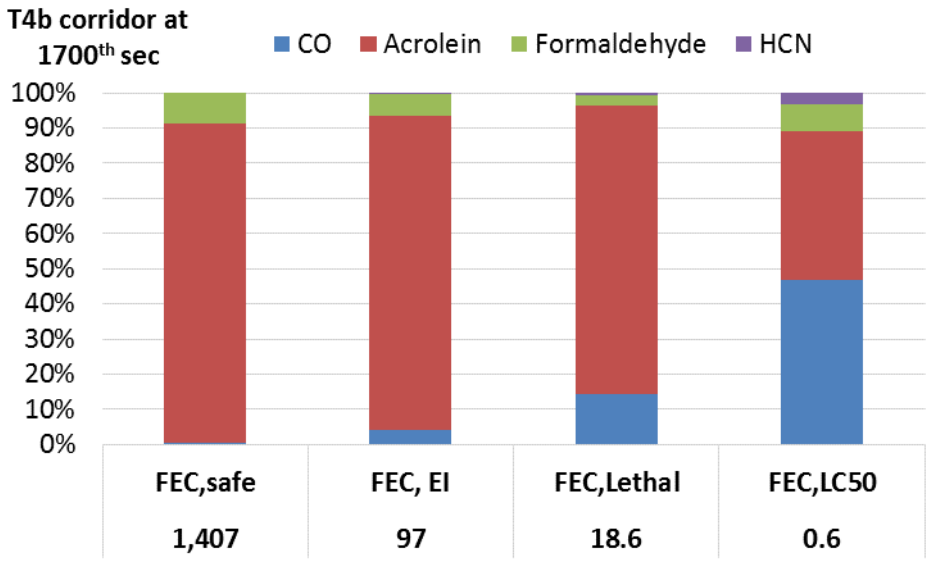

Figure 5-84: The main toxic products measured in the corridor during Test 4b at 1700th second in respect to their contribution to the overall Fractional Effective Concentration (FEC).

Table 5-5 presents the gas concentration measurements in the corridor for the second single point measurement (2400th second) and their corresponding yields based on the emission-based equivalence ratio (EBER) at the point of sampling that was 0.45. Ratios to the relevant exposure thresholds are presented. The composition of the overall fractional effective concentration (FEC) are presented in Figure 5-85. These data are useful for studying situations of exposure away from the room of origin where the required dilution rate is indicated by the FEC values for different levels of exposure effects.

Table 5-5: Concentrations of major combustion emissions measured in the corridor during Test 4b at 2400th second, with their ratios to relevant toxic exposure thresholds and mass yield data for each species.

Species	Conc. [ppm]	R-Safe	R-Escape impairment	R-Lethal	R-LC50	Yield [g/g]
CO	4,106	21	9.8	6.8	0.72	0.0497
Acrolein	87	2,889	197	34.7	0.58	0.0021
Formaldehyde	28	94	4.7	0.4	0.04	0.0004
HCN	19	7.6	1.1	0.9	0.12	0.0002
THC	1,853					0.0129

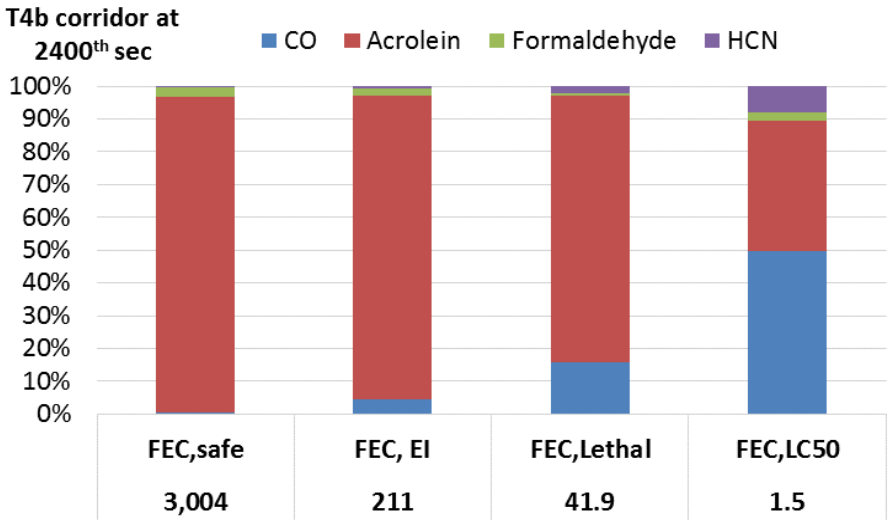

Figure 5-85: The main toxic products measured in the corridor during Test 4b at 2400th second in respect to their contribution to the overall Fractional Effective Concentration (FEC).

The measurements from inside the room were analysed separately, for the gap measurements (due to sampling from the corridor, not for the room) the data points were linked based on before and after switching in order to estimate these measurements. Due to the fact that the room was not completely confined from ventilation, the data were treated as a dynamic online gas measurements. The combustion emission-based equivalence ratio (EBER) was calculated as a function of time and is presented at the top of Figure 5-86. The EBER shows that the fire was lean throughout Test 4b with a 0.8 peak around the 2200th second. Main toxic species measured at this stage (T4b) are presented as well in Figure 5-86. Oxygenated hydrocarbons peaked before the 2200th second while SO_2 and HCN peaked at that point. It is suspected that sulphur origin was from the storage door that had insulation materials as an inner layer. Oxygen levels dropped to 9% around the 2200th second. Corresponding mass yields are presented in Figure 5-87.

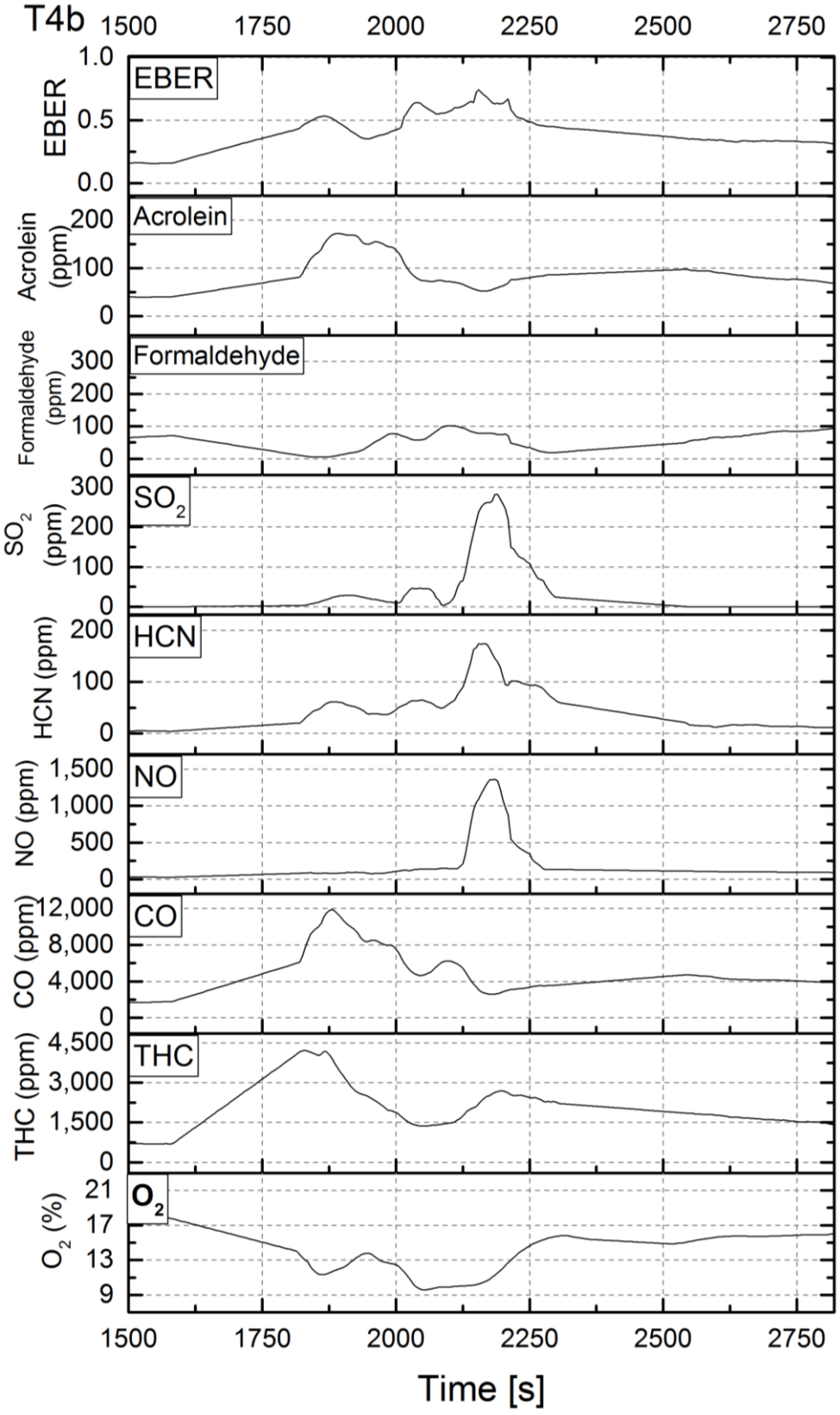

Figure 5-86: Combustion toxic products concentrations in volume basis in line with equivalence ratio and Oxygen concentration for Test 4b.

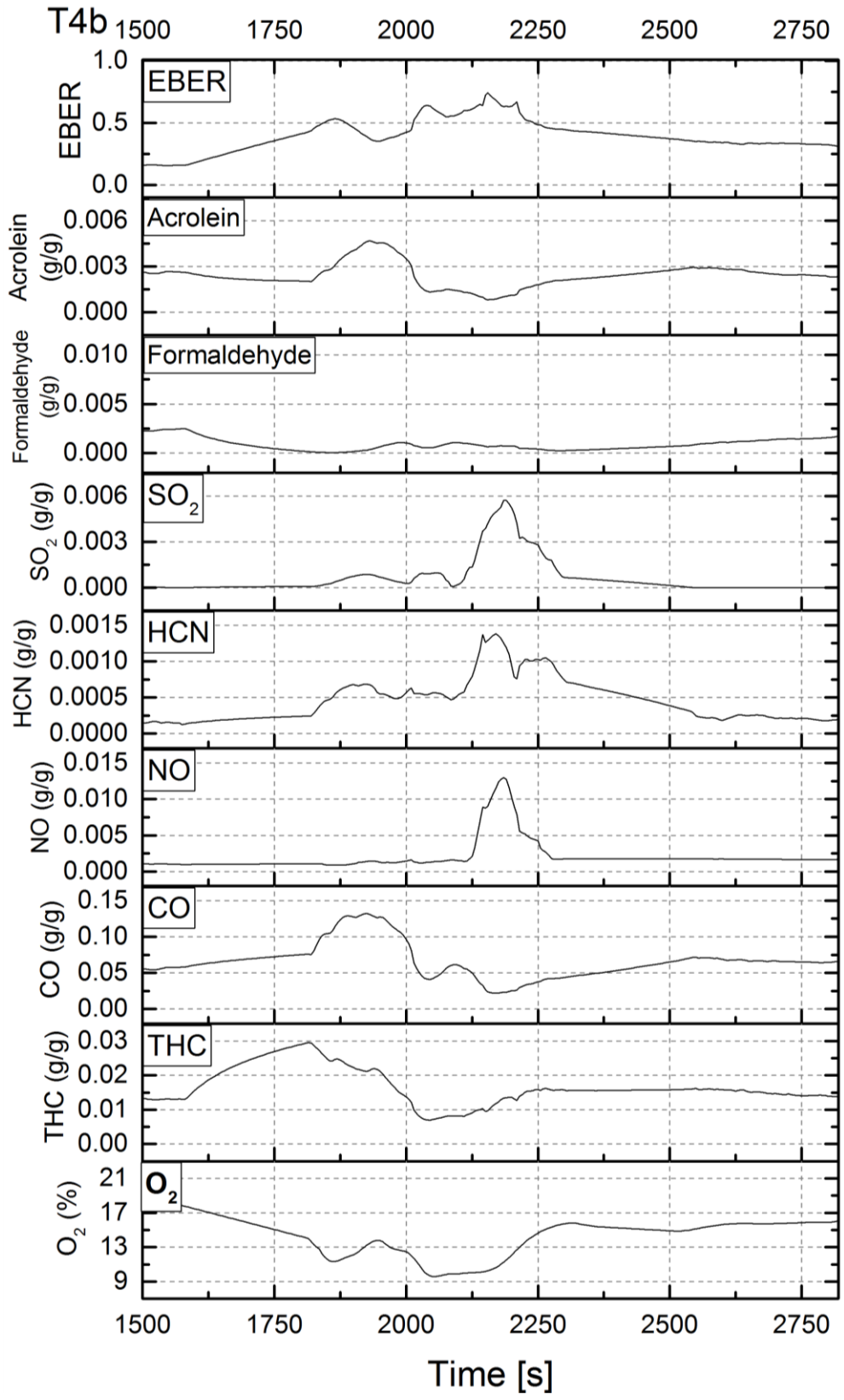

Figure 5-87: Combustion toxic products mass yields in line with equivalence ratio and Oxygen concentration for Test 4b.

The instantaneous fractional effective concentration FEC for different levels were calculated in accordance with the guidelines presented earlier in section 2.3 to demonstrate the health effects of the smoke produced at the point of sampling. Firstly, FEC safe that is important for designing purposes to ensure a safe environment in protected structures such as corridors and staircases. This value (total FEC safe) is the dilution factor required to achieve a safe environment as discussed earlier in section 2.3.

Figure 5-88 presents FEC for safe level by the combustion products concentrations from Test 4b in the stacked graph (Figure 5-86). Figure 5-89 shows the composition of the contributing toxic emissions by percentage, where acrolein is dominating throughout Test 4b, Sulphur dioxide contribution peaked at the 2200th second reaching about 40%, formaldehyde was contributing approximately 10% to the total influence of the smoke based on the safe exposure thresholds.

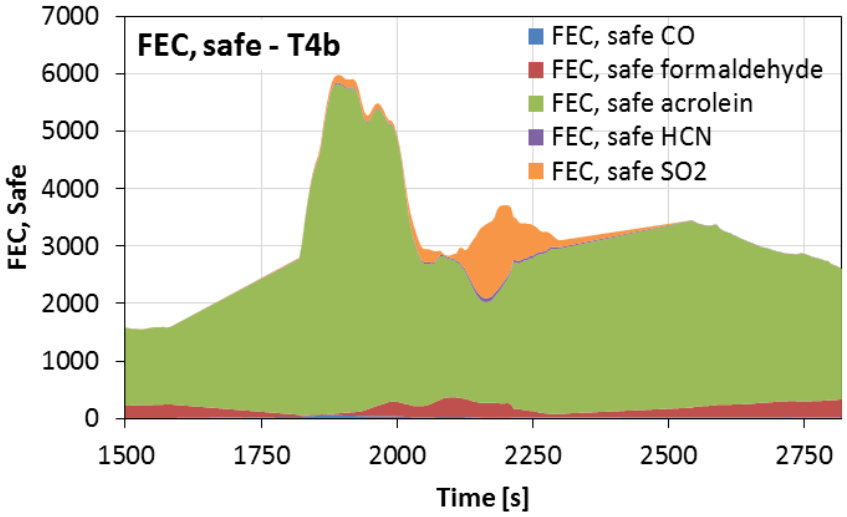

Figure 5-88: Instantaneous total fractional effective concentration (FEC) for safe level during Test 4b.

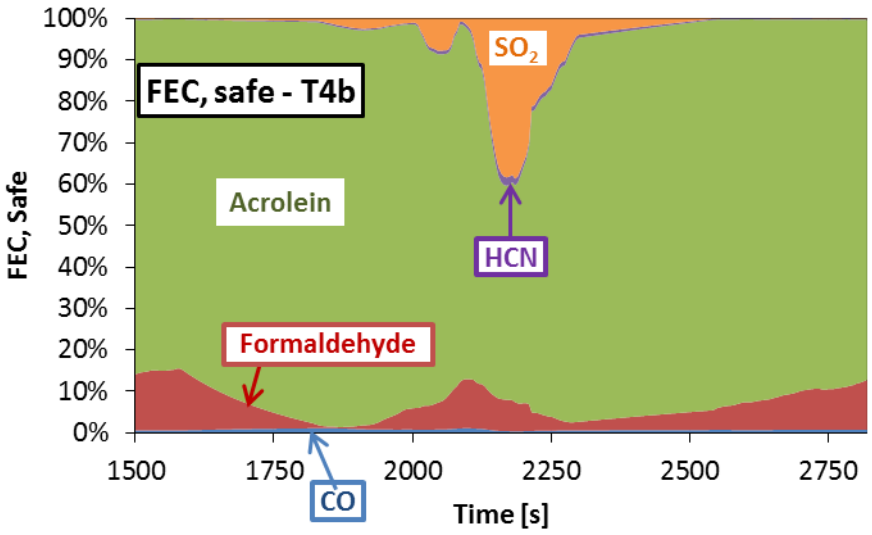

Figure 5-89: Major toxic emissions contribution by species to the fractional effective concentration for safe level in Test 4b.

Secondly, FEC for escape impairment (EI) that is important for post-accident investigations to understand the development of the evacuation plan and the point where victims were trapped. Figure 5-90 shows FEC for escape impairment from Test 4b in the stacked graph (Figure 5-86). While Figure 5-91 shows the composition of the contributing toxic emissions by percentage based on escape impairment exposure thresholds.

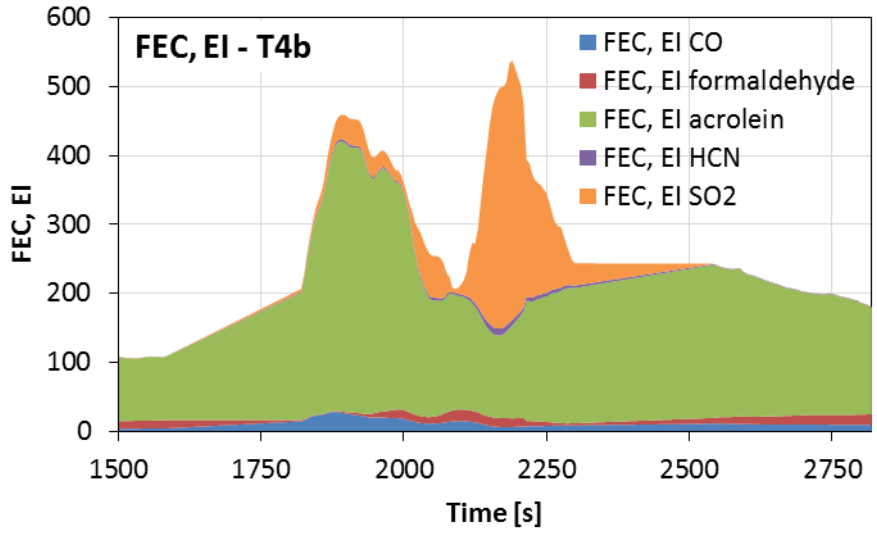

Figure 5-90: Instantaneous total fractional effective concentration (FEC) for escape impairment (EI) level during Test 4b.

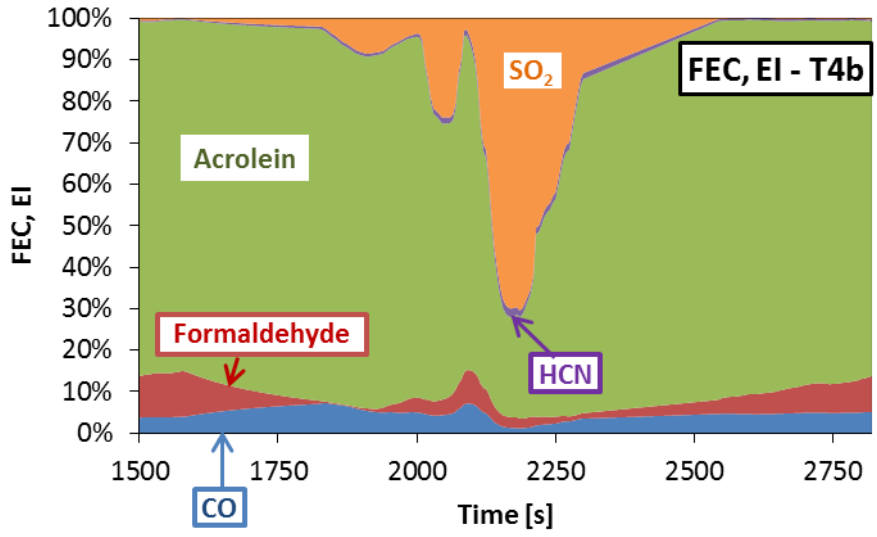

Figure 5-91: Major toxic emissions contribution by species to the fractional effective concentration for escape impairment (EI) level in Test 4b.

Thirdly, FEC for lethality that is useful for post-accident investigations. Figure 5-92 shows the instantaneous FEC for lethality from Test 4b in the stacked graph (Figure 5-86). The total value for lethal FEC reached 90. Figure 5-93 shows the composition of the contributing toxic emissions by percentage based on lethal exposure thresholds discussed in section 2.3.

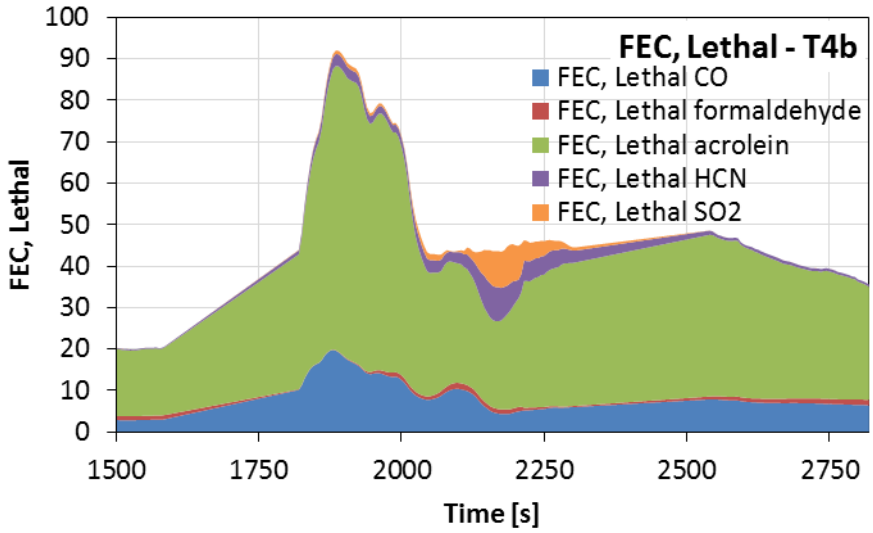

Figure 5-92: Instantaneous total fractional effective concentration (FEC) for lethal level during Test 4b.

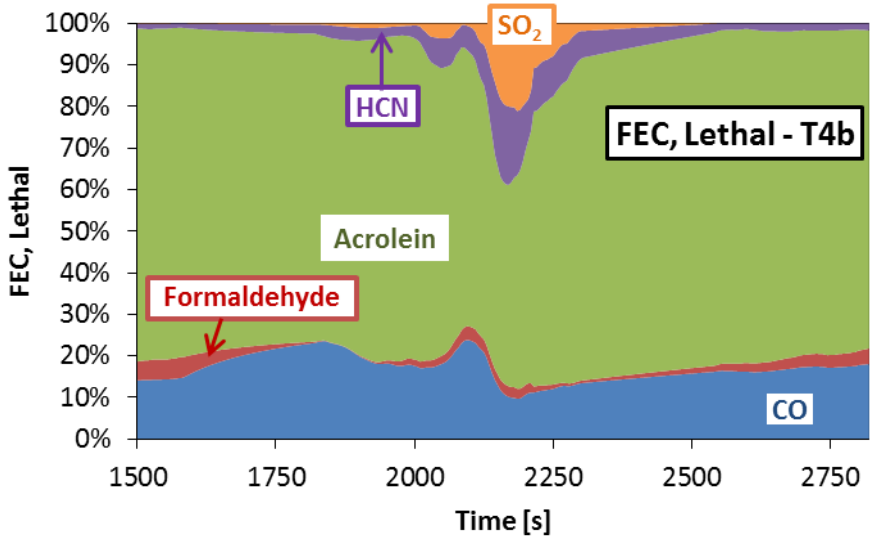

Figure 5-93: Major toxic emissions contribution by species to the fractional effective concentration for lethal level in Test 4b.

Finally, FEC for lethality based on the values purposed by ISO 13344 for LC50 the lethal concentration for half the population, as discussed earlier in section 2.3. Figure 5-94 shows the instantaneous FEC for lethality (based on LC50) from Test 4b in the stacked graph (Figure 5-86). The total value for lethal FEC reached 3.5. Figure 5-95 shows the composition of the contributing toxic emissions by percentage based on lethal exposure thresholds of LC50. The comparison between FEC for lethality based on the most conservative threshold shown in Figure 5-92 and Figure 5-93 on one hand and FEC for lethality based on LC50 shown in Figure 5-94 and Figure 5-95 on the other, is important to demonstrate the difference between the two. As discussed earlier in section 2.3, the most conservative threshold database for lethality used was AEGL-3_{30min} is defined to be the minimum exposure to cause life-threatening health damage or death, while LC50 is defined to be the concentrations that cause death to half the population.

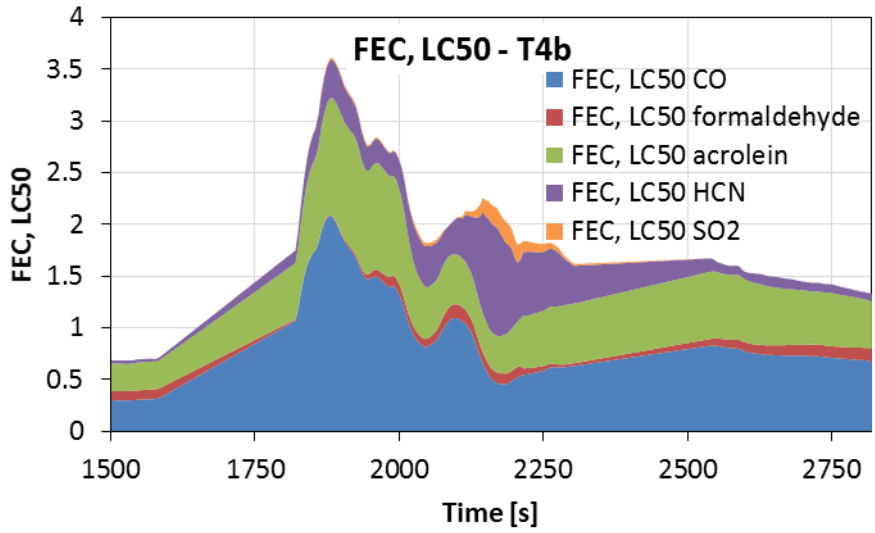

Figure 5-94: Instantaneous total fractional effective concentration (FEC) for lethal level (using LC50 values) during Test 4b.

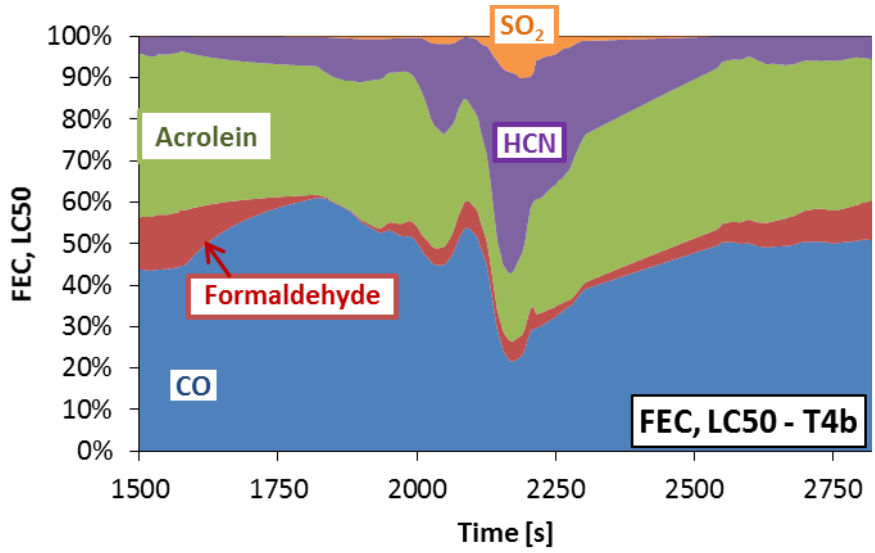

Figure 5-95: Major toxic emissions contribution by species to the fractional effective concentration for lethal level (using LC50 values) in Test 4b.

5.4.3 Results and analysis for the third part of Test 4 (T4c)

5.4.3.1 Thermal environment – Test 4c

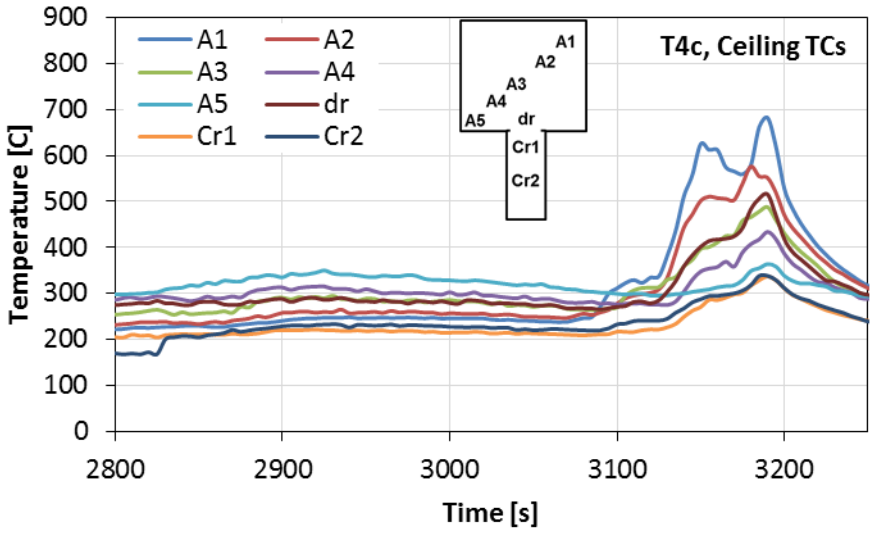

5.4.3.2 Toxic environment – Test 4c

During Test 4c the gas sampling system was set on the central sampling line inside the room for the total duration of T4c. The combustion emission-based equivalence ratio (EBER) was calculated as a function of time and is presented at the top of Figure 5-86. The EBER shows that the fire was lean throughout Test 4c with a 0.8 peak around the 3150th second. Main toxic species measured at this stage (T4c) are presented as well in Figure 5-96. Oxygen levels dropped to 8% around the 3150th second. Corresponding mass yields are presented in Figure 5-97.

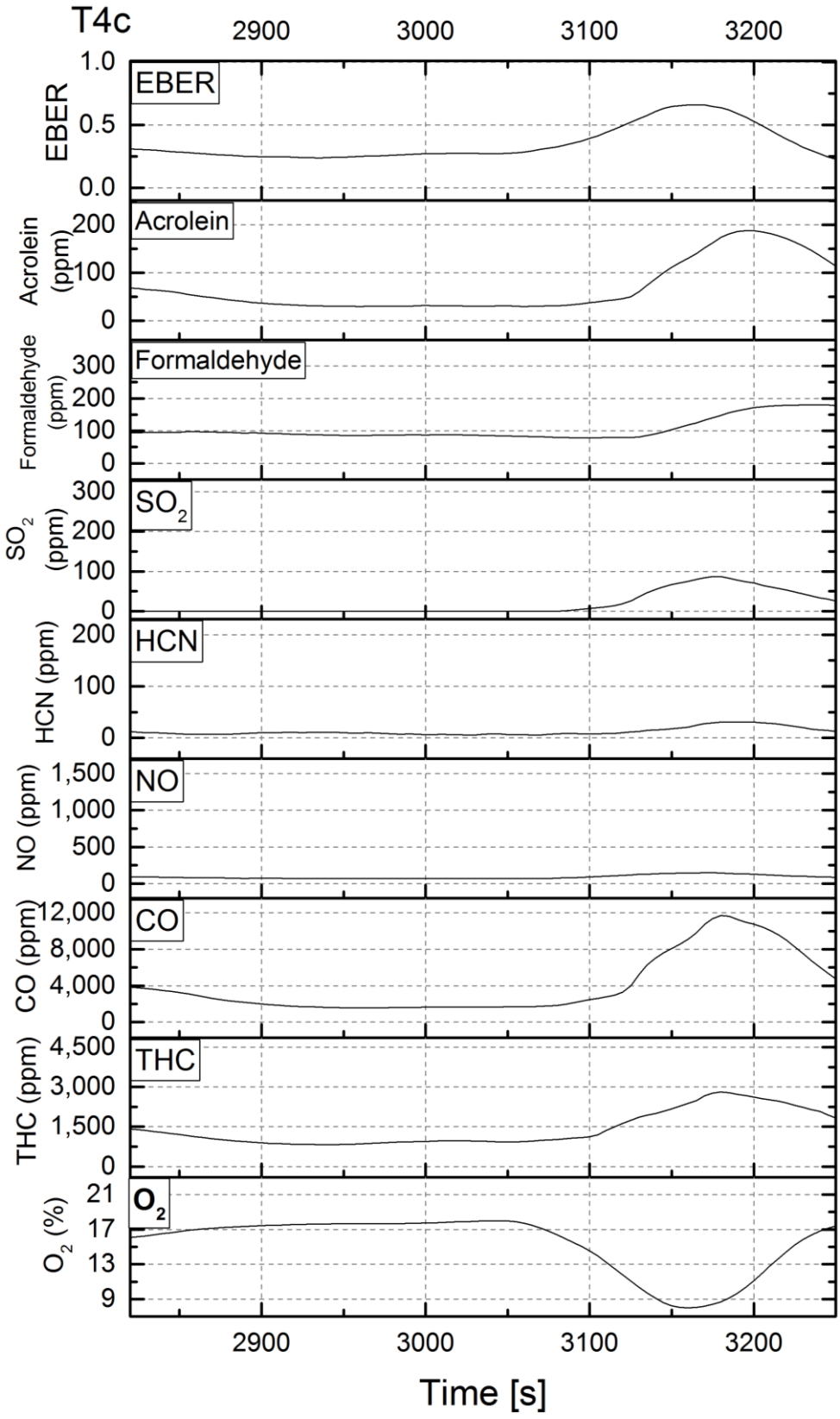

Figure 5-96: Combustion toxic products concentrations in volume basis in line with equivalence ratio and Oxygen concentration for Test 4a.

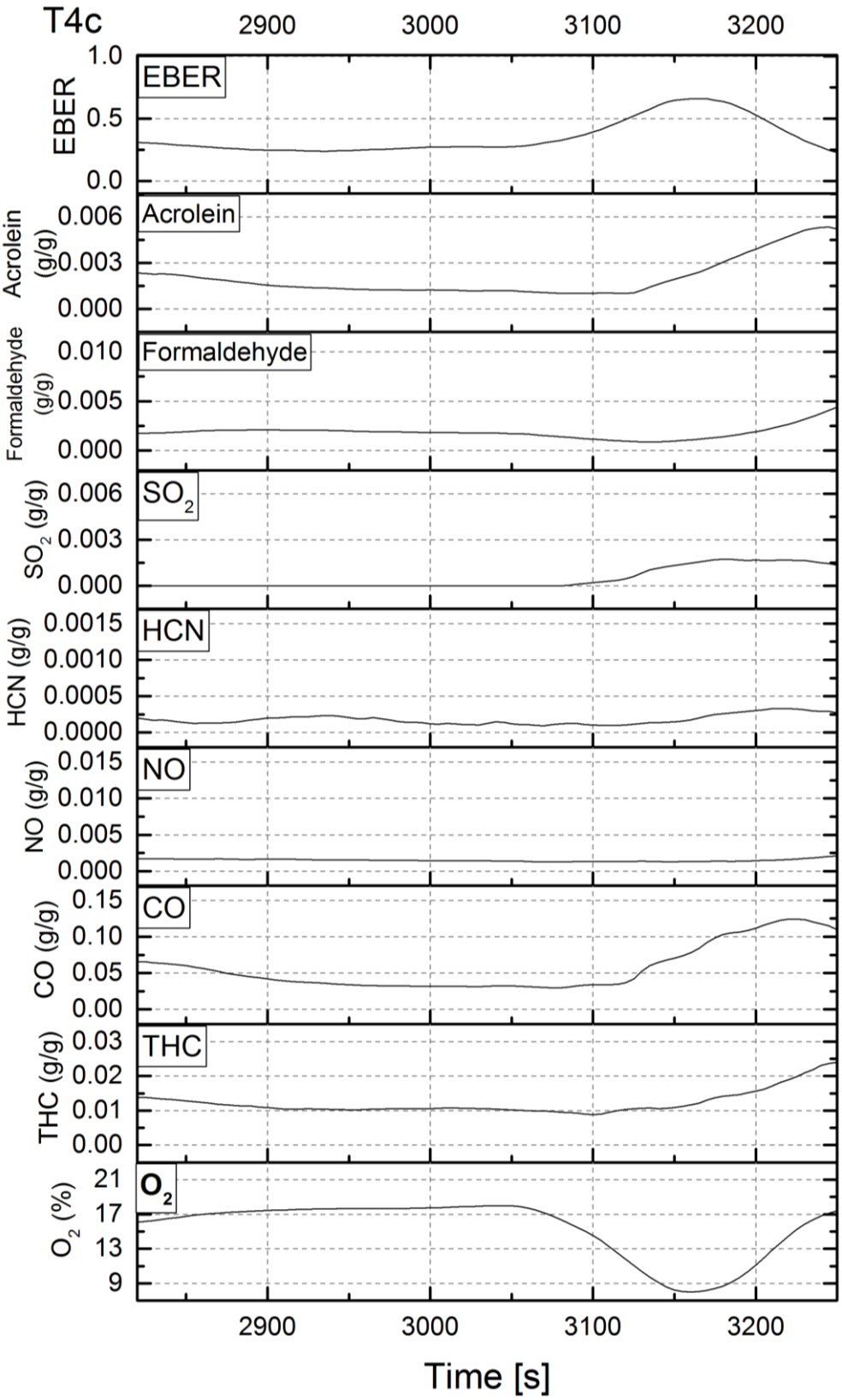

Figure 5-97: Combustion toxic products mass yields in line with equivalence ratio and Oxygen concentration for Test 4c.

The instantaneous fractional effective concentration FEC for different levels were calculated in accordance with the guidelines presented earlier in section 2.3 to demonstrate the health effects of the smoke produced at the point of sampling. Firstly, FEC safe that is important for designing purposes to ensure a safe environment in protected structures such as corridors and staircases. This value (total FEC safe) is the dilution factor required to achieve a safe environment as discussed earlier in section 2.3.

Figure 5-98 presents FEC for safe level by the combustion products concentrations from Test 4c in the stacked graph (Figure 5-96). Figure 5-99 shows the composition of the contributing toxic emissions by percentage, where acrolein is dominating while formaldehyde is contributing 10-20% to the total influence of the smoke based on the safe exposure thresholds.

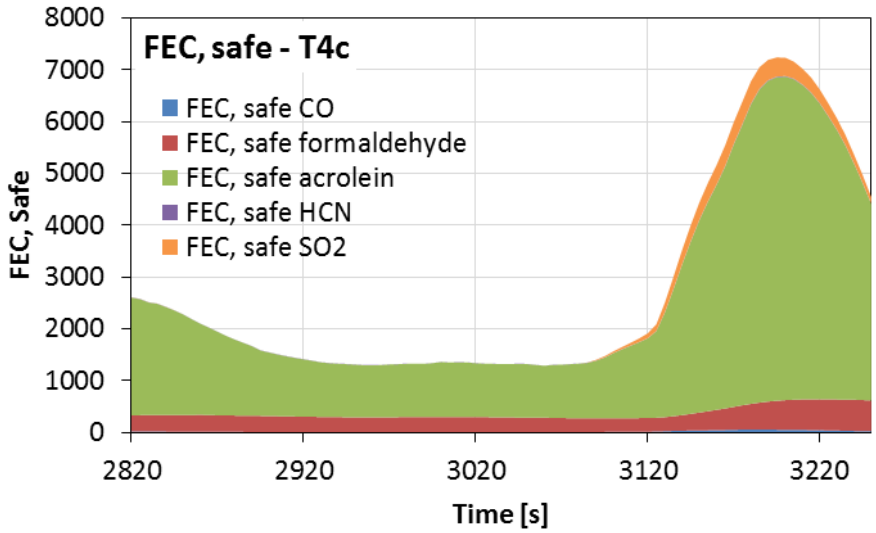

Figure 5-98: Instantaneous total fractional effective concentration (FEC) for safe level during Test 4c.

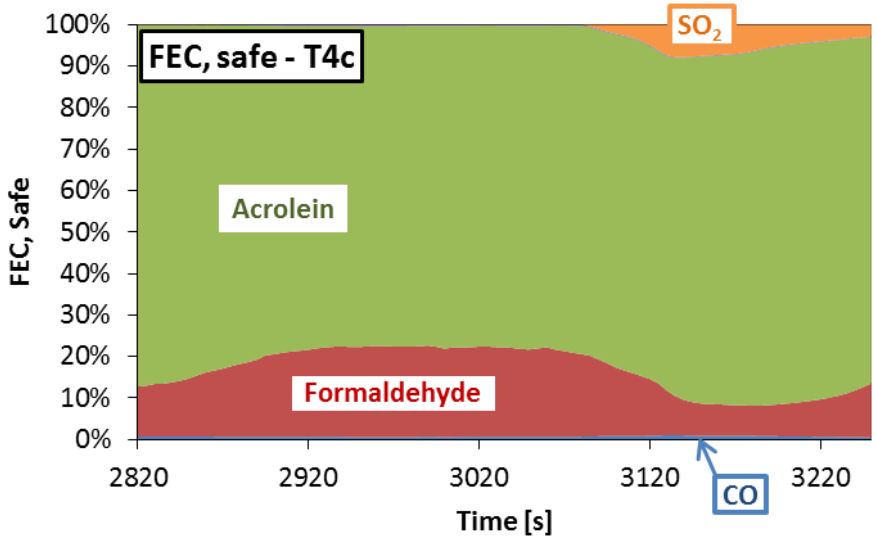

Figure 5-99: Major toxic emissions contribution by species to the fractional effective concentration for safe level in Test 4c.

Secondly, FEC for escape impairment (EI) that is important for post-accident investigations to understand the development of the evacuation plan and the point where victims were trapped. Figure 5-100 shows FEC for escape impairment from Test 4c in the stacked graph (Figure 5-96). While Figure 5-101 shows the composition of the contributing toxic emissions by percentage based on escape impairment exposure thresholds.

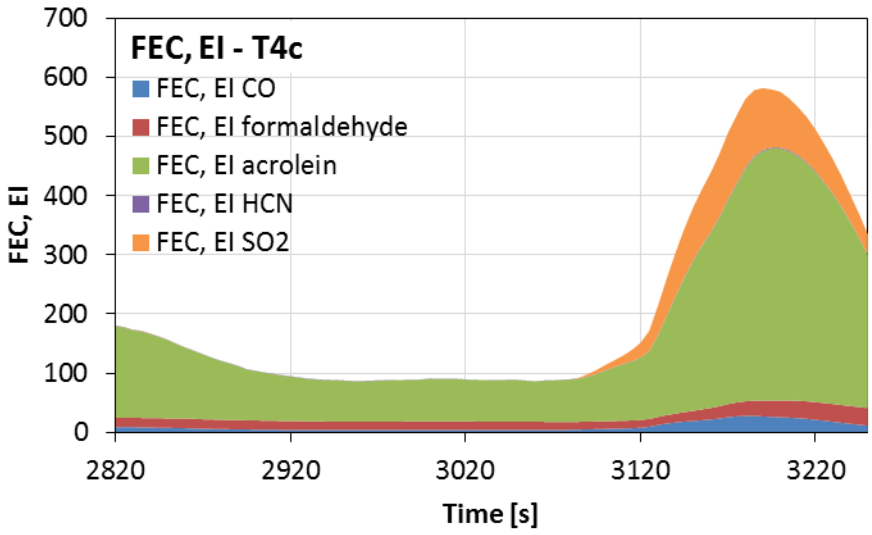

Figure 5-100: Instantaneous total fractional effective concentration (FEC) for escape impairment (EI) level during Test 4c.

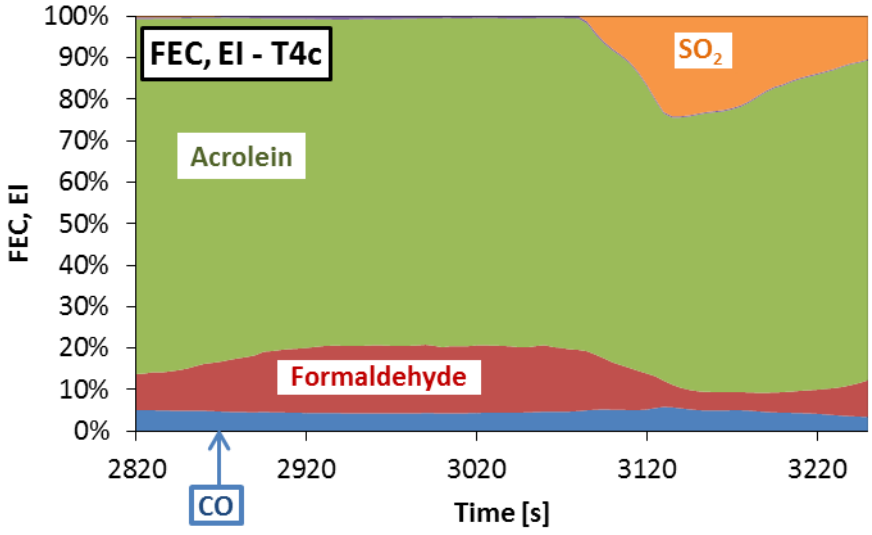

Figure 5-101: Major toxic emissions contribution by species to the fractional effective concentration for escape impairment (EI) level in Test 4c.

Thirdly, FEC for lethality that is useful for post-accident investigations. Figure 5-102 shows the instantaneous FEC for lethality from Test 4c in the stacked graph (Figure 5-96). The total value for lethal FEC reached 100. Figure 5-103 shows the composition of the contributing toxic emissions by percentage based on lethal exposure thresholds discussed in section 2.3.

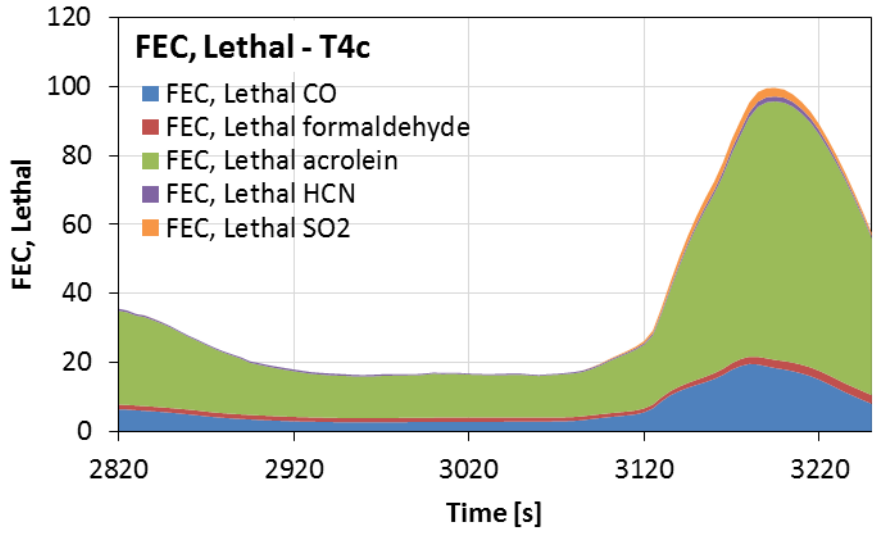

Figure 5-102: Instantaneous total fractional effective concentration (FEC) for lethal level during Test 4c.

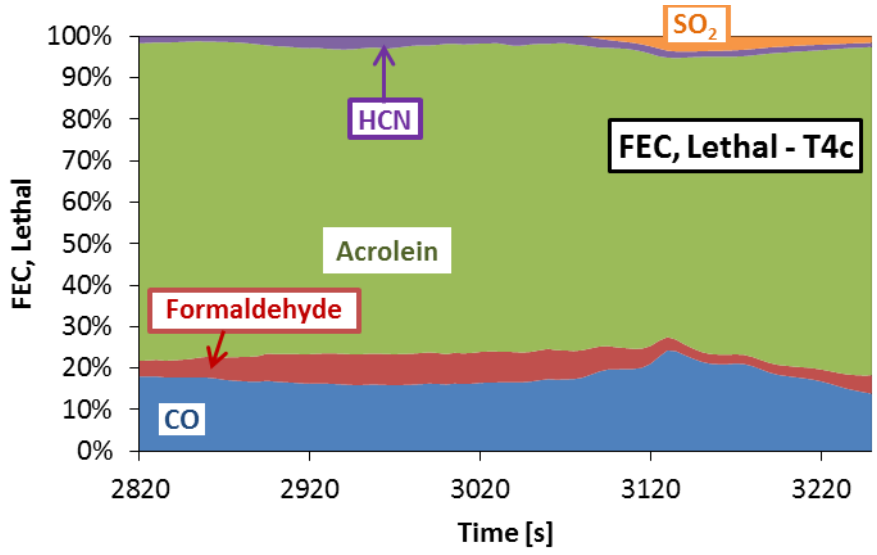

Figure 5-103: Major toxic emissions contribution by species to the fractional effective concentration for lethal level in Test 4c.

Finally, FEC for lethality based on the values purposed by ISO 13344 for LC50 the lethal concentration for half the population, as discussed earlier in section 2.3. Figure 5-104 shows the instantaneous FEC for lethality (based on LC50) from Test 4c in the stacked graph (Figure 5-96). The total value for lethal FEC reached 3.6. Figure 5-105 shows the composition of the contributing toxic emissions by percentage based on lethal exposure

thresholds of LC50. The comparison between FEC for lethality based on the most conservative threshold shown in Figure 5-102 and Figure 5-103 on one hand and FEC for lethality based on LC50 shown in Figure 5-104 and Figure 5-105 on the other, is important to demonstrate the difference between the two. As discussed earlier in section 2.3, the most conservative threshold database for lethality used was AEGL-3_{30min} is defined to be the minimum exposure to cause life-threatening health damage or death, while LC50 is defined to be the concentrations that cause death to half the population.

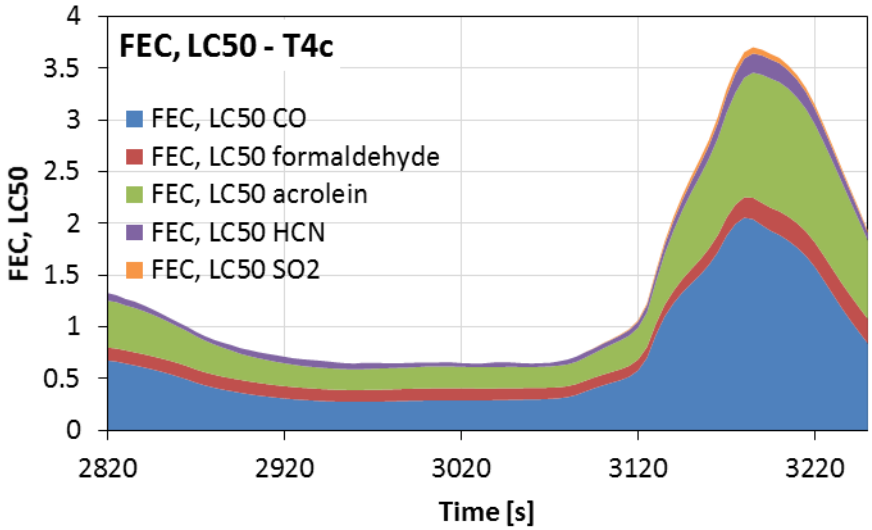

Figure 5-104: Instantaneous total fractional effective concentration (FEC) for lethal level (using LC50 values) during Test 4c.

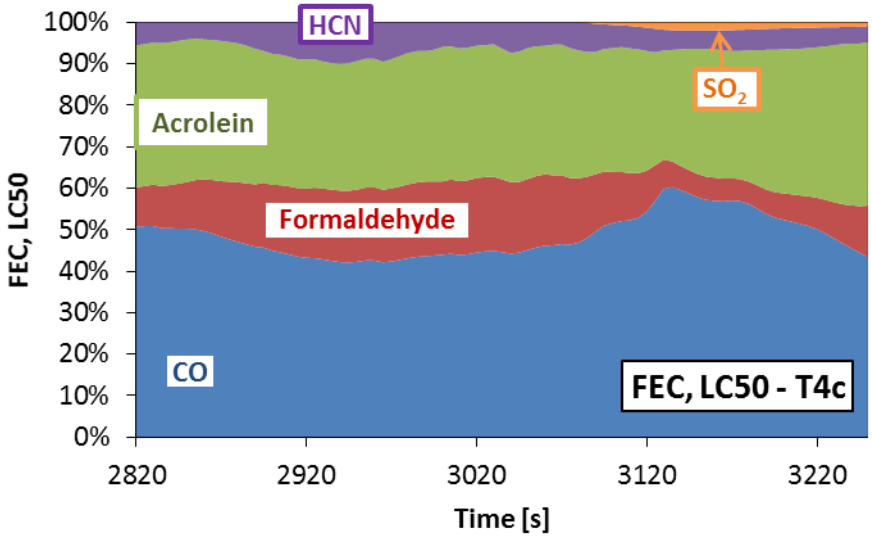

Figure 5-105: Major toxic emissions contribution by species to the fractional effective concentration for lethal level (using LC50 values) in Test 4c.

5.5 Settee

The test was intended to be a simulation of a single item from living rooms furniture which was a three-person-settee shown in Figure 3-23. The settee used for this test was complying with furniture regulations and was fully fire retarded. The test had two scenarios; firstly (T2a), a door closed scenario where shortly after ignition the only door to the room was closed in order to restrict ventilation. Secondly (T2b), with the door fully open which happened after T2a and the fuel needed to be ignited using an external ignition source.

The equivalent elemental analysis of the settee used was estimated in Table 3-8, to be 52.18% carbon, 5.6% hydrogen, 2.41% nitrogen and 39.81% oxygen. The room setup is shown in Figure 3-23, a full description of the room setup and fuel was discussed earlier (see section 3.2.5.2). The initial (for T2a) ignition source used was 250 ml of meths poured into the left-hand corner of the settee, as can be seen in the picture shown in Figure 5-107. While the same ignition method used for the second part of the test (T2b) applied at the other (right-hand) corner.

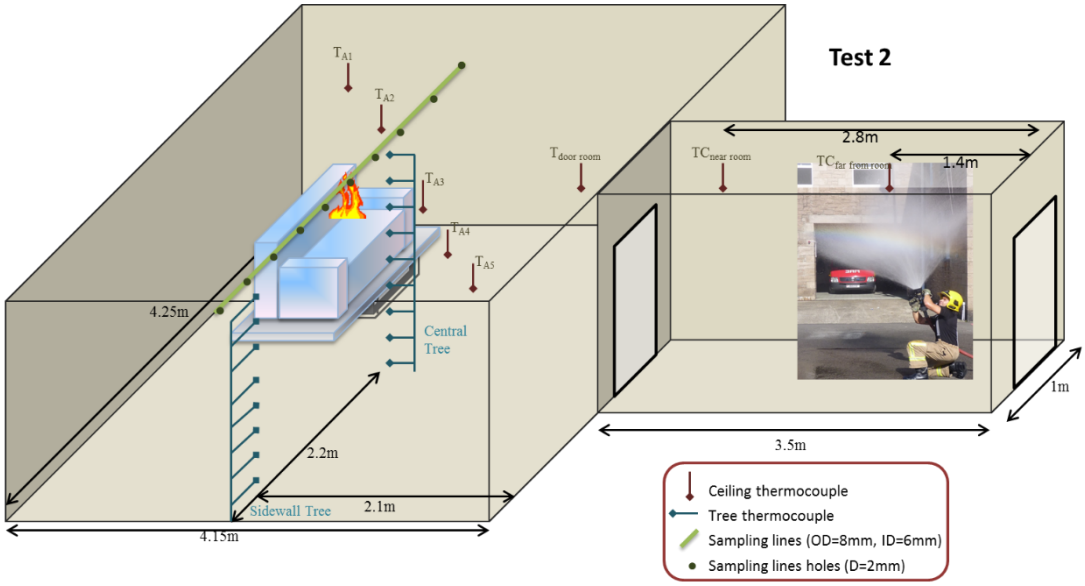

Figure 5-106: Test 2 full setup showing fire load, instrumentation and fire-fighting entrance.

Figure 5-107: Picture of the fire in Test 2, few seconds after ignition from inside the room before closing the door.

The fire load was ignited 100 seconds (1min 40sec) from the start of logging. The door was shut 80 seconds later (3min). Then after temperatures dropped in the compartment below 50 C the door was opened at the 3390th second (56min 30sec). Then the second part of the test (T2b) started by igniting the settee again at the 4825th second (80min 25sec), after about ten minutes the fire propagated to reach flaming fully involved fire. The fire-fighting activities started at the 5820th seconds (97min). The time line for Test 2 is graphically demonstrated in Figure 5-108 and measurements of mass of the fire load throughout the test is shown in Figure 5-109.

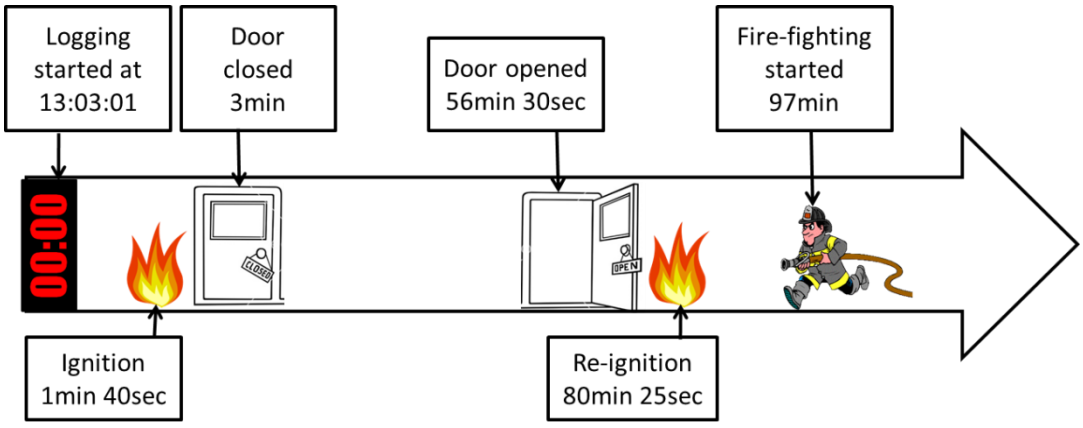

Figure 5-108: Timeline of the main events for Test 2.

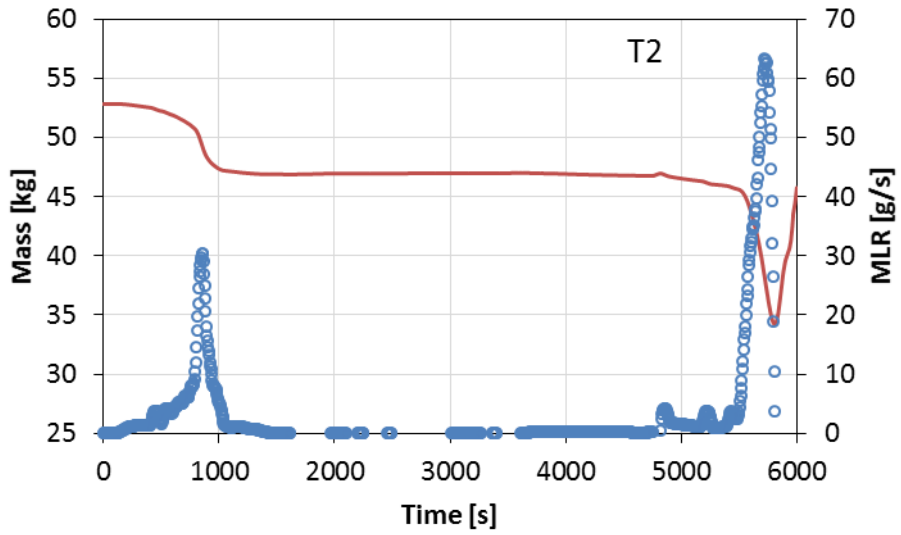

Figure 5-109: Total mass of the fire load (Red) and mass loss rate (Blue) for Test 2.

5.5.1 Results and analysis for the first part of Test 2 (T2a)

During this part of the test the fire started initially with a well ventilated flaming fire (ISO stage 2) until oxygen available was used (reaching peak temperatures and heat release rate). Deprived oxygen levels at this point were unable to sustain the fire at the same burning rate so it transformed to be under-ventilated pre-flashover flaming fire (ISO stage 3a). With more oxygen being used, oxygen reached the level to be unable to sustain a flaming fire to transform to a slower non-flaming smouldering fire (ISO stage 1a) until the fire was completely self-extinguished. In the following sections thermal and toxic environments results and analysis for this phase (T2a) are discussed.

5.5.1.1 Mass loss and heat release rate (HRR) – Test 2a

Heat release rate can be quantified by the use of mass loss data and calorific values of the materials. And can be corrected for inefficiencies using the mass yields data of incomplete combustion products. A calorific value of 18 MJ/kg were used for the settee to produce Figure 5-110. The correction of the HRR data is based on inefficiency as derived from unburnt hydrocarbons and carbon monoxide measurements shown in Table 5-6. Initially, the burning rate was propagating rapidly (due to the existence of the fire load and oxidizing agent). Then, the level of oxygen dropped (due to the lack of ventilation) and the fire slowed down. Till eventually it was unable to sustain any flaming fires, to transform to a smouldering fire with a very slow burning rate.

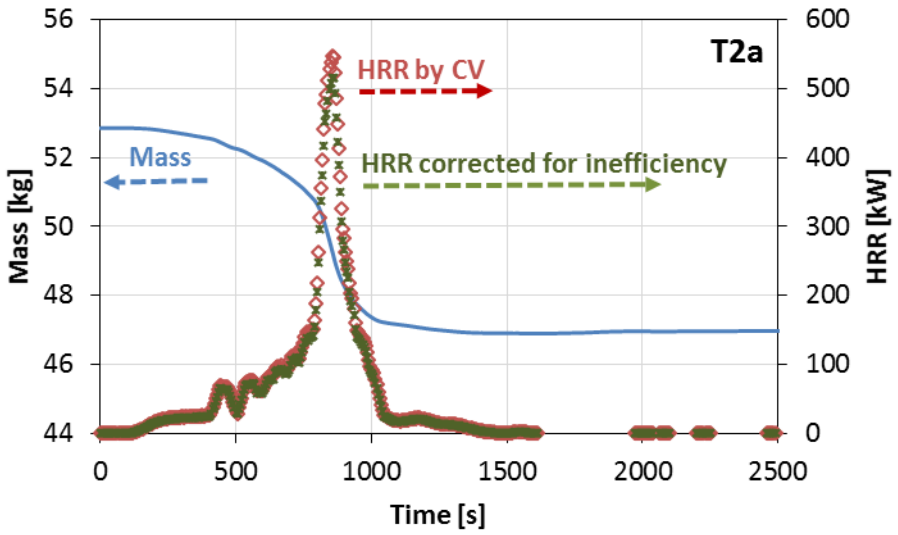

Figure 5-110: Mass change with time and associated HRR based on the mass loss rate for Test 2a. Also shown is an adjusted HRR, based on inefficiency of combustion as derived from the unburnt hydrocarbons and CO measurements.

5.5.1.2 Thermal environment – Test 2a

Temperature inside the room followed similar patterns to the HRR discussed above. Figure 5-111 shows temperature measured at the ceiling level, where temperatures at the highest point dropped to lower than 100 C just after the 1200 seconds mark. Before opening the door to end the first part of Test 2, the vertical temperature gradient throughout the room showed very little variation (less than 25 C), demonstrated in Figure 5-112.

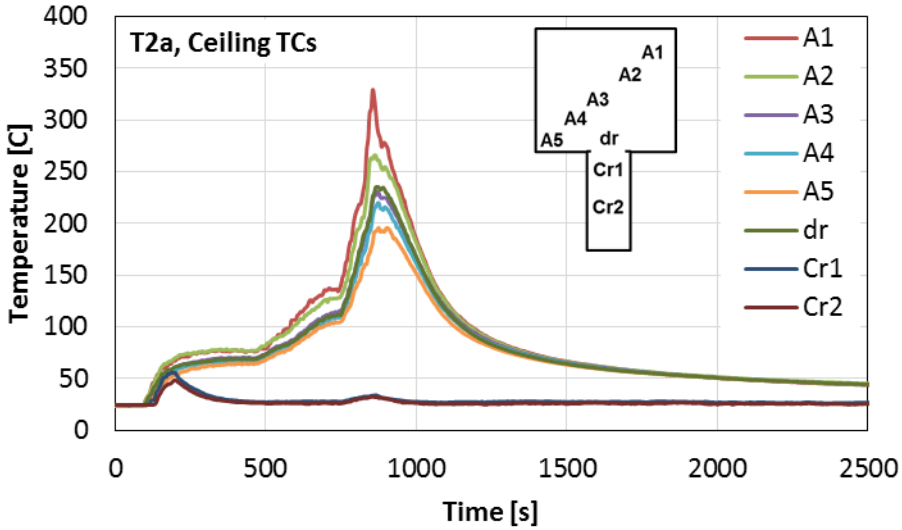

Figure 5-111: Ceiling layer temperature measurements at different positions inside the compartment and corridor during Test 2a.

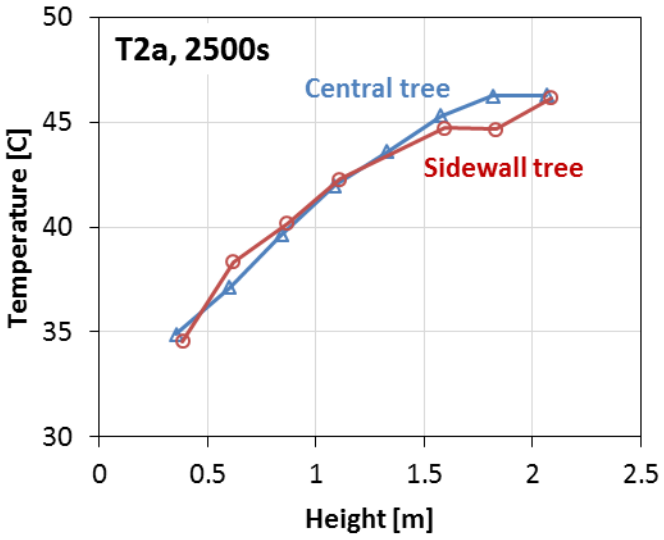

Figure 5-112: Vertical temperature variation at the 2500th second from central and sidewall thermocouple trees.

5.5.1.3 Toxic environment – Test 2a

Gas analyses for products from the first part of the test (T2a), while the door was closed, cannot be treated as a dynamic process due to the lack of exhaust and fresh air supply, which is important for sustaining a flaming combustion. So the gas concentration measurements given by the instruments in that period were for a static situation of the fire where the smoke is accumulating in the room space. So for the purpose of establishing yield data, concentration measurements were taken at the point when the fire died down and before opening the door.

Table 5-6: Concentrations of major combustion emissions produced in Test 2a at the 2500th second, with their ratios to relevant toxic exposure thresholds. and average mass yield data for each species.

Species	Conc. [ppm]	R-Safe	R-Escape impairment	R-Lethal	R-LC50	Yield [g/g]
CO	4,606	23	11	7.7	0.8	0.0402
Acrolein	241	8,058	549	97	1.6	0.0042
Formaldehyde	75	250	13	1.1	0.1	0.0007
THC	2,832					0.0141

At that point (2500th second), the deviation for the vertical temperature gradient was minimal between top and bottom thermocouples (less than 25 ^{0}C), hence it was assumed that the collected sample was representative of the whole 41 m^{3} compartment. And by quantifying the total mass of fuel burnt during that period (5.9 kg), then mass yields of each toxic gas can be quantified, as presented in Table 5-6. The fractional effective concentration of the sampled gas in respect to the different levels of effects discussed earlier in section 2.3 were established the contribution of each species is demonstrated in Figure 5-113.

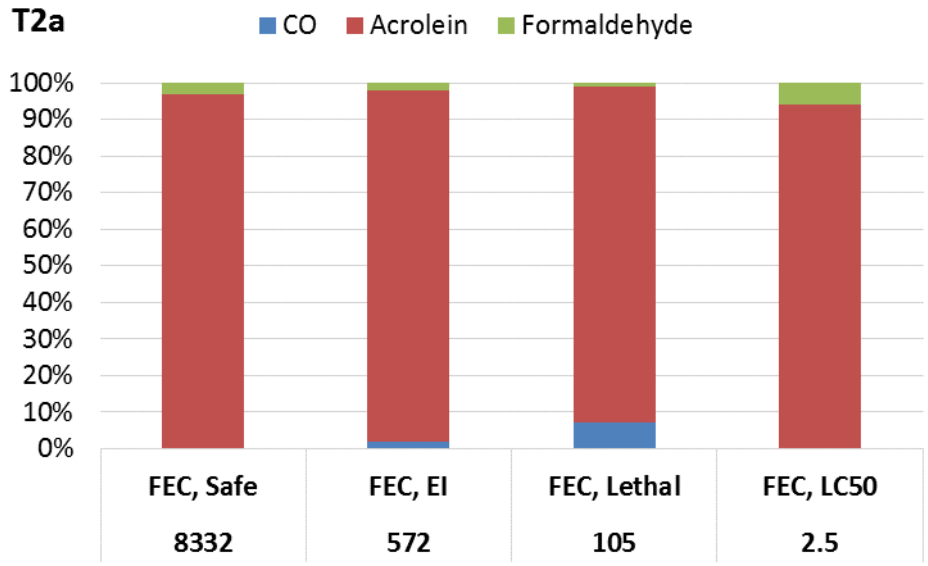

Figure 5-113: The main toxic products released in Test 2a in respect to their contribution to the overall Fractional Effective Concentration (FEC).

5.5.2 Results and analysis for the second part of Test 2 (T2b)

As discussed earlier Test 2b started by reigniting the settee, after opening the door allowing unlimited supply of air to the fire. The fire took ten minutes to propagate to propagate into a well ventilated flaming fire. The fire was left for about 8 minutes before the start of the fire-fighting activities (5820th second on the global timeline). The following sections present the results for that part of the test (T2b) by discussing the thermal and toxic environment produced within the compartment.

5.5.2.1 Mass loss and heat release rate (HRR) – Test 2b

Using the calorific value approach combined with the mass loss data, online heat release rate (HRR) is established. Additionally, using the incomplete combustion products measurements carbon monoxide and total unburnt hydrocarbons. During Test 2b, about 12 kg of the fire load was consumed giving a peak corrected HRR of 1MW, demonstrated in Figure 5-114. In terms of inefficiency, Figure 5-115 shows the combustion peaked at about 17% at the same point that peak HRR was reached.

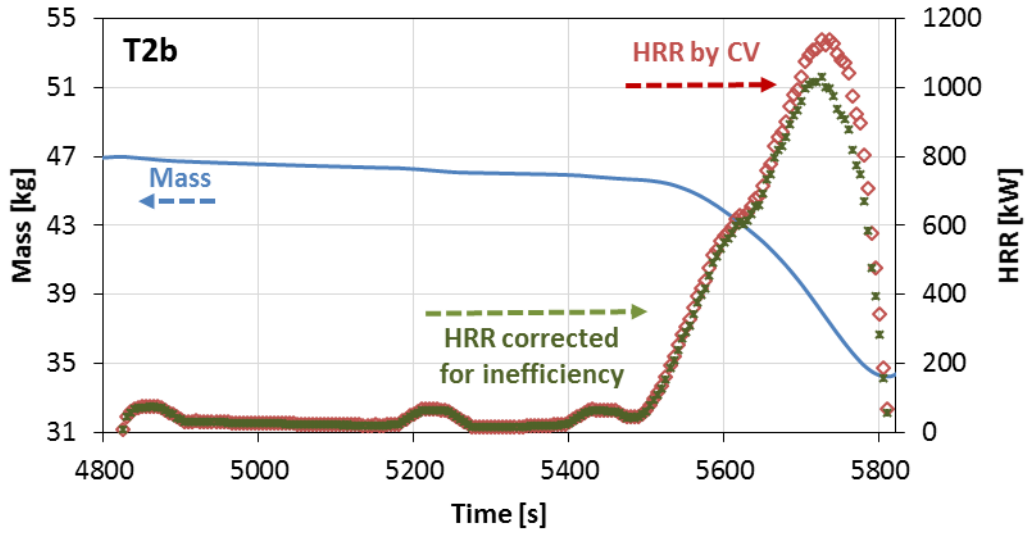

Figure 5-114: Mass change with time and associated HRR based on the mass loss rate for Test 2b. Also shown is an adjusted HRR, based on inefficiency of combustion as derived from the unburnt hydrocarbons and CO measurements.

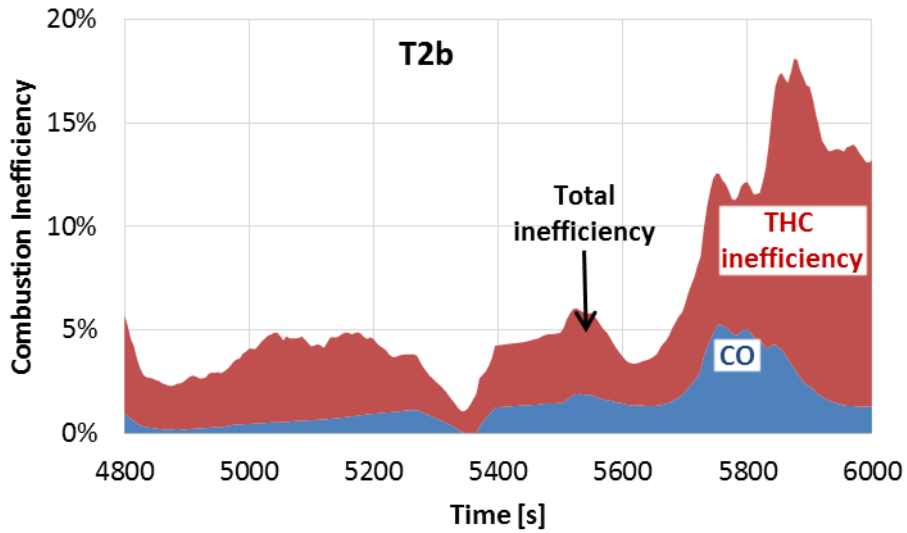

Figure 5-115: Total combustion inefficiency as a function of time with contributions from CO and THC for Test 2b.

5.5.2.2 Thermal environment – Test 2b

Temperatures inside the room followed a similar pattern as the HRR shown in Figure 5-114 where upper layer temperature peaked at 4350th second and started stabilising afterwards, as can be seen in Figure 5-116.

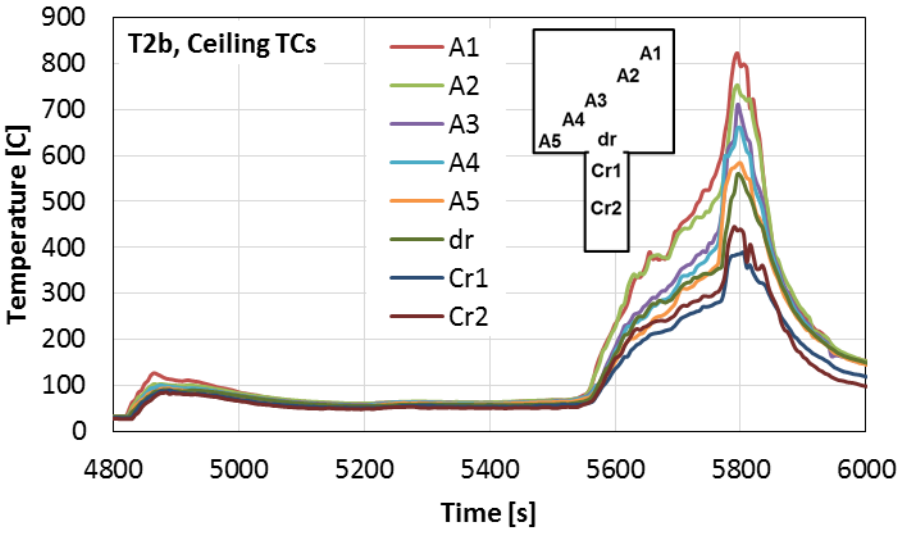

Figure 5-116: Temperature profile at ceiling level across the room and corridor for Test 2b.

5.5.2.3 Toxic environment – Test 2b

The combustion emission-based equivalence ratio (EBER) was calculated as a function of time and is presented at the top of Figure 5-119. The EBER shows that the fire lean and reached unity at the initiation point of fire-fighting activities. Measurements of the concentrations of the combustion products are presented in Figure 5-119.

In general the fire was fuel controlled, air supplied to the compartment was in excess creating a lean combustion as shown by the equivalence ratio values. However, the fire development was obstructed by fire-fighting, if the fire-fighting activities were delayed for another five minutes it is highly likely that a flashover might have been achieved. Carbon monoxide and THC showed similar behaviour with a rapid increase after 40 seconds reaching steady high levels during the steady state period of the fire. Acrolein and formaldehyde showed a reduction of concentrations during the steady state phase. This occurred at the same time as the oxygen was reduced to its minimum value and flashover occurred. Aldehydes form at low temperatures in the presence of hydrocarbons and oxygen. Oxygen levels measured in the sampled smoke show that a major drop of oxygen level to 3% was observed between (5500^{th} – 5850^{th} seconds) this is the same time when peak HRR and temperatures inside the compartment, shown in Figure 5-114 and Figure 5-116.

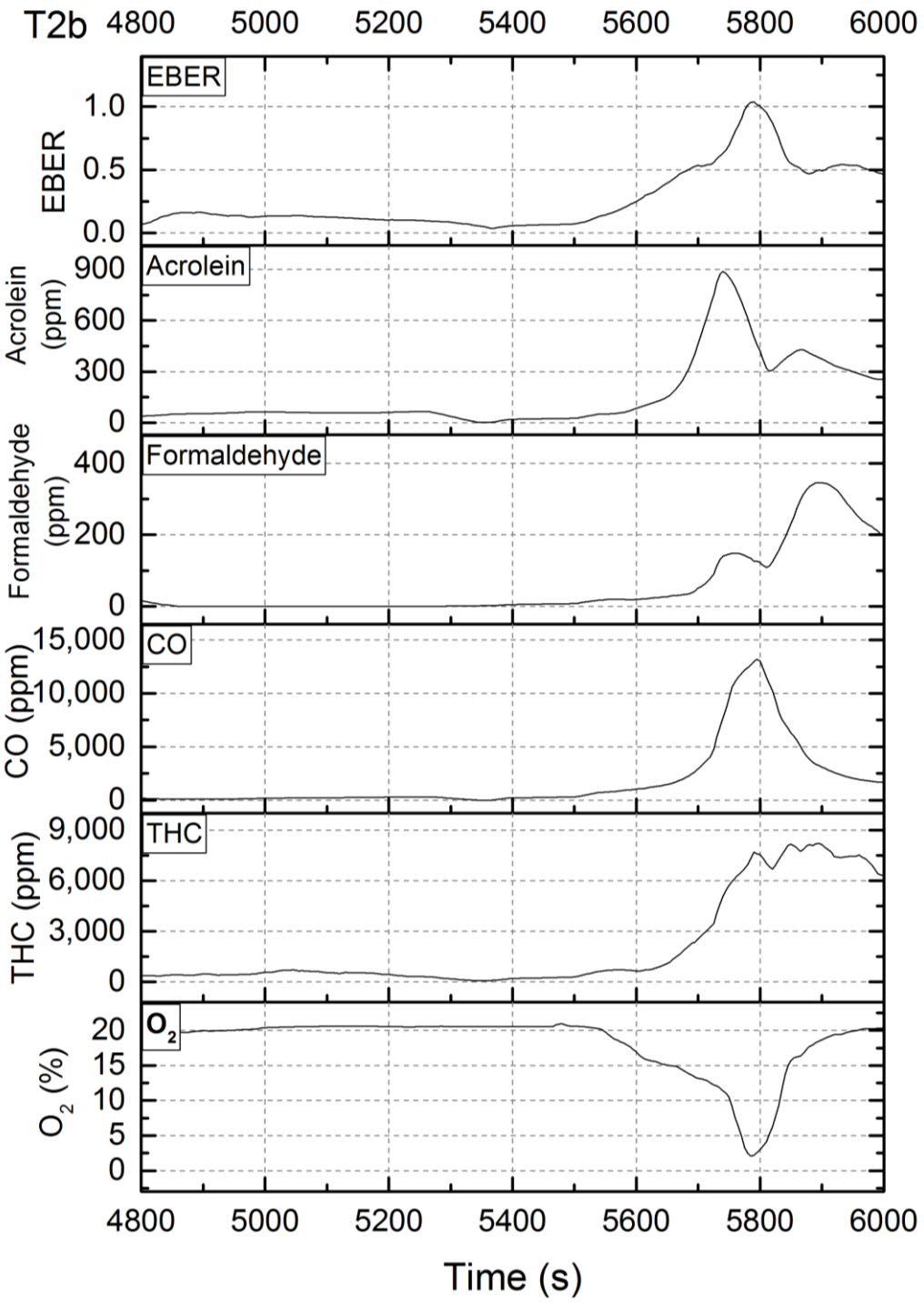

Figure 5-117: Combustion toxic products concentrations in volume basis in line with equivalence ratio and Oxygen concentration for Test 2b.

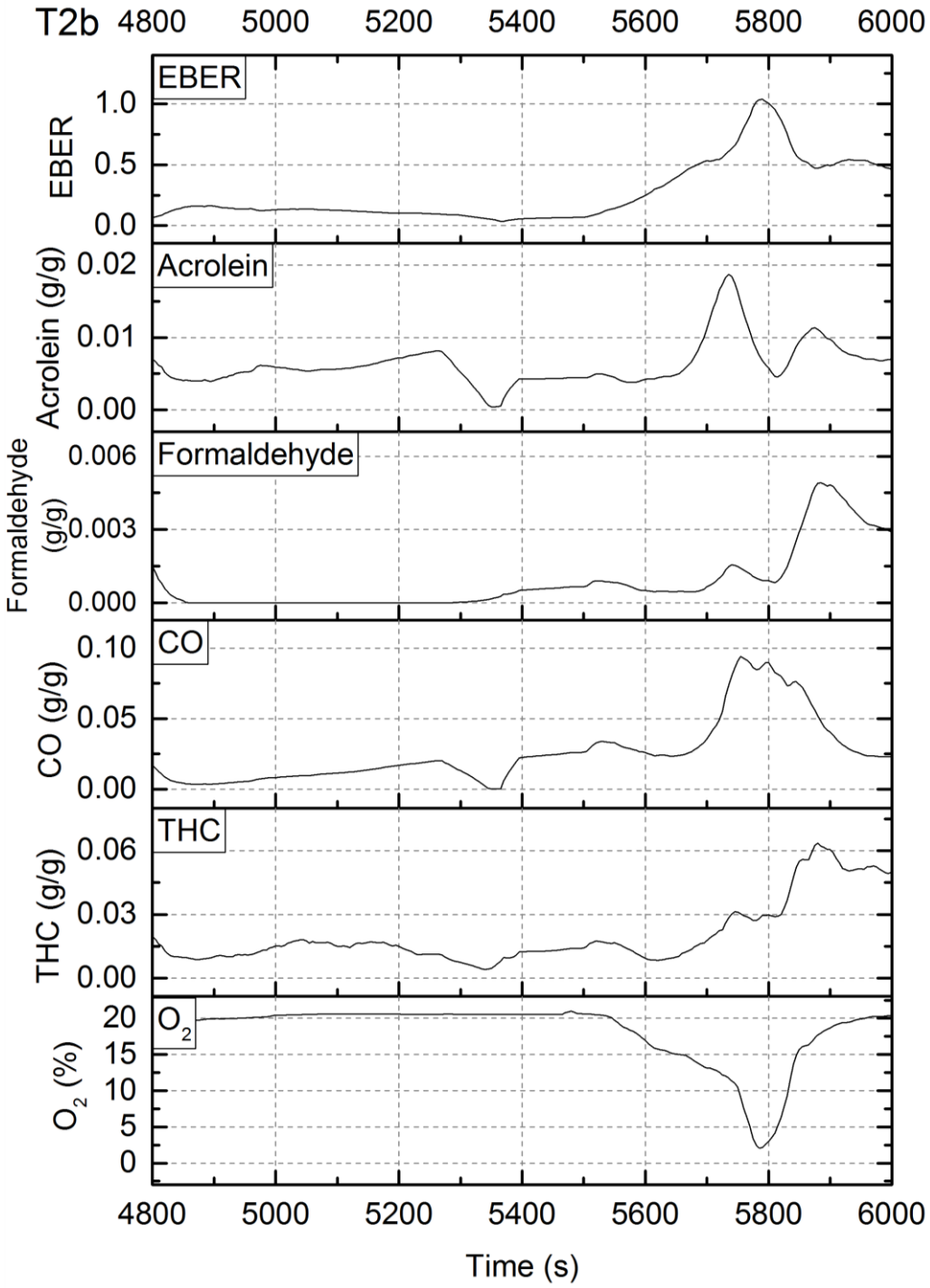

Figure 5-118: Combustion toxic products mass yields in line with equivalence ratio and Oxygen concentration for Test 2b.

The instantaneous fractional effective concentration FEC for different levels were calculated in accordance with the guidelines presented earlier in section 2.3 to demonstrate the health effects of the smoke produced at the point of sampling. Firstly, FEC safe that is important for designing purposes to ensure a safe environment in protected structures such as corridors and staircases. This value (total FEC safe) is the dilution factor required to achieve a safe environment as discussed earlier in section 2.3.

Figure 5-119 presents FEC for safe level by the combustion products from Test 2b in the stacked graph (Figure 5-117). Figure 5-120 shows the composition of the contributing toxic emissions by percentage, where acrolein is the dominating contributor of the smoke influence based on the safe exposure thresholds.

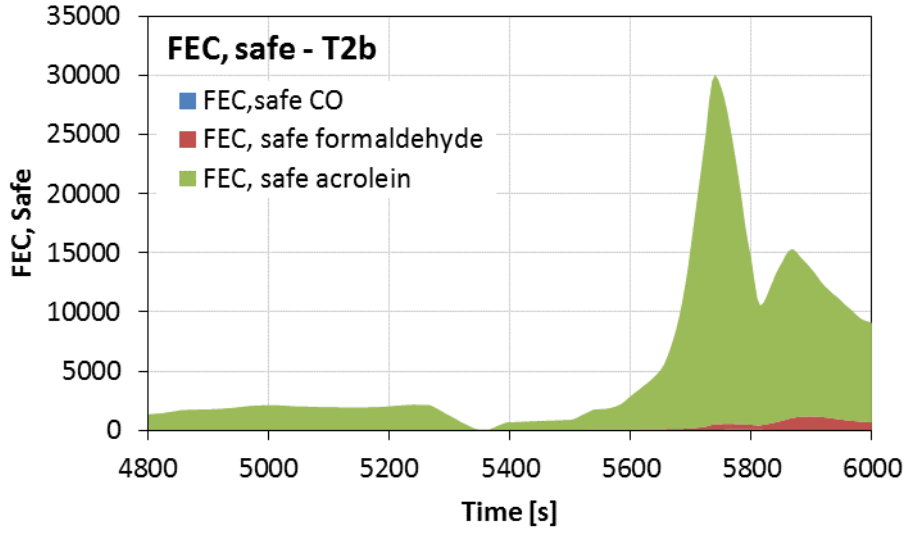

Figure 5-119: Instantaneous total fractional effective concentration (FEC) for safe level during Test 2b.

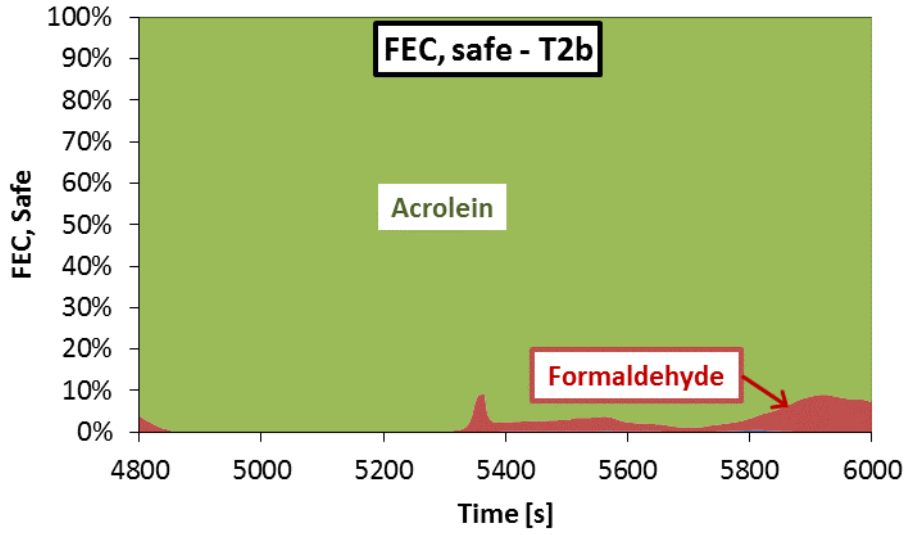

Figure 5-120: Major toxic emissions contribution by species to the fractional effective concentration for safe level in Test 2b.

Secondly, FEC for escape impairment (EI) that is important for post-accident investigations to understand the development of the evacuation plan and the point where victims were trapped. Figure 5-121 shows FEC for escape impairment from Test 1b in the stacked graph (Figure 5-117). While Figure 5-122 shows the composition of the contributing toxic emissions by percentage based on escape impairment exposure thresholds.

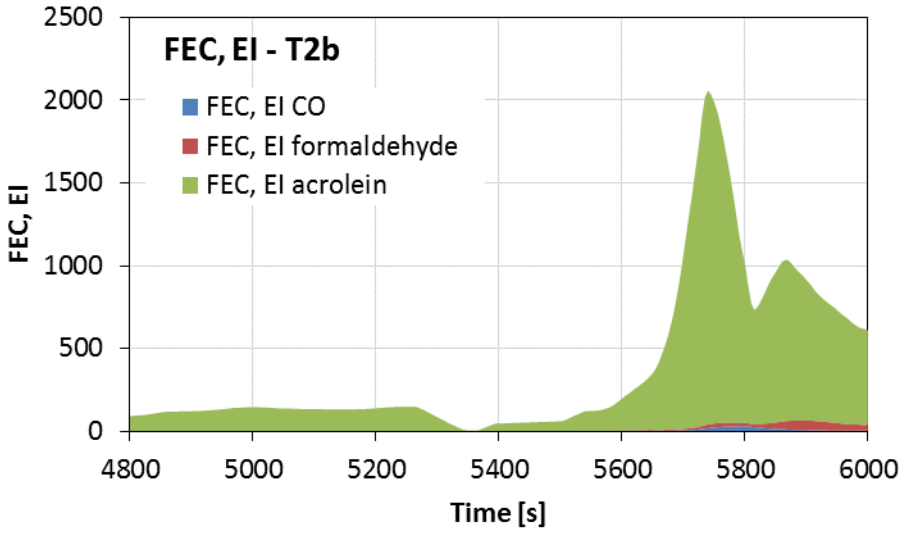

Figure 5-121: Instantaneous total fractional effective concentration (FEC) for escape impairment (EI) level during Test 2b.

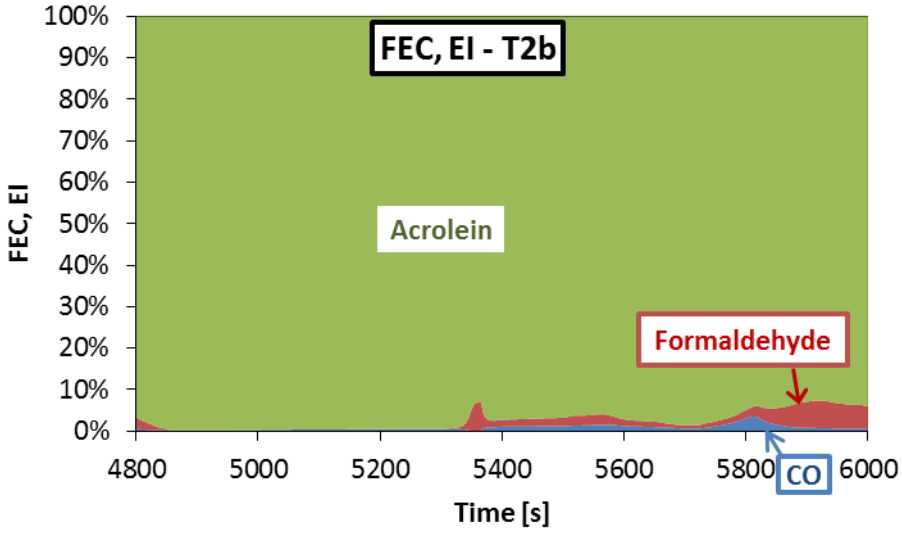

Figure 5-122: Major toxic emissions contribution by species to the fractional effective concentration for escape impairment (EI) level in Test 2b.

Thirdly, FEC for lethality that is useful for post-accident investigations. Figure 5-123 shows the instantaneous FEC for lethality from Test 2b in the stacked graph (Figure 5-117). The total value for lethal FEC peaked at around 350 in (at 5800th second). Figure 5-124 shows the composition of the contributing toxic emissions by percentage based on lethal exposure thresholds discussed in section 2.3.

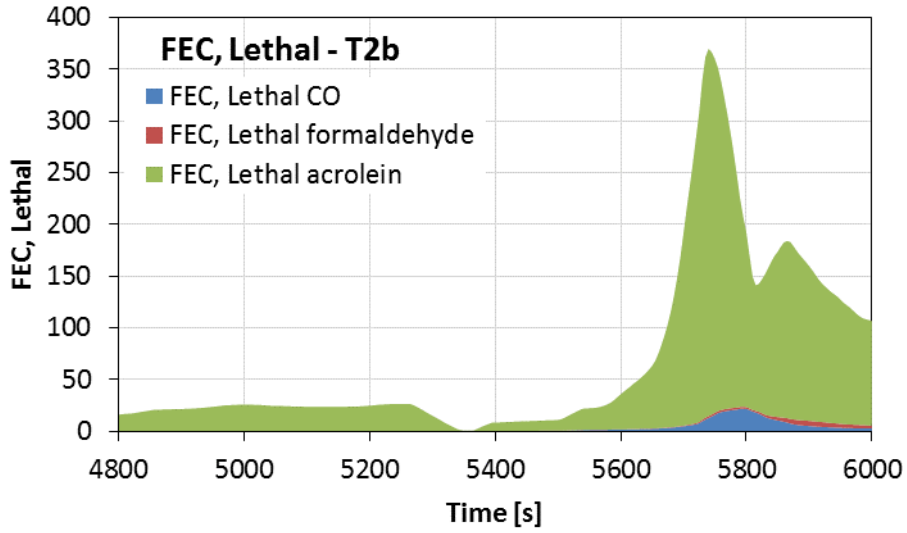

Figure 5-123: Instantaneous total fractional effective concentration (FEC) for lethal level during Test 2b.

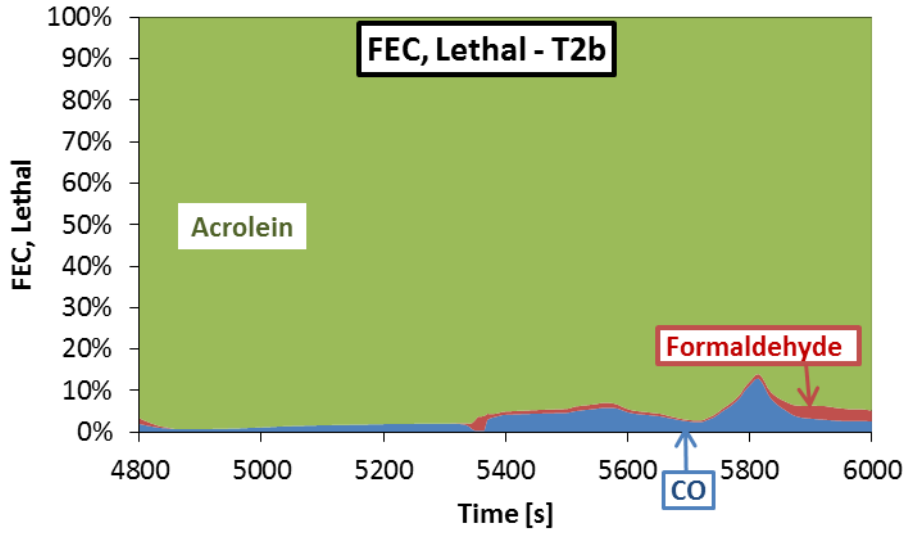

Figure 5-124: Major toxic emissions contribution by species to the fractional effective concentration for lethal level in Test 2b.

Finally, FEC for lethality based on the values purposed by ISO 13344 for LC50 the lethal concentration for half the population, as discussed earlier in section 2.3. Figure 5-125 shows the instantaneous FEC for lethality (based on LC50) from Test 1b in the stacked graph (Figure 5-117). The total value for lethal FEC peaked above 7 in (at 5800th second). Figure 5-126 shows the composition of the contributing toxic emissions by percentage based on lethal exposure thresholds of LC50. The comparison between FEC for lethality based on the most conservative threshold shown in Figure 5-123 and Figure 5-124 on one hand and FEC for lethality based on LC50 shown in Figure 5-125 and Figure 5-126 on the other, is important to demonstrate the difference between the two. As discussed earlier in section 2.3,

the most conservative threshold database for lethality used was AEGL-3_{30min} is defined to be the minimum exposure to cause life-threatening health damage or death, while LC50 is defined to be the concentrations that cause death to half the population.

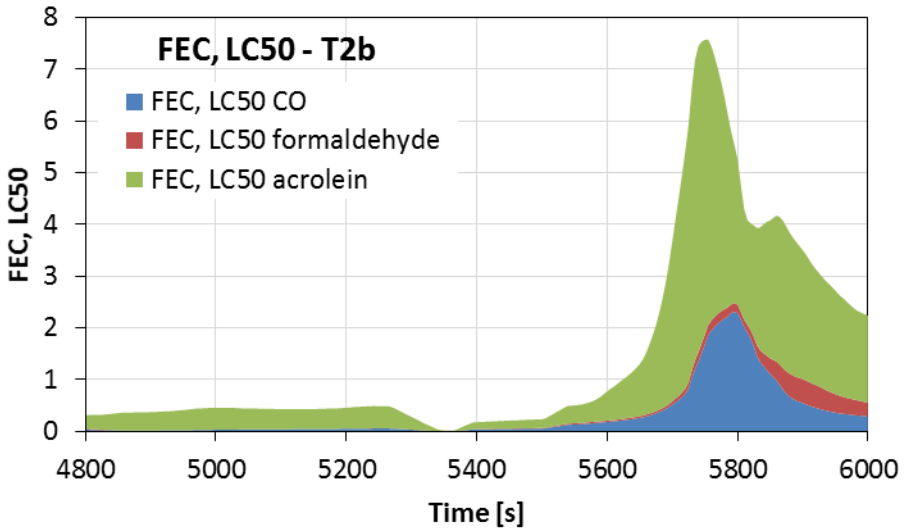

Figure 5-125: Instantaneous total fractional effective concentration (FEC) for lethal level (using LC50 values) during Test 2b.

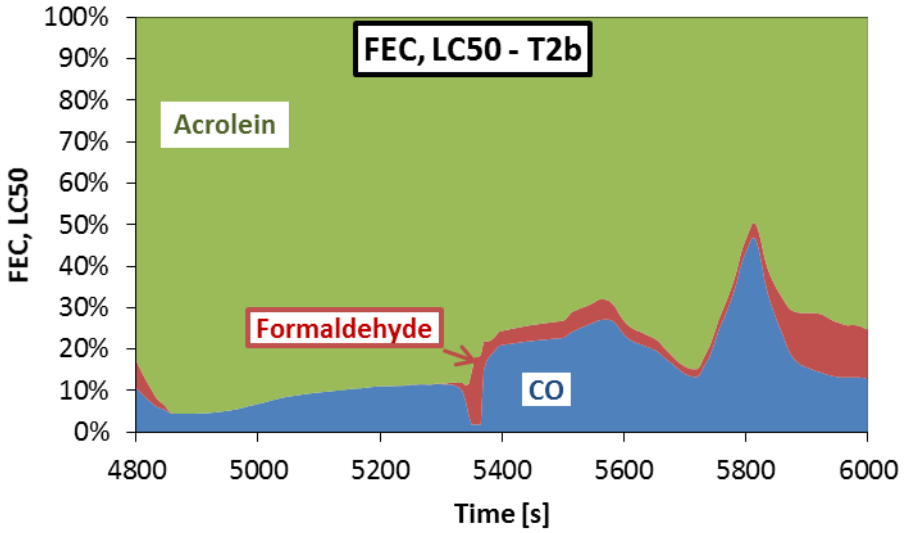

Figure 5-126: Major toxic emissions contribution by species to the fractional effective concentration for lethal level (using LC50 values) in Test 2b.

5.6 Living room furniture

The test was designed to simulate a home living-room fire and measure the effectiveness of fire-fighting tactics on a fully developed post-flashover fire, in terms of temperature and toxic emissions within the compartment. The effect of almost complete air restriction was also simulated at the start of the test before allowing the fire to develop. The fuel load was typical living-room furniture and was distributed around the room as shown in Figure 5-127.

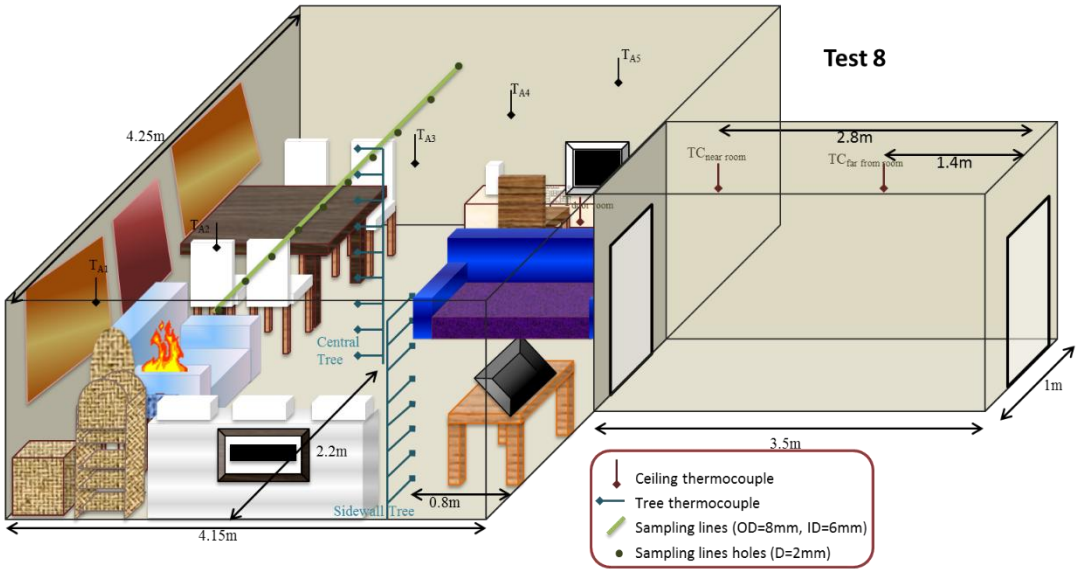

Figure 5-127: Test 8 full setup showing fire load distribution, instrumentation and ignition location.

Figure 5-128: Picture of the initial ignition in Test 8, few seconds after ignition from inside the room before closing the door.

Figure 5-129 and Figure 5-130 illustrate the main events in the development of the fire in relation to the profiles of average temperatures of hot and cold layers in addition to the room

average temperature. Time 0 indicates the start of the data logging. The white single seat sofa was ignited 75 seconds on, using 500ml of white spirit poured on the right arm of the sofa. The door was kept open till the 330th second, when it was shut. The fire developed to its peak temperature at around 840th second. Then it started decaying due to the limited amount of oxygen available (reached a minimum value of 11% O_2). At this stage, if the door had been left shut for longer the fire would have extinguished itself.

This happened in other tests that are not presented here and based on this experience, as soon as the hot layer temperature dropped to 100 °C, the door was opened on the 1105th second. After opening the door the temperature of the room kept descending till it reached 50 °C, then by 1550s the fire re-established itself and the temperature started rising exponentially. With the help of the continuous supply of fresh air through the open door, the fire developed to reach flashover at 1700s. Fire-fighting started after about 5 minutes from flashover. These events during the fire development are marked on Figure 5-130, Figure 5-134, and Figure 5-135.

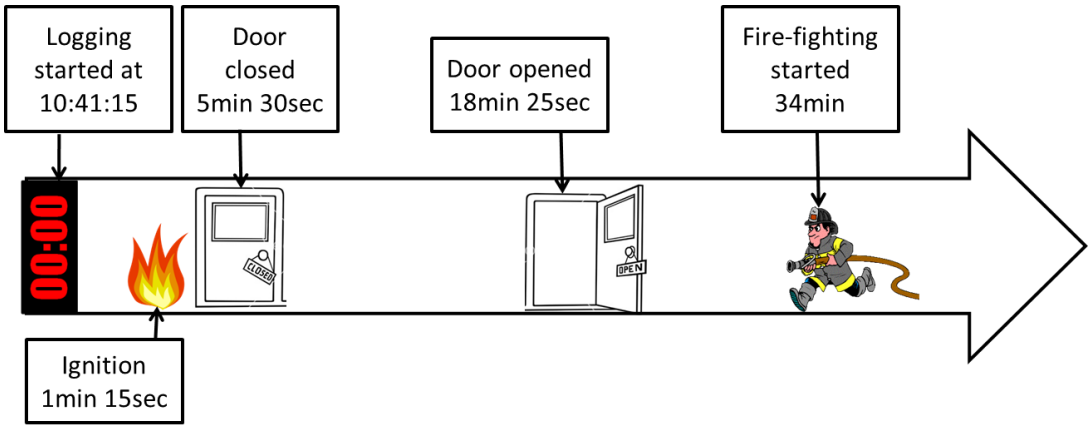

Figure 5-129: Timeline of the main events for Test 8.

5.6.1 Thermal environment – Test 8

Ventilation to the compartment was controlled by the single door, illustrated in Figure 5-127. As described earlier and illustrated in Figure 5-130, by controlling ventilation to the compartment, it was evident that the fire would have extinguish itself if the door was kept closed at the first stage. Figure 5-130 also illustrates the flashover point which was monitored by the flashover targets (pieces of paper on floor level underneath the lowest thermocouple of the central vertical tree). Figure 5-130 also illustrates carpet contribution average temperature of the cold layer in comparison to other tests without any combustible flooring materials.

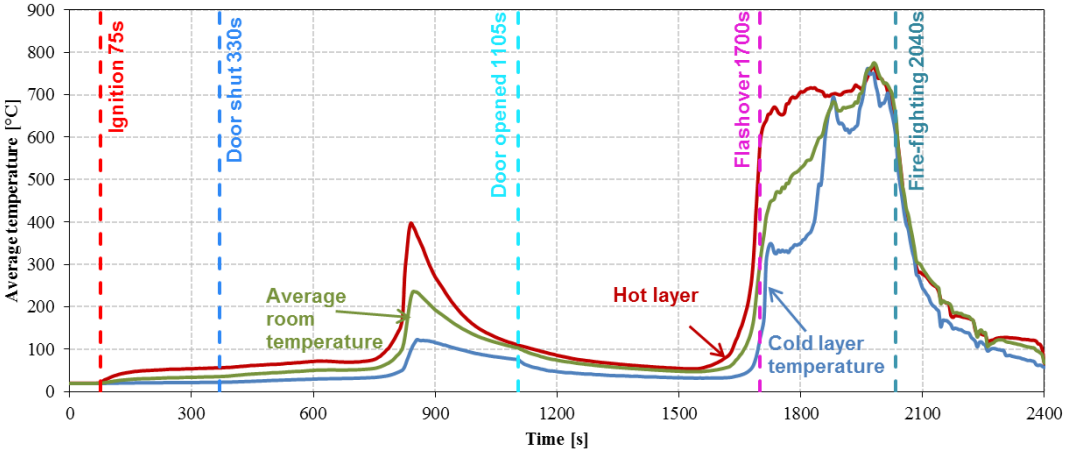

Figure 5-130: Compartment temperatures and fire events for Test 8. (Average hot layer temperate: is based on top two thermocouples from each of the two vertical tree in addition to six thermocouples fixed on the ceiling inside the room (approximately from 1.8m to 2.2m height),

Figure 5-131 and Figure 5-132 show the vertical temperature profile at the two vertical trees; central and near-sidewall. The curves represent fixed time step of 50 seconds, from the start of the self-reignition till just before the setoff of the fire-fighting activities. Near-sidewall vertical temperature profiles are more representative of defining smoke layer depth than the central vertical temperature profiles, as a consequence of not being exposed to the air entrainment dynamics created by the air supply through the corridor which was the case with the latter. Figure 5-132 shows that smoke layer was formulating above 1.6 m from the floor level just before flashover, and then dropped to 0.6 m level after flashover.

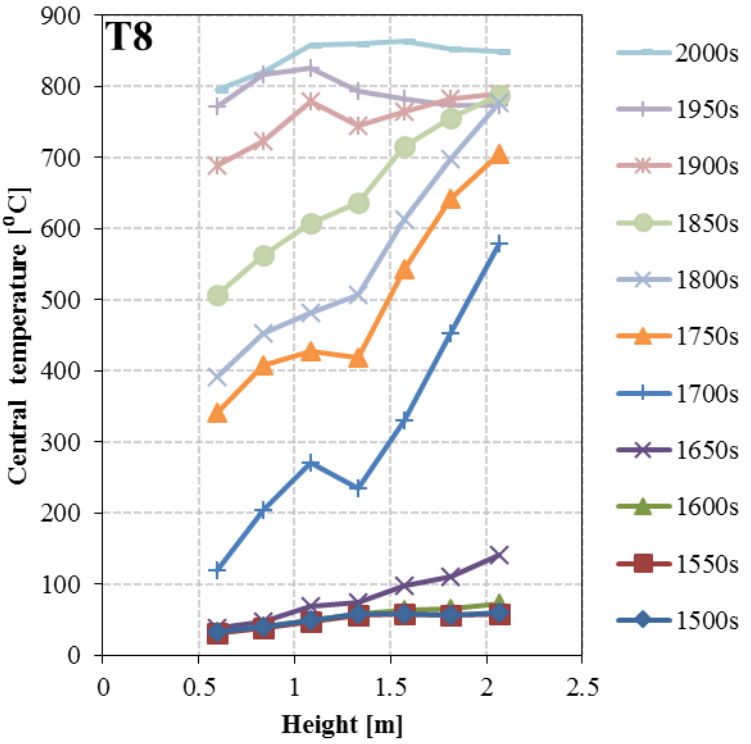

Figure 5-131: Vertical temperature profiles measured by the central tree at different time-steps of the fire (note: Flashover occurred at the 1700th second).

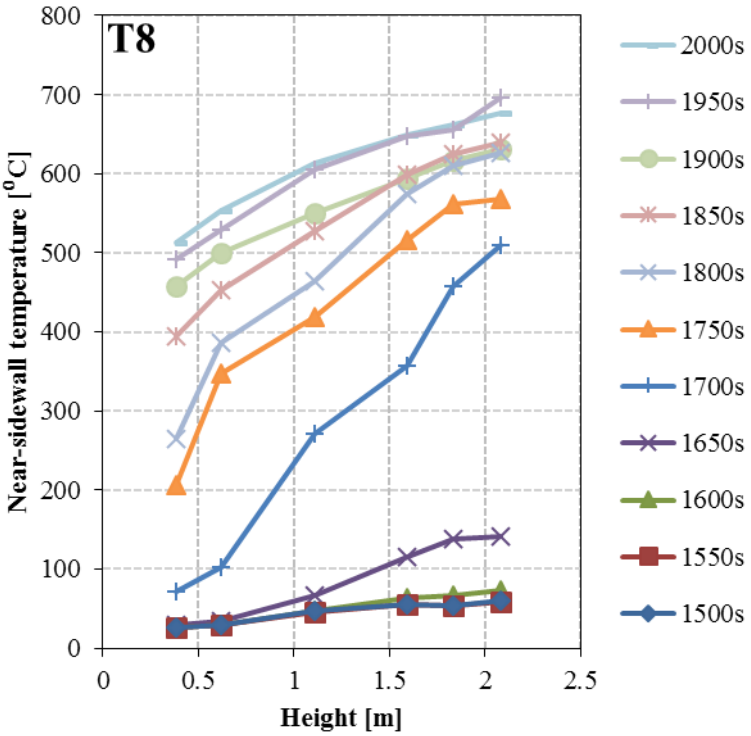

Figure 5-132: Vertical temperature profiles measured by the sidewall tree at different time-steps of the fire (note: Flashover occurred at the 1700th second).

Unlike the other tests presented in this chapter, because of the distributed fire load, it was not possible to monitor the mass loss rate in Test 8 and because of the variable type of fuel it

was not possible to have a representative elemental fuel composition. Thus an evaluation of the HRR and of the combustion efficiency in the same way as was performed in the other tests were not possible for this test.

However, a reasonable estimate of the HRR was obtained by utilizing the correlation between the effective HRR and the temperature in the compartment obtained from the timber pallet Test 3b.

Several researchers [288, 338, 339] have shown that based on fundamentals, the hot layer or ceiling jet temperature rise above ambient (ΔT) is proportional to the HRR to the power of 2/3. Conversely $HRR \propto (\Delta T)^{3/2}$. The proportionality constant would be dependent on the heat transfer properties of the compartment materials and the size of the ventilation openings. Since these were almost identical between the two tests then the proportionality constant could be obtained as shown in Figure 5-133.

Figure 5-134 shows an estimate of the effective HRR based on a reference Test 3b where HRR was measured based mass loss rate (MLR) and then corrected for inefficiency to produce actual HRR.

The average hot layer temperature was taken from the average of five ceiling thermocouples, two top thermocouples from the central vertical tree and the top thermocouple from the sidewall vertical tree.

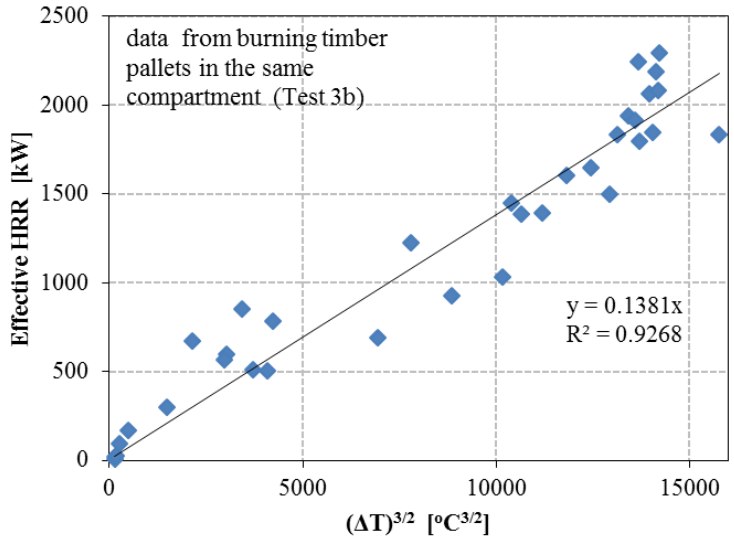

Figure 5-133: Correlation between effective HRR and hot layer temperature from Test 3b.

Calculation of the heat flux at floor level from the hot layer and at 1.2 m above floor level – representing radiation received by fire fighters helmets and at temperature of 700 °C and using view factors between finite parallel plates [325] and an emissivity of 0.8 give values of 31 kW/m^2 and 41 kW/m^2 at floor and helmet level respectively. These are very high heat fluxes which even with protective gear could only be withstood for a few seconds. This is

consistent with the reports of discomfort from the fire-fighting team on entry. Significant cooling of the hot gas layer would be needed to reduce the heat flux to manageable levels.

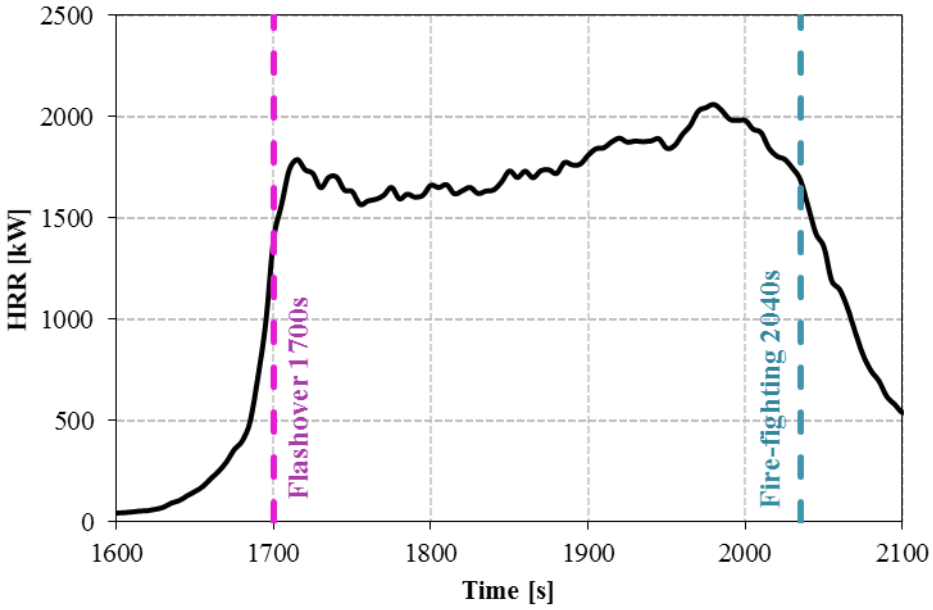

Figure 5-134: Estimated Effective HRR curve for the flashover and post-flashover fire for Test 8.

5.6.2 Toxic environment – Test 8

The heated on-line FTIR analyser used in these tests was calibrated for the simultaneous identification of over 50 species. The most significant of these along with the oxygen levels (measured using a paramagnetic analyser) are shown in Figure 5-135. They are shown to be well in excess (by one or two orders of magnitude) of the USA Environmental Protection Agency (EPA) AEGL-$2_{10\ min}$ (acute exposure guideline level 2 for 10 minutes) also marked on Figure 5-135 for acrolein, HCN and CO. AEGL-$2_{10\ min}$ is a critical limit defined as having long-lasting health effects or impairment of escape threshold limits [147].

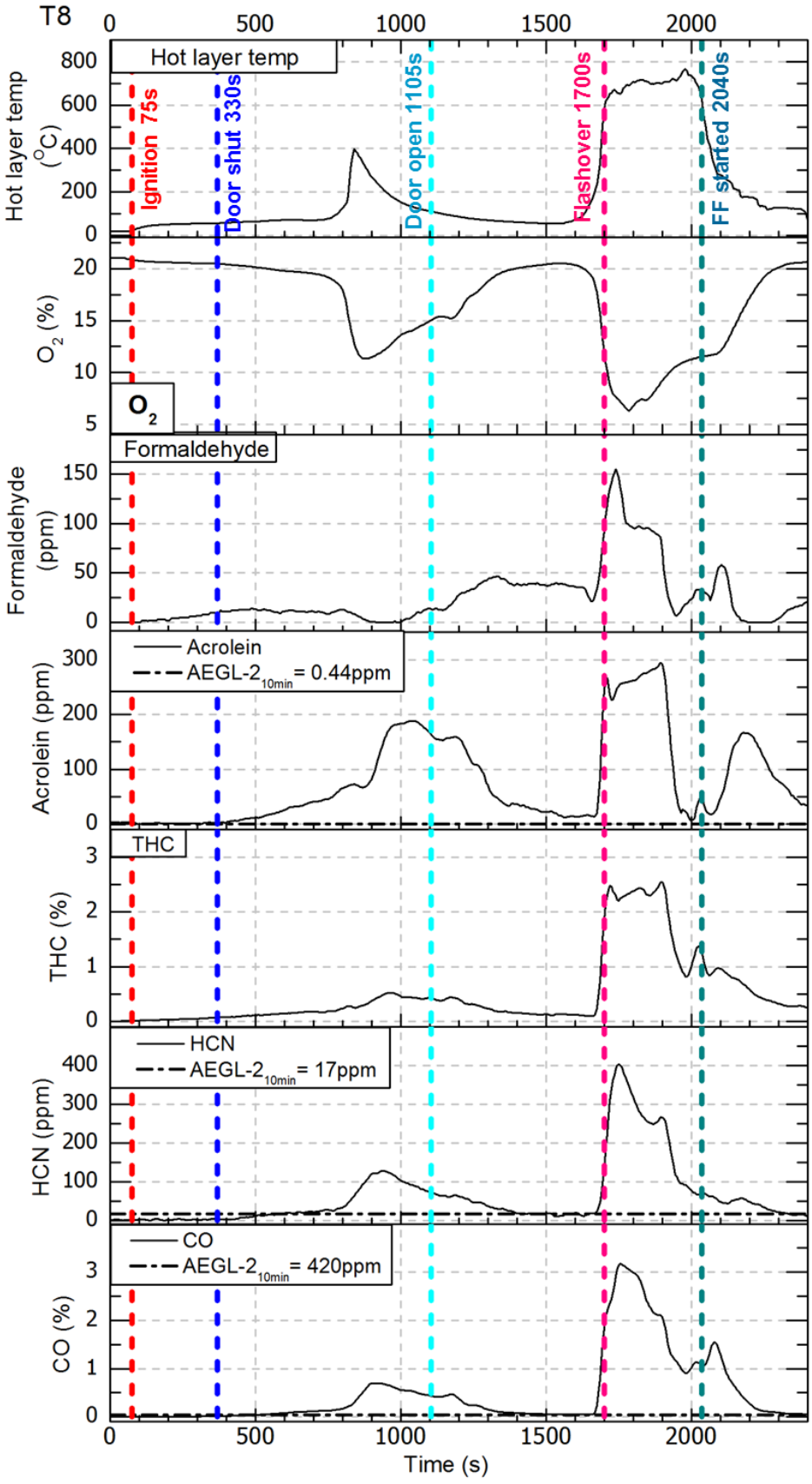

Figure 5-135: Hot layer temperature and concentrations (v/v) of O_2, Formaldehyde, acrolein, total hydrocarbons (THC), HCN and CO as a function of time. Also escape impairment threshold limits (AEGL-2_{10min}) are marked.

Of interest is the near extinguishment of the fire during the “door shut” phase at about 11% Oxygen levels. By comparison during the fully developed phase with the door open the fire burnt intensely at oxygen levels as low as 6% with no sign of imminent extinguishment. This can be attributed to the significantly different compartment temperatures for the two cases. In the door shut case the maximum hot layer temperature was around 400^{o}C, while in the open-door case the temperature is almost twice that underlining the importance of compartment temperature on the effective oxygen levels for fire extinguishment. The reduction in oxygen levels on both occasions was associated with a strong increase of incomplete combustion products and toxic emissions.

In both cases the buildup of combustion products and the deepening of the smoke layer resulted in some self inerting of the fire which in turn resulted in an increase in oxygen levels. In combination with the high temperatures for the case of door-open case and also the onset of flaming combustion of the carpet at floor level this seems to have resulted in some burnout and reduction of concentration of incomplete combustion species such as acrolein, total hydrocarbons, between 1800 and 2000s.

On the onset of fire-fighting operations an increase of CO and THC was recorded before they quickly starting to fall, while a significant and persistent increase of acrolein was recorded in association with the reductions of the compartment temperatures.

The instantaneous fractional effective concentration FEC for different levels were calculated in accordance with the guidelines presented earlier in section 2.3 to demonstrate the health effects of the smoke produced at the point of sampling. Firstly, FEC safe that is important for designing purposes to ensure a safe environment in protected structures such as corridors and staircases. This value (total FEC safe) is the dilution factor required to achieve a safe environment as discussed earlier in section 2.3.

Figure 5-136 presents FEC for safe level by the combustion products from Test 8b in the stacked graph (Figure 5-135). Figure 5-137 shows the composition of the contributing toxic emissions by percentage, where acrolein is the dominating contributor of the smoke influence based on the safe exposure thresholds.

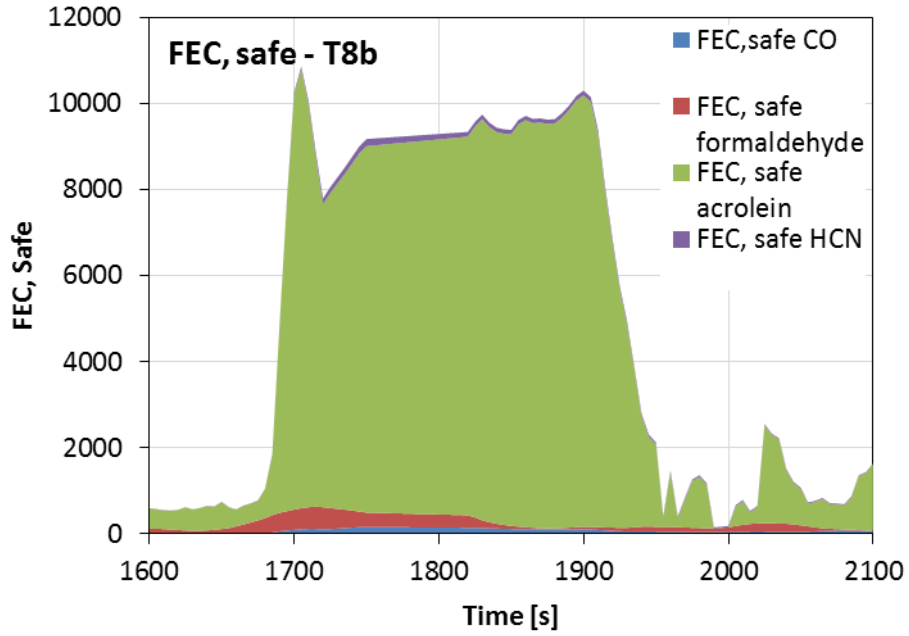

Figure 5-136: Instantaneous total fractional effective concentration (FEC) for safe level during Test 8b.

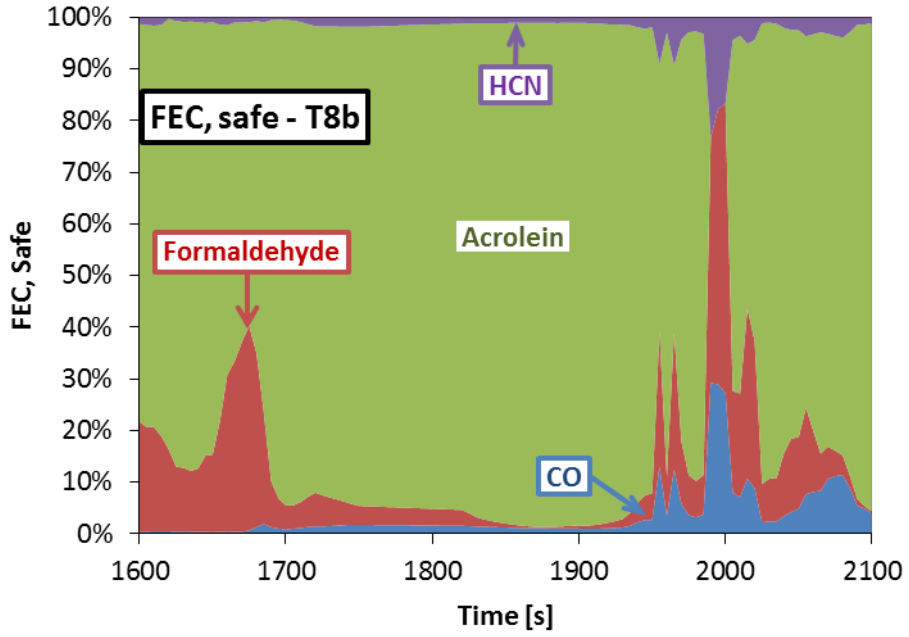

Figure 5-137: Major toxic emissions contribution by species to the fractional effective concentration for safe level in Test 8b.

Secondly, FEC for escape impairment (EI) that is important for post-accident investigations to understand the development of the evacuation plan and the point where victims were trapped. Figure 5-138 shows FEC for escape impairment from Test 8b in the stacked graph (Figure 5-135). While Figure 5-139 shows the composition of the contributing toxic emissions by percentage based on escape impairment exposure thresholds.

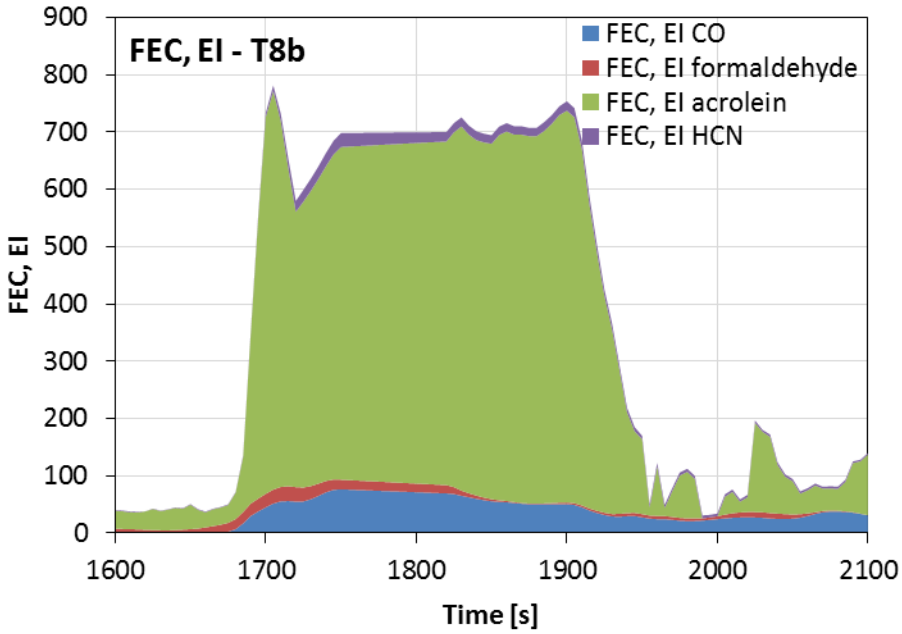

Figure 5-138: Instantaneous total fractional effective concentration (FEC) for escape impairment (EI) level during Test 8b.

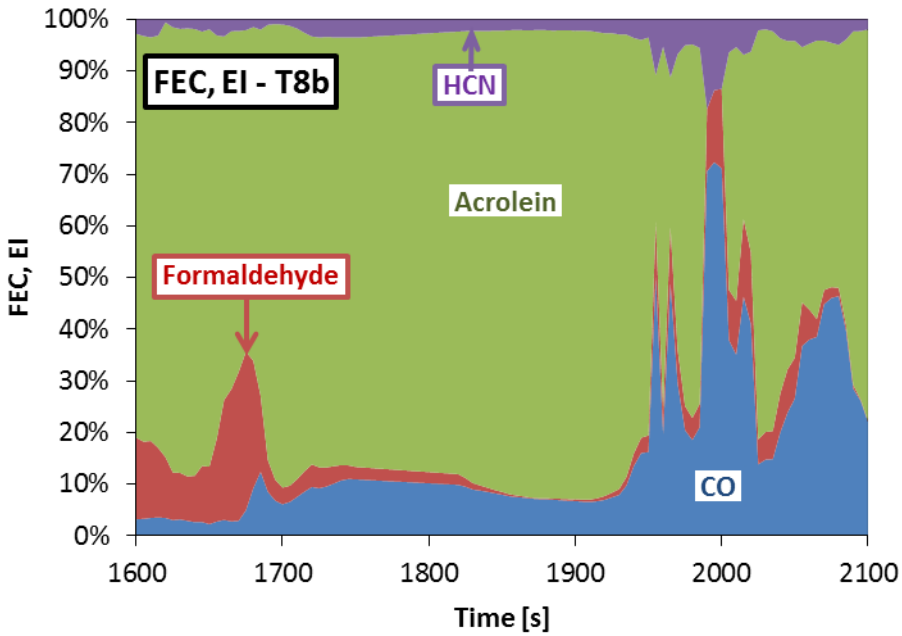

Figure 5-139: Major toxic emissions contribution by species to the fractional effective concentration for escape impairment (EI) level in Test 8b.

Thirdly, FEC for lethality that is useful for post-accident investigations. Figure 5-140 shows the instantaneous FEC for lethality from Test 8b in the stacked graph (Figure 5-135). The total value for lethal FEC peaked at around 170. Figure 5-141 shows the composition of the contributing toxic emissions by percentage based on lethal exposure thresholds discussed in section 2.3.

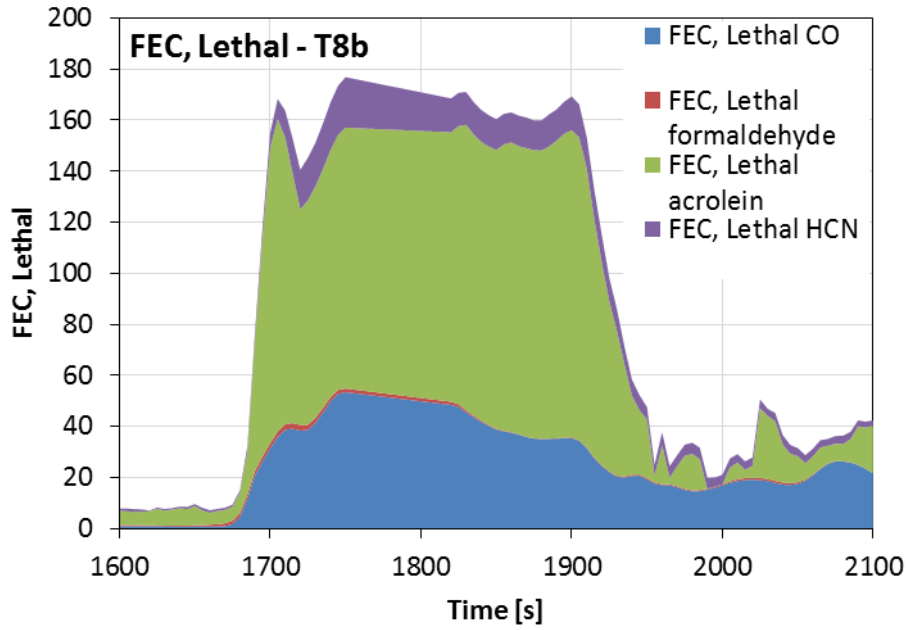

Figure 5-140: Instantaneous total fractional effective concentration (FEC) for lethal level during Test 8b.

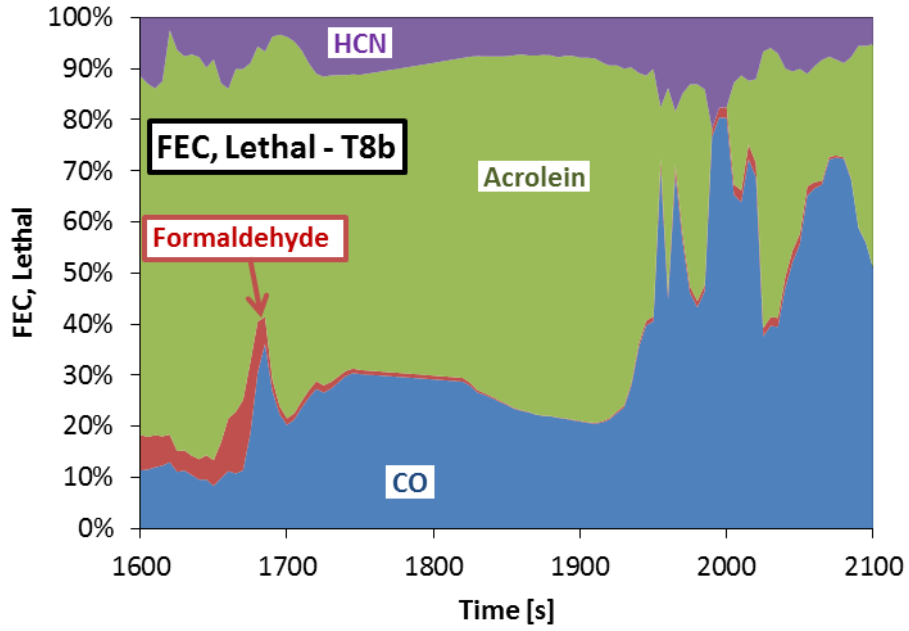

Figure 5-141: Major toxic emissions contribution by species to the fractional effective concentration for lethal level in Test 8b.

Finally, FEC for lethality based on the values purposed by ISO 13344 for LC50 the lethal concentration for half the population, as discussed earlier in section 2.3. Figure 5-142 shows the instantaneous FEC for lethality (based on LC50) from Test 8b in the stacked graph (Figure 5-135). The total value for lethal FEC peaked to reach 10. Figure 5-143 shows the composition of the contributing toxic emissions by percentage based on lethal exposure thresholds of LC50. The comparison between FEC for lethality based on the most conservative threshold shown in Figure 5-140 and Figure 5-141 on one hand and FEC for lethality based on LC50 shown in Figure 5-142 and Figure 5-143 on the other, is important

to demonstrate the difference between the two. As discussed earlier in section 2.3, the most conservative threshold database for lethality used was AEGL-3_{30min} is defined to be the minimum exposure to cause life-threatening health damage or death, while LC50 is defined to be the concentrations that cause death to half the population.

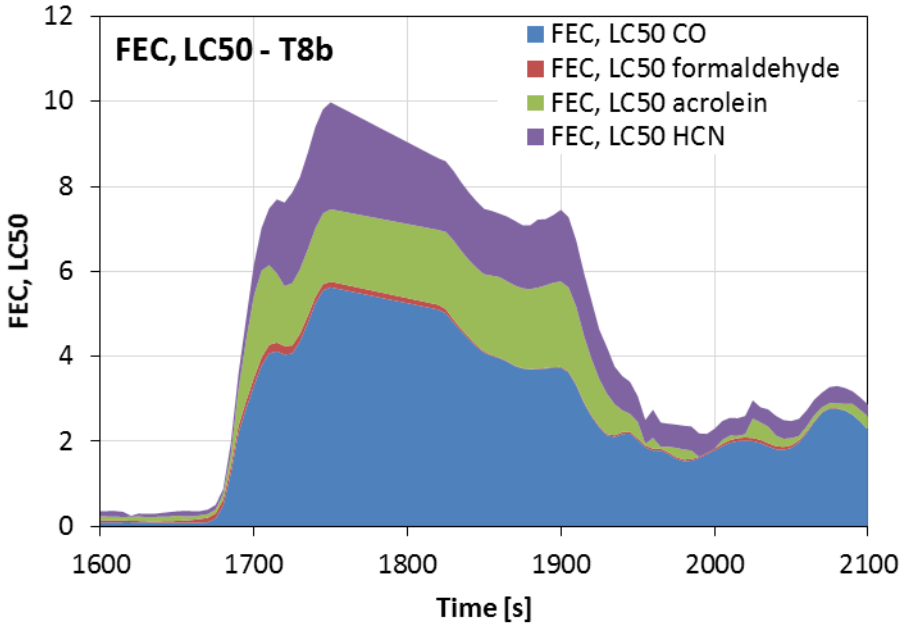

Figure 5-142: Instantaneous total fractional effective concentration (FEC) for lethal level (using LC50 values) during Test 8b.

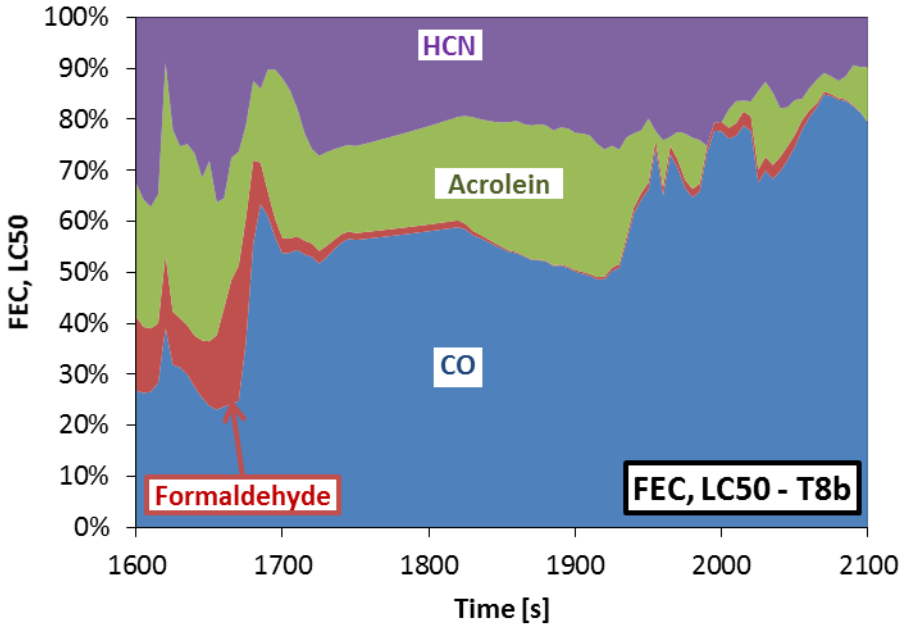

Figure 5-143: Major toxic emissions contribution by species to the fractional effective concentration for lethal level (using LC50 values) in Test 8b.

5.7 Diesel pool I

The test simulates an oil spillage fire in a compartment for industrial application. A tray with the dimensions 1.2 x 1.2 m^2. It was mounted on the top of the weighting platform in the near corner to the door. The ventilation for the compartment was restricted to smaller than quarter of the door as shown in Figure 3-34 (total area of ventilation was (0.28 x 0.82 = 0.23 m^2). The ventilation was expected to keep the HRR to a maximum value of 340 kW based on the fire dynamics calculations explained in [289]. No fire-fighting activity was required as the test was planned for the diesel to burn out by the end of the test, however fire-fighting teams were on standby.

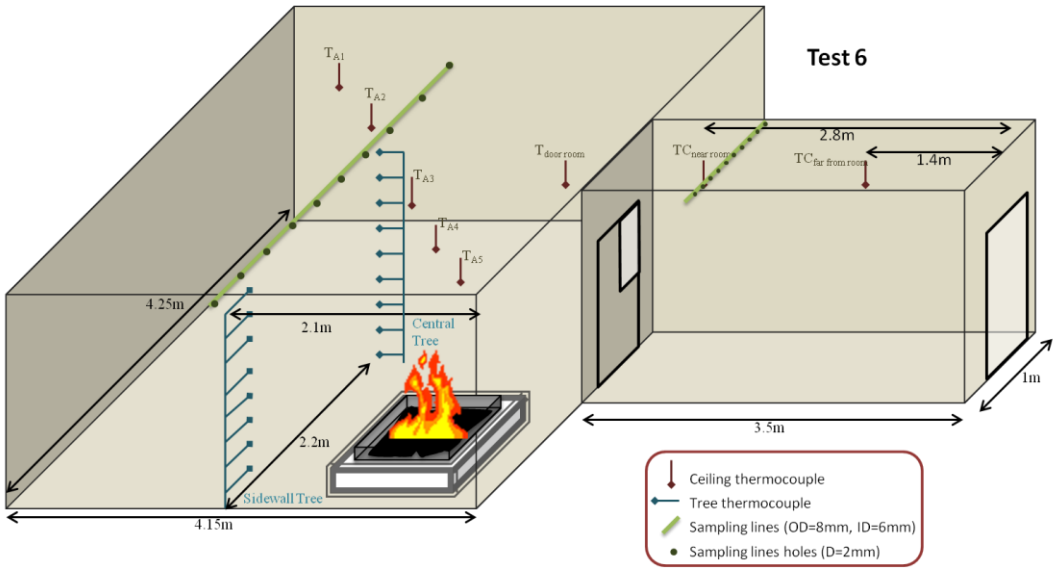

Figure 5-144: Test 6 full setup showing fire load, instrumentation and ventilation openings.

Figure 5-145: Picture of the pool ignition in Test 6 showing torch ignitor appears on the left hand side. The photo was taken from inside the room before closing the door.

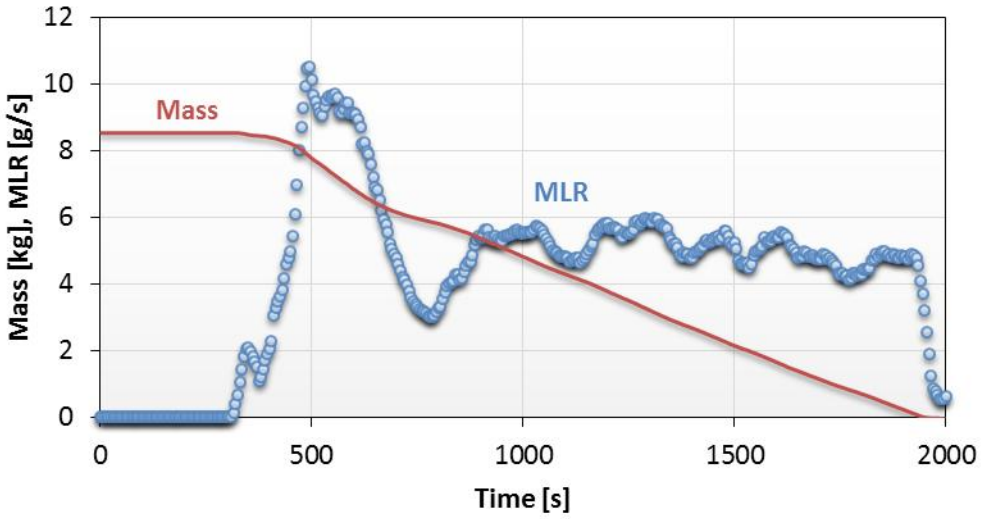

Figure 5-146: Total mass of the fire load (Red) and mass loss rate (Blue) for Test 6 from start till fire-fighting.

5.7.1 Mass loss and heat release rate (HRR) – Test 6

Using the calorific value approach combined with the mass loss data, online heat release rate (HRR) is established. Additionally, using the incomplete combustion products measurements carbon monoxide and total unburnt hydrocarbons, inefficiency is estimated. During Test 6, 8.5 kg of diesel was consumed giving a peak HRR of just above 450 kW and a steady state HRR between 200 – 250 kW, demonstrated in Figure 5-147. In terms of inefficiency, Figure 5-148 shows the combustion inefficiency observed in Test 6 was very low (below 6%).

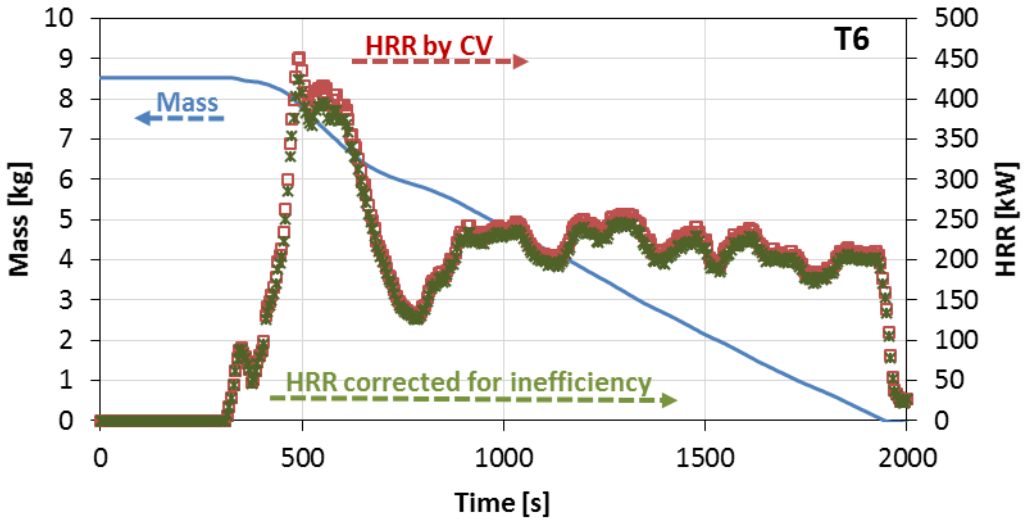

Figure 5-147: Mass change with time and associated HRR based on the mass loss rate for Test 6. Also shown is an adjusted HRR, based on inefficiency of combustion as derived from the unburnt hydrocarbons and CO measurements.

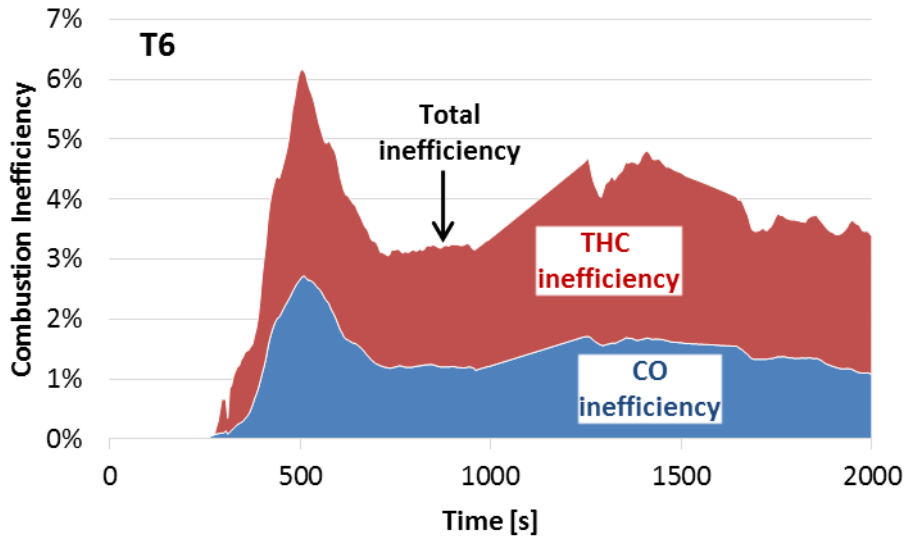

Figure 5-148: Total combustion inefficiency as a function of time with contributions from CO and THC for Test 6.

5.7.2 Thermal environment – Test 6

Temperatures inside the room followed a similar pattern as the HRR profile shown earlier, where the upper layer temperature peaked initially reaching 700 ^{0}C above the fire then started stabilising afterwards around 300 ^{0}C, as can be seen in Figure 5-149. Vertical thermocouple trees showed similar patterns to those at the upper layer showing a stabilised value for each height, as demonstrated in Figure 5-150 and Figure 5-151.

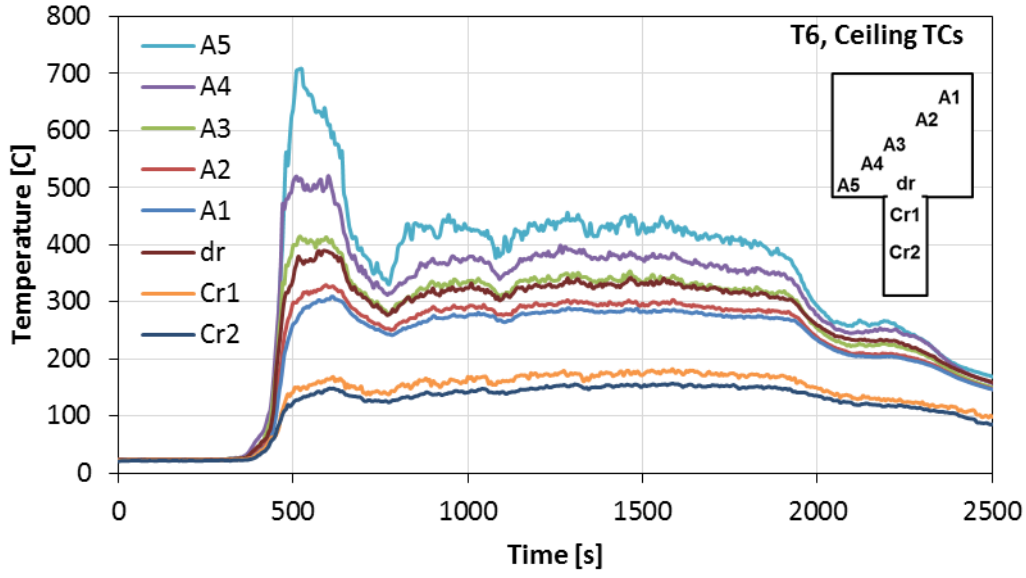

Figure 5-149: Ceiling layer temperature measurements at different positions inside the compartment and corridor during Test 6.

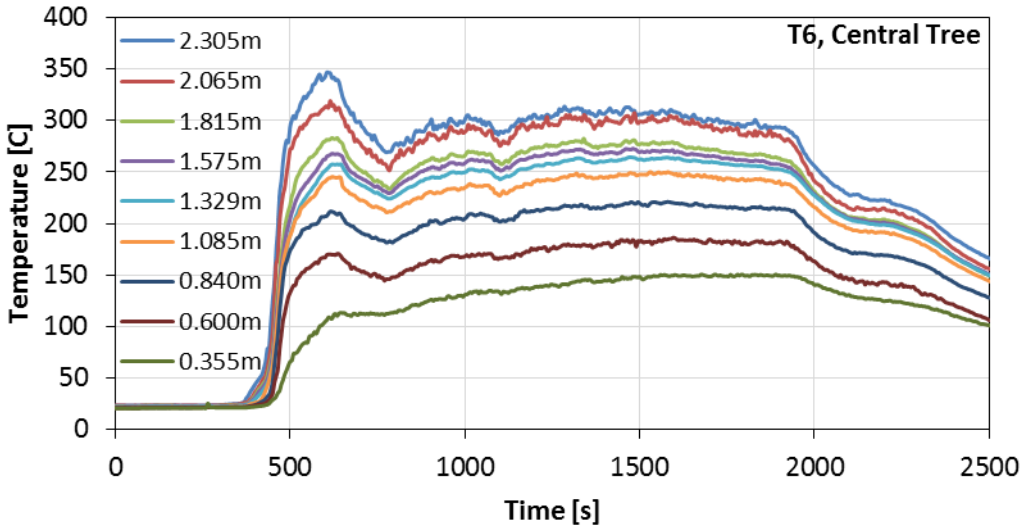

Figure 5-150: Temperatures at different heights from floor level in the fire room as measured by the central vertical thermocouple tree during test 6.

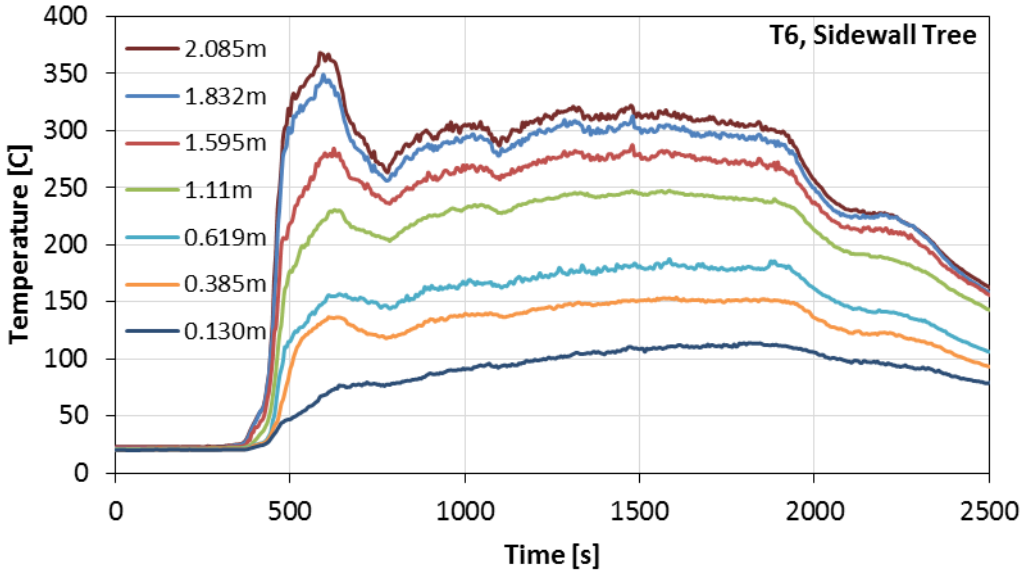

Figure 5-151: Temperatures at different heights from floor level in the fire room as measured by the vertical thermocouple tree on the sidewall of the compartment during test 6.

5.7.3 Toxic environment – Test 6

During Test 6 the gas sampling system was mainly set on the central sampling line inside the room and switched to sample from the corridor briefly twice during test 6 (between 950th – 1250th seconds and 1450th – 1650th seconds). Measurements from both periods were almost identical (due to the steady burning rate), so the single point measurements at the 1200th second was chosen to be representative of the toxic environment in the corridor during the steady state period of test 6. Table 5-7 presents the gas concentration measurements in the corridor and their corresponding yields based on the emission-based

equivalence ratio (EBER) at the point of sampling that was 0.49. Ratios to the relevant exposure thresholds are presented. The composition of the overall fractional effective concentration (FEC) are presented in Figure 5-152. These data useful for studying situations of smoke exposure in rooms away from the room of origin, where the required dilution rate is indicated by the FEC values for different levels of exposure effects.

Table 5-7: Concentrations of major combustion emissions measured in the corridor during Test 6 at 1200th second, with their ratios to relevant toxic exposure thresholds and mass yield data for each species.

Species	Conc. [ppm]	R-Safe	R-Escape impairment	R-Lethal	R-LC50	Yield [g/g]
CO	2,189	11	5.2	3.6	0.38	0.0649
Acrolein	19	641	44	7.7	0.13	0.0014
Formaldehyde	75	249	12	1.1	0.1	0.0010
THC	1,804					0.0059

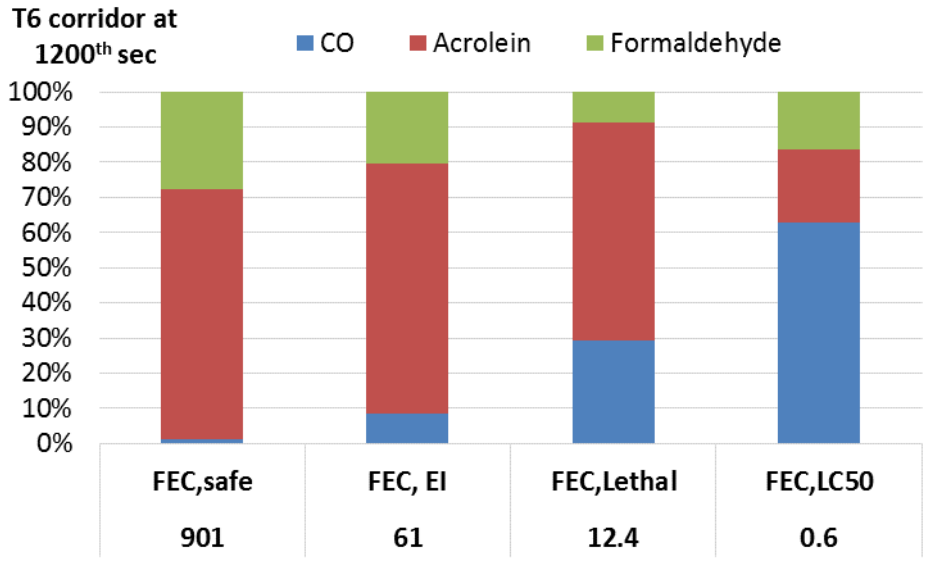

Figure 5-152: The main toxic products measured in the corridor during Test 6 at 1200th second in respect to their contribution to the overall Fractional Effective Concentration (FEC).

The measurements from inside the room were analysed separately, for the gap measurements (due to sampling from the corridor, not for the room) the data points were linked based on before and after switching in order to estimate these measurements. Due to the fact that the room was not completely confined from ventilation, the data were treated as a dynamic online gas measurements. The combustion emission-based equivalence ratio (EBER) was calculated as a function of time and is presented at the top of Figure 5-153. The EBER shows that the fire was lean throughout Test 6 with a value of 0.7 during the steady

state period. Main toxic species measured at this stage (T6) are presented as well in Figure 5-153. Oxygen levels dropped to 6% at the HRR peak point, and stabilised around 9% during the steady state period. Corresponding mass yields are presented in Figure 5-154.

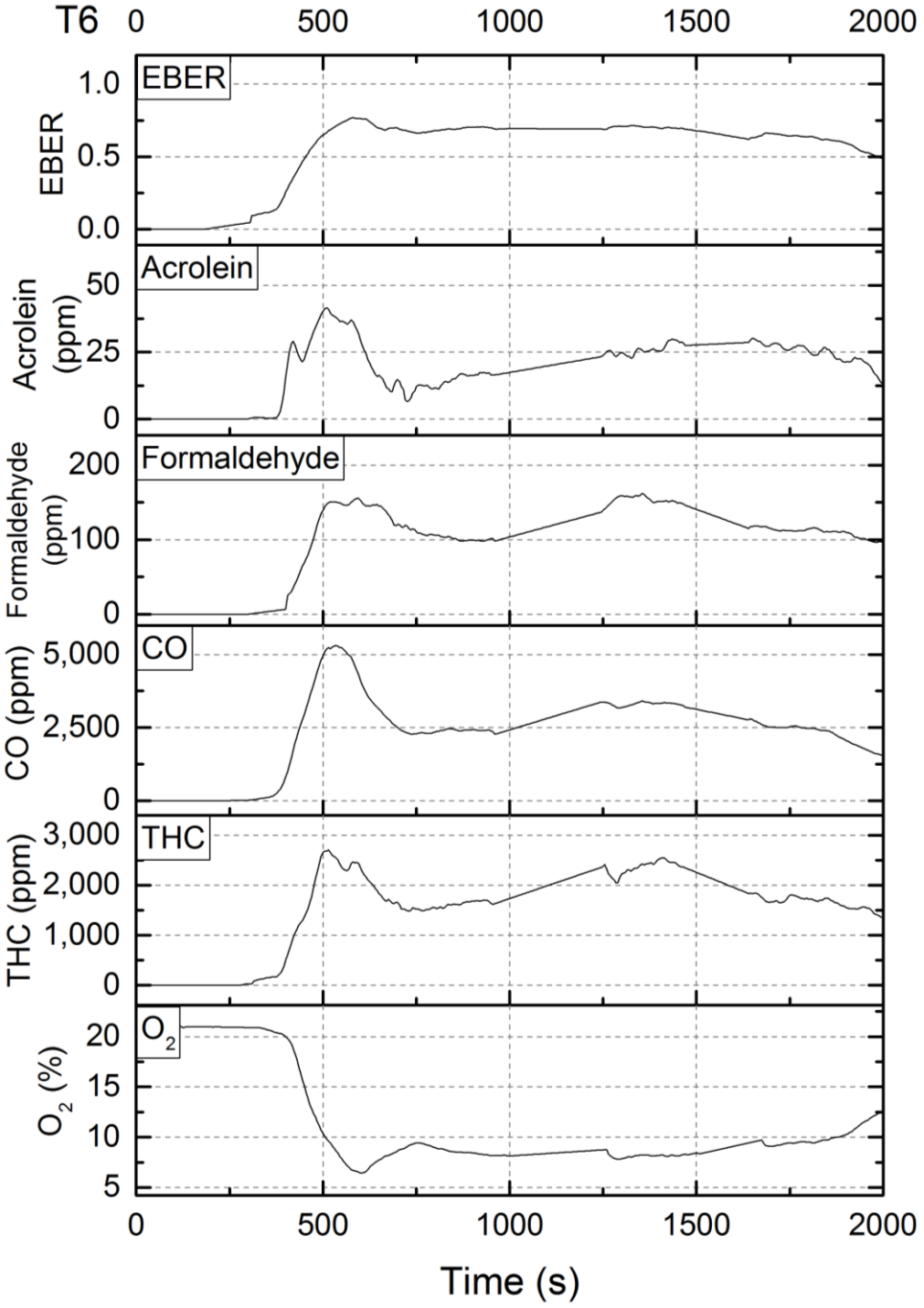

Figure 5-153: Combustion toxic products concentrations in volume basis in line with equivalence ratio and Oxygen concentration for Test 6.

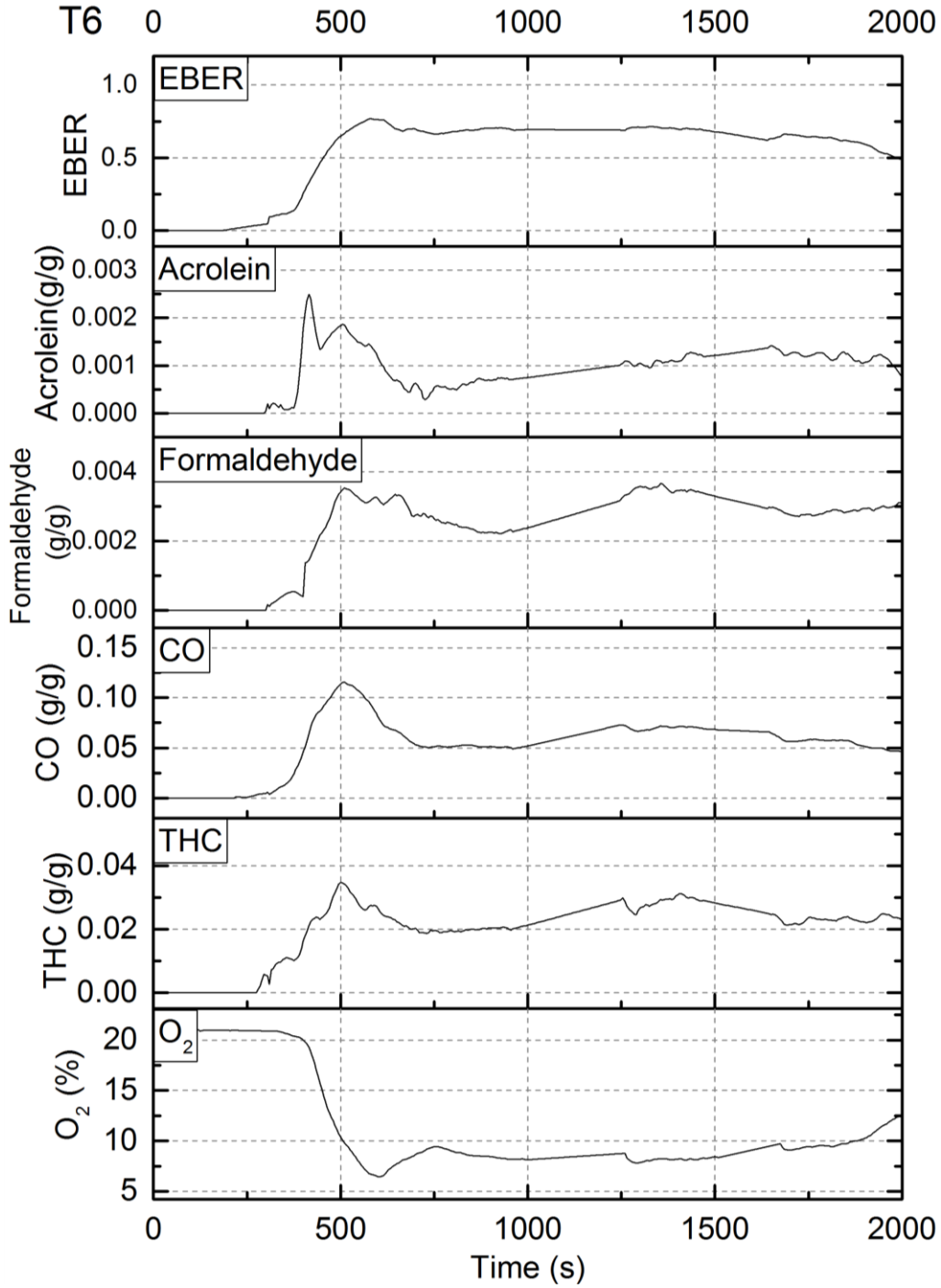

Figure 5-154: Combustion toxic products mass yields in line with equivalence ratio and Oxygen concentration for Test 6.

The instantaneous fractional effective concentration FEC for different levels were calculated in accordance with the guidelines presented earlier in section 2.3 to demonstrate the health effects of the smoke produced at the point of sampling. Firstly, FEC safe that is important for designing purposes to ensure a safe environment in protected structures such as corridors and staircases. This value (total FEC safe) is the dilution factor required to achieve a safe environment as discussed earlier in section 2.3.

Figure 5-155 presents FEC for safe level by the combustion products from Test 6 in the stacked graph (Figure 5-153). Figure 5-156 shows the composition of the contributing toxic emissions by percentage, where acrolein is the dominating contributor of the smoke influence based on the safe exposure thresholds and followed by formaldehyde.

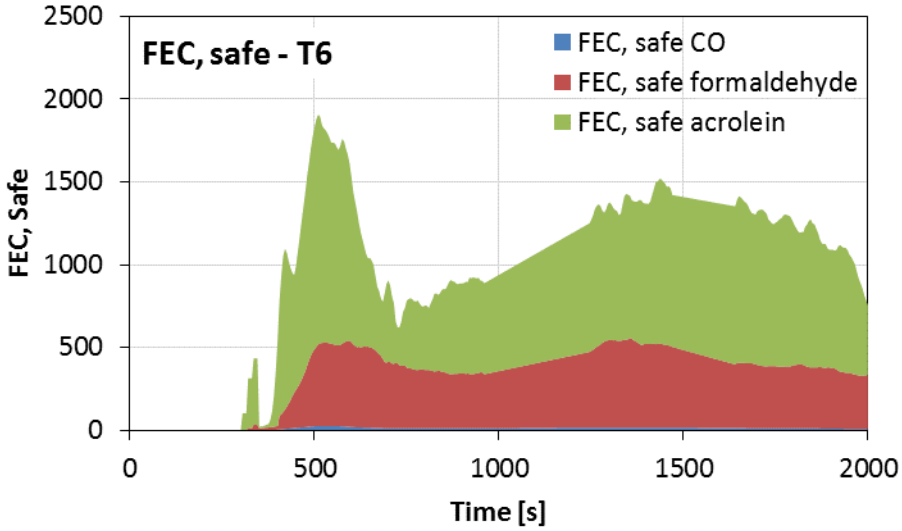

Figure 5-155: Instantaneous total fractional effective concentration (FEC) for safe level during Test 6.

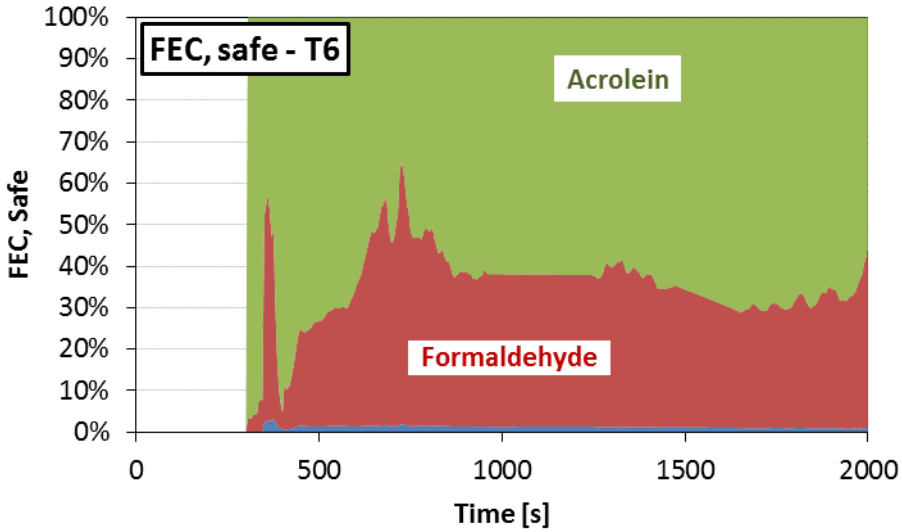

Figure 5-156: Major toxic emissions contribution by species to the fractional effective concentration for safe level in Test 6.

Secondly, FEC for escape impairment (EI) that is important for post-accident investigations to understand the development of the evacuation plan and the point where victims were trapped. Figure 5-157 shows FEC for escape impairment from Test 6 in the stacked graph (Figure 5-153). While Figure 5-158 shows the composition of the contributing toxic emissions by percentage based on escape impairment exposure thresholds.

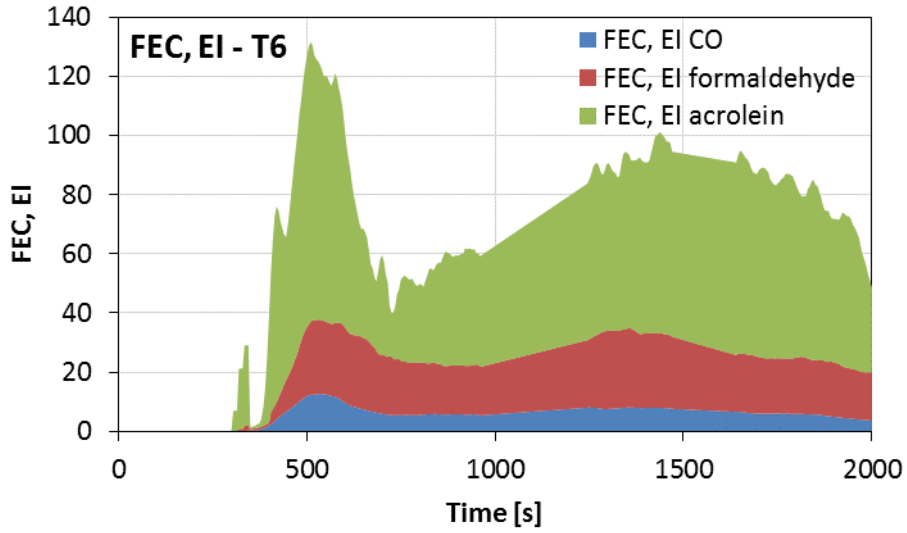

Figure 5-157: Instantaneous total fractional effective concentration (FEC) for escape impairment (EI) level during Test 6.

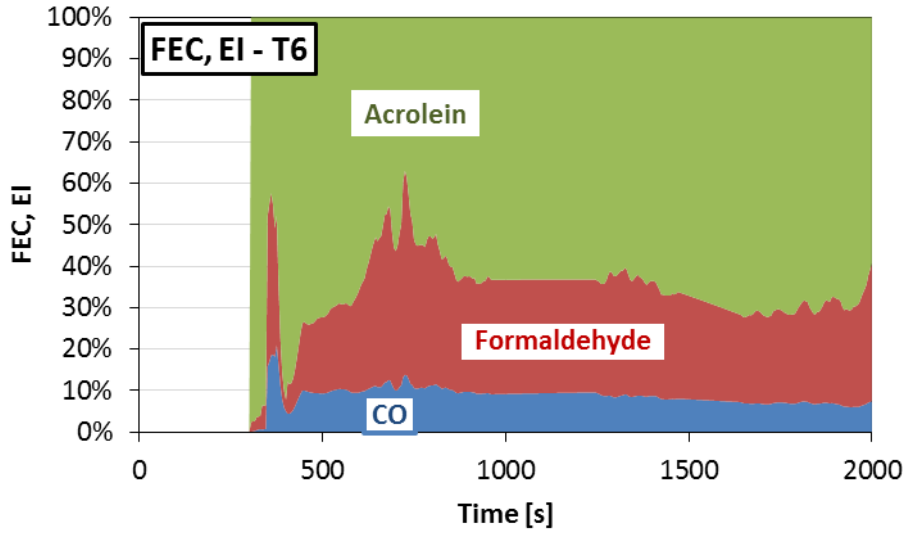

Figure 5-158: Major toxic emissions contribution by species to the fractional effective concentration for escape impairment (EI) level in Test 6.

Thirdly, FEC for lethality that is useful for post-accident investigations. Figure 5-159 shows the instantaneous FEC for lethality from Test 6 in the stacked graph (Figure 5-153). The total value for lethal FEC peaked by reaching 25. Figure 5-160 shows the composition of the contributing toxic emissions by percentage based on lethal exposure thresholds discussed in section 2.3.

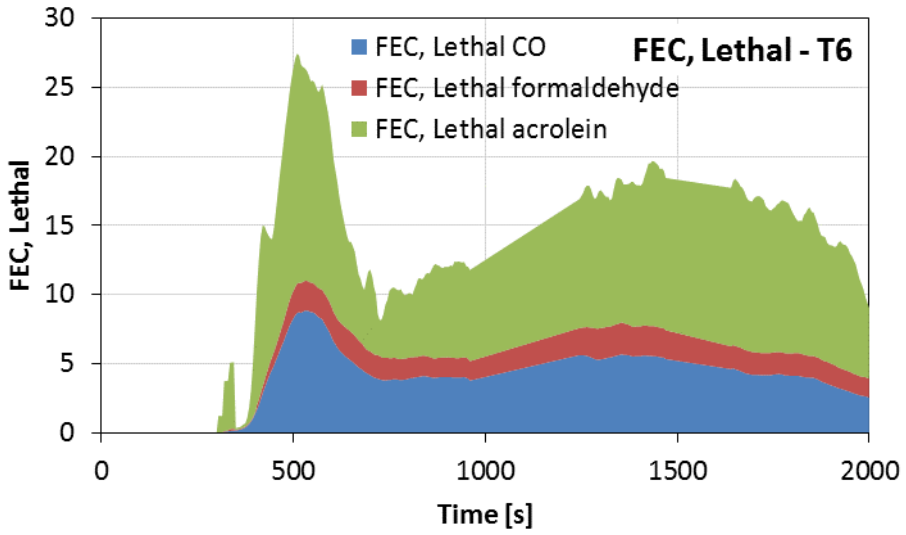

Figure 5-159: Instantaneous total fractional effective concentration (FEC) for lethal level during Test 6.

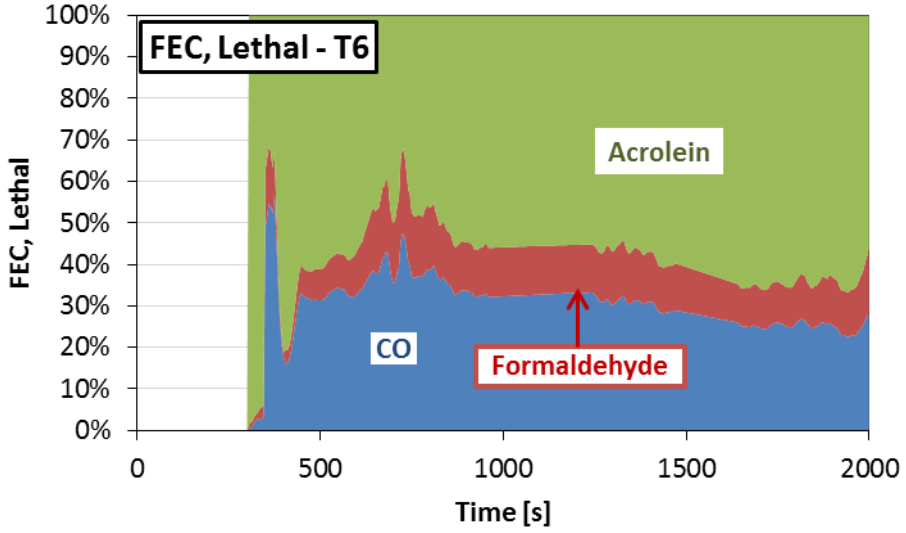

Figure 5-160: Major toxic emissions contribution by species to the fractional effective concentration for lethal level in Test 6.

Finally, FEC for lethality based on the values purposed by ISO 13344 for LC50 the lethal concentration for half the population, as discussed earlier in section 2.3. Figure 5-161 shows the instantaneous FEC for lethality (based on LC50) from Test 6 in the stacked graph (Figure 5-153). The total value for lethal FEC peaked reaching 1.4. Figure 5-162 shows the composition of the contributing toxic emissions by percentage based on lethal exposure thresholds of LC50. The comparison between FEC for lethality based on the most conservative threshold shown in Figure 5-159 and Figure 5-160 on one hand and FEC for lethality based on LC50 shown in Figure 5-161 and Figure 5-162 on the other, is important to demonstrate the difference between the two. As discussed earlier in section 2.3, the most conservative threshold database for lethality used was AEGL-3_{30min} is defined to be the minimum exposure to cause life-threatening health damage or death, while LC50 is defined to be the concentrations that cause death to half the population.

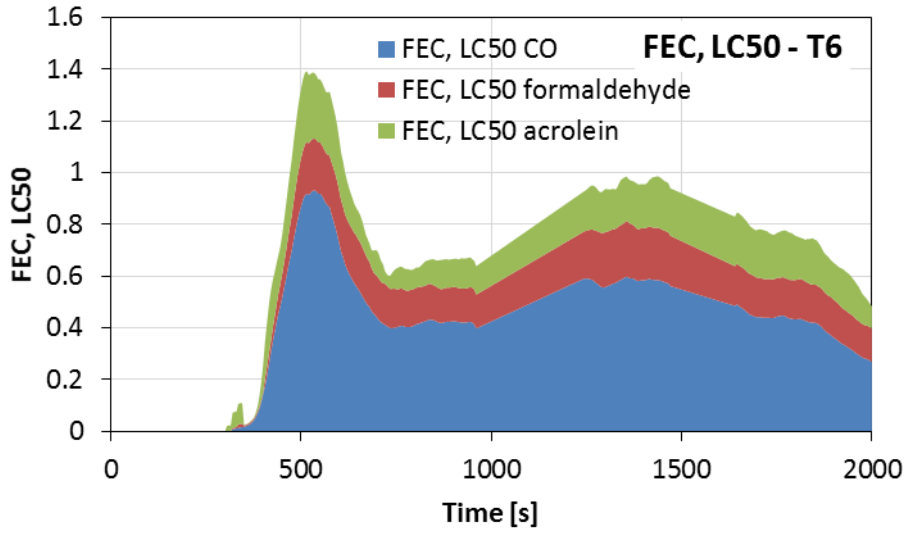

Figure 5-161: Instantaneous total fractional effective concentration (FEC) for lethal level (using LC50 values) during Test 6.

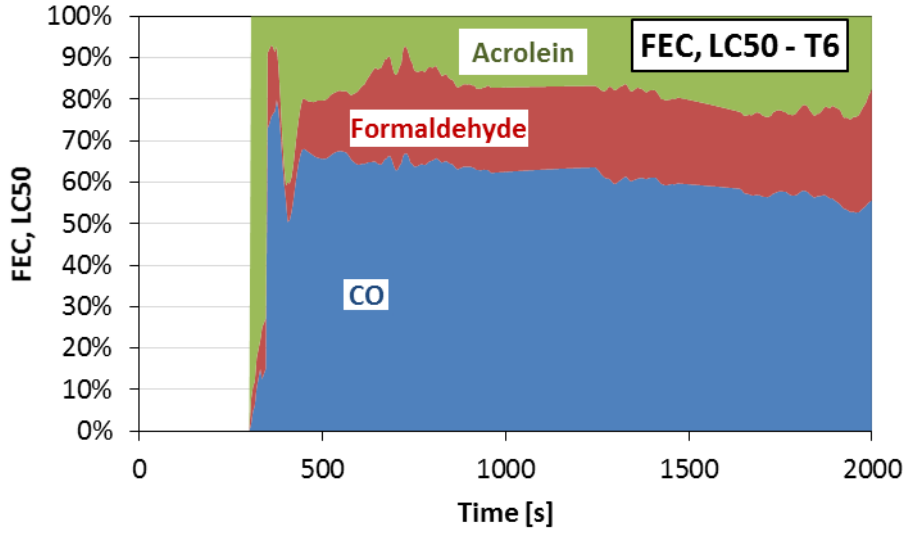

Figure 5-162: Major toxic emissions contribution by species to the fractional effective concentration for lethal level (using LC50 values) in Test 6.

5.8 Diesel pool II

Using the same compartment and tray as test 6 this test was conducted however the amount of diesel was doubled to be 16.2 kg and the ventilation opening was doubled by extending the opening to double the height for the total area of opening to be 0.28 x 1.64 = 0.46 m^2. During the test due to the excessive heat of the previous tests the fire managed to penetrate the plasterboard ceiling above the weighting platform which eventually collapsed on the tray and weighting platform, at this stage the test was suspended. The control room had to be evacuated due to the risk of the fire spreading through the roof space. The available data are presented here.

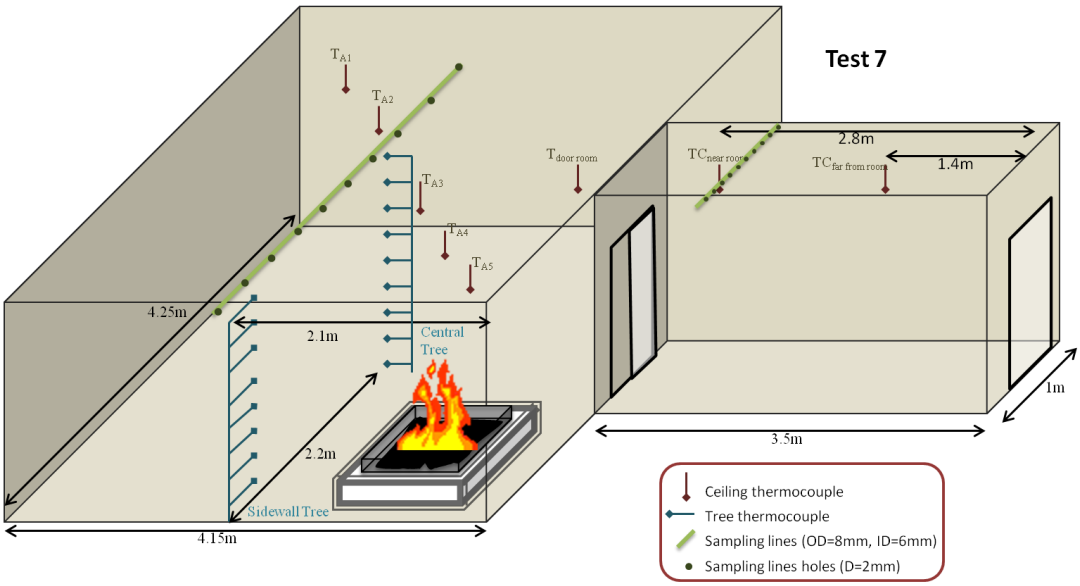

Figure 5-163: Test 7 full setup showing fire load, instrumentation and ventilation openings.

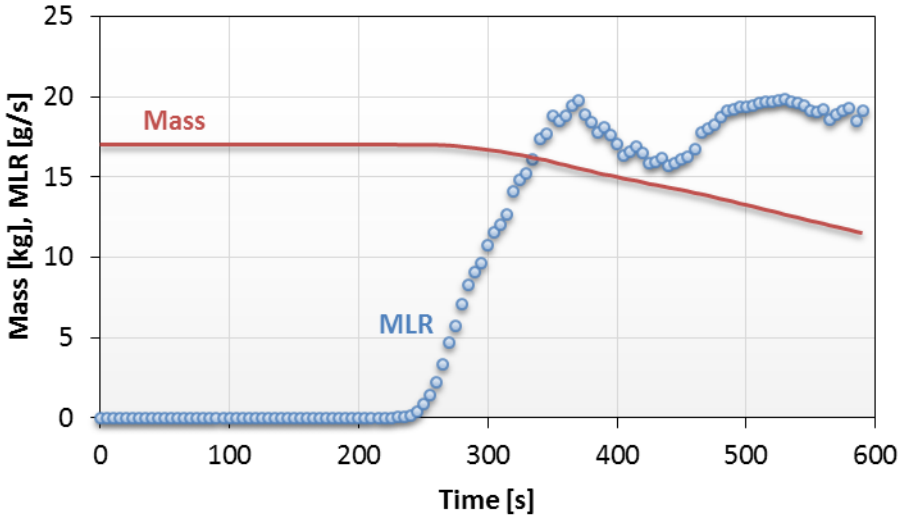

Figure 5-164: Total mass of the fire load (Red) and mass loss rate (Blue) for Test 7.

5.8.1 Mass loss and heat release rate (HRR) – Test 7

The mass data retrieved were valid up to the 600th second as after that weight platform observed sudden increase in weight, that can be explained by the plasterboard ceiling falling on the pool fire. Consequently only the initial 600 seconds of the mass are used for HRR analysis. Using the calorific value approach combined with the available mass loss data, online heat release rate (HRR) is established for the first 600 second. Additionally, using the incomplete combustion products measurements carbon monoxide and total unburnt hydrocarbons, inefficiency is estimated. The peak corrected HRR observed in T7 reached over 700 kW, demonstrated in Figure 5-165. In terms of inefficiency, Figure 5-166 shows high combustion inefficiency were measured during T7 reaching 18%.

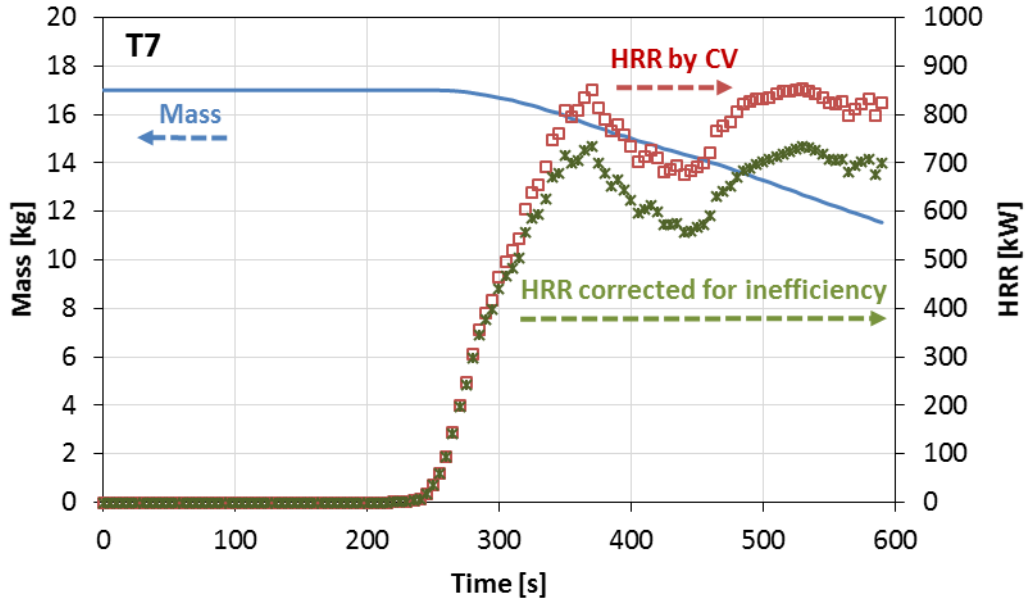

Figure 5-165: Mass change with time and associated HRR based on the mass loss rate for Test 7. Also shown is an adjusted HRR, based on inefficiency of combustion as derived from the unburnt hydrocarbons and CO measurements.

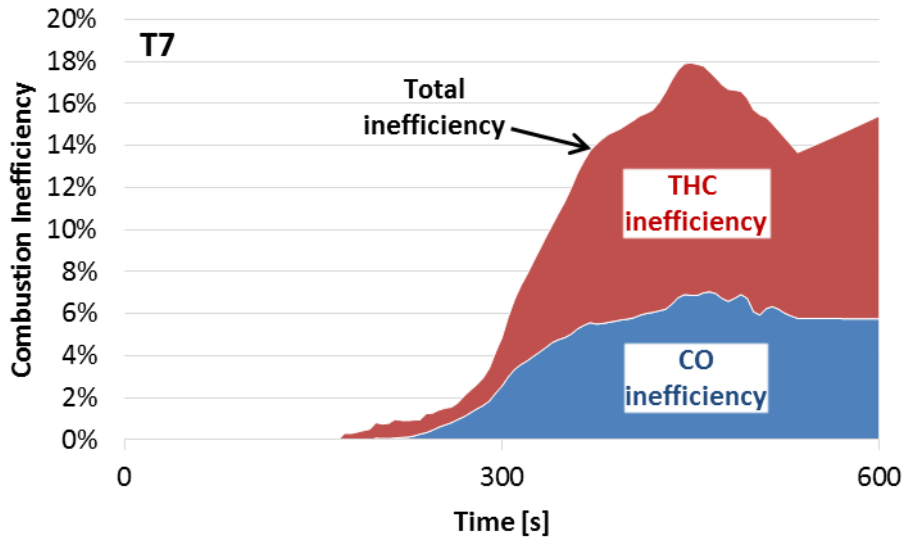

Figure 5-166: Total combustion inefficiency as a function of time with contributions from CO and THC for Test 7.

5.8.2 Thermal environment – Test 7

Temperature data were logged by the system up to the 1200th second as presented in the following figures. Highest temperature observed by thermocouples inside the room reached levels above 950 C, these levels of heat proved to be too intense for the ceiling plasterboard to stay intact. In general temperatures observed inside the compartment during Test 7 (with half door opening) were almost double those observed inside the room during Test 6 (with quarter door opening).

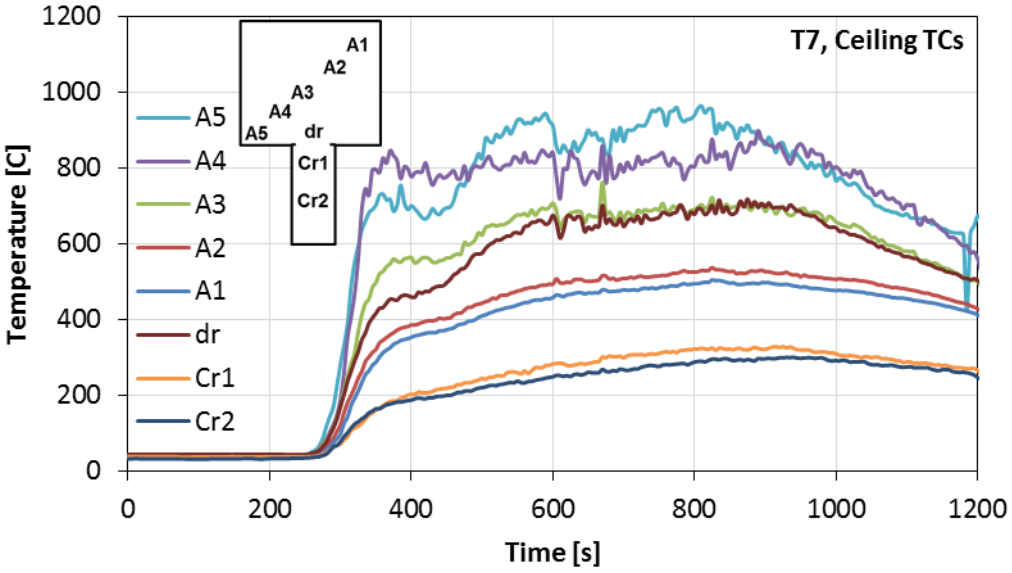

Figure 5-167: Ceiling layer temperature measurements at different positions inside the compartment and corridor during Test 7.

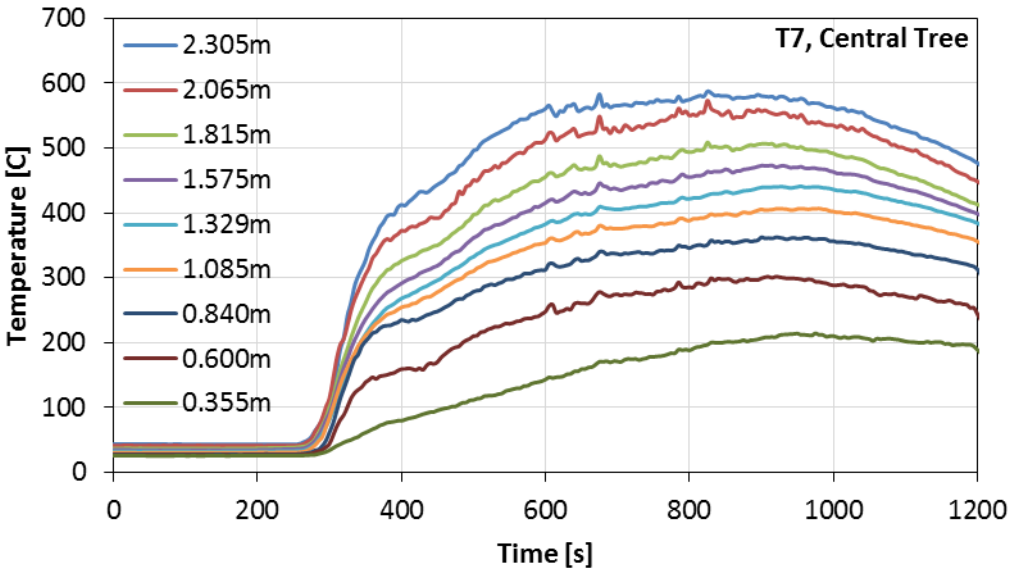

Figure 5-168: Temperatures at different heights from floor level in the fire room as measured by the central vertical thermocouple tree during test 7.

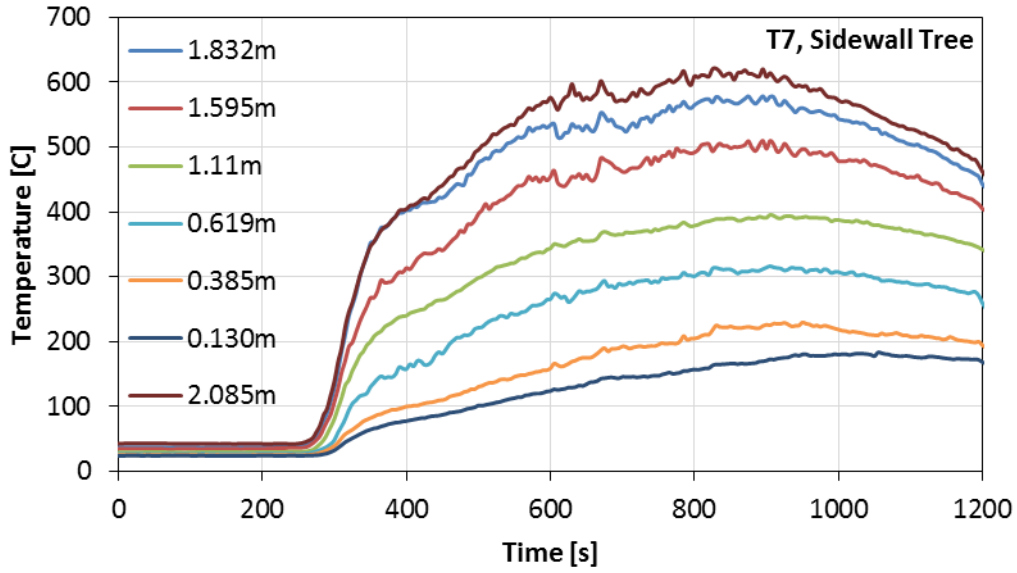

Figure 5-169: Temperatures at different heights from floor level in the fire room as measured by the vertical thermocouple tree on the sidewall of the compartment during test 7.

5.8.3 Toxic environment – Test 7

During Test 7 the gas sampling system was mainly set on the central sampling line inside the room and switched to sample from the corridor briefly once during test 7 (between 550th – 750th seconds). The single point measurements at the 700th second was chosen to be representative of the toxic environment in the corridor during the steady state period of test 7. Table 5-8 presents the gas concentration measurements in the corridor and their corresponding yields based on the emission-based equivalence ratio (EBER) at the point of sampling that was 0.59. Ratios to the relevant exposure thresholds are presented. The composition of the overall fractional effective concentration (FEC) are presented in Figure 5-170. These data useful for studying situations of smoke exposure in rooms away from the room of origin, where the required dilution rate is indicated by the FEC values for different levels of exposure effects.

Table 5-8: Concentrations of major combustion emissions measured in the corridor during Test 7 at 700th second, with their ratios to relevant toxic exposure thresholds and mass yield data for each species.

Species	Conc. [ppm]	R-Safe	R-Escape impairment	R-Lethal	R-LC50	Yield [g/g]
CO	7,388	37	18	12	1.3	0.1846
Acrolein	87	2,898	198	35	0.6	0.0014
Formaldehyde	95	317	16	1.4	0.1	0.0010
Benzene	425	170	0.85	0.08		0.0296
THC	10,535					0.0059

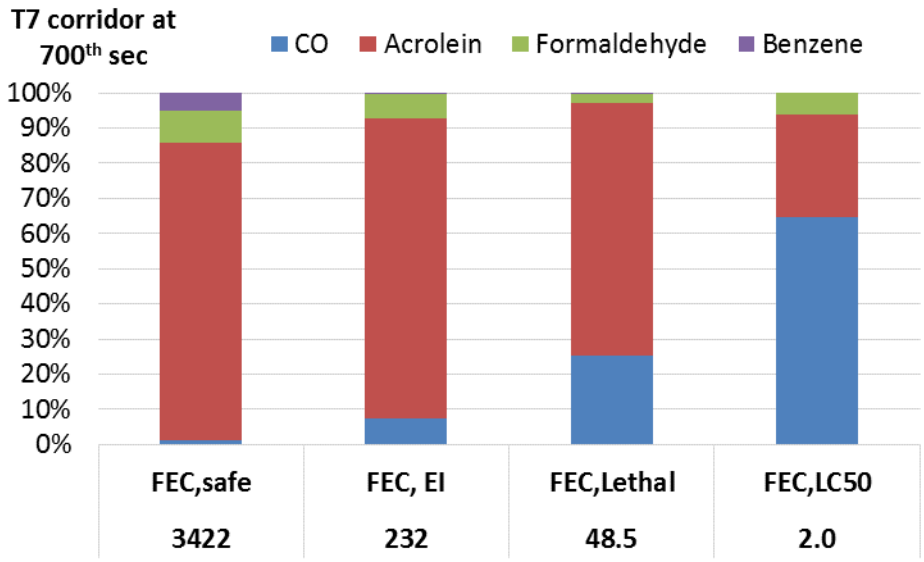

Figure 5-170: The main toxic products measured in the corridor during Test 7 at 700th second in respect to their contribution to the overall Fractional Effective Concentration (FEC).

The measurements from inside the room were analysed separately from corridor measurements, for the gap measurements (due to sampling from the corridor, not for the room) the data points were linked based on before and after switching in order to estimate these measurements. Retrieved data from the gas analysis measurements were recorded until the 900th second. The combustion emission-based equivalence ratio (EBER) was calculated as a function of time and is presented at the top of Figure 5-171. The EBER shows that the fire rapidly started to burn rich within 5 minutes from ignition. Major toxic species measured at this test (T7) are presented as well in Figure 5-171. Oxygen levels dropped to 2% at the HRR peak point. Corresponding mass yields are presented in Figure 5-172.

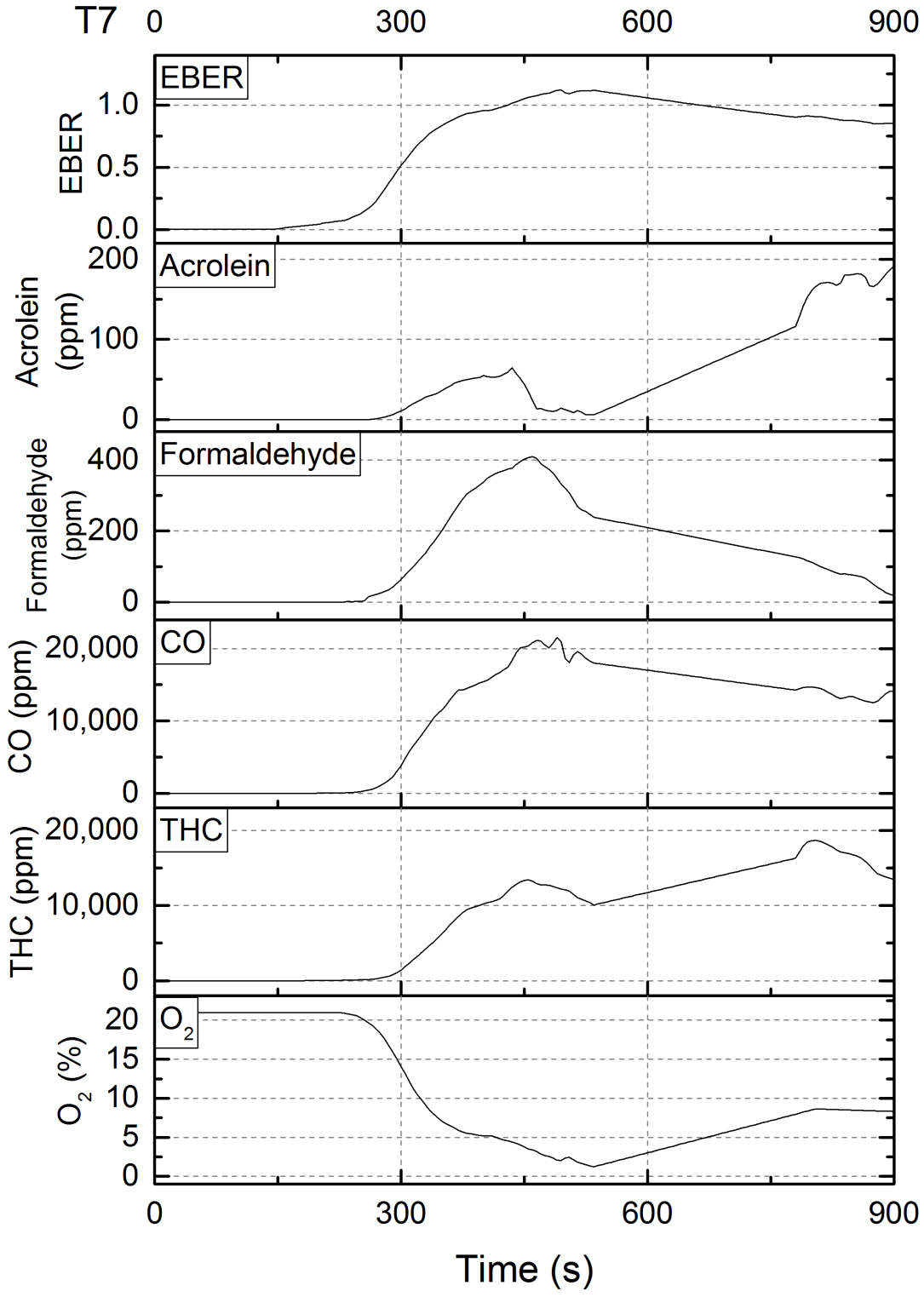

Figure 5-171: Combustion toxic products concentrations in volume basis in line with equivalence ratio and Oxygen concentration for Test 7.

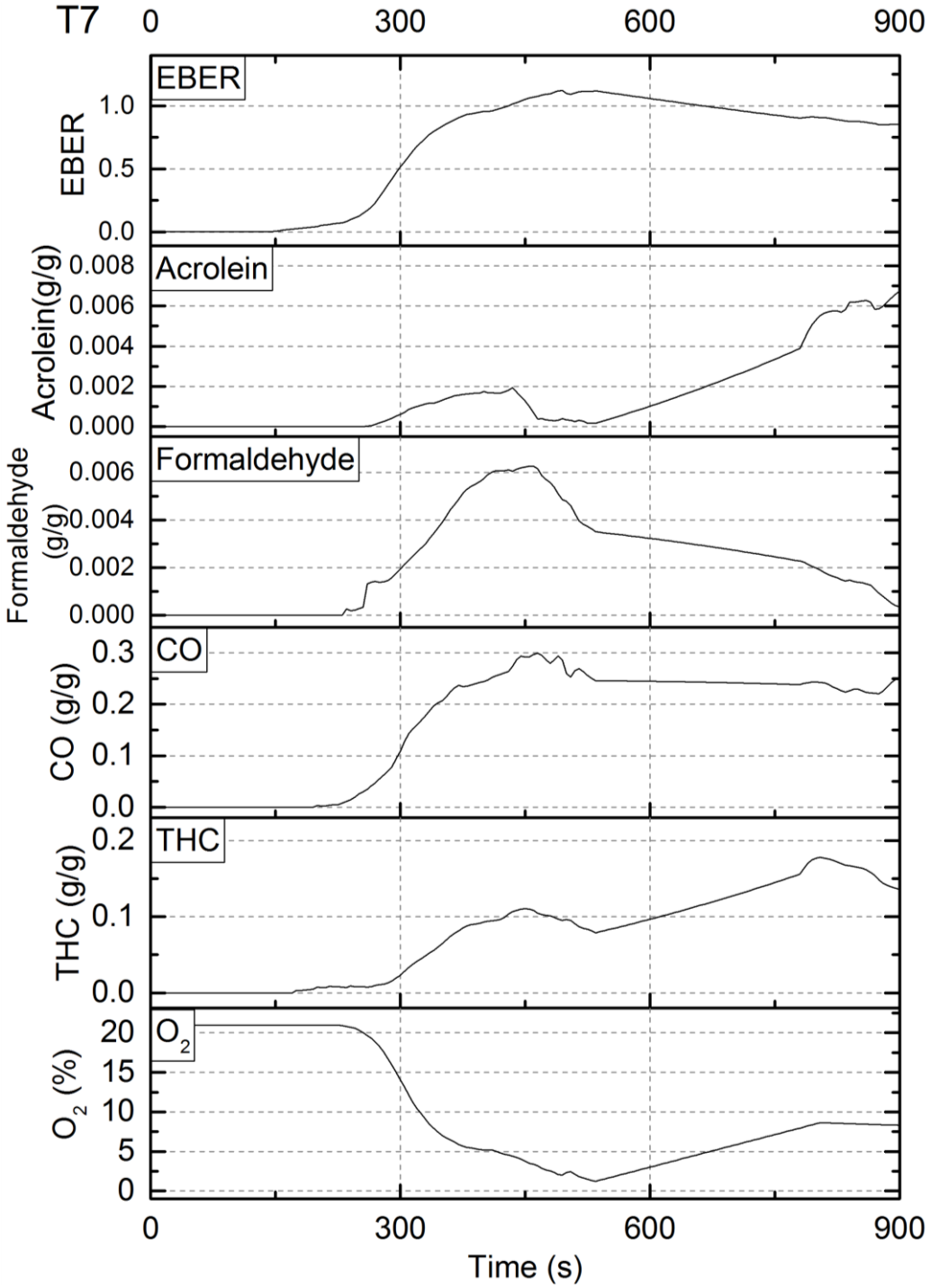

Figure 5-172: Combustion toxic products mass yields in line with equivalence ratio and Oxygen concentration for Test 7.

The instantaneous fractional effective concentration FEC for different levels were calculated in accordance with the guidelines presented earlier in section 2.3 to demonstrate the health effects of the smoke produced at the point of sampling. Firstly, FEC safe that is important for designing purposes to ensure a safe environment in protected structures such as corridors and staircases. This value (total FEC safe) is the dilution factor required to achieve a safe environment as discussed earlier in section 2.3.

Figure 5-173 presents FEC for safe level by the combustion products from Test 7 in the stacked graph (Figure 5-171). Figure 5-174 shows the composition of the contributing toxic emissions by percentage, where acrolein is the dominating contributor of the smoke influence based on the safe exposure thresholds and followed by formaldehyde.

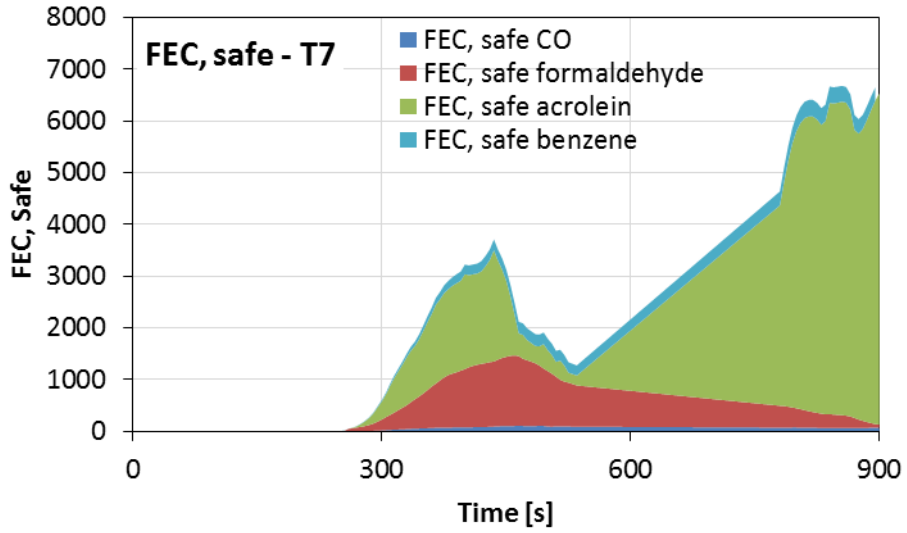

Figure 5-173: Instantaneous total fractional effective concentration (FEC) for safe level during Test 7.

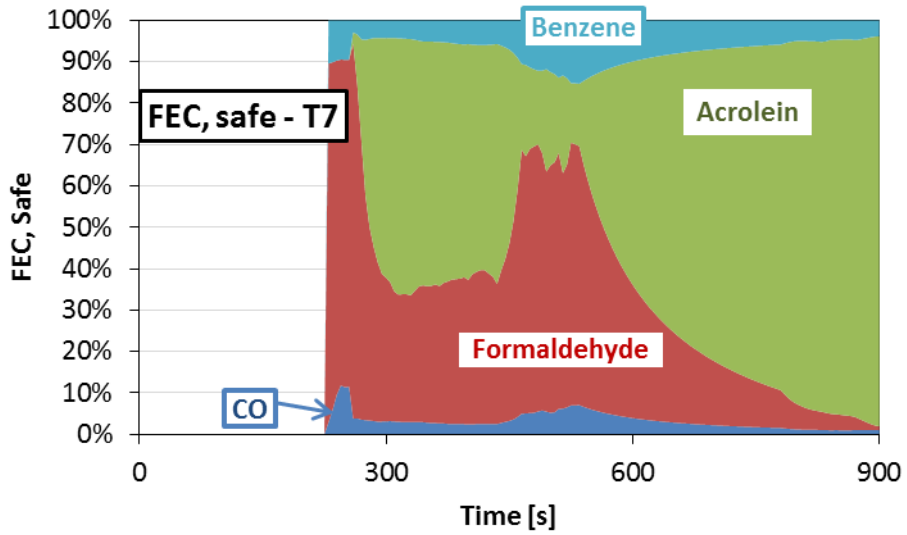

Figure 5-174: Major toxic emissions contribution by species to the fractional effective concentration for safe level in Test 7.

Secondly, FEC for escape impairment (EI) that is important for post-accident investigations to understand the development of the evacuation plan and the point where victims were

trapped. Figure 5-175 shows FEC for escape impairment from Test 7 in the stacked graph (Figure 5-171). While Figure 5-176 shows the composition of the contributing toxic emissions by percentage based on escape impairment exposure thresholds.

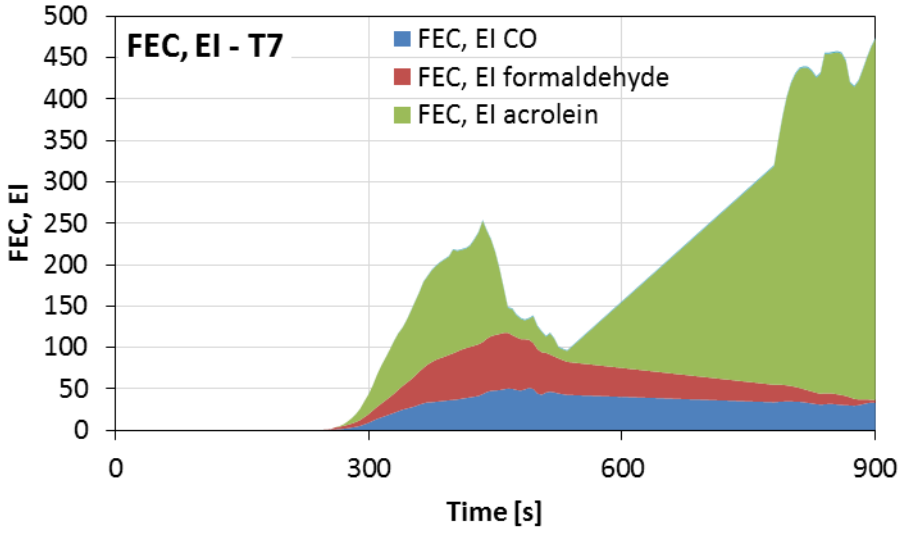

Figure 5-175: Instantaneous total fractional effective concentration (FEC) for escape impairment (EI) level during Test 7.

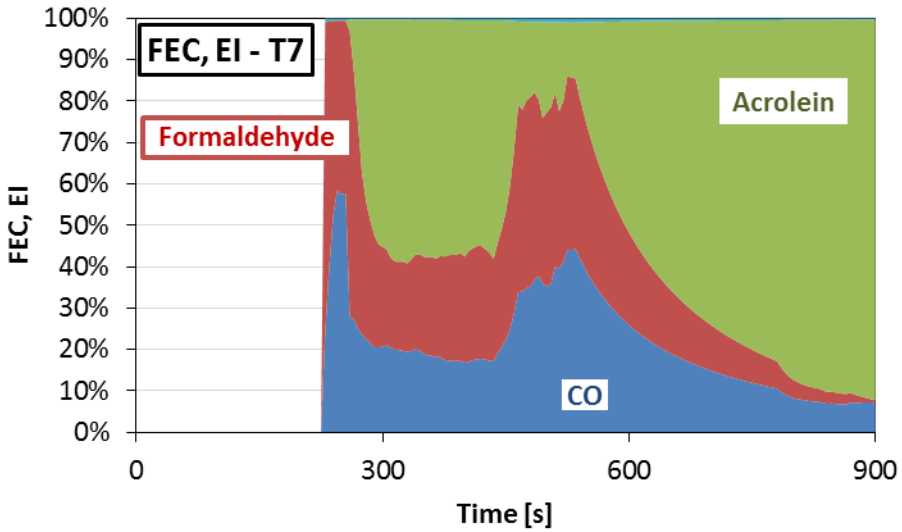

Figure 5-176: Major toxic emissions contribution by species to the fractional effective concentration for escape impairment (EI) level in Test 7.

Thirdly, FEC for lethality that is useful for post-accident investigations. Figure 5-177 shows the instantaneous FEC for lethality from Test 7 in the stacked graph (Figure 5-171). The total value for lethal FEC reached 100. Figure 5-178 shows the composition of the contributing toxic emissions by percentage based on lethal exposure thresholds discussed in section 2.3.

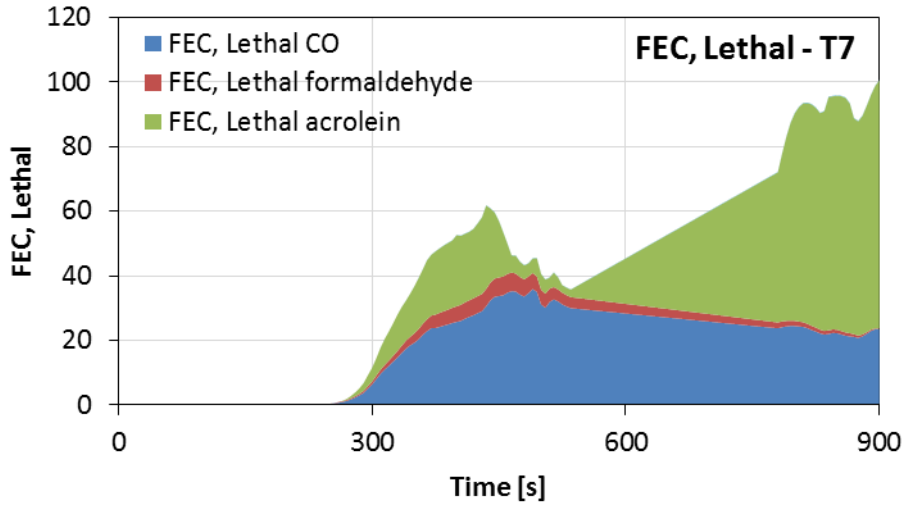

Figure 5-177: Instantaneous total fractional effective concentration (FEC) for lethal level during Test 7.

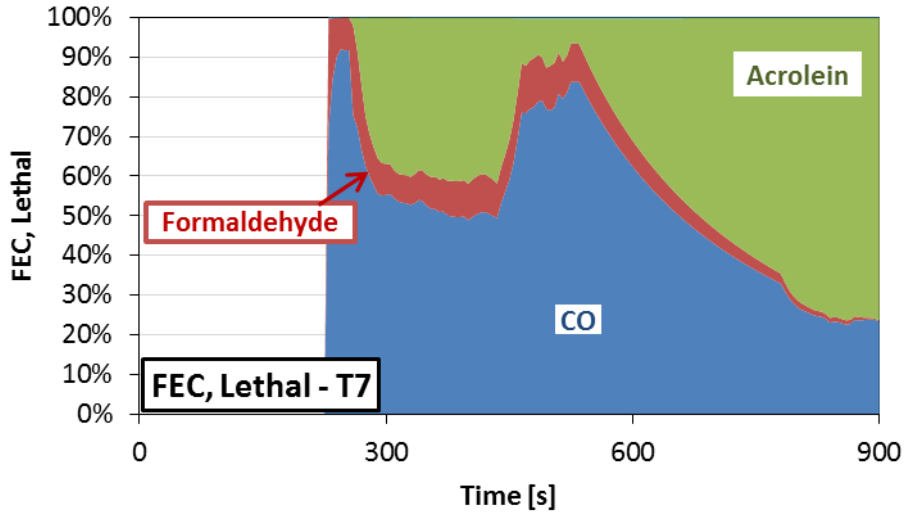

Figure 5-178: Major toxic emissions contribution by species to the fractional effective concentration for lethal level in Test 7.

Finally, FEC for lethality based on the values purposed by ISO 13344 for LC50 the lethal concentration for half the population, as discussed earlier in section 2.3. Figure 5-179 shows the instantaneous FEC for lethality (based on LC50) from Test 7 in the stacked graph (Figure 5-171). The total value for lethal FEC peaked reaching values larger than 4. Figure 5-180 shows the composition of the contributing toxic emissions by percentage based on lethal exposure thresholds of LC50. The comparison between FEC for lethality based on the most conservative threshold shown in Figure 5-177 and Figure 5-178 on one hand and FEC for lethality based on LC50 shown in Figure 5-179 and Figure 5-180 on the other, is important to demonstrate the difference between the two. As discussed earlier in section 2.3, the most conservative threshold database for lethality used was AEGL-3_{30min} is defined to be

the minimum exposure to cause life-threatening health damage or death, while LC50 is defined to be the concentrations that cause death to half the population.

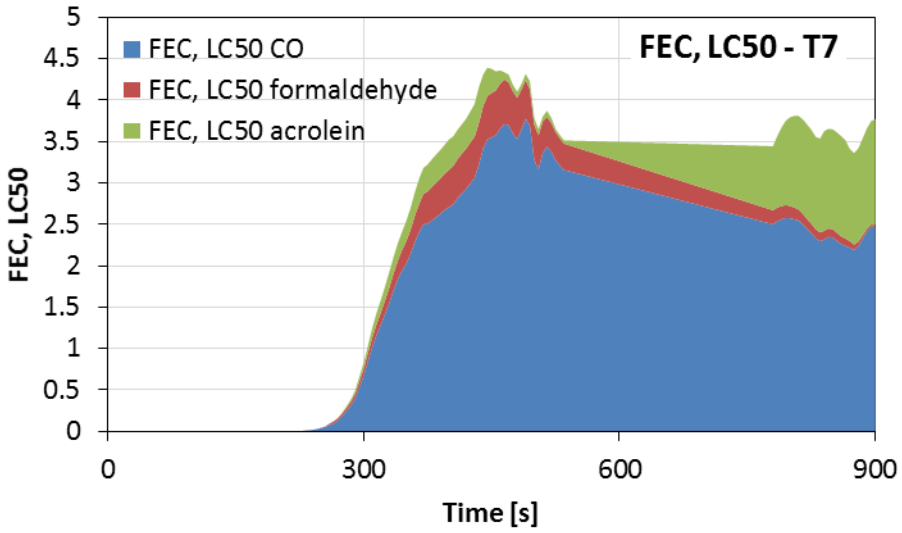

Figure 5-179: Instantaneous total fractional effective concentration (FEC) for lethal level (using LC50 values) during Test 7.

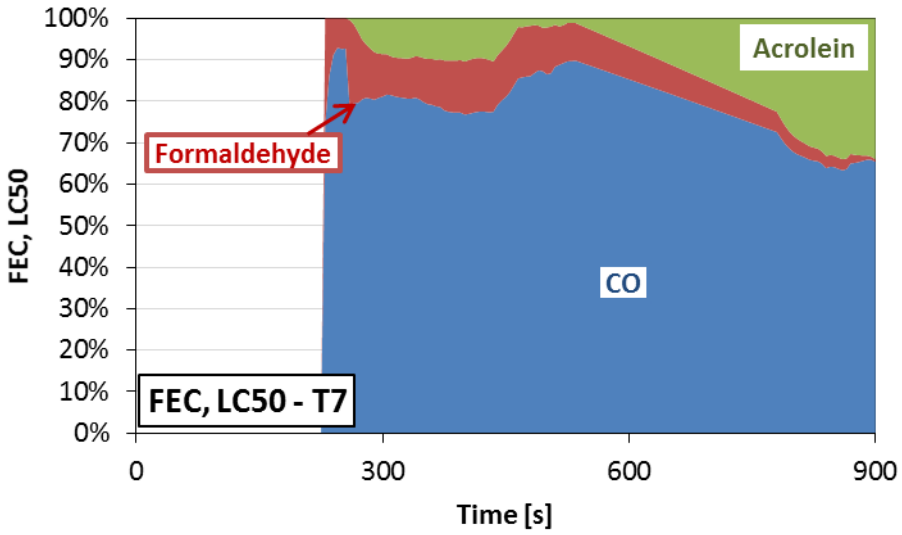

Figure 5-180: Major toxic emissions contribution by species to the fractional effective concentration for lethal level (using LC50 values) in Test 7.

Chapter 6
Small Scale Testing – Modified Cone Calorimeter

Utilising bench-scale testing apparatuses in establishing toxic yield data is required for assessing toxic hazards from different materials. As discussed in the literature section 2.5,

6.1 Investigation into the introduction of the raw sampling to the standard open cone calorimeter by using the chimney

Series of tests were conducted to investigate the effects of introducing the raw sampling support in the form of a chimney as shown in Figure 6-1. The main benefit of installing the chimney, beside enabling raw sampling, is to restrict any further dilution till the combustion products are cooled to inactive temperatures in order to minimise or eliminate any post reactions from the diluting air. This chimney is made of stainless steel with an internal diameter of 8 cm and height of 21 cm. Two thermocouples have been added to detect any invisible combustion or exothermic reactions in the chimney or the hood space. The first (chimney) thermocouple was added in the chimney at a fixed location 90 mm above the raw sampling point. The second (hood) thermocouple was added in the space above the centre of the chimney and has adjustable location in respect to the top of the chimney. The position of this thermocouple is critical, as it is important to measure the space when the exhaust flow interacts with air entrained in the hood as early as possible.

The work was carried out for the freely ventilated fire using pine wood (determined elemental formula $CH_{1.6}O_{0.73}$ with stoichiometric air to fuel ratio $AFR_{st}=5.62\ g_{air}/g_{fuel}$) as the fire load in the form of five 20×20 mm square 100 mm long sticks of pine wood side by side in the sample holder subjected to the heat radiated by the conical heater.

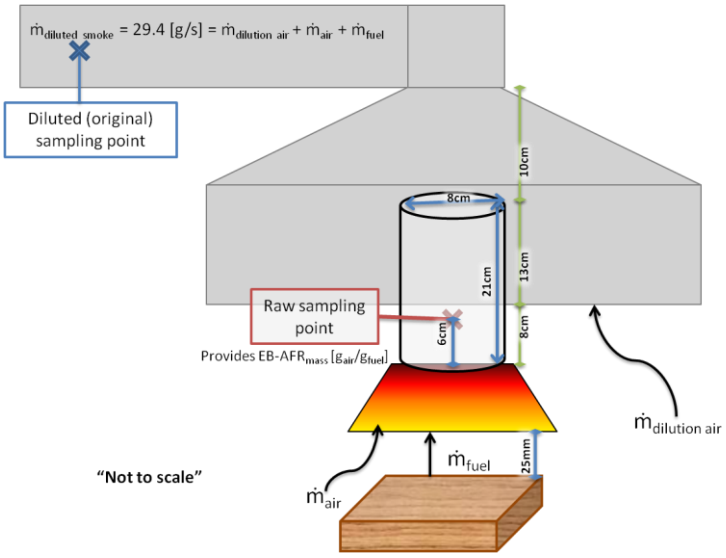

Figure 6-1: Mass flow balance for the cone calorimeter with the chimney.

6.1.1 Determination of dilution ratio and the flow through the chimney.

Using the emission based equivalence ratio model, ratio between fuel and air is multiplied by the fuel MLR to quantify air flow rate. The mass flow through the chimney = mass of air + fuel volatiles

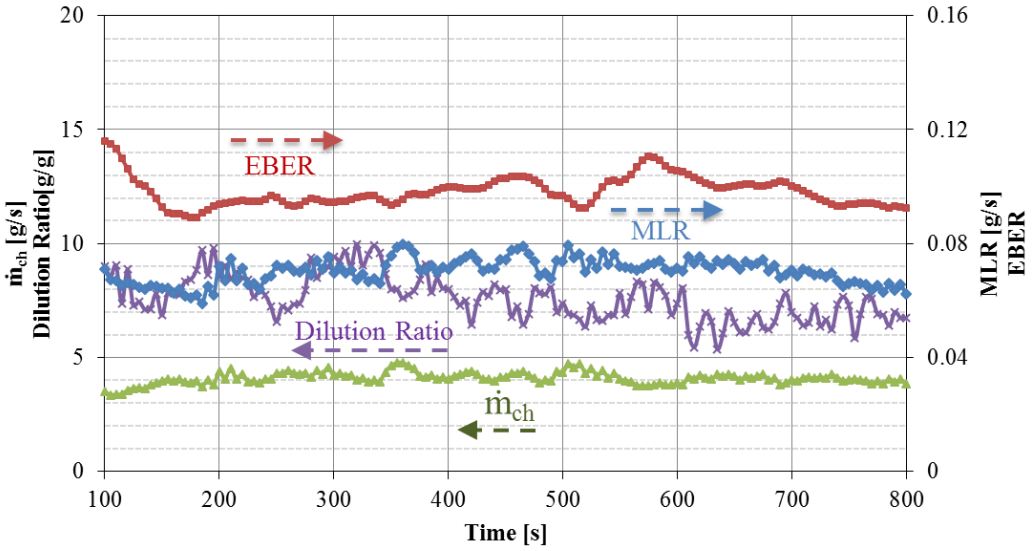

Figure 6-2: Standard cone calorimeter test for burning pine wood sample with 50kW/m2 heat flux and chimney positioned above the conical heater. The graph shows the steady state period (post 100s), the Dilution ratio factor (between raw and standard diluted sampling points) and other related variables; MLR is the mass burning rate of the wood sample in g/s, EBER is the emission based equivalence ratio at the raw sampling point. Mass flow rate through the chimney m_{ch} in g/s was measured based on F/A ratio derived from EBER and MLR. Dilution ratio was measured by dividing mch by total mass flow rate measured at the standard diluted sampling point of the cone calorimeter.

In this work the air flow through the cone (and chimney) was calculated using the EBER of the combustion products to find the air to fuel ratio EB-AFR. Using the MLR data, the air entering the cone would be assumed to equal the air involved in the combustion plus the mass of products from the fuel.

Figure 6-2 shows a time dependent functions for air flowing through chimney, dilution ratio and MLR. Furthermore, average EB-AFR for the test was found 50.9 g_a/g_f and the average MLR was 0.07 g/s giving an average air flowing through chimney of 3.56 g/s. accordingly average mass flow ratio (dilution ratio) at the two sampling points was 8.1.

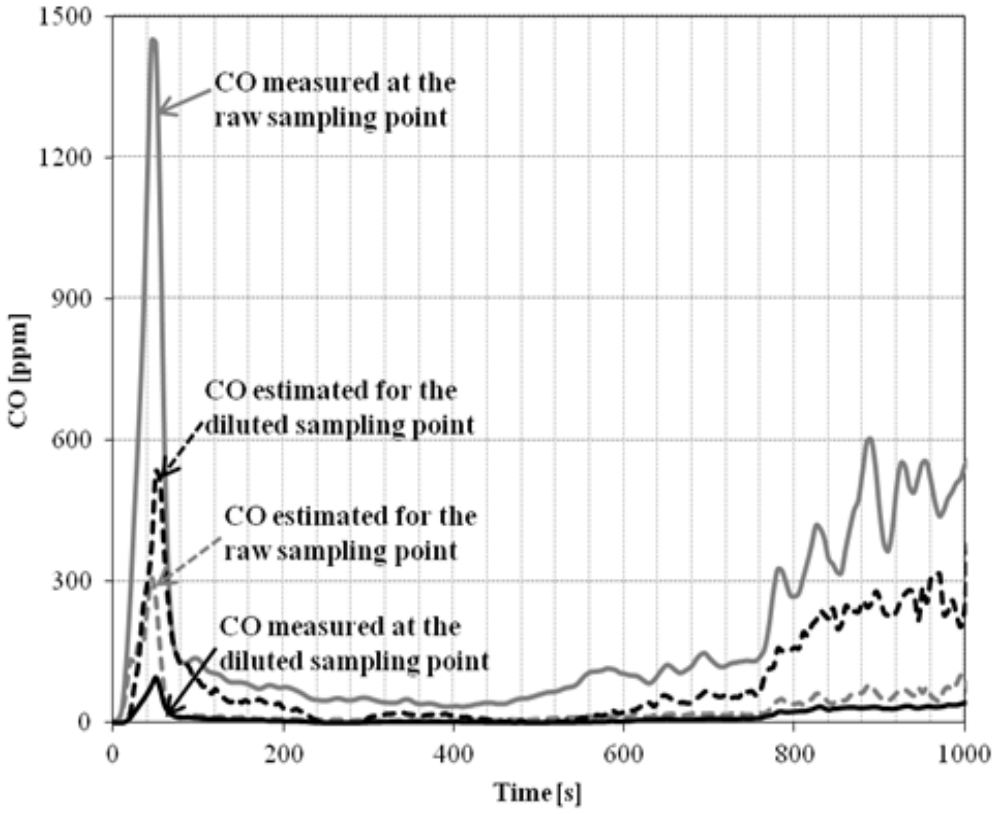

Figure 6-3: CO actual concentrations at diluted and raw sampling points with estimated concentrations using the dilution ratio factor.

It is important to highlight that mass flow ratio found, depends on the rate of air supplied to the combustion area and can be influenced by different setups (e.g. using controlled atmosphere box) the mass flow dilution ratio can be higher by a factor of 50 depending on the air supplied to the box. To evaluate the use of such a characteristic quantity (mass flow based dilution ratio), CO measurements from diluted and raw sampling points for the same test were compared. In Figure 6-3 the average mass flow based dilution ratio between the two sampling points was used to estimate the concentration of CO at the both points and to be compared with actual measurements. The results show that he estimated CO concentration for the raw sample was lower than what was measured, this is an evidence of post-oxidation.

6.1.1.1 Influence on ignition time

To assess the effect of the chimney addition on the tests results, two tests setups were used, with and without the chimney, using the standard test setup for the same fire load (five pine wood sticks) and the primary results were compared to assess the effect of the chimney on the combustion. Auto-ignition time is recorded manually when a visible flame is seen. It is a key indicator for the combustion behaviour. Results shown in Table 5 2 suggests that adding the chimney would delay auto-ignition time, which is attributed to the enhancement of air

entrainments through the cone and chimney and above the surface of the sample creating a cooling effect.

Table 6-1: Chimney influence on ignition time

	With chimney [s]	**Without chimney [s]**
1st test	53	26
2nd test	54	26
3rd test	46	22
4th test	57	22
Average	52.5	24

6.1.1.2 Influence on the heat release rate and mass loss rate

The Heat release rate given by the cone calorimeter is based on the oxygen levels sampled from the ring sampler in the exhaust duct. Variations in the HRR would indicate variations in the way and rate oxygen is consumed by the combustion process and therefore would be a reasonable indicator of the chimney affecting the combustion process compared to the standard set-up test. A comparison between the HRR behaviour for both setups is shown in Figure 6-4. Appending the chimney would result in later ignition with a lower first peak and produce higher HRR in the steady state stage. The higher peak is a result of the earlier ignition as most of the initial decomposed fuel would burn before flowing away from the flaming space. The higher HRR in the steady state stage with chimney mounted is another result of air enhancement bringing more fresh air to the combustion space which develops the combustion more.

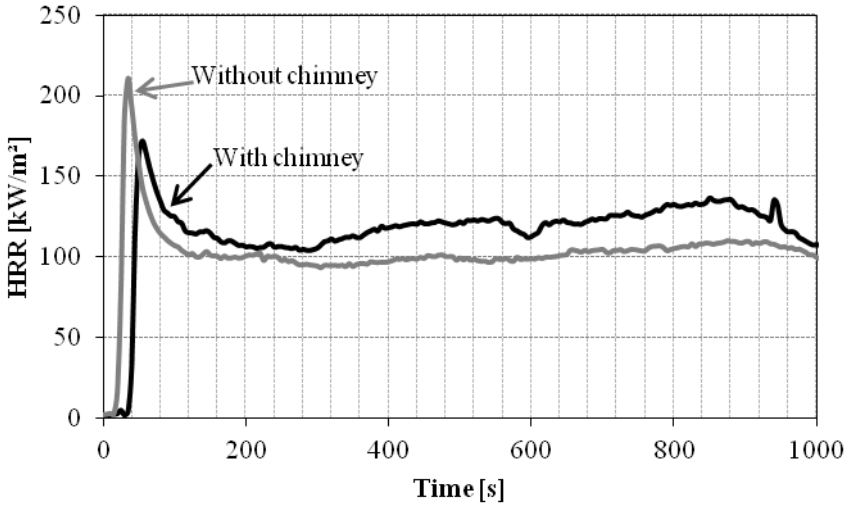

Figure 6-4: average HRR from four tests without chimney and another four tests with chimney.

The Mass Loss Rate and normalised Mass loss of the sample are based on the mass loss of the sample recorded by sensitive load cell which the sample is placed upon. It represents loss of mass from sample by devolatilisation and decomposition due to the heat from the cone and flames above the sample.

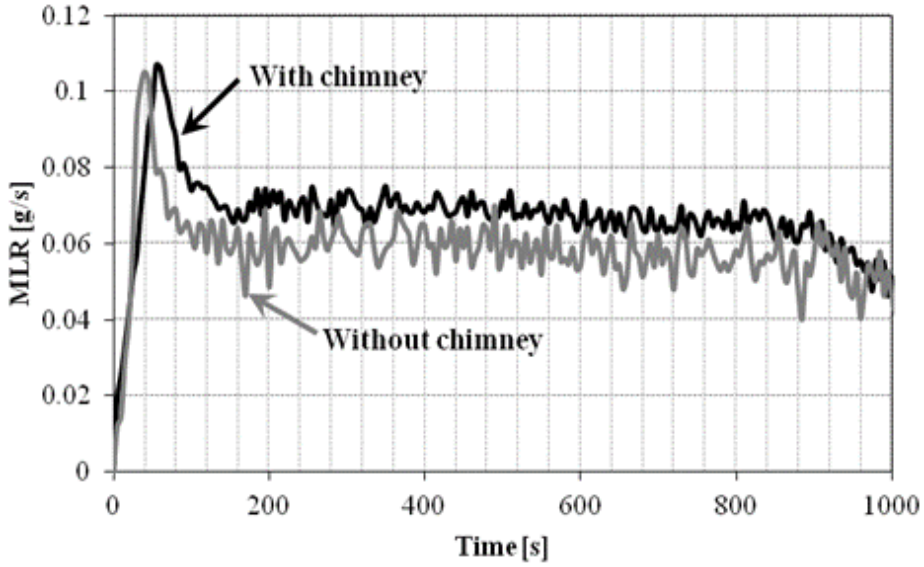

Figure 6-5: Influence of the chimney, on mass loss rates from burning pine wood in the standard cone calorimeter.

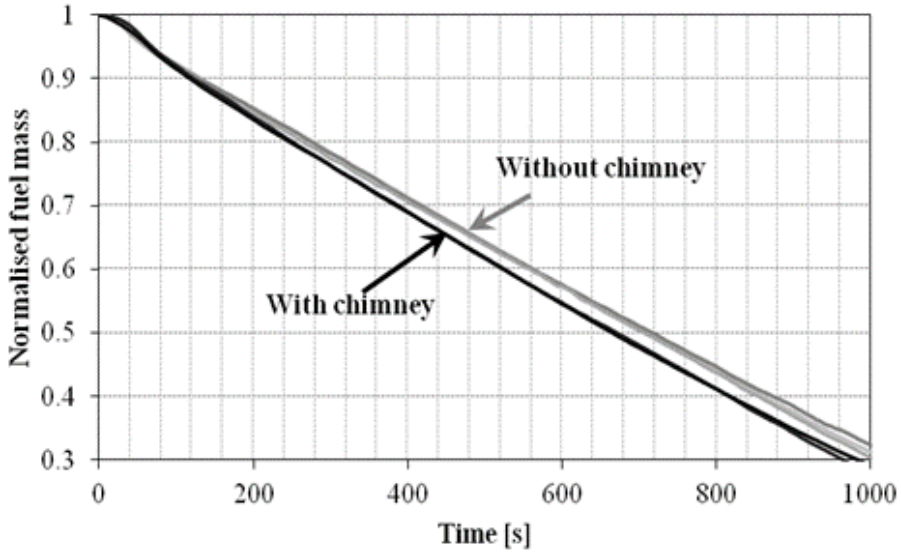

Figure 6-6: Influence of the chimney, on the normalised mass profile from burning pine wood in the standard cone calorimeter. (four tests with chimney and another four without)

The mass loss rate initial peak value was the same for both setups with a prospective delay due to ignition shown in Figure 6-5. The sample was losing mass quicker when the chimney is appended as the chimney physical effect was enhancing air movement into the combustion area causing quicker burning rate decomposing more fuel.

6.1.2 Comparison of mass yields and concentrations measured at the two sampling points

Carbon monoxide yields measured at the diluted and the raw sampling points are presented in Figure 6-7. It shows that the chimney restricts further oxidation of CO even in the diluted sample.

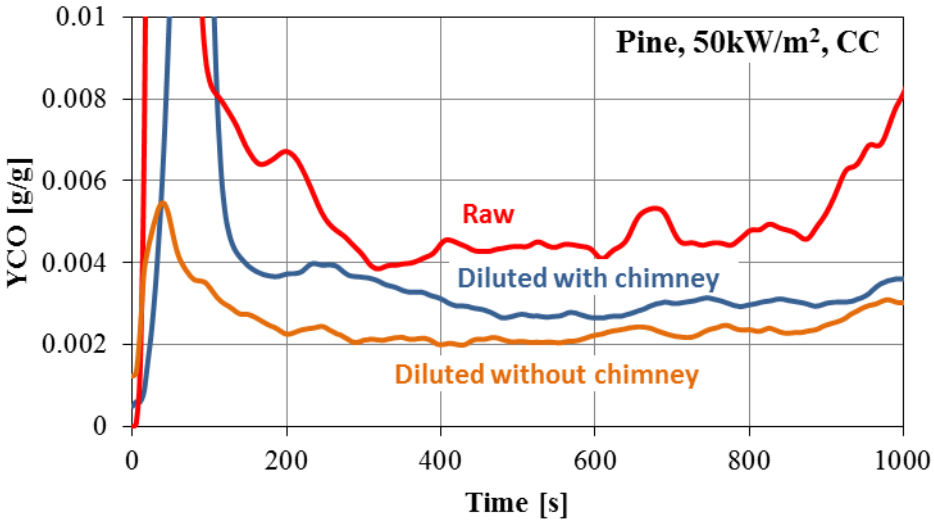

Figure 6-7: carbon monoxide mass yields measured in standard cone calorimeter test at different sampling points.

6.1.3 Temperature profile of the smoke products through the chimney

As discussed earlier in section 2.1.6, the temperature of the combustion products play a crucial part in determining the reactivity of these species for further oxidation. Temperatures measured at the point discharge from the chimney and inside the chimney are shown in Figure 6-8.

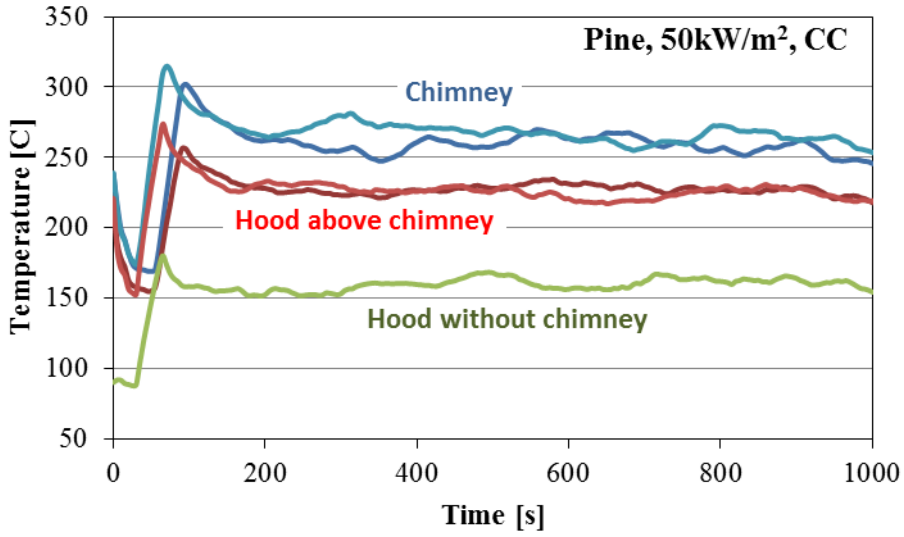

Figure 6-8: Temperatures inside the chimney and the hood (4 cm above the chimney).

6.2 Deploying the Controlled Atmosphere Cone Calorimeter (CACC)

The controlled atmosphere enclosure is used in the cone calorimeter to simulate restricted ventilation conditions. For raw sampling the chimney described above is used. However some of the above conclusions of the influence of the chimney are not applicable when used with the CACC.

First, the dilution ratio when deploying the controlled atmosphere enclosure is much higher than 8.1 found for the standard CC. This is because the supply rate of primary air to the combustion zone inside the box is restricted.

Second, the temperature variation inside the chimney and outside it is influenced by the flow rate, as with higher flow rates more heat is transferred while low flow rates lose more heat before reaching the dilution point outside the chimney as demonstrated in Figure 6-9.

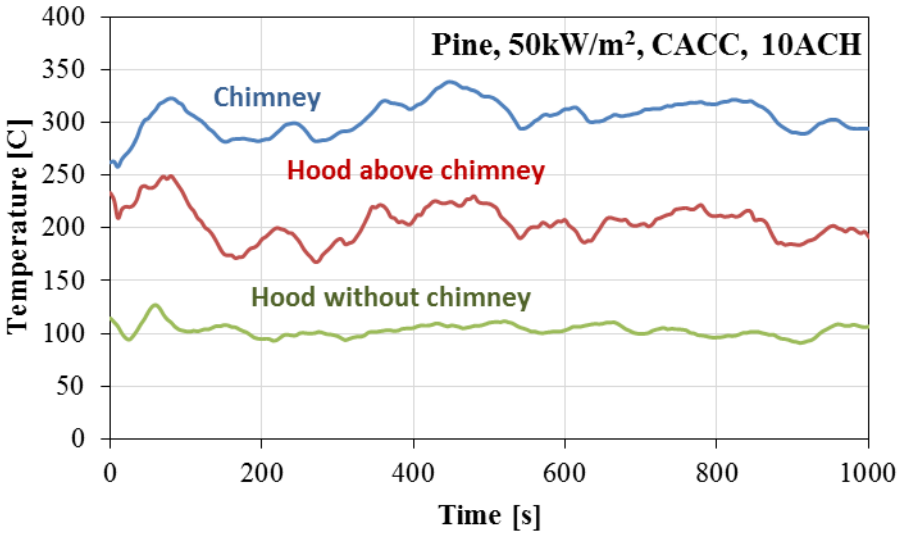

Figure 6-9: Temperatures inside the chimney and the hood (4 cm above the chimney). During CACC tests.

Third, the mass burning rate is slower due to the restriction of air supply as shown in Figure 6-10. It is shown that slower burning rates are measured with lower the air supply rate.

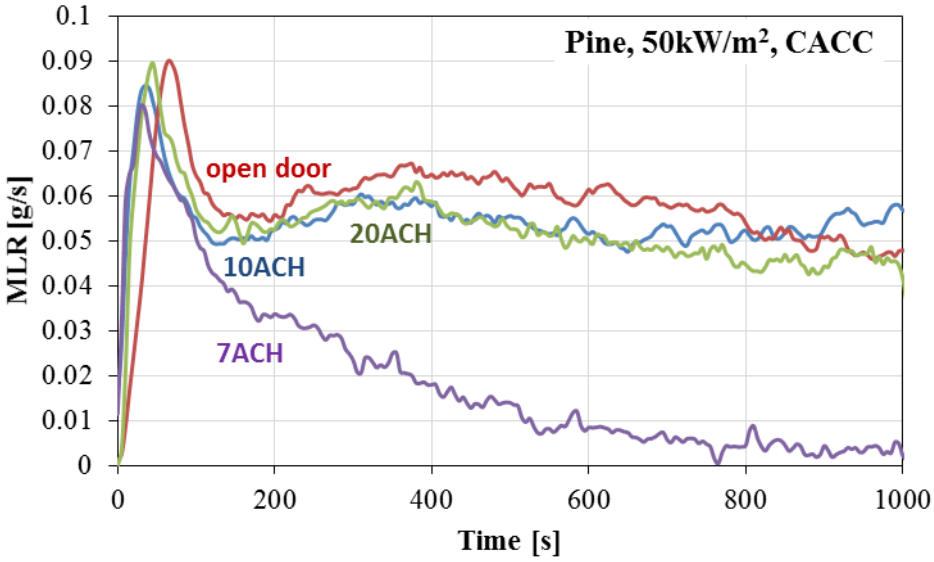

Figure 6-10: on mass loss rates from burning pine wood in CACC at different ventilation conditions.

Fourth, quicker ignition times are observed when deploying the controlled atmosphere enclosure, see. This caused by the lower flow rate around the sample, causing higher temperatures and volatiles produced not driven away as quickly as the open fire.

Table 6-2: Ignition times for burning wood in CACC at different ventilation conditions

	Ignition time [s]	Flameout time [s]
Open door	52	1,458
20 ACH	16	2,047
10 ACH	9	1,387
7 ACH	4	324

Finally, the emission based equivalence ratios measured in the CACC (see Figure 6-11) are higher than those measured in the open standard cone calorimeter tests. Although the measurements observed are lean, an increase in mass yields of incomplete combustion products is observed as can be seen in Figure 6-12 for carbon monoxide, Figure 6-13 for mass yield of formaldehyde, and Figure 6-14 for mass yields measurements of total hydrocarbons.

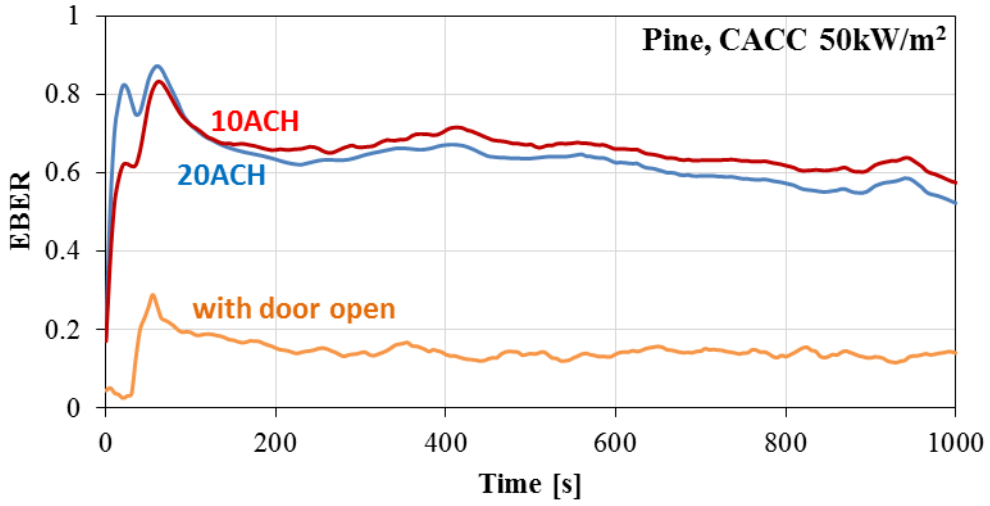

Figure 6-11: Emission based Equivalence ratio measured in CACC at different ventilation conditions.

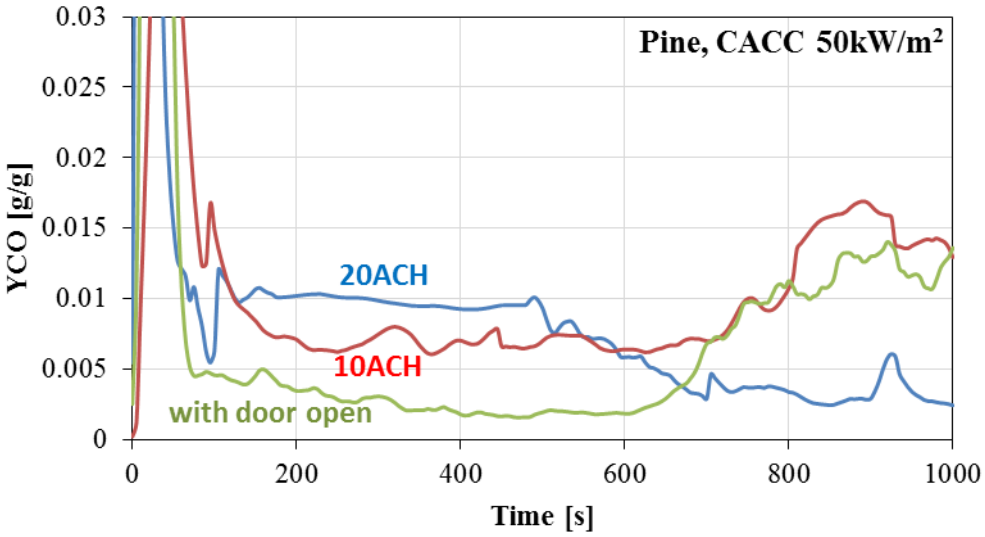

Figure 6-12: yields of carbon monoxide measured in CACC at different ventilation conditions.

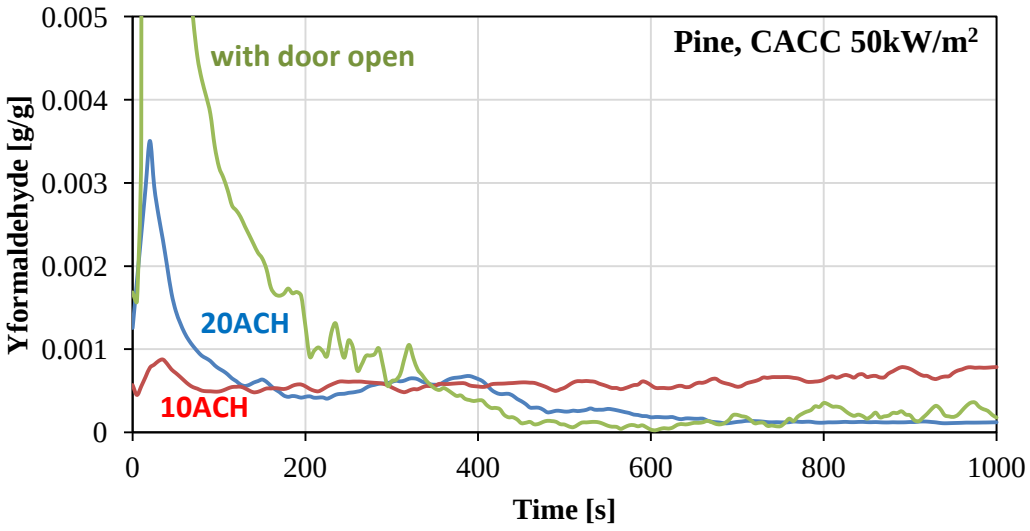

Figure 6-13: yields of formaldehyde measured in CACC at different ventilation conditions.

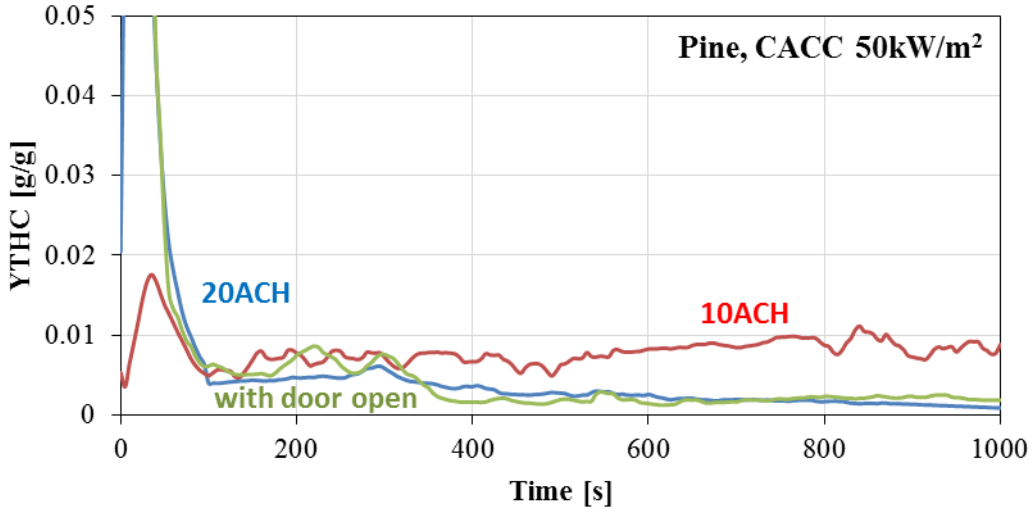

Figure 6-14: yields of total hydrocarbons measured in CACC at different ventilation conditions.

Chapter 7
Comparison of Toxic Product Yields from Small Scale to Full Scale Wood Burning Tests

The mass yields of major toxic emissions produced from burning wood at different scales measured in this work were compared with other measurements in the literature at different scales. These sources are

- Firstly, four sets of yield data for different fire species were reported by Aljumaiah et al. [242] from burning wood in a 1.6m^3 fire compartment at different (metered) air supply rates. As discussed earlier, only tests with 11, 21, and 37 ACH achieved fully developed flaming fires, while the 5 ACH test self-extinguished after burning 15% of the mass.
- CO yield data reported by Gottuk et al. [246] from burning wood in the 2.2m^3 compartment.
- Beyler's 1.6m^3 hood [65] where by controlling the supply of air, variation of equivalence ratios were achieved (no details of the rate of supplied air to the compartment were reported).
- Finally, widely used Tewarson empirical correlations [52], discussed in Chapter 2. Tewarson's correlations are based on yield measurements for wood, at different equivalence ratios using the bench-scale fire propagation apparatus.

Figure 7-1 shows good agreement between Tewarson's correlation and Aljumaiah's et al. data at the lower ventilation rate. However, for a significant number of data for apparently larger compartments and/or larger ventilation rates there is significant deviation from Tewarson's correlation which starts at equivalence ration of 0.5 and higher where the correlation significantly underpredicts the data. There is good agreement between the present data and those of Gottuk and Beyler for equivalence ratios of 0.5 to 1.3. Their data does not extend beyond Φ of 1.6 while the pre-sent data extend up to Φ of approximately 2, where yields of CO approaching 0.3 were measured. Some of Aljumaiah's data at the highest ventilation rate give comparable yields but at much higher Φ of 2.5.

Figure 7-2 shows the total hydrocarbon yields and shows reasonable agreement of the Tewarsons correlation with the reported data only at ϕ of 1.6 to 1.8. However, at lower ϕ the correlation shows lower THC yields than the other experimental data. The majority of the experimental data show no yields exceeding 0.05 even at high equivalence ratios while the Tewarson correlation exceeds this apparent threshold yield value

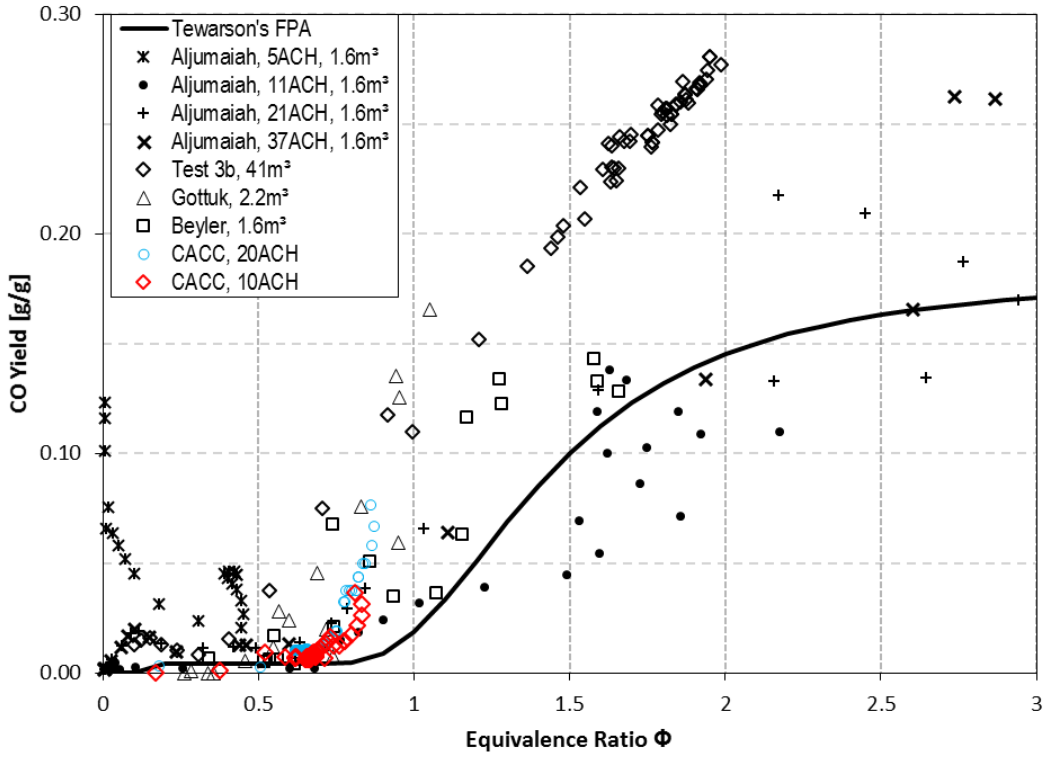

Figure 7-1: Carbon monoxide yields as a function of equivalence ratio for the present experiment compared to other wood yield data from smaller compartment tests [242, 246] and to Tewarson's correlation [52].

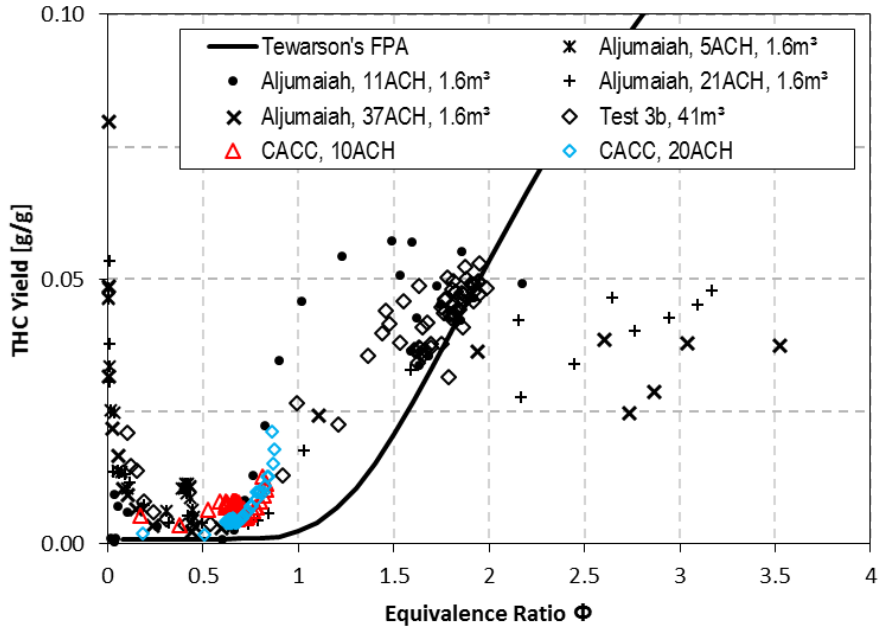

Figure 7-2: Total hydrocarbon yields as a function of equivalence ratio for the present experiment compared to other wood yield data from smaller compartment tests [242, 246] and to Tewarson's correlation [52].

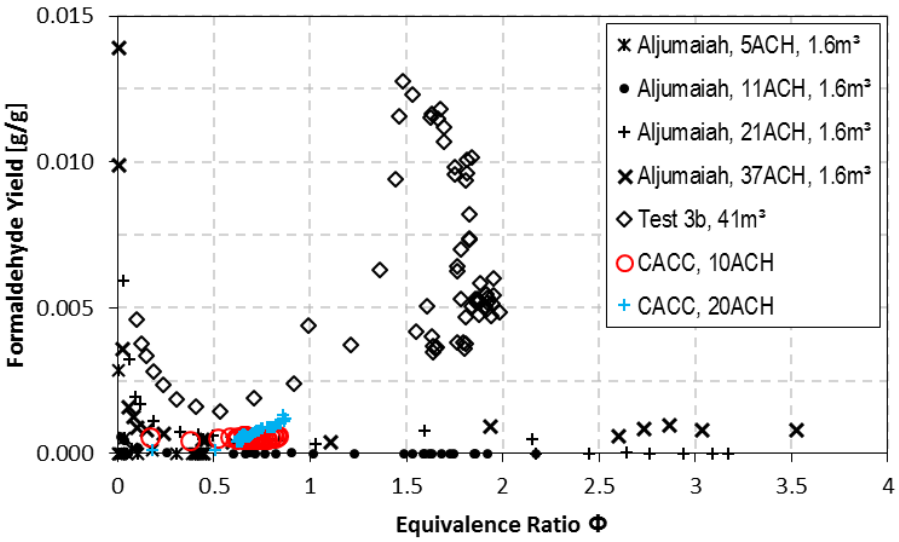

Figure 7-3: Formaldehyde yields as a function of equivalence ratio for the present experiment compared to other wood yield data from smaller compartment tests [242, 246].

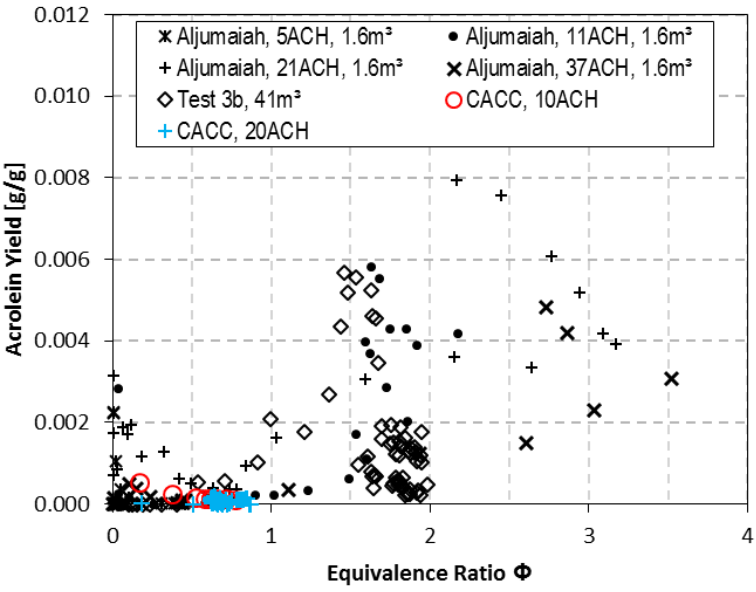

Figure 7-4: Acrolein yields as a function of equivalence ratio for the present experiments compared to other wood yield data from smaller compartment tests [242, 246].

Figure 7-3 shows that formaldehyde yields at the full scale tests were higher than those measured in the small scale wood tests. The small scale tests did not produce data at ER>1. As an oxygenated hydrocarbon, formaldehyde usually forms at lower temperatures and with the excess of oxygen in the reaction. It can be seen that this is supported at high equivalence ratios by Aljumaiah's data but the present data from the Jersey test show high formaldehyde yields for ER values between 1 and 2 and peaking at ER of 1.5.

Figure 7-4 shows good agreement between the full scale acrolein yields data and the reduced 1.6 m^3 compartment yields. Since acrolein would only form at low temperatures,

the size of the compartment and its effect on the temperature was not a significant influence on the production of acrolein.

Valuable full scale toxic yield measurements are reported as a function of equivalence ratio for a wood compartment fire with one door open. CO, acrolein, formaldehyde and unburnt hydrocarbons were the main toxic species produced by this compartment wood fire. The concentrations of the first three emissions in the layer were several times higher than the threshold limits for incapacitation and death. Good agreement was demonstrated between CO yields from the present tests and other data in the literature for equivalence ratios of 0.5 and 1.3 and these were higher than the widely accepted Tewarson correlation results for the same fuel. The present CO yields reached a maximum approaching 0.3 g/g which is significantly higher than those recommended in the standards and used in fire modelling. For the THC yields the Tewarson correlation was in agreement over a narrow range of Φ of 1.6 to 1.8, and was lower than the other data for lower Φ, while it showed significantly higher yields for THC at values of Φ higher than 2, where all the other data suggested that yields THC were limited to below 0.05 g/g.

Yields reported here are important for modelling fires in buildings for the purpose of assessing the hazard associated with fire effluents and its influence on the means of escape.

The modified enclosed cone calorimeter tests struggled to produce environments with ER larger than 1. The yield data at lower equivalence ratios show good reasonable agreement with the other datasets.

Chapter 8
Conclusions and future work

8.1 Main findings and conclusions

The literature review established that fire toxicity is governed by three factors; Equivalence ratio, temperature and fuel type. Wood was found to be the most common fuel in residential buildings. The need for an emission based equivalence ratio was established. Assessments methods for toxic hazards from fires were reviewed and a new approach with four different levels of harm was proposed and used in the experimental part of the thesis. The review of the common testing and measurement models were reviewed and the potential held by the bench scale testing apparatus controlled atmosphere cone calorimeter CACC was highlighted. A database of published experimental toxic yields was constructed highlighting the lack of data for large scale experiments, restricted ventilation rates, and mass yields of irritant gases.

The experimental sampling difficulties and the advantages of heated sampling systems allowing for raw sampling of combustion products were discussed. Such sampling techniques combined with more accessible FTIR gas analysis systems offers a powerful analytical capability for species emissions in transient fire analysis and this is the main instrumentation that was used in this work..

An emission based equivalence ratio (EBER) model suitable for the more complex fuels encountered in fire research was developed and validated. By quantifying the mass based fuel to air ratio (or air to fuel ratio) from the measured volumetric species concentration then toxic mass yields can be determined without the need to collect and meter the flows in and out or even the mass burning rates. usually achieved by having collecting hood with a constant blowing fan.. The use of EBER is demonstrated in the experimental work and it opens up the capability of producing toxic yields in wider range of tests.

8.1.1 Main findings from the full scale tests

The Jersey full scale tests burning **wooden pallets** resulted in the following main findings,

- The first part of Test 3 (T3a), had the door closed, the fire extinguished itself after consuming the oxygen in the room peaking at 700 kW. That fire produced toxic combustion products with a combined harm level 256 times the lethal threshold limit.

- The second part of Test 3 (T3b) with the door open, freely supplying air to the fire, it reached flashover conditions within 155 seconds from ignition transferring the fire from lean, fuel-controlled to ventilation-controlled, rich fire.
- The thermal environment of T3b was analysed during the fire-fighting activities concluding that if the fire fighters were delayed inside by 10 seconds, their protective equipment (PPE) could have been damaged.
- The toxic environment was influenced by the fire-fighting activities initially increasing the production of incomplete toxic combustion products due the starvation of air incurred by fire fighters blocking the only path for air supply when crawling through the corridor.
- The toxic hazards by the combustion products measured in the test were assessed using the fractional effective concentration approach for different levels, this showed that the irritant gases acrolein and formaldehyde are the major contributor for causing impairment of escape. While carbon monoxide and hydrogen cyanide were key contributor to lethality if that mixture of combustion products were inhaled by a victim.
- Test 5 was a repeat of T3b, it was found that the second target fuel pile reached a pyrolysis rate of 3.4 g/m^2s without igniting due to the reduced oxygen environment which requires the pyrolysis rate to reach higher than 7 g/m^2s. Toxic and thermal environments were similar to Test 3b.

Tests in the same compartment arrangement using **cotton linen and towels** as the main fire load (common scenario for storage rooms in residential buildings), resulted in the following main findings;

- The first part of test 1 (T1a) with the door closed, the fire produced a very toxic environment, by consuming 8.5 kg of the fire load with the available oxygen, reached toxic gas concentrations 1,300 times the impairment of escape threshold limit. This scenario is very common for fire victims who die while asleep. Then the fire slowed down to sustain a smouldering fire for about an hour. After that, the fire re-established itself when enough air was supplied after opening the door for the second part of the test (T1b).
- During the second part of Test 1 (T1b), the fire was burning lean and efficient throughout T1b and the peak HRR reached was 700 kW. The thermal environment of T1b was much cooler than those of the wooden pallets tests. The emission produced during the peak HRR was less toxic due to the efficient burning of the fire giving FEC based on LC50 less than 1 as shown in Figure 5-65.
- Test 4 used similar setup where cotton towels were the main fire load, but here other fire loads were available in the room. The fire expanded to involve storage door and curtains were fixed on the opposite wall. The involvement of these fuels yielded

different composition from toxic emissions produced in Test 1. These tests (T1 and T4) highlighted that cotton burn efficiently and produce relatively low toxic emissions while the flaming fire remains localised. However its most dangerous feature (observed in these tests) was its ability to continue burning as a smouldering fire for long times and the potential threat of spreading fire to other materials with higher potential toxic hazard, as shown in T4 in contrast to T1.

The full scale tests using **typical furniture materials** showed the following;

- With the single item test (three-person-settee) and the door closed shortly after ignition - first part of the test (T2a) - the fire behaved in the same way as in the other closed door fires where it was developing till the available oxygen was consumed, then it died down till eventually extinguished itself. After opening the door, the fire was completely out and another external ignition had to be introduced for the second part of the settee test (T2b) to start. The fire developed slowly reaching 1 MW before fire-fighting intervened to extinguish the fire. However, no flashover was reached and the fire was lean for most of the time reaching EBER of 1 just before the start of fire-fighting activities. The toxic environment contribution was dominated by the organic irritants acrolein for both parts of Test 2.
- A fully furnished living room was burnt using the same setup was used. Firstly, closing the door after ignition for the first part of the test (T8a), where the fire died down after the upper layer reached a peak temperature of 400 C. The door was opened to start the second part of the test (T8b) where the smoke was cleared from the room within few minutes however the fire needed about 10 minutes before developing into a very intense fire reaching post-flashover condition to burn on every combustible surface in the room including the carpet. In terms of the thermal conditions, it was extremely hot inside especially after flashover, where temperature measured at 0.6 m height (the supposedly cold layer) reached 800 C. Effective heat release rate was estimated to have reached 2 MW, based on temperature measurements correlated to the wooden pallets test effective HRR and temperatures measured previously. High levels of organic irritants were the leading contributor to the risk of impairment of escape, in addition contributing to lethality of the smoke alongside the asphyxiant gases CO and HCN.

The last pair of tests from the large scale experiments were **diesel pool** fires with limited ventilation, simulating oil spillage fire in a compartment for industrial application. The main findings were as follows;

- The first test (T6) had 0.23 m^3 opening in the door, allowing for enough air burn 340 kW fire. the fire lasted for about 25 minutes to burn 8.5 kg of diesel with steady state MLR of 5.5 g/s and HRR of 240 kW. The fire was burning lean during the steady state phase with EBER value of 0.7. The hottest temperature measured was

around 450 C during the steady state. High yields (for a lean fire) of unburnt hydrocarbons were observed in T6, the organic irritant acrolein was the dominant toxic hazard.

- Another test (T7) was conducted with a larger opening (0.46 m^2), allowing for more air to enter the compartment. The reached an environment with EBER just above 1, temperatures inside the compartment reached 800 C. Before stopping the test after the collapse of part of the ceiling above the fire pool, lethal levels of carbon monoxide were measured inside the room and in the corridor as well.

8.1.2 Main findings from the modified Cone Calorimeter tests

Further investigations for testing at smaller scale were conducted to explore the potential of the modified cone calorimeter (CACC). These investigations concluded the following;

- Raw sampling is very useful for bench-scale experiment for two reasons,
    - It avoids avoid low concentration measurements (below detection limit) and
    - It avoids further oxidation not part of the defined test conditions.
- Raw sampling was introduced to the standard cone calorimeter by using a chimney above the conical heater. This was shown to influence the combustion in two ways; firstly by increasing the flow through the combustion zone and chimney (the chimney effect) and secondly , by losing heat before the air mixing and dilution at the chimney exit . These effects consequently influence the MLR, HRR, dilution ratio, post-oxidation, concentrations and mass yields measured.
- The chimney influence on the controlled atmosphere cone calorimeter is different from the one with the standard cone calorimeter. The main difference is the chimney effect which is restricted by the controlled supply of air to the enclosure.
- By utilising measurements from the raw sampling point, useful mass yield data is obtained for incomplete combustion products.
- The EBER analysis of the wood modified cone tests showed clearly that the set up in its present configuration was unable to produce EBER values greater than 1 which would be representative of the full scale ventilation controlled environments encountered in practice.

8.1.3 Comparison of toxic yields at different scales

Finally a comparison of mass yields of major toxic emissions produced from burning wood at different scales measured in this work were compared with other measurements in the literature. And it was concluded that,

- It was possible to measure comparable carbon monoxide and total hydrocarbons yields in smaller scale tests for lean fires. However rich fires are harder to reproduce in the small l scale tests considered here.

- It was even more difficult to measure organic irritants in the bench sale testing especially if dilution was part analysis system.

8.2 Recommendations and future work

Emission based equivalence ratio (EBER) is a very useful tool for fire research and its wider adoption would allow for flexibility of measurements from different positions within standard tests or real scale experiments. The value of the tool should be demonstrated to the community through more publications of analysed data.

Raw sampling has many advantages, however it needs careful understanding of the implications of such sampling points and certain experimental requirements such as heating sampling systems are very important for a meaningful measurements.

Smoke particulates produced from fires have acute effects of reducing visibility. Also, those particulates can act as carrier for other toxic chemical emissions and metals adsorbed on its surface, which poses a long term health hazard for those exposed to fire regularly (e.g. fire-fighters) and also for reduction of air quality as a result of large fires that sustain themselves for lengthy periods (e.g. wild fires and industrial disasters). Developing analysis method for measuring particulates and adsorbed chemicals from different fire conditions and fuels is an important step to enable assessing such hazard.

The Full scale tests in this work provide very detailed analysis of real fires that are rarely reported in the literature to this depth. The data lends itself to using CFD modelling for validation of developments in modelling toxic emissions and calculated toxic yields.

The toxic exposure assessment method, used throughout this thesis for demonstrating the influence smoke products to achieve different threshold levels - from safe to lethal is very useful for fire safety design purposes as well as for forensic fire investigation purposes. It requires further validation and refinement, as well as developing a consensus and acceptance amongst the interested parties.

The modified controlled atmosphere cone calorimeter has not fulfilled its expectations based on the current state of development. It is the author's opinion that the potential for a useful bench scale tool remains and but requires further careful analysis of the data produced so far and consequent further modification to the apparatus and the methodology.

Appendix A

Wood

Species	Yield [g/g]	Ventilation	Notes	Ref
CO	0.004 (red oak)	Free	FPA	[340]
	0.004 (Douglas fir)	Free	FPA	[340]
	0.005 (pine)	Free	FPA	[340]
	0.091 (DF)	Restricted	Full	[341]
	0.072 (DF)	Restricted	Full	[341]
	0.12 (DF)	Restricted	Full	[341]
	0.2 (DF)	Restricted	NBS cup furnace	[341]
	0.03-0.04 (DF)	Free	SwRI/NIST	[341]
	0.005 (DF)	Free	CC 35kW/m^2	[341]
	0.003 (DF)	Free	CC 50kW/m^2	[341]
	0.003 (DF)	Free	CC 75kW/m^2	[341]
	0.013 (DF) (avg.)	Free	Furniture Calor.	[341]
	0.012 (DF)(steady)	Free	Furniture Calor.	[341]
	0.10-0.14	Vitiated	Tube furnace	[113]
	0.005-0.01	Well-vent.	Tube furnace	[113]
	0.16(ParticleBoard)	Rest. 10L/m	CACC 50kW/m^2	[222]
	0.075 (PB)	Rest. 20L/m	CACC 50kW/m^2	[222]
	0.05 (PB)	Rest. 30L/m	CACC 50kW/m^2	[222]
	0.025 (PB)	Rest. 50L/m	CACC 50kW/m^2	[222]
	0.005 (PB)	Rest.110L/m	CACC 50kW/m^2	[222]
	0.005 (PB)	Rest.130L/m	CACC 50kW/m^2	[222]
	0.005 (PB)	Rest.150L/m	CACC 50kW/m^2	[222]
	0.005 (PB)	Rest.170L/m	CACC 50kW/m^2	[222]
	0.05-0.09 (PB)	Vitiat.10%O_2	CACC 50kW/m^2	[222]
	0.05-0.09 (PB)	Vitiat.15%O_2	CACC 50kW/m^2	[222]
	0.035 (PB)	Vitiat.17%O_2	CACC 50kW/m^2	[222]
	0.01 (PB)	Vitiat.18%O_2	CACC 50kW/m^2	[222]
	0.008 (PB)	Vitiat.19%O_2	CACC 50kW/m^2	[222]
	0.004 (PB)	Vitiat.21%O_2	CACC 50kW/m^2	[222]

	0.002-0.15 (MDF)	Rest(Varied)	Tube furnace	[204]
	0.007-0.23 (MDF)	Rest(Varied)	ISO Room	[204]
	0.050 (plywood)	Free	CC 35kW/m^2	[110]
	0.087- 0.093 (DF)	Free	CC 35kW/m^2	[259]
	0.071 - 0.092 (Ponderosa Pine)	Free	CC 35kW/m^2	[259]
	0.017-0.023 (DF)	Free	CC 15kW/m^2 no flame	[259]
	0.13 (Ponderosa Pine)	Free	CC 15kW/m^2 no flame	[259]
CO2	1.27 (red oak)	Free	FPA	[340]
	1.31 (Douglas fir)	Free	FPA	[340]
	1.33 (pine)	Free	FPA	[340]
	1.2 (DF)	Restricted	Full	[341]
	1.2 (DF)	Restricted	Full	[341]
	1.8 (DF)	Restricted	Full	[341]
	1.3-1.5 (DF)	Restricted	NBS cup furnace	[341]
	1.0-1.8 (DF)	Free	SwRI/NIST	[341]
	0.9 (DF)	Free	CC 35kW/m^2	[341]
	1.0 (DF)	Free	CC 50kW/m^2	[341]
	1.0 (DF)	Free	CC 75kW/m^2	[341]
	1.6 (DF) (avg.)	Free	Furniture Calor.	[341]
	1.6 (DF)(steady)	Free	Furniture Calor.	[341] [113]
	0.7-0.8	Vitiated	Tube furnace	[113]
	1.3-1.8	Well-vent.	Tube furnace	[204]
	0.85-1.7 (MDF)	Rest(Varied)	Tube furnace	[204]
	0.60-1.2 (MDF)	Rest(Varied)	ISO Room	[110]
	2.0 (plywood)	Free	CC 35kW/m^2	[259]
	0.9-1.0 (DF)	Free	CC 35kW/m^2	[259]
	1.15-1.47 (Ponderosa Pine)	Free	CC 35kW/m^2	[259]
	0.0 (DF)	Free	CC 15kW/m^2 no flame	[259]
	0.05-0.14 (Ponderosa Pine)	Free	CC 15kW/m^2 no flame	

Hydrocarbons	0.001 (red oak)	Free	FPA	[340]
	0.001 (Douglas fir)	Free	FPA	[340]
	0.001 (pine)	Free	FPA	[340]
	0.01-0.11 (MDF)	Rest(Varied)	Tube furnace	[204]
	0.02-0.08 (MDF)	Rest(Varied)	ISO Room	[204]
Particulates (smoke/ Soot)	0.015 (red oak)	Free	FPA	[340]
	0.015 (hemlock)	Free	FPA	[340]
	33 [m^3/kg] (DF)	Restricted	Full	[341]
	46 [m^3/kg] (DF)	Restricted	Full	[341]
	59 [m^3/kg] (DF)	Restricted	Full	[341]
	0.0024	Free	CC 35kW/m^2	[110]
	0.002-0.021 (MDF)	Rest(Varied)	Tube furnace	[204]
	0.010-0.041 (MDF)	Rest(Varied)	ISO Room	[204]
Isocyanates	$3x10^{-5}$-$4x10^{-5}$	Vitiated	Tube furnace	[113]
	$2x10^{-5}$-$3x10^{-5}$	Well-vent.	Tube furnace	[113]
HCN	0.000-0.001 (MDF)	Rest(Varied)	Tube furnace	[204]
	0.001-0.005 (MDF)	Rest(Varied)	ISO Room	[204]

Rubber

Species	Yield [g/g]	Ventilation	Notes	Ref
CO	0.067 (Nitrile rubber)	Free	CC 35kW/m^2	[110]
CO_2	1.7 (Nitrile rubber)	Free	CC 35kW/m^2	[110]
Particulates (Soot/Smoke)	0.0246 (Nitrile rubber)	Free	CC 35kW/m^2	[110]
HCN	0.006 (Nitrile rubber)	Free	CC 35kW/m^2	[110]
HCl	0.082 (Nitrile rubber)	Free	CC 35kW/m^2	[110]
SO_2	0.023 (Nitrile rubber)	Free	CC 35kW/m^2	[110]
NH_3	0.011 (Nitrile rubber)	Free	CC 35kW/m^2	[110]

Hydraulic oils

Species	Yield [g/g]	Ventilation	Notes	Ref
CO	0.097-0.10 (Cooking oil)	Free	CC 35kW/m^2	[259]
	0.055-0.093 (Cooking oil)	Free	CC 15kW/m^2 no flame	[259]
CO_2	2.2-2.3 (Cooking oil)	Free	CC 35kW/m^2	[259]
	0.61-1.3 (Cooking oil)	Free	CC 15kW/m^2 no flame	[259]

Pool fires

Species	Yield [g/g]	Ventilation	Notes	Ref
CO	0.185-0.296 (kerosene)	Rest.	Pool RSE 1.6 m^3	[244]
	0.239-0.788 (Heptene)	Rest.	Pool RSE 1.6 m^3	[244]
	0.101-0.519 (Diesel)	Rest.	Pool RSE 1.6 m^3	[244]
	0.185-0.566 (Toluene)	Rest.	RSE 1.6 m^3	[244]
Hydrocarbons	0.156-0.553 (kerosene)	Rest.	RSE 1.6 m^3	[244]
	0.019-0.326 (Heptene)	Rest.	RSE 1.6 m^3	[244]
	0.038-0.165 (Diesel)	Rest.	RSE 1.6 m^3	[244]
	0.028-0.279 (Toluene)	Rest.	RSE 1.6 m^3	[244]

Polyurethane Foam – Sandwich panels

Species	Yield [g/g]	Ventilation	Notes	Ref
CO	0.010 (flexible GM21)	Free	FPA	[340]
	0.031 (flexible GM23)	Free	FPA	[340]
	0.028 (flexible GM25)	Free	FPA	[340]
	0.042 (flexible GM27)	Free	FPA	[340]
	0.031 (rigid GM29)	Free	FPA	[340]
	0.038 (rigid GM31)	Free	FPA	[340]
	0.025 (rigid GM35)	Free	FPA	[340]
	0.024 (rigid GM37)	Free	FPA	[340]
	0.046 (rigid GM41)	Free	FPA	[340]
	0.051 (rigid GM43)	Free	FPA	[340]
	0.200 (Building products Rigid PU)	Free	FPA	[340]
	0.14 (RPU)	Restricted	Full	[341]
	0.12 (RPU)	Restricted	Full	[341]
	0.10 (RPU)	Restricted	Full	[341]
	0.2 (RPU)	Restricted	NBS cup furnace	[341]
	0.09-0.12 (RPU)	Free	SwRI/NIST	[341]
	0.06 (RPU)	Free	CC 35kW/m^2	[341]
	0.08 (RPU)	Free	CC 50kW/m^2	[341]
	0.04 (RPU)	Free	CC 75kW/m^2	[341]
	0.08 (RPU) (avg.)	Free	Furniture Calor.	[341]
	0.06 (RPU)steady)	Free	Furniture Calor.	[341]
	0.001 (PU)(no flame)	Free	CC 10kW/m^2	[342] via [343]
	0.065 (PU)	Free	CC 20kW/m^2	[342] via [343]
	0.055 (PU)	Free	CC 30kW/m^2	[342] via [343]
	0.014 (PU)	Free	CC 35kW/m^2	[110] via [343]
	0.037 (PU)	Free	CC 35kW/m^2	[259] via [343]
	0.058 (PU)	Free	CC 40kW/m^2	[342] via [343]
	0.059 (PU)	Free	CC 50kW/m^2	[342] via [343]
	0.054 (PU)	Free	CC 60kW/m^2	[342]
	0.056 (PU)	Free	CC 70kW/m^2	[342]
	0.009 (PUNIII)	Free	CC 10kW/m^2	[342]

	0.007 (PUNIII)	Free	CC 20kW/m^2	[342]
	0.003 (PUNIII)	Free	CC 30kW/m^2	[342]
	0.003 (PUNIII)	Free	CC 40kW/m^2	[342]
	0.028 (PUNIII)	Free	CC 50kW/m^2	[342]
	0.031 (PUNIII)	Free	CC 60kW/m^2	[342]
	0.023 (PUNIII)	Free	CC 70kW/m^2	[342]
	0.036 (PU)	Free	CC 10kW/m^2	[343]
	0.029 (PU)	Free	CC 20kW/m^2	[343]
	0.018 (PU)	Free	CC 30kW/m^2	[343]
	0.016 (PU)	Free	CC 40kW/m^2	[343]
	0.019 (PU)	Free	CC 50kW/m^2	[343]
	0.024 (PU) (avrg)	Free	CC 10-50kW/m^2	[343]
	0.05-0.17	Vitiated	Tube furnace	[113]
	0.07-0.09	Well-vent.	Tube furnace	[113]
	0.12 (rigid PU)	Free	CC 35kW/m^2	[110]
CO2	1.55 (flexible GM21)	Free	FPA	[340]
	1.51 (flexible GM23)	Free	FPA	[340]
	1.50 (flexible GM25)	Free	FPA	[340]
	1.57 (flexible GM27)	Free	FPA	[340]
	1.52 (rigid GM29)	Free	FPA	[340]
	1.53 (rigid GM31)	Free	FPA	[340]
	1.58 (rigid GM35)	Free	FPA	[340]
	1.63 (rigid GM37)	Free	FPA	[340]
	1.18 (rigid GM41)	Free	FPA	[340]
	1.11 (rigid GM43)	Free	FPA	[340]
	1.1 (Building products Rigid PU)	Free	FPA	[340]
	2.2 (RPU)	Restricted	Full	[341]
	1.5 (RPU)	Restricted	Full	[341]
	2.2 (RPU)	Restricted	Full	[341]
	1.6-2.6 (RPU)	Restricted	NBS cup furnace	[341]
	0.6-0.8 (RPU)	Free	SwRI/NIST	[341]
	1.1 (RPU)	Free	CC 35kW/m^2	[341]
	1.2 (RPU)	Free	CC 50kW/m^2	[341]

	1.2 (RPU)	Free	CC 75kW/m^2	[341]
	2.1 (RPU) (avg.)	Free	Furniture Calor.	[341]
	1.4 (RPU)steady)	Free	Furniture Calor.	[341]
	0.37 (PU)(no flame)	Free	CC 10kW/m^2	[342] via [343]
	3.05 (PU)	Free	CC 20kW/m^2	[342] via [343]
	2.59 (PU)	Free	CC 30kW/m^2	[342] via [343]
	2.43 (PU)	Free	CC 35kW/m^2	[110] via [343]
	1.26 (PU)	Free	CC 35kW/m^2	[259] via [343]
	2.62 (PU)	Free	CC 40kW/m^2	[342] via [343]
	2.72 (PU)	Free	CC 50kW/m^2	[342] via [343]
	2.08 (PU)	Free	CC 60kW/m^2	[342]
	2.04 (PU)	Free	CC 70kW/m^2	[342]
	2.16 (PUNIII)	Free	CC 10kW/m^2	[342]
	2.82 (PUNIII)	Free	CC 20kW/m^2	[342]
	1.95 (PUNIII)	Free	CC 30kW/m^2	[342]
	2.14 (PUNIII)	Free	CC 40kW/m^2	[342]
	2.34 (PUNIII)	Free	CC 50kW/m^2	[342]
	2.50 (PUNIII)	Free	CC 60kW/m^2	[342]
	2.21 (PUNIII)	Free	CC 70kW/m^2	[342]
	2.69 (PU)	Free	CC 10kW/m^2	[343]
	2.17 (PU)	Free	CC 20kW/m^2	[343]
	2.15 (PU)	Free	CC 30kW/m^2	[343]
	2.32 (PU)	Free	CC 40kW/m^2	[343]
	2.31 (PU)	Free	CC 50kW/m^2	[343]
	2.33 (PU) (avrg)	Free	CC 10-50kW/m^2	[343]
	1.6 (rigid PU)	Free	CC 35kW/m^2	[110]
Hydrocarbons	0.002 (flexible GM21)	Free	FPA	[340]
	0.005 (flexible GM23)	Free	FPA	[340]
	0.005 (flexible GM25)	Free	FPA	[340]
	0.004 (flexible GM27)	Free	FPA	[340]
	0.003 (rigid GM29)	Free	FPA	[340]
	0.002 (rigid GM31)	Free	FPA	[340]
	0.001 (rigid GM35)	Free	FPA	[340]
	0.001 (rigid GM37)	Free	FPA	[340]

	0.004 (rigid GM41)	Free	FPA	[340]
	0.004 (rigid GM43)	Free	FPA	[340]
	0.104 (PU)	Free	CC 10kW/m^2	[343]
	0.062 (PU)	Free	CC 20kW/m^2	[343]
	0.018 (PU)	Free	CC 30kW/m^2	[343]
	0.028 (PU)	Free	CC 40kW/m^2	[343]
	0.032 (PU)	Free	CC 50kW/m^2	[343]
	0.049 (PU) (avrg)	Free	CC 10-50kW/m^2	[343]
Particulates (smoke/ Soot)	0.131 (flexible GM21)	Free	FPA	[340]
	0.227 (flexible GM23)	Free	FPA	[340]
	0.194 (flexible GM25)	Free	FPA	[340]
	0.198 (flexible GM27)	Free	FPA	[340]
	0.130 (rigid GM29)	Free	FPA	[340]
	0.125 (rigid GM31)	Free	FPA	[340]
	0.104 (rigid GM35)	Free	FPA	[340]
	0.113 (rigid GM37)	Free	FPA	[340]
	360 [m^3/kg] (RPU)	Restricted	Full	[341]
	200 [m^3/kg] (RPU)	Restricted	Full	[341]
	270 [m^3/kg] (RPU)	Restricted	Full	[341]
HCN	0.009 (RPU)	Restricted	Full	[341]
	0.005 (RPU)	Restricted	Full	[341]
	0.011 (RPU)	Restricted	Full	[341]
	0.016-0.020 (RPU)	Restricted	NBS cup furnace	[341]
	0.002-0.004 (RPU)	Free	SwRI/NIST	[341]
	0.005 (RPU)	Free	CC 35kW/m^2	[341]
	0.005 (RPU)	Free	CC 50kW/m^2	[341]
	0.004 (RPU)	Free	CC 75kW/m^2	[341]
	0.0015 (PU)	Free	CC 35kW/m^2	[110] via [343]
	0.01-0.012	Vitiated	Tube furnace	[113]
	0.005-0.01	Well-vent.	Tube furnace	[113]
	0.014 (rigid PU)	Free	CC 35kW/m^2	[110]
NO	0.011 (Flexible PU)	Free	CC 35kW/m^2	[110] via [343]
	0.003 (PU)	Free	CC 10kW/m^2	[343]

	0.004 (PU)	Free	CC 20kW/m^2	[343]
	0.002 (PU)	Free	CC 30kW/m^2	[343]
	0.003 (PU)	Free	CC 50kW/m^2	[343]
	0.003 (PU) (avrg)	Free	CC 10-50kW/m^2	[343]
	0.003-0.004	Vitiated	Tube furnace	[113]
	0.002-0.004	Well-vent.	Tube furnace	[113]
	0.010 (rigid PU)	Free	CC 35kW/m^2	[110]
H_2O	0.92 (PU)	Free	CC 10kW/m^2	[343]
	1.54 (PU)	Free	CC 20kW/m^2	[343]
	0.61 (PU)	Free	CC 30kW/m^2	[343]
	0.78 (PU)	Free	CC 50kW/m^2	[343]
	0.96 (PU) (avrg)	Free	CC 10-50kW/m^2	[343]
Isocyanates	0.0019-0.0028	Vitiated	Tube furnace	[113]
	0.0007-0.0035	Well-vent.	Tube furnace	[113]
NH_3	0.0008-0.0011	Vitiated	Tube furnace	[113]
	0.0005-0.0011	Well-vent.	Tube furnace	[113]
HCl	0.010 (rigid PU)	Free	CC 35kW/m^2	[110]

List of References

1. DCLG, *Fire Statistics: Great Britain April 2013 to March 2014*. 2015, Department for Communities and Local Government: London.
2. FEMA, *Civilian Fire Fatalities in Residential Buildings (2011-2013)*, N.F.D.C. U.S. Fire Administration, Editor. 2015, FEMA: Emmitsburg, Maryland.
3. Drysdale, D., *An introduction to fire dynamics*. 2nd ed. 1999, Chichester ; New York: Wiley. xviii, 451 p.
4. Karlsson, B. and J.G. Quintiere, *Enclosure fire dynamics*. Environmental and energy engineering series. 2000, Boca Raton, FL: CRC Press. 315 p.
5. Quintiere, J.G., *Fundamentals of fire phenomena*. 2006, Chichester: John Wiley. xix, 439 p.
6. BS EN ISO 13943, *Fire safety — Vocabulary (ISO 13943:2008)*. 2010, British Standard Institution: London.
7. Purser, D.A., *Combustion Toxicity*, in *SFPE handbook of fire protection engineering*, M.J. Hurley, et al., Editors. 2016, Springer New York. p. 2207-2307.
8. Birky, M.M., et al., *Fire fatality study*. Fire and Materials 1979. **3**(4): p. 211-217.
9. Bright, R.G. *Reconstruction of a Tragedy: The Beverly Hills Supper Club Fire, Southgate, Kentucky, May 28, 1977. An Analysis of the Development and Spread of Fire from the Room of Fire Origin (Zebra Room) to the Cabaret Room - Appendix C, Richard Bright's Analysis*. 1977.
10. Wallace, D., *DANGERS OF POLYVINYL-CHLORIDE WIRE INSULATION DECOMPOSITION. 1. LONG-TERM HEALTH IMPAIRMENTS-STUDIES OF FIREFIGHTERS OF THE 1975 NEW YORK TELEPHONE FIRE AND OF SURVIVORS OF THE 1977 BEVERLY HILLS SUPPER CLUB FIRE*. Journal of Combustion Toxicology, 1981. **8**(NOV): p. 205-223.
11. Gregg, B.G., *Beverly Hills Supper Club Litigation*, in *Cincinnati Magazine*. 2001, Emmis Communications: Cincinnati, OH. p. 148.
12. Quaranta, R. *L'incendio al cinema Statuto di Torino, 30 anni fa*. il Post, 2013.
13. Zancan, N. *Io e il rogo allo Statuto dannazione senza fine*. la Repubblica Torino 2008 20/10/2015]; Available from: http://torino.repubblica.it/dettaglio/io-e-il-rogo-allo-statuto-dannazione-senza-fine/1414607/1.
14. tailstrike.com. *19 August 1980 - Saudi 163*. Cockpit Voice Recorder Database 2015 [cited 2015 October 20,]; Available from: http://www.tailstrike.com/190880.htm.
15. PCV, *SV 163 Aircraft Accident Report* 1980, Presidency of Civil Aviation: Jeddah, Saudi Arabia.
16. airlines.net-Aviation forums. *Manchester Airport Disaster 1985*. 2005 21/10/2015]; Available from: http://www.airliners.net/aviation-forums/general_aviation/read.main/2286529/.
17. Air Accidents Investigation Branch, *Report on the accident to Boeing 737-236 series 1, G-BGJL at Manchester International Airport on 22 August 1985*. 1988, Department of Transport.
18. Clark County Nevada Fire Department. *MGM Grand Hotel Fire - Nov. 21, 1980*. 2010 [cited 2013 January 5,]; Available from: http://www.clarkcountynv.gov/depts/fire/Pages/MGMHotelFire.aspx.

19. Best, R. and D. Demers, *Investigation report on the MGM grand hotel fire - November 21, 1980*. 1982, NFPA.
20. Emmons, H.W., *Why Fire Model - the Mgm Fire and Toxicity Testing.* Fire Safety Journal, 1988. **13**(2-3): p. 77-85.
21. Oliver, M. *MGM Grand Set to Battle Its Insurers : Case Expected to Last 8 to 10 Months, Cost $342,000 a Day to Try*. Los Angeles Times, 1985.
22. Lockhart, B., *Inquiry into the deaths of Rosepark care home fire fatalities - 31 January 2004*, Sheriffdom of South Strathclyde Dumfries and Galloway, Editor. 2011.
23. BRE Ltd, *Experimental research for Scottish Building Standards Agency following the fire at the Rosepark Care Home, Glasgow, 31st January 2004*. 2004, The Scottish Government.
24. Wallace, D., *In the Mouth of the Dragon: Toxic fires in the age of plastics*. 1990, Garden City, NY: Avery Pub Group.
25. Port, B. *Three Decades after an Infamous New York Telephone Co. Blaze, Cancer Ravages Heroes*. NY Daily News, 2004.
26. FEMA, *Civilian Fire Injuries in Residential Buildings (2011-2013)*, N.F.D.C. U.S. Fire Administration, Editor. 2015, FEMA: Emmitsburg, Maryland.
27. Purser, D.A., *Fire Toxicity and Toxic Hazard Analysis*, in *6th International Seminar on Fire and Explosion Hazards*, F. Tamanini, Editor. 2010: Univesity of Leeds.
28. DCLG, *Fire Statistics United Kingdom, 2007*. 2009, Department for Communities and Local Government: London.
29. DCLG, *Fire Statistics United Kingdom, 2008*. 2010, Department for Communities and Local Government: London.
30. DCLG, *Fire Statistics Great Britain, 2010 to 2011*. 2011, Department for Communities and Local Government: London.
31. DCLG, *Fire Statistics Great Britain, 2011 to 2012*. 2012, Department for Communities and Local Government: London.
32. DCLG, *Fire Statistics Great Britain, 2012 to 2013*. 2013, Department for Communities and Local Government: London.
33. Hall Jr, J.R., *Fatal effects of fire*, in *Quincy, MA: National Fire Protection Association*. 2011, National Fire Protection Association.
34. Forth, E., *The Furniture and Furnishings (Fire) (Safety) Regulations 1988*, in *1324*, Parliamentary Under-Secretary of State, Editor. 1988, The National Archives.
35. US Congress, *U.S. Flammable Fabrics Act*, in *Public Law 90-189*, Senate and House of Representatives of the United States of America in Congress, Editor. 1967.
36. Purser, D.A., *Toxicity Assessment of Combustion Products*, in *SFPE Handbook of Fire Protection Engineering*, P.J. DiNenno, Editor. 2002, National Fire Protection Association & Society of Fire Protection Engineers: Quincy, Mass. & Bethesda, Md.
37. BS 7974, *Application of fire safety engineering principles to the design of buildings — Code of practice*. 2001, British Standards Institution: London.
38. PD 7974-0, *Application of fire safety engineering principles to the design of buildings — Part 0: Guide to design framework and fire safety engineering procedures*. 2002, British Standards Institution: London.

39. PD 7974-1, *Application of fire safety engineering principles to the design of buildings - Part 1: Initiation and development of fire within the enclosure of origin (Sub-system 1)*. 2003, British Standards Institution: London.
40. PD 7974-2, *Application of fire safety engineering principles to the design of buildings — Part 2: Spread of smoke and toxic gases within and beyond the enclosure of origin (Sub-system 2)*. 2002, British Standards Institution: London.
41. PD 7974-3, *Application of fire safety engineering principles to the design of buildings — Part 3: Structural response and fire spread beyond the enclosure of origin (Sub-system 3)*. 2003, British Standards Institution: London.
42. PD 7974-4, *Application of fire safety engineering principles to the design of buildings — Part 4: Detection of fire and activation of fire protection systems (Sub-system 4)*. 2003, British Standards Institution: London.
43. PD 7974-5, *Application of fire safety engineering principles to the design of buildings — Part 5: Fire and rescue service intervention (Sub-system 5)*. 2014, British Standards Institution: London.
44. PD 7974-6, *Application of fire safety engineering principles to the design of buildings — Part 6: Human factors: Life safety strategies — Occupant evacuation, behaviour and condition (Sub-system 6)*. 2004, British Standards Institution: London.
45. Purser, D.A., *Hazards from smoke and irritants*, in *Fire Toxicity*, A. Stec and R. Hull, Editors. 2010, Woodhouse Publishing Ltd.: Cambridge.
46. Purser, D.A., *Application of human and animal exposure studies to human fire safety*, in *Fire Toxicity*, A. Stec and R. Hull, Editors. 2010, Woodhouse Publishing Ltd.: Cambridge.
47. Purser, D.A., *Toxic hazard calculation models for use with fire effluent data*, in *Fire Toxicity*, A. Stec and R. Hull, Editors. 2010, Woodhouse Publishing Ltd.: Cambridge.
48. Gwynne, S.M.V., D. Purser, and D.L. Boswell, *Pre-Warning Staff Delay: A Forgotten Component in ASET/RSET Calculations*, in *Pedestrian and Evacuation Dynamics*, R.D. Peacock, E.D. Kuligowski, and J.D. Averill, Editors. 2011, Springer US. p. 243-253.
49. Babrauskas, V., J.M. Fleming, and B. Don Russell, *RSET/ASET, a flawed concept for fire safety assessment.* Fire and Materials 2010. **34**(7): p. 341-355.
50. Chow, W., *Six points to note in applying timeline analysis in performance-based design for fire safety provisions in the Far East.* International Journal on Engineering Performance-Based Fire Codes, 2011. **10**(1): p. 1-5.
51. McGrattan, K., S. Hostikka, and J.E. Floyd, *Fire dynamics simulator, user's guide*. NIST special publication, 2014. **1019**.
52. Alpert, R.L., *Ceiling Jet Flows*, in *SFPE Handbook of Fire Protection Engineering*, P.J. DiNenno, et al., Editors. 2008, National Fire Protection Association & Society of Fire Protection Engineers: Quincy, Massachusetts. p. 18-31.
53. Gann, R.G., et al., *Smoke component yields from room-scale fire tests*. 2003: US Department of Commerce, National Institute of Standards and Technology.
54. The chartered institution of building services engineers, *CIBSE - Guide B: Heating, ventilating, air conditioning and refrigeration*. 2005, The chartered institution of building services engineers: London.

55. Fantronix. *Recommended Air Change Rates*. 2012 [cited 2013 May 3rd]; Available from: http://www.fantronix.com/acatalog/Recommended_Air_Change_Rates.html.
56. Watkin Hire. *Guide to ventilation ranges (ACH)*. 2009 [cited 2013 May 3rd]; Available from: http://www.watkinshire.co.uk/blog/ventilation-hire/ventilation-rates-air-changes-per-hour.
57. Blomqvist, P. and M. Simonson-McNamee, *Estimation of CO2-emissions from fires in dwellings, schools and cars in the Nordic countries*. 2009, SP Technical Research Institute of Sweden.
58. BS ISO 19706, *Guidelines for assessing the fire threat to people*. 2007, Bristish Standards Institution: London.
59. Hull, R., *Bench-scale generation of fire effluents*, in *Fire Toxicity*, A. Stec and R. Hull, Editors. 2010, Woodhouse Publishing Ltd.: Cambridge.
60. Hull, R. and A. Stec, *An international standardised framework for prediction of fire gas toxicity*, in *Fire Toxicity*, A. Stec and R. Hull, Editors. 2010, Woodhouse Publishing Ltd.: Cambridge.
61. Purser, D.A., A. Stec, and R. Hull, *Fire senarios and combustion conditions*, in *Fire Toxicity*, A. Stec and R. Hull, Editors. 2010, Woodhouse Publishing Ltd.: Cambridge.
62. Forell, B., *A methodology to assess species yields of compartment fires by means of an extended global equivalence ratio concept*. 2007, Techn. Univ., Inst. für Baustoffe, Massivbau und Brandschutz.
63. Pitts, W., *The global equivalence ratio concept and the formation mechanisms of carbon monoxide in enclosure fires.* Progress in Energy and Combustion Science, 1995. **21**: p. 197-237.
64. Gottuk, D.T. and B.Y. Lattimer, *Effect of Combustion Conditions on Species Production*, in *SFPE handbook of fire protection engineering*, P.J. DiNenno, Editor. 2002, National Fire Protection Association & Society of Fire Protection Engineers: Quincy, Mass. & Bethesda, Md.
65. Beyler, C.L., *Development and burning of a layer of products of incomplete combustion generated by a buoyant diffusion flame*. 1983, Harvard University.
66. Zukoski, E.E., et al., *Species production and heat release rates in two-layered natural gas fires.* Combustion and Flame 1991. **83**(3): p. 325-332.
67. Wang, Z., F. Jia, and E.R. Galea, *Predicting toxic gas concentrations resulting from enclosure fires using local equivalence ratio concept linked to fire field models.* Fire and Materials 2007. **31**(1): p. 27-51.
68. Fardell, P., et al., *Fires reduced oxygen conditions.* Interflam, Interscience Communications Ltd., London, UK, 2004: p. 129-142.
69. Hietaniemi, J., R. Kallonen, and E. Mikkola, *Burning characteristics of selected substances: production of heat, smoke and chemical species.* Fire and Materials 1999. **23**(4): p. 171-185.
70. Tewarson, A., *Generation of Heat and Chemical Compounds in Fires*, in *SFPE Handbook of Fire Protection Engineering*. 2002, NFPA: Quincy, Massachusetts.
71. ASTM E2058, *Standard Test Methods for Measurement of Material Flammability Using a Fire Propagation Apparatus (FPA)*. 2010, ASTM International: West Conshohocken, PA.
72. ISO 19700, *Controlled equivalence ratio method for the determination of hazardous components of fire effluents*. 2007, International Organization for Standardization: Geneva.

73. BS 7990, *Tube furnace method for the determination of toxic product yields in fire effluents*. 2003, British Standard Institution: London.
74. Tewarson, A., *Fully developed enclosure fires of wood cribs.* Symposium (International) on Combustion, 1985. **20**(1): p. 1555-1566.
75. Li, H., et al. *Impact of Traffic Conditions and Road Geometry on Real World Urban Emissions Using a SI Car*. in *SAE Technical Paper Series*. 2007. Detroit.
76. BS ISO 5660-1, *Reaction-to-fire tests - Heat release, smoke production and mass loss rate - Part 1: Heat release rate (cone calorimeter method) and smoke production rate (dynamic measurement)*. 2015, Bristish Standards Institution: London.
77. Pitts, W.M. *Reactivity of product gases generated in idealized enclosure fire environments*. in *Symposium (International) on Combustion* 1992. Elsevier.
78. Pitts, W.M., *Application of thermodynamic and detailed chemical kinetic modeling to understanding combustion product generation in enclosure fires.* Fire Safety Journal, 1994. **23**(3): p. 271-303.
79. Purser, D.A., *Chapter 12 Dioxins and Other Carcinogens*, in *Toxicology, Survival and Health Hazards of Combustion Products*. 2016, The Royal Society of Chemistry. p. 382-410.
80. Wakefield, J.C., *Chapter 4 Products of Combustion and Toxicity from Specific Types of Fires*, in *Toxicology, Survival and Health Hazards of Combustion Products*. 2016, The Royal Society of Chemistry. p. 79-107.
81. Aldhous, P., *Oil-well climate catastrophe?* Nature, 1991. **349**(6305): p. 96-96.
82. COMAH. *Buncefield: Why did it happen?* 2011; Available from: http://www.hse.gov.uk/comah/buncefield/buncefield-report.pdf.
83. Waite, T., C. Keshishian, and V. Murray, *Chapter 18 Buncefield Fire*, in *Toxicology, Survival and Health Hazards of Combustion Products*. 2016, The Royal Society of Chemistry. p. 553-573.
84. NASA. *Fire and Smoke maps, NASA*. 2016 [cited 2016 1 January]; Available from: http://www.nasa.gov/mission_pages/fires/main/index.html.
85. McAllister, J.L., *Chapter 17 Health Effects in Groups Exposed to Wildland and Urban Fires*, in *Toxicology, Survival and Health Hazards of Combustion Products*. 2016, The Royal Society of Chemistry. p. 535-552.
86. Purser, D.A., *Asphyxiant components of fire effluents*, in *Fire Toxicity*, A. Stec and R. Hull, Editors. 2010, Woodhouse Publishing Ltd.: Cambridge.
87. Alarie, Y., *Toxicity of Fire Smoke.* Critical Reviews in Toxicology, 2002. **32**(4): p. 259-289.
88. Hartzell, G.E., *Overview of combustion toxicology.* Toxicology, 1996. **115**(1–3): p. 7-23.
89. Levin, B.C. and E.D. Kuligowski, *Toxicology of Fire and Smoke*, in *Inhalation Toxicology, Second Edition*. 2005, CRC Press. p. 205-228.
90. Speitel, L.C., *Toxicity Assessment of Combustion Gases and Development of a Survival Model*. 1995, DTIC Document.
91. Group Discussion, *New research avenues in combustion toxicology.* Toxicology, 1996. **115**(1–3): p. 185-200.
92. Kuligowski, E.D., *Compilation of data on the sublethal effects of fire effluent.* NIST Technical Note, 2009. **1644**: p. 18.
93. Maynard, R.L., I. Myers, and J.A.S. Ross, *Chapter 9 Carbon Monoxide*, in *Toxicology, Survival and Health Hazards of Combustion Products*. 2016, The Royal Society of Chemistry. p. 260-309.

94. Purser, D., *Interactions Among Carbon Monoxide, Hydrogen Cyanide, Low Oxygen Hypoxia, Carbon Dioxide, and Inhaled Irritant Gases*, in *Carbon Monoxide Toxicity*. 2000, CRC Press. p. 157-191.
95. National Research Council. *Carbon Monoxide Acute Exposure Guideline Levels*. Acute Exposure Guideline Levels for Selected Airborne Chemicals 2010; Available from: http://www.ncbi.nlm.nih.gov/books/NBK220007/.
96. Pach, J., et al., *Various factors influencing the clinical picture and mortality in acute carbon monoxide poisoning.* Folia Medica Cracoviensia, 1978. **20**(1): p. 159-167.
97. BS ISO 13344, *Estimation of the lethal toxic potency of fire effluents*. 2004, British Standard Institution: London.
98. Purser, D.A., *Chapter 10 Hydrogen Cyanide-Physiological Effects of Acute Exposure during Fires*, in *Toxicology, Survival and Health Hazards of Combustion Products*. 2016, The Royal Society of Chemistry. p. 310-360.
99. Purser, D.A., P. Grimshaw, and K.R. Berrill, *Intoxication by Cyanide in Fires: A Study in Monkeys using Polyacrylonitrile.* Archives of Environmental Health: An International Journal, 1984. **39**(6): p. 394-400.
100. Baud, F.J., et al., *Elevated Blood Cyanide Concentrations in Victims of Smoke Inhalation.* New England Journal of Medicine, 1991. **325**(25): p. 1761-1766.
101. National Research Council. *Hydrogen Cyanide Acute Exposure Guideline Levels*. Acute Exposure Guideline Levels for Selected Airborne Chemicals 2002; Available from: http://www.ncbi.nlm.nih.gov/books/NBK207601/.
102. Moritz, A.R., *Death Due to Conflagration.* New England Journal of Medicine, 1949. **240**(22): p. 901-902.
103. Baker, D.J., *Chapter 16 Acute Lung Injury Following Inhalation of Irritant Products of Combustion*, in *Toxicology, Survival and Health Hazards of Combustion Products*. 2016, The Royal Society of Chemistry. p. 514-534.
104. Purser, D., *Behavioural impairment in smoke environments.* Toxicology, 1996. **115**(1–3): p. 25-40.
105. Wakefield, J.C., *Chapter 13 Irritant Gases*, in *Toxicology, Survival and Health Hazards of Combustion Products*. 2016, The Royal Society of Chemistry. p. 411-427.
106. Purser, D.A., *Toxic product yields and hazard assessment for fully enclosed design fires.* Polymer International 2000. **49**(10): p. 1232-1255.
107. Buckley, L.A., et al., *Respiratory tract lesions induced by sensory irritants at the RD50 concentration.* Toxicology and Applied Pharmacology 1984. **74**(3): p. 417-429.
108. Hilado, C.J., *Flammability handbook for plastics*. Vol. 5th. 1998, Lancaster, Pa: Technomic Pub. Co.
109. ISO 13571, *Life-threatening components of fire -- Guidelines for the estimation of time available for escape using fire data*. 2007, International Organization for Standardization.
110. Hertzberg, T., et al., *Particles and isocyanates from fires*. 2003, SP Swedish National Testing and Research Institute, Fire Technology.
111. BS EN 13823, *Reaction to fire tests for building products. Building products excluding floorings exposed to the thermal attack by a single burning item*. 2010, Bristish Standards Institution: London.
112. BS ISO TR 9705-2, *Reaction to fire tests. Full scale room tests for surface products. Technical background and guidance*. 2001, Bristish Standards Institution: London.

113. Blomqvist, P., et al., *Detailed determination of smoke gas contents using a small-scale controlled equivalence ratio tube furnace method.* Fire and Materials, 2007. **31**(8): p. 495-521.
114. EEA. *Emission inventory guidebook.* 2013; Available from: http://www.eea.europa.eu/publications/emep-eea-guidebook-2013.
115. Kang, C.-M., D. Gold, and P. Koutrakis, *Downwind O_3 and $PM_{2.5}$ speciation during the wildfires in 2002 and 2010.* Atmospheric Environment, 2014. **95**: p. 511-519.
116. Purser, D.A. and J.L. McAllister, *Assessment of Hazards to Occupants from Smoke, Toxic Gases, and Heat*, in *SFPE handbook of fire protection engineering*, M.J. Hurley, et al., Editors. 2016, Springer New York. p. 2308-2428.
117. Lundquist, P., L. Rammer, and B. Sörbo, *The role of hydrogen cyanide and carbon monoxide in fire casualties: A prospective study.* Forensic Science International, 1989. **43**(1): p. 9-14.
118. Anybody. *Colours represent the exit taken by survivors. Red crosses show fatalities.* British Airtours Flight 28M 2008 [cited 2015 October 20,]; Available from: https://commons.wikimedia.org/wiki/File:Britair28m.png.
119. Altman, P.L., R.M. Grebe, and D.D. Katz, *Handbook of respiration*. 1958, Philadelphia: Saunders.
120. Alarie, Y., *Irritating Properties of Airborne Materials to the Upper Respiratory Tract.* Archives of Environmental Health: An International Journal, 1966. **13**(4): p. 433-449.
121. Alarie, Y., *Sensory irritation of the upper airways by airborne chemicals.* Toxicology and Applied Pharmacology, 1973. **24**(2): p. 279-297.
122. Alarie, Y. and H.E. Stokinger, *Sensory Irritation by Airborne Chemicals.* CRC Critical Reviews in Toxicology, 1973. **2**(3): p. 299-363.
123. Tsuchiya, Y. and K. Sumi, *Thermal decomposition products of polyvinyl chloride.* Journal of Applied Chemistry, 1967. **17**(12): p. 364-366.
124. Tsuchiya, Y. and K. Sumi, *Evaluation of the toxicity of combustion products.* Journal of Fire and Flammability, 1972. **3**(1): p. 46-50.
125. Purser, D.A. and K.R. Berrill, *Effects of carbon monoxide on behavior in monkeys in relation to human fire hazard.* Arch Environ Health, 1983. **38**(5): p. 308-15.
126. Purser, D.A., *A Bioassay Model for Testing the Incapacitating Effects of Exposure To Combustion Product Atmospheres Using Cynomolgus Monkeys.* Journal of Fire Sciences, 1984. **2**(1): p. 20-36.
127. Purser, D., *Validation of additive models for lethal toxicity of fire effluent mixtures.* Polymer Degradation and Stability 2012. **97**(12): p. 2552-2561.
128. Purser, D.A. and W.D. Woolley, *Biological Studies of Combustion Atmospheres.* Journal of Fire Sciences, 1983. **1**(2): p. 118-144.
129. Levin, B.C., et al., *Further Development of a Test Method for the Assessment of the Acute Inhalation Toxicity of Combustion Products*. 1982, National Burea of Standards (now NIST): Washington, DC.
130. Levin, B.C., *New research avenues in toxicology: 7-gas N-gas model, toxicant suppressants, and genetic toxicology.* Toxicology, 1996. **115**(1–3): p. 89-106.
131. Levin, B.C., *New Approaches to Toxicity: A Seven-Gas Predictive Model and Toxicant Suppressants.* Drug and Chemical Toxicology 1997. **20**(4): p. 271-280.

132. Hartzell, G.E., D.N. Priest, and W.G. Switzer, *Modeling of Toxicological Effects of Fire Gases: Ii. Mathematical Modeling of Intoxication of Rats By Carbon Monoxide and Hydrogen Cyanide.* Journal of Fire Sciences, 1985. **3**(2): p. 115-128.
133. Hartzell, G.E., W.G. Switzer, and D.N. Priest, *Modeling of Toxicological Effects of Fire Gases: V. Mathematical Modeling of Intoxication of Rats By Combined Carbon Monoxide and Hydrogen Cyanide Atmospheres.* Journal of Fire Sciences, 1985. **3**(5): p. 330-342.
134. Hartzell, G.E. and H.W. Emmons, *The Fractional Effective Dose Model for Assessment of Toxic Hazards in Fires.* Journal of Fire Sciences, 1988. **6**(5): p. 356-362.
135. Kaplan, H.L., A.F. Grand, and G.E. Hartzell, *Toxicity and the smoke problem.* Fire Safety Journal, 1984. **7**(1): p. 11-23.
136. Babrauskas, V., et al., *Toxic potency measurement for fire hazard analysis*. NIST special publication 827. 1991, Gaithersburg, MD: U.S. Dept. of Commerce. xi, 107 p.
137. Nielsen, G.D., P. Wolkoff, and Y. Alarie, *Sensory irritation: risk assessment approaches.* Regulatory toxicology and pharmacology : RTP, 2007. **48**(1): p. 6-18.
138. Schaper, M., *Development of a database for sensory irritants and its use in establishing occupational exposure limits.* Am Ind Hyg Assoc J, 1993. **54**(9): p. 488-544.
139. Brüning, T., et al., *Sensory irritation as a basis for setting occupational exposure limits.* Archives of Toxicology, 2014. **88**(10): p. 1855-1879.
140. Kaplan, H.L. and G.E. Hartzell, *Modeling of Toxicological Effects of Fire Gases: I. Incapacitating Effects of Narcotic Fire Gases.* Journal of Fire Sciences, 1984. **2**(4): p. 286-305.
141. Kaplan, H.L., et al., *Effects of Combustion Gases On Escape Performance of the Baboon and the Rat.* Journal of Fire Sciences, 1985. **3**(4): p. 228-244.
142. Kaplan, H.L., et al., *Studies of the Effects of Hydrogen Chloride and Polyvinylchloride (PVC) Smoke in Rodents.* Journal of Fire Sciences, 1993. **11**(6): p. 512-552.
143. HSE, *EH40/2005 Workplace Exposure Limits: Containing the List of Workplace Exposure Limits for Use with the Control of Substances Hazardous to Health Regulations (As Amended)*. 2011, HSE Books.
144. OSHA. *Permissible Exposure Limits*. 2015; Available from: https://www.osha.gov/dsg/annotated-pels/index.html.
145. ACGIH, *6th edition of the Documentation of the Threshold Limit Values and Biological Exposure Indices*. 1997, ACGIH: Cincinnati.
146. NIOSH, *Immediately Dangerous To Life or Health Concentrations (IDLH)*. 1994, NIOSH.
147. National Research Council, *Acute Exposure Guideline Levels for Selected Airborne Chemicals*. 2015: The National Academies Press.
148. National Research Council. *Formaldehyde Interim Acute Exposure Guideline Levels*. Acute Exposure Guideline Levels for Selected Airborne Chemicals 2008; Available from: http://www.epa.gov/sites/production/files/2014-07/documents/formaldehyde_tsd_interim_07_2008.v1_0.pdf.
149. National Research Council. *Acrolein Acute Exposure Guideline Levels*. Acute Exposure Guideline Levels for Selected Airborne Chemicals 2010; Available from: http://www.ncbi.nlm.nih.gov/books/NBK220013/.

150. National Research Council. *Sulphur Dioxide Acute Exposure Guideline Levels*. Acute Exposure Guideline Levels for Selected Airborne Chemicals 2010; Available from: http://www.ncbi.nlm.nih.gov/books/NBK219999/.
151. National Research Council. *Ammonia Acute Exposure Guideline Levels*. Acute Exposure Guideline Levels for Selected Airborne Chemicals 2010; Available from: http://www.ncbi.nlm.nih.gov/books/NBK207883/.
152. Levin, B.C., et al., *Effects of exposure to single or multiple combinations of the predominant toxic gases and low oxygen atmospheres produced in fires.* Fundamental and Applied Toxicology, 1987. **9**(2): p. 236-250.
153. BS ISO 19701, *Methods for sampling and analysis of fire effluents*. 2013, International Organization for Standardization: Geneva.
154. Jahnke, J.A., *Continuous emission monitoring*. 2000: John Wiley & Sons.
155. International Light Tech. *NDIR Gas Sensors*. 2015; Available from: http://www.intl-lighttech.com/sites/default/files/pdf/application/ndir-gas-sensor.pdf.
156. Luma Sense Tech. *Non-dispersive Infrared (NDIR) Technology*. 2015; Available from: http://www.lumasenseinc.com/EN/solutions/techoverview/ndir/.
157. Fuji Electric, *NDIR Type Infrared gas Analyzer*. 2011, Fuji Electric Co., Ltd.: Japan.
158. Yokogawa Electric Corporation. *NDIR Type Infrared gas analyzer (5-Component analyzer)*. 2006; Available from: https://www.yokogawa.com/an/download/general/GS11G02N01-01E.pdf.
159. CFR, *NDIR analyzer calibration and*

checks., in *40 CFR § 92.120*, Code of Federal Regulations, Editor. 2011: USA,.
160. Clarke, A., *Industrial Air Pollution Monitoring: Gaseous and Particulate Emissions*. Vol. 8. 1998: Springer Science & Business Media.
161. Systech, *Paramagnetic Cells*, S.I. Ltd, Editor. 2010.
162. Laird, C.K. and I. Verhappen, *18 - Chemical analysis: Gas analysis*, in *Instrumentation Reference Book (Third Edition)*, W. Boyes, Editor. 2003, Butterworth-Heinemann: Burlington. p. 382-413.
163. Servomex. *Paramagnetic Oxygen Analysis*. 2014; Available from: http://www.servomex.com/80257434005926FF/en/paramagnetic-oxygen-analysis.
164. Mikkola, E. *Practise of FTIR analysis for fire gases (SAFIR)*. in *Flame Retardants*. 2000.
165. Hakkarainen, T., et al., *Smoke gas analysis by Fourier transform infrared spectroscopy – summary of the SAFIR project results.* Fire and Materials, 2000. **24**(2): p. 101-112.
166. Guillaume, E., et al., *Effect of gas cell pressure in FTIR analysis of fire effluents.* Fire and Materials 2014.
167. Hakkarainen, T., et al., *Smoke gas analysis by Fourier transform infrared spectroscopy*, in *The SAFIR Project*. 1999, Technical Research Centre of Finland, VTT: Espoo. p. 81.
168. Speitel, L.C., *Fourier Transform Infrared Analysis of Combustion Gases.* Journal of Fire Sciences 2002. **20**(5): p. 349-371.
169. ISO 19702, *Toxicity testing of fire effluents — Guidance for analysis of gases and vapours in fire effluents using FTIR gas analysis*. 2006, International Organization for Standardization: Geneva.

170. ISO 19702, *Guidance for sampling and analysis of toxic gases and vapours in fire effluents using Fourier Transform Infrared (FTIR) spectroscopy*. 2015, International Organization for Standardization: Geneva.
171. Andrews, G.E., et al. *FTIR Investigations Of Toxic Gases In Air Starved Enclosed Fires.* in *Eighth International Symposium on Fire Safety Science*. 2005. Beijing: International Association for Fire Safety Science.
172. BS ISO 27368, *Analysis of blood for asphyxiant toxicants. Carbon monoxide and hydrogen cyanide*. 2008, International Organization for Standardization: Geneva.
173. Babrauskas, V., et al., *The phi meter: A simple, fuel-independent instrument for monitoring combustion equivalence ratio.* Review of Scientific Instruments 1994. **65**(7): p. 2367-2375.
174. Lönnermark, A., et al., *TOXFIRE 45 – Fire Characteristics and Smoke Gas Analyses in Under-ventilated Large-scale Combustion Experiments – Tests in the ISO 9705 Room.* SP Swedish National Testing and Research Institute, 1996(SP Report 1996:45).
175. Lönnermark, A. and V. Babrauskas, *TOXFIRE 49 – Fire Characteristics and Smoke Gas Analyses in Under-ventilated Large-scale Combustion Experiments – Theoretical Background and Calculations.* SP Swedish National Testing and Research Institute, 1996(SP Report 1996:49).
176. Hull, T.R. and K.T. Paul, *Bench-scale assessment of combustion toxicity—A critical analysis of current protocols.* Fire Safety Journal, 2007. **42**(5): p. 340-365.
177. Beitel, J.J., et al., *Overview of Smoke Toxicity Testing and Regulations*. 1998, DTIC Document.
178. BS ISO TR 9122-4, *Toxicity testing of fire effluents. The fire model (furnaces and combustion apparatus used in small-scale testing).* 1993, Bristish Standards Institution: London.
179. Babrauskas, V., *Fire safety improvements in the combustion toxicity area: is there a role for LC50 tests?* Fire and Materials, 2000. **24**(2): p. 113-119.
180. Babrauskas, V., *Toxic Hazard from Fires: A Simple Assessment Method.* Fire Safety Journal, 1993(20): p. 1-14.
181. Babrauskas, V., et al., *A methodology for obtaining and using toxic potency data for fire hazard analysis.* Fire Safety Journal, 1998. **31**(4): p. 345-358.
182. Guillaume, E., A. Camillo, and T. Rogaume, *Application and Limitations of a Method Based on Pyrolysis Models to Simulate Railway Rolling Stock Fire Scenarios.* Fire Technology 2013. **50**(2): p. 317-348.
183. BS EN 45545-2, *Railway application: Fire protection on railway vehicles — Part 2: Requirements for fire behaviour of materials and components*. 2013, Bristish Standards Institution: London.
184. Babrauskas, V., et al., *The Role of Bench-Scale Test Data in Assessing Real-Scale Fire Toxicity*, in *NIST Technical Note 1284*. 1991, NIST.
185. Debanne, S.M., H.S. Haller, and D.Y. Rowland, *A Statistical Comparison of Test Protocols Used in the Assessment of Combustion Product Toxicity.* Journal of Fire Sciences, 1987. **5**(6): p. 416-434.
186. Packham, S.C. and M.B. Crawford, *An Evaluation of Smoke Toxicity and Toxic Hazard of Electrical Nonmetallic Tubing Combustion Products.* Journal of Fire Sciences, 1984. **2**(1): p. 37-59.
187. NFPA 269, *Standard Test Method for Developing Toxic Potency Data for Use in Fire Hazard Modeling*. 2012, National Fire Protection Association: Quincy, MA.

188. ASTM E1678, *Standard Test Method for Measuring Smoke Toxicity for Use in Fire Hazard Analysis*. 2010, ASTM International: West Conshohocken, PA.
189. Babrauskas, V., et al., *Large-Scale Validation of Bench-Scale Fire Toxicity Tests.* Journal of Fire Sciences, 1991. **9**(2): p. 125-148.
190. Marsh, N.D., et al., *Smoke component yields from bench-scale fire tests: 1. NFPA 269 / ASTM E 1678.* NIST Technical Note 2013. **1760**.
191. Lee, T., *Interlaboratory evaluation of smoke density chamber*. Vol. 708. 1971: US National Bureau of Standards.
192. BS EN 2824, *Aerospace series. Burning behaviour of non-metallic materials under the influence of radiating heat and flames. Determination of smoke density and gas components in the smoke of materials. Test equipment apparatus and media*. 2011, Bristish Standards Institution: London.
193. BS EN 2825, *Aerospace series — Burning behaviour of non metallic materials under the influence of radiating heat and flames — Determination of smoke density*. 2011, Bristish Standards Institution: London.
194. BS EN 2826, *Aerospace series — Burning behaviour of non metallic materials under the influence of radiating heat and flames — Determination of gas components in the smoke*. 2011, Bristish Standards Institution: London.
195. BS 6401, *Method for measurement, in the laboratory, of the specific optical density of smoke generated by materials*. 1983, Bristish Standards Institution: London.
196. ASTM E662, *Standard Test Method for Specific Optical Density of Smoke Generated by Solid Materials*. 2010, ASTM International: West Conshohocken, PA.
197. BS EN ISO 5659-2, *Plastics - Smoke generation. Part 2: Determination of optical density by a single-chamber test*. 2012, British Standard Institution: London.
198. IMO MSC 41 (64), *Interim standard for measuring smoke and toxic products of combustion.* International Maritime Organisation.
199. FTT. *NBS Smoke Density Chamber - Product Catalogue*. 2016; Available from: http://www.fire-testing.com/sdc.
200. Alarie, Y.C. and R.C. Anderson, *Toxicologic and acute lethal hazard evaluation of thermal decomposition products of synthetic and natural polymers.* Toxicology and Applied Pharmacology 1979. **51**(2): p. 341-362.
201. Herpol, C. and P. Vandevelde, *Use of toxicity test results and confrontation of some toxicity test methods with fire scenarios.* Fire Safety Journal, 1981. **4**(4): p. 271-280.
202. IEC 60695-7-50, *Fire hazard testing - Part 7-50: Toxicity of fire effluent - Estimation of toxic potency - Apparatus and test method*. 2002, International Electrotechnical Commission: Geneva.
203. Stec, A.A., *Fire Toxicity and its Measurments*, in *Centre for Materials Research and Innovation*. 2007, Univerisity of Bolton: Bolton.
204. Stec, A.A., et al., *Comparison of toxic product yields from bench-scale to ISO room.* Fire Safety Journal 2009. **44**(1): p. 62-70.
205. Marsh, N.D., R.G. Gann, and M.R. Nyden, *Smoke component yields from bench-scale fire tests: 2. ISO 19700 Controlled Equivalence Ratio Tube Furnace.* NIST Technical Note 2013. **1761**.

206. Hull, T.R., A.A. Stec, and K. Lebek, *Characterisation of the steady state tube furnace (ISO TS 19700) for fire toxicity assessment.* Polymer Degradation and Stability, 2008. **93**(11): p. 2058-2065.
207. Stec, A.A., et al., *Fire Toxicity Assessment: Comparison of Asphyxiant Yields from Laboratory and Large Scale Flaming Fires.* Fire Safety Science, 2014. **11**: p. 404-418.
208. ASTM E2058, *Standard Test Methods for Measurement of Synthetic Polymer Material Flammability Using a Fire Propagation Apparatus (FPA)*. 2010, ASTM International: West Conshohocken, PA.
209. BS ISO 12136, *Reaction to fire tests — Measurement of material properties using a fire propagation apparatus*. 2011, Bristish Standards Institution: London.
210. Khan, M.M. and R.G. Bill, *Comparison of flammability measurements in vertical and horizontal exhaust duct in the ASTM E-2058 fire propagation apparatus.* Fire and Materials, 2003. **27**(6): p. 253-266.
211. Calogine, D., et al., *Gaseous effluents from the combustion of nanocomposites in controlled-ventilation conditions.* Journal of Physics: Conference Series, 2011. **304**(1): p. 012019.
212. ASTM E1354, *Standard test method for heat and visible smoke release rates for materials and products using an oxygen consumption calorimeter*. 2010, ASTM International: West Conshohocken, PA.
213. FTT, *User's Guide for the Cone Calorimeter*. 2001, East Grinstead, UK: Fire Testing Technology Limited.
214. Babrauskas, V., et al., *A cone calorimeter for controlled-atmosphere studies.* Fire and Materials 1992. **16**(1): p. 37-43.
215. Mulholland, G., et al., *The effect of oxygen concentration on CO and smoke produced by flames.* Fire safety science, 1991. **3**: p. 585-594.
216. Marquis, D., E. Guillaume, and D. Lesenechal, *Accuracy (Trueness and Precision) of Cone Calorimeter Tests with and Without a Vitiated Air Enclosure.* Procedia Engineering, 2013. **62**(0): p. 103-119.
217. Hermouet, F., et al. *Development of an experimental design methodology adapted to Controlled Atmosphere Cone Calorimeter in order to evaluate the thermal degradation of solid materials in the context of tunnel fires*. in *Proceedings of the 6th International Symposium on Tunnel Safety and Security, Marseille, France*. 2014.
218. Guillaume, E., D.M. Marquis, and C. Chivas, *Experience plan for controlled-atmosphere cone calorimeter by Doehlert method.* Fire and Materials, 2012: p. n/a-n/a.
219. Werrel, M., et al., *The calculation of the heat release rate by oxygen consumption in a controlled-atmosphere cone calorimeter.* Fire and Materials, 2014. **38**(2): p. 204-226.
220. Marquis, D.M., et al., *Usage of controlled-atmosphere cone calorimeter to provide input data for toxicity modelling.* Proceeding in the 12th. International Fire and Material., San Francisco, 2011.
221. Hermouet, F., et al. *Evaluation of the thermal decomposition of solid materials in tunnel related conditions with a Controlled Atmosphere Cone Calorimeter*. in *Proceedings of the 3rd International conference on Fire in Vehicles, Berlin, Germany*. 2014.
222. Werrel, M., et al. *Use and Benefit of a Controlled-Atmosphre Cone Calorimeter*. in *13th International Conference on Fire and Material*. 2013. San Francisco, CA: Interscience Communications Ltd.

223. Marsh, N.D., et al., *Smoke component yields from bench-scale fire tests: 3. ISO 5660-1 / ASTM E 1354 with Enclosure and Variable Oxygen Concentration.* NIST Technical Note 2013. **1762**.
224. Alarifi, A.A., et al., *Ignition and Toxicity Evaluation of Selected Aircraft Interior Materials Using the Cone Calorimeter and FTIR Analysis*, in *InterFlam2013*. 2013, Interscience Communications Limited: Royal Holloy College, University of London, UK. p. 37-48.
225. Andrews, G.E., et al., *Aircraft Blanket Ignition and Toxic Emission in Simulated Aircraft Cabin Fires Using the Cone Calorimeter*, in *Fire & Materials*. 2015, Interscience Communications: San Francisco, CA.
226. FTT. *Cone Calorimeter - Product Catalogue*. 2016; Available from: http://www.fire-testing.com/cone-calorimeter-dual.
227. Axelsson, J., et al., *Uncertainties in measuring heat and smoke release rates in the room/corner test and the SBI.* SP RAPPORT, 2001.
228. Babrauskas, V., et al., *Upholstered furniture heat release rates measured with a furniture calorimeter*. Vol. 82-2604. 1982: US Department of Commerce, National Bureau of Standards.
229. Babrauskas, V. and J. Krasny, *Upholstered furniture transition from smoldering to flaming.* Journal of forensic sciences, 1997. **42**: p. 1029-1031.
230. Beyler, C.L., *Major species production by diffusion flames in a two-layer compartment fire environment.* Fire Safety Journal 1986. **10**(1): p. 47-56.
231. Toner, S.J., *Entrainment, chemistry, and structure of fire plumes*. 1987, California Institute of Technology.
232. Cetegen, B.M., E.E. Zukoski, and T. Kubota, *Entrainment in the Near and Far Field of Fire Plumes.* Combustion Science and Technology 1984. **39**(1-6): p. 305-331.
233. Zukoski, E., et al., *Combustion Processes In Two-layered Configuations.* Fire safety science, 1989. **2**: p. 295-304.
234. Morehart, J.H., E.E. Zukoski, and T. Kubota, *Chemical species produced in fires near the limit of flammability.* Fire Safety Journal 1992. **19**(2–3): p. 177-188.
235. Gottuk, D., *Generation of Carbon Monoxide in Compartment Fires. National Institute of Standards and Technology*. 1992, Viginia Polytechnic Institute and State University.
236. Bryner, N.P., E.L. Johnsson, and W.M. Pitts, *Carbon monoxide production in compartment fires: Reduced-scale enclosure test facility*. 1994: National Institute of Standards and Technology, Building and Fire Research Laboratory.
237. Bundy, M., et al., *Measurements of Heat and Combustion Products in Reduced-scale Ventilation-lmited Compartment Fires*. 2007: US Department of Commerce, Technology Administration, Building and Fire Research Laboratory, National Institute of Standards and Technology.
238. Andrews, G. and J. Ledger, *Enclosed Pool Fires in Low Ventilation Enclosures: Flame Temperatures and Global Heat Loss Using Gas Analysis.* Fire Safety Science, 2000. **6**: p. 591-602.
239. Andrews, G., J. Ledger, and H. Phylaktou. *Pool fires in a low ventilation enclosure*. in *INSTITUTION OF CHEMICAL ENGINEERS SYMPOSIUM SERIES*. 2000. Institution of Chemical Engineers; 1999.
240. Aljumaiah, O., et al. *Toxic Emissions from Folded Cotton Towel Fires in a Low Ventilation Compartment*. in *6th International Seminar on Fire and Explosion Hazards*. 2010. Leeds: Research Publishing Services.

241. Aljumaiah, O., et al. *Air Starved Acrylic Curtain Fire Toxic Gases using an FTIR.* in *6th International Seminar on Fire and Explosion Hazards*. 2010. Leeds: Research Publishing Services.
242. Aljumaiah, O., et al. *Air Starved Wood Crib Compartment Fire Heat Release and Toxic Gas Yields*. in *10th International Symposium on Fire Saftey Science*. 2011. Maryland, USA: IAFSS.
243. Aljumaiah, O.A.O., *Combustion products from ventilation controlled fires: toxicity assessment and modelling*. 2012, The University of Leeds.
244. Aljumaiah, O., et al. *Fuel Volatility Effects on Pool Fires in Compartments with Low Ventilation*. in *11 IAFSS*. 2014. Canterbury, NZ: IAFSS.
245. Andrews, G., et al. *Toxic Gas Measurements Using FTIR for Combustion of COH Materials in Air Starved Enclosed Fires*. in *Proceedings of the European Combustion Institute Meeting*. 2007.
246. Gottuk, D.T., R.J. Roby, and C.L. Beyler, *A study of carbon monoxide and smoke yields from compartment fires with external burning.* Symposium (International) on Combustion 1992. **24**(1): p. 1729-1735.
247. Lattimer, B.Y., *The Transport of High Concentrations of Carbon Monoxide to Location Remote from the Burning Compartment*. 1997, Viginia Polytechnic Institute and State University. p. 350.
248. Lattimer, B.Y., U. Vandsburger, and R.J. Roby, *The transport of carbon monoxide from a burning compartment located on the side of a hallway.* Symposium (International) on Combustion, 1996. **26**(1): p. 1541-1547.
249. Ko, G.H., et al., *Mixture fraction analysis of combustion products in the upper layer of reduced-scale compartment fires.* Combustion and Flame, 2009. **156**(2): p. 467-476.
250. Floyd, J.E. and K.B. McGrattan. *Multiple parameter mixture fraction with two step combustion chemistry for large eddy simulation*. in *International Interflam Conference, 11th Proceedings*. 2007.
251. Floyd, J.E., *Multi-Parameter, Multiple Fuel Mixture Fraction Combustion Model for Fire Dynamics Simulator.* Report GCR, 2011: p. 08-920.
252. Blomqvist, P., P. Lindberg, and M. Mansson, *TOXFIRE 47- Fire characteristics and smoke gas analysis in under-ventilated large-scale combustion experiments, FTIR measurements.* SP Swedish National Testing and Research Institute, 1996. **47**(SP Report 1996:47).
253. Månsson, M., et al., *TOXFIRE 44 – Fire Characteristics and Smoke Gas Analyses in Under-ventilated Large-scale Combustion Experiments.* SP Swedish National Testing and Research Institute, 1996(SP Report 1996:44).
254. Lönnermark, A., et al., *TOXFIRE 46- Fire characteristics and smoke gas analysis in under-ventilated large-scale combustion experiments, Storage Confifuration Tests.* SP Swedish National Testing and Research Institute, 1996. **46**(SP Report 1996:46).
255. Mansson, M., I. Isaksson, and L. Rosell, *TOXFIRE 48- Fire characteristics and smoke gas analysis in under-ventilated large-scale combustion experiments, Adsorbents and Soot Measurements.* SP Swedish National Testing and Research Institute, 1996. **48**(SP Report 1996:48).
256. Blomqvist, P. and A. Lönnermark, *Characterization of the combustion products in large-scale fire tests: comparison of three experimental configurations.* Fire and Materials, 2001. **25**(2): p. 71-81.
257. Lock, A., et al., *Experimental study of the effects of fuel type, fuel distribution, and vent size on full-scale underventilated compartment fires in*

an ISO 9705 room. 2008: US Department of Commerce, National Institute of Standards and Technology.
258. Marsh, N.D. and R.G. Gann, *Smoke component yields from bench-scale fire tests: 4. Comparison with room fire results.* NIST Technical Note 2013. **1763**.
259. Fabian, T.Z. and D.G. Pravinray, *Smoke characterization project*. 2007, Fire Protection Research Foundation/Underwriters Laboratories, Incorporated.
260. Alarifi, A.A., et al., *Effects of fire-fighting on a fully developed compartment fire: Temperatures and emissions.* Fire Safety Journal 2014. **68**(0): p. 71-80.
261. ISO 5660, *Reaction-to-fire tests - Heat release, smoke production and mass loss rate - Part 1: Heat release rate (cone calorimeter method)*. 2002, Bristish Standards Institution: London.
262. Marquis, D.M. and É. Guillaume. *Effects of under-ventilated conditions on the reaction-to-fire of a polyisocyanurate foam*. in *Fire and Materials 2013 - 13th International Conference and Exhibition, Conference Proceedings*. 2013.
263. Tewarson, A., *Generations of Heat and Chemical Compounds in Fires*, in *SFPE Handbook of Fire Protection Engineering*, P.J. DiNenno, Editor. 2002, National Fire Protection Association: Quincy, Mass. & Bethesda, Md.
264. Gevantman, L., *Solubility of selected gases in water.* Nitric oxide (NO), 2000. **308**(3.348): p. 10-4.
265. IUPAC, *IUPAC-NIST Solubility Database, Version 1.1 -NIST Standard Reference Database 106* 2015, National Institute of Standards and Technology.
266. Yalkowsky, S.H., Y. He, and P. Jain, *Handbook of aqueous solubility data*. 2010: CRC press.
267. NIOSH, *NIOSH pocket guide to chemical hazards (2005-149)*. 3rd ed. 2007: DHHS (NIOSH) Publishing.
268. Stegemann, S., et al., *When poor solubility becomes an issue: From early stage to proof of concept.* European Journal of Pharmaceutical Sciences 2007. **31**(5): p. 249-261.
269. MAC, *The MAC Humidity/Moisture Handbook*. 2011.
270. Andrews, G.E., J. Ledger, and H.N. Phylaktou. *Enclosed Pool Fires in Low Ventilation Enclosures: Flame Temperatures and Global Heat Loss Using Gas Analysis*. in *Sixth International Symposium on Fire Safety Science*. 2000. Poitiers: International Association for Fire Safety Science.
271. Chan, S.H., *An Exhaust Emissions based Air-Fuel Ratio Calculation For Internal Combustion Engines.* IMech Auto Eng., 1996. **210**: p. 273-280.
272. Ishibe, T., et al., *Absorption of nitrogen dioxide and nitric oxide by soda lime.* British journal of anaesthesia, 1995. **75**(3): p. 330-333.
273. Fuji Electric, *Paramagnetic Oxygen Analyzer*. 2011, Fuji Electric Co., Ltd.: Japan.
274. Servomex, *1400B Gas Analyser - Instruction Manual*. 1994, Fuji Electric Co., Ltd.: Japan.
275. Daham, B., et al., *Application of a portable FTIR for measuring on-road emissions*, in *SAE Technical Paper 2005-01-0676*. 2005.
276. Li, H., et al., *Evaluation of a FTIR emission measurement system for legislated emissions using a SI car*. 2006, SAE Technical Paper.
277. Gasmet Technologies Oy, *Gasmet Calcmet for Windows - User's guide and refernce manual*. 2010, Helsinki, Fi: Gasmet Technologies Oy. 172 p.
278. Andrews, G.E. 2012.

279. Alarifi, A.A., et al. *Toxic Gas Emissions from a Timber-Pallet-Stack Fire in a Full Scale Compartment*. in *10th Asia-Oceania Symposium on Fire Science and Technology*. 2015. Tsukuba, Japan.
280. Alarifi, A.A., et al. *Developing and post-flashover fires in a full scale room. Thermal environment, toxic emissions and effects of fire-fighting tactics*. in *2nd European Symposium in Fire Safety Science*. 2015. Nicosia, Cyprus.
281. Andrews, G.E., et al. *Toxic Gases in simulated aircraft interior fires using FTIR analysis*. in *5th International Conference on Fire and Explosion Hazards*. 2008. Edinburgh.
282. Hartmann&Braun, *Operating Instructions URAS 10E - NDIR Industrial Photometer*. 1999.
283. Blevins, L.G., *Behavior of bare and aspirated thermocouples in compartment fires*, in *National Heat Transfer Conference, 33rd Proceedings*, M.K. Jensen, Di Marzo, M., Editor. 1999: Albuquerque, New Mexico, USA. p. 15-17.
284. Pitts, W.M., et al., *Temperature uncertainties for bare-bead and aspirated thermocouple measurements in fire environments.* ASTM Special Technical Publication, 2003. **1427**: p. 3-15.
285. Mingchun Luo, *Effects of Radiation on Temperature Measurement in a Fire Environment.* Journal of Fire Sciences 1997. **15**(6): p. 443-461.
286. Waterman, T.E., *Room flashover—Criteria and synthesis.* Fire Technology 1968. **4**(1): p. 25-31.
287. Babrauskas, V., *Full-scale burning behavior of upholstered chairs*. 1979, NIST Interagency.
288. Drysdale, D., *Ch.4: Diffusion flames and fire plumes*, in *An introduction to fire dynamics*. 2011, John Wiley & Sons.
289. Drysdale, D., *Ch.10: The Post-flashover Compartment Fire*, in *An introduction to fire dynamics*. 2011, John Wiley & Sons.
290. BS EN 1991-1-2, *Eurocode 1: Actions on structures — Part 1-2: General actions — Actions on structures exposed to fire*. 2002, Bristish Standards Institution: London.
291. Babrauskas, V., *Ignition handbook : principles and applications to fire safety engineering, fire investigation, risk management and forensic science*. 2003, Issaquah, WA: Fire Science Publishers. viii, 1116 p.
292. Babrauskas, V., *Development of the cone calorimeter—A bench-scale heat release rate apparatus based on oxygen consumption.* Fire and Materials 1984. **8**(2): p. 81-95.
293. Huggett, C., *Estimation of rate of heat release by means of oxygen consumption measurements.* Fire and Materials, 1980. **4**(2): p. 61-65.
294. ISO 5660-1, *Fire tests on building materials and structures - part 1: Method of measuring the rate of heat release of products*. 1993, Bristish Standards Institution: London.
295. Babrauskas, V. and Fire Retardant Chemicals Association (U.S.), *Fire hazard comparison of fire-retarded and non-fire-retarded products*. NBS special publication. 1988, Gaithersburg, MD & Washington, DC: U.S. Dept. of Commerce. xiii, 86 p.
296. Kallonen, R., *Smoke Gas Analysis by FTIR Method. Preliminary Investigation.* Journal of Fire Sciences, 1990. **8**(5): p. 343-360.
297. Hietaniemi, J. and R. Kallonen, *Small Scale Cone Calorimeter Experiments*, in *Assessment of Fires in Chemical Warehouses - An overview of the*

TOXFIRE project, K.E. Petersen and F. Markert, Editors. 1999, Risø National Laboratory: Roskilde, Denmark.
298. BS EN ISO 13927, *Plastics. Simple heat release test using a conical radiant heater and a thermopile detector*. 2015, British Standard Institution: London.
299. ASTM D5373, *Standard Test Methods for Determination of Carbon, Hydrogen and Nitrogen in Analysis Samples of Coal and Carbon in Analysis Samples of Coal and Coke*. 2010, ASTM International: West Conshohocken, PA.
300. ASTM D3176, *Standard Practice for Ultimate Analysis of Coal and Coke*. 2010, ASTM International: West Conshohocken, PA.
301. ASTM D3180, *Standard Practice for Calculating Coal and Coke Analyses from As-Determined to Different Bases*. 2010, ASTM International: West Conshohocken, PA.
302. ASTM D7582, *Standard Test Methods for Proximate Analysis of Coal and Coke by Macro Thermogravimetric Analysis*. 2010, ASTM International: West Conshohocken, PA.
303. ASTM D3172, *Standard Practice for Proximate Analysis of Coal and Coke*. 2010, ASTM International: West Conshohocken, PA.
304. ASTM D3173, *Standard Test Method for Moisture in the Analysis Sample of Coal and Coke*. 2010, ASTM International: West Conshohocken, PA.
305. ASTM D3174, *Standard Test Method for Ash in the Analysis Sample of Coal and Coke from Coal*. 2010, ASTM International: West Conshohocken, PA.
306. ASTM D3175, *Standard Test Method for Volatile Matter in the Analysis Sample of Coal and Coke*. 2010, ASTM International: West Conshohocken, PA.
307. Mettler Toledo, *Thermal Analysis of Polymers*, A. Hammer, Editor. 2013: Greifensee, Switzerland.
308. Erdman, N., et al., *Multispectral Imaging in an FEG-SEM*, in *Advanced Materials & Processes*. 2009, ASM International.
309. Thermo Scientific, *Flash 2000 Elemental Analyzer - Operating Manual*. 2008: Cambridge, UK.
310. BS ISO 1928, *Solid mineral fuels -- Determination of gross calorific value by the bomb calorimetric method and calculation of net calorific value*. 2009, Bristish Standards Institution: London.
311. Channiwala, S.A. and P.P. Parikh, *A unified correlation for estimating HHV of solid, liquid and gaseous fuels.* Fuel, 2002. **81**(8): p. 1051-1063.
312. Janssens, M. and W.J. Parker, *Oxygen consumption calorimetry*. Heat Release in Fires, 1992: p. 31-59.
313. Taylor, C.F., *Internal-Combustion Engine in Theory and Practice, Volume 2 - Combustion, Fuels, Materials, Design (2nd Edition, Revised)*. MIT Press.
314. Spindt, R.S., *Air-fuel ratios from exhaust gas analysis*. 1965, SAE Technical Paper.
315. Wood, L.A., *The use of dew-point temperature in humidity calculations.* J. Research, 1970.
316. d'Alleva, B. and W. Lovell, *Relation of exhaust gas composition to air-fuel ratio*. 1936, SAE Technical Paper.
317. Silvis, W.M., *The algorithmic structure of the air/fuel ratio calculation*. 1997, Horriba Technical Report.
318. Chan, S. and J. Zhu, *Exhaust emission based air-fuel ratio model (I): Literature reviews and modelling*. 1996, SAE Technical Paper.

319. Chan, S. and J. Zhu, *Exhaust Emission Based Air-Fuel Ratio Model (II): Divergence Analysis and Emission Estimations*. 1996, SAE Technical Paper.
320. Chan, S.H., *An Exhaust Emissions based Air-Fuel Ratio Calculation For Internal Combustion Engines.* Proceedings of the Institution of Mechanical Engineers, Part D: Journal of Automobile Engineering, 1996. **210**: p. 273-280.
321. Alpert, R.L. and E.J. Ward, *Evaluation of unsprinklered fire hazards.* Fire Safety Journal, 1984. **7**(2): p. 127-143.
322. Wang, Y., E. Zalok, and G. Hadjisophocleous, *An Experimental Study of Smoke Movement in Multi-Storey Buildings.* Fire Technology 2011. **47**(4): p. 1141-1169.
323. Delichatsios, M.A., *Piloted ignition times, critical heat fluxes and mass loss rates at reduced oxygen atmospheres.* Fire Safety Journal, 2005. **40**(3): p. 197-212.
324. Walton, W.D. and P.H. Thomas, *Estimating Temperatures in Compartment Fires*, in *SFPE Handbook of Fire Protection Engineering*, P.J. DiNenno, Editor. 2002, National Fire Protection Association & Society of Fire Protection Engineers: Quincy, Mass. & Bethesda, Md.
325. Ehlert, J.R. and T.F. Smith, *View factors for perpendicular and parallel rectangular plates.* Journal of Thermophysics and Heat Transfer, 1993. **7**(1): p. 173-175.
326. DCLG, *Measurements of the Firefighting Environment*. 1994, Department for Communities and Local Government: London.
327. National Research Council, *Acute Exposure Guideline Levels for Selected Airborne Chemicals*. 2000: The National Academies Press.
328. Shi, L. and M.Y.L. Chew, *Experimental study of carbon monoxide for woods under spontaneous ignition condition.* Fuel, 2012. **102**(0): p. 709-715.
329. Babrauskas, V., *The generation of CO in bench-scale fire tests and the prediction for real-scale fires.* Fire and Materials, 1995. **19**(5): p. 205-213.
330. Bustamante Valencia, L., et al., *Analysis of principal gas products during combustion of polyether polyurethane foam at different irradiance levels.* Fire Safety Journal, 2009. **44**(7): p. 933-940.
331. Luche, J., et al., *Characterization of thermal properties and analysis of combustion behavior of PMMA in a cone calorimeter.* Fire Safety Journal, 2011. **46**(7): p. 451-461.
332. Aljumaiah, O., et al. *Ghosting Flames in a Low Ventilation Compartment with Kerosene Pool Fires*. in *International Congress Combustion and Fire Dynamics*. 2010. Santander, Spain: University De Cantabria.
333. Aljumaiah, O., et al. *Wood Crib Fires under High Temperature Low Oxygen Conditions*. in *6th International Seminar on Fire and Explosion Hazards*. 2010. Leeds: Research Publishing Services.
334. Purser, J.A., et al., *Repeatability and reproducibility of the ISO/TS 19700 steady state tube furnace.* Fire Safety Journal 2013. **55**(0): p. 22-34.
335. Andersson, B., F. Markert, and G. Holmstedt, *Combustion products generated by hetero-organic fuels on four different fire test scales.* Fire Safety Journal, 2005. **40**(5): p. 439-465.
336. Hull, T.R., K. Lebek, and K.T. Paul. *Correlation of toxic product yields from tube furnace tests and large scale fires*. in *8th Int. Symp. on Fire Saf. Sc.* 2005. Beijing; China: IAFSS.

337. Stec, A.A. and J. Rhodes, *Smoke and hydrocarbon yields from fire retarded polymer nanocomposites.* Polymer Degradation and Stability, 2011. **96**(3): p. 295-300.
338. Alpert, R.L., *Calculation of response time of ceiling-mounted fire detectors.* Fire Technology 1972. **8**(3): p. 181-195.
339. Custer, R.L.P., *Dynamics of Compartment Fire Growth*, in *Fire Protection Handbook*, A.E. Cote, et al., Editors. 2008, National Fire Protection Association: Quincy, Massachusetts. p. 49-58.
340. Tewarson, A., *SFPE Handbook of Fire Protection Engineering, chapter Generation of Heat and Gaseous, Liquid, and Solid Products in Fires.* National Fire Protection Association, Quincy, Massachusetts, 2008. **18**.
341. Babrauskas, et al., *NIST Technical Report 1284: The Role of Bench-Scale Test Data in Assessing Real-Scale Fire Toxicity*, U.S.D.o. Commerce, Editor. 1991, NIST: Gaithersburg.
342. Kotresh, T., et al., *Effect of heat flux on the burning behaviour of foam and foam/Nomex III fabric combination in the cone calorimeter.* Polymer Testing 2006. **25**(6): p. 744-757.
343. Valencia, L.B., et al., *Analysis of principal gas products during combustion of polyether polyurethane foam at different irradiance levels.* Fire Safety Journal 2009. **44**(7): p. 933-940.